SEED DORMANCY, GERMINATION AND PRE-HARVEST SPROUTING

EDITED BY: Chengdao Li, Hiro Nonogaki and Jose Barrero
PUBLISHED IN: Frontiers in Plant Science

frontiers Research Topics

ISSN 1664-8714
ISBN 978-2-88945-762-5
DOI 10.3389/978-2-88945-762-5

About Frontiers

Frontiers is more than just an open-access publisher of scholarly articles: it is a pioneering approach to the world of academia, radically improving the way scholarly research is managed. The grand vision of Frontiers is a world where all people have an equal opportunity to seek, share and generate knowledge. Frontiers provides immediate and permanent online open access to all its publications, but this alone is not enough to realize our grand goals.

Frontiers Journal Series

The Frontiers Journal Series is a multi-tier and interdisciplinary set of open-access, online journals, promising a paradigm shift from the current review, selection and dissemination processes in academic publishing. All Frontiers journals are driven by researchers for researchers; therefore, they constitute a service to the scholarly community. At the same time, the Frontiers Journal Series operates on a revolutionary invention, the tiered publishing system, initially addressing specific communities of scholars, and gradually climbing up to broader public understanding, thus serving the interests of the lay society, too.

Dedication to Quality

Each Frontiers article is a landmark of the highest quality, thanks to genuinely collaborative interactions between authors and review editors, who include some of the world's best academicians. Research must be certified by peers before entering a stream of knowledge that may eventually reach the public - and shape society; therefore, Frontiers only applies the most rigorous and unbiased reviews.
Frontiers revolutionizes research publishing by freely delivering the most outstanding research, evaluated with no bias from both the academic and social point of view. By applying the most advanced information technologies, Frontiers is catapulting scholarly publishing into a new generation.

What are Frontiers Research Topics?

Frontiers Research Topics are very popular trademarks of the Frontiers Journals Series: they are collections of at least ten articles, all centered on a particular subject. With their unique mix of varied contributions from Original Research to Review Articles, Frontiers Research Topics unify the most influential researchers, the latest key findings and historical advances in a hot research area! Find out more on how to host your own Frontiers Research Topic or contribute to one as an author by contacting the Frontiers Editorial Office: researchtopics@frontiersin.org

SEED DORMANCY, GERMINATION AND PRE-HARVEST SPROUTING

Topic Editors:
Chengdao Li, Murdoch University, Australia
Hiro Nonogaki, Oregon State University, United States
Jose Barrero, CSIRO, Australia

Pre-harvest sprouting (PHS) and late-maturity alpha-amylase (LMA) are two of the biggest grain quality defects that grain growers encounter. About 50 percent of the global wheat crop is affected by pre-harvest sprouting to various degrees. Pre-harvest sprouting is a genetically-based quality defect and results in the presence of alpha-amylase in otherwise sound mature grain. It can range from perhaps undetectable to severe damage on grain and is measured by the falling numbers or alpha-amylase activity. This is an international issue, with sprouting damage lowering the value of crops to growers, seed and grain merchants, millers, maltsters, bakers, other processors, and ultimately the consumer. As such it has attracted attention from researchers in many biological and non-biological disciplines. The 13th International Symposium on Pre-Harvest Sprouting in Cereals was held 18-20 September, 2016 in Perth to discuss current findings of grain physiology, genetic pathways, trait expression and screening methods related to pre-harvest sprouting and LMA. This event followed the previous symposium in 2012 in Canada.

Citation: Li, C., Nonogaki, H., Barrero, J., eds. (2019). Seed Dormancy, Germination and Pre-harvest Sprouting. Lausanne: Frontiers Media.
doi: 10.3389/978-2-88945-762-5

Table of Contents

IV. GENES FOR SEED DORMANCY

V. GENETIC ENGINEERING OF SEED DORMANCY AND GERMINATION

VI. ALPHA-AMYLASE, LATE MATURITY ALPHA-AMYLASE AND PRE-HARVEST SPROUTING

VII. ABSTRACTS OF THE 13TH INTERNATIONAL SYMPOSIUM ON PRE-HARVEST SPROUTING IN CEREALS

frontiers in Plant Science

EDITORIAL
published: 30 November 2018
doi: 10.3389/fpls.2018.01783

Editorial: Seed Dormancy, Germination, and Pre-harvest Sprouting

Hiroyuki Nonogaki[1], *Jose M. Barrero*[2] *and Chengdao Li*[3]*

[1] Department of Horticulture, Oregon State University, Corvallis, OR, United States, [2] Commonwealth Scientific and Industrial Research Organisation, Agriculture and Food, Canberra, ACT, Australia, [3] Western Barley Genetics Alliance, Murdoch University, Murdoch, WA, Australia

Keywords: dormancy, seed germination, pre-harvest sprouting, late maturity alpha-amylase, functional genes, QTL

Editorial on the Research Topic

Seed Dormancy, Germination and Pre-harvest Sprouting

Seed germination is the first critical step of the plant life cycle and the foundation of agricultural production. In contrast, seed dormancy prevents seedling emergence in a wrong season or place in wild species. In cereal crops, the lack of dormancy results in pre-harvest sprouting (PHS) under particular conditions of humidity and temperature, which triggers reserve mobilization, mainly starch degradation by α-amylase (Bewley et al., 2013), and reduces grain quality. Annual losses from PHS are likely to approach $1 billion U.S. dollars worldwide (Black et al., 2006).

International Symposium on Pre-harvest Sprouting in Cereals gathered scientists investigating seed dormancy and PHS and staged an excellent opportunity for discussion between basic and applied researchers for the common goal-PHS prevention. This Research Topic: *Seed Dormancy, Germination, and Pre-harvest Sprouting* collected full papers and abstracts from the symposium and also other highly relevant papers submitted to the Journal. The collection also covers another grain quality defect that is often confounded with PHS: Late Maturity α-Amylase (LMA). This Research Topic serves as a reference book for PHS and LMA, in addition to the previous reviews for LMA and PHS (Mares and Mrva, 2014; Rodríguez et al., 2015).

Seed germination is promoted by GA. One way to prevent PHS is to understand the mechanisms of germination promotion by GA and block that pathway. Nelson et al. compared the transcriptomics of the *sleepy1-2* (*sly1-2*), a GA signaling mutant, and wild-type seeds and found dormancy-promoting stored transcripts. Mutations in these genes weaken seed dormancy and therefore their enhancement has potential to prevent PHS.

Another approach to strengthen seed dormancy is to reinforce ABA metabolism or signaling. Nonogaki and Nonogaki enhanced expression of *nine-cis-epoxycarotenoid dioxygenase* (*NCED*) and caused hyperdormancy. While the proof of concept was tested in Arabidopsis, the gene construct was created using a sorghum *NCED* and a wheat promoter. Therefore, the genetic tool is ready for direct translation into crops. *FUSCA3* (*FUS3*) enhances ABA biosynthesis in Arabidopsis (Gazzarrini et al., 2004). Sun et al. has found that *Triticum aestivum FUS3* (*TaFUS3*) interacts with TaSPA (STORAGE PROTEIN ACTIVATOR) (Albani et al., 1997). While the TaFUS3 analysis was not performed in the context of direct regulation of *NCED* expression, the interaction of TaFUS3 and TaSPA to transactivate gene expression advanced our understanding of the FUS3 function in ABA regulation.

ABI5 is involved in ABA signaling in seeds and regulated by nitric oxide (NO) (Nonogaki, 2017). Signorelli and Considine provided their perspectives about the action of reactive nitrogen species

Edited and reviewed by:
Alma Balestrazzi, University of Pavia, Italy

***Correspondence:**
Chengdao Li
c.li@murdoch.edu.au

Specialty section:
This article was submitted to Plant Breeding, a section of the journal Frontiers in Plant Science

Received: *02 October 2018*
Accepted: *16 November 2018*
Published: *30 November 2018*

Citation:
Nonogaki H, Barrero JM and Li C (2018) Editorial: Seed Dormancy, Germination, and Pre-harvest Sprouting. Front. Plant Sci. 9:1783. doi: 10.3389/fpls.2018.01783

and the free radicals with an emphasis on post-translational modification. Understanding this pathway is also critical for PHS prevention and potentially more important for seed germination recovery from PHS-resistant crops because NO promotes germination.

The progresses in basic science are now ready to be translated into crops. However, the fundamental mechanism may have diversified among various crops. Therefore, species-specific case studies are also necessary. Das et al. performed metabolomic analysis using PHS-susceptible and -resistant wheat grains and presented significant differences in small molecule profiles. These profiles, together with proteomic and transcriptomic profiles, will identify crop-specific responses that might not be found in Arabidopsis. Benech-Arnold and Rodriguez shared their experience in PHS research in sorghum. While they also found a GA-ABA balance as the core mechanism of dormancy, GA deactivation, rather than ABA biosynthesis, turned out to be a critical factor for PHS resistance in sorghum. Their finding exemplifies the importance of comparative analyses between species. New QTL analyses in other crops offer a basis for cloning novel genes. Li et al. identified 43 QTL associated with low temperature seed germination of maize while Lee et al. identified 39 candidate SNPs for PHS by re-sequencing 21 representative accessions of rice. These new loci in maize and rice could potentially shed light on hidden pathways of seed dormancy and PHS. In the past, the rice QTL analysis for PHS identified *Seed dormancy 4* (*Sdr4*), which was not found from Arabidopsis (Sugimoto et al., 2010). Likewise, the analysis of the barley *Qsd1* identified the critical role of alanine aminotransferase in seed dormancy regulation through a yet-unknown pathway (Sato et al., 2016). Thus, more discoveries are anticipated from the crop QTL analyses.

This Research Topic also addresses inter- and intraspecies differences in dormancy and PHS mechanisms by using wild, local or synthetic species. Nakamura et al. crossed the wild barley to a malting barley and highlighted the importance of maternal effects. Dale et al. crossed *Aegilops tauschii* with a hexaploid PHS-susceptible white-grain wheat and generated a synthetic octaploid wheat. By using the advanced backcross population, they identified dormancy-associated QTLs. In addition to wild or synthetic species, it is also important to use varieties of local origin for addressing geographical and climate differences of PHS responses in a global scale. Sydenham and Barnard conducted QTL analysis of the South African wheat cultivars while Zhou et al. performed genome-wide association study of the large germplasm collection of Chinese landraces.

The ultimate goal of PHS research is to secure grain quality. Zhang and Li employed genomic approaches to compare α-amylase genes in cereals, including promoters. The information is a great resource to understand the "behavior" of the starch-degrading enzyme and regulate its expression for grain quality. Unusual α-amylase activity in late maturing wheat grains, so-called LMA, is a genetic defect and considered a negative trait for grain quality. However, Newberry et al. are now raising question about the traditional view about LMA. They observed little correlation between LMA and the end product functionality and concluded that LMA has limited impact on bread baking. Martinez et al. even demonstrated inconsistency between some falling number and PHS traits. These new discoveries could be a game changer in breeding programs.

Finally, another important aspect of PHS studies is the synergy between basic and applied science. As discussed for *Sdr4* and *Qsd1*, crop research revealed the presence of novel pathways of seed dormancy, which was not known in model species. The *mitogen-activated protein kinase kinase 3*(*TaMKK3*) is emerging as a novel seed dormancy regulator in crops (Nakamura et al., 2016; Torada et al., 2016). Shorinola et al. analyzed a causal relation between TaMKK3 and PHS in the global germplasm and confirmed its significance for seed dormancy. TaMKK3 also offers a new target pathway to be investigated in basic seed dormancy research using Arabidopsis. Thus, PHS studies are advancing both basic seed biology and applied crop science.

AUTHOR CONTRIBUTIONS

All authors listed have made a substantial, direct and intellectual contribution to the work, and approved it for publication.

FUNDING

The project is partially supported by the Grain Research and Development Corporation for CL (UMU00046).

REFERENCES

Albani, D., Hammond-Kosack, M. C., Smith, C., Conlan, S., Colot, V., Holdsworth, M., et al. (1997). The wheat transcriptional activator SPA: a seed-specific bZIP protein that recognizes the GCN4-like motif in the bifactorial endosperm box of prolamin genes. *Plant Cell* 9, 171–184. doi: 10.1105/tpc.9.2.171

Bewley, J. D., Bradford, K. J., Hilhorst, H. W. M., and Nonogaki, H. (2013). *Seeds: Physiology of Development, Germination and Dormancy*. New York, NY: Springer.

Black, M., Bewley, J. D., and Halmer, P. (2006). *Encyclopedia of Seeds-Science, Technology and Uses*. Wallingford: CABI.

Gazzarrini, S., Tsuchiya, Y., Lumba, S., Okamoto, M., and McCourt, P. (2004). The transcription factor *FUSCA3* controls developmental timing in *Arabidopsis* through the hormones gibberellin and abscisic acid. *Dev. Cell* 7, 373–385. doi: 10.1016/j.devcel.2004.06.017

Mares, D. J., and Mrva, K. (2014). Wheat grain preharvest sprouting and late maturity alpha-amylase. *Planta* 240, 1167–1168. doi: 10.1007/s00425-014-2172-5

Nakamura, S., Pourkheirandish, M., Morishige, H., Kubo, Y., Nakamura, M., Ichimura, K., et al. (2016). Mitogen-activated protein kinase kinase 3 regulates seed dormancy in barley. *Curr. Biol.* 26, 775–781. doi: 10.1016/j.cub.2016.01.024

Nonogaki, H. (2017). Seed biology updates–Highlights and new discoveries in seed dormancy and germination research. *Front. Plant Sci.* 8:524. doi: 10.3389/fpls.2017.00524

Rodríguez, M. V., Barrero, J. M., Corbineau, F., Gubler, F., and Benech-Arnold, R. L. (2015). Dormancy in cereals (not too much, not so little): about the mechanisms behind this trait. *Seed Sci. Res.* 25, 99–119. doi: 10.1017/S0960258515000021

Sato, K., Yamane, M., Yamaji, N., Kanamori, H., Tagiri, A., Schwerdt, J. G., et al. (2016). Alanine aminotransferase controls seed dormancy in barley. *Nat. Commun.* 7:11625. doi: 10.1038/ncomms11625

Sugimoto, K., Takeuchi, Y., Ebana, K., Miyao, A., Hirochika, H., Hara, N., et al. (2010). Molecular cloning of *Sdr4*, a regulator involved in seed dormancy and domestication of rice. *Proc. Natl. Acad. Sci. U.S.A.* 107, 5792–5797. doi: 10.1073/pnas.0911965107

Torada, A., Koike, M., Ogawa, T., Takenouchi, Y., Tadamura, K., Wu, J., et al. (2016). A causal gene for seed dormancy on wheat chromosome 4A encodes a MAP kinase kinase. *Curr. Biol.* 26, 782–787. doi: 10.1016/j.cub.2016.01.063

Conflict of Interest Statement: The authors declare that the research was conducted in the absence of any commercial or financial relationships that could be construed as a potential conflict of interest.

frontiers in Plant Science

ORIGINAL RESEARCH
published: 22 December 2017
doi: 10.3389/fpls.2017.02158

Biology in the Dry Seed: Transcriptome Changes Associated with Dry Seed Dormancy and Dormancy Loss in the *Arabidopsis* GA-Insensitive *sleepy1-2* Mutant

Sven K. Nelson[1†], Tohru Ariizumi[2†] and Camille M. Steber[1,2,3*]*

[1] Molecular Plant Sciences Program, Washington State University, Pullman, WA, United States, [2] Department of Crop and Soil Science, Washington State University, Pullman, WA, United States, [3] Wheat Health, Genetics, and Quality Research Unit, United States Department of Agriculture–Agricultural Research Service, Pullman, WA, United States

OPEN ACCESS

Edited by:
Jose Maria Barrero,
Commonwealth Scientific and Industrial Research Organisation (CSIRO), Australia

Reviewed by:
Christophe Bailly,
Université Pierre et Marie Curie, France
Eiji Nambara,
University of Toronto, Canada

***Correspondence:**
Sven K. Nelson
sven.nelson@ars.usda.gov
Camille M. Steber
csteber@wsu.edu

†Present address:
Sven K. Nelson,
United States Department of Agriculture – Agricultural Research Service and Interdisciplinary Plant Group, University of Missouri, Columbia, MO, United States
Tohru Ariizumi,
Department of Life and Environmental Science, University of Tsukuba, Tsukuba, Japan

Specialty section:
This article was submitted to Plant Breeding, a section of the journal Frontiers in Plant Science

Received: 04 October 2017
Accepted: 06 December 2017
Published: 22 December 2017

Citation:
Nelson SK, Ariizumi T and Steber CM (2017) Biology in the Dry Seed: Transcriptome Changes Associated with Dry Seed Dormancy and Dormancy Loss in the Arabidopsis GA-Insensitive sleepy1-2 Mutant. Front. Plant Sci. 8:2158. doi: 10.3389/fpls.2017.02158

Plant embryos can survive years in a desiccated, quiescent state within seeds. In many species, seeds are dormant and unable to germinate at maturity. They acquire the capacity to germinate through a period of dry storage called after-ripening (AR), a biological process that occurs at 5–15% moisture when most metabolic processes cease. Because stored transcripts are among the first proteins translated upon water uptake, they likely impact germination potential. Transcriptome changes associated with the increased seed dormancy of the GA-insensitive *sly1-2* mutant, and with dormancy loss through long *sly1-2* after-ripening (19 months) were characterized in dry seeds. The *SLY1* gene was needed for proper down-regulation of translation-associated genes in mature dry seeds, and for AR up-regulation of these genes in germinating seeds. Thus, *sly1-2* seed dormancy may result partly from failure to properly regulate protein translation, and partly from observed differences in transcription factor mRNA levels. Two positive regulators of seed dormancy, DELLA *GAI* (*GA-INSENSITIVE*) and the histone deacetylase *HDA6/SIL1* (*MODIFIERS OF SILENCING1*) were strongly AR-down-regulated. These transcriptional changes appeared to be functionally relevant since loss of *GAI* function and application of a histone deacetylase inhibitor led to decreased *sly1-2* seed dormancy. Thus, after-ripening may increase germination potential over time by reducing dormancy-promoting stored transcript levels. Differences in transcript accumulation with after-ripening correlated to differences in transcript stability, such that stable mRNAs appeared AR-up-regulated, and unstable transcripts AR-down-regulated. Thus, relative transcript levels may change with dry after-ripening partly as a consequence of differences in mRNA turnover.

Keywords: SLY1, Arabidopsis, dormancy, dry after-ripening, germination, seeds, transcriptome, DELLA

INTRODUCTION

Plant colonization of dry land was made possible by the evolution of seeds as a means of propagation. The plant embryo encapsulated in orthodox seeds can survive long periods in a desiccated, quiescent state, allowing time for dispersal (reviewed in Bewley et al., 2013). Osmoprotectants like LEA (Late Embryogenesis Abundant) proteins and non-reducing sugars

protect desiccated seeds from cellular damage due to destabilization of membranes and proteins. Non-reducing sugars and compatible solutes replace water in dry seeds at 5–15% moisture, resulting in a "glassy state" that allows only gradual molecular movement (Buitink and Leprince, 2004). Ribosomes are inactive in dry seeds, but form polysomes without *de novo* translation during water uptake or imbibition (Spiegel and Marcus, 1975; Rajjou et al., 2004). mRNAs transcribed during seed maturation are stored in dry seeds, and likely play an important role in determining whether or not a seed can germinate because they encode the earliest proteins translated during seed germination (Marcus and Feeley, 1964; Dure and Waters, 1965; Waters and Dure, 1965, 1966; Chen et al., 1968; Gordon and Payne, 1976; Ishibashi et al., 1990; Almoguera and Jordano, 1992).

Seed dormancy is an adaptation that prevents seed germination even when immediate environmental conditions are favorable (Finch-Savage and Leubner-Metzger, 2006). Seed dormancy prevents germination out of season, allows time for seed dispersal, and increases the variation in the timing of germination (reviewed in Koornneef and Alonso-Blanco, 2000; Venable, 2007; Poisot et al., 2011). Seed dormancy is established during embryo maturation, the final stage of seed development. Dormancy can be relieved through a period of dry storage called after-ripening, through moist chilling (cold stratification), or through seed coat scarification. The after-ripening time required for dormancy loss depends on genotype, and can be perturbed through altered function of dormancy-regulating genes (Ariizumi and Steber, 2007; Chiang et al., 2011; Kendall et al., 2011; reviewed in Koornneef and Alonso-Blanco, 2000; reviewed in Nonogaki, 2014). This genetic variation is particularly important in cereal crops where lack of seed dormancy can lead to problems with preharvest sprouting, the germination of grain on the mother plant when cool and rainy conditions occur before harvest (reviewed by Rodríguez et al., 2015). Informed genetic strategies may allow us to increase seed dormancy sufficiently to prevent preharvest sprouting without causing problems with poor germination and emergence when winter crops are planted in the fall with little after-ripening.

The word "germination" refers both to a process and an event. The germination process has been divided into three phases (reviewed in Bewley et al., 2013). During Phase I, rapid water uptake (imbibition) leads to cellular rehydration associated with expression of genes involved in seed maturation and desiccation tolerance such as LEAs, small heat shock proteins (smHSPs) and oxidoreductases. During Phase II, water uptake plateaus and the seed undergoes essential processes, including DNA repair, initiation of transcription and translation, mitochondrial repair, respiration, initiation of stored nutrient mobilization, DNA synthesis, and cell expansion. Phase III begins with germination the event (germination *per se*), defined by embryonic root emergence. Phase III also includes post-germinative events such as completion of nutrient mobilization, cell division, and seedling growth. Living dormant seeds do not reach Phase III, but they do imbibe water and enter Phase II. This paper will refer to ungerminated seed in Phase I or II as "imbibing seeds" to distinguish them from seeds undergoing germination *per se*.

Understanding how dormancy loss through after-ripening occurs in a dry and metabolically quiescent seed is one of the great mysteries of plant science (reviewed in Koornneef and Alonso-Blanco, 2000; Bewley et al., 2013). Changes during dry seed storage regulate germination potential once the seed is imbibed, yet the severe water deficit in dry seeds likely inhibits most biological processes, including transcription and translation. Transcriptome studies have observed differential accumulation of stored dry seed mRNAs with after-ripening of multiple species (Comai and Harada, 1990; Bove et al., 2005; Leubner-Metzger, 2005; Cadman et al., 2006; Leymarie et al., 2007; Oracz et al., 2007; Bazin et al., 2011; Chitnis et al., 2014; Meimoun et al., 2014). The changes in transcript levels with dry seed after-ripening may result from transcription or differential mRNA turnover. Based on inhibitor studies, protein translation, but not gene transcription, is required for seed germination (Spiegel and Marcus, 1975; Rajjou et al., 2004). This emphasizes the importance of stored mRNAs, since translation of stored mRNA is necessary and sufficient for seed germination.

Some have hypothesized that localized moisture conditions may allow active transcription in dry seeds, while others maintain this is unlikely. Hydrogen proton NMR microimaging of dry seeds detected possible moisture pockets proposed to make dry seed transcription possible (Leubner-Metzger, 2005). Polysome profiles of nuclei isolated from dry seeds of *Brassica napus* suggested active transcription, albeit at 8% of the rate observed during seed maturation (Comai and Harada, 1990). However, non-transcriptional processes likely cause apparent changes in relative transcript abundances during dry seed after-ripening (reviewed in Bewley et al., 2013). Differential RNA turnover may be triggered by mRNA oxidation resulting from oxygen diffusion into dry seeds (Oracz et al., 2007). Dry seed after-ripening of sunflower (*Helianthus annuus*) was associated with differential transcript levels, including 24 after-ripening-down-regulated mRNAs preferentially targeted for destruction by mRNA oxidation (Bazin et al., 2011). Oxidative reactions have also been implicated in dormancy regulation through lipid peroxidation, carbonylation of specific proteins, or oxidation of disulfide bonds to alter protein structure (Alkhalfioui et al., 2007a,b; Oracz et al., 2007). Regardless of the mechanisms causing changes in the dry seed transcriptome with after-ripening, it is important to consider whether changes can impact germination capacity.

The plant hormones abscisic acid (ABA) and gibberellin (GA) act antagonistically to regulate seed dormancy and germination (reviewed in Finkelstein et al., 2008). While ABA promotes seed dormancy, GA stimulates germination. ABA establishes dormancy during seed maturation (Karssen et al., 1983; Lefebvre et al., 2006; Okamoto et al., 2006), while GA biosynthesis and signaling are required for Arabidopsis seed dormancy loss and germination (Koornneef and van der Veen, 1980; Steber et al., 1998; Iuchi et al., 2007; Willige et al., 2007; Hauvermale et al., 2015). ABA-insensitive or biosynthesis mutants rescue the failure

to germinate in GA biosynthesis or GA-insensitive mutants (Karssen and Laçka, 1986; Steber et al., 1998). Thus, GA acts upstream of ABA to stimulate germination.

Gibberellin stimulates seed germination, stem elongation, and flowering by negatively regulating the DELLA (Asp-Glu-Leu-Leu-Ala) repressors of GA responses (reviewed in Hauvermale et al., 2012). GA-binding stimulates the protein–protein interaction between the GID1 (GA-INSENSITIVE DWARF1) GA receptors and DELLA protein. Formation of the GID1-GA-DELLA complex causes either DELLA inactivation or destruction via the ubiquitin-proteasome pathway (McGinnis et al., 2003; Dill et al., 2004; Ariizumi et al., 2008, 2011, 2013; Wang et al., 2009; Ariizumi and Steber, 2011). The Arabidopsis *SLEEPY1* (*SLY1*) gene encodes the F-box subunit of an SCF (Skp, Cullin, F-box) E3 ubiquitin ligase that directly binds to and ubiquitinates DELLA upon formation of the GID1-GA-DELLA complex. Thus, GA causes SCF^{SLY1} to polyubiquitinate, and thereby, target DELLA for destruction by the 26S proteasome. Arabidopsis has five DELLA proteins, *RGA* (*REPRESSOR OF GA1-3*), *GAI* (*GA-INSENSITIVE1*), *RGL1*, *RGL2*, and *RGL3* (*RGA-LIKE*). The failed seed germination of the GA biosynthesis mutant *ga1-3* in the light was strongly rescued by loss of the DELLA *RGL2* (Cao et al., 2005). However, rescue of *ga1-3* germination in the dark, also required loss of DELLAs *RGA* and *GAI*. The GA-insensitive gain-of-function mutation *gai-1* was associated with reduced GA sensitivity during germination in the dark, and reduced germination on ABA in the ABA-insensitive *ABI1-1* mutant background (Koornneef et al., 1985; Ariizumi et al., 2013). DELLAs are thought to repress GA responses through transcriptional regulation via interaction with DNA-binding proteins such as PHYTOCHROME-INTERACTING FACTORS, PIF3, PIF4, and PIF1.

Loss of *SLY1* leads to overaccumulation of DELLA repressors of seed germination associated with increased seed dormancy (Steber et al., 1998; McGinnis et al., 2003; Ariizumi and Steber, 2007). The Arabidopsis GA-insensitive *sly1-2* mutation is a 2-bp deletion leading to loss of the last 40 amino acids of the 151 amino acid protein. Seeds of *sly1-2* have strong initial seed dormancy, but acquire the ability to germinate either with *GID1* gene overexpression (*GID1-OE*) or with 1–2 years of dry after-ripening (Ariizumi and Steber, 2007; Ariizumi et al., 2013). In contrast, Landsberg *erecta* (L*er*) wild-type seeds fully after-ripen within 2 weeks. Neither after-ripening nor *GID1-OE* result in reduced accumulation of DELLA repressors of seed germination. Thus, GA signaling can occur without DELLA-proteolysis leading to increased germination potential. There are three GA receptor genes in Arabidopsis, *GID1a*, *GID1b*, and *GID1c*. *GID1b* protein has higher affinity for GA_4 and for DELLA protein than GID1a and GID1c (Nakajima et al., 2006; Yamamoto et al., 2010). This is likely the reason that *GID1b-OE* rescues *sly1-2* seed germination and plant height phenotypes better than *GID1a-OE* and *GID1c-OE* (Ariizumi et al., 2008, 2013; Hauvermale et al., 2014).

This paper examines the pattern of transcript accumulation in dry seeds associated with increased seed dormancy and dormancy loss in the GA-insensitive *sly1-2 (sleepy1-2)* mutant of Arabidopsis. Transcripts involved in protein translation were *sly1*-up-regulated in dry seeds, and *sly1*-down-regulated upon seed imbibition. Thus, it appears that *SLY1* may be needed both to down-regulate protein translation during seed development, and to up-regulate translation during germination. The importance of protein translation during seed germination has been well characterized (Galland et al., 2014; Layat et al., 2014). This agrees with our previous research showing that increasing germination capacity with after-ripening is associated with increased abundance of protein translation-associated genes (Nelson and Steber, 2017). In that study, the transcriptional changes associated with *sly1-2* dormancy and dormancy loss were quite different during early and late Phase II of seed imbibition. Based on this result, we postulated that earlier transcriptome differences most likely regulate whether a seed can or cannot germinate. By this rationale, transcriptome differences in dry seeds should play key roles in dormancy and dormancy loss since the stored transcripts in dry seeds are likely the first transcripts to impact germination potential. Consistent with this notion, mutations in two genes showing down-regulation with dry seed after-ripening, the DELLA *GAI* and the histone deacetylase *HDA6*, led to decreased seed dormancy. This suggests that *GAI* and histone deacetylation may establish and maintain seed dormancy.

MATERIALS AND METHODS

Plant Materials and Growth Conditions

Arabidopsis thaliana ecotype Landsberg *erecta* (L*er*) wild-type and mutant lines used in this study including *ga1-3*, *sly1-2*, *sly1-2 GID1b-OE*, *gai-1*, *gai-t6*, *sly1-2 gai-t6*, and *sil1* all in the L*er* background were described previously (Peng and Harberd, 1993; Peng et al., 1997; Furner et al., 1998; Steber et al., 1998; Ariizumi et al., 2008). All lines were grown under fluorescent lights in a Conviron® growth chamber according to McGinnis et al. (2003). Harvested seeds were stored at room temperature and low humidity (≈15–30%) in open tubes for dry after-ripening treatments.

The standard practice of harvesting seeds after the entire plant has turned brown (fully desiccated) was used in all cases, except where indicated that harvest occurred at "near maturity." Since all parts of a plant do not turn brown simultaneously, harvesting fully brown plants means that some portion of the seeds collected have been after-ripening on the plant for up to a few weeks. In order to obtain dormant seeds for wild-type or when expecting germination rates higher than wild-type, seeds were harvested when the mother plants were partially brown and partially green. By collecting only seeds that fell freely from dry siliques and sifting seeds through a fine mesh, we ensured that only brown (desiccated) seeds were collected for use in assays.

Microarray Seeds

This study used the same seed batches examined previously during imbibition to investigate starting state transcriptomes of L*er* wt, *sly1-2*(D), *sly1-2*(AR), and *sly1-2 GID1b-OE* (Nelson and Steber, 2017). Two-week-old L*er* wt, *sly1-2*, *sly1-2 GID1b-OE* were grown side-by side, while 19-month-old *sly1-2* was

grown in advance to allow comparison of dormant to non-dormant *sly1-2*. All seeds for microarray analysis were collected from fully brown plants. The *GID1b*-overexpression allele in the *sly1-2* background is a translational fusion of *HA:GID1b* on the 35S cauliflower mosaic virus promoter. Growth and storage conditions are described further in Nelson and Steber (2017).

L*er* After-ripening Time Course

A single batch of L*er* wt seeds was harvested "near maturity" to collect dormant seeds for an after-ripening time course. Freshly harvested seeds were stored in open tubes overnight before collecting dormant, 0 week after-ripened (0wkAR), seeds for germination and RT-qPCR assays. Seeds from the same batch were collected for RT-qPCR and germination assays each day for 14 days.

GAI Mutant Germination Assays

Seeds of L*er* wt, *gai-1*, *gai-t6*, and *sly1-2 gai-t6* were grown side-by-side and harvested at near maturity. Freshly harvested seeds were stored in open tubes overnight before collecting dormant 0wkAR seeds for germination assays.

sil1/*hda6* Mutant Germination Assay

The *hda6* loss of function mutant in the L*er* background, *sil1* was a kind gift from Dr. Jong-Myong Kim at the RIKEN Plant Science Center in Yokohama, JAPAN. L*er* wt and *sil1* seeds used for germination assays were grown side-by-side and harvested at near maturity to obtain dormant seeds. Freshly harvested seeds were stored in open tubes overnight before collecting dormant 0wkAR seeds for the germination assay. Seeds were stored for an additional 14 days in open tubes then collected for the 2wkAR germination assay.

Germination on Tricostatin A

Seeds of L*er* wt, *ga1-3*, and *sly1-2* seeds were harvested from fully brown plants. Seeds were stored for 2 weeks with the exception of long after-ripened *sly1-2*, which was stored for more than 1 year.

Germination Experiments

For all germination screens, seeds were sterilized with 70% ethanol and 0.01% SDS for 5 min followed by 10% bleach and 0.01% SDS for 10 min, washed, and plated on 0.8% agar plates containing 0.5× MS salts (Sigma–Aldrich) and 5 mM MES [2-(*N*-morpholino)ethanesulfonic acid], pH 5.5 (referred to as MS-agar plates). Germination was scored daily. Germination of the same batch of seeds used for microarray analysis was performed as in Nelson and Steber (2017). For the L*er* after-ripening time course germination of at 0wkAR, 1wkAR, and 2wkAR was scored for three replicates of 100 seeds each after cold stratification for 4 days at 4°C in the dark. L*er* after-ripening time course seeds were the seeds used for the RT-qPCR time course for *AHb1* gene expression in L*er* wt. For the comparison of *GAI* mutants, germination was scored for three replicates of 70–100 seeds each both with and without cold stratification for 4 days at 4°C in the dark. For *sil1* mutants, because we expected higher germination efficiency than wild-type would be difficult to capture, each plate was divided into two halves with L*er* wt plated on one side and *sil1* plated on the other for side-by-side comparison. For the same reason, three replicates of 70 seeds each for each of three biologically independent batches of L*er* wt and *sil1* at 0 and 2 weeks of after-ripening were scored both with and without cold stratification for 4 days at 4°C in the dark. The tricostatin A (TSA) dose response experiments were performed for 2–4 replicates of about 30–90 seeds each. Tricostatin A (TSA) was added to plates at 0, 0.5, 1, 2, 4, and 6 μM concentrations and germination was recorded for 2–4 replicates of about 30–90 seeds.

Total RNA Isolation from Dry Seeds

RNA extractions for microarray and RT-qPCR were performed as in Nelson and Steber (2017). Briefly, 20 mg of dry seed per sample were flash frozen in liquid nitrogen and RNA was isolated using a phenol-chloroform based extraction method optimized for extraction from tough tissues, such as dry seeds (Nelson and Steber, Unpublished). The extraction method is based on the Oñate-Sánchez and Vicente-Carbajosa (2008) with additional steps to prevent phenol contamination and increase yield. RNA quantity and quality were determined using a NanoDrop ND-2000c spectrophotometer (Thermo Scientific) and gel electrophoresis using RNA denatured at 70°C for 5 min in a formaldehyde dye. For six samples selected from RNA used in the L*er* after-ripening time course RT-qPCR experiment, quality and quality were also determined using the Agilent 2100 bioanalyzer with the RNA 6000 Nano Kit [RNA integrity number (RIN) = 9.0–9.3].

Microarray and Data Analysis

Microarray analysis of RNA from dry seeds was performed in triplicate using the Affymetrix ATH1 oligonucleotide-based DNA microarray chip (22,810 genes represented). For each replicate of L*er* wt (stored dry for 2 weeks), dormant *sly1-2* (stored dry for 2 weeks), after-ripened *sly1-2* (stored dry for 19 months), and *sly1-2 GID1b-OE* (stored dry for 2 weeks), 2 μg of RNA was processed by the Molecular Biology and Genomics Core Laboratory at Washington State University biotin-labeled cRNA synthesis, ATH1 chip hybridization, and chip scanning[1]. The LIMMA package as part of the Bioconductor suite of tools in the R was used for data analysis as described previously (Gentleman et al., 2004; Smyth, 2005; R Core Team, 2016; Nelson and Steber, 2017). Raw data files are available at ArrayExpress[2] (Kolesnikov et al., 2015) under accession number E-MTAB-6135. Background correction and normalization was performed by Robust Multi-array Average (RMA), control probesets removed, and significance determined by False Discovery Rate (FDR) with $\alpha = 0.05$ (Benjamini and Hochberg, 1995; Irizarry et al., 2003).

Reanalysis of published microarray datasets was conducted using the same methods as above to facilitate fair comparison. The raw dataset from Finch-Savage et al. (2007) was obtained from NASCarrays[3], and dataset from Kendall et al. (2011) was obtained from ArrayExpress. In Finch-Savage et al. (2007) dry seeds of freshly harvested and 120 days after-ripened Cvi

[1]http://crb.wsu.edu/core-laboratories/molecular-biology-and-genomics-core

[2]http://www.ebi.ac.uk/arrayexpress

[3]http://arabidopsis.info/affy

wild-type from independent seed batches were analyzed. The Kendall et al. (2011) study compared dry seeds of L*er* wt and *ft-1* collected from dehisced siliques. When referring to the differential regulation in A relative to B, or AvsB, up in AvsB means up-regulated in A (or down-regulated in B), whereas down in AvsB means down-regulated in A (or up-regulated in B).

Gene Ontology, Gene Family, and TAGGIT Ontology Analyses

Analysis for enrichment in gene categories was performed by (1) looking for global enrichment of genes in standard gene ontology (GO) categories, (2) looking for global enrichment of genes in specific gene families (GF), and (3) looking for enrichment of genes within a specific set of seed dormancy and germination related gene categories (TAGGIT). GO biological process and GF enrichment was performed using the BioMaps tool as part of the VirtualPlant 1.3 suite of online tools for analysis of genomic data[4] (Katari et al., 2010). Enrichment was determined for a list of differentially regulated genes against the whole genome using a Fisher Exact Test with FDR correction for multiple comparisons using a p-value cutoff of $p < 0.01$ (Fisher, 1922). For each significantly enriched category a value for enrichment expected by chance (Expected), was presented for comparison to observed enrichment values (Observed).

For seed germination and dormancy specific GO classifications, the *TAGGITontology* and *TAGGITplot* R functions that we developed previously based on the Carrera et al. (2007) TAGGIT categorizations were used (Nelson and Steber, 2017). These functions are publicly available through github as part of the microarray Tools R package[5]. TAGGIT uses 26 categories defined for their involvement in seed dormancy and germination and matches genes to categories based on lists of AGI locus identifiers in combination with a gene description search for specific keywords. For simplicity, "more up-regulation" or "more down-regulation" in a category refers to a higher degree of enrichment in either the up-regulated gene fraction, or in the down-regulated gene fraction, respectively.

One of the concerns about comparisons of dry seed gene datasets is that differential regulation may be random background due to differences in seed batches. To confirm that the differences in category enrichment identified by TAGGIT could not emerge from a random dataset due to unexpected bias in the computational algorithm, a non-overlapping random set of 330 up- and 430 down-regulated genes was analyzed by TAGGIT (Supplementary Figure 1). This random dataset showed low category enrichments and only small changes between up- and down-regulation datasets, indicating that the differential enrichment in TAGGIT categories observed for *sly1-2* and Cvi dry seed datasets were non-random.

Transcription Factor Gene Identification in R

To determine the number of transcription-factor-coding mRNAs (TF-mRNAs) in a given geneset a list of Arabidopsis transcription factors was compiled based on the combined databases of PlnTFDB[6], AtTFDB[7], and PlantTFDB[8], since each database contained some unique entries (Supplementary Table 1; Davuluri et al., 2003; Palaniswamy et al., 2006; Pérez-Rodríguez et al., 2009; Zhang et al., 2014). This list contains both true DNA-binding transcription factors and transcription co-factors. In order to categorize a list of TF-mRNAs into transcription factor families, an R function called *countTFs* was written for this study (Supplementary Figure 2). *countTFs* is available for public use as part of the microarrayTools R package through github[9].

PlantGSEA Transcription Factor Target Analysis

The web-based Plant GeneSet Enrichment Analysis toolkit (PlantGSEA[10]) with the Transcription Factor Targets (TFT) dataset was used to determine enrichment for known targets of transcription factors within differentially regulated genesets (Yilmaz et al., 2010; Lai et al., 2012; Yi et al., 2013). This toolkit uses published ChIP-seq or ChIP-chip data to identify "Confirmed" or "Unconfirmed" transcription factor targets. Targets that are "unconfirmed" were only identified by a single experimental approach, while "confirmed" targets were identified by two or more approaches with *in vivo* evidence. The "All" category includes both confirmed and unconfirmed targets. Enrichment of transcription factor targets was determined using a Fisher statistical test with the Yekutieli (FDR under dependency) correction for multiple testing adjustment with $\alpha = 0.05$ (Fisher, 1922; Benjamini and Yekutieli, 2001). To prevent falsely high enrichment for transcription factors with few known targets a 5 hit minimum cutoff was used.

RT-qPCR Analysis

RT-qPCR analysis was performed using gene-specific primers for *GAI*, *HDA6*, *DOG1*, *SLY1*, *MFT*, *HSFA9*, and *AHb1* for comparison to microarray results. RT-qPCR was also performed for L*er* wt dry seeds at 0, 2, and 4 weeks of after-ripening to determine if an increase in *AHb1* mRNAs could be seen with after-ripening. Primers for *SLY1* were selected to allow binding of both the *sly1-2* mutant and native *SLY1* transcript, since the ATH1 chip cannot distinguish between *SLY1* and *sly1-2* transcripts. The ProScript® M-MuLV First Strand cDNA synthesis kit (New England Biolabs) was used for cDNA synthesis from 1 μg of total RNA and the LightCycler FastStart DNA Master SYBR Green I kit (Roche) was used for qPCR. The QuantPrime online tool[11] was used for primer design with the exception of the previously published *DOG1*, *GAI*, and *HSFA9* (Zhang and Zhu, 2011; Nomoto et al., 2012; Guan et al., 2013). Primer sequence and annealing temperatures are presented in Supplementary Figure 3. Dilution curves were used to calculate reaction efficiencies; all efficiencies were

[4]www.virtualplant.org

[5]https://github.com/bakuhatsu/microarrayTools

[6]http://plntfdb.bio.uni-potsdam.de/v3.0/

[7]http://arabidopsis.med.ohio-state.edu/AtTFDB/

[8]http://planttfdb.cbi.pku.edu.cn

[9]https://github.com/bakuhatsu/microarrayTools

[10]http://structuralbiology.cau.edu.cn/PlantGSEA/

[11]http://www.quantprime.de

within 10% of each other and ±10% of 100% efficiency. qPCR conditions were: 10 min at 95°C (initial denature), then 45 cycles of 10 s at 95°C (denaturation), 5 s at the primer-specific annealing temperature (see Supplementary Figure 3), and 10 s at 72°C (extension). Data was analyzed using the Delta–Delta *C*t method with three replicates per gene or timepoint using the AKR2B (*ANKYRIN REPEAT-CONTAINING 2B*; *At2g17390*) reference gene (Livak and Schmittgen, 2001; Hruz et al., 2011). Statistical testing was performed by pairwise *t*-test with Bonferroni–Holm correction for multiple comparisons with $\alpha = 0.07$ (Supplementary Figure 4; Holm, 1979).

RESULTS

Strategies for Examining Mechanisms of *sly1-2* Dormancy and Dormancy Loss in Dry Seeds

In order to ask specific questions regarding the initial transcriptome state of dormant and non-dormant *sly1-2* seeds, an Affymetrix® oligonucleotide-based microarray transcriptome analysis was conducted on dry seeds of: (a) wild-type L*er* (WT) stored for 2 weeks, (b) dormant *sly1-2* stored for 2 weeks [*sly1-2*(D)], (c) after-ripened *sly1-2* stored for 19 months [*sly1-2*(AR)], and d) *sly1-2 GID1b-overexpressed* (*sly1-2 GID1b-OE*) stored for 2 weeks (**Figure 1C**). L*er* WT reached 96% germination after 1 day, whereas *sly1-2*(D) did not germinate even after 7 days of imbibition (**Figure 1B**). *sly1-2* germination was rescued by long after-ripening for 19 months (51% germination by 7 days), and by *GID1b-OE* (73% by 7 days). The same seed stocks were previously used in an imbibed seed microarray study, including a "0h" timepoint taken immediately after cold stratification for 4 days at 4°C in the dark, and a "12h" timepoint (4 days at 4°C, followed by 12h at 22°C in the light) (**Figure 1A**; Nelson and Steber, 2017). Time points examined and comparisons made between this and previous studies are summarized in **Figures 1C,D**.

Stored mRNA Transcriptome Differences Associated with the *sly1-2* Dormancy Phenotype

The *sly1-2*(D) to wild-type L*er* (*sly1-2* DvsWT) comparison identified 794 transcript differences associated with the *sly1-2* seed dormancy phenotype (**Figure 2A**). Since the comparison of another mutation affecting germination, *ft-1* (*flowering locus t-1*), to L*er* wt dry seeds detected no transcriptome differences (Chiang et al., 2009; Kendall et al., 2011), these changes in dry seed transcript levels were likely effects of the *sly1* mutation during seed development, maturation, or during the 2 weeks of dry after-ripening. The *sly1-2* DvsWT comparison had more negative $\log_2$-fold changes (logFCs) (517 *sly1*-down-regulated) than positive (277 *sly1*-up-regulated) (**Figure 2A**), resulting in an adjusted Fisher-Pearson standardized moment coefficient skewed toward down-regulation (G1 = −0.56, vs.

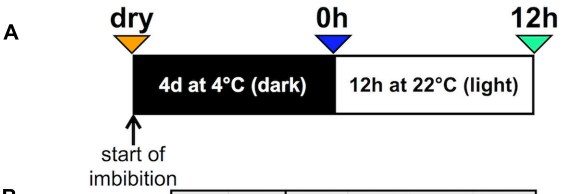

B

	0h	12h	1 d	3 d	5 d	7 d	
Ler (wt)	0%	0%	96%	98%	99%	99%	WT
sly1-2(D)	0%	0%	0%	0%	0%	0%	D
sly1-2(AR)	0%	0%	19%	43%	51%	51%	AR
sly1-2 GID1b-OE	0%	0%	0%	19%	53%	73%	GID

C

	genotype	dry storage		germinate	this study	Nelson and Steber, 2017	
		2 wk	19 mo		dry	0h	12h
WT	wild-type	X		X	X	X	X
D	*sly1-2*	X			X	X	X
AR	*sly1-2*		X	X	X	X	X
GID	*sly1-2 GID1b-OE*	X		X	X	X	X

D

Comparison	timepoint	original data
DvsWT	dry, 0h, 12h	current study; Nelson and Steber, 2017
GIDvsD	dry, 0h, 12h	current study; Nelson and Steber, 2017
sly1-2 **ARvsD**	dry, 0h, 12h	current study; Nelson and Steber, 2017
ARvsWT	dry, 0h, 12h	current study; Nelson and Steber, 2017
Cvi **ARvsD**	dry	Finch-Savage et al., 2007
ft-1 vs L*er* wt	dry	Kendall et al., 2011

FIGURE 1 | Microarray experimental design. **(A)** Seeds in this study were examined at the "dry" (orange) timepoint in dry seeds. Comparisons were also made to Nelson and Steber (2017) "0h" (blue) timepoint after cold stratification in the dark for 4 days at 4°C and the "12h" (green) timepoint with cold stratification and 12h in the light at 22°C. **(B)** Germination of seeds used for microarray analysis. The same batches of seeds as in Nelson and Steber (2017) were imbibed on MS-agar plates for 4 days at 4°C, then moved to the light at 22°C and scored for germination. **(C)** L*er* wt, *sly1-2*(D), and *sly1-2 GID1b-OE* seed batches were 2 weeks old, while *sly1-2*(AR) was 19 months old seed. **(D)** Experimental comparisons made in this paper, including comparisons from reanalysis of data from Finch-Savage et al. (2007) and Kendall et al. (2011).

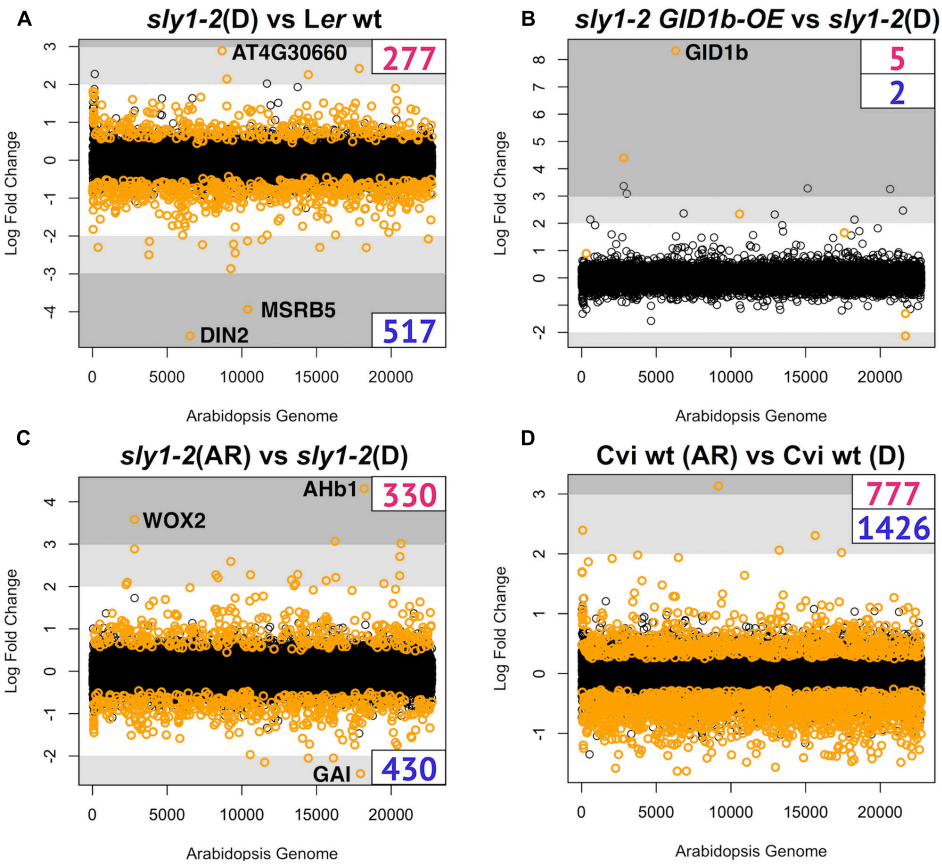

FIGURE 2 | Genome wide expression plots. Plots indicate skew, chromosomal distribution, and magnitude of **(A)** dry seed *sly1*-regulated transcriptome differences, **(B)** dry seed *sly1-2 GID1b-OE* vs. *sly1-2*(D) differences, **(C)** differences after-ripened (AR) and dormant (D) *sly1-2* dry seeds *sly1-2,* and **(D)** differences between after-ripened (AR) and dormant (D) Cvi. Genes with significant differences are indicated in orange (based on FDR $p < 0.05$). Up-regulation is indicated by positive $\log_2$-fold change (logFC) and down-regulation with negative. Shaded area mark the ±2 and ±3 logFC to allow comparison of magnitude and skew between genesets.

G1 = 0 if symmetrical) (Joanes and Gill, 1998). Plots comparing normalized intensities showed transcriptome differences across a wide range of signal intensities, indicating that significance was not an artifact of small changes at low intensities (Supplementary Figure 5A). The *sly1-2* F-box mutation results in an inability to degrade DELLA transcriptional regulators (Nelson and Steber, 2016). Thus, negative DELLA regulation in *sly1* mutants may directly or indirectly cause the reduced accumulation of many transcripts during dry seed development. Not surprisingly, some of the top 50 differentially regulated genes were seed-related genes such as a LEA and seed storage proteins (**Figure 3A**). Of the top 50 DELLA/*sly1*-regulated genes in dry seeds, 21 were similarly regulated at the previously published 0h and 12h imbibed timepoints (Nelson and Steber, 2017).

The differentially abundant genes in the dry seed *sly1-2* DvsWT comparison were characterized using BioMaps GO and gene family (GF) to look for biological process enrichment[12] (Supplementary Figures 6A–C; Katari et al., 2010). There was significant up-regulation of two ribosomal GF, and down-regulation of the glycosyltransferase gene family, including genes involved in auxin and ABA hormone signaling (Supplementary Figure 6A; Yonekura-Sakakibara, 2009). Many *sly1*-up-regulated GO categories were also related to protein translation, ribonucleoprotein complex and ribosome biogenesis (Supplementary Figure 6B). The *sly1*-down-regulated GO categories included stress or stimuli responses related to seed dormancy such as response to ABA, abiotic stress, and oxidation/reactive oxygen species (Supplementary Figure 6C; reviewed in Graeber et al., 2012).

Transcriptome Differences Associated with Rescue of *sly1-2* Germination by Long After-ripening and *GID1b-OE*

The fact that *sly1* mutants have increased seed dormancy suggests that *SLY1*-directed DELLA destruction is needed for dormancy loss and germination. However, the germination of *sly1-2* seeds is partly rescued by *GID1* overexpression and by long after-ripening without any decrease in DELLA protein accumulation

[12] www.virtualplant.org

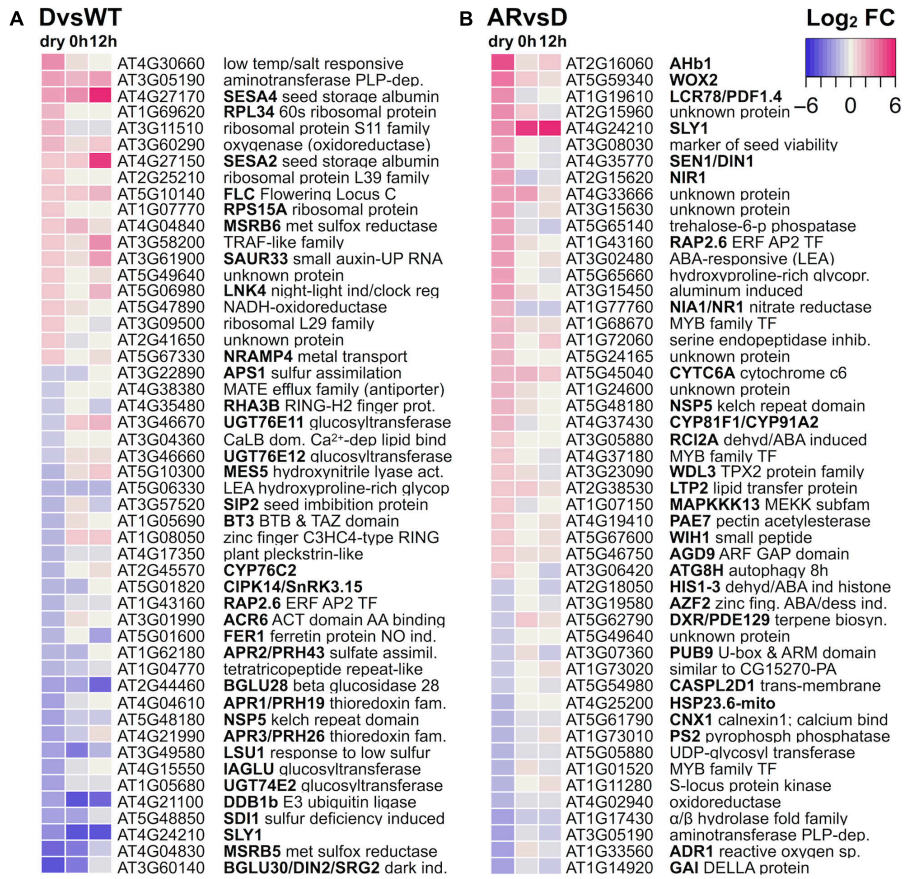

FIGURE 3 | The top 50 largest $\log_2$-fold change differences in and their transcriptome differences in imbibed seeds. Differences are plotted as a heat map of dry seed values with comparison to the same comparison at 0h and 12h imbibition timepoints from Nelson and Steber (2017). **(A)** Between *sly1-2*(D) and L*er* wt dry seeds (DvsWT) and **(B)** between after-ripened and dormant *sly1-2* (ARvsD) dry seeds. Throughout this work, up-regulation is indicated in red and down-regulation in blue.

(**Figure 1B**; Ariizumi and Steber, 2007; Ariizumi et al., 2008). We previously learned that *sly1-2* rescue by *GID1b-OE* was associated with far fewer changes in expression than rescue by long after-ripening in imbibing seeds (Nelson and Steber, 2017). We made a similar observation in dry seeds (**Figures 1B,C** and **Table 1**). There were 770 genes with different transcript abundances between D and AR *sly1-2* dry seed, 330 up-regulated and 430 down-regulated with after-ripening of *sly1-2* (*sly1-2* ARvsD). In contrast, only 7 genes showed differential accumulation with *GID1b*-overexpression in *sly1-2* (GIDvsD) dry seeds (**Figure 2B**).

While more transcripts showed decreased rather than increased levels with after-ripening, the dataset was slightly skewed toward AR-up-regulation (G1 = 0.35), likely due to stronger up-regulation of fewer transcripts (**Figure 2C**). For example, there were 20 up-regulated transcripts with logFCs from 2 to 4.3, whereas only 4 of the down-regulated transcripts had logFCs greater than 2. This is consistent with observations made during dry after-ripening of the dormant ecotype Cvi; where there were 777 up- and 1426 down-regulated transcripts in the Cvi ARvsD comparison (**Figure 2D**). Since the plotted normalized intensities of *sly1-2* ARvsD showed significant differences (red) over a wide range of intensities, the small number of transcripts highly up-regulated do not appear to be artifacts of comparing low intensity values (Supplementary Figure 5B). Many of the *sly1-2* ARvsD transcriptome changes observed in dry seeds were also seen at 0h and 12h of imbibition, but with lower logFCs (**Figure 3B**). The most up-regulated gene was the *AHb1* (*Arabidopsis nonsymbiotic Hemoglobin1*; Abbruzzetti et al., 2011) gene involved in oxidative stress response, whereas the most down-regulated gene was the DELLA *GAI*. It is interesting that *GAI* was up-regulated in the *sly1-2* DvsWT dry seed comparison and down-regulated with dry after-ripening (**Figure 3B**). This suggests that *GAI* plays a role in *sly1-2* dormancy that is reversed with long after-ripening. BioMaps gene family analysis and GO analysis showed that many of the dry seed *sly1*-regulated terms (*sly1-2* DvsWT) were oppositely AR-regulated (Supplementary Figures 6A–C; Katari et al., 2010). The *sly1*-down-regulated stimuli response terms, including ABA and abiotic stress, were AR-up-regulated in dry *sly1-2* seeds (Supplementary Figure 7A). Only translation and terms related to cellular/metabolic processes were *sly1*-up- and AR-down-regulated (Supplementary Figures 6A,B, 7B).

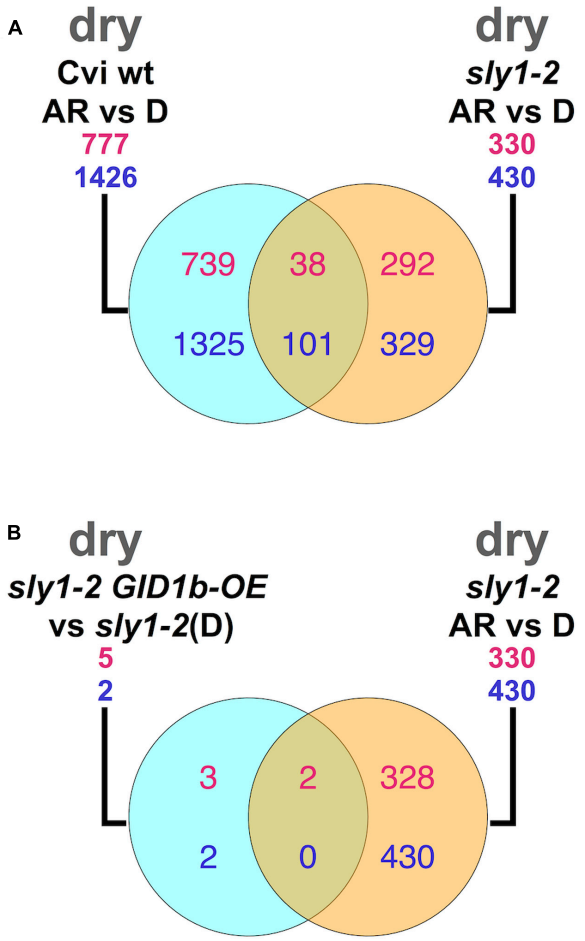

FIGURE 4 | Comparisons between dry transcriptome datasets. **(A)** The overlap between *sly1-2* and Cvi dry seed after-ripening regulated datasets. Cvi dataset is from Finch-Savage et al. (2007). **(B)** The overlap between dry seed *GID1b-OE*-regulated and after-ripening regulated mRNAs.

TABLE 1 | Complete table of *sly1-2 GID1b-OE* vs. *sly1-2*(D) differentially regulated genes across all three imbibition timepoints.

ID	Gene	dry[a]	0h[a]	12h[a]
At3g63010	GID1b	8.32	8.58	8.28
At5g59310	LTP4	4.40	–	–
At4g02380	LEA5	2.34	–	–
At1g21630	EF hand family	1.65	2.77	2.95
At1g44575	NPQ4	0.89	–	–
At5g46050	PTR3	–	1.26	–
At5g54070	HSFA9	–	–	1.34
At4g09610	GASA2	–	–	1.29
At3g45970	EXPL1	–	–	1.01
At2g34740	A PP2C	–	–	0.97
At3g22490	A LEA	–	–	0.91
At5g45690	Unknown protein	–	–	0.83
At2g46240	BAG6	−2.13	−2.69	−3.19
At2g46250	Myosin heavy chain related	−1.31	−1.80	−3.39
At1g17430	α/β hydrolase fold family	–	−1.10	–
At5g01740	NTF2 family	–	−1.07	–
At5g48850	SDI1	–	−1.06	–
At5g58860	HORST	–	−1.00	–
At1g09200	Histone H3.1	–	−0.93	–
At1g22760	PAB3	–	−0.90	–
At5g56580	ANQ1/MKK6	–	−0.83	–
At1g56190	Phosphoglycerate kinase	–	−0.79	–
At5g15230	GASA4[b]	–	–	−1.51
At5g07480	KUOX1	–	–	−1.28
At2g44800	Oxidoreductase	–	–	−1.13
At2g40880	CYSA	–	–	−0.77
At2g16060	AHb1/GLB1	–	–	−0.73

[a] *sly1-2 GID1b-OE vs. sly1-2(D) log_2 fold changes.*
[b] *log_2 fold change of −1.51 ± 0.56, significant based on RT-qPCR.*

The significant overlap between AR-regulated genes in Cvi and *sly1-2*, despite the fact that *sly1-2* is in the L*er* ecotype, suggests that these changes are biologically relevant (**Figure 4A**). The direct overlap of *sly1-2* and Cvi AR-regulated transcriptome changes identified a list of genes associated with both Cvi wt and *sly1-2* dormancy loss (Supplementary Table 2). There were 38 up- and 101 down-regulated transcripts in *sly1-2* and Cvi with after-ripening. This smaller dataset included genes that are AR-regulated in both *sly1-2* and Cvi wt. This dataset included many genes related to ABA or GA signaling and germination. Among them, the DELLA *GAI*, 5 members of the ABA PP2C (Protein Phosphatase Type 2C) family genes, *MFT* (*MOTHER OF FT AND TFL*), and *HDA6* (*HISTONE DEACETYLASE6*) were all AR-down-regulated.

GID1b-OE rescue of *sly1-2* germination was associated with only seven differentially abundant transcripts in dry seeds, 5 up- and 2 down-regulated (**Table 1**). Since *GID1b* is overexpressed on the 35S promoter, it was not surprising that the most up-regulated gene was *GID1b* itself. Among the remaining 6 genes, 3 were similarly regulated at 0h and 12h of imbibition, including: the up-regulated *At1g21630* (EF hand family) gene, and down-regulated *At2g46250* (myosin heavy-chain related) and *BAG6* (*BCL-2-Associated Anthogene6*) genes. When the dataset was compared to the dry seed transcriptome changes with after-ripening of *sly1-2*, *LTP4* and *LEA5/SAG21* were *GID1b-OE*- and AR-up-regulated (**Figure 4B**). *LTP4* encodes a phospholipid transfer protein localized to the cell wall, while *LEA5/SAG21* encodes a senescence-associated protein with a role in oxidative stress tolerance (Arondel et al., 2000; Hundertmark and Hincha, 2008). Both *LTP4* and *LEA5/SAG21* are also ABA-induced transcripts.

Protein Translation and Gene Transcription Are Major Gene Categories Regulated by *SLY1* and After-ripening

TAGGIT seed-related ontology analysis was used to compare gene enrichment in seed-specific categories for genes differentially regulated in DvsWT, *sly1-2* ARvsD (current study, L*er* ecotype), and ecotype Cvi ARvsD dry seed comparisons (**Figures 1D**, **5**; Carrera et al., 2007; Finch-Savage et al., 2007; Nelson and Steber, 2017). It is interesting that the protein translation category accounted for 25% of the *sly1*-up-regulated genes (DvsWT; **Figure 5A**) given that the translation category

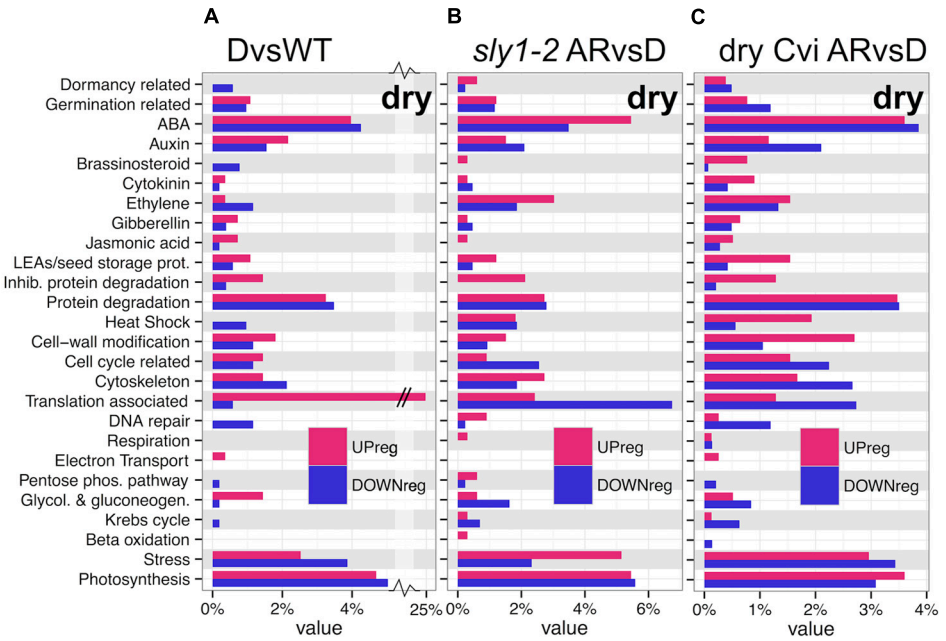

FIGURE 5 | TAGGIT gene ontology analysis of *sly1-* and after-ripening-regulated transcriptome differences in dry seeds. **(A)** *sly1-2* DvsWT dry seed transcriptome differences. **(B)** Differences with after-ripening of *sly1-2* dry seeds. **(C)** Differences with after-ripening of Cvi dry seeds. The value on the *x*-axis shows the percentage of either the total up-regulated or total down-regulated genes within a dataset.

was among the most highly *sly1*-down-regulated at 0h and 12h of seed imbibition in our previous study (Supplementary Figure 8; Nelson and Steber, 2017). The translation category was also strongly down-regulated with after-ripening of both *sly1-2* and Cvi dry seeds (**Figures 5B,C**). In contrast, the translation category showed strong up-regulation with after-ripening of imbibed L*er* wt but not *sly1-2* seeds (Nelson and Steber, 2017). Thus, it appears that the *SLY1* gene is needed both to down-regulate protein translation-associated genes during seed development and to up-regulate protein translation genes during seed germination.

It appears that dry after-ripening involves similar mechanisms in *sly1-2* and Cvi since many TAGGIT categories, such as auxin, ethylene, LEAs, inhibition of protein degradation, cell wall, and cell cycle, showed similar regulation in both experiments (**Figures 5B,C**). TAGGIT analysis of a randomly generated dataset confirmed that TAGGIT profiles similar to those observed for *sly1-2* ARvsD and Cvi ARvsD were unlikely to happen by chance, suggesting that this agreement has functional relevance (Supplementary Figure 1). However, there was not perfect agreement in all *sly1-2* and Cvi categories. For example, ABA was strongly up-regulated in *sly1-2*, but slightly down-regulated in Cvi, while the cytoskeleton category was up-regulated in *sly1-2* but down-regulated in Cvi. Since these categories were similarly regulated in *sly1-2* and L*er* during late Phase II, they may result from either the *sly1* mutation or ecotype differences (Nelson and Steber, 2017).

The first proteins translated from stored mRNAs may activate or block transcriptional cascades leading to germination. Thus, we examined if differentially expressed transcription-factor-encoding mRNAs (TF-mRNAs) are among the AR-regulated genes in dry seeds using a combined list of Arabidopsis transcription factors compiled from the PlnTFDB, AtTFDB, and PlantTFDB databases (Davuluri et al., 2003; Palaniswamy et al., 2006; Pérez-Rodríguez et al., 2009; Jin et al., 2013). This analysis revealed 27 transcription-factor-encoding mRNAs (TF-mRNAs) up-regulated and 42 TF-mRNAs down-regulated with dry after-ripening (Supplementary Figure 9C). Categorization of genes by transcription factor families using the *countTFs* R function, written for this study (see Section "Materials and Methods"), revealed that transcription factor families strongly regulated with *sly1-2* after-ripening included AP2-EREBP, ARF (Auxin Response Factors), C3H (Cys3His zinc fingers), GRAS, and MYB-related families (Supplementary Figure 9D).

Since 2 weeks of dry after-ripening is sufficient to stimulate wild-type L*er* but not in *sly1-2* germination, we examined changes in TF-mRNA accumulation in the *sly1-2* DvsWT dry seed comparison. Of the 794 *sly1*-regulated transcripts, 53 TF-mRNAs were *sly1*-down-regulated, while only 10 TF-mRNAs were up-regulated (**Figure 6** and Supplementary Figure 9A). Thus, a major effect of the *sly1* mutation appears to be loss of TF-mRNAs that may be translated during imbibition. When these TF-mRNAs were examined at 0h and 12h, most of the dry seed *sly1*-down-regulated genes were not similarly regulated at 0h or 12h, while 7 of the 10 *sly1*-up-regulated genes were similarly regulated at 0h or 12h of imbibition (**Figure 6**). The *sly1*-down-regulated TF-mRNAs families included AP2-EREBP (APETALA2 and ethylene-responsive element binding proteins), bHLHs (basic helix-loop-helix), C2H2 zinc fingers, and MYB-related family

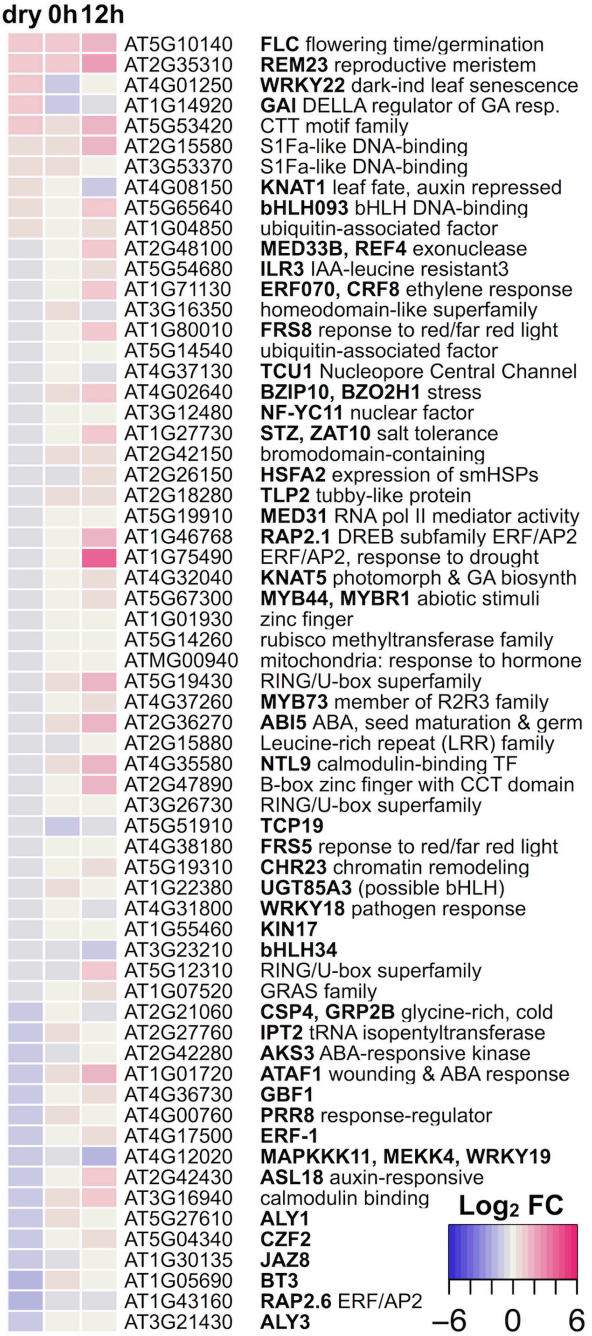

FIGURE 6 | Heat map of all dry seed *sly1-2* DvsWT differentially regulated transcription factors showing their expression changes in dry seeds, at 0h, and at 12h of imbibition.

transcription factors (Supplementary Figure 9B). The DELLA *GAI* was among the *sly1*-up-regulated TF-mRNAs. Thus, DELLA accumulation in *sly1-2* may promote *GAI* expression, possibly through feed-forward regulation (Zentella et al., 2007).

In addition to TF-mRNAs, the Plant GeneSet Enrichment Analysis (PlantGSEA) tool was used to look for enrichment of known transcription factor targets within the dataset of stored mRNA differences in the *sly1-2* DvsWT dry seed comparison (Yilmaz et al., 2010; Lai et al., 2012; Yi et al., 2013). Targets of the bHLH transcription factor PIF1/PIL5 (PHYTOCHROME INTERACTING FACTOR1/PIF3-LIKE5) were strongly enriched in the *sly1*-down-regulated geneset, representing 9% of the *sly1*-down-regulated genes in dry seeds (Supplementary Figure 10). Thus, PIF1/PIL5 may represent a *SLY1*-dependent regulator of seed dormancy.

An Association between mRNA Stability and Changes in Relative Transcript Levels with Dry After-ripening

Seed dormancy is relieved by after-ripening during dry storage. Little metabolic activity is possible in a dry seed, suggesting that differences in transcript turnover rates rather than active transcription may cause the changes in transcript abundances observed with dry after-ripening. Data analysis was used to explore whether apparent up- or down-regulation of stored mRNA was associated with differences in transcript stability. If a small number of stable or protected mRNAs degrade more slowly than the ribosomal RNA, microarray of apparently equal RNA amounts would indicate that these stable genes were up-regulated. A previous study identified genome-wide mRNA stabilities for 13,012 transcripts by measuring transcriptome changes over time after L*er* cell cultures were treated with the transcriptional inhibitor Actinomycin D (Narsai et al., 2007). This included mRNA half-life values for 99 of the 139 *sly1-2* and Cvi AR-regulated transcripts. A heatmap of these 99 AR-regulated transcript changes was plotted in decreasing order of mRNA half-life to examine whether lower intrinsic mRNA stability was associated with decreasing mRNA levels with dry after-ripening (**Figure 7A**). Although mRNA stability alone cannot account for all up- and down-regulation, shorter half-life mRNAs appeared more AR-down-regulated and longer half-life mRNAs appeared more AR-up-regulated. Similarly, when the AR-regulated transcripts were categorized by half-life range, a larger percentage of stable mRNAs (12–24 h or 6–12 h half-life) were up-regulated, whereas more unstable mRNAs (1–3 h half-life) were down-regulated (**Figures 7B,C**). This trend for high stability mRNAs to be up-regulated and lower stability mRNAs to be down-regulated was not seen at *sly1-2* ARvsD 0h and 12h timepoints, indicating that mRNA stability is not the major determinant of transcript levels in imbibing seeds (Supplementary Figures 11A–C). The dry transcriptome counterexamples where mRNA stability was high, yet transcript levels were low or vice versa may be transcripts subject to more active regulation, such as protection by an RNA-binding proteins or targeted mRNA oxidation.

Comparison of Differential Regulation of Stored mRNAs by RT-qPCR and Microarray

RT-qPCR analysis was used to validate transcript level differences identified by microarray in the *sly1-2* ARvsD and/or DvsWT comparisons (**Figure 8**). For comparison, both RT-qPCR and microarray expression were plotted relative to the

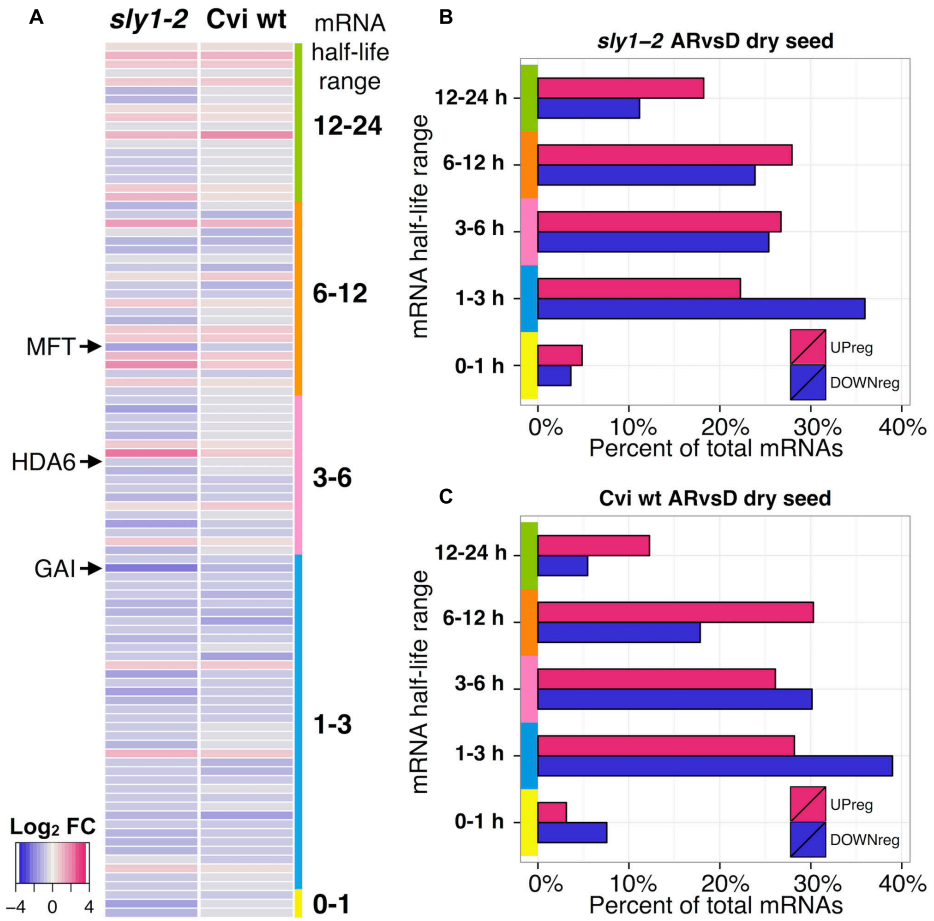

FIGURE 7 | Transcriptome differences categorized based on inherent mRNA stability. **(A)** Heat map of genes differentially regulated in dry seeds with after-ripening of both *sly1-2* and Cvi wt. Genes are plotted in order of high to low mRNA stability determined based on the half-life scores from Narsai et al. (2007). **(B,C)** Plots of fractions of after-ripening-up- and down-regulated genes in each half life range stability category. **(B)** For *sly1-2* dry seed transcriptome changes. **(B)** For Cvi dry seed transcriptome changes. There was a correlation of higher stability with up-regulation and lower stability with down-regulation in dry seed datasets. Both datasets had few genes with half-life in the 0–1 h range.

constitutively expressed control gene *AKR2B* (*ANKYRIN REPEAT-CONTAINING 2B, At2g17390*) (Hruz et al., 2011). RT-qPCR confirmed that *GAI*, *HDA6*, *MFT*, and *HSFA9* (*HEAT SHOCK FACTOR A9*) were AR-down-regulated, while *GAI* and *MFT* were *sly1*-up-regulated in dry seeds (**Figure 8A**). As in imbibed seeds, the *SLY1*/*sly1-2* transcript was AR-up-regulated and *sly1*-down-regulated in dry seeds (Nelson and Steber, 2017). The dormancy-associated *DOG1* (*DELAY OF GERMINATION1*) gene was AR-up-regulated in the *sly1-2* microarray analysis, but just outside of statistical significance ($p = 0.071$) by RT-qPCR. Conversely, *DOG1* was AR-down-regulated in Cvi wt (Finch-Savage et al., 2007). Finally, the *AHb1* transcript was highly AR-up-regulated based both on microarray and RT-qPCR ($p = 8 \times 10^{-4}$) analysis in *sly1-2* (**Figure 8B**).

Since *AHb1* was not significantly up-regulated with ecotype Cvi dry after-ripening, it may be the case that AR-up-regulation of *AHb1* is dependent on the L*er* ecotype. Thus, an after-ripening time course examined if *AHb1* was up-regulated with dry after-ripening of wild-type L*er*. RNA was isolated from dry L*er* seeds immediately after harvest at maturity (0 weeks after-ripened, 0wkAR), then after-ripened for 1 (1wkAR) and 2 weeks (2wkAR). *AHb1* mRNA levels showed an increasing trend with AR, and a significant increase from 0wkAR to 2wkAR by RT-qPCR analysis (**Figure 8C** and Supplementary Figure 12). Thus, *AHb1* is up-regulated with dry after-ripening in the L*er* ecotype, both in WT and *sly1-2* seeds.

Functional Analysis of DELLA *GAI* and *HDA6*, Genes Down-regulated with Dry After-ripening

Dormancy loss due to dry seed after-ripening may result from degradation of transcripts encoding strong negative regulators of seed germination. For example, DELLA family genes are known to negatively regulate Arabidopsis seed germination. Both DELLA *GAI* and the histone deacetylase *HDA6* were down-regulated with dry after-ripening of both *sly1-2* and Cvi seeds. In addition, *GAI* was up-regulated in the *sly1-2* DvsWT dry seed

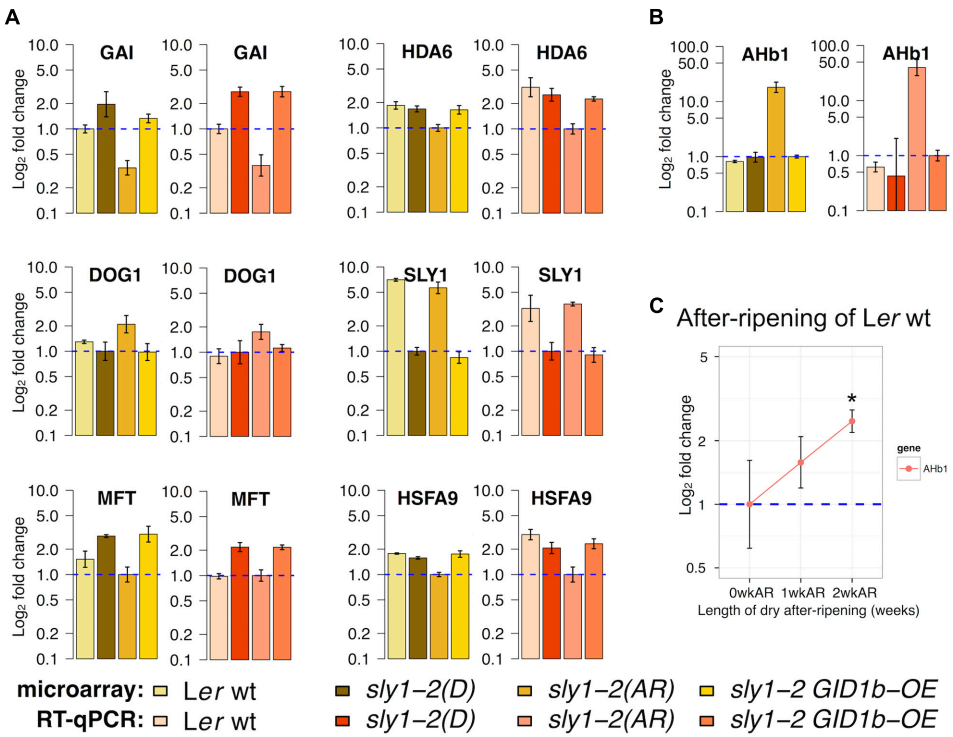

FIGURE 8 | Comparing RT-qPCR analyses of transcriptome differences with those measured by microarray. **(A)** Plots for a selection of genes with differential regulation in both ARvsD and DvsWT comparisons and **(B)** plots for *AHb1*, the most AR-up-regulated gene in *sly1-2* dry seeds. Both microarray (brown) and RT-qPCR (orange) relative expression are shown relative to the same calibrator, set to height of 1 and indicated by the blue dotted-line. For this comparison, RMA normalized microarray data was analyzed using the ddCT method relative to the same constitutively expressed AKR2B control gene used for analysis of RT-qPCR data. **(C)** L*er* wt was harvested "near maturity" and seeds were collected for RT-qPCR to examine transcript levels of *AHb1* at 0, 1, and 2 weeks of after-ripening (0, 1, and 2wkAR). Asterisk indicates significance relative to 0wkAR ($p = 0.04$). For all RT-qPCR experiments, statistical significance was determined by pairwise *t*-test with Bonferroni–Holm correction for multiple comparisons (see Supplementary Figure 4 for *p*-values). Error bars represent SD.

comparison, indicating that *GAI* mRNA expression is associated with seed dormancy and negatively regulated by *SLY1* and after-ripening. To examine whether the down-regulation of these mRNAs with dry after-ripening is functionally relevant, the effect of mutant alleles on seed dormancy and dormancy loss were examined.

Based on double mutant studies with *ga1-3*, DELLA *GAI* was believed to play a less important role in repressing seed germination than DELLA *RGL2* (Lee et al., 2002; Tyler et al., 2004; Cao et al., 2005). While *RGL2*, *RGL3* and *GAI* transcript levels were high in imbibing WT, *sly1-2(D)*, *sly1-2(AR)*, and *sly1-2 GID1b-OE* seeds, the fact that only *GAI* and *RGL3* transcript levels were high in dry seeds suggests that *GAI* may be more important in dry seed after-ripening (Supplementary Figure 13). Furthermore, *GAI* was the only DELLA transcript differentially regulated with after-ripening in dry *sly1-2* seeds, showing AR-down-regulation in both *sly1-2* and Cvi wt seeds. Consistent with the notion that *GAI* regulates seed dormancy, *gai-t6* had a higher and *gai-1* a lower germination rate than wild-type L*er* seeds when seed germination was examined in highly dormant fresh seeds harvested at near maturity (**Figures 9A,B**). Cold stratification improved germination for all lines, but *gai-t6* consistently germinated faster than wild-type, while *gai-1* germinated slower. If elevated *GAI* mRNA levels in *sly1-2* seeds stimulate dormancy, then we would expect *gai-t6* to rescue *sly1-2* seed germination. Indeed, while dormant *sly1-2* seeds failed to germinate even with cold stratification, the *sly1-2 gai-t6* double mutant germinated without cold stratification reaching 25% with 16 days of incubation (**Figures 9C,D**). Taken together, these results suggest that *GAI* plays an early role in the negative regulation of seed germination.

If *HDA6* stimulates seed dormancy in wild-type L*er*, then we would expect *hda6* mutants to be less dormant than wild-type. The germination phenotype of the *HDA6* allele in the L*er* background called *sil1* (*modifiers of silencing1*) was examined in seeds harvested near maturity to maximize dormancy. Seeds of *sil1* germinated more efficiently than wild-type L*er* in three biologically independent batches of seeds at 0 and 2 weeks of after-ripening, both with and without cold stratification (**Figures 10A,B** and Supplementary Figures 14A,B). This suggests that histone deacetylation by *HDA6* stimulates seed dormancy, presumably by inhibiting the expression of genes needed for germination.

If histone deacetylation stimulates the seed dormancy of GA mutants, then inhibition of histone deacetylation should rescue the germination of GA-insensitive *sly1-2* and of the

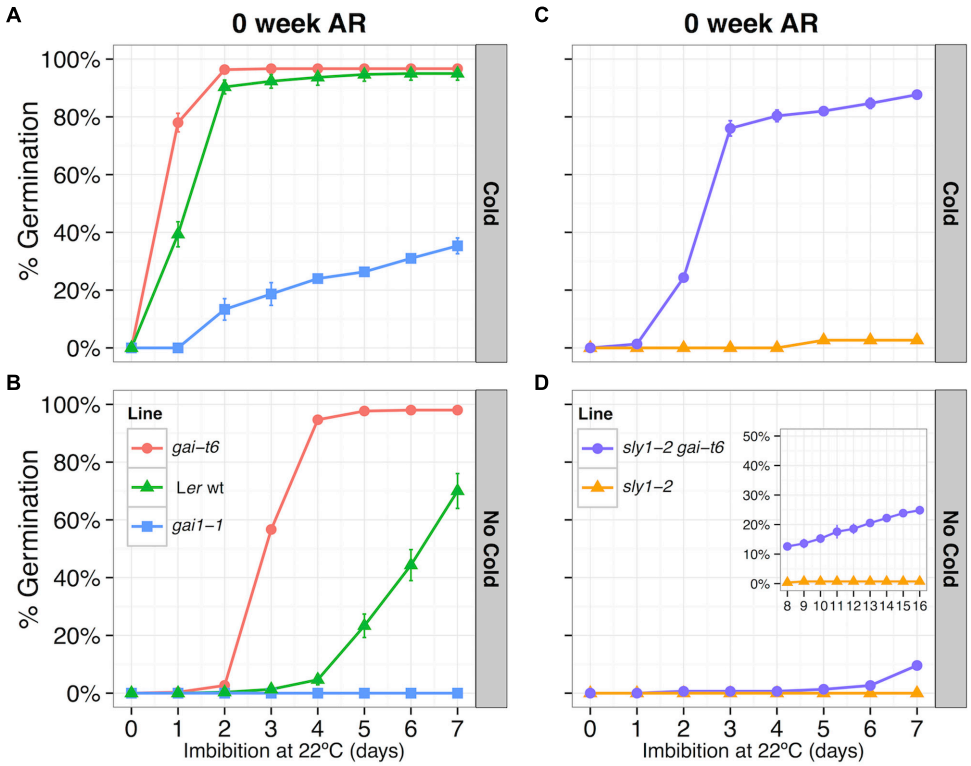

FIGURE 9 | Examining the role of *GAI* in the regulations of seed germination based on germination screens using freshly harvested seeds collected at near maturity. **(A,B)** Comparing of L*er* wt, *gai-1* (gain of function allele), and *gai-t6* germination: **(A)** with cold stratification for 4 days at 4°C, before moving to the light at 22°C where germination was scored daily ("Cold"), and **(B)** without cold, seeds placed directly at 22°C and germination scored daily ("No Cold"). Loss of *GAI* function leads to an increase in germination and gain of *GAI* function leads to increased dormancy. **(C,D)** Comparing *sly1-2* and *sly1-2 gai-t6* germination **(C)** with cold stratification, and **(D)** without cold stratification. Loss of *GAI* function caused partial rescue of *sly1-2* seed germination.

GA biosynthesis mutant *ga1-3*. This was examined using a specific inhibitor of histone deacetylases called tricostatin A (TSA) (Yoshida et al., 1995). TSA rescued the germination of dormant and after-ripened *sly1-2* in a dose-dependent manner (**Figure 11**). Interestingly, TSA also stimulated the germination of *ga1-3* seeds, suggesting that GA functions in part by relieving transcriptional repression by histone deacetylases. TSA rescued germination most efficiently at 2 μM (76%), and showed decreasing germination at 4 and 6 μM TSA. It may be that histone deacetylation and TSA alter the expression of other positive or negative regulators of germination at different concentrations.

DISCUSSION

DELLA-Directed Seed Dormancy in *sly1-2*

There are many mechanisms contributing to seed dormancy. The *sly1* mutant has increased dormancy due to overaccumulation of DELLA proteins, the negative regulators of GA responses and seed germination. Thus, comparing *sly1-2* vs. WT (DvsWT) defined transcriptome differences associated with DELLA-imposed seed dormancy.

The majority (65%) of these genes were down-regulated in *sly1-2*, suggesting that a major effect of *sly1* loss/increased DELLA is decreased transcript abundance (**Figure 2A**). DELLA proteins act in concert with DNA-binding proteins to regulate transcription (Oh et al., 2004, 2006, 2007; Gallego-Bartolomé et al., 2010). Thus, it is interesting that the DELLA-interactor PIF1/PIL5 is a regulator of many highly *sly1*-down-regulated transcripts (Supplementary Figure 10). PIF-regulated genes were expected to be among *SLY1*/DELLA-regulated genes because DELLA proteins bind PIF3 and PIF4, inhibiting PIF DNA-binding and transcriptional activation while promoting PIF3 protein degradation by the 26S proteasome (de Lucas et al., 2008; Feng et al., 2008; Li et al., 2016). PIF1/PIL5 is a known DELLA interactor whose negative regulation of germination is relieved by light (Oh et al., 2004, 2006, 2007; Gallego-Bartolomé et al., 2010). Thus, it is appears that DELLA overaccumulation in *sly1-2* seeds during development or maturation may cause transcriptional repression of PIF1/PIL5-regulated gene targets accounting for some of the down-regulation of stored mRNAs in dry seeds.

Transcription factors produced early in seed imbibition are ideal candidates to initiate the transcriptional cascades leading to or blocking germination *per se*. There were 5-times more *sly1*-down-regulated than *sly1*-up-regulated TF-mRNAs (Supplementary Figure 9). This suggests that

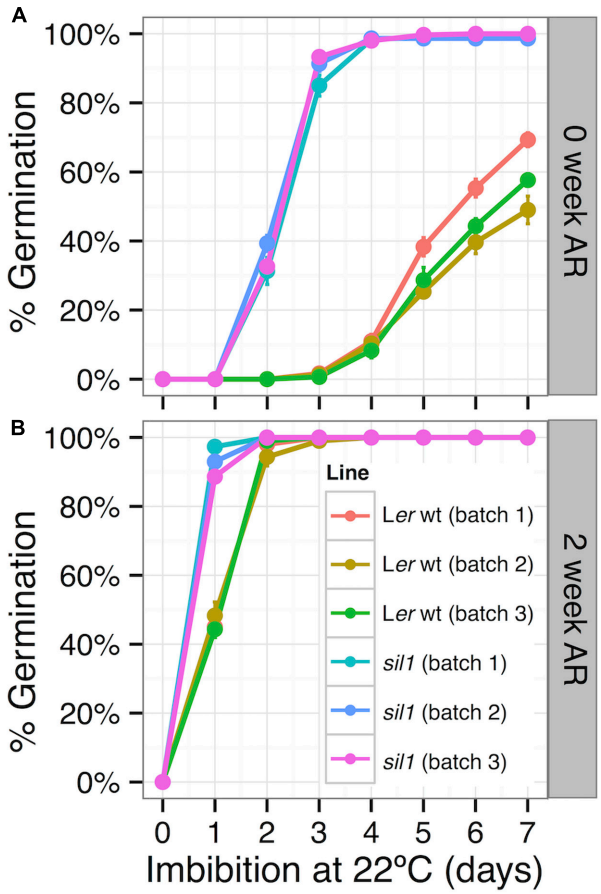

FIGURE 10 | A germination screen was performed to compare germination of *sil1* and L*er* wt harvested at near maturity. Seeds were germinated at two timepoints, **(A)** freshly harvested (0 week AR), and **(B)** 2 weeks old (2 weeks AR). Three biologically independent batches of seed were assayed to clearly capture the *HDA6* loss of function phenotype in *sil1*. To minimize dormancy release, seeds were placed directly at 22°C and germination was scored daily. Freshly harvested *sil1* seed germinated more efficiently than wild-type, both at 0 and at 2 weeks of after-ripening.

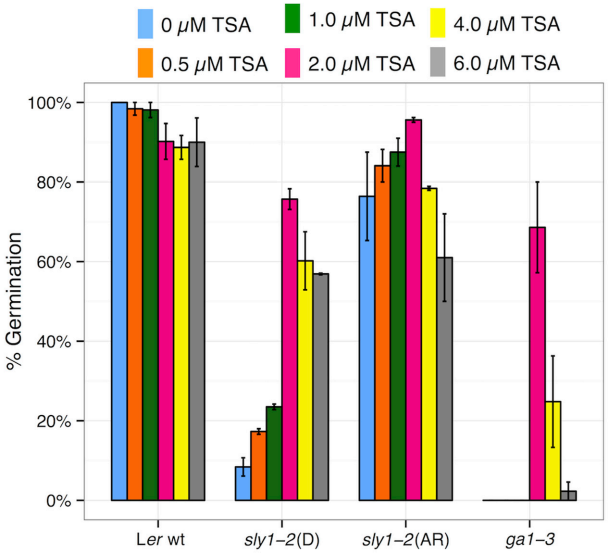

FIGURE 11 | Germination of L*er* wt, *sly1-2*(D), *sly1-2*(AR), and *ga1-3* was conducted on varying concentrations of the histone deacetylase inhibitor, tricostatin A (TSA). TSA stimulated germination of both dormant *sly1-2* and of *ga1-3*. Rescue of germination was most efficient at 2.0 μM TSA.

DELLA overaccumulation in *sly1* leads to lower expression of transcription factors. Known regulators of germination, *ABI5* (*ABA-INSENSITIVE5*) and DELLA *GAI* are examples of major *sly1*-regulated TF-mRNAs (**Figure 6**; Koornneef et al., 1985; Lopez-Molina et al., 2002). Thus, different levels of germination-promoting or -inhibiting TFs in *sly1-2* and WT may be one mechanism allowing wild-type L*er*, but not *sly1-2*, seeds to germinate at 2 weeks of after-ripening.

While it is tempting to believe that dry seed transcriptional differences in *sly1-2*(D) compared to WT arise entirely during development or maturation, these differences may also arise during 2 weeks of dry storage. For example, transcripts may be degraded at different rates in different genotypes, either faster or slower in the *sly1-2* mutant than in WT. Since *sly1-2* requires 1–2 years to reach a germination rate similar to WT after-ripened for 2 weeks, it is possible that some germination-inhibiting transcripts require more time to degrade or oxidize in *sly1-2* than in WT. It could also be the case that germination-promoting transcripts are less protected in *sly1-2*. Investigation of DvsWT transcriptome differences during development and maturation might help to differentiate transcriptome differences arising during development from those arising during dry storage.

Evidence for the Functional Relevance of Dry Seed Transcriptome Changes

While it may be argued that changes in the dry seed transcriptome are merely artifacts of mRNA oxidation/damage over time, the results of this study provide circumstantial evidence that some of these changes are of regulatory importance in dormancy loss. First, similar changes occurred with dry after-ripening in two different ecotypes. Second, transcription factors known to function in dormancy, dormancy loss, and GA signaling were among the AR-differentially regulated genes. And third, mutations in two of these differentially regulated genes resulted in altered seed dormancy and germination.

The overlap in the *sly1-2* and Cvi ARvsD comparisons suggested that dry seed transcriptome changes are not due to random degradation of transcripts as seeds age, but may represent dormancy-loss mechanisms. Of the 770 stored mRNAs that were differentially regulated with after-ripening in dry *sly1-2* seeds, 12% of the AR-up-regulated and 23% of the AR-down-regulated were similarly regulated in Cvi wt (**Figure 4A**). Since *sly1-2* is a mutation in the L*er* rather than the Cvi ecotype, differences between these two ARvsD comparisons may result either from ecotype differences or the *sly1-2* mutation. Interestingly, the regulation of TAGGIT gene categories was similar in *sly1-2* and Cvi wt dry seed after-ripening (**Figures 5B,C**). The partial overlap in the *sly1-2* and Cvi

ARvsD comparisons may simply suggest that the seed dormancy of the two genotypes results from only partially overlapping mechanisms. In other words, there are multiple ways to acquire and to lose seed dormancy.

Even transcripts that are AR-regulated in *sly1-2* but not Cvi may function in after-ripening of the L*er* ecotype. For example, the *AHb1* transcript was not AR-up-regulated in Cvi, but was strongly AR-up-regulated transcript in dry seeds of *sly1-2* and L*er*. *AHb1* (also called Arabidopsis class 1 phytoglobin or *pgb1*) protects roots from severe oxidative stress (Hill et al., 2016; Mira et al., 2017). Thus, it may play a similar role in dry seeds. There appears to be a link between class 1 phytoglobin expression and seed dormancy/germination in barley (Ma et al., 2016). Dormancy can also be rescued without a large change at the transcriptome level, as evident by *GID1b-OE* rescue of *sly1-2* seed germination, where only 27 genes were differentially regulated at any of the three timepoints investigated (**Table 1**). Of these, the *AHb1* transcript was down-regulated at 12h of imbibition. Future research will need to examine if *AHb1* is needed to stimulate *sly1-2* germination in early Phase I, but not in Phase II of germination.

Transcription factors produced early in seed imbibition are ideal candidates to initiate the transcriptional cascades leading to or blocking germination *per se*. Thus, it is interesting that transcription factors known to control dormancy and dormancy loss were among the AR-regulated genes. ABA hormone establishes dormancy, ethylene can break dormancy in *ga1-1,* and auxin has been implicated in dormancy and dormancy release (Finkelstein et al., 2008; Karssen et al., 1989). In light of this, it is interesting that TAGGIT ontology analysis found that 9% of TFs were ABA-related, 12% were ethylene-related, and 7% were auxin-related (Supplementary Figure 9C). For example, ABA related protein phosphatase genes, *HAB2* (*HOMOLOGY TO ABI2*), *AHG3* (*ABA-HYPERSENSITIVE GERMINATION3*), and *HAI3* (*HIGHLY ABA-INDUCED PP2C GENE3*) were among transcripts down-regulated with *sly1-2* after-ripening (Supplementary Table 2; Finkelstein et al., 2008). Moreover, the negative regulator of germination and GA signaling, DELLA *GAI* was also AR-down-regulated in dry *sly1* seeds (**Figure 6**; Koornneef et al., 1985). Examination of mutations in two *sly1* AR-downregulated genes resulted in altered seed dormancy, allowing us to conclude that the decreased transcript levels of *GAI* and *HDA6* are likely to increase germination.

GAI Regulation of Seed Dormancy

The DELLA *GAI* was the most AR-down-regulated gene in dry *sly1-2* seeds, suggesting a more important role in seed germination than previously believed. The DELLA *RGL2* is considered the major DELLA repressing seed germination, since *rgl2* mutations best rescue *ga1-3* germination in the light (Tyler et al., 2004; Cao et al., 2005). DELLA *GAI* also functions as a negative regulator of germination, since the *ga1-3 gai-t6 rgl2-1* triple but not the *ga1-3 rgl2-1* double mutant can germinate in the dark. DELLAs RGL2 and RGA mRNA and protein levels do not decrease with *sly1-2* after-ripening, whereas *GAI* mRNA levels decrease with dry after-ripening of *sly1* and Cvi (Supplementary Figure 13; Ariizumi and Steber, 2007). Mutant analysis confirmed that DELLA repressor *GAI* is a positive regulator of seed dormancy or a negative regulator of germination. Loss of function allele, *gai-t6*, increased germination, whereas gain-of-function allele *gai-1* promoted dormancy in the L*er* ecotype (**Figures 9A,B**). Moreover, the *gai-t6* mutation was able to partly rescue *sly1-2* germination without cold stratification, and strongly rescue *sly1-2* germination with cold stratification (**Figures 9C,D**). Thus, AR-down-regulation of *GAI* in dry *sly1-2* seeds likely results in increased germination potential since *GAI* acts as a positive regulator of *sly1-2* dormancy.

Previous work showed that *gai-1* has reduced germination potential compared to wild-type L*er* in cold-stratified seeds (Koornneef et al., 1985; Ariizumi et al., 2013). Moreover, *gai-t6* caused slightly increased germination without cold stratification, and slightly decreased germination with cold stratification of the low-dormancy ecotype Columbia-0 (Col) (Boccaccini et al., 2014). Thus, our model is that *GAI* transcript down-regulation with dry after-ripening increases germination potential by reducing GAI repressor levels during early imbibition. Further research will need to measure DELLA GAI protein levels during early seed imbibition.

Control of Seed Dormancy by Histone Modification

Chromatin modifications regulate developmental processes including dormancy by altering gene transcription (reviewed in Nonogaki, 2014). Since 65% of the differentially-regulated transcripts in *sly1-2* (DvsWT) were down-regulated, it was interesting that rescue of *sly1-2* seed germination by long after-ripening was associated with down-regulation of the *HDA6* histone deacetylase because histone deacetylases repress gene transcription. Histone deacetylation represses gene expression through heterochromatin formation, whereas histone acetylation promotes gene expression and has been implicated in seed dormancy release by stimulating gene expression needed for seed germination. Our hypothesis was that *HDA6* down-regulation with after-ripening of *sly1-2* and Cvi breaks dormancy through increased expression of germination-promoting transcripts. The notion that *HDA6* stimulates seed dormancy was supported by the observation that loss of *HDA6* in the *sil1* mutant decreased seed dormancy in freshly harvested seeds (**Figure 10**). In addition to the *hda6/sil1* mutant, the histone deacetylase mutants *hda9* and *hda19* also exhibited reduced seed dormancy (Wang et al., 2013; van Zanten et al., 2014). *HDA9* is down-regulated with imbibition, but neither *HDA9* nor *HDA19* were down-regulated with *sly1-2* after-ripening. *HDA6* also appears to function in ABA and salt stress response, as *hda6* and *hda19* mutants were hypersensitive to ABA and salt inhibition of germination (Chen and Wu, 2010; Chen et al., 2010; Luo et al., 2012).

The increased seed dormancy associated with reduced GA signaling appears to be partially due to gene repression by histone deacetylation. The GA biosynthesis mutant *ga1-3* fails to germinate, and never regains the ability to germinate through after-ripening. Interestingly, the inhibitor of histone deacetylase

activity TSA partly rescued the germination not only of *sly1-2* but of *ga1-3* seeds (**Figure 11**). The increased seed dormancy in *sly1-2* is rescued by long after-ripening, whereas the seed dormancy of the GA biosynthesis in *ga1-3* is not. No GA signaling can occur in *ga1-3*, whereas some GA signaling can occur in *sly1-2* mutants that cannot trigger DELLA destruction (Ariizumi and Steber, 2007; Ariizumi et al., 2013). Thus, DELLA-proteolysis independent GA signaling may be sufficient for *HDA6* down-regulation with *sly1* after-ripening. Taken together, this suggests that histone deacetylation maintains dormancy in GA mutants and that TSA-treatment may bypass GA signaling to relieve seed dormancy by allowing histone acetylation. This is consistent with previous studies suggesting that histone deacetylation stimulates and TSA relieves seed dormancy (Yoshida et al., 1995; Yano et al., 2013; van Zanten et al., 2014). Future work will need to examine whether down-regulation of *HDA6* with after-ripening is associated with altered histone acetylation of HDA6 targets.

SLY1 and GA Signaling Regulate Protein Translation

Our *sly1-2* transcriptome studies indicate that regulation of translation-associated gene expression is one of the major roles of GA signaling in seeds (Nelson and Steber, 2017). Inhibitor studies showed that translation, not gene transcription, is required for seed germination *per se* (Rajjou et al., 2004). Thus, regulation of translation-associated genes is an excellent strategy for determining whether or not a seed can germinate. Consistent with this notion, previous studies found that translation-associated genes were strongly up-regulated with seed imbibition and Cvi after-ripening (Nakabayashi et al., 2005; Dekkers et al., 2016). Differentially regulated translation-associated genes in this and other studies included ribosomal subunits and translation initiation and elongation factors. The translation-associated category was strongly AR-up-regulated in imbibing L*er* wild-type seeds, but not well AR-up-regulated in imbibing *sly1-2* seeds (Dekkers et al., 2016; Nelson and Steber, 2017). The positive regulator of GA signaling, *SLY1*, was needed to up-regulate translation-associated genes with after-ripening of imbibed seeds (Nelson and Steber, 2017). Moreover, protein translation-associated transcripts were strongly GA-up-regulated and DELLA-down-regulated, indicating that regulation of translation-associated genes is a general function of GA signaling (Nelson and Steber, 2017). Previous work showed that after-ripening was associated with higher protein translation after 24h of imbibition in *H. annuus* (Layat et al., 2014). After-ripening can also be associated with increased translation of specific transcripts (Layat et al., 2014; Basbouss-Serhal et al., 2015). One possibility is that the increased mRNA accumulation of specific translation initiation factors with after-ripening is responsible for recruitment of specific transcripts. Future work will need to determine if dormant *ga1-3* and *sly1-2* seeds have either a general defect in protein translation or an inability to translate specific transcripts.

In contrast to imbibed seeds, translation-associated genes were strongly AR-down-regulated in dry *sly1-2* and Cvi seeds (**Figures 5B,C**). Although not as much as in DvsWT, translation-associated mRNAs accounted for 12% of the up-regulated transcripts in the *sly1-2* ARvsWT dry seed comparison (**Figure 5A**). This indicates that *SLY1* is not a requirement for this decrease with after-ripening, but that loss of *SLY1* resulted in a higher starting-point during seed maturation. Thus, it appears that *SLY1* is needed for down-regulation of translation-associated transcripts during seed maturation, since the translation-associated category accounted for 25% of the *sly1*-up-regulated genes in dry seeds (**Figure 5A**). This suggests that SLY1 may serve as a kind of shutdown signal to down-regulate translation associated genes during seed maturation to prepare for the quiescent state. In this context, it is interesting to note that *sly1-2* mutant seeds exhibit a mild decrease in survival of long-term storage (Ariizumi and Steber, 2007). Future work should examine the early imbibition proteome to determine if translation-associated proteins over-accumulate in *sly1-2* seeds during early imbibition. If too much of early translation is devoted to translation-associated gene expression, there may be limited amino acids available for protein synthesis of other important early-translated transcripts.

Differences in mRNA Stability Correlate to Changes in Transcript Levels with Dry After-ripening

If changes in the dry seed transcriptome increase germination potential, then how can a quiescent, dry seed differentially regulate these changes in transcript levels? If we assume that *de novo* transcription is very unlikely in dry seeds, then such changes must be regulated through degradation that preferentially targets certain mRNAs over others. Genes that are up-regulated in transcriptome analyses may be those that are more stable or more well protected than the majority of the transcriptome, while those that are down-regulated are those that are less stable or otherwise more prone to degradation (i.e., targeted for degradation via mRNA oxidation or other mechanisms) than the majority. Consistent with this notion, comparison of dry seed AR-regulation with Arabidopsis mRNA stability, showed a correlation between AR-up-regulation and higher mRNA stability, as well as AR-down-regulation and lower mRNA stability (**Figure 7**). This is consistent with a previous study showing RNA degradation during dry after-ripening of sunflower seeds and Arabidopsis (Bazin et al., 2011; Basbouss-Serhal et al., 2017). Imbibed seeds did not show a correlation between mRNA stability and AR-regulation (Supplementary Figures 11A–C). In fact, in early Phase II (0h) there appeared to be a negative correlation between mRNA stability and AR-regulation, possibly indicating increased transcription of mRNAs that were not present in dry seeds at the time of imbibition due to lower stability.

Novel mechanisms may control those transcripts whose dry seed accumulation cannot be explained by differences in mRNA stability. Such genes may be regulated by other factors that increase or reduce the chances of degradation in a real seed. Future work should examine whether the subcellular localization

of transcripts or RNA-binding proteins determine whether transcripts appear to be AR-up- or AR-down-regulated in dry seeds, as opposed to *de novo* transcription. Genes like *At3g23090* that have low stability mRNAs, but are up-regulated with after-ripening would be good candidates for such studies.

CONCLUSION

How dormancy is lost in dry, metabolically inactive seeds is a fascinating question. This study took some first steps toward addressing this question by identifying transcriptional mechanisms underlying dormancy and dormancy loss in dry seeds of the GA-insensitive mutant, *sly1-2*. Our general model is that dry after-ripening of seeds leads to down-regulation of transcripts that negatively regulate seed germination. Loss of function mutations in two of these strongly AR-down-regulated transcripts, *GAI* and *HDA6*, resulted in increased germination potential (**Figures 9**, **10**). The AR-down-regulation of these two transcripts and of other transcription factors suggests that the control of gene transcription and of histone acetylation is one major mechanism controlling dormancy and after-ripening of dry seeds. The *sly1* seed dormancy phenotype was strongly associated with decreased abundance of transcription factor mRNAs, and generally skewed toward transcriptome down-regulation. Thus, it appears that over-accumulation of DELLA repressors has the general effect of down-regulating dry seed transcript abundances. There is one major counterexample to this observation; genes associated with protein translation were strongly up-regulated in dry dormant *sly1-2* seeds compared to wild type accounting for 25% of the *sly1*-up-regulated transcripts. Translation-associated genes are the major class of GA and *SLY1*-regulated transcripts in seeds (**Figures 5A,B**; Nelson and Steber, 2017). Ribosomes are inactive in dry seeds, and must be reactivated in order to germinate (Bewley et al., 2013). *SLY*1 is needed to down-regulate protein translation-genes during seed maturation and to up-regulate protein translation-genes with after-ripening during seed imbibition. Future work will need to examine if the increased dormancy of *sly1-2* and *ga1-3* results largely from inability to efficiently up-regulate protein translation.

AUTHOR CONTRIBUTIONS

CS provided the initial research design and obtained funding. TA performed the TSA experiments for **Figure 11**. SN performed all remaining experiments and bioinformatics analyses. Both CS and SN contributed to the research and analysis design, and to the writing of this article.

FUNDING

This research was funded by National Science Foundation (NSF) Award 0850981 and USDA-ARS project 424575 (to CS).

ACKNOWLEDGMENTS

We would like to thank J. Kim, T. To, and the M. Seki lab at the RIKEN Plant Science Center in Yokohama for providing *sil1* seeds and advice for the *sil1* experiments. We thank the members of the Steber lab, A. Hauvermale, S. Martinez, K. Tuttle, and T. Harris, for helpful suggestions about the research and manuscript. Thanks are also due to M. Neff, H. Hellmann, A. McCubbin, and P. Okubara for helpful comments on the manuscript.

SUPPLEMENTARY MATERIAL

The Supplementary Material for this article can be found online at: https://www.frontiersin.org/articles/10.3389/fpls.2017.02158/full#supplementary-material

REFERENCES

Abbruzzetti, S., Faggiano, S., Spyrakis, F., Bruno, S., Mozzarelli, A., Astegno, A., et al. (2011). Oxygen and nitric oxide rebinding kinetics in nonsymbiotic hemoglobin AHb1 from *Arabidopsis thaliana*. *IUBMB Life* 63, 1094–1100. doi: 10.1002/iub.546

Alkhalfioui, F., Renard, M., and Montrichard, F. (2007a). Unique properties of NADP-thioredoxin reductase C in legumes. *J. Exp. Bot.* 58, 969–978. doi: 10.1093/jxb/erl248

Alkhalfioui, F., Renard, M., Vensel, W. H., Wong, J., Tanaka, C. K., Hurkman, W. J., et al. (2007b). Thioredoxin-linked proteins are reduced during germination of *Medicago truncatula* seeds. *Plant Physiol.* 144, 1559–1579. doi: 10.1104/pp.107.098103

Almoguera, C., and Jordano, J. (1992). Developmental and environmental concurrent expression of sunflower dry-seed-stored low-molecular-weight heat-shock protein and Lea mRNAs. *Plant Mol. Biol.* 19, 781–792. doi: 10.1007/BF00027074

Ariizumi, T., Hauvermale, A. L., Nelson, S. K., Hanada, A., Yamaguchi, S., and Steber, C. M. (2013). Lifting DELLA repression of Arabidopsis seed germination by nonproteolytic gibberellin signaling. *Plant Physiol.* 162, 2125–2139. doi: 10.1104/pp.113.219451

Ariizumi, T., Lawrence, P. K., and Steber, C. M. (2011). The role of two f-box proteins, *SLEEPY1* and *SNEEZY*, in Arabidopsis gibberellin signaling. *Plant Physiol.* 155, 765–775. doi: 10.1104/pp.110.166272

Ariizumi, T., Murase, K., Sun, T.-P., and Steber, C. M. (2008). Proteolysis-independent downregulation of DELLA repression in *Arabidopsis* by the gibberellin receptor GIBBERELLIN INSENSITIVE DWARF1. *Plant Cell* 20, 2447–2459. doi: 10.1105/tpc.108.058487

Ariizumi, T., and Steber, C. M. (2007). Seed germination of GA-insensitive *sleepy1* mutants does not require RGL2 protein disappearance in *Arabidopsis*. *Plant Cell* 19, 791–804. doi: 10.1105/tpc.106.048009

Ariizumi, T., and Steber, C. M. (2011). Mutations in the F-box gene *SNEEZY* result in decreased *Arabidopsis* GA signaling. *Plant Signal. Behav.* 6, 831–833. doi: 10.4161/psb.6.6.15164

Arondel, V., Vergnolle, C., Cantrel, C., and Kader, J. (2000). Lipid transfer proteins are encoded by a small multigene family in *Arabidopsis thaliana*. *Plant Sci.* 157, 1–12. doi: 10.1016/S0168-9452(00)00232-6

Basbouss-Serhal, I., Leymarie, J., and Bailly, C. (2015). Fluctuation of Arabidopsis seed dormancy with relative humidity and temperature during dry storage. *J. Exp. Bot.* 67, 119–130. doi: 10.1093/jxb/erv439

Basbouss-Serhal, I., Pateyron, S., Cochet, F., Leymarie, J., and Bailly, C. (2017). 5′ to 3′ mRNA decay contributes to the regulation of Arabidopsis seed germination by dormancy. *Plant Physiol.* 173, 1709–1723. doi: 10.1104/pp.16.01933

Bazin, J., Langlade, N., Vincourt, P., Arribat, S., Balzergue, S., El-Maarouf-Bouteau, H., et al. (2011). Targeted mRNA oxidation regulates sunflower seed dormancy alleviation during dry after-ripening. *Plant Cell* 23, 2196–2208. doi: 10.1105/tpc.111.086694

Benjamini, Y., and Hochberg, Y. (1995). Controlling the false discovery rate: a practical and powerful approach to multiple testing. *J. R. Stat. Soc. B Methodol.* 57, 289–300.

Benjamini, Y., and Yekutieli, D. (2001). The control of the false discovery rate in multiple testing under dependency. *Ann. Stat.* 29, 1165–1188. doi: 10.1186/1471-2105-9-114

Bewley, J. D., Bradford, K. J., Hilhorst, H. W. M., and Nonogaki, H. (2013). *Seeds: Physiology of Development, Germination and Dormancy*. New York, NY: Springer. doi: 10.1007/978-1-4614-4693-4

Boccaccini, A., Santopolo, S., Capauto, D., Lorrai, R., Minutello, E., Belcram, K., et al. (2014). Independent and interactive effects of DOF affecting germination 1 (DAG1) and the Della proteins GA insensitive (GAI) and repressor of ga1-3 (RGA) in embryo development and seed germination. *BMC Plant Biol.* 14:200. doi: 10.1186/s12870-014-0200-z

Bove, J., Lucas, P., Godin, B., Ogé, L., Jullien, M., and Grappin, P. (2005). Gene expression analysis by cDNA-AFLP highlights a set of new signaling networks and translational control during seed dormancy breaking in *Nicotiana plumbaginifolia*. *Plant Mol. Biol.* 57, 593–612. doi: 10.1007/s11103-005-0953-8

Buitink, J., and Leprince, O. (2004). Glass formation in plant anhydrobiotes: survival in the dry state. *Cryobiology* 48, 215–228. doi: 10.1016/j.cryobiol.2004.02.011

Cadman, C. S., Toorop, P. E., Hilhorst, H. W., and Finch-Savage, W. E. (2006). Gene expression profiles of Arabidopsis Cvi seeds during dormancy cycling indicate a common underlying dormancy control mechanism. *Plant J.* 46, 805–822. doi: 10.1111/j.1365-313X.2006.02738.x

Cao, D., Hussain, A., Cheng, H., and Peng, J. (2005). Loss of function of four DELLA genes leads to light- and gibberellin-independent seed germination in *Arabidopsis*. *Planta* 223, 105–113. doi: 10.1007/s00425-005-0057-3

Carrera, E., Holman, T., Medhurst, A., Peer, W., Schmuths, H., Footitt, S., et al. (2007). Gene expression profiling reveals defined functions of the ATP-Binding cassette transporter COMATOSE late in phase II of germination. *Plant Physiol.* 143, 1669–1679. doi: 10.1104/pp.107.096057

Chen, D., Sarid, S., and Katchalski, E. (1968). Studies on the nature of messenger RNA in germinating wheat embryos. *Proc. Natl. Acad. Sci. U.S.A.* 60, 902–909. doi: 10.1073/pnas.60.3.902

Chen, L.-T., Luo, M., Wang, Y.-Y., and Wu, K. (2010). Involvement of *Arabidopsis* histone deacetylase HDA6 in ABA and salt stress response. *J. Exp. Bot.* 61, 3345–3353. doi: 10.1093/jxb/erq154

Chen, L.-T., and Wu, K. (2010). Role of histone deacetylases HDA6 and HDA19 in ABA and abiotic stress response. *Plant Signal. Behav.* 5, 1318–1320. doi: 10.4161/psb.5.10.13168

Chiang, G. C. K., Bartsch, M., Barua, D., Nakabayashi, K., Debieu, M., Kronholm, I., et al. (2011). DOG1 expression is predicted by the seed-maturation environment and contributes to geographical variation in germination in *Arabidopsis thaliana*. *Mol. Ecol.* 20, 3336–3349. doi: 10.1111/j.1365-294X.2011.05181.x

Chiang, G. C. K., Barua, D., Kramer, E. M., Amasino, R. M., and Donohue, K. (2009). Major flowering time gene, FLOWERING LOCUS C, regulates seed germination in *Arabidopsis thaliana*. *Proc. Natl. Acad. Sci. U.S.A.* 106, 11661–11666. doi: 10.1073/pnas.0901367106

Chitnis, V. R., Gao, F., Yao, Z., Jordan, M. C., Park, S., and Ayele, B. T. (2014). After-ripening induced transcriptional changes of hormonal genes in wheat seeds: the cases of brassinosteroids, ethylene, cytokinin and salicylic acid. *PLOS ONE* 9:e87543. doi: 10.1371/journal.pone.0087543

Comai, L., and Harada, J. J. (1990). Transcriptional activities in dry seed nuclei indicate the timing of the transition from embryogeny to germination. *Proc. Natl. Acad. Sci. U.S.A.* 87, 2671–2674. doi: 10.1073/pnas.87.7.2671

Davuluri, R. V., Sun, H., Palaniswamy, S. K., Matthews, N., Molina, C., Kurtz, M., et al. (2003). AGRIS: Arabidopsis gene regulatory information server, an information resource of Arabidopsis *cis*-regulatory elements and transcription factors. *BMC Bioinformatics* 4:25. doi: 10.1186/1471-2105-4-25

de Lucas, M., Davière, J.-M., Rodríguez-Falcón, M., Pontin, M., Iglesias-Pedraz, J. M., Lorrain, S., et al. (2008). A molecular framework for light and gibberellin control of cell elongation. *Nature* 451, 480–484. doi: 10.1038/nature06520

Dekkers, B. J. W., Pearce, S. P., van Bolderen-Veldkamp, R. P. M., Holdsworth, M. J., and Bentsink, L. (2016). Dormant and after-ripened *Arabidopsis thaliana* seeds are distinguished by early transcriptional differences in the imbibed state. *Front. Plant Sci.* 7:1323. doi: 10.3389/fpls.2016.01323

Dill, A., Thomas, S. G., Hu, J., Steber, C. M., and Sun, T.-P. (2004). The Arabidopsis F-box protein SLEEPY1 targets gibberellin signaling repressors for gibberellin-induced degradation. *Plant Cell* 16, 1392–1405. doi: 10.1105/tpc.020958

Dure, L., and Waters, L. (1965). Long-lived messenger RNA: evidence from cotton seed germination. *Science* 147, 410–412. doi: 10.1126/science.147.3656.410

Feng, S., Martinez, C., Gusmaroli, G., Wang, Y., Zhou, J., Wang, F., et al. (2008). Coordinated regulation of *Arabidopsis thaliana* development by light and gibberellins. *Nature* 451, 475–479. doi: 10.1038/nature06448

Finch-Savage, W. E., Cadman, C. S. C., Toorop, P. E., Lynn, J. R., and Hilhorst, H. W. M. (2007). Seed dormancy release in Arabidopsis Cvi by dry after-ripening, low temperature, nitrate and light shows common quantitative patterns of gene expression directed by environmentally specific sensing. *Plant J.* 51, 60–78. doi: 10.1111/j.1365-313X.2007.03118.x

Finch-Savage, W. E., and Leubner-Metzger, G. (2006). Seed dormancy and the control of germination. *New Phytol.* 171, 501–523. doi: 10.1111/j.1469-8137.2006.01787.x

Finkelstein, R., Reeves, W., Ariizumi, T., and Steber, C. M. (2008). Molecular aspects of seed dormancy. *Annu. Rev. Plant Biol.* 59, 387–415. doi: 10.1146/annurev.arplant.59.032607.092740

Fisher, R. A. (1922). On the interpretation of X2 from contingency tables, and the calculation of P. *J. R. Stat. Soc.* 85, 87–94. doi: 10.2307/2340521

Furner, I. J., Sheikh, M. A., and Collett, C. E. (1998). Gene silencing and homology-dependent gene silencing in Arabidopsis: genetic modifiers and DNA methylation. *Genetics* 149, 651–662.

Galland, M., Huguet, R., Arc, E., Cueff, G., Job, D., and Rajjou, L. (2014). Dynamic proteomics emphasizes the importance of selective mRNA translation and protein turnover during *Arabidopsis* seed germination. *Mol. Cell. Proteomics* 13, 252–268. doi: 10.1074/mcp.M113.032227

Gallego-Bartolomé, J., Minguet, E. G., Marín, J. A., Prat, S., Blázquez, M. A., and Alabadí, D. (2010). Transcriptional diversification and functional conservation between DELLA proteins in Arabidopsis. *Mol. Biol. Evol.* 27, 1247–1256. doi: 10.1093/molbev/msq012

Gentleman, R. C., Carey, V. J., Bates, D. M., Bolstad, B., Dettling, M., Dudoit, S., et al. (2004). Bioconductor: open software development for computational biology and bioinformatics. *Genome Biol.* 5:R80. doi: 10.1186/gb-2004-5-10-r80

Gordon, M. E., and Payne, P. I. (1976). In vitro translation of the long-lived messenger ribonucleic acid of dry seeds. *Planta* 130, 269–273. doi: 10.1007/BF00387832

Graeber, K., Nakabayashi, K., Miatton, E., Leubner-Metzger, G., and Soppe, W. J. J. (2012). Molecular mechanisms of seed dormancy. *Plant Cell Environ.* 35, 1769–1786. doi: 10.1111/j.1365-3040.2012.02542.x

Guan, Q., Wen, C., Zeng, H., and Zhu, J. (2013). A KH domain-containing putative RNA-binding protein is critical for heat stress-responsive gene regulation and thermotolerance in Arabidopsis. *Mol. Plant* 6, 386–395. doi: 10.1093/mp/sss119

Hauvermale, A. L., Ariizumi, T., and Steber, C. M. (2012). Gibberellin signaling: a theme and variations on DELLA repression. *Plant Physiol.* 160, 83–92. doi: 10.1104/pp.112.200956

Hauvermale, A. L., Ariizumi, T., and Steber, C. M. (2014). The roles of the GA receptors *GID1a, GID1b,* and *GID1c* in *sly1*-independent GA signaling. *Plant Signal. Behav.* 9:e28030. doi: 10.4161/psb.28030

Hauvermale, A. L., Tuttle, K. M., Takebayashi, Y., Seo, M., and Steber, C. M. (2015). Loss of *Arabidopsis thaliana* seed dormancy is associated with increased accumulation of the GID1 GA hormone receptors. *Plant Cell Physiol.* 56, 1773–1785. doi: 10.1093/pcp/pcv084

Hill, R., Hargrove, M., and Arredondo-Peter, R. (2016). Phytoglobin: a novel nomenclature for plant globins accepted by the globin community at the 2014 XVIII conference on oxygen-binding and sensing proteins. *F1000Res.* 5:212. doi: 10.12688/f1000research.8133.1

Holm, S. (1979). A simple sequentially rejective multiple test procedure. *Scand. J. Stat.* 6, 65–70. doi: 10.2307/4615733

Hruz, T., Wyss, M., Docquier, M., Pfaffl, M. W., Masanetz, S., Borghi, L., et al. (2011). RefGenes: identification of reliable and condition specific reference genes for RT-qPCR data normalization. *BMC Genomics* 12:156. doi: 10.1186/1471-2164-12-156

Hundertmark, M., and Hincha, D. K. (2008). LEA (late embryogenesis abundant) proteins and their encoding genes in *Arabidopsis thaliana*. *BMC Genomics* 9:118. doi: 10.1186/1471-2164-9-118

Irizarry, R. A., Hobbs, B., Collin, F., Beazer-Barclay, Y. D., Antonellis, K. J., Scherf, U., et al. (2003). Exploration, normalization, and summaries of high density oligonucleotide array probe level data. *Biostatistics* 4, 249–264. doi: 10.1093/biostatistics/4.2.249

Ishibashi, N., Yamauchi, D., and Minamikawa, T. (1990). Stored mRNA in cotyledons of *Vigna unguiculata* seeds: nucleotide sequence of cloned cDNA for a stored mRNA and induction of its synthesis by precocious germination. *Plant Mol. Biol.* 15, 59–64. doi: 10.1007/BF00017724

Iuchi, S., Suzuki, H., Kim, Y.-C., Iuchi, A., Kuromori, T., Ueguchi-Tanaka, M., et al. (2007). Multiple loss-of-function of Arabidopsis gibberellin receptor AtGID1s completely shuts down a gibberellin signal. *Plant J.* 50, 958–966. doi: 10.1111/j.1365-313X.2007.03098.x

Jin, J., Zhang, H., Kong, L., Gao, G., and Luo, J. (2013). PlantTFDB 3.0: a portal for the functional and evolutionary study of plant transcription factors. *Nucleic Acids Res.* 42, D1182–D1187. doi: 10.1093/nar/gkt1016

Joanes, D. N., and Gill, C. A. (1998). Comparing measures of sample skewness and kurtosis. *J. R. Stat. Soc. D* 47, 183–189. doi: 10.1111/1467-9884.00122

Karssen, C. M., Brinkhorst-van der Swan, D. L., Breekland, A. E., and Koornneef, M. (1983). Induction of dormancy during seed development by endogenous abscisic acid: studies on abscisic acid deficient genotypes of *Arabidopsis thaliana* (L.) Heynh. *Planta* 157, 158–165. doi: 10.1007/BF00393650

Karssen, C. M., and Laçka, E. (1986). "A revision of the hormone balance theory of seed dormancy: studies on gibberellin and/or abscisic acid-deficient mutants of *Arabidopsis thaliana*," in *Plant Growth Substances 1985* (Berlin: Springer), 315–323. doi: 10.1007/978-3-642-71018-6_41

Karssen, C. M., Zagorski, S., Kepczynski, J., and Groot, S. P. C. (1989). Key role for endogenous gibberellins in the control of seed germination. *Ann. Bot.* 63, 71–80. doi: 10.1093/oxfordjournals.aob.a087730

Katari, M. S., Nowicki, S. D., Aceituno, F. F., Nero, D., Kelfer, J., Thompson, L. P., et al. (2010). VirtualPlant: a software platform to support systems biology research. *Plant Physiol.* 152, 500–515. doi: 10.1104/pp.109.147025

Kendall, S. L., Hellwege, A., Marriot, P., Whalley, C., Graham, I. A., and Penfield, S. (2011). Induction of winter seed dormancy in *Arabidopsis* summer annuals requires the parallel regulation of *DOG1* and hormone metabolism by temperature and CBF transcription factors. *Plant Cell* 23, 2568–2580. doi: 10.1105/tpc.111.087643

Kolesnikov, N., Hastings, E., Keays, M., Melnichuk, O., Tang, Y. A., Williams, E., et al. (2015). ArrayExpress update–simplifying data submissions. *Nucleic Acids Res.* 43, D1113–D1116. doi: 10.1093/nar/gku1057

Koornneef, M., and Alonso-Blanco, C. (2000). *Dormancy in Plants: From Whole Plant Behaviour to Cellular Control*. Wallingford: CABI.

Koornneef, M., Elgersma, A., Hanhart, C. J., van Loenen-Martinet, E. P., van Rijn, L., and Zeevaart, J. A. D. (1985). A gibberellin insensitive mutant of *Arabidopsis thaliana*. *Physiol. Plant.* 65, 33–39. doi: 10.1111/j.1399-3054.1985.tb02355.x

Koornneef, M., and van der Veen, J. H. (1980). Induction and analysis of gibberellin sensitive mutants in *Arabidopsis thaliana* (L.) Heynh. *Theor. Appl. Genet.* 58, 257–263. doi: 10.1007/BF00265176

Lai, L., Liberzon, A., Hennessey, J., Jiang, G., Qi, J., Mesirov, J. P., et al. (2012). AraPath: a knowledgebase for pathway analysis in Arabidopsis. *Bioinformatics* 28, 2291–2292. doi: 10.1093/bioinformatics/bts421

Layat, E., Leymarie, J., El-Maarouf-Bouteau, H., Caius, J., Langlade, N., and Bailly, C. (2014). Translatome profiling in dormant and nondormant sunflower (*Helianthus annuus*) seeds highlights post-transcriptional regulation of germination. *New Phytol.* 204, 864–872. doi: 10.1111/nph.13002

Lee, S., Cheng, H., King, K. E., Wang, W., He, Y., Hussain, A., et al. (2002). Gibberellin regulates *Arabidopsis* seed germination via *RGL2*, a *GAI/RGA*-like gene whose expression is up-regulated following imbibition. *Genes Dev.* 16, 646–658. doi: 10.1101/gad.969002

Lefebvre, V., North, H., Frey, A., Sotta, B., Seo, M., Okamoto, M., et al. (2006). Functional analysis of Arabidopsis *NCED6* and *NCED9* genes indicates that ABA synthesized in the endosperm is involved in the induction of seed dormancy. *Plant J.* 45, 309–319. doi: 10.1111/j.1365-313X.2005.02622.x

Leubner-Metzger, G. (2005). beta-1,3-Glucanase gene expression in low-hydrated seeds as a mechanism for dormancy release during tobacco after-ripening. *Plant J.* 41, 133–145. doi: 10.1111/j.1365-313X.2004.02284.x

Leymarie, J., Bruneaux, E., Gibot-Leclerc, S., and Corbineau, F. (2007). Identification of transcripts potentially involved in barley seed germination and dormancy using cDNA-AFLP. *J. Exp. Bot.* 58, 425–437. doi: 10.1093/jxb/erl211

Li, K., Yu, R., Fan, L.-M., Wei, N., Chen, H., and Deng, X. W. (2016). DELLA-mediated PIF degradation contributes to coordination of light and gibberellin signalling in *Arabidopsis*. *Nat. Commun.* 7:11868. doi: 10.1038/ncomms11868

Livak, K. J., and Schmittgen, T. D. (2001). Analysis of relative gene expression data using real-time quantitative PCR and the $2^{-\Delta\Delta C_T}$ method. *Methods* 25, 402–408. doi: 10.1006/meth.2001.1262

Lopez-Molina, L., Mongrand, S., McLachlin, D. T., Chait, B. T., and Chua, N.-H. (2002). ABI5 acts downstream of ABI3 to execute an ABA-dependent growth arrest during germination. *Plant J.* 32, 317–328. doi: 10.1046/j.1365-313X.2002.01430.x

Luo, M., Wang, Y.-Y., Liu, X., Yang, S., Lu, Q., Cui, Y., et al. (2012). HD2C interacts with HDA6 and is involved in ABA and salt stress response in *Arabidopsis*. *J. Exp. Bot.* 63, 3297–3306. doi: 10.1093/jxb/ers059

Ma, Z., Marsolais, F., Bykova, N. V., and Igamberdiev, A. U. (2016). Nitric oxide and reactive oxygen species mediate metabolic changes in barley seed embryo during germination. *Front. Plant Sci.* 7:138. doi: 10.3389/fpls.2016.00138

Marcus, A., and Feeley, J. (1964). Activation of protein synthesis in the imbibition phase of seed germination. *Proc. Natl. Acad. Sci. U.S.A.* 51, 1075–1079. doi: 10.1073/pnas.51.6.1075

McGinnis, K. M., Thomas, S. G., Soule, J. D., Strader, L. C., Zale, J. M., Sun, T.-P., et al. (2003). The Arabidopsis *SLEEPY1* gene encodes a putative F-box subunit of an SCF E3 ubiquitin ligase. *Plant Cell* 15, 1120–1130. doi: 10.1105/tpc.010827

Meimoun, P., Mordret, E., Langlade, N. B., Balzergue, S., Arribat, S., Bailly, C., et al. (2014). Is gene transcription involved in seed dry after-ripening? *PLOS ONE* 9:e86442. doi: 10.1371/journal.pone.0086442

Mira, M. M., Huang, S., Kapoor, K., Hammond, C., Hill, R. D., and Stasolla, C. (2017). Expression of Arabidopsis class 1 phytoglobin (*AtPgb1*) delays death and degradation of the root apical meristem during severe PEG-induced water deficit. *J. Exp. Bot.* 68, 5653–5668. doi: 10.1093/jxb/erx371

Nakabayashi, K., Okamoto, M., Koshiba, T., Kamiya, Y., and Nambara, E. (2005). Genome-wide profiling of stored mRNA in *Arabidopsis thaliana* seed germination: epigenetic and genetic regulation of transcription in seed. *Plant J.* 41, 697–709. doi: 10.1111/j.1365-313X.2005.02337.x

Nakajima, M., Shimada, A., Takashi, Y., Kim, Y.-C., Park, S.-H., Ueguchi-Tanaka, M., et al. (2006). Identification and characterization of Arabidopsis gibberellin receptors. *Plant J.* 46, 880–889. doi: 10.1111/j.1365-313X.2006.02748.x

Narsai, R., Howell, K. A., Millar, A. H., O'Toole, N., Small, I., and Whelan, J. (2007). Genome-wide analysis of mRNA decay rates and their determinants in *Arabidopsis thaliana*. *Plant Cell* 19, 3418–3436. doi: 10.1105/tpc.107.055046

Nelson, S. K., and Steber, C. M. (2016). "Gibberellin hormone signal perception: down-regulating DELLA repressors of plant growth and development," in *Annual Plant Reviews: The Gibberellins*, Vol. 49, eds P. Hedden and S. G. Thomas (Chichester: John Wiley & Sons), 153–188. doi: 10.1002/9781119210436.ch6

Nelson, S. K., and Steber, C. M. (2017). Transcriptional mechanisms associated with seed dormancy and dormancy loss in the gibberellin-insensitive *sly1-2* mutant of *Arabidopsis thaliana*. *PLOS ONE* 12:e0179143. doi: 10.1371/journal.pone.0179143

Nomoto, Y., Nomoto, Y., Kubozono, S., Miyachi, M., Yamashino, T., Nakamichi, N., et al. (2012). A circadian clock- and PIF4-mediated double coincidence mechanism is implicated in the thermosensitive photoperiodic control of plant architectures in *Arabidopsis thaliana*. *Plant Cell Physiol.* 53, 1965–1973. doi: 10.1093/pcp/pcs141

Nonogaki, H. (2014). Seed dormancy and germination—emerging mechanisms and new hypotheses. *Front. Plant Sci.* 5:233. doi: 10.3389/fpls.2014.00233

Oh, E., Kim, J., Park, E., Kim, J.-I., Kang, C., and Choi, G. (2004). PIL5, a phytochrome-interacting basic helix-loop-helix protein, is a key negative regulator of seed germination in *Arabidopsis thaliana*. *Plant Cell* 16, 3045–3058. doi: 10.1105/tpc.104.025163

Oh, E., Yamaguchi, S., Hu, J., Yusuke, J., Jung, B., Paik, I., et al. (2007). PIL5, a phytochrome-interacting bHLH protein, regulates gibberellin responsiveness by binding directly to the *GAI* and *RGA* promoters in *Arabidopsis* seeds. *Plant Cell* 19, 1192–1208. doi: 10.1105/tpc.107.050153

Oh, E., Yamaguchi, S., Kamiya, Y., Bae, G., Chung, W.-I., and Choi, G. (2006). Light activates the degradation of PIL5 protein to promote seed germination through gibberellin in Arabidopsis. *Plant J.* 47, 124–139. doi: 10.1111/j.1365-313X.2006.02773.x

Okamoto, M., Kuwahara, A., Seo, M., Kushiro, T., Asami, T., Hirai, N., et al. (2006). CYP707A1 and CYP707A2, which encode abscisic acid 8'-hydroxylases, are indispensable for proper control of seed dormancy and germination in Arabidopsis. *Plant Physiol.* 141, 97–107. doi: 10.1104/pp.106.079475

Oñate-Sánchez, L., and Vicente-Carbajosa, J. (2008). DNA-free RNA isolation protocols for *Arabidopsis thaliana*, including seeds and siliques. *BMC Res. Notes* 1:93. doi: 10.1186/1756-0500-1-93

Oracz, K., El-Maarouf-Bouteau, H., Farrant, J. M., Cooper, K., Belghazi, M., Job, C., et al. (2007). ROS production and protein oxidation as a novel mechanism for seed dormancy alleviation. *Plant J.* 50, 452–465. doi: 10.1111/j.1365-313X.2007.03063.x

Palaniswamy, S. K., James, S., Sun, H., Lamb, R. S., Davuluri, R. V., and Grotewold, E. (2006). AGRIS and AtRegNet. A platform to link cis-regulatory elements and transcription factors into regulatory networks. *Plant Physiol.* 140, 818–829. doi: 10.1104/pp.105.072280

Peng, J., Carol, P., Richards, D. E., King, K. E., Cowling, R. J., Murphy, G. P., et al. (1997). The *Arabidopsis GAI* gene defines a signaling pathway that negatively regulates gibberellin responses. *Genes Dev.* 11, 3194–3205. doi: 10.1101/gad.11.23.3194

Peng, J., and Harberd, N. P. (1993). Derivative alleles of the Arabidopsis gibberellin-insensitive (gai) mutation confer a wild-type phenotype. *Plant Cell* 5, 351–360. doi: 10.1105/tpc.5.3.351

Pérez-Rodríguez, P., Riaño-Pachón, D. M., Corrêa, L. G. G., Rensing, S. A., Kersten, B., and Mueller-Roeber, B. (2009). PlnTFDB: updated content and new features of the plant transcription factor database. *Nucleic Acids Res.* 38, D822–D827. doi: 10.1093/nar/gkp805

Poisot, T., Bever, J. D., Nemri, A., Thrall, P. H., and Hochberg, M. E. (2011). A conceptual framework for the evolution of ecological specialisation. *Ecol. Lett.* 14, 841–851. doi: 10.1111/j.1461-0248.2011.01645.x

R Core Team (2016). *R: A Language and Environment for Statistical Computing*. Vienna: R Foundation for Statistical Computing.

Rajjou, L., Gallardo, K., Debeaujon, I., Vandekerckhove, J., Job, C., and Job, D. (2004). The effect of alpha-amanitin on the Arabidopsis seed proteome highlights the distinct roles of stored and neosynthesized mRNAs during germination. *Plant Physiol.* 134, 1598–1613. doi: 10.1104/pp.103.036293

Rodríguez, M. V., Barrero, J. M., Corbineau, F., Gubler, F., and Benech-Arnold, B. R. L. (2015). Dormancy in cereals (not too much, not so little): about the mechanisms behind this trait. *Seed Sci. Res.* 25, 99–119. doi: 10.1017/S0960258515000021

Smyth, G. (2005). "Limma: linear models for microarray data," in *Bioinformatics and Computational Biology Solutions using R and Bioconductor*, ed. R. Gentleman (Berlin: Springer), 397–420. doi: 10.1007/0-387-29362-0_23

Spiegel, S., and Marcus, A. (1975). Polyribosome formation in early wheat embryo germination independent of either transcription or polyadenylation. *Nature* 256, 228–230. doi: 10.1038/256228a0

Steber, C. M., Cooney, S. E., and McCourt, P. (1998). Isolation of the GA-response mutant *sly1* as a suppressor of *ABI1-1* in *Arabidopsis thaliana*. *Genetics* 149, 509–521.

Tyler, L., Thomas, S. G., Hu, J., Dill, A., Alonso, J. M., Ecker, J. R., et al. (2004). DELLA proteins and gibberellin-regulated seed germination and floral development in Arabidopsis. *Plant Physiol.* 135, 1008–1019. doi: 10.1104/pp.104.039578

van Zanten, M., Zöll, C., Wang, Z., Philipp, C., Carles, A., Li, Y., et al. (2014). HISTONE DEACETYLASE 9 represses seedling traits in *Arabidopsis thaliana* dry seeds. *Plant J.* 80, 475–488. doi: 10.1111/tpj.12646

Venable, D. L. (2007). Bet hedging in a guild of desert annuals. *Ecology* 88, 1086–1090. doi: 10.1890/06-1495

Wang, F., Zhu, D., Huang, X., Li, S., Gong, Y., Yao, Q., et al. (2009). Biochemical insights on degradation of *Arabidopsis* DELLA proteins gained from a cell-free assay system. *Plant Cell* 21, 2378–2390. doi: 10.1105/tpc.108.065433

Wang, Z., Cao, H., Sun, Y., Li, X., Chen, F., Carles, A., et al. (2013). *Arabidopsis* paired amphipathic helix proteins SNL1 and SNL2 redundantly regulate primary seed dormancy via abscisic acid-ethylene antagonism mediated by histone deacetylation. *Plant Cell* 25, 149–166. doi: 10.1105/tpc.112.108191

Waters, L., and Dure, L. (1965). Ribosomal-RNA synthesis in the absence of ribosome synthesis in germinating cotton seeds. *Science* 149, 188–191. doi: 10.1126/science.149.3680.188

Waters, L. C., and Dure, L. S. (1966). Ribonucleic acid synthesis in germinating cotton seeds. *J. Mol. Biol.* 19, 1–27. doi: 10.1016/S0022-2836(66)80046-3

Willige, B. C., Ghosh, S., Nill, C., Zourelidou, M., Dohmann, E. M. N., Maier, A., et al. (2007). The DELLA domain of GA INSENSITIVE mediates the interaction with the GA INSENSITIVE DWARF1A gibberellin receptor of *Arabidopsis*. *Plant Cell* 19, 1209–1220. doi: 10.1105/tpc.107.051441

Yamamoto, Y., Hirai, T., Yamamoto, E., Kawamura, M., Sato, T., Kitano, H., et al. (2010). A rice *gid1* suppressor mutant reveals that gibberellin is not always required for interaction between its receptor, GID1, and DELLA proteins. *Plant Cell* 22, 3589–3602. doi: 10.1105/tpc.110.074542

Yano, R., Takebayashi, Y., Nambara, E., Kamiya, Y., and Seo, M. (2013). Combining association mapping and transcriptomics identify HD2B histone deacetylase as a genetic factor associated with seed dormancy in *Arabidopsis thaliana*. *Plant J.* 74, 815–828. doi: 10.1111/tpj.12167

Yi, X., Du, Z., and Su, Z. (2013). PlantGSEA: a gene set enrichment analysis toolkit for plant community. *Nucleic Acids Res.* 41, W98–W103. doi: 10.1093/nar/gkt281

Yilmaz, A., Mejia-Guerra, M. K., Kurz, K., Liang, X., Welch, L., and Grotewold, E. (2010). AGRIS: the Arabidopsis gene regulatory information server, an update. *Nucleic Acids Res.* 39, D1118–D1122. doi: 10.1093/nar/gkq1120

Yonekura-Sakakibara, K. (2009). Functional genomics of family 1 glycosyltransferases in *Arabidopsis*. *Plant Biotechnol.* 26, 267–274. doi: 10.5511/plantbiotechnology.26.267

Yoshida, M., Horinouchi, S., and Beppu, T. (1995). Trichostatin A and trapoxin: novel chemical probes for the role of histone acetylation in chromatin structure and function. *Bioessays* 17, 423–430. doi: 10.1002/bies.950170510

Zentella, R., Zhang, Z.-L., Park, M., Thomas, S. G., Endo, A., Murase, K., et al. (2007). Global analysis of DELLA direct targets in early gibberellin signaling in *Arabidopsis*. *Plant Cell* 19, 3037–3057. doi: 10.1105/tpc.107.054999

Zhang, H., and Zhu, J.-K. (2011). RNA-directed DNA methylation. *Curr. Opin. Plant Biol.* 14, 142–147. doi: 10.1016/j.pbi.2011.02.003

Zhang, J., Duan, X., Ding, F., Ma, H., Zhang, T., and Yang, Y. (2014). Salinity induced the changes of root growth and antioxidative responses in two wheat cultivars. *Protoplasma* 251, 771–780. doi: 10.1007/s00709-013-0579-7

Conflict of Interest Statement: The authors declare that the research was conducted in the absence of any commercial or financial relationships that could be construed as a potential conflict of interest.

frontiers in Plant Science

ORIGINAL RESEARCH
published: 12 July 2017
doi: 10.3389/fpls.2017.01203

Unraveling Key Metabolomic Alterations in Wheat Embryos Derived from Freshly Harvested and Water-Imbibed Seeds of Two Wheat Cultivars with Contrasting Dormancy Status

Aayudh Das[1,2], Dea-Wook Kim[3], Pramod Khadka[2†], Randeep Rakwal[4] and Jai S. Rohila[2†]*

[1] Department of Plant Biology, University of Vermont, Burlington, VT, United States, [2] Department of Biology and Microbiology, South Dakota State University, Brookings, SD, United States, [3] National Institute of Crop Science, Rural Development Administration, Wanju-gun, South Korea, [4] Faculty of Health and Sport Sciences, University of Tsukuba, Tsukuba, Japan

OPEN ACCESS

Edited by:
Hiroyuki Nonogaki,
Oregon State University,
United States

Reviewed by:
Belay T. Ayele,
University of Manitoba, Canada
Karl Kunert,
University of Pretoria, South Africa
Joshua L. Heazlewood,
University of Melbourne, Australia

***Correspondence:**
Jai S. Rohila
jai.rohila@ars.usda.gov

†Present address:
Pramod Khadka,
Department of Biology, University of Virginia, Charlottesville, VA, United States
Jai S. Rohila,
Dale Bumpers National Rice Research Center, United States Department of Agriculture – Agricultural Research Service, Stuttgart, AR, United States

Specialty section:
This article was submitted to Crop Science and Horticulture, a section of the journal Frontiers in Plant Science

Received: 29 March 2017
Accepted: 26 June 2017
Published: 12 July 2017

Citation:
Das A, Kim D-W, Khadka P, Rakwal R and Rohila JS (2017) Unraveling Key Metabolomic Alterations in Wheat Embryos Derived from Freshly Harvested and Water-Imbibed Seeds of Two Wheat Cultivars with Contrasting Dormancy Status. Front. Plant Sci. 8:1203. doi: 10.3389/fpls.2017.01203

Untimely rains in wheat fields during harvest season can cause pre-harvest sprouting (PHS), which deteriorates the yield and quality of wheat crop. Metabolic homeostasis of the embryo plays a role in seed dormancy, determining the status of the maturing grains either as dormant (PHS-tolerant) or non-dormant (PHS-susceptible). Very little is known for direct measurements of global metabolites in embryonic tissues of dormant and non-dormant wheat seeds. In this study, physiologically matured and freshly harvested wheat seeds of PHS-tolerant (cv. Sukang, dormant) and PHS-susceptible (cv. Baegjoong, non-dormant) cultivars were water-imbibed, and the isolated embryos were subjected to high-throughput, global non-targeted metabolomic profiling. A careful comparison of identified metabolites between Sukang and Baegjoong embryos at 0 and 48 h after imbibition revealed that several key metabolic pathways [such as: lipids, fatty acids, oxalate, hormones, the raffinose family of oligosaccharides (RFOs), and amino acids] and phytochemicals were differentially regulated between dormant and non-dormant varieties. Most of the membrane lipids were highly reduced in Baegjoong compared to Sukang, which indicates that the cell membrane instability in response to imbibition could also be a key factor in non-dormant wheat varieties for their untimely germination. This study revealed that several key marker metabolites (e.g., RFOs: glucose, fructose, maltose, and verbascose), were highly expressed in Baegjoong after imbibition. Furthermore, the data showed that the key secondary metabolites and phytochemicals (vitexin, chrysoeriol, ferulate, salidroside and gentisic acid), with known antioxidant properties, were comparatively low at basal levels in PHS-susceptible, non-dormant cultivar, Baegjoong. In conclusion, the results of this investigation revealed

that after imbibition the metabolic homeostasis of dormant wheat is significantly less affected compared to non-dormant wheat. The inferences from this study combined with proteomic and transcriptomic studies will advance the molecular understanding of the pathways and enzyme regulations during PHS.

Keywords: wheat, metabolomic profile, pre-harvest sprouting, PHS, raffinose, oligosaccharide, oxalate

INTRODUCTION

Pre-harvest sprouting (PHS) in wheat refers to the germination of physiologically mature seeds inside the spike, but before the crop is harvested (Sorrells and Sherman, 2007; Shu et al., 2015). It occurs due to periods of rainfall that cause excess humidity and warm temperatures in the field during seed maturation. Post-anthesis, wheat grains achieve maximum mass within a month, and then they undergo drying phase with rapid and gradual water loss and continue their ripening process. As a result, the endosperm cells succumb, and the embryo becomes dormant during this period (Thomason et al., 2009), which helps to prevent untimely germination of freshly matured seeds during short spells of conditions in fields that may even be very much favorable for seed germination (Née et al., 2017). During the post-green revolution period, for uniform and rapid seed germination at sowing wheat breeders have directly or indirectly applied genetic selections in the development of modern varieties that could have resulted in lowering the dormancy levels in wheat, and thus probably have decreased tolerance of wheat to PHS. Occurrence of PHS in wheat is determined by several factors, mainly: (i) inherent dormancy levels, (ii) duration and severity of humidity in the field, (iii) field temperature during high humidity period, (iv) growth phase of the maturing grain, and (v) spike morphology (Singh et al., 2014; Tuttle et al., 2015). The prevalence of PHS in the same cultivar could fluctuate from year-to-year depending on climatic conditions. Typical characteristics of PHS include swelling of the grain, splitting of the seed coat, discoloration of grain, and emergence of root and shoot (Thomason et al., 2009). PHS adversely affects milling properties, grain quality, seed viability and seedling vigor (Morgan, 2005). Pre-harvest germination of seeds causes degradation of protein and starch in endosperm and as a result the quality of wheat grains is reduced, which ultimately produces low-quality flour (Groos et al., 2002; Fakthongphan et al., 2016). PHS confines the end-use applications of wheat due to this downgraded grain and flour quality. A decreased test weight of the harvested crop is also a result of sprouting and is triggered by the conversion of starch to glucose by the α-amylase enzyme (Mares and Mrva, 2014; Kondhare et al., 2015). In China, the world's largest wheat producer, almost 25 million hectares of wheat are affected by PHS (Liu et al., 2016); thus putting the PHS on a list that causes more than $1 billion loss per year to farmers on a global basis.

Seed dormancy level and seed germination rate are the two key processes involved in PHS, which are largely regulated by a series of complex biochemical processes in seed, and are controlled by genetic factors with substantial environmental influences (Koornneef et al., 2002; Nonogaki et al., 2010). Recent progress in functional genomics approaches such as transcriptomics, proteomics, and metabolomics have enhanced our limited knowledge of PHS (Gao and Ayele, 2014; Dong et al., 2015). Imbibition of dry seed reestablishes the molecular processes and eventually breaks the seed dormancy (Manz et al., 2005). Transcriptomics and proteomics studies in plants have also increased our current understanding on the dynamic relationship between transcripts and proteins during seed maturation and their amendments after imbibition (Nakabayashi et al., 2005; Chibani et al., 2006; Holdsworth et al., 2008). A comparative proteomic analysis was carried out by Kamal et al. (2009) in seeds of PHS-resistant (cv. Keumgang) and PHS-susceptible (cv. Jinpum) wheat. The researchers identified 73 differentially expressed proteins between the resistant and susceptible cultivar, which fall under nine broad functional categories: metabolism, storage, photosynthesis, amino acid, allergy, stress, protein synthesis, enzyme, and hypothetical protein. Another proteomic study consisting of a transgenic PHS-resistant wheat [reduced Thioredoxin h (trx h) expression] and wild-type PHS-susceptible wheat (cv. Yumai 18), after 48 h of imbibition, identified 16 differential abundant proteins (Guo et al., 2011). They suggest that trx h gene, along with other proteins such as Serpin, 14-3-3, and WRKY6 transcription factor might be a key determinant for seed germination. It possibly will increase the activity of thiocalsin by reducing disulfide groups and inhibiting Serpin, and might be playing a role during PHS in wheat especially by promoting proteins degradation. Recently, transcriptomic investigations of dormant and non-dormant pea seeds has identified 148 differentially expressed genes (Hradilová et al., 2017). Metabolomic analysis of separated seed coats from pea genotypes revealed significantly higher contents of proanthocyanidins (dimer and trimer of gallocatechin), quercetin, and myricetin rhamnosides and hydroxylated fatty acids in dormant compared to non-dormant seeds. The transcriptomic studies have also demonstrated that various transcription factors are differentially expressed in wheat during seed development and first 48 h of post-imbibition germination (Wilson et al., 2005; Wan et al., 2008). The authors suggest that the majority of the transcripts required for germination after imbibition may accumulate in the embryo during seed maturation or at least prior to germination. Abscisic acid (ABA) has also been reported to be associated with seed dormancy. Gao et al. (2012) meticulously performed comparative transcriptomic analysis between dormant and after-ripened seeds in both dry and water-imbibed states. The study found a total of 3067 probesets, grouped into 16 clusters, which show differential expression of fivefolds or higher. Of these, only 58 probesets showed differential expression between dry after-ripened and dormant seeds, and 36 probesets were found to be regulated by dormancy only. Overall, this microarray study identified several

biological processes such as: jasmonate biosynthesis, cell wall modifications, epigenetic mechanisms that could be critical in germination of water-imbibed, after-ripened wheat seeds when dormancy status is at low level in wheat seeds. An excellent review by Nonogaki (2014) on seed dormancy and seed germination research has highlighted a complex biological fact that there is a risk of over-simplifying molecular functions as positive and negative regulators because a single gene product could employ a negative feedback while serving as a positive regulator. Quantitative trait loci (QTL) analyses in wheat have shown that seed dormancy is regulated by major loci on chromosome 4A (Shorinola et al., 2016; Torada et al., 2016), chromosomes 5D, 3A, and 3D (Zhou et al., 2017). Approaches using map-based cloning have revealed that the TaMFT gene in wheat directly affects PHS through seed dormancy (Liu S. et al., 2013). Moreover, TaSdr genes were established to be key regulators of seed dormancy and PHS (Zhang et al., 2014). These evidences and more detailed discussions elsewhere such as by Zhou et al. (2017) suggest that either loss or reduced seed dormancy are the two key regulatory factors to determine the PHS phenotype in wheat. It has also been suggested that the occurrence of pre-harvest α-amylase in wheat seeds points toward the fluctuation of major plant hormones, including abscisic acid (ABA) and gibberellins (GAs), which play key roles in grain development. In the past two decades, research has been focused on breeding PHS-resistant varieties through identification of QTLs that confer PHS tolerance to wheat (Kulwal et al., 2004, 2005; Lohwasser et al., 2005; Torada et al., 2005; Chen et al., 2008; Gao et al., 2013; Cao et al., 2016; Shorinola et al., 2016), but very little is known at the level of metabolome. The metabolome is downstream of transcriptome and proteome, and cannot be predicted directly by the genomic information (Hong et al., 2016); and one of its attraction is in providing reliable molecular markers because metabolites are dynamically and comparatively closest to the observed phenotypes compared to the transcripts and proteins. Further, metabolomics studies can complement the insights drawn from transcriptomics and proteomics studies and may suggest a direct link between a gene and the function of the metabolic network (Fiehn et al., 2000). On a molecular breeding assignment the QTL mapping relies heavily on precise phenotyping of the trait, and metabolite profiling is proficient to provide a novel and precise phenotyping tool to plant breeders in the form of metabolite variants. Thus the developments in metabolomics offer great promise to plant breeding programs by developing metabolic markers, metabolic quantitative trait loci (mQTL), as well as to basic biology programs by contributing substantial knowledge toward the understanding of various cellular mechanisms (Nambara and Nonogaki, 2012; Herrmann and Schauer, 2013).

Metabolomics is comparatively a new branch of high-throughput functional genomics that has the potential to uncover the differential accumulation of metabolites or small molecules at global level within a cell at a given time (Weckwerth, 2010). Global metabolomics via the use of mass spectrometry (MS) permits the identification of 1000s of metabolites associated with a specific treatment (Patti et al., 2012). Metabolomics delivers an improved gateway of measuring biochemical activity directly by monitoring the substrates and products that are converted throughout the cellular metabolism of the plant (Saito and Matsuda, 2010). Quantitative measurements of the metabolites in the cell convey an extensive outlook of the functional status of the plant tissue, which can be useful for the assessment of gene functions (Ramalingam et al., 2015). A global metabolomics approach also provides a powerful tool to study the temporal regulation of various metabolic pathways. Although the effects of PHS conditions on wheat have been the subject of intense research at the levels of quantitative genetics, physiology, molecular biology, and genomics, no detailed metabolomics-based study has been performed yet on wheat embryos related to PHS and/or seed dormancy (Zanetti et al., 2000; Kulwal et al., 2004; Carvalho and Beleia, 2015; Shu et al., 2015). Recent studies have started to emerge on infrared spectroscopy-based metabolomic profiling, which assesses the length of the germination process in barley and wheat (Burke et al., 2016). A recent excellent report recommended using the near-infrared spectroscopy to the grain industry to detect instances of germination in cereal seeds at a very early stage where symptoms of germination are not visible to human eyes, and thus barely sprouted grains can be noticed (Jones, 2017). Moreover, another study by Liu et al. (2016) used the metabolomic approach to define various metabolites from 20-days-post-anthesis to after 30-days-post-harvest ripening which were induced by introduction of *anti-trx-s* gene in wheat that facilitate PHS-resistance. They noticed that in freshly matured seeds, most metabolites of glycolysis, TCA cycle, choline metabolism, biosynthesis of proteins, nucleotides and fatty acids were at significantly lower levels in transgenic than in wild-type wheat.

We hypothesized that if the PHS-tolerant and PHS-susceptible wheat genotypes are water-imbibed, they may show differential accumulation of metabolites in the excised embryos, and this knowledge may shed light on germination and PHS mechanisms. To identify dormancy-associated metabolomic alterations in wheat embryos that are also associated with PHS, we carried out metabolomic profiling of two Korean wheat cultivars (*Triticum aestivum* L.) that possess contrasting phenotypes for PHS in the field; Sukang is a PHS-tolerant cultivar (PHS rate of 0.2% compared to a check variety 'Keumkang,' which has a PHS rate of 30.4%) and Baegjoong is PHS-susceptible cultivar (PHS rate of 23.9% compared to 'Keumkang') (Park et al., 2008, 2009). Parents of the two cultivars are genetically distant, but they show similar agronomical characteristics for growth duration, date of heading and maturity dates (Park et al., 2008). In terms of flour characteristics, the two varieties have different levels of protein content but similar characteristics in the high molecular weight glutenin subunit (HMW-GS) composition (Park et al., 2009). The objective of this study was to compare metabolomic profiles of embryos from the water-imbibed wheat seeds, and find key processes where the two wheat cultivars, which contrast in PHS tolerance after imbibition, differ and by data analyses and previous reports to get insights into the metabolomic activities of PHS-tolerant cv. Sukang over PHS-susceptible cv. Baegjoong. An in-depth metabolomic insight can complement the knowledge gained from other fields such as plant physiology, genetics, transcriptomics and proteomics to elucidate the physiological

and biochemical mechanisms involved in PHS tolerance in wheat as well as in other cereals (Das et al., 2015, 2016).

A metabolomic analysis of primary metabolites using liquid chromatography (LC) and gas chromatography (GC) coupled with MS allowed us to identify differentially expressed metabolites (such as carbohydrates, amino acids, lipids, oxalate, different plant hormones and their precursors) in response to water-imbibition of dormant and non-dormant wheat seeds. This study offers new knowledge for facilitating the development metabolite markers that can be utilized along with DNA markers to design PHS-resistant wheat varieties in future.

MATERIALS AND METHODS

Plant Materials

Two wheat cultivars Sukang (PHS-tolerant) and Baegjoong (PHS-susceptible) were grown in a field experiment with three replicated plots in a complete randomized design. Spikes of each wheat cultivar were harvested at physiological maturity (Calderini et al., 2000), and air-dried at room temperature until seed moisture content reached approximately 12%. After hand-threshing, morphologically sound seeds that show similar size, color, health, and maturity levels were selected and surface sterilized with 50% bleach solution. Fifty seeds from each replication were placed crease down in Petri dishes (90 mm diameter) with two layers of Whatman No. 3 filter paper with 6 ml of sterile distilled water and incubated at 20°C for 48 h in dark (Nyachiro et al., 2002). For this investigation, we selected 48 h time point for imbibition based on Yu et al. (2014) where they have described three distinct phases during seed germination process that commences with imbibition: a rapid initial uptake phase (0–12 hours after imbibition [HAI]), a plateau phase (12–24 HAI), and a further water uptake phase (24–48 HAI). After imbibition treatment, all the seeds were lyophilized. Embryos from more than 120 seeds were isolated manually with the help of a scalpel and ground in liquid nitrogen using a mortar and pestle. The pulverized material was stored at −80°C until metabolomic profiling.

Metabolomic Profiling

The metabolomic profiling in this study was focused on wheat embryos harvested at 0 and 48 h time points. The embryonic tissue samples were submitted to the Metabolon, Inc. (Durham, NC, United States). The sample preparation and analysis process was carried out essentially as described previously (Evans et al., 2009; Oliver et al., 2011; Tripathi et al., 2016; Das et al., 2017). Briefly, the samples were extracted in 400 μl of methanol using an automated liquid handling system, and the resulting samples were split into independent aliquots for analysis on three MS instrument platforms: GC/MS and two UPLC/MS platforms-where one was optimized for positive ionizations, and another platform was optimized for negative ionizations. Three controls were also prepared with the experimental samples: (i) pooled samples from three biological replications served as one technical replicate; (ii) ultra-pure water was used as a blank; (iii) a cocktail of quality control (QC) standards that included pooled samples, ultra-pure water and an aliquot of solvents used for extraction. Instrumentation derived variability was determined by calculating the median relative standard deviation (RSD) for the standards and overall process variability was calculated by measuring the median RSD for all metabolites present in the pooled matrix.

As described by Evans et al. (2009) in details, the Metabolon's LC/MS portion of the platform was based on a Waters ACQUITY ultra-performance liquid chromatography (UPLC) and a Thermo Scientific Q-Exactive high resolution/accurate mass spectrometer interfaced with a heated electrospray ionization (HESI-II) source and the Orbitrap mass analyzer was operated at 35,000 mass resolution. The dried sample extract were reconstituted in acidic or basic LC-compatible solvents and were divided into three aliquots. First aliquot was analyzed using acidic positive ion optimized conditions, and were eluted from C18 column (Waters UPLC BEH C18-2.1 mm × 100 mm, 1.7 μm) using water and methanol containing 0.1% formic acid. Second aliquot was analyzed using basic negative ion optimized conditions, were eluted from separate but similar C18 column using methanol and water with 6.5 mM ammonium bicarbonate. The third aliquot was analyzed via negative ionization following elution from a HILIC column (Waters UPLC BEH Amide 2.1 mm × 150 mm, 1.7 μm) using a gradient consisting of water and acetonitrile with 10 mM ammonium formate. The MS analysis alternated between MS and data-dependent MS^2 scans using dynamic exclusion, and the scan range was from 80 to 1000 mass to charge ratio (*m/z*).

The same embryonic samples were also derivatized under dried nitrogen using bistrimethyl-silyltrifluoroacetamide and analyzed by GC-MS. Derivatized samples were separated on a 5% diphenyl/95% dimethyl polysiloxane fused silica column (20 m × 0.18 mm ID; 0.18 μm film thickness) with helium as carrier gas and a temperature ramp from 60° to 340°C in a 17.5 min period. The samples were analyzed on a Thermo-Finnigan Trace DSQ fast-scanning single-quadrupole mass spectrometer using electron impact ionization (EI) and operated at unit mass resolving power. The scan range was from 50 to 750 m/z. The MS data was normalized and the metabolite quantification was performed by calculating the area-under-the-curve. Further, the MS peaks were also processed for QC using Metabolon's hardware and software. For peak identification the Metabolon maintains a library based on authenticated standards that contains the retention time/index (RI), mass to charge ratio (*m/z*), and chromatographic data including MS/MS spectral data. Compounds were identified by comparisons to Metabolon's library entries of purified standards (Dehaven et al., 2010) and their recurrent unknown entities. The biochemical identifications in this study were based on three criterion: retention index within a narrow RI window of the proposed identification, accurate mass match to the library +/− 0.005 amu, and the MS/MS forward and reverse scores between the experimental data and authentic standards. The MS/MS scores are based on a comparison of the

ions present in the experimental spectrum to the ions present in the library spectrum.

Statistical and Computational Analysis

Since all the treatments were comprised of three replicates ($n = 3$ for all groups), the statistical significance of the results was evaluated using Welch's two sample t-test and a level of significance of $p \leq 0.05$ for two group comparisons. The matched pair t-test was used to test whether two unknown means are different from paired observations from the same subjects. Principal component analysis (PCA), which is an unsupervised analysis and reduces the dimension of the data, was performed using R 3.3.1 software[1] to reveal the variability and significance of the dataset that can show- how the metabolites are differentially expressed in Sukang and Baegjoong seeds when imbibed in water.

For the clustering of the data, the log2-transformed accumulation values of the metabolites were used, and the heat map included the hierarchical clustering of the metabolites using Gene Cluster 3.0 software (de Hoon et al., 2004). The clusters were visualized using JAVA TREEVIEW software (Saldanha, 2004). MapMan application software (MapMan Version 3.5.1R2) was used to understand the metabolic distribution and metabolic regulation in response to PHS. Different metabolic networks were portrayed using the MetScape 3.1 plugin for Cytoscape software, version 3.0.1, and for ID referencing, we used the KEGG database (Kanehisa and Goto, 2000; Shannon et al., 2003; Karnovsky et al., 2012). The data analysis was done using R package ggplot2 (Wickham, 2016).

[1]https://www.R-project.org

RESULTS AND DISCUSSION

PHS Phenotype and Differential Accumulation of Metabolites in Sukang and Baegjoong in Response to Water-Imbibition

Before examining the differential accumulation of metabolites in the embryos of Sukang and Baegjoong, we checked the sprouting behavior of the two cultivars. **Figure 1** shows the phenotypic differences between Sukang and Baegjoong after 24 and 48 h of water-imbibition. Early seed germination was observed in Baegjoong at 24 h of imbibition, whereas Sukang remained dormant even after 48 h of imbibition. Earlier physiological studies had also shown the pre-mature germination in Baegjoong compared to Sukang (Park et al., 2008, 2009).

The analyses of the metabolomic profiling data of isolated embryos from these imbibed seeds showed that in response to water-imbibition, the metabolites were differentially accumulated between the two varieties at both time points (**Figure 2** and Supplementary Table S1). The metabolomic profiling revealed a concurrent detection of 409 metabolites that fall under several broad functional categories, such as carbohydrates, amino acids, lipids, cofactors, nucleotides, peptides, and secondary metabolites. Supplementary Figure S1 shows a PCA plot of all of the sample's metabolites. The two cultivars were widely separated at the analyzed time points due to the general differences in the abundance of metabolite levels. However, it is important to note that for overall metabolite profiling, the Baegjoong embryo at 0 h (BEM-00) is similar to the Sukang embryo at 0 h (SEM-00), but the SEM-00 and BEM-00 were clearly differentiated from the Sukang embryo at

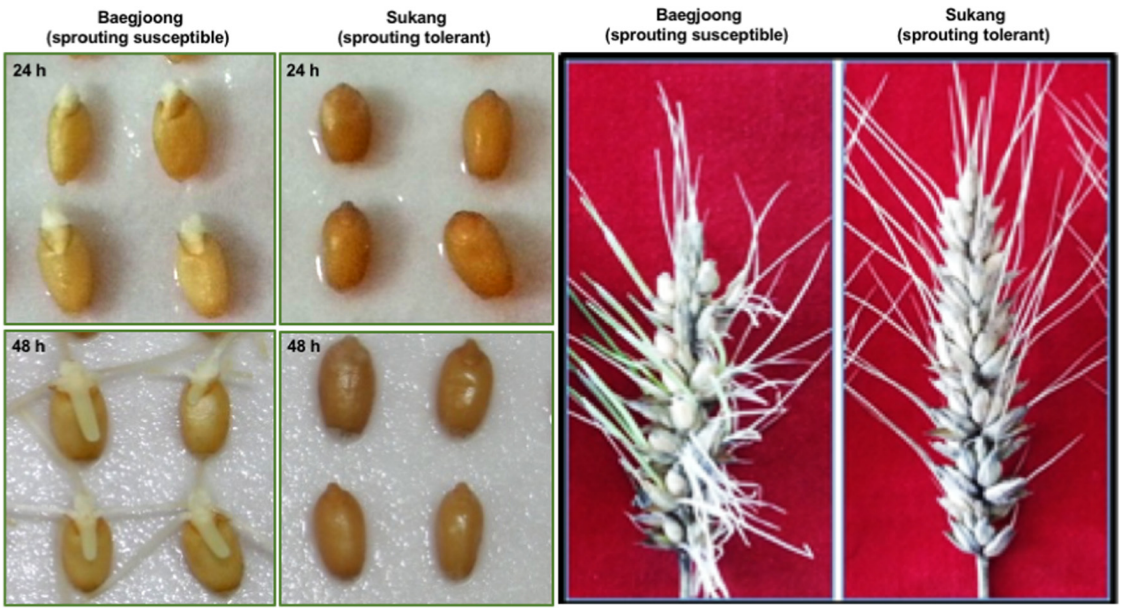

FIGURE 1 | The phenotypic differences of Baegjoong and Sukang after imbibition in water. The seeds of both cultivars used in this experiment were freshly harvested. **Left panel** shows Baegjoong and Sukang seeds after 24 and 48 h of imbibition. The **Right panel** shows the phenotype of the whole spike.

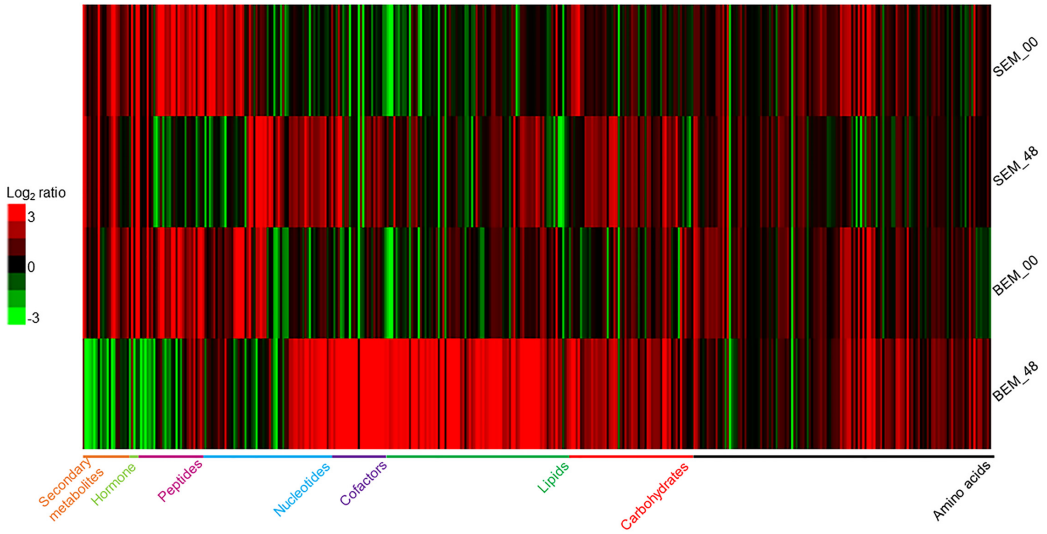

FIGURE 2 | The heat map shows the differential expression of metabolites in wheat embryos at two different time points (0 and 48 h) of imbibition as detected by LC/GC–MS. [S-Sukang; B-Baegjoong; and EM-embryo]. Heat map was developed using Gene Cluster 3.0 and visualized by using JAVA TREEVIEW.

48 h (SEM-48) and the Baegjoong embryo at 48 h (BEM-48), respectively.

The disparity in the general number of metabolites in Baegjoong was apparent in the strong skewing of the statistical results when the cultivars were compared to each other (**Figure 2**). In this study, 409 metabolites were found to be significantly accumulated between the two cultivars, and the majority of metabolites were significantly higher in Baegjoong. On the other hand, it seems very likely that the metabolites, whose abundance was relatively higher in Sukang (such as lipids: glycerophosphorylcholine, 1-linoleoyl-GPI, 1-palmitoyl-GPA, glycerol 3-phosphate, 1-oleoyl-GPA, and 1-linoleoyl-GPS; raffinose family of oligosaccharides (RFO's): fructose, galactitol, mannitol, mannose, and myo-inositol; and secondary metabolites like ferulate) might be notable for PHS-resistance. It is also to be noted that overall mean value for the accumulated metabolites did not change in Sukang in response to 48 h of imbibition, whereas Baegjoong showed a significantly higher mean value for the accumulated metabolites (Supplementary Figure S2), probably due to significant changes in the metabolic homeostasis of Baegjoong. A MapMan (Thimm et al., 2004) based analysis (Supplementary Figures S3A,B) mapped 101 metabolites out of 409, and it showed a clear difference between the two varieties in various metabolic processes that were affected by the water-imbibition of wheat seeds.

Lipid and Oxalate Metabolism during PHS

Cellular membranes are an integral part of cell organelles. Phospholipids are the backbone of the cellular membranes and can serve as a precursor for the generation of secondary lipids during many developmental processes (Fuller, 2006). Interestingly, at 48 h, most of the phospholipids were highly expressed in Sukang, and comparatively very few in Baegjoong. Baegjoong showed decreasing levels of membrane lipids and lysolipids between the 0 and 48 h time window (**Figure 3A** and Supplementary Table S2). At the same time, Sukang showed increasing levels of many lysolipids. The pattern suggests membrane instability and/or improperly timed membrane turnover/apoptosis during seed maturation of Baegjoong, a PHS-susceptible cultivar. A structurally diverse range of plant lipids, including fatty acids, contributes to a range of biological processes, such as membrane structure, primary and secondary metabolism, and extracellular and intracellular signaling in plants (Horn and Chapman, 2014). Lipid metabolism greatly affects seed development, dormancy, and germination (Penfield et al., 2007). Defects in β-oxidation can affect the seed dormancy levels of seeds, and, as determined from the metabolite levels in this study, the β-oxidation process in Baegjoong is significantly enhanced, which could have resulted in oxidation of many fatty acids. Moreover, higher levels of lipid peroxidation cause membrane damage (Wang et al., 2012), and this proposition is also supported in our analysis by compromised levels of most of the phospholipids, e.g., oxylipins and glycerolipids. Similar to other abiotic stressors, pre-mature seed germination may also induce the production of reactive oxygen species (ROS) and other cytotoxic compounds (Bailly et al., 2008). These stress-induced compounds could further lead to the breakdown of lipids.

We also found that in response to water-imbibition, there is an elevation of 18:1 (cis-vaccenate, oleate, linoleate, and linolenate) polyunsaturated fatty acids in Sukang. It is known that phospholipase A2 (PLA_2) mediates signaling cascades during developmental processes (Verlotta et al., 2013) and increased levels of free fatty acids, such as linoleate, linolenate, and palmitate, suggests that this reversal effect for pre-mature germination is mediated by increased PLA_2 activity, which is

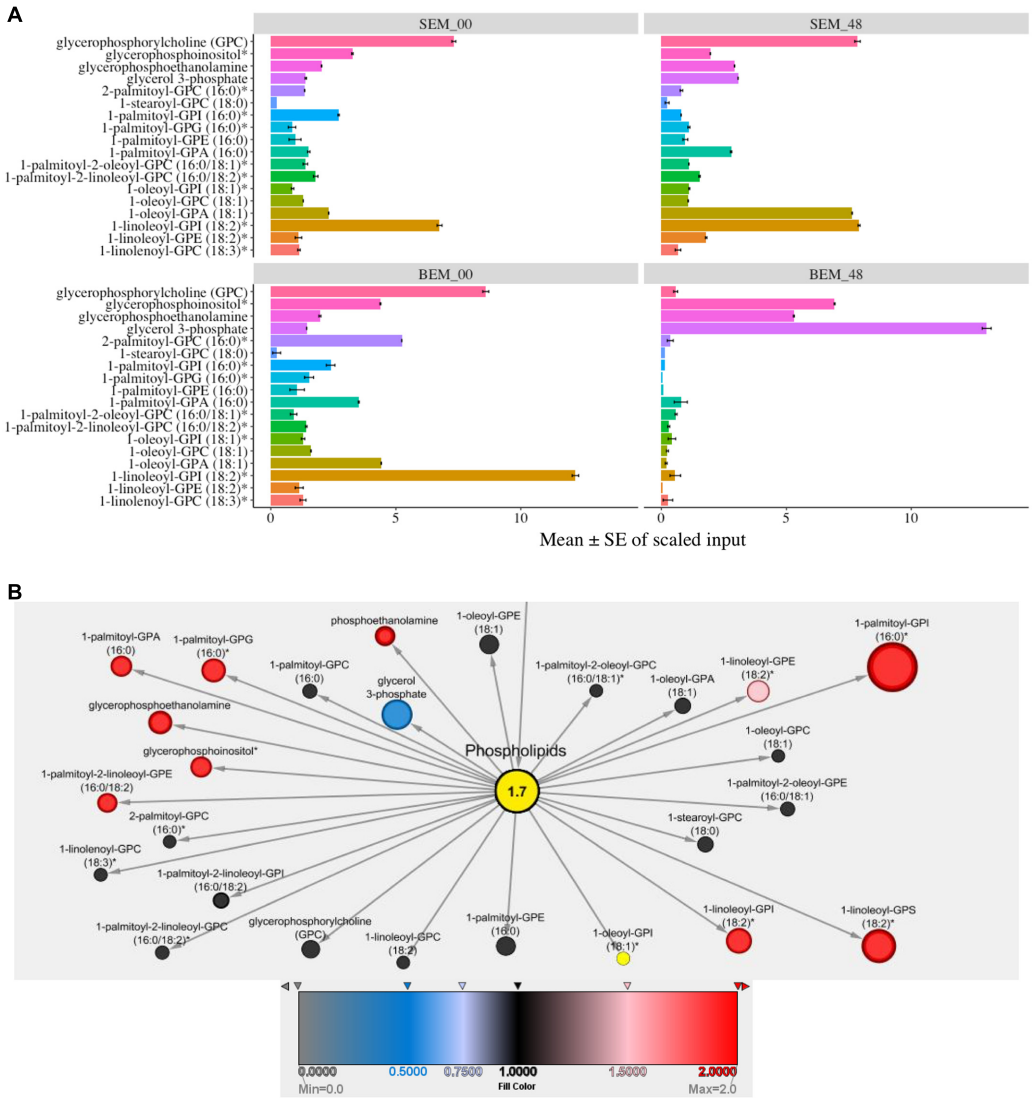

FIGURE 3 | Differential expression of lipids. **(A)** Mean values ± SE of scaled input of membrane lipids in SEM compared to BEM at 48 and 0 h. Error bars represent standard error (SE), data was accumulated from three replicates. For *p*-values see Supplementary Table S2 [S-Sukang; B-Baegjoong; and EM-embryo]. **(B)** Lipidomic interactions of all the input candidates in the study are shown using MetScape 3 software, along with their predicted interaction partners where the phospholipid has a centralized place.

steadily detected in Baegjoong (Supplementary Figure S4 and Table S1).

From a systems biology perspective, and for a better understanding of functional lipidomic interactions occurring in cell during PHS, we used Metscape to look through an overall scenario of all of the phospholipids and fatty acids during PHS. **Figure 3B** shows the putative lipidomic interaction of all of the input candidates in this study as well as their predicted partners. This study revealed various carbohydrates participating in glycolysis, TCA cycle, pentose phosphate pathway and other significant biological processes as well as functionally interacting with related compounds, which would eventually exert an effect on the biological and cellular processes when the wheat seeds are exposed to high humidity through rains in field or water-imbibition in lab experiments.

In Baegjoong, one compound, oxalate, stands out as showing the largest cultivar-related difference. Oxalate is a dianion that is synthesized by partial oxidation of the carbohydrates in plants (Osmond, 1967), and could be one of the key metabolites playing a crucial role during seed germination. In this metabolomic profiling, at 0 and 48 h, oxalate shows a major alteration between the two cultivars (**Figure 4**). Oxalate formation can be induced by metabolic precursors, such as glyoxylate, isocitrate, oxaloacetate, and ascorbate (Nakata, 2003; Xu et al., 2006). During developmental processes, oxalate oxidase can be involved in the production of ROS in plant tissues (Voothuluru and Sharp, 2013; Baxter et al., 2014). Germin (a type of oxalate oxidase),

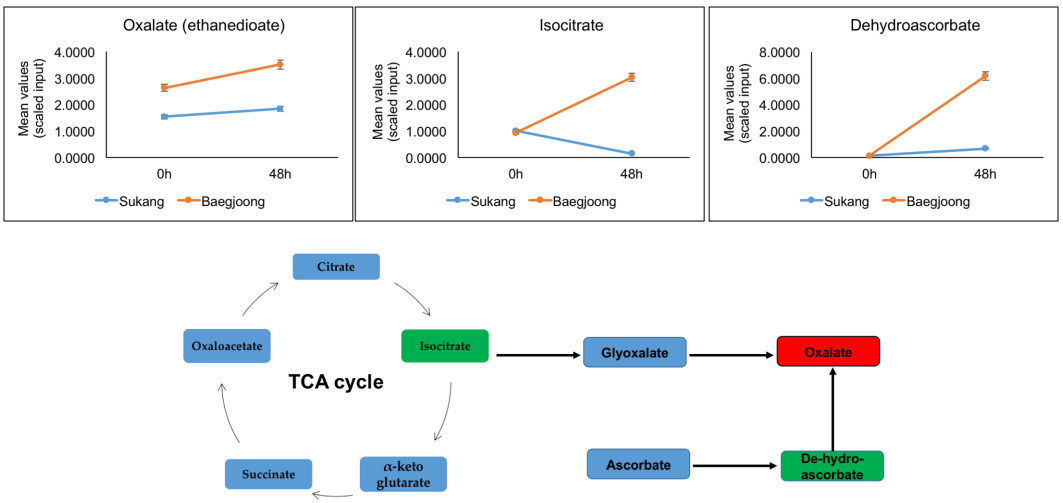

FIGURE 4 | Differential expression of oxalate (red box) and its precursors (green box) in Sukang and Baegjoong. The figure shows that at 0 and 48 h the oxalate and its precursors are elevated in Baegjoong, but not in Sukang. Error bars represent ± SE, data was accumulated from three replicates.

which is a major protein in wheat embryos and a marker for seed germination, seems to be involved in regulating seed dormancy status of the seed (Caliskan and Cuming, 1998). Berna and Bernier (1999) showed that the expression of wheat germin gene is stimulated during seed germination. In wheat root tips, a high level of oxalate oxidase expression generates excess amount of H_2O_2, which induces cell death and is required for cell wall crosslinking (Caliskan and Cuming, 1998; Berna and Bernier, 1999; Delisle et al., 2001; Baxter et al., 2014). Thus, comparatively higher abundance of oxalate in Baegjoong may suggest a lack of oxalate oxidase activity or an increased level of lipid degradation in this cultivar. It has been suggested that oxalate catabolism in *Arabidopsis* may determine the fate of seed germination (Foster et al., 2012). Based on the previous findings and by correlating our metabolic profiling derived results, we expect that a higher level of oxalate in Baegjoong may have induced seed germination after imbibition; therefore, sprouting occurs rapidly when seed encounters high humidity in field. In contrast, a comparatively lower level of oxalate in Sukang, may have delayed the seed germination and can prevent PHS.

Differential Accumulation of Hormone and Hormone-Related Compounds

Auxins (e.g., indole-3-acetic acid, IAA) and amino acids (e.g., tryptophan), play key roles in balancing seed dormancy and seed germination rates (Ramaih et al., 2003). Metabolomic profiling of the two cultivars detected variable abundance of many auxin-related compounds in Baegjoong in the 48 h samples (**Figure 5**). Interestingly, the precursor amino acid tryptophan was induced showing higher accumulation at 48 h after water-imbibition, whereas Sukang did not show any significant changes. Indoleacetate abundance did not change much in the Sukang samples but showed a steep reduction in Baegjoong at 48 h after water-imbibition. Three IAA catabolites were also detected, including indole-3-carboxylate, which showed a similar pattern at 48 h to IAA but with two other metabolites (indoleacetyl-aspartate and 2-oxindole-3-acetate) showing much higher levels in Baegjoong at 48 h time point. Serotonin, another potential regulatory molecule, which acts as a natural auxin, exhibited a similar pattern (**Figure 5** and Supplementary Table S3) (Pelagio-Flores et al., 2011).

Ethylene is one of the key plant hormones that controls dormancy in various plants (Corbineau et al., 2014). Cyano-alanine is a co-product of ethylene biosynthesis (Yip and Yang, 1988, 1998). Consistent with previous reports, our metabolomic profiling shows that after water-imbibition of seeds, there is no change in abundance for cyano-alanine in Sukang embryos, but over time, it increased in Baegjoong embryos (**Figure 6** and Supplementary Table S3). Additionally, methionine and *S*-adenosyl-methionine, which are involved in ethylene biosynthesis and the Yang cycle, are also abundant in the Baegjoong embryos but accumulated at reduced levels in Sukang. Several reports indicate that ABA maintains seed dormancy in accordance with other hormones, genes and metabolites in plants, such as wheat and *Arabidopsis* (Liu X. et al., 2013; Martinez et al., 2016). Walker-Simmons (1987) compared the sprouting-susceptible and sprouting-resistant wheat cultivars and found a 25% lower ABA level in sprouting-susceptible cultivars compared to sprouting-resistant cultivars, which indicated the potential of ABA in inhibiting embryonic germination effectively in the sprouting-resistant cultivar. In our metabolic profiling, putatively detected ABA had a very small peak and thus could not be confirmed with statistical significance. However, ions believed to come from ABA were found only in the first time point of the Sukang samples (none at 48 h), and were not detected at all in Baegjoong samples at any time points (Supplementary Figure S5). Additionally, two major ABA precursors, i.e., mevalonate and mevalonolactone, are higher at 0 h in Sukang and were gradually reduced following the water imbibition treatment. In contrast, for Baegjoong, both of

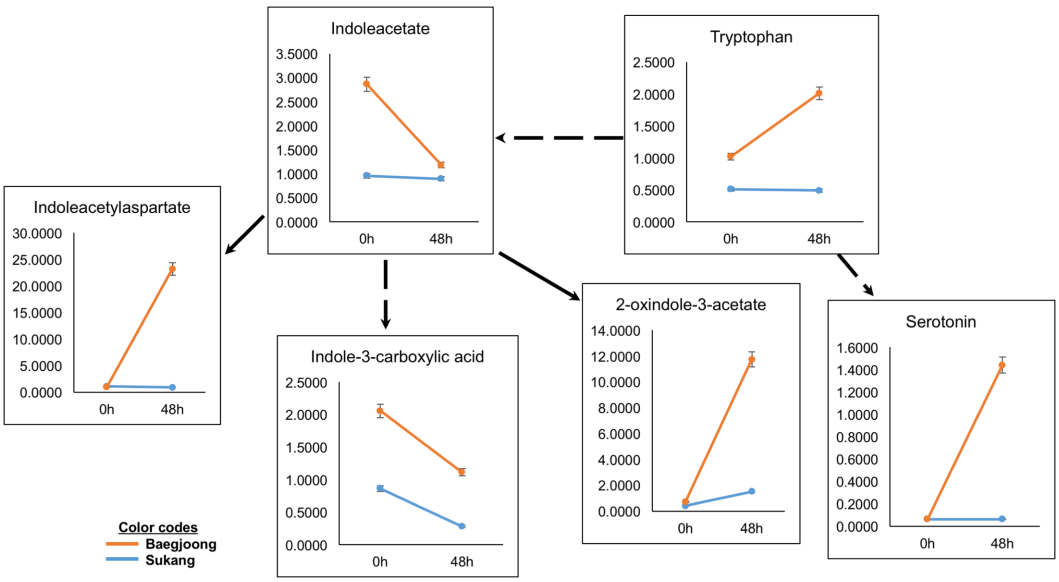

FIGURE 5 | Differential expression of auxin-related compounds in Sukang and Baegjoong after 48 h of imbibition. Broken arrow emphasizes that more than one step is involved in the process. Error bars represent ± SE, data was accumulated from three replicates.

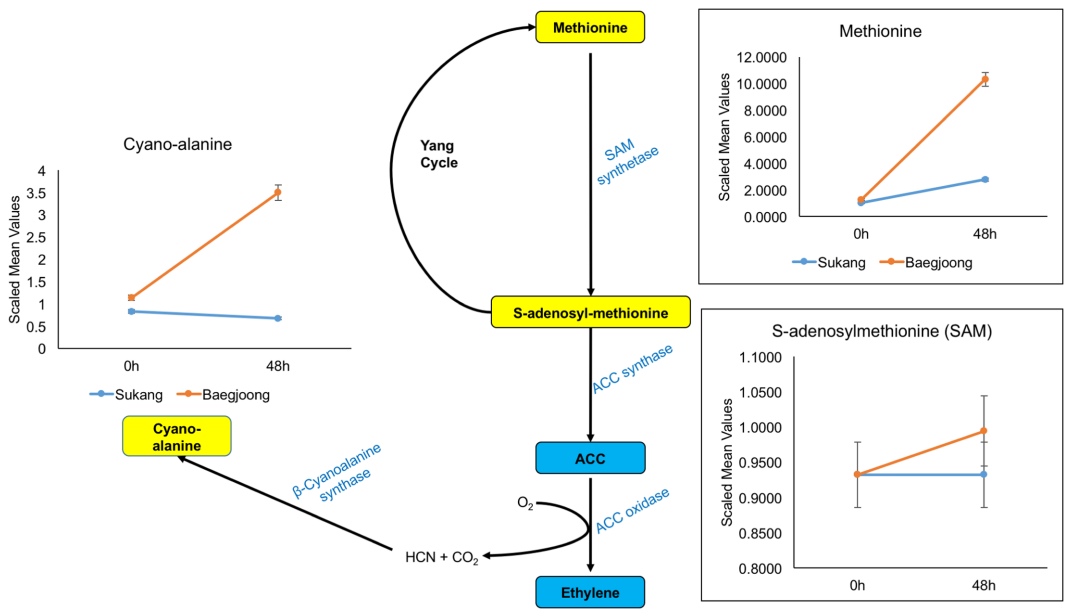

FIGURE 6 | Differential expression of cyano-alanine and ethylene precursors in Sukang and Baegjoong after imbibition in water. The figure demonstrates that methionine and *S*-adenosyl-methionine, which are involved in ethylene biosynthesis and the Yang cycle, are differentially expressed after imbibition (48 h) in both cultivars [ACC, 1-aminocyclopropane-carboxylate]. Error bars represent ± SE, data was accumulated from three replicates.

these ABA precursors are accumulated at much lower levels (Supplementary Figure S5).

It has been reported that in potato, ethylene treatment rapidly inhibits sprout growth in a completely reversible manner (Rylski et al., 1974). Specifically, auxin-treated tubers show dose-dependent enhancement of ethylene production and an inhibition of sprout growth (Suttle, 2003). Although, ethylene promotes germination in dormant seeds, it does so in cooperation with ABA, which is the primary facilitator of seed dormancy (Koornneef et al., 2002; Gubler et al., 2005). Our metabolic profiling also elucidates that how ethylene precursors and ethylene-related metabolites are regulated in response to imbibition in these two wheat cultivars. Because ethylene is considered to be an aging hormone, a higher

level of ethylene expression might induce senescence (Schaller, 2012), and in Baegjoong, it might be signaling an after-ripening effect to trigger the PHS (Carrera et al., 2008). In this study, ABA-mediated responses during PHS show a similar result to previous reports (Kashiwakura et al., 2016). It is evident that ABA can be directly synthesized from trans-farnesyl pyrophosphate or isopentenyl diphosphate (IPP) from mevalonic acid (Rohmer et al., 1993; Hirai et al., 2000; Milborrow, 2001). Thus, the observed enhancement of mevalonate and mevalonolactone levels at 48 h in Baegjoong (Supplementary Figure S5) suggests that water-imbibition might be inducing seed sprouting subsequently, which may lead to PHS in field. Although, it is also true that ABA synthesis is similarly regulated downstream of the mevalonate pathway mainly at steps catalyzed by NCED (9-cis-epoxycarotenoid dioxygenase) and ABA8′OH (ABA8′ hydroxylase), but it does not reflect in our findings (Seiler et al., 2011; Finkelstein, 2013).

Alterations in the Carbohydrate and Amino Acid Metabolism

Figures 7A,B show the data and pathways associated with carbohydrate metabolism, including the RFO pathway (also see Supplementary Table S4). RFOs are abundant in plant seeds and are synthesized through the involvement of a set of galactosyltransferases that successively transfer galactose units from galactinol to sucrose. RFOs accumulate during seed development and promptly decrease during seed germination (Peterbauer and Richter, 2001). While most of these metabolites are higher in Baegjoong samples at 48 h, there are several exceptions that may be informative for future PHS experiments.

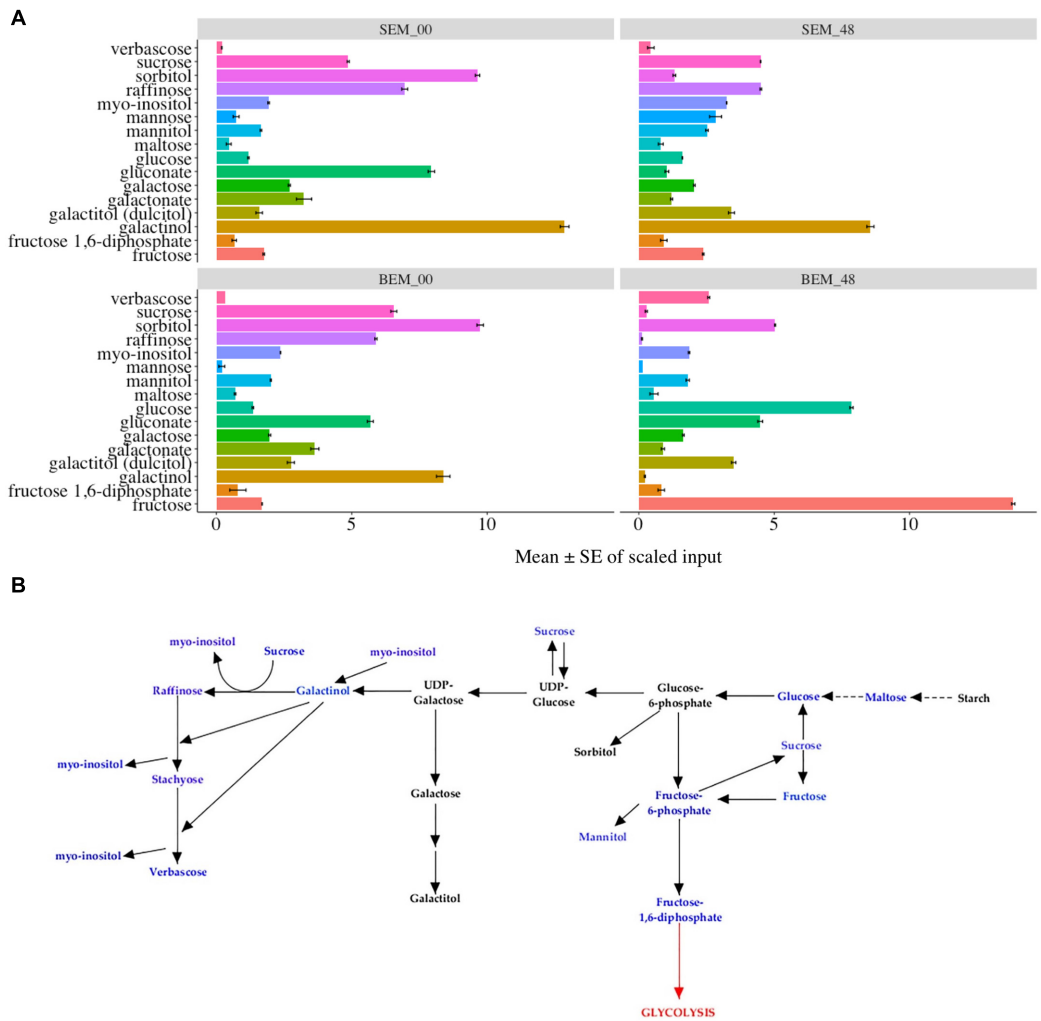

FIGURE 7 | Differential expression of carbohydrate pathways. **(A)** Mean value ± SE in the raffinose family oligosaccharides (RFOs), which are involved in carbohydrate metabolism in SEM compared to BEM (0 and 48 h time points are shown) [S-Sukang; B-Baegjoong; and EM-embryo]. Error bars represent ± SE, data was accumulated from three replicates. See Supplementary Table S5 for *p*-values. **(B)** Differential expression of RFOs. Blue font indicates carbohydrates that were detected in the study, and black font indicates adjoining carbohydrates, based on KEGG database, in the same pathway. Error bars represent ± SE, data was accumulated from three replicates.

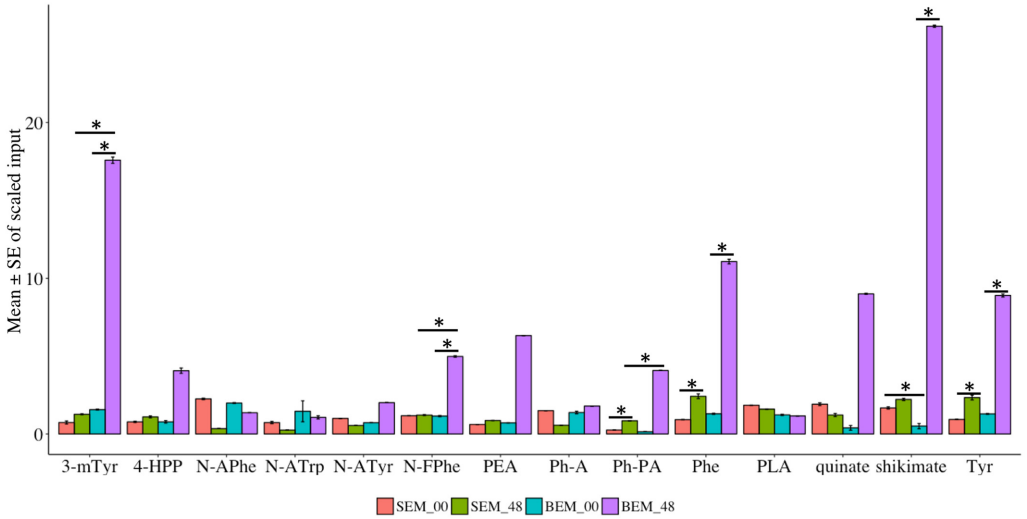

FIGURE 8 | Metabolomic alterations in the precursor compounds of the aromatic amino acid biosynthetic pathway in Sukang and Baegjoong after 48 h of imbibition. Error bars represent ± SE, data was accumulated from three replicates. *Indicates $p < 0.05$, for more information see Supplementary Table S6. 4-HPP, 4-hydroxyphenylpyruvate; PLA, phenyllactate; *N*-FPhe, *N*-formylphenylalanine; *N*-APhe, *N*-acetylphenylalanine; *N*-ATrp, *N*-acetyltryptophan; *N*-ATyr, *N*-acetyltyrosine; 3-mTry, 3-methoxytyrosine; Ph-A, phenylacetate; Ph-PA, phenylpyruvate; PEA, phenethylamine; Phe, phenylalanine; Tyr, tyrosine; Trp, tryptophan.

First, sucrose and other metabolites of the RFO pathway (such as galactinol, raffinose, gluconate, and galactose) all start at much higher levels in Sukang samples but then decrease sharply at the 48 h time point. In contrast, glucose, fructose, maltose (breakdown product of starch), and verbascose levels increase at 48 h in Baegjoong samples. In other words, most of the major carbohydrates that are involved in RFO are greatly affected in the PHS-susceptible cultivar Baegjoong, but Sukang shows a constant level of carbohydrate expression in terms of hexose sugar. Simsek et al. (2014) used a scanning electron microscope, and observed intact starch granules in non-sprouted wheat varieties; but found that the starch granules are degraded in sprouted varieties due to the high α-amylase activity. Consistent with this finding, high level of breakdown products of starch, such as glucose, fructose, maltose, and verbascose were observed in Baegjoong embryos after 48 h of water-imbibition. In this study, we showed that individual hexose sugars, starches and their precursors in the RFO family are affected by 48 h of water-imbibition. The TCA cycle is a crucial respiratory pathway that is essential for energy delivery to different organelles and for the maintenance of various physiological functions (Fernie et al., 2004). Our study indicates that after imbibition, the abundance level of several metabolites of TCA cycle such as citrate, fumarate, isocitrate, malate, succinate, and cis-aconitate are significantly increased in the PHS-susceptible cultivar Baegjoong at 48 h compared to those in Sukang (Supplementary Figure S6). We believe that the increased level of metabolites of the TCA cycle in the Baegjoong could have a major impact on the energy synthesis with rapid sugar utilization, and thus it may have a correlating effect on the poor quality of wheat grains after imbibition. The exceptions to this include sucrose, hexose diphosphate isobar (fructose-1,6-diphosphate, F-1,6-DP), and three higher order oligosaccharides: the RFO verbascose, stachyose (tetrasaccharide of galactose units), and raffinose (tetrasaccharide of galactose, glucose, and fructose units). While a higher F-1,6-DP may indicate higher activity in the glycolytic pathway, and although other compounds in the pathway were not increased, the other metabolites are consistent with the observation that Baegjoong samples contains higher levels of polysaccharides.

Amino acids are fundamental compounds that independently or synergistically influence the physiological activities of plants (Causin, 1996). Most importantly, amino acids are building blocks for active plant proteins, which are involved in major cellular and molecular functions (Rai, 2002). Specifically, plant nitrogen metabolism is highly regulated by the major amino acids, which have a potential role in the assimilation of nutrients (Buchanan et al., 2015). Our metabolic profiling indicated that 137 metabolites related to either amino acids or their conjugates and metabolism are differentially expressed during imbibition in Baegjoong and Sukang (Supplementary Figure S7 and Table S5). These metabolites fall into one of the following categories: serine family phosphoglycerate-derived amino acids, aromatic amino acid (PEP-derived), aspartate family of amino acids (OAA derived), glutamate family of amino acids (alpha-keto-glutarate-derived), branched chain amino acids (both OAA-derived and pyruvate-derived), amines-polyamines and amino acids that are involved in glutathione metabolism. Globally, amino acid metabolism was highly altered in the PHS-susceptible cultivar Baegjoong compared to PHS-tolerant Sukang from the 0 to 48 h time points (Supplementary Figure S7). The present investigation showed that aromatic amino acid metabolism was induced in the PHS-susceptible Baegjoong at 48 h, whereas the changes were very little in the PHS-tolerant Sukang (**Figure 8** and

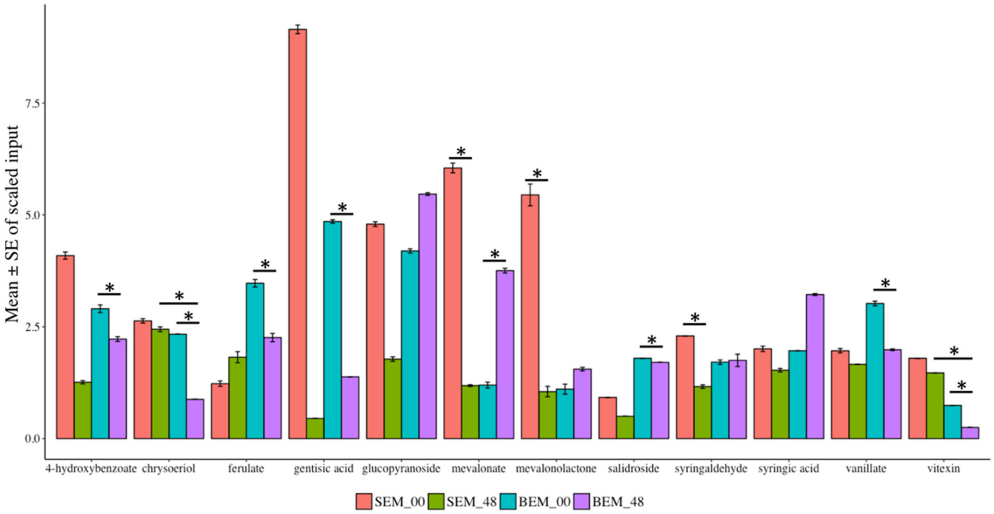

FIGURE 9 | Mean scaled inputs of secondary metabolites and wheat phytochemicals in SEM compared to BEM after 48 h of imbibition compared to 0 h [S-Sukang; B-Baegjoong; and EM-embryo]. Error bars represent ± SE, data was accumulated from three replicates. *Indicates $p < 0.05$, for more information see Supplementary Table S7.

Supplementary Table S6). Interestingly, shikimate, one of the precursor compounds of the aromatic amino acid biosynthetic pathway, was greatly induced in Baegjoong after 48 h of imbibition. The shikimate pathway has the potential to affect other biosynthetic pathways, such as tryptophan, tyrosine, and phenylalanine (Maeda and Dudareva, 2012). Affected aromatic amino acid metabolism may compromise essential precursors which are required for the synthesis of a wide range of secondary metabolites essential for various biological processes (Tzin and Galili, 2010). The oxidized form of cysteine and several other catabolites of amino acids fit this criterion. Phosphoenolpyruvate (PEP) is the main precursor of the aromatic amino acids, and chorismate is the branch point for the synthesis of major aromatic amino acids such as: tryptophan, tyrosine, and phenylalanine (Salter et al., 1986).

Differential Accumulation of the Secondary Metabolites

Various reports have shown that wheat phytochemicals, such as phenolics, tocopherols, carotenoids, and isoflavonoids have crucial antioxidant activity (Zhou et al., 2004). In this study, numerous secondary metabolites (such as alkaloids, benzenoids, flavonoids, and phenylpropanoids) as well as phytochemicals were found to be highly reduced in abundance after 48 h of water-imbibition in PHS-susceptible Baegjoong compared to the PHS-tolerant Sukang when compared to their initial levels at 0 h (**Figure 9** and Supplementary Table S7).

The major secondary metabolites, including vitexin, vanillate, chrysoeriol, 4-hydroxybenzoate, salidroside and gentisic acid, were reduced significantly at the 48 h time point in Baegjoong (**Figure 9**). Previous reports showed that salidroside, which is a phenylethanoid glycoside and was identified in *Rhodiola sachalinensis*, has a potential radical-scavenging function and antioxidant activity at cellular level (Li and Chen, 2001; Yu et al., 2007). We also identified significant differential accumulation of key flavonoids, vitexin, and chrysoeriol, which are also prominent antioxidants. Most importantly, numerous phenylpropanoids (ferulate, syringaldehyde, and vanillate) are more or less constant in Sukang, but reduced in Baegjoong. Considering this observation, it is evident that PHS reduces the phytochemicals along with their antioxidant activity in wheat seeds.

CONCLUSION

In general, the baselines for small molecules' abundance were observed at a much higher level in Sukang, which is a PHS-tolerant wheat cultivar, compared to Baegjoong, which is PHS-susceptible. Baegjoong exhibited signs of increased membrane degradation, which were probably the result of high PLA_2 abundance at the 48 h time point. Baegjoong also had much higher levels of oxalate at both time points, and the reason for this could be due to a higher lipid degradation (with isocitrate lyase feeding the glyoxylate cycle) and/or from a lower level of oxalate oxidase activity. The precursors of several hormones were found to be differentially regulated between Sukang and Baegjoong at 48 h. For example, in Baegjoong the precursors for IAA were found highly reduced, while the ethylene precursors were found to be highly expressed, which could be responsible for rapid seed germination and eventually it will accelerate the PHS (Keçpczyński and Keçpczyńska, 1997; Matilla, 2000). Although, this metabolic profiling derived information does not reflect the targeted IAA, GA or ethylene levels, it certainly signifies that their precursors or related metabolites have a role to play in response to imbibition. An analysis of

the oligosaccharide pathways suggested that Baegjoong contains higher levels of oligosaccharide polymers. Thus, we expect that Baegjoong have a greater amounts of cell wall material, starches, and other polysaccharides, or complex lipids. All of these elements would contribute to the mass, but may precipitate during methanol extraction or for some unknown reasons could not be detected in the analysis (Maharjan and Ferenci, 2003). We also discussed the importance of lipid and oxalate metabolism and how it can affect the seed dormancy. We identified various phospholipids, oxalate and their precursor metabolites in the pathways which are differentially expressed in the two cultivars contrasting for PHS trait. A future study with targeted metabolomics approach can explain if lipid peroxidation occurs during PHS and whether oxalate oxidase can be involved in the production of ROS, which determines the fate of seed dormancy. It is interesting to note that during this study the effects of water-imbibition might be different between the two cultivars. At the time of embryo harvest, while the PHS-susceptible Baegjoong (non-dormant) seeds were at the post-germination stage, the PHS-resistant Sukang (dormant) seeds might be at pre-germination stage. Therefore, this metabolomic profile may also be reflecting physiological stage differences. To distinguish between the metabolites that are specifically the cause of PHS characteristic or the consequences of PHS further ultra-focused experiments are needed. Nonetheless, this study reveals the global scenario of metabolic alterations in two unique wheat cultivars in response to water-imbibition and identifies potential key marker metabolites enriching our understanding of PHS-mechanisms at metabolomic levels.

Current knowledge of metabolomics or chemical biology can be utilized to differentiate the genetic and biochemical mechanisms underlying PHS and seed dormancy (Nonogaki and Nonogaki, 2017). There is a huge scope of applying plant metabolomics toward improving the crop quality and food safety assessment as well as plant metabolic engineering. Plant metabolomics can provide meaningful insight into the numbers of identified metabolites and their associations with each other, and which reflects the agronomic importance of various traits. Thus, metabolomic profile-based knowledge can be used for the generation of more rational models to link specific pathway(s) with quality associated traits (Carreno-Quintero et al., 2013). For example, with this metabolomic profile of imbibed wheat seeds, a more promising study can be performed with the help of the resulting phenotypes with pathway specific metabolites, which will reveal how variation in metabolites abundance/expression can deploy certain phenotypes. One of the potential applications of our metabolomics study would be to generate PHS-resistant varieties by employing metabolomic markers and mQTLs in wheat breeding programs with an overarching aim for improving food security. According to an estimate, the crop yield trends are not encouraging to meet the future food security requirements. It is estimated that the current global wheat yield is increasing at a rate of 0.9% per year, which is far less than the required 2.4% per year to meet projected demands by 2050 (Ray et al., 2013). Pre-harvest sprouted seeds have poor germination at planting, and an inferior crop stand at germination results in comparatively poor yield at the crop harvest. New varieties with better PHS tolerance and with rapid and uniform germination rates at planting will certainly boost wheat yields; and thus will contribute toward improving world's food security. This metabolic profiling-based finding, especially pathway-based metabolites, can be a guide for the seed dormancy re-programming in wheat to generate PHS-tolerant varieties. Moreover, insights from this metabolic profile can be combined with proteomic and transcriptomic evaluations to gain better understanding of the molecular pathways and enzyme regulations during PHS, which will lead us toward a clearer understanding of various metabolic regulations and cellular mechanisms affecting the PHS.

AUTHOR CONTRIBUTIONS

D-WK, RR, and JR designed the experiments. AD, D-WK, and PK performed the experiments. AD, D-WK, PK, RR, and JR analyzed the results and wrote the manuscript.

ACKNOWLEDGMENTS

JR and D-WK acknowledge support from Cooperative Research Program for Agriculture Science & Technology Development (Project no. PJ01149902), Rural Development Administration, Republic of Korea. JR also acknowledges the USDA hatch project (SD00H541-15). We sincerely acknowledge Dr. Anna McClung for discussion, encouragement, and constructive comments during the writing of this manuscript. The U.S. Department of Agriculture-Agricultural Research Service (USDA-ARS), is an equal opportunity/affirmative action employer and all agency services are available without discrimination. Mention of commercial products and organizations in this manuscript is solely to provide specific information. It does not constitute endorsement by USDA-ARS over other products and organizations not mentioned.

SUPPLEMENTARY MATERIAL

The Supplementary Material for this article can be found online at: http://journal.frontiersin.org/article/10.3389/fpls.2017.01203/full#supplementary-material

REFERENCES

Bailly, C., El-Maarouf-Bouteau, H., and Corbineau, F. (2008). From intracellular signaling networks to cell death: the dual role of reactive oxygen species in seed physiology. *C. R. Biol.* 331, 806–814. doi: 10.1016/j.crvi.2008.07.022

Baxter, A., Mittler, R., and Suzuki, N. (2014). ROS as key players in plant stress signalling. *J. Exp. Bot.* 65, 1229–1240. doi: 10.1093/jxb/ert375

Berna, A., and Bernier, F. (1999). Regulation by biotic and abiotic stress of a wheat germin gene encoding oxalate oxidase, a H2O2-producing enzyme. *Plant Mol. Biol.* 39, 539–549. doi: 10.1023/A:1006123432157

Buchanan, B. B., Gruissem, W., Vickers, K., and Jones, R. L. (2015). *Biochemistry and Molecular Biology of Plants*. Hoboken, NJ: John Wiley & Sons.

Burke, M., Small, D. M., Antolasic, F., Hughes, J. G., Spencer, M. J. S., Blanch, E. W., et al. (2016). Infrared spectroscopy-based metabolomic analysis for the detection of preharvest sprouting in grain. *Cereal Chem. J.* 93, 444–449. doi: 10.1094/CCHEM-01-16-0005-R

Calderini, D. F., Abeledo, L. G., and Slafer, G. A. (2000). Physiological maturity in wheat based on kernel water and dry matter. *Agron. J.* 92, 895–901. doi: 10.2134/agronj2000.925895x

Caliskan, M., and Cuming, A. C. (1998). Spatial specificity of H2O2-generating oxalate oxidase gene expression during wheat embryo germination. *Plant J.* 15, 165–171. doi: 10.1046/j.1365-313X.1998.00191.x

Cao, L., Hayashi, K., Tokui, M., Mori, M., Miura, H., and Onishi, K. (2016). Detection of QTLs for traits associated with pre-harvest sprouting resistance in bread wheat (*Triticum aestivum* L.). *Breed. Sci.* 66, 260–270. doi: 10.1270/jsbbs.66.260

Carreno-Quintero, N., Bouwmeester, H. J., and Keurentjes, J. J. (2013). Genetic analysis of metabolome–phenotype interactions: from model to crop species. *Trends Genet.* 29, 41–50. doi: 10.1016/j.tig.2012.09.006

Carrera, E., Holman, T., Medhurst, A., Dietrich, D., Footitt, S., Theodoulou, F. L., et al. (2008). Seed after-ripening is a discrete developmental pathway associated with specific gene networks in Arabidopsis. *Plant J.* 53, 214–224. doi: 10.1111/j.1365-313X.2007.03331.x

Carvalho, P. D. T., and Beleia, A. D. P. (2015). Physicochemical changes and enzymatic activity of pre-harvest sprouting wheat. *Rev. Ciênc. Agron.* 46, 524–531. doi: 10.5935/1806-6690.20150034

Causin, H. F. (1996). The central role of amino acids on nitrogen utilization and plant growth. *J. Plant Physiol.* 149, 358–362. doi: 10.1016/S0176-1617(96)80134-9

Chen, C.-X., Cai, S.-B., and Bai, G.-H. (2008). A major QTL controlling seed dormancy and pre-harvest sprouting resistance on chromosome 4A in a Chinese wheat landrace. *Mol. Breed.* 21, 351–358. doi: 10.1007/s11032-007-9135-5

Chibani, K., Ali-Rachedi, S., Job, C., Job, D., Jullien, M., and Grappin, P. (2006). Proteomic analysis of seed dormancy in Arabidopsis. *Plant Physiol.* 142, 1493–1510. doi: 10.1104/pp.106.087452

Corbineau, F., Xia, Q., Bailly, C., and El-Maarouf-Bouteau, H. (2014). Ethylene, a key factor in the regulation of seed dormancy. *Front. Plant Sci.* 5:539. doi: 10.3389/fpls.2014.00539

Das, A., Eldakak, M., Paudel, B., Kim, D.-W., Hemmati, H., Basu, C., et al. (2016). Leaf proteome analysis reveals prospective drought and heat stress response mechanisms in soybean. *BioMed Res. Int.* 2016:23. doi: 10.1155/2016/6021047

Das, A., Paudel, B., and Rohila, J. S. (2015). "Potentials of proteomics in crop breeding," in *Advances in Plant Breeding Strategies: Breeding, Biotechnology and Molecular Tools*, eds J. M. Al-Khayri, S. M. Jain, and D. V. Johnson (Berlin: Springer), 513–537. doi: 10.1007/978-3-319-22521-0_18

Das, A., Rushton, P. J., and Rohila, J. S. (2017). Metabolomic profiling of soybeans (*Glycine max* L.) reveals the importance of sugar and nitrogen metabolism under drought and heat stress. *Plants* 6:21. doi: 10.3390/plants6020021

de Hoon, M. J., Imoto, S., Nolan, J., and Miyano, S. (2004). Open source clustering software. *Bioinformatics* 20, 1453–1454. doi: 10.1093/bioinformatics/bth078

Dehaven, C., Evans, A. M., Dai, H., and Lawton, K. A. (2010). Organization of GC/MS and LC/MS metabolomics data in to chemical libraries. *J. Cheminform.* 2:9. doi: 10.1186/1758-2946-2-9

Delisle, G., Champoux, M., and Houde, M. (2001). Characterization of oxalate oxidase and cell death in Al-sensitive and tolerant wheat roots. *Plant Cell Physiol.* 42, 324–333. doi: 10.1093/pcp/pce041

Dong, K., Zhen, S., Cheng, Z., Cao, H., Ge, P., and Yan, Y. (2015). Proteomic analysis reveals key proteins and phosphoproteins upon seed germination of wheat (*Triticum aestivum* L.). *Front. Plant Sci.* 6:107. doi: 10.3389/fpls.2015.01017

Evans, A. M., Dehaven, C. D., Barrett, T., Mitchell, M., and Milgram, E. (2009). Integrated, nontargeted ultrahigh performance liquid chromatography/electrospray ionization tandem mass spectrometry platform for the identification and relative quantification of the small-molecule complement of biological systems. *Anal. Chem.* 81, 6656–6667. doi: 10.1021/ac901536h

Fakthongphan, J., Graybosch, R. A., and Baenziger, P. S. (2016). Combining ability for tolerance to pre-harvest sprouting in common wheat (L.). *Crop Sci.* 56, 1025–1035. doi: 10.2135/cropsci2015.08.0490

Fernie, A. R., Carrari, F., and Sweetlove, L. J. (2004). Respiratory metabolism: glycolysis, the TCA cycle and mitochondrial electron transport. *Curr. Opin. Plant Biol.* 7, 254–261. doi: 10.1016/j.pbi.2004.03.007

Fiehn, O., Kopka, J., Dormann, P., Altmann, T., Trethewey, R. N., and Willmitzer, L. (2000). Metabolite profiling for plant functional genomics. *Nat. Biotechnol.* 18, 1157–1161. doi: 10.1038/81137

Finkelstein, R. (2013). Abscisic acid synthesis and response. *Arabidopsis Book* 11:e0166. doi: 10.1199/tab.0166

Foster, J., Kim, H. U., Nakata, P. A., and Browse, J. (2012). A previously unknown Oxalyl-CoA synthetase is important for oxalate catabolism in Arabidopsis. *Plant Cell* 24, 1217–1229. doi: 10.1105/tpc.112.096032

Fuller, M. (2006). "Towards the improvement of global environment and food," in *Abiotic Stress Tolerance in Plants*, eds K. Rai and T. Takabe (Dordrecht: Springer), 267.

Gao, F., and Ayele, B. T. (2014). Functional genomics of seed dormancy in wheat: advances and prospects. *Front. Plant Sci.* 5:458. doi: 10.3389/fpls.2014.00458

Gao, F., Jordan, M. C., and Ayele, B. T. (2012). Transcriptional programs regulating seed dormancy and its release by after-ripening in common wheat (*Triticum aestivum* L.). *Plant Biotechnol. J.* 10, 465–476. doi: 10.1111/j.1467-7652.2012.00682.x

Gao, X., Hu, C., Li, H., Yao, Y., Meng, M., Dong, J., et al. (2013). Factors affecting pre-harvest sprouting resistance in wheat (*Triticum aestivum* L.): a review. *J. Anim. Plant Sci.* 23, 556–565.

Groos, C., Gay, G., Perretant, M.-R., Gervais, L., Bernard, M., Dedryver, F., et al. (2002). Study of the relationship between pre-harvest sprouting and grain color by quantitative trait loci analysis in a white × red grain bread-wheat cross. *Theor. Appl. Genet.* 104, 39–47. doi: 10.1007/s001220200004

Gubler, F., Millar, A. A., and Jacobsen, J. V. (2005). Dormancy release, ABA and pre-harvest sprouting. *Curr. Opin. Plant Biol.* 8, 183–187. doi: 10.1016/j.pbi.2005.01.011

Guo, H., Zhang, H., Li, Y., Ren, J., Wang, X., Niu, H., et al. (2011). Identification of changes in wheat (*Triticum aestivum* L.) seeds proteome in response to anti–trx s gene. *PLoS ONE* 6:e22255. doi: 10.1371/journal.pone.0022255

Herrmann, A., and Schauer, N. (2013). "Metabolomics-assisted plant breeding," in *The Handbook of Plant Metabolomics*, eds W. Weckwerth and G. Kahl (Weinheim: Wiley-VCH Verlag GmbH & Co. KGaA), 245–254. doi: 10.1002/9783527669882.ch13

Hirai, N., Yoshida, R., Todoroki, Y., and Ohigashi, H. (2000). Biosynthesis of abscisic acid by the non-mevalonate pathway in plants, and by the mevalonate pathway in fungi. *Biosci. Biotechnol. Biochem.* 64, 1448–1458. doi: 10.1271/bbb.64.1448

Holdsworth, M. J., Finch-Savage, W. E., Grappin, P., and Job, D. (2008). Post-genomics dissection of seed dormancy and germination. *Trends Plant Sci.* 13, 7–13. doi: 10.1016/j.tplants.2007.11.002

Hong, J., Yang, L., Zhang, D., and Shi, J. (2016). Plant metabolomics: an indispensable system biology tool for plant science. *Int. J. Mol. Sci.* 17:767. doi: 10.3390/ijms17060767

Horn, P. J., and Chapman, K. D. (2014). Lipidomics in situ: insights into plant lipid metabolism from high resolution spatial maps of metabolites. *Prog. Lipid Res.* 54, 32–52. doi: 10.1016/j.plipres.2014.01.003

Hradilová, I., Trněný, O., Válková, M., Cechová, M., Janská, A., Prokešová, L., et al. (2017). A combined comparative transcriptomic, metabolomic, and anatomical analyses of two key domestication traits: pod dehiscence and seed dormancy in pea (*Pisum* sp.). *Front. Plant Sci.* 8:542. doi: 10.3389/fpls.2017.00542

Jones, O. A. (2017). Assessing pre-harvest sprouting in cereals using near-infrared spectroscopy-based metabolomics. *NIR News* 28, 15–19.

Kamal, A. H. M., Kim, K.-H., Shin, D.-H., Seo, H.-S., Shin, K.-H., Park, C.-S., et al. (2009). Proteomics profile of pre-harvest sprouting wheat by using MALDI-TOF mass spectrometry. *Plant Omics* 2:110.

Kanehisa, M., and Goto, S. (2000). KEGG: kyoto encyclopedia of genes and genomes. *Nucleic Acids Res.* 28, 27–30. doi: 10.1093/nar/28.1.27

Karnovsky, A., Weymouth, T., Hull, T., Tarcea, V. G., Scardoni, G., Laudanna, C., et al. (2012). Metscape 2 bioinformatics tool for the analysis and visualization of metabolomics and gene expression data. *Bioinformatics* 28, 373–380. doi: 10.1093/bioinformatics/btr661

Kashiwakura, Y.-I., Kobayashi, D., Jikumaru, Y., Takebayashi, Y., Nambara, E., Seo, M., et al. (2016). Highly sprouting-tolerant wheat grain exhibits extreme dormancy and cold imbibition-resistant accumulation of abscisic acid. *Plant Cell Physiol.* 57, 715–732. doi: 10.1093/pcp/pcw051

Keçpczyński, J., and Keçpczyńska, E. (1997). Ethylene in seed dormancy and germination. *Physiol. Plant.* 101, 720–726. doi: 10.1111/j.1399-3054.1997.tb01056.x

Kondhare, K., Farrell, A., Kettlewell, P., Hedden, P., and Monaghan, J. (2015). Pre-maturity α-amylase in wheat: the role of abscisic acid and gibberellins. *J. Cereal Sci.* 63, 95–108. doi: 10.1038/srep05355

Koornneef, M., Bentsink, L., and Hilhorst, H. (2002). Seed dormancy and germination. *Curr. Opin. Plant Biol.* 5, 33–36. doi: 10.1016/S1369-5266(01)00219-9

Kulwal, P. L., Kumar, N., Gaur, A., Khurana, P., Khurana, J. P., Tyagi, A. K., et al. (2005). Mapping of a major QTL for pre-harvest sprouting tolerance on chromosome 3A in bread wheat. *Theor. Appl. Genet.* 111, 1052–1059. doi: 10.1007/s00122-005-0021-4

Kulwal, P. L., Singh, R., Balyan, H. S., and Gupta, P. K. (2004). Genetic basis of pre-harvest sprouting tolerance using single-locus and two-locus QTL analyses in bread wheat. *Funct. Integr. Genomics* 4, 94–101. doi: 10.1007/s10142-004-0105-2

Li, H.-B., and Chen, F. (2001). Preparative isolation and purification of salidroside from the Chinese medicinal plant Rhodiola sachalinensis by high-speed counter-current chromatography. *J. Chromatogr. A* 932, 91–95. doi: 10.1016/S0021-9673(01)01232-8

Liu, C., Ding, F., Hao, F., Yu, M., Lei, H., Wu, X., et al. (2016). Reprogramming of seed metabolism facilitates pre-harvest sprouting resistance of wheat. *Sci. Rep.* 6:20593. doi: 10.1038/srep20593

Liu, S., Sehgal, S. K., Li, J., Lin, M., Trick, H. N., Yu, J., et al. (2013). Cloning and characterization of a critical regulator for preharvest sprouting in wheat. *Genetics* 195, 263–273. doi: 10.1534/genetics.113.152330

Liu, X., Zhang, H., Zhao, Y., Feng, Z., Li, Q., Yang, H.-Q., et al. (2013). Auxin controls seed dormancy through stimulation of abscisic acid signaling by inducing ARF-mediated ABI3 activation in Arabidopsis. *Proc. Natl. Acad. Sci. U.S.A.* 110, 15485–15490. doi: 10.1073/pnas.1304651110

Lohwasser, U., Röder, M. S., and Börner, A. (2005). QTL mapping of the domestication traits pre-harvest sprouting and dormancy in wheat (*Triticum aestivum* L.). *Euphytica* 143, 247–249. doi: 10.1016/j.cub.2016.01.063

Maeda, H., and Dudareva, N. (2012). The shikimate pathway and aromatic amino acid biosynthesis in plants. *Annu. Rev. Plant Biol.* 63, 73–105. doi: 10.1146/annurev-arplant-042811-105439

Maharjan, R. P., and Ferenci, T. (2003). Global metabolite analysis: the influence of extraction methodology on metabolome profiles of *Escherichia coli*. *Anal. Biochem.* 313, 145–154. doi: 10.1016/S0003-2697(02)00536-5

Manz, B., Müller, K., Kucera, B., Volke, F., and Leubner-Metzger, G. (2005). Water uptake and distribution in germinating tobacco seeds investigated in vivo by nuclear magnetic resonance imaging. *Plant Physiol.* 138, 1538–1551. doi: 10.1104/pp.105.061663

Mares, D. J., and Mrva, K. (2014). Wheat grain preharvest sprouting and late maturity alpha-amylase. *Planta* 240, 1167–1178. doi: 10.1007/s00425-014-2172-5

Martinez, S. A., Tuttle, K. M., Takebayashi, Y., Seo, M., Campbell, K. G., and Steber, C. M. (2016). The wheat ABA hypersensitive ERA8 mutant is associated with increased preharvest sprouting tolerance and altered hormone accumulation. *Euphytica* 212, 1–17. doi: 10.1007/s10681-016-1763-6

Matilla, A. J. (2000). Ethylene in seed formation and germination. *Seed Sci. Res.* 10, 111–126. doi: 10.1017/S096025850000012X

Milborrow, B. (2001). The pathway of biosynthesis of abscisic acid in vascular plants: a review of the present state of knowledge of ABA biosynthesis. *J. Exp. Bot.* 52, 1145–1164. doi: 10.1093/jxb/52.359.1145

Morgan, G. (2005). *Pre-harvest Sprouting in wheat. Texas Co-operative Extension E-336*. Available at: http://counties.agrilife.org/taylor/files/2015/01/E336-Pre-Harvest-Sprouting-in-Wheat.pdf

Nakabayashi, K., Okamoto, M., Koshiba, T., Kamiya, Y., and Nambara, E. (2005). Genome-wide profiling of stored mRNA in *Arabidopsis thaliana* seed germination: epigenetic and genetic regulation of transcription in seed. *Plant J.* 41, 697–709. doi: 10.1111/j.1365-313X.2005.02337.x

Nakata, P. A. (2003). Advances in our understanding of calcium oxalate crystal formation and function in plants. *Plant Sci.* 164, 901–909. doi: 10.1016/S0168-9452(03)00120-1

Nambara, E., and Nonogaki, H. (2012). Seed biology in the 21st century: perspectives and new directions. *Plant Cell Physiol.* 53, 1–4. doi: 10.1093/pcp/pcr184

Née, G., Xiang, Y., and Soppe, W. J. J. (2017). The release of dormancy, a wake-up call for seeds to germinate. *Curr. Opin. Plant Biol.* 35, 8–14. doi: 10.1016/j.pbi.2016.09.002

Nonogaki, H. (2014). Seed dormancy and germination-emerging mechanisms and new hypotheses. *Front. Plant Sci.* 5:233. doi: 10.3389/fpls.2014.00233

Nonogaki, H., Bassel, G. W., and Bewley, J. D. (2010). Germination-still a mystery. *Plant Sci.* 179, 574–581. doi: 10.1016/j.plantsci.2010.02.010

Nonogaki, M., and Nonogaki, H. (2017). Prevention of preharvest sprouting through hormone engineering and germination recovery by chemical biology. *Front. Plant Sci.* 8:90. doi: 10.3389/fpls.2017.00090

Nyachiro, J. M., Clarke, F. R., Depauw, R. M., Knox, R. E., and Armstrong, K. C. (2002). Temperature effects on seed germination and expression of seed dormancy in wheat. *Euphytica* 126, 123–127. doi: 10.1023/A:1019694800066

Oliver, M. J., Guo, L., Alexander, D. C., Ryals, J. A., Wone, B. W., and Cushman, J. C. (2011). A sister group contrast using untargeted global metabolomic analysis delineates the biochemical regulation underlying desiccation tolerance in *Sporobolus stapfianus*. *Plant Cell* 23, 1231–1248. doi: 10.1105/tpc.110.082800

Osmond, C. (1967). Acid metabolism in Atriplex I. Regulation of oxalate synthesis by the apparent excess cation absorption in leaf tissue. *Aust. J. Biol. Sci.* 20, 575–588. doi: 10.1071/BI9670575

Park, C. S., Heo, H. Y., Kang, M. S., Kim, H. S., Park, H. H., Park, J. C., et al. (2009). A new wheat variety, "Sukang" with good noodle quality, resistant to winter hardiness and pre-harvest sprouting. *Korean J. Breed. Sci.* 41, 44–50.

Park, C. S., Heo, H. Y., Kang, M. S., Lee, C. K., Park, K. G., Park, J. C., et al. (2008). A new white wheat variety, "Baegjoong" with high yield, good noodle quality and moderate to pre-harvest sprouting. *Korean J. Breed. Sci.* 40, 153–158.

Patti, G. J., Yanes, O., and Siuzdak, G. (2012). Metabolomics: the apogee of the omics trilogy. *Nat. Rev. Mol. Cell Biol.* 13, 263–269. doi: 10.1038/nrm3314

Pelagio-Flores, R., Ortíz-Castro, R., Méndez-Bravo, A., Macías-Rodríguez, L., and López-Bucio, J. (2011). Serotonin, a tryptophan-derived signal conserved in plants and animals, regulates root system architecture probably acting as a natural auxin inhibitor in *Arabidopsis thaliana*. *Plant Cell Physiol.* 52, 490–508. doi: 10.1093/pcp/pcr006

Penfield, S., Pinfield-Wells, H., and Graham, I. A. (2007). "Lipid metabolism in seed dormancy," in *Annual Plant Reviews: Seed Development, Dormancy and Germination*, Vol. 27, eds K. J. Bradford and H. Nonogaki (Oxford: Blackwell Publishing Ltd), 133–152. doi: 10.1002/9780470988848.ch6

Peterbauer, T., and Richter, A. (2001). Biochemistry and physiology of raffinose family oligosaccharides and galactosyl cyclitols in seeds. *Seed Sci. Res.* 11, 185–197.

Rai, V. K. (2002). Role of amino acids in plant responses to stresses. *Biol. Plant.* 45, 481–487. doi: 10.1023/A:1022308229759

Ramaih, S., Guedira, M., and Paulsen, G. M. (2003). Relationship of indoleacetic acid and tryptophan to dormancy and preharvest sprouting of wheat. *Funct. Plant Biol.* 30, 939–945. doi: 10.1071/FP03113

Ramalingam, A., Kudapa, H., Pazhamala, L. T., Weckwerth, W., and Varshney, R. K. (2015). Proteomics and metabolomics: two emerging areas for legume improvement. *Front. Plant Sci.* 6:1116. doi: 10.3389/fpls.2015.01116

Ray, D. K., Mueller, N. D., West, P. C., and Foley, J. A. (2013). Yield trends are insufficient to double global crop production by 2050. *PLoS ONE* 8:e66428. doi: 10.1371/journal.pone.0066428

Rohmer, M., Knani, M., Simonin, P., Sutter, B., and Sahm, H. (1993). Isoprenoid biosynthesis in bacteria: a novel pathway for the early steps leading to isopentenyl diphosphate. *Biochem. J.* 295, 517–524. doi: 10.1042/bj2950517

Rylski, I., Rappaport, L., and Pratt, H. K. (1974). Dual effects of ethylene on potato dormancy and sprout growth. *Plant Physiol.* 53, 658–662. doi: 10.1104/pp.53.4.658

Saito, K., and Matsuda, F. (2010). Metabolomics for functional genomics, systems biology, and biotechnology. *Annu. Rev. Plant Biol.* 61, 463–489. doi: 10.1146/annurev.arplant.043008.092035

Saldanha, A. J. (2004). Java treeview-extensible visualization of microarray data. *Bioinformatics* 20, 3246–3248. doi: 10.1093/bioinformatics/bth349

Salter, M., Knowles, R. G., and Pogson, C. I. (1986). Quantification of the importance of individual steps in the control of aromatic amino acid metabolism. *Biochem. J.* 234, 635–647. doi: 10.1042/bj2340635

Schaller, G. E. (2012). Ethylene and the regulation of plant development. *BMC Biol.* 10:9. doi: 10.1186/1741-7007-10-9

Seiler, C., Harshavardhan, V. T., Rajesh, K., Reddy, P. S., Strickert, M., Rolletschek, H., et al. (2011). ABA biosynthesis and degradation contributing to ABA homeostasis during barley seed development under control and terminal drought-stress conditions. *J. Exp. Bot.* 62, 2615–2632. doi: 10.1093/jxb/erq446

Shannon, P., Markiel, A., Ozier, O., Baliga, N. S., Wang, J. T., Ramage, D., et al. (2003). Cytoscape: a software environment for integrated models of biomolecular interaction networks. *Genome Res.* 13, 2498–2504. doi: 10.1101/gr.1239303

Shorinola, O., Bird, N., Simmonds, J., Berry, S., Henriksson, T., Jack, P., et al. (2016). The wheat Phs-A1 pre-harvest sprouting resistance locus delays the rate of seed dormancy loss and maps 0.3 cM distal to the PM19 genes in UK germplasm. *J. Exp. Bot.* 67, 4169–4178. doi: 10.1093/jxb/erw194

Shu, K., Meng, Y., Shuai, H., Liu, W., Du, J., Liu, J., et al. (2015). Dormancy and germination: how does the crop seed decide? *Plant Biol.* 17, 1104–1112. doi: 10.1111/plb.12356

Simsek, S., Ohm, J.-B., Lu, H., Rugg, M., Berzonsky, W., Alamri, M. S., et al. (2014). Effect of pre-harvest sprouting on physicochemical properties of starch in wheat. *Foods* 3, 194–207. doi: 10.3390/foods3020194

Singh, A. K., Knox, R. E., Clarke, J. M., Clarke, F. R., Singh, A., Depauw, R. M., et al. (2014). Genetics of pre-harvest sprouting resistance in a cross of Canadian adapted durum wheat genotypes. *Mol. Breed.* 33, 919–929. doi: 10.1007/s11032-013-0006-y

Sorrells, M., and Sherman, J. (2007). *Pre-harvest Sprouting*. Available at: http://maswheat.ucdavis.edu/education/PDF/facts/PHS.pdf [Accessed June 23, 2017].

Suttle, J. C. (2003). Auxin-induced sprout growth inhibition: role of endogenous ethylene. *Am. J. Potato Res.* 80, 303–309. doi: 10.1007/BF02854314

Thimm, O., Bläsing, O., Gibon, Y., Nagel, A., Meyer, S., Krüger, P., et al. (2004). Mapman: a user-driven tool to display genomics data sets onto diagrams of metabolic pathways and other biological processes. *Plant J.* 37, 914–939. doi: 10.1111/j.1365-313X.2004.02016.x

Thomason, W. E., Hughes, K. R., Griffey, C. A., Parrish, D. J., and Barbeau, W. E. (2009). "Understanding pre-harvest sprouting of wheat," in *Virginia Cooperative Extension*, (Blacksburg, VA: Virginia Tech).

Torada, A., Ikeguchi, S., and Koike, M. (2005). Mapping and validation of PCR-based markers associated with a major QTL for seed dormancy in wheat. *Euphytica* 143, 251–255. doi: 10.1007/s10681-005-7872-2

Torada, A., Koike, M., Ogawa, T., Takenouchi, Y., Tadamura, K., Wu, J., et al. (2016). A causal gene for seed dormancy on wheat chromosome 4A encodes a MAP kinase kinase. *Curr. Biol.* 26, 782–787. doi: 10.1016/j.cub.2016.01.063

Tripathi, P., Rabara, R. C., Reese, R. N., Miller, M. A., Rohila, J. S., Subramanian, S., et al. (2016). A toolbox of genes, proteins, metabolites and promoters for improving drought tolerance in soybean includes the metabolite coumestrol and stomatal development genes. *BMC Genomics* 17:1–22. doi: 10.1186/s12864-016-2420-0

Tuttle, K. M., Martinez, S. A., Schramm, E. C., Takebayashi, Y., Seo, M., and Steber, C. M. (2015). Grain dormancy loss is associated with changes in ABA and GA sensitivity and hormone accumulation in bread wheat, *Triticum aestivum* (L.). *Seed Sci. Res.* 25, 179–193. doi: 10.1017/S0960258515000057

Tzin, V., and Galili, G. (2010). New insights into the shikimate and aromatic amino acids biosynthesis pathways in plants. *Mol. Plant* 3, 956–972. doi: 10.1093/mp/ssq048

Verlotta, A., Liberatore, M. T., Cattivelli, L., and Trono, D. (2013). Secretory phospholipases A2 in durum wheat (*Triticum durum* Desf.): gene expression, enzymatic activity, and relation to drought stress adaptation. *Int. J. Mol. Sci.* 14, 5146–5169. doi: 10.3390/ijms14035146

Voothuluru, P., and Sharp, R. E. (2013). Apoplastic hydrogen peroxide in the growth zone of the maize primary root under water stress. I. Increased levels are specific to the apical region of growth maintenance. *J. Exp. Bot.* 64, 1223–1233. doi: 10.1093/jxb/ers277

Walker-Simmons, M. (1987). ABA levels and sensitivity in developing wheat embryos of sprouting resistant and susceptible cultivars. *Plant Physiol.* 84, 61–66. doi: 10.1104/pp.84.1.61

Wan, Y., Poole, R. L., Huttly, A. K., Toscano-Underwood, C., Feeney, K., Welham, S., et al. (2008). Transcriptome analysis of grain development in hexaploid wheat. *BMC Genomics* 9:121. doi: 10.1186/1471-2164-9-121

Wang, L., Ma, H., Song, L., Shu, Y., and Gu, W. (2012). Comparative proteomics analysis reveals the mechanism of pre-harvest seed deterioration of soybean under high temperature and humidity stress. *J. Proteomics* 75, 2109–2127. doi: 10.1016/j.jprot.2012.01.007

Weckwerth, W. (2010). Metabolomics: an integral technique in systems biology. *Bioanalysis* 2, 829–836. doi: 10.4155/bio.09.192

Wickham, H. (2016). *Ggplot2: Elegant Graphics for Data Analysis*. Berlin: Springer. doi: 10.1007/978-3-319-24277-4

Wilson, I. D., Barker, G. L. A., Lu, C., Coghill, J. A., Beswick, R. W., Lenton, J. R., et al. (2005). Alteration of the embryo transcriptome of hexaploid winter wheat (*Triticum aestivum* cv. Mercia) during maturation and germination. *Funct. Integr. Genomics* 5, 144–154. doi: 10.1007/s10142-005-0137-2

Xu, H.-W., Ji, X.-M., He, Z.-H., Shi, W.-P., Zhu, G.-H., Niu, J.-K., et al. (2006). Oxalate accumulation and regulation is independent of glycolate oxidase in rice leaves. *J. Exp. Bot.* 57, 1899–1908. doi: 10.1093/jxb/erj131

Yip, W.-K., and Yang, S. F. (1988). Cyanide metabolism in relation to ethylene production in plant tissues. *Plant Physiol.* 88, 473–476. doi: 10.1104/pp.88.2.473

Yip, W. K., and Yang, S.-F. (1998). Ethylene biosynthesis in relation to cyanide metabolism. *Bot. Bull. Acad. Sin.* 39, 1–7.

Yu, P., Hu, C., Meehan, E. J., and Chen, L. (2007). X-ray crystal structure and antioxidant activity of salidroside, a phenylethanoid glycoside. *Chem. Biodivers.* 4, 508–513. doi: 10.1002/cbdv.200790043

Yu, Y., Guo, G., Lv, D., Hu, Y., Li, J., Li, X., et al. (2014). Transcriptome analysis during seed germination of elite Chinese bread wheat cultivar Jimai 20. *BMC Plant Biol.* 14:20. doi: 10.1186/1471-2229-14-20

Zanetti, S., Winzeler, M., Keller, M., Keller, B., and Messmer, M. (2000). Genetic analysis of pre-harvest sprouting resistance in a wheat x spelt cross. *Crop Sci.* 40, 1406–1417. doi: 10.2135/cropsci2000.4051406x

Zhang, Y., Miao, X., Xia, X., and He, Z. (2014). Cloning of seed dormancy genes (TaSdr) associated with tolerance to pre-harvest sprouting in common wheat and development of a functional marker. *Theor. Appl. Genet.* 127, 855–866. doi: 10.1007/s00122-014-2262-6

Zhou, K., Su, L., and Yu, L. (2004). Phytochemicals and antioxidant properties in wheat bran. *J. Agric. Food Chem.* 52, 6108–6114. doi: 10.1021/jf049214g

Zhou, Y., Tang, H., Cheng, M., Dankwa, K., Chen, Z., Li, Z., et al. (2017). Genome-wide association study for pre-harvest sprouting resistance in a large germplasm collection of Chinese wheat landraces. *Front. Plant Sci.* 8:401. doi: 10.3389/fpls.2017.00401

Conflict of Interest Statement: The authors declare that the research was conducted in the absence of any commercial or financial relationships that could be construed as a potential conflict of interest.

frontiers in Plant Science

REVIEW
published: 15 June 2018
doi: 10.3389/fpls.2018.00811

Pre-harvest Sprouting and Grain Dormancy in *Sorghum bicolor*: What Have We Learned?

Roberto L. Benech-Arnold[1,2] and María V. Rodríguez[2,3]*

[1] *Cátedra de Cultivos Industriales, Departamento de Producción Vegetal, Facultad de Agronomía, Universidad de Buenos Aires, Buenos Aires, Argentina,* [2] *Instituto de Fisiología y Ecología Vinculado a la Agricultura, Consejo Nacional de Investigaciones Científicas y Técnicas, Facultad de Agronomía, Universidad de Buenos Aires, Buenos Aires, Argentina,* [3] *Cátedra de Fisiología Vegetal, Departamento de Biología Aplicada y Alimentos, Facultad de Agronomía, Universidad de Buenos Aires, Buenos Aires, Argentina*

The possibility of obtaining sorghum grains with quality to match the standards for a diversity of end-uses is frequently hampered by the susceptibility to pre-harvest sprouting (PHS) displayed by many elite genotypes. For these reasons, obtaining resistance to PHS is considered in sorghum breeding programs, particularly when the crop is expected to approach harvest maturity under rainy or damp conditions prevalence. As in other cereals, the primary cause for sprouting susceptibility is a low dormancy prior to crop harvest; in consequence, most research has focused in understanding the mechanisms through which the duration of dormancy is differentially controlled in genotypes with contrasting sprouting behavior. With this aim two tanninless, red-grained inbred lines were used as a model system: IS9530 (sprouting resistant) and Redland B2 (sprouting susceptible). Redland B2 grains are able to germinate well before reaching physiological maturity (PM) while IS9530 ones can start to germinate at 40–45 days after pollination, well after PM. Results show that the anticipated dormancy loss displayed by Redland B2 grains is related reduced embryo sensitivity to abscisic acid (ABA) and increased levels of GA upon imbibition. In turn, transcriptional data showed that ABA signal transduction is impaired in Redland B2, which appears to have an impact on GA catabolism, thus affecting the overall GA/ABA balance that regulates germination. QTL analyses were conducted to test whether previous candidate genes were located in a dormancy QTL, but also to identify new genes involved in dormancy. These analyses yielded several dormancy QTL and one of them located in chromosome 9 (qGI-9) was consistently detected even across environments. Fine mapping is already in progress to narrow down the number of candidate genes in qGI-9.

Keywords: *Sorghum bicolor*, grain sorghum, pre-harvest sprouting, seed dormancy, abscisic acid, dormancy QTL

OPEN ACCESS

Edited by:
Hiroyuki Nonogaki,
Oregon State University,
United States

Reviewed by:
Shingo Nakamura,
Institute of Crop Science (NARO),
Japan
Jirui Wang,
Sichuan Agricultural University, China

****Correspondence:***
Roberto L. Benech-Arnold
benech@agro.uba.ar

Specialty section:
This article was submitted to Plant Breeding, a section of the journal Frontiers in Plant Science

Received: *18 April 2018*
Accepted: *25 May 2018*
Published: *15 June 2018*

Citation:
Benech-Arnold RL and Rodríguez MV (2018) Pre-harvest Sprouting and Grain Dormancy in Sorghum bicolor: What Have We Learned? Front. Plant Sci. 9:811. doi: 10.3389/fpls.2018.00811

INTRODUCTION

Grain sorghum [*Sorghum bicolor* (L.) Moench] is a grass species cultivated for its grain which is used for feeding both humans and animals. Also known as *durra*, *jowari*, or *milo*, sorghum can grow under harsher conditions and therefore may be better than maize or sugarcane in some environments. Sorghum originated in Northern Africa but is now cultivated widely in tropical

and subtropical environments to the point that it has become the fifth most important cereal of the world after rice, wheat, maize, and barley. Sorghum grains for human consumption are used to make flat breads and beverages and also for malting and brewery. As in many other crops, the sorghum grain is also required to perform as the propagule for a new crop. The possibility of obtaining grains with quality to match the standards for these end-uses is frequently hampered by the susceptibility to pre-harvest sprouting (PHS) displayed by many elite genotypes. Indeed, untimely germination in the mother plant promotes reserve mobilization and/or leads to either immediate loss of seed viability or to a large reduction in seed longevity (Del Fueyo et al., 2003). In addition, sorghum sprouts accumulate toxic amounts of cyanide (Ikediobi et al., 1988). For these reasons, obtaining resistance to PHS is one of the main objectives in sorghum breeding programs, particularly when the crop is expected to approach harvest maturity under rainy or damp conditions prevalence. As in other cereals, the primary cause for sprouting susceptibility is a low dormancy prior to crop harvest (see Rodríguez et al., 2015). Consequently, efforts have been directed to understand the mechanisms through which the duration of dormancy is differentially controlled in genotypes with contrasting sprouting behavior. In this review paper, we discuss the current understanding of the mechanisms that impose dormancy to the sorghum grain, and mention on-going work directed toward breeding for PHS tolerance.

WHERE IS DORMANCY LOCATED IN THE SORGHUM GRAIN?

The sorghum grain is a caryopsis (Waniska and Rooney, 2002). Depending on the genotype, this caryopsis may be "naked" or covered to different extents by the hulls (consisting of the glumellae – lemma and palea – and the glumes). The grain comprises an embryo, reserve tissue (corneous and starchy endosperm, surrounded by the aleurone layer), and the seed coat (nucellus and testa) fused to the pericarp. As in other cereals, the external structures of the sorghum grain, including testa, pericarp, and hulls, can impose dormancy to the underlying embryo. These structures may accumulate various phenolic compounds, such as phenolic acids, coumarins, flavonoids, and tannins (Glennie, 1981; Dykes et al., 2009). Increased pigmentation has been frequently associated with deeper dormancy in cereals like rice, wheat, barley, and maize (as discussed in Rodríguez et al., 2015). Flavonoid compounds may have an inhibitory effect *per se*, as chemically active inhibitors of germination, or through an effect on permeability to gas exchange in the imbibed seed (as discussed in Rodríguez et al., 2015). Nevertheless, genetic studies have usually found that pigmentation-related loci that co-locate with loci for PHS or germination traits correspond with transcriptional regulators rather than structural genes involved in pigment biosynthesis. Red colored grains accumulate phlobaphenes or anthocyanins in the pericarp. Regulation of phlobaphene synthesis is exerted by R2R3-MYB transcriptional factors, as encoded by the *P1* gene in maize and *Yellow seed1* in sorghum (Kambal and Bate-Smith, 1976; Boddu et al., 2005; Ibraheem et al., 2015), whereas regulation of anthocyanin synthesis is controlled by transcriptional complexes consisting of R2R3-MYB, basic-helix-loop-helix (bHLH), and WD-repeat (WDR) proteins (MBW complex; Liu et al., 2015). Mutations in some of these genes can affect dormancy through pleiotropic effects on different pathways. In weedy red rice, SD7-1 (a BHLH-type regulator) activates simultaneously flavonoid and abscisic acid (ABA) synthesis genes in the developing seed, conferring red color and deep dormancy (Gu et al., 2011). Maize VIVIPAROUS-1 (VP1) is required for ABA signal transduction in the developing grain, and also regulates the expression of *C1* (encoding an R2R3 MYB factor) that promotes anthocyanin synthesis in the aleurone (McCarty et al., 1989). Loss-of-function alleles of *Tamyb10* (red pericarp, R-1 loci) in wheat and *Hvmyb10* in barley fail to accumulate proanthocyanidins in the testa and contribute to reduce grain sensitivity to ABA and dormancy (Himi et al., 2002; Himi and Noda, 2005). Sorghum grains can accumulate variable levels of flavonoids, including phlobaphenes in the outer pericarp and proanthocyanidines (condensed tannins) in the underlying testa (Cheng et al., 2009). Accumulation of tannins in the testa is independent of pericarp color and is controlled by Tannin1, a WD40-type transcriptional regulator (Wu et al., 2012). In a study with 42 sorghum hybrids by Harris and Burns (1970), a negative correlation between germination index and astringent tannin content was observed. Also, among tannin-less sorghums, red grained varieties are usually more resistant to PHS than genotypes with yellow and white grains, although no strict correlation has been demonstrated so far. A direct role for *Tannin1* and *Yellow seed1* in dormancy remains to be tested. Because condensed tannins are considered to reduce the nutritional value of the sorghum grain, research on PHS tolerance has focused on tannin-less sorghum varieties.

As reported for other cereals, the inability of the sorghum grains to germinate at harvest or before [*i.e.*, from 20 days after pollination (DAP) onward] is due to a complex interplay between coat- and embryo-based dormancy, with the former playing a major role in the overall contribution to grain dormancy. Removal of the covering structures (i.e., pericarp, testa and endosperm) results in a reduced expression of dormancy at a wide range of temperatures even with embryos isolated as early as 15 DAP (Benech-Arnold et al., 1991; Steinbach et al., 1995). However, different responsiveness to inhibitory factors such as ABA, as well as different accumulation of promoting factors such as gibberellins (GAs), support that embryo-related factors are relevant in the expression of different levels of coat-imposed dormancy.

THE SYSTEM REDLAND B2 – IS9530

During the last 25 years, studies on the physiological and genetic bases of PHS resistance in sorghum were conducted using two inbred, red-grained lines as a model system: IS9530, a tall, tannin-less line derived from ICRISAT breeding program, and Redland B2 (originally registered as Redlan, or BTx378), an also tannin-less, three-dwarf derivative line, resulting from the

US Sorghum Conversion Program (Stephens et al., 1967). During this program, sorghums were substituted with several height and maturity genes to obtain short, early forms in temperate zones. Despite their different background, both IS9530 and RedlandB2 display similar phenology at our latitude under sowing dates taking place between the last week of November and the first week of December. The sprouting behavior of these two inbred lines, however, is contrasting: the Redland B2 line is susceptible to PHS, while the IS9530 one is resistant. The nature of this contrasting behavior relies on the anticipated exit from dormancy of the Redland B2 grains which are able to germinate well before reaching physiological maturity (PM); IS9530 grains, in contrast, can start to germinate at 40–45 DAP, well after PM (**Figure 1**; Steinbach et al., 1995, 1997). Isolated embryos from both lines can germinate very quickly even before 20 DAP (**Figure 1**) demonstrating that the different capacity to germinate during development is the result of dormancy differentially imposed by the presence of the seed coat tissues. The pattern of dormancy release during grain filling normally shows two phases in Redland B2 grains: an early one which is not observed in IS9530 grains, starting around 15–20 DAP and reaching a plateau prior to PM (30–35 DAP), and a second one starting after PM and coinciding with the beginning of exit from dormancy in IS9530 grains (**Figure 1**). Susceptibility to PHS in Redland B2, then, is related to precocious grain dormancy loss, while resistance in IS9530 can be associated to a more persistent dormancy (Steinbach et al., 1995). It is well known, as in many other species, that the expression of dormancy in sorghum depends on the incubation temperature: dormancy is very much expressed at low incubation temperatures (i.e., 15–20°C), while it is barely expressed at high temperatures (i.e., 30–35°C; Benech-Arnold et al., 2003). For these reasons, differences in the sprouting behavior between these two lines are exacerbated when damp conditions prior to harvest are combined with mild ambient temperatures (20°C or below) that favor the expression of dormancy.

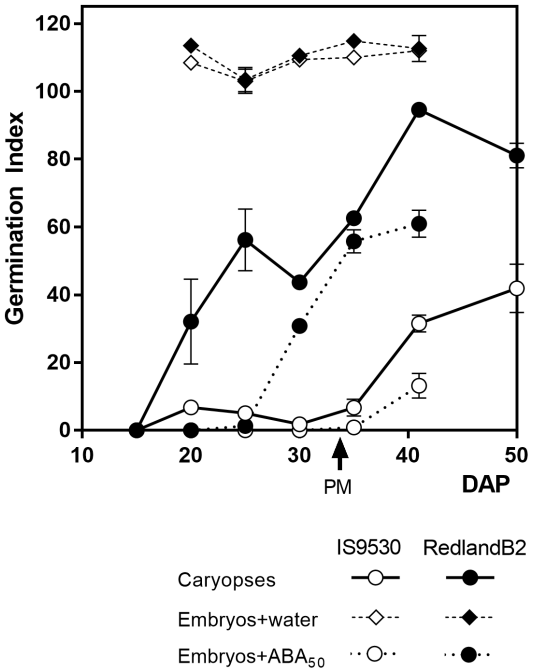

FIGURE 1 | Germination index for sorghum lines IS9530 and RedlandB2. Caryopses were harvested on different days after pollination (DAP) and incubated for 12 days in water at 25°C (circles with solid lines). Embryos were dissected and incubated at 25°C in distilled water (diamonds) or 50 μM ABA (circles with dashed lines). Each data point is the mean value of two biological replicates (i.e., field plots) each one assessed in triplicate. Bars indicate SE of mean. Time of physiological maturity is indicated with an arrow. Experimental details are described in Rodríguez et al. (2009). Adapted from data first published by Rodríguez et al. (2009) and reproduced by permission of Oxford University Press (doi: 10.1093/aob/mcp184).

HORMONAL REGULATION OF DORMANCY IN THE DEVELOPING SORGHUM GRAIN

A crucial role for ABA in the imposition of physiological dormancy in the developing seed has been demonstrated in many species (Finkelstein et al., 2002). Mutant seeds of *Arabidopsis* and maize that are ABA-deficient or ABA-insensitive germinate precociously (Robichaud et al., 1980; Karssen et al., 1983). No sorghum mutants for ABA synthesis or metabolism have been reported, but application of the ABA-synthesis inhibitor fluridone during early seed development accelerated dormancy release in dormant IS9530 sorghum line (Steinbach et al., 1997), as expected from earlier experiments with fluridone that produced vivipary in maize (Fong et al., 1983). However, embryos from the more dormant line IS9530 were found to have a similar ABA content throughout development to embryos from the less dormant line Redland B2 (Steinbach et al., 1995). Embryonic content of ABA decreased gradually during phase two of imbibition, but this decrease was similar for both lines and did not relate with their germination response (Rodríguez et al., 2009). The seed coats were found to delay ABA leakage from the embryo to the medium, as ABA content decreased rapidly when isolated embryos were incubated in water (Gualano et al., 2007). This is due to the fact that ABA easily leaks from the naked embryo into the incubation medium, and suggests that the covers impose dormancy to the embryo, at least in part, by reducing ABA leakage. Instead, suppression of germination of Redland B2 embryos required ABA concentrations 10-fold higher than those required for inhibiting germination of IS 9530 embryos; moreover, this difference was maintained throughout the whole developmental period and even beyond PM (**Figure 1**; Steinbach et al., 1995). These results confirmed that the observed differences in responsiveness to ABA are due to functional differences in the ABA signaling pathway and not in embryonic ABA concentration (Gualano et al., 2007).

It has been known for a long time that GAs promote germination of dormant seeds in many species, antagonizing the inhibitory effect of ABA. Both ABA and GA also act antagonistically in the inception of dormancy during early development. Application of paclobutrazol, a GA biosynthesis inhibitor to young sorghum panicles, reduced GA content during development and delayed dormancy release for several weeks

in Redland B2 grains (Steinbach et al., 1997). Moreover, the incubation of immature IS9530 grains coming from fluridone-treated panicles, in the presence of GA_{4+7}, resulted in a pattern of exit from dormancy throughout development that resembled that of Redland B2 grains (Steinbach et al., 1997). Indeed, the first phase of dormancy release displayed by Redland B2 grains but not by IS 9530 ones (**Figure 1**), was mimicked by combining low ABA content with exogenous GA supplementation. These results suggested that the anticipated dormancy release displayed by Redland B2 grains was not only related to a low embryo responsiveness to ABA, but also to a high GA content or, alternatively, to a high capacity to synthesize GA *de novo* upon imbibition. Similar to observations of ABA content in developing grains of these two genotypes, no correlation was found between natural endogenous GA content and dormancy (Benech-Arnold et al., 2000). Instead, analysis of GA content in these same sorghum lines revealed that, in Redland B2, but not in IS 9530, GA_4 content increased during imbibition and before completion of germination (Pérez-Flores et al., 2003). This increase in GA_4 was directly related to a reduction in catabolite GA_{34} (Rodríguez et al., 2012) suggesting that GA catabolism has an active role in regulating GA_4 levels. Taken together, these results suggest that the anticipated dormancy loss displayed by Redland B2 grains is related to a reduced embryo sensitivity to ABA and increased levels of GA upon imbibition. Therefore, both GA metabolism (in particular, GA catabolism) and ABA signaling appeared as the main components of the ABA/GA balance regulating the germination response in developing grains of both lines. A candidate gene approach was followed to assess and identify potential regulatory sites at the transcriptional level that would lead to the observed differences at the physiological level.

EXPRESSION OF SEVERAL ABA SIGNALING GENES AND A GA CATABOLISM GENE IS UPREGULATED IN IMBIBED, DORMANT IS9530 GRAINS BEFORE – BUT NOT AFTER – PM

Expression analyses were conducted for several candidate genes involved in ABA signaling and GA metabolism (Rodríguez et al., 2009, 2012). Orthologous sequences for the candidate genes in sorghum were obtained by searching the sorghum genome published by Paterson et al. (2009). Consistently with differences in sensitivity to ABA, a transient and coordinated up-regulation of *SbABI3/VP1*, *SbABI4*, *SbABI5*, and *SbPKABA1* (together with SbABI5 protein levels) occurred in imbibed grains of IS9530, but not in RedlandB2. This "induction" pattern in IS9530 was observed in immature grains (30 DAP), but after PM expression of these genes decreased rapidly and similarly in both lines (Rodríguez et al., 2009). This synchronous expression of main ABA signaling genes is in agreement with published results in Arabidopsis, where extensive cross-regulation has been demonstrated among VP1/ABI3, ABI4, and ABI5 (Lopez-Molina et al., 2002; Reeves et al., 2011).

Transcriptional analysis of several sorghum genes encoding putative GA synthesis enzymes (*SbEKO, SbEKAH, SbGA20ox2, SbGA20ox3*, and *SbGA3ox1*) showed, on the other hand, a transient increase in dormant grains (IS9530) during the first 2–3 days of grain imbibition, which did not occur in Redland B2 (Rodríguez et al., 2012). This evidence appears to be in contradiction with changes in GA_4 levels in both lines. However, simultaneously with this enhanced expression of GA synthesis genes in dormant IS9530 grains, expression of GA inactivation genes *SbGA 2-oxidase1* and *Sb GA 2-oxidase3 (SbGA2ox1 and SbGA2ox3)* was also increased This observation, together with a negative association between embryo content of active GA_4 and its corresponding catabolite GA_{34}, supported the notion that GA_4 levels remain low in dormant IS9530 grains as a result of a prominent catabolic activity by GA2-oxidases, which, in turn, is reduced in RedlandB2. On the other hand, incubation of dormant grains in 100 μM GA_3 promoted germination but did not reduce the expression of most key GA synthesis genes, ruling out the idea of a negative feedback regulatory mechanism driven by active GAs. In addition, and in contrast to other reports which show a feed-forward mechanism affecting expression of *GA2-oxidase* genes by active GA levels in Arabidopsis (Ogawa et al., 2003; Rieu et al., 2008), expression of sorghum *SbGA2-ox1* and *SbGA2-ox3* was downregulated by exogenously applied GA_3 (Rodríguez et al., 2012). The similar expression profiles obtained for *SbABI4*, *SbABI5* (together with SbABI5 protein abundance), and *SbGA2-oxidase* genes suggested the existence of a possible functional link between both pathways. This, together with the presence of an ABA-responsive complex (ABRC) conformed by *cis*-regulatory elements related to ABA (ABRE, RY repeat, and CE) in the 5′ regulatory region of *GA-2ox3*, suggested a possible interaction between ABA signaling pathway and GA catabolism (Rodríguez et al., 2009, 2012). This interaction was tested by Cantoro et al. (2013). In this work, SbABI4 and SbABI5 proteins were shown to interact *in vitro* with a fragment of the *SbGA2-ox3* promoter containing the above-mentioned ABRC. Both transcription factors were able to bind the promoter, although not simultaneously, suggesting that they might compete for the same *cis*-acting regulatory sequences. A biological role for these interactions in the expression of dormancy of sorghum grains was proposed: either SbABI4 and/or SbABI5 activate transcription of the *SbGA2-oxidase3* gene *in vivo* and promote SbGA2-oxidase3 protein accumulation; this would result in active degradation of GA_4, thus preventing germination of dormant grains. A comparative analysis of the 5′-regulatory region of *GA2-oxidase* genes from both monocots and dicots showed that *GA2-oxidase* genes with an ABRC in their promoter region are exclusive to a conserved sub-group found in monocots (sub-group M3, according to Cantoro et al., 2016) to which *SbGA2-ox3* belongs. Conservation of the ABRC in closely related GA2-oxidases from *Brachypodium distachyon* and rice suggests that these species might share the same regulatory mechanism as proposed for grain sorghum.

In summary, physiological evidence (showing similar endogenous ABA levels but contrasting response to exogenous ABA) and transcriptional data (showing different expression levels of ABA signaling genes but also of ABI5 protein levels)

support that ABA signal transduction is impaired in Redland B2. Reduced ABA signaling appears to have an impact on GA catabolism, thus affecting the overall GA/ABA balance that regulates germination.

GENETIC APPROACH: MAPPING OF "OLD" CANDIDATE AND "NEW" DORMANCY GENES

Quantitative trait loci (QTL) analyses were conducted to investigate the genetic bases of the contrasting dormancy phenotypes in both sorghum inbred lines IS 9530 and Redland B2. This approach would allow testing whether previous candidate genes are located in a dormancy QTL, but also would lead to the identification of new genes involved in dormancy. The first genetic study was done by Lijavetzky et al. (2000) with an F_2 mapping population derived from a cross between IS9530 x Redland B2. These authors used RFLP, RAPDs, and AFLP markers, and reported a putative association between *SbVP1* and a dormancy QTL in likage group "E" (Carrari et al., 2003). To further confirm and expand these results, a new mapping population was obtained from the same sorghum parents, the genetic map was constructed using SSR markers, and phenotypic data were obtained at 34 (before PM) and 45 (after PM) DAP (Cantoro et al., 2016). In this work, six QTLs were identified for seed dormancy (**Figure 2**) in 42 DAP grains (qGI-1, qGI-3, qGI-4, qGI-6, qGI-7, and qGI-9) which were successfully anchored on the *S. bicolor* genome assembly v2.1 (Paterson et al., 2009) through QTL flanking SSR physical position. The number of genes within these intervals ranged from 75 (*qGI-9*) to 547 (*qGI-3*). No epistasis was detected for the identified QTL. Interestingly, *SbABI3/VP1* located within qGI-3, which makes it a good candidate to be the causal gene for this QTL. Allelic variants for *SbVP1* were found to exist in RedlandB2 and IS9530 (Carrari et al., 2001). The sorghum *VP1* gene encodes a 699 amino acid predicted protein, and sequences

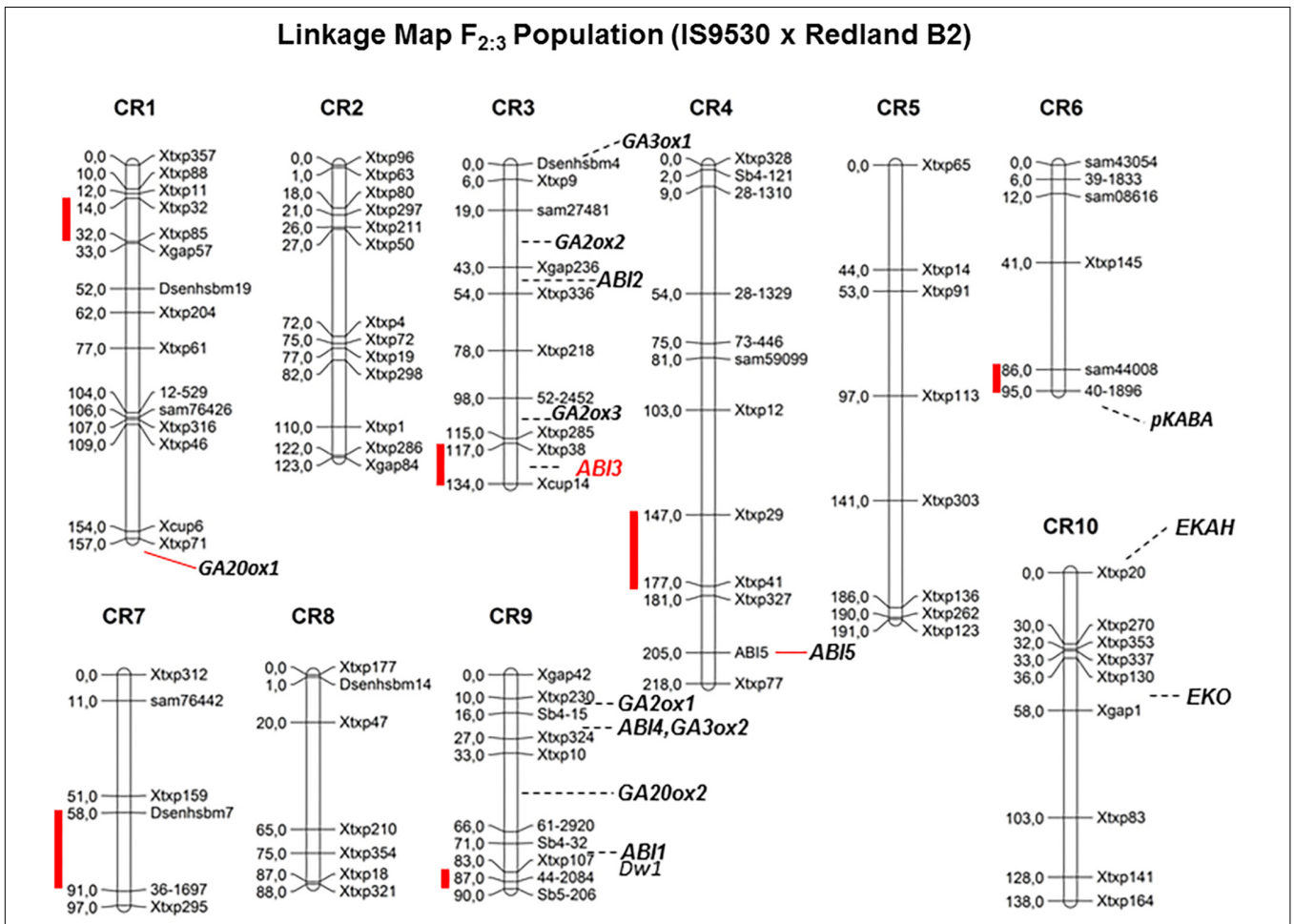

FIGURE 2 | Genetic linkage map for F2 grain sorghum population, derived from IS9530 and RedlandB2 inbred lines, built with 96 SSRs segregation analysis (Adapted from Cantoro et al. (2016), by permission from Springer, Euphytica, ®2016). Red bars indicate position of dormancy related QTL as reported by Cantoro et al. (2016). Marker names are shown on the right side of each chromosome and genetic distances between markers (in cM) are indicated on the left side. Positions of *Dwarf1*, and ABA signaling and GA metabolism candidate genes are shown.

obtained for RedlandB2 and IS9530 differ in two residues at positions 341 (Gly/Cys, within the repression domain) and 448 (Pro/Ser; Carrari et al., 2001). These replacements might result in different biological functions, particularly the one located in the repression domain (Hoecker et al., 1995). Interestingly, in Arabidopsis seeds of *abi3* mutants, ABI5 expression was greatly reduced (Lopez-Molina et al., 2002), while ectopic expression of maize *VP1* in Arabidopsis *abi3* background inhibited *ABI1/ABI2* induction by ABA (Suzuki et al., 2003). An altered functionality of Redland B2 *SbVP1* allele appears as a possible cause for the altered expression of other ABA signaling genes as observed in imbibed, developing grains. Future experiments will test whether sorghum allelic variants for *SbVP1* have different activation/repression activity, together with fine mapping for this QTL. In parallel, synteny analysis of all detected QTL was also carried out and, besides *VP1*, no previous dormancy-related *loci* reported in other cereals were found to locate with sorghum QTLs reported by our group (Cantoro et al., 2016).

Ongoing work relies on a recombinant inbred line (RIL) population derived from the F_3 mapping population used by Cantoro et al. (2016). This population was phenotyped recently for several dormancy-related traits, including sprouting in the field which occurred naturally in 2016. A new set of SNP markers was used, and due to an unbalanced coverage in several chromosome regions, QTL detection was limited to chromosome 9. Using two-year phenotypic data obtained before and after PM, qGI-9 (as reported by Cantoro et al., 2016) was identified again in this new RIL population. Improved marker coverage is expected to allow detection of previous dormancy QTLs including qGI-3. Interestingly, the region containing the dormancy *locus* in qGI-9 is very close to *DWARF-1*, a gene regulating plant stature and recently cloned by two groups (Hilley et al., 2016; Yamaguchi et al., 2016). Sorghum DW1 protein positively regulates brassinosteroid (BR) signaling and plant stature by inhibiting a negative regulator of BR signaling, BIN2 (Hirano et al., 2017). The genomic region in chromosome 9 carrying the loss-of-function dw1 allele has been introduced into many elite lines during the Sorghum Conversion Program to reduce plant stature, including RedlandB2 and BTx623. As the Standard Yellow Milo background (where the *dw1* mutation originated; Quinby and Karper, 1961) displays very low dormancy prior to harvest, it is likely that a low-dormancy allele was introduced together with the *dw1* allele during breeding for reduced height. Low heterozygocity along this region of chromosome 9 in a large GWAS panel (Morris et al., 2013) suggests that, if both *dw1* and the qGI-9 causal gene are linked, then many elite parental lines harbor this low dormancy allele. Current work involves the obtention of NILs for fine mapping of both qGI-3 and qGI-9 and genotyping by sequencing (GBS) of parental lines. Both strategies are aimed to narrow down the number of candidate genes in these regions and identify DNA polymorphisms in these genes. Future studies including transcriptomic analysis of developing grains for both parental lines are expected to help identify potential transcriptional variants (due to polymorphisms in the promoter region) among the candidate genes within each QTL. Strategies based on the combination of genetic and genomic tools have accelerated the process leading to identify a solid, causal gene for a QTL. An example of this is the identification of MOTHER OF FT (MFT) as the causal gene of a dormancy QTL (QPhs.ocs-3A.1) in wheat by Nakamura et al. (2011). Confirmation of the role of the proposed candidate genes for qGI-9 and qGI-3 in the dormancy phenotype will require functional testing either in sorghum or in other model organisms.

AUTHOR CONTRIBUTIONS

All authors listed above made a substantial, direct and intellectual contribution to this work. RB-A and MR discussed the contents and wrote the first version of the manuscript. MR corrected the revised version. Both authors read and approved the final version for publication.

FUNDING

This work was financed with grant no. PICT 2013 1357 from the Agencia Nacional de Promoción Científica y Tecnológica, Argentina.

REFERENCES

Benech-Arnold, R. L., Enciso, S., Sánchez, R. A., Carrari, F., Pérez-Flores, L., Iusem, N., et al. (2000). "Involvement of ABA and GAs in the regulation of dormancy in developing sorghum seeds," in *Seed Biology: Advances and Applications*, eds M. Black, K. J. Bradford, and J. V. ázquez-Ramos (Wallingford: CABI Publishing), 101–111. doi: 10.1079/9780851994048.0101

Benech-Arnold, R. L., Fenner, M., and Edwards, P. J. (1991). Changes in germinability, ABA levels and ABA embryonic sensitivity in developing seeds of *Sorghum bicolor* induced by water stress under grain filling. *New Phytol.* 118, 339–347. doi: 10.1111/j.1469-8137.1991.tb00986.x

Benech-Arnold, R. L., Rodriguez, M. V., Sánchez, R. A., Carrari, F., Pérez-Flores, L. J., Osuna-Fernández, H. R., et al. (2003). "Physiological and molecular aspects of the control of dormancy and germination in developing sorghum caryopses," in *The Biology of Seeds: Recent Research Advances*, eds G. Nicolás, K. J. Bradford, D. Come, and H. W. Pritchard (Oxon: CAB International), 11–23.

Boddu, J., Svabek, C., Ibraheem, F., Jones, A. D., and Chopra, S. (2005). Characterization of a deletion allele of a sorghum Myb gene, yellow seed1 showing loss of 3-deoxyflavonoids. *Plant Sci.* 169, 542–552. doi: 10.1016/j.plantsci.2005.05.007

Cantoro, R., Crocco, C. D., Benech-Arnold, R. L., and Rodríguez, M. V. (2013). *In vitro* binding of *Sorghum bicolor* transcription factors ABI4 and ABI5 to a conserved region of a GA 2-*OXIDASE* promoter: possible role of this interaction in the expression of seed dormancy. *J. Exp. Bot.* 64, 5721–5735. doi: 10.1093/jxb/ert347

Cantoro, R., Fernández, L. G., Cervigni, G. D. L., Rodríguez, M. V., Gieco, J. O., Paniego, N., et al. (2016). Seed dormancy QTL identification across a *Sorghum bicolor* segregating population. *Euphytica* 211, 41–56. doi: 10.1007/s10681-016-1717-z

Carrari, D., Benech-Arnold, R. L., Osuna-Fernández, R., Hopp, E., Sánchez, R., Iusem, N., et al. (2003). Genetic mapping of the *Sorghum bicolor* VP1 gene and its relationship with pre-harvest sprouting resistance. *Genome* 46, 253–258. doi: 10.1139/g02-129

Carrari, F., Perez-Flores, L. J., Lijavetzky, D., Enciso, S., Sánchez, R. A., Benech-Arnold, R. L., et al. (2001). Cloning and expression of a sorghum gene with homology to maize VP1. Its potential involvement in pre-harvest

sprouting resistance. *Plant Mol. Biol.* 45, 631–640. doi: 10.1023/A:1010648420669

Cheng, S., Sun, Y., and Halgreen, L. (2009). The relationships of sorghum kernel pericarp and testa characteristics with tannin content. *Asian J. Crop Sci.* 1, 1–5.

Del Fueyo, P. A., Sánchez, R. A., and Benech-Arnold, R. L. (2003). Seed longevity in two sorghum varieties with contrasting dormancy level prior to harvest. *Seed Sci. Technol.* 31, 639–650. doi: 10.15258/sst.2003.31.3.13

Dykes, L., Seitz, L. M., Rooney, W. L., and Rooney, L. W. (2009). Flavonoid composition of red sorghum genotypes. *Food Chem.* 116, 313–317. doi: 10.1016/j.foodchem.2011.03.020

Finkelstein, R. R., Gampala, S. S. L., and Rock, C. D. (2002). Abscisic acid signaling in seeds and seedlings. *Plant Cell* 14(Suppl. 1), S15–S45. doi: 10.1105/tpc.010441

Fong, F., Smith, J. D., and Koehler, D. E. (1983). Early events in maize seed development. *Plant Physiol.* 73, 899–901. doi: 10.1104/pp.73.4.899

Glennie, C. W. (1981). Preharvest changes in polyphenols, peroxidase, and polyphenol oxidase in Sorghum grain. *J. Agric. Food Chem.* 29, 33–36. doi: 10.1021/jf00103a009

Gu, X. Y., Foley, M. E., Horvath, D. P., Anderson, J. V., Feng, J., Zhang, L., et al. (2011). Association between seed dormancy and pericarp color is controlled by a pleiotropic gene that regulates abscisic acid and flavonoid synthesis in weedy red rice. *Genetics* 189, 1515–1524. doi: 10.1534/genetics.111.131169

Gualano, N., Carrari, F., Rodríguez, M. V., Pérez-Flores, L., Sánchez, R. A., Iusem, N. D., et al. (2007). Reduced embryo sensitivity to ABA in sprouting susceptible sorghum (*Sorghum bicolor*) variety is associated with an altered ABA signalling. *Seed Sci. Res.* 17, 81–90. doi: 10.1017/S0960258507708115

Harris, H. B., and Burns, R. E. (1970). Influence of tannin content on pre-harvest seed germination in sorghum. *Agronomy J.* 62, 835–836. doi: 10.2134/agronj1970.00021962006200060051x

Hilley, J., Truong, S., Olson, S., Morishige, D., and Mullet, J. (2016). Identification of D*w1*, a regulator of sorghum stem internode length. *PLoS One* 11:e0151271. doi: 10.1371/journal.pone.0151271

Himi, E., Mares, D. J., Yanagisawa, A., and Noda, K. (2002). Effect of grain color gene (R) on grain dormancy and sensitivity of the embryo to abscisic acid (ABA) in wheat. *J. Exp. Bot.* 3, 1569–1574. doi: 10.1093/jxb/erf005

Himi, E., and Noda, K. (2005). Red grain color gene (R) of wheat is a Myb-type transcription factor. *Euphytica* 143, 239–242. doi: 10.1007/s10681-005-7854-4

Hirano, K., Kawamura, M., Araki-Nakamura, S., Fujimoto, H., Ohmae-Shinohara, K., Yamaguchi, M., et al. (2017). Sorghum DW1 positively regulates brassinosteroid signaling by inhibiting the nuclear localization of BRASSINOSTEROID INSENSITIVE 2. *Sci. Rep.* 7, 126. doi: 10.1038/s41598-017-00096-w

Hoecker, U., Vasil, I. K., and McCarty, D. R. (1995). Integrated control of seed maturation and germination programs by activator and repressor functions of Viviparous-1 of maize. *Genes Develop.* 9, 2459–2469. doi: 10.1101/gad.9.20.2459

Ibraheem, F., Gaffoor, I., Tan, Q., Shyu, C., and Chopra, S. (2015). A sorghum MYB transcription factor induces 3-Deoxyanthocyanidins and enhances resistance against leaf blights in maize. *Molecules* 20, 2388–2404. doi: 10.3390/molecules20022388

Ikediobi, C. O., Olugboji, O., and Okoh, P. N. (1988). Cyanide profile of component parts of sorghum (*Sorghum bicolor* L. Moench) sprouts. *Food Chem.* 27, 167–175. doi: 10.1016/0308-8146(88)90059-3

Kambal, A. E., and Bate-Smith, E. C. (1976). A genetic and biochemical study on pericarp pigments in a cross between two cultivars of grain sorghum, *Sorghum bicolor*. *Heredity* 37, 413–416. doi: 10.1038/hdy.1976.106

Karssen, C. M., Brinkhorst-van der Swan, D. L. C., Breekland, A. E., and Koornneef, M. (1983). Induction of dormancy during seed development by endogenous abscisic acid: studies on abscisic acid deficient genotypes of *Arabidopsis thaliana* (L.) Heynh. *Planta* 157, 158–165. doi: 10.1007/BF00393650

Lijavetzky, D., Martínez, M. C., Carrari, F., and Hopp, E. H. (2000). QTL analysis and mapping of pre-harvest sprouting resistance in Sorghum. *Euphytica* 112, 125–135. doi: 10.1023/A:1003823829878

Liu, J., Osbourn, A., and Ma, P. (2015). MYB transcription factors as regulators of phenylpropanoid metabolism in plants. *Mol. Plant* 8, 689–708. doi: 10.1016/j.molp.2015.03.012

Lopez-Molina, L., Mongrand, S., McLachlin, D. T., Chait, B. T., and Chua, N. H. (2002). ABI5 acts downstream of ABI3 to execute an ABA-dependent growth arrest during germination. *Plant J.* 32, 317–328. doi: 10.1046/j.1365-313X.2002.01430.x

McCarty, D. R., Carson, C. B., Stinard, P. S., and Robertson, D. S. (1989). Molecular analysis of Viviparous-1, an abscisic acid-insensitive mutant of maize. *Plant Cell* 1, 523–532. doi: 10.1105/tpc.1.5.523

Morris, G. P., Ramu, P., Deshpande, S. P., Hash, C. T., Shah, T., Upadhyaya, H. D., et al. (2013). Population genomic and genome-wide association studies of agroclimatic traits in sorghum. *Proc. Natl. Acad. Sci. U.S.A.* 110, 453–458. doi: 10.1073/pnas.1215985110

Nakamura, S., Abe, F., Kawahigashi, H., Nakazono, K., Tagiri, A., Matsumoto, T., et al. (2011). A wheat homolog of MOTHER OF FT AND TFL1 acts in the regulation of germination. *Plant Cell* 23, 3215–3229. doi: 10.1105/tpc.111.088492

Ogawa, M., Hanada, A., Yamauchi, Y., Kuwahara, A., Kamiya, Y., and Yamaguchi, S. (2003). Gibberellin biosynthesis and response during Arabidopsis seed germination. *Plant Cell* 15, 1591–1604. doi: 10.1105/tpc.011650

Paterson, A. H., Bowers, J. E., Bruggmann, R., Dubchak, I., Grimwood, J., Gundlach, H., et al. (2009). The *Sorghum bicolor* genome and the diversification of grasses. *Nature* 457, 551–556. doi: 10.1038/nature07723

Pérez-Flores, L. J., Carrari, F., Osuna-Fernández, H. R., Enciso, S., Stanelloni, R., Sánchez, R. A., et al. (2003). Expression analysis of a GA 20-oxidase in embryos from two sorghum lines with contrasting dormancy: possible participation of this gene in the hormonal control of germination. *J. Exp. Bot.* 54, 2071–2079. doi: 10.1093/jxb/erg233

Quinby, J. R., and Karper, R. E. (1961). Inheritance of duration of growth in the milo group of sorghum. *Crop Sci.* 1, 8–10. doi: 10.2135/cropsci1961.0011183X000100010004x

Reeves, W. M., Lynch, T. J., Mobin, R., and Finkelstein, R. R. (2011). Direct targets of the transcription factors ABA-Insensitive ABI4 and ABI5 reveal synergistic action by ABI4 and several bZIP ABA response factors. *Plant Mol. Biol.* 75, 347–363. doi: 10.1007/s11103-011-9733-9

Rieu, W. I., Eriksson, S., Powers, S. J., Gong, F., Griffiths, J., Woolley, L., et al. (2008). Genetic analysis reveals that C19-GA 2-oxidation is a major gibberellin inactivation pathway in *Arabidopsis*. *Plant Cell* 20, 2420–2436. doi: 10.1105/tpc.108.058818

Robichaud, C. S., Wong, J., and Sussex, I. M. (1980). Control of in vitro growth of viviparous embryo mutants of maize by abscisic acid. *Dev. Genet.* 1, 325–330. doi: 10.1002/dvg.1020010405

Rodríguez, M. V., Barrero, J., Corbineau, F., Gubler, F., and Benech-Arnold, R. (2015). Dormancy in cereals (not too much, not so little): About the mechanisms behind this trait. *Seed Sci. Res.* 25, 99–119. doi: 10.1017/S0960258515000021

Rodríguez, M. V., Mendiondo, G. M., Cantoro, R., Auge, G. A., Luna, V., Masciarelli, O., et al. (2012). Expression of seed dormancy in grain sorghum lines with contrasting pre-harvest sprouting behavior involves differential regulation of gibberellin metabolism genes. *Plant Cell Physiol.* 53, 64–80. doi: 10.1093/pcp/pcr154

Rodríguez, M. V., Mendiondo, G. M., Maskin, L., Gudesblat, G. E., Iusem, N. D., and Benech-Arnold, R. L. (2009). Expression of ABA signalling genes and ABI5 protein levels in imbibed *Sorghum bicolor* caryopses with contrasting dormancy and at different developmental stages. *Ann. Bot.* 104, 975–985. doi: 10.1093/aob/mcp184

Steinbach, H. S., Benech-Arnold, R. L., Kristof, G., Sanchez, R. A., and Marcucci Poltri, S. (1995). Physiological basis of pre-harvest sprouting resistance in *Sorghum bicolor* (L.) Moench. ABA levels and sensitivity in developing embryos of sprouting resistant and susceptible varieties. *J. Exp. Bot.* 45, 701–709. doi: 10.1093/jxb/46.6.701

Steinbach, H. S., Benech-Arnold, R. L., and Sánchez, R. A. (1997). Hormonal regulation of dormancy in developing Sorghum seeds. *Plant Physiol.* 113, 149–154. doi: 10.1104/pp.113.1.149

Stephens, J. C., Miller, F. R., and Rosenow, D. T. (1967). Conversion of alien sorghums to early combine genotypes. *Crop Sci.* 7:396. doi: 10.2135/cropsci1967.0011183X000700040036x

Suzuki, M., Ketterling, M. G., Li, Q.-B., and Mc Carty, D. R. (2003). Viviparous1 alters global gene expression patterns through regulation of abscisic acid signaling. *Plant Physiol.* 132, 1664–1677. doi: 10.1104/pp.103.022475

Waniska, A. R. D., and Rooney, W. (2002). "Structure and chemistry of the sorghum caryopsis," in *Sorghum Origin, History, Technology, and Production*, eds C. Wayne Smith and R. A. Frederiksen (Hoboken, NJ: Wiley Series in Crop Science), 45–53.

Wu, Y., Li, X., Xiang, W., Zhu, C., Lin, Z., Wu, Y., et al. (2012). Presence of tannins in sorghum grains is conditioned by different natural alleles of *Tannin1*. *Proc. Natl. Acad. Sci. U.S.A.* 109, 10281–10286. doi: 10.1073/pnas.1201700109

Yamaguchi, M., Fujimoto, H., Hirano, K., Araki-Nakamura, S., Ohmae-Shinohara, K., Fujii, A., et al. (2016). Sorghum D*w1*, an agronomically important gene for lodging resistance, encodes a novel protein involved in cell proliferation. *Sci. Rep.* 6:28366. doi: 10.1038/srep28366

Conflict of Interest Statement: The authors declare that the research was conducted in the absence of any commercial or financial relationships that could be construed as a potential conflict of interest.

frontiers in Plant Science

ORIGINAL RESEARCH
published: 06 April 2017
doi: 10.3389/fpls.2017.00401

Genome-Wide Association Study for Pre-harvest Sprouting Resistance in a Large Germplasm Collection of Chinese Wheat Landraces

*Yong Zhou[1], Hao Tang[1], Meng-Ping Cheng[1], Kwame O. Dankwa[1], Zhong-Xu Chen[1], Zhan-Yi Li[1], Shang Gao[1], Ya-Xi Liu[1], Qian-Tao Jiang[1], Xiu-Jin Lan[1], Zhi-En Pu[1], Yu-Ming Wei[1], You-Liang Zheng[1,2], Lee T. Hickey[3] and Ji-Rui Wang[1]**

[1] Triticeae Research Institute, Sichuan Agricultural University, Chengdu, China, [2] Ministry of Education Key Laboratory for Crop Genetic Resources and Improvement in Southwest China, Sichuan Agricultural University, Ya'an, China, [3] Queensland Alliance for Agriculture and Food Innovation, The University of Queensland, Brisbane, QLD, Australia

OPEN ACCESS

Edited by:
Chengdao Li,
Murdoch University, Australia

Reviewed by:
Awais Rasheed,
International Maize and Wheat Improvement Center, Mexico
Hamid Khazaei,
University of Saskatchewan, Canada

***Correspondence:**
Ji-Rui Wang
wangjirui@gmail.com

Specialty section:
This article was submitted to Crop Science and Horticulture, a section of the journal Frontiers in Plant Science

Received: *01 February 2017*
Accepted: *09 March 2017*
Published: *06 April 2017*

Citation:
Zhou Y, Tang H, Cheng M-P, Dankwa KO, Chen Z-X, Li Z-Y, Gao S, Liu Y-X, Jiang Q-T, Lan X-J, Pu Z-E, Wei Y-M, Zheng Y-L, Hickey LT and Wang J-R (2017) Genome-Wide Association Study for Pre-harvest Sprouting Resistance in a Large Germplasm Collection of Chinese Wheat Landraces. Front. Plant Sci. 8:401. doi: 10.3389/fpls.2017.00401

Pre-harvest sprouting (PHS) is mainly caused by the breaking of seed dormancy in high rainfall regions, which leads to huge economic losses in wheat. In this study, we evaluated 717 Chinese wheat landraces for PHS resistance and carried out genome-wide association studies (GWAS) using to 9,740 DArT-seq and 178,803 SNP markers. Landraces were grown across six environments in China and germination testing of harvest-ripe grain was used to calculate the germination rate (GR) for each accession at each site. GR was highly correlated across all environments. A large number of landraces (194) displayed high levels of PHS resistance (i.e., mean GR < 0.20), which included nine white-grained accessions. Overall, white-grained accessions displayed a significantly higher mean GR (42.7–79.6%) compared to red-grained accessions (19.1–56.0%) across the six environments. Landraces from mesic growing zones in southern China showed higher levels of PHS resistance than those sourced from xeric areas in northern and north-western China. Three main quantitative trait loci (QTL) were detected by GWAS: one on 5D that appeared to be novel and two co-located with the grain color transcription factor *Tamyb10* on 3A and 3D. An additional 32 grain color related QTL (GCR-QTL) were detected when the set of red-grained landraces were analyzed separately. GCR-QTL occurred at high frequencies in the red-grained accessions and a strong correlation was observed between the number of GCR-QTL and GR ($R^2 = 0.62$). These additional factors could be critical for maintaining high levels of PHS resistance and represent targets for introgression into white-grained wheat cultivars. Further, investigation of the origin of haplotypes associated with the three main QTL revealed that favorable haplotypes for PHS resistance were more common in accessions from higher rainfall zones in China. Thus, a combination of natural and artificial selection likely resulted in landraces incorporating PHS resistance in China.

Keywords: wheat, landrace, pre-harvest sprouting, GWAS, haplotypes, geographic distribution

INTRODUCTION

Pre-harvest sprouting (PHS) is defined as the germination of grains within mature spikes on the mother plant before harvest (Nyachiro, 2012). In wheat (*Triticum aestivum* L.), PHS is mainly caused by the breaking or lack of seed dormancy under humid and wet conditions, which leads to huge economic losses due to decreased grain weight and end-use quality (Zhang and Liu, 1989; Kulwal et al., 2012). Thus, seed dormancy (SD) has been considered the major factor that determines PHS resistance (Bewley and Black, 1982; Mares and Mrva, 2001; Finch-Savage and Leubner-Metzger, 2006). The world's major wheat production regions, including Canada, Australia, and China, experience regular losses due to PHS (Rajjou et al., 2012). In China, PHS is a major abiotic constraint that reduces yield and production quality of wheat grain and has affected about 24.91 million ha of wheat fields (Xiao et al., 2002). Therefore, breeding for PHS-resistant cultivars is of great importance in China. The Chinese Academy of Agricultural Sciences (CAAS) has defined 10 wheat-growing zones in China, according to wheat type, varietal reactions to temperature, wheat-growing season and other factors (He et al., 2001). PHS is common in zones III-YTS (Middle and Low Yangtze Valleys Autumn-Sown Spring Wheat Zone), IV-SAS (Southern Autumn-Sown Spring Wheat Zone), V-SWAS (Southwestern Autumn-Sown Spring Wheat Zone), and VI-NES (Northeastern Spring Wheat Zone) (Jin, 1996; He et al., 2000; Xiao et al., 2002; Yuan et al., 2003; Liu L. et al., 2013).

A total of 110 quantitative trait loci (QTL) or loci associated with resistance to PHS in wheat have been reported in 24 previous mapping studies (Supplementary Table S1). These studies have either evaluated PHS resistance directly by testing whole intact spikes in misting chambers or simulated rain events in the field (Somyong et al., 2014; Albrecht et al., 2015), or germination testing of harvest-ripe grain under controlled conditions (Somyong et al., 2014; Zhang et al., 2014; Lin et al., 2015). According to biparental genetic linkage analyses, all 21 chromosomes of wheat reportedly harbor QTL for PHS resistance (Mohan et al., 2009; Cabral et al., 2014; Cao et al., 2016; Fakthongphan et al., 2016), but the most consistently detected regions are located on the group three chromosomes (Kato et al., 2001; Osa et al., 2003; Kulwal et al., 2004; Mori et al., 2005; Liu and Bai, 2010) and Chr 4A (Mares et al., 2005; Chen et al., 2008; Singh et al., 2010; Cabral et al., 2014). The PHS resistance genes underpinning the 3A, 3B, and 3D regions are considered to be tightly linked or pleiotropic with red seed coat color determined by dominant R alleles (Himi et al., 2011). Thus, red-grained wheat cultivars typically display superior levels of PHS resistance. However, the major QTL on Chr 4AL is not associated with grain color (Mares et al., 2005; Tan et al., 2006; Chen et al., 2008; Imtiaz et al., 2008; Ogbonnaya et al., 2008; Singh et al., 2010; Liu et al., 2011; Cabral et al., 2014) and the underlying casual gene for grain dormancy (MKK3) was recently cloned by Torada et al. (2016).

Several genome-wide association studies (GWAS) have also reported candidate loci associated with PHS resistance (Supplementary Table S1). Jaiswal et al. (2012) used 250 simple sequence repeat (SSR) markers to scan 242 common wheat accessions and identified 30 markers associated with PHS, including eight previously reported markers. Kulwal et al. (2012) scanned 198 white winter wheat accessions using 1,166 Diversity Array Technology (DArT) and SSR markers, and identified eight QTL on seven chromosomes, including a novel QTL on Chr 7BS. Rehman Arif et al. (2012) reported 70 DArT markers positioned on 11 chromosomes were associated with PHS and SD in a collection of 96 winter wheat cultivars. Albrecht et al. (2015) carried out GWAS for a panel of 124 European winter wheat accessions using DArT and SSR markers, and detected five QTLs on Chr 1B, 1D (two QTL), 3D, and 5D.

Chinese wheat landraces display higher PHS resistance than improved cultivars (Wang et al., 2011; Liu et al., 2014), thus present valuable genetic resources for identifying candidate loci associated with PHS resistance that could be used in modern breeding programs. In the present study, a collection of 717 wheat landraces from major wheat-growing zones in China were phenotyped for PHS resistance over 4 years (2012–2015) at three locations. In order to identify markers that are closely positioned to new or known candidate genes and QTL, the accessions were genotyped using high density DArT-seq and single nucleotide polymorphism (SNP) arrays. We investigate the frequency of favorable alleles for PHS resistance in landraces originating from different wheat-growing regions in China.

MATERIALS AND METHODS

Chinese Wheat Landraces

Seven hundred and seventeen wheat landraces from 10 major wheat-growing zones in China were obtained from the CAAS (Supplementary Table S2 and **Figure 1**). The landraces were evaluated from 2012 to 2015 at experimental farms at Wenjiang (30°42′41.1″N 103°52′06.7″E), Chongzhou (30°32′39.9″N 103°39′08.6″E), and Ya'an (29°58′39.9″N 102°59′21.9″E) in Sichuan.

Phenotyping for PHS Resistance

We evaluated PHS resistance by performing germination tests of harvest-ripe grain under controlled conditions (Somyong et al., 2014; Zhang et al., 2014; Lin et al., 2015). At each site, wheat spikes were harvested at physiological maturity (i.e., after loss of green pigmentation in the spikes and peduncles). The spikes were air-dried at room temperature for 7 days, avoiding direct sunlight and high temperature. Spikes were then stored at -20°C to preserve grain dormancy (Mares, 1983). Once samples of all accessions had been collected, threshing was performed by hand to aviod damaging the seed coat or embryos. Germination testing was conducted at 20 ± 1°C for 7 days and used three replicate petri dishes lined with filter paper for each accession, where each petri dish contained 50 grains. Germination was defined as the rupture of the grain coat by the emerging radicle. Germination was recorded over a period of 7 days and used to calculate cumulative percentage germination or germination rate (GR) to estimate the degree of SD (Osa et al., 2003; Mori et al., 2005; Torada et al., 2005). A GR apoproaching 100% indicates low levels of grain dormancy or PHS resistance (i.e., all grains germinated), whereas a GR approaching 0% indicates high

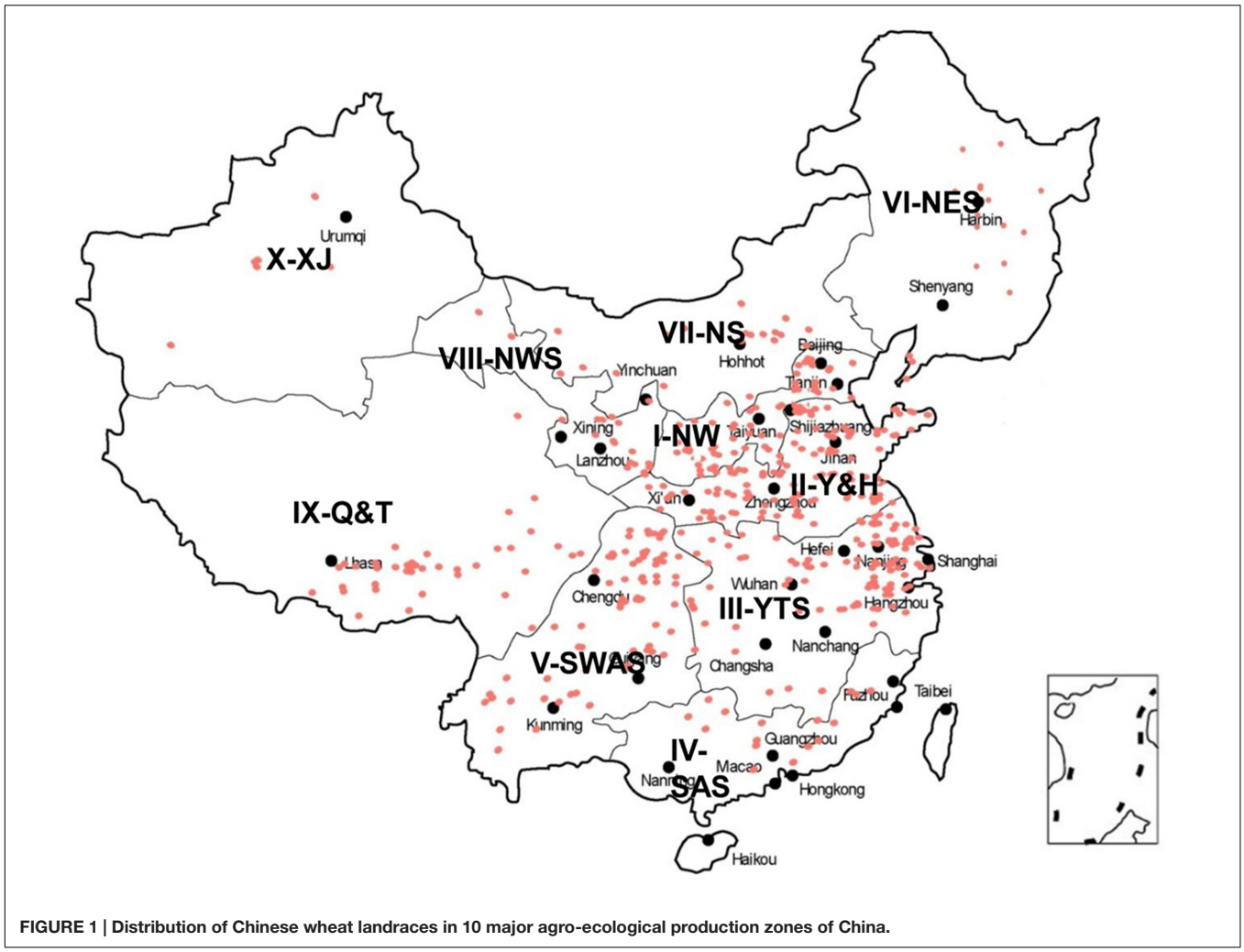

FIGURE 1 | Distribution of Chinese wheat landraces in 10 major agro-ecological production zones of China.

levels of grain dormancy or PHS resistance. One-Way Analysis of variance (ANOVA) of GR for accessions derived from the 10 Chinese wheat-growing zones, which was performed by Duncan's multiple test in each phenotyping tested environment. Two-tailed Pearson product-moment correlation coefficient tests were also carried out for GR obtained across the six environments (Fieller et al., 1957).

Genotyping

The collection of 717 wheat landraces was genotyped using the DArT-seq (Diversity Arrays Technology, Canberra, ACT, Australia) genotyping-by-sequencing (GBS) platform. A subset of 272 landraces, that were representative of the genetic diversity, was also genotyped using the Axiom® Wheat660 SNP array (Affymetrix[1], Santa Clara, CA, USA). A total of 89,284 probes from the DArT-seq (DArT and DArT_GBS) and 630,517 probes from the Wheat660 SNP arrays were used for genotyping. Markers with maximum missing values of 10% were discarded and only those with minor allele frequency (MAF) $\geq$ 0.05 were used for further analyses.

Genome-Wide Association Study (GWAS) for PHS Resistance

Compressed mixed linear model (Wang et al., 2005; Zhang Z. et al., 2010) accounting for the population structure (Pritchard, et al., 2000) and familial relationship (Li et al., 2013) was used to examine the association between markers and PHS phenotype using Tassel 4.0 (Bradbury et al., 2007). Population structure was assessed using the Bayesian clustering algorithm implemented by Structure 2.3.4 (Pritchard et al., 2000; Falush et al., 2003; Hubisz et al., 2009). An admixture model with 10 replicates for each number of genetic clusters (K, ranging from 1 to 10) and 10,000 iterations of burn-in followed by 10,000 MCMC iterations was used. The outputs of the genetic cluster analysis were extracted in STRUCTURE HARVESTER (Earl and vonHoldt, 2012) and the optimal alignment of the 10 iterations was determined using CLUMPP (Jakobsson and Rosenberg, 2007).

Four separated GWAS analyses were performed with four sets of STRUCTURE data in this study: (1) association analysis for

[1]http://www.affymetrix.com/catalog/prod850001/AFFY/Axiom%26%23174%3B-Wheat-Genotyping-Arrays#1_3

717 Chinese landrace wheat accessions using DArT-seq markers, (2) association analysis for 272 accessions using Wheat660 SNP markers, (3) association analysis for 77 white-grained accessions by Wheat660 SNP markers, and (4) association analysis for 186 red-grained accessions by Wheat660 SNP markers. GWAS sets 3 and 4 were conducted to explore the possibility of detecting QTL specific to the white- and red-grained germaplsm pools, termed grain colour releated QTL (GCR-QTL). The threshold for significant marker-trait associations was set at $-\log_{10}(0.01/n$, where $n =$ number of markers) for GWAS sets 1 and 2, and $-\log_{10}$ (0.001/n, where $n =$ number of markers) for GWAS sets 3 and 4, which roughly equates to a Bonferroni correction (Weisstein, 2004; Su et al., 2016). Manhattan plots were generated using the qqman R package (Turner, 2014) in R i386 3.0.3 (R Core Team, 2014). Markers detected in at least two environments were used for QTL determine, and markers positioned with a 10 Mb region were considered the same QTL region. Markers associated with PHS resistance in this study were compared with QTL, loci and genes previously reported in the literature using a genetic map including 90K SNP, expressed sequence tag, SSR and DArT markers was reported by Cabral et al. (2014). The chromosomal locations of the 90K SNPs (Supplementary Table S7), DArT-seq markers and Wheat660 SNP markers were determined using the wheat 'Chinese Spring' survey sequence version 2.28[2].

Estimation of Haplotype Effects

Haplotype analyses were carried out for major QTL detcted in GWAS sets 1 and 2. Popart 1.7[3] (Leigh and Bryant, 2015) was used to carry out haplotype analyses, and accessions with missing values were not included. The minimum spanning networks method was used to show the relationship between haplotypes and Median-joining networks for inferring intraspecific phylogenies (Bandelt et al., 1999). In each of the test environments, analysis of vairance (ANOVA) was conducted by taking genotypes as fixed effects and environments as random effect using SPSS version 16.0 (SPSS Inc., Chicago, IL, USA). 'Favorable' haplotpyes (allele and allelic combinations) were those that significantly lowered GR (increasing PHS resistance) compared to alternative haplotypes based on ANOVA. Thus, alterntive haplotypes were considered 'unfavorable' haplotpyes for PHS resistance. Accessions genotyped with the Wheat660 SNP array were used to determine the number of favorable haplotypes in each accession for haplotype pyramiding analysis. The frequency of favorable haplotpyes in the landrace collection was determined as the proportion of accessions that carried the favorable haplotpye.

RESULTS

Variation for PHS Resistance in Chinese Wheat Landraces

Pre-harvest sprouting resistance was evaluated for a collection of 717 landraces grown at three locations (Chongzhou, Wenjiang, and Ya'an) from 2012 to 2015 (**Figure 1** and Supplementary Table S2). Most accessions displayed relatively stable phenotypes across the six environments (**Figure 2A**). The lowest mean GR (24.8%) was recorded in 2014 at Wenjiang, whereas the highest mean GR (60.8%) was recorded in 2012 at Ya'an (Supplementary Table S3). The GR was highly correlated across environments ($r = 0.54$–0.80) based on the two-tailed Pearson product-moment correlation coefficient test (Fieller et al., 1957) (**Table 1**). A total of 194 landraces exhibited a mean GR $< 20.0\%$, of which 23 landraces displayed consistently dormant phenotypes across all six environments (Supplementary Table S2). Overall, white-grained accessions displayed significantly higher GR (mean range 47.2–79.6%) compared to red-grained accessions (mean range 19.1–56.0%) across all test environments ($p = 8.52\text{E-}28$–$9.88\text{E-}13$). Most landraces from wheat-growing zones III-YTS, IV-SAS, and V-SWAS, which are high rainfall regions in southern China, had red colored grain and displayed a significantly lower mean GR than landraces from other wheat-growing zones (**Figure 2B** and Supplementary Table S4). No accessions from zone IV-SAS were white-grained and only 8.5 and 7.9% of landraces from zones III-YTS and V-SWAS, respectively, produced white grains. Only a small number of landraces with white grains showed a mean GR $< 20.0\%$ across all six environments (i.e., Baitiaoyu, Baikangyangmai, Xiaoganmai, Baixu, Xiaoqingmang, Tuotuomai, Hechuanmai, Changxuxuqiaomai, and Dabaili). In contrast, 43.1 and 40.3% of landraces from zones I-NW and II-Y&H were red-grained and exhibited a significantly higher mean GR, respectively. Although higher percentages of accessions with red grains were from zones VIII-NWS and IX-Q&T, landraces from these two regions displayed lower levels of PHS resistance.

In order to investigate variation for PHS resistance associated with the origin of Chinese landraces, the mean GR obtained by accessions from each of the 10 zones were compared. Accessions from high rainfall zones III-YTS, IV-SAS, and V-SWAS showed a significantly lower mean GR than accessions derived from the other seven zones in at least three environments (**Figure 2B**). Further, accessions from zone IX-Q&T showed a significantly higher mean GR than accessions from other zones in at least three environments (**Figure 2B**). Accessions from zone IV-SAS displayed the lowest mean GR across all six environments (6.0–20.9%), however, this was similar to accessions from zones III-YTS (12.0–30.0%) and V-SWAS (13.1–36.9%). Accessions from zone VI-NES showed a significantly higher GR (15.5–58.8%) compared to accessions from zone IV-SAS in two of the six environments (i.e., Wenjiang in 2013 and Chongzhou in 2014). But accessions from zone VI-NES exhibited similar levels of PHS resistance with those from zones III-YTS and V-SWAS in all environments except Wenjiang in 2013. Accessions from zone I-NW (30.7–8.1%), II-Y&H (30.0–56.0%), VII-NS (29.4–66.0%), VIII-NWS (27.9–70.4%), IX-Q&T (58.9–80.8%), and X-XJ (35.7–70.7%) showed a significantly higher mean GR than accessions from zone IV-SAS in all test environments. Overall, accessions from zone IX-Q&T showed the highest mean GR compared to accessions from all other nine zones, but the mean GR was only deemed significantly higher in two of the six

[2]ftp://ftp.ensemblgenomes.org/pub/release-28/plants/fasta/triticum_aestivum/dna/
[3]http://popart.otago.ac.nz

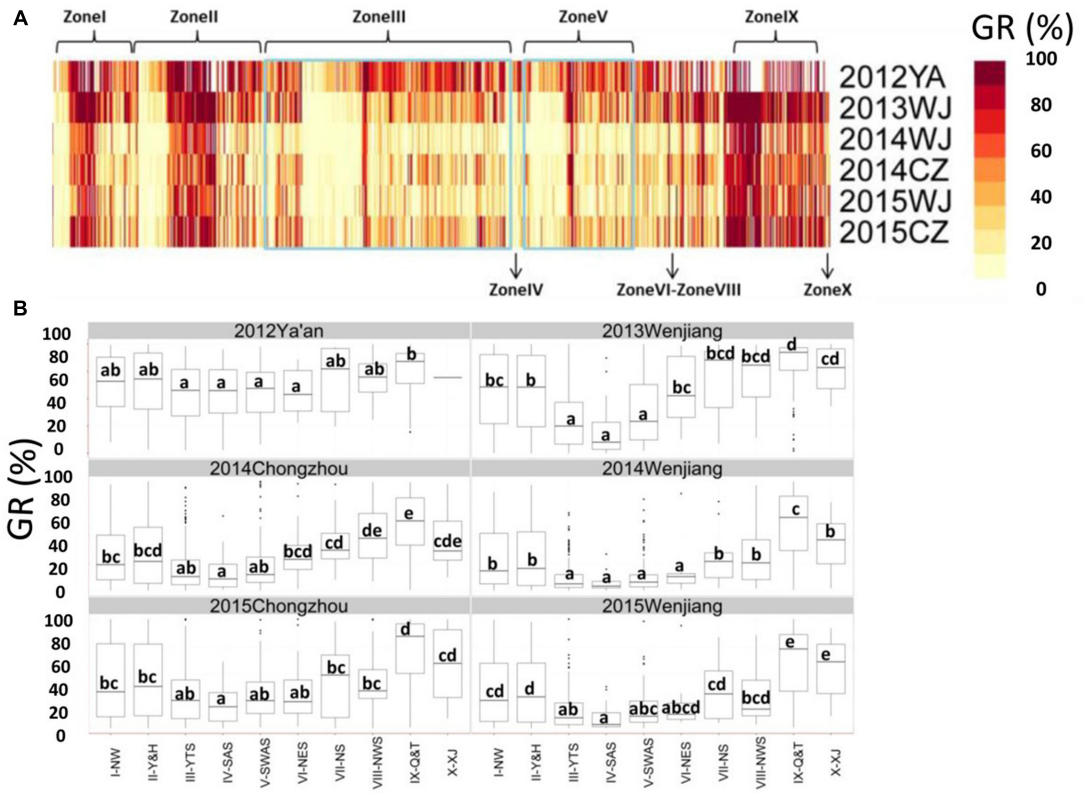

FIGURE 2 | Phenotypic analysis for germination rate (GR) obtained by Chinese wheat landraces. (A) GR of Chinese wheat landraces grown from 2012 to 2015 at Wenjiang, Chongzhou, and Ya'an; **(B)** Box plot for GR obtained by accessions grouped according to origin (i.e., the 10 major agro-ecological production zones of China). The middle horizontal line within each box represents the mean GR and vertical lines mark the range from 5 to 95% of the total GR within each group.

TABLE 1 | Pearson product-moment correlation coefficient (PPCC) of germination rate among all measured environments.

Correlations	2012 Ya'an	2013 Wenjiang	2014 Wenjiang	2014 Chongzhou	2015 Wenjiang	2015 Chongzhou
2012 Ya'an						
2013 Wenjiang	0.56**					
2014 Wenjiang	0.54**	0.70**				
2014 Chongzhou	0.55**	0.68**	0.69**			
2015 Wenjiang	0.56**	0.69**	0.81**	0.68**		
2015 Chongzhou	0.62**	0.68**	0.74**	0.68**	0.77**	

***Correlation is significant at the 0.01 level (2-tailed).*

test environments. Overall, analysis of germination data using harvest-ripe grain collected from six environments revealed that wheat landraces originating from high rainfall zones in China (III-YTS, IV-SAS, and V-SWAS) displayed superior levels of PHS resistance.

GWAS for PHS in Chinese Wheat Landraces

A total of 9,740 polymorphic markers with MAF $\geq$ 0.05 were selected from 89,284 DArT-seq markers for Bayes structure analysis and GWAS using 717 landrace accessions. Out of the 717 accessions, 272 that were representative of the genetic diversity were selected and genotyped using the Axiom® Wheat660 SNP array (Supplementary Table S2). From the Wheat660 SNP array, 178,803 polymorphic SNP markers with MAF $\geq$ 0.05 were selected out of 630,517 total SNP markers. This subset of SNP markers were used for Bayes structure analysis and GWAS. Based on the genetic clusters analysis in Structure Harvester, $K = 5$ provided the highest peaks in both DArT-seq and Wheat660 data sets.

Genome-wide association studies detected three highly significant DArT-seq and seven highly significant SNP markers. These markers satisfied the threshold for significance applied in this study; a $-\log_{10}$P value $>$ 6.55 [$-\log_{10}$ (0.01/178803)] (Su et al., 2016) and were detected in at least two test

environments. The chromosome position of these 10 highly associated markers revealed three main QTL regions that potentially contain PHS resistance genes (**Figure 3A**, **Table 2**, and Supplementary Table S5). QTL1 and QTL3 were represented by only one marker each, while QTL2 comprised eight markers. SNP marker AX-111578083 located at 173.81 Mb was linked with QTL1 on Chr 3A. This marker was detected in all environments with the exception of 2012Ya'an and explained 11.5–25.1% of the phenotypic variation. SNP marker AX-109028892 located at 39.36 Mb was linked with QTL 3 on Chr 5D. This marker was identified in three environments; 2013Wenjiang, 2015Wenajiang, and 2015Chongzhou and explained 11.5–12.0% of the phenotypic variation. The eight markers associated with QTL2 on Chr 3D consisted of three DArT-seq markers and five Wheat660 SNP markers. The three DArT-seq markers; A11134, A36351, and A36269 were located at 110.99 Mb, 111.54 Mb, and 113.89 Mb, respectively. They were detected in 4, 5, and 6 environments and explained 4.4–8.8% of the phenotypic variation, respectively. The five SNP markers; AX-111204246, AX-108879360, AX-111624595, AX-110772653, and AX-95124645 were located at 112.35 Mb, 112.36 Mb, 112.63 Mb, 112.80 Mb, and 113.74 Mb on Chr 3D and explained 11.7–19.3% of the phenotypic variation, respectively (**Table 2** and Supplementary Table S5). SNP markers AX-111204246 and AX-95124645 were associated in two environments, while AX-111624595 and AX-110772653 were associated in four environments, and AX-108879360 was associated in three environments.

Among the three main QTL identified, QTL3 on Chr 5D appears to be novel (**Figure 3D**, **Tables 2**, and Supplementary Table S7) while QTL1 and QTL2 were located in close proximity to known genes or previously reported QTL for grain dormancy or PHS resistance in wheat (**Figures 3B,C** and Supplementary Table S7). QTL1 was positioned close to the *Tamyb10* gene located at 174.1 Mb on Chr 3A which is significantly associated with grain color and germination (Himi et al., 2011; Dong et al., 2015; Lin et al., 2015). SNP maker AX-111578083 linked to QTL1 was positioned only 0.3 Mb away from *Tamyb10* (**Figure 3B**). At least three QTL have been previously mapped within the region spanning 102.3–119.3 Mb on Chr 3D and includes the *R-loci* (Groos et al., 2002; Fofana et al., 2009; Rasul et al., 2009). QTL2 identified in this study (110.99–113.89 Mb, located near the *R-loci* region) also overlaps with major QTL previously reported on Chr 3D (**Figure 3C**). Overall, three main QTL for PHS resistance detected in Chinese wheat landraces were located on Chromosomes 3A, 3D, and 5D.

Haplotype Analyses for Main QTL Confering PHS Resistance

Each main QTL detcted in the panel of 717 landraces (i.e., QTL1, QTL2, and QTL3) had two haplotypes; one favorable and another unfavorable for PHS reisitance. Haplotype A for QTL1 (QTL1-HAP-A) was observed in 71 accessions, where the mean GR ranged from 60.9 to 89.5% across all evironments (**Table 3** and **Figure 4**). Whereas, haplotype G for QTL1 (QTL1-HAP-G) was observed in 109 accessions that showed an average GR of 9.0–38.8% (**Table 3** and **Figure 4**). From the ANOVA results, the GR of accessions from haplotpye G was significantly lower than that of haplotpye A. Therefore, QTL1-HAP-G was defined as the favorable haplotype and QTL1-HAP-A as the unfavorable haplotype for PHS resistance. Haplotype TGTAC in QTL2 (QTL2-HAP-TGTAC) was present in 30 accessions showing an avgerage GR of 67.7–94.2% (**Table 3** and **Figure 4**). On the other hand, haplotype CACTT for QTL2 (QTL2-HAP-CACTT) was observed in 176 accessions showing a significantly lower average GR of 20.1–42.4% (**Table 3** and **Figure 4**). Hence the QTL2-HAP-CACTT was defined as the favorable haplotype and QTL2-Hap-TGTAC as the unfavorable haplotpye for PHS resistance. Haplotpye G for QTL3 (QTL3-HAP-G) was observed in 74 accessions showing an average GR of 59.2–83.2% across the enviornments (**Table 3** and **Figure 4**). In contrast, haplotype A for QTL3 (QTL3-HAP-A) was present in 179 accessions which showed a significantly lower average GR of 21.7–35.5% (**Table 3** and **Figure 4**), hence QTL3-HAP-A was defined as the favorable haplotype and QTL3-HAP-G as the unfavorable haplotpye for PHS resistance.

Geographic Distribution of Main QTL for PHS Reisitance

To investigate the geographic distribution of the three main QTL, the frequency of the six haplotypes was determined for landraces sourced from 9 of the 10 Chinese wheat-growing zones (**Figure 5**).

High frequencies (94.4–100%) of the favorable haplotype for QTL1 (QTL1-HAP-G) were observed in landraces from zones III-YTS, IV-SAS, V-SWAS, and IX-Q&T. Half of the accessions originating from zones VII-NS and VIII-NWS carried the QTL1-HAP-G favorable haplotype, while only 18.2 and 30.7% of accessions from zones I-NW and II-Y&H carried it. More than 50% of all accessions carried the favorable haplotype for QTL2 (QTL2-HAP-CACTT) in all test zones. The frequencies of QTL2-HAP-CACTT were 53.3, 73.9, and 94.4% in landraces from zones II-Y&H, I-NW, and III-YTS, respectively. All accessions from zones IV-SAS, V-SWAS, VIII-NWS, and IX-Q&T had the favorable haplotype QTL2-HAP-CACTT. None of the accessions in zone VII-NS carried the favorable haplotype for QTL3 (QTL3-HAP-A). The QTL3-HAP-A favorable haplotype occurred in 33.3, 47.2, and 50.0% of accessions from zones I-NW, II-Y&H, and X-XJ. High frequencies of QTL3-HAP-A were observed in zones III-YTS, IV-SAS, V-SWAS, VIII-NWS, and IX-Q&T. More than 80% of all accessions from zones III-YTS, IV-SAS, V-SWAS, VIII-NWS, and IX-Q&T had all three favorable haplotypes. Overall, the frequency of favorable haplotypes for main QTL contributing PHS resistance in Chinese wheat landraces varied depending on their geographical origin (**Figure 5**).

Additional Grain Colour Related QTL (GCR-QTL)

To investigate QTL that may have been masked by the main QTL associated with grain color (e.g., QTL1 on 3A and QTL2 on 3D) GWAS was repeated for red- and white-grained accessions

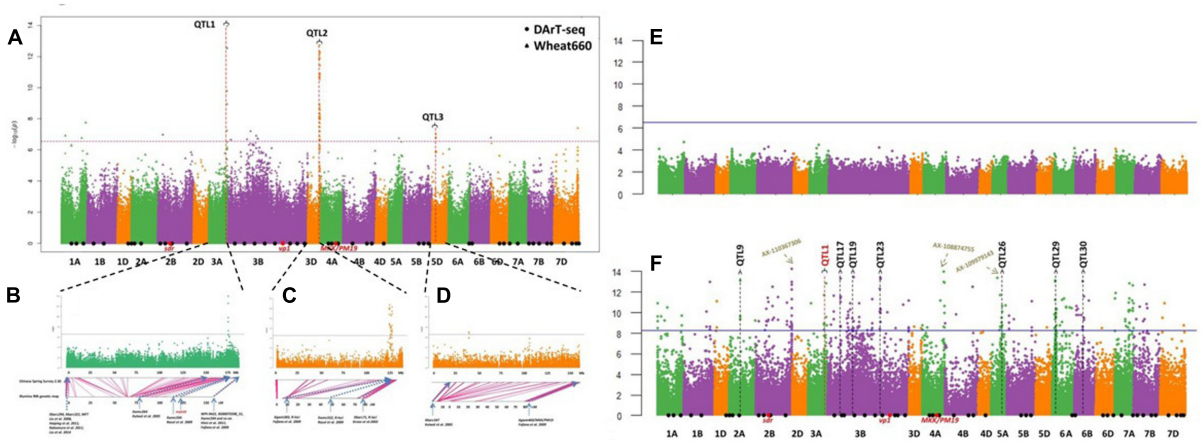

FIGURE 3 | Manhattan plots of genome-wide association studies (GWAS) results for pre-harvest sprouting (PHS) resistance in Chinese wheat landraces. (A) Three main quantitative trait loci (QTL) identified by GWAS set 1 DArT-seq and 2 Wheat660; **(B)** QTL1 on Chr 3A and co-locating previously reported QTL; **(C)** QTL2 on Chr 3D and co-locating previously reported QTL; **(D)** QTL3 on Chr 5D and co-locating previously reported QTL; **(E)** GWAS results of GWAS set 3 77 white-grained accessions; **(F)** GWAS results of set 4 186 red-grained accessions.

separately. Among the 272 accessions that were genotyped using Wheat660 SNP array (Supplementary Table S2), 186 accessions were red-grained, and 77 accessions were white-grained, while 9 accessions didn't have any color information in Chinese Crop Germplasm Resources Information System.

Firstly, 178,803 polymorphic SNP markers were used for Bayes structure analysis of the two germplasm sets. $K = 4$ and $K = 2$ showed the highest peak in both white- and red-grained accessions, respectively. Next, compressed mixed linear model accounting for the population structure and familial relationship was then used to examine marker-trait assoications within both groups. In the white-grained accessions, no marker was found to be significantly associated with GR (**Figure 3E**). However, in the red-grained group, a total of 46 significant markers obtained $-\log_{10}$P values > 8.25 [$-$log10(0.001/178803)] in at least two environments (**Figure 3F** and Supplementary Table S6). This resulted in the detection of 32 GCR-QTL for PHS resistance within the red-grained sub-group, of which 20 QTL were previously reported, as indicated in **Table 2**. Eleven GCR-QTL were detected in the A genome, 20 GCR-QTL in the B genome, but only 1 GCR-QTL was detected in the D genome. In addition, some markers displayed high $-\log_{10}$P values (> 8.25) in only one environment (e.g., AX-110367306, AX-108874755, and AX-109979143), therefore were not selected for further analysis (**Figure 3F**).

By determining the presence/absence of the favorable haplotype for each of the 32 GCR-QTL in the 186 red-grained wheat accessions, the total number of favorable haplotypes in each landrace was calculated. Interestingly, a highly significant correlation was observed between the number of favorable haplotypes occurring in landrace accessions and the mean GR obtained across all six environments ($R^2 = 0.62$; **Figure 6**). Red-grained landraces were highly enriched with favorable haplotypes for GCR-QTL. For instance, 135 of the 186 red-grained landraces carried more than 20 favorable haplotypes.

DISCUSSION

We have characterized the largest number of wheat landraces for PHS resistance to date – providing new insight into the genetic architecture of this important trait and the geographical distribution of favorable haplotypes across the wheat-growing zones in China.

Genome-wide association studies using germination data collected across six environments identified three main QTL in the collection of 717 landraces, plus 32 GCR-QTL when the red-grained accessions were analyzed separately. However, this is not the first study to report genes/QTL for PHS resistance in Chinese wheat landraces (Zhang H.P. et al., 2010; Zhang et al., 2014, 2017; Wang et al., 2011). For example, QTL located on Chr 4A in the landrace Tuotuomai and QTL on Chr 3A and 3B in the landrace Wanxianbaimaizi are reported to be associated with PHS resistance (Chen et al., 2008; Zhang H.P. et al., 2010). It is clear that Chinese wheat landraces provide a useful source of PHS resistance to develop modern cultivars incorporating PHS resistance.

So far, seven genes associated with PHS have also been cloned in wheat, including: *TaVp1* (Nakamura and Toyama, 2001; Chang et al., 2010, 2011; Wang et al., 2011), *TaMFT* (Nakamura et al., 2011), *TaPHS1* (Liu S. et al., 2013; Liu et al., 2015), *TaSdr* (Zhang et al., 2014, 2017), *TaPm19* (Barrero et al., 2015), *Tamyb10* (Dong et al., 2015; Wang et al., 2016), and *TaMKK3* (Torada et al., 2016). Some of them (i.e., *TaVp1*, *TaMFT*, *TaPHS1,* and *TaSdr*) have been used to test PHS in Chinese cultivars by developing KASP markers (Rasheed et al., 2016). In this study, highly significant main QTL were positioned on the group 3 chromosomes. Positioned in close proximity to the strong signals detected on Chr 3A (QTL1) and Chr 3D (QTL2), is the grain color transcription factor *Tamyb10*, known to be associated with PHS resistance (Groos et al., 2002; Dong et al., 2015). *Tamyb10* is located at the distal region of the long arm of Chr 3A, 3B,

TABLE 2 | Summary of quantitative trait loci (QTL) results from genome-wide association studies (GWAS) of pre-harvest sprouting (PHS) resistance in Chinese wheat landraces.

QTL	Locus	Marker	Mb	Env.	−log10P	R2	Reference
QTL1[#]	3A	AX-111578083	173.81	5	7.23 ~ 13.95[a]	11.5–25.1%	*Tamyb10-A1*
QTL2[#]	3D	A11134 ~ A36269	110.99 ~ 113.89	6	6.58 ~ 12.74	4.4–19.3%	*Tamyb10-D1*
QTL3[#]	5D	AX-109028892	39.36	3	6.79 ~ 7.00	11.5–12%	
GCR-QTL1[$]	1A	AX-110008090	0.35	2	9.14 ~ 10.86	21.8–33.8%	Mohan et al., 2009
GCR-QTL2[$]	1A	AX-94464571	233.53	2	8.75 ~ 9.68	23.5–30.6%	Singh et al., 2010
GCR-QTL3[$]	1B	AX-109866527	221.04	3	8.62 ~ 10.1	23–23.6%	Jaiswal et al., 2012
GCR-QTL4[$]	1B	AX-109555236	248.86	2	8.58 ~ 12.96	19.6–25.7%	
GCR-QTL5[$]	1D	AX-111775865	20.07	2	8.53 ~ 11.11	19.6–34.3%	
GCR-QTL6[$]	2A	AX-109973468	104.07	3	9.36 ~ 13.08[a]	21.2–31.2%	Mohan et al., 2009; Jaiswal et al., 2012
GCR-QTL7[$]	2B	AX-94693825 ~ AX-110478651	102.36 ~ 118.23	2	8.72 ~ 11.40	21.4–34.6%	Kumar et al., 2009; Zhang et al., 2014
GCR-QTL8[$]	2B	AX-110645544	160.78	2	10.62 ~ 12.48	21.5–29.5%	Kumar et al., 2009; Zhang et al., 2014
GCR-QTL9[$]	2B	AX-109008046	209.62	2	9.27 ~ 11.48	25.6–32.9%	Kumar et al., 2009; Zhang et al., 2014
GCR-QTL10[$]	2B	AX-111478580	296.90	3	8.82 ~ 10.93	21.9–29.7%	
GCR-QTL11[$]	2B	AX-110610210 ~ AX-111741521	338.83 ~ 340.34	3	8.42 ~ 12.95	22.1–30.1%	
GCR-QTL12[$]	3A	AX-109376167 ~ AX-111037462	151.44 ~ 152.19	2	8.81 ~ 11.67	19.3–35.7%	Rasul et al., 2009
GCR-QTL13[$]	3A	AX-111578083	173.81	2	9.51 ~ 12.81	22.4–37.1%[b]	*Tamyb10-A1*
GCR-QTL14[$]	3B	AX-111495497	56.99	3	9.35 ~ 11.6	23.1–31.3%	Jaiswal et al., 2012
GCR-QTL15[$]	3B	AX-110619077 ~ AX-111560777	121.63 ~ 126.95	3	8.59 ~ 13.27[a]	20.7–35.2%	Mares et al., 2009; Chang et al., 2010; Zhang H.P. et al., 2010
GCR-QTL16[$]	3B	AX-108930833	197.07	2	8.51 ~ 10.11	28.1–29.1%	Mares et al., 2009; Chang et al., 2010; Zhang H.P. et al., 2010
GCR-QTL17[$]	3B	AX-109353822	249.91	2	8.19 ~ 13.42[a]	19.3–37.3%[b]	Mares et al., 2009; Chang et al., 2010; Zhang H.P. et al., 2010
GCR-QTL18[$]	3B	AX-111819945	286.02	2	8.46 ~ 8.63	19.3–20.2%	Mares et al., 2009; Chang et al., 2010; Zhang H.P. et al., 2010
GCR-QTL19[$]	3B	AX-110978491	299.58	3	8.59 ~ 10.86	19.6–27.9%	Mares et al., 2009; Chang et al., 2010; Zhang H.P. et al., 2010
GCR-QTL20[$]	3B	AX-111529538	421.31	2	6.58 ~ 11.29	15–26.6%	Mares et al., 2009; Chang et al., 2010; Zhang H.P. et al., 2010
GCR-QTL21[$]	3B	AX-109861314 ~ AX-111106200	494.35 ~ 505.33	3	8.37 ~ 13.36[a]	19–36.5%[b]	Jaiswal et al., 2012; Cabral et al., 2014
GCR-QTL22[$]	3B	AX-111194600	767.96	2	8.15 ~ 8.52	19.4–21.1%	Rehman Arif et al., 2012; Jaiswal et al., 2012
GCR-QTL23[$]	4A	AX-109919526	0.58	2	8.3 ~ 8.76	21.6–25.1%	
GCR-QTL24[$]	4A	AX-111634210	208.43	3	8.53 ~ 12.86	19.5–36.4%[b]	Albrecht et al., 2015; Lin et al., 2015; Torada et al., 2016
GCR-QTL25[$]	5A	AX-109844264 ~ AX-111698406	100.05 ~ 103.36	2	8.46 ~ 10.60	21–28.5%	
GCR-QTL26[$]	5B	AX-89623229	19.77	3	8.43 ~ 9.66	19.1–23.1%	
GCR-QTL27[$]	6A	AX-111007766 ~ AX-111732156	23.31 ~ 31.33	2	8.52 ~ 13.06[a]	19.4–34.9%	
GCR-QTL28[$]	6B	AX-109834362	79.00	3	8.32 ~ 13.05[a]	20.4–37.4%[b]	
GCR-QTL29[$]	6B	AX-108844376	92.71	2	9.3 ~ 11.53	22.1–31.6%	
GCR-QTL30[$]	7A	AX-110909277 ~ AX-111486355	136.77 ~ 141.52	3	8.27 ~ 12.8	18.7–36%	
GCR-QTL31[$]	7A	AX-110478067	170.37	3	10.15 ~ 12.65	24.4–34%	
GCR-QTL32[$]	7B	AX-110932737	102.42	2	9.32 ~ 12.66	22.3–35.3%	Cabral et al., 2014

[#]*indicates a main QTL identified using all accessions;* [$]*indicates a grain color related QTL (GCR-QTL) identified in the red-grained group;* [a]*indicates the* $-log_{10}P$ *value is higher than 13;* [b]*indicates the QTL explained more than 36% of the phenotypic variance.*

TABLE 3 | Phenotypes (GR) and frequencies of haplotypes (or alleles) for the three main QTL identified via GWAS using all accessions.

Main QTL	Haplotpye	Frequency of Hap	GR 2012 Ya'an	GR 2013 Wenjiang	GR 2014 Wenjiang	GR 2014 Chongzhou	GR 2015 Wenjiang	GR 2015 Chongzhou
QTL1	Hap-A[a]	60.6%	38.8%	15.8%	9.0%	12.6%	10.7%	17.7%
	Hap-G[b]	39.4%	89.5%	85.2%	63.9%	63.8%	60.9%	73.4%
QTL2	Hap-CACTT[a]	85.4%	42.4%	31.3%	20.1%	25.4%	23.5%	29.0%
	Hap-TGTAC[b]	14.6%	94.2%	91.4%	71.6%	67.7%	68.8%	77.1%
QTL3	Hap-A[a]	70.8%	30.1%	32.5%	21.7%	26.2%	24.0%	30.1%
	Hap-G[b]	29.2%	71.8%	83.2%	59.7%	60.7%	59.1%	71.8%

[a]*Favorable haplotpye,* [b]*Unfavorable haplotpye determined by ANOVA test.*

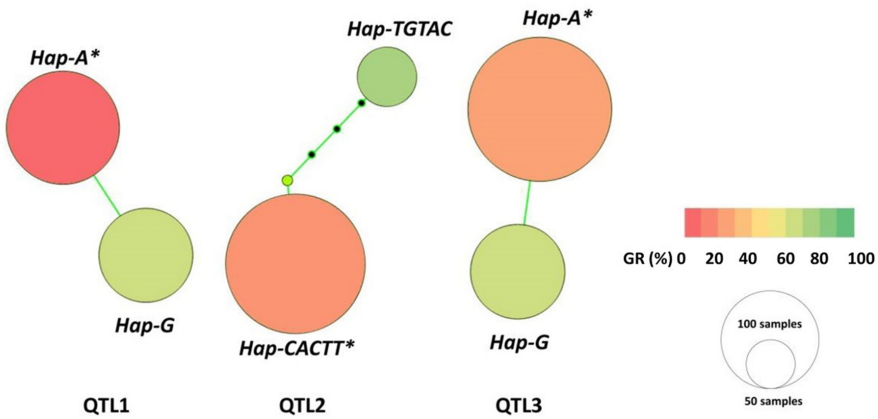

FIGURE 4 | Haplotype networks for the three main QTL. The nodes represent variants for the haplotype blocks, with sizes proportional to the number of genotypes carrying the respective variant and colors indicating phenotypic means among genotypes carrying the specific haplotype variant. *The germination rate for accessions carrying the favorable haplotype is significantly lower than accessions carrying the unfavorable haplotype ($p < 0.01$).

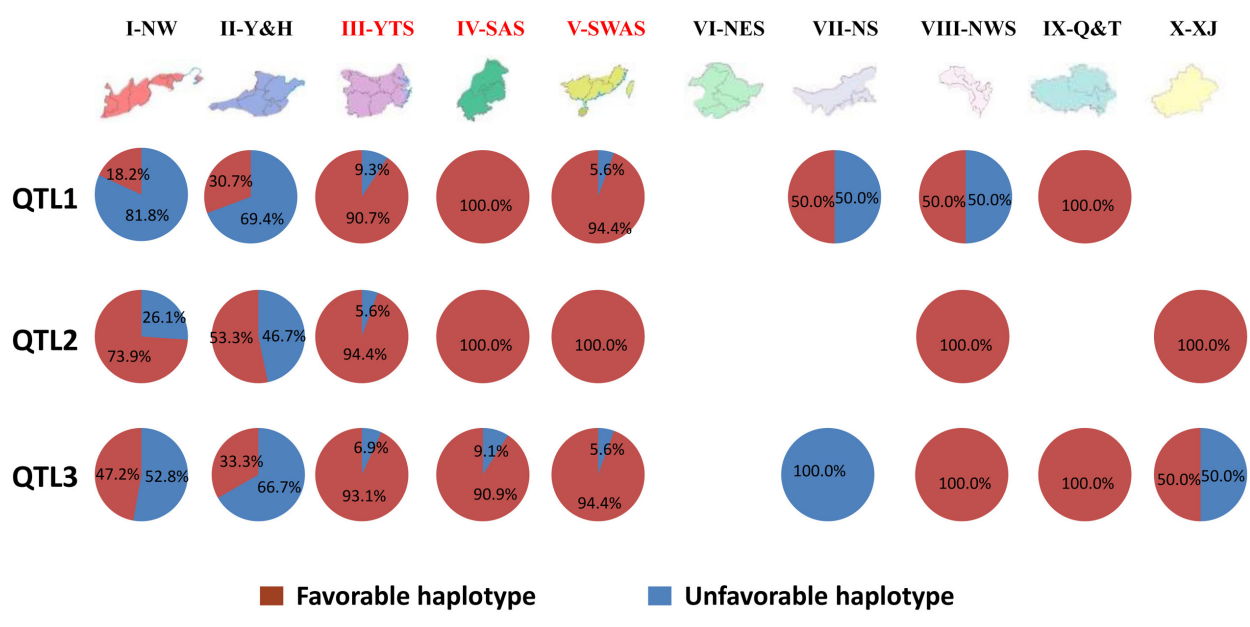

FIGURE 5 | Geographic distribution of haplotypes for the three main QTL in 10 Chinese Wheat-growing Zones.

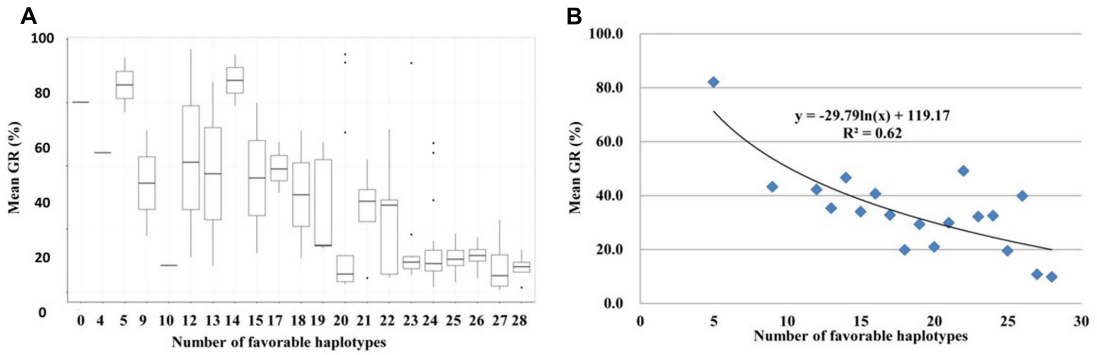

FIGURE 6 | Pyramiding effect of favorable haplotypes for 32 grain color related QTL (GCR-QTL) in red-grained landrace accessions. (A) Box plot for GR obtained by accessions grouped according to favorable haplotype numbers. The middle horizontal line within each box represents the mean GR and vertical lines mark the range from 5 to 95% of the total GR within each group. **(B)** Regression analysis with GR and the number of favorable haplotypes.

and 3D, as reported by Himi and Noda (2005) and Himi et al. (2011). *Tamyb10* is considered a strong candidate for the *R-1* gene, which regulates grain color and SD in wheat (Groos et al., 2002) by regulating both ABA and anthocyanin accumulation (Medina-Puche et al., 2014). Although *Tamyb10-D1* has not been mapped on the 'Chinese Spring' survey sequence, it is likely that the strong signal of *R-loci* on Chr 3D in the current study is *Tamyb10-D1*. Recently, a molecular investigation of allelic variation in *Tamyb10* provided information on grain color and GR in Chinese wheat (Wang et al., 2016) and *Aegilops tauschii* (Dong et al., 2015). In this study, two genes associated with grain color (*Tamyb10-A1* and *Tamyb10-D1*) were positioned in close proximity to PHS-resistant QTL (**Figure 3A**). However, a QTL was not detected in the region harboring the B genome ortholog *Tamyb10-B1*, which was detected in U.S. winter wheat (Lin et al., 2016). Two color-related genes showed the strongest signals, thus grain color appears to play an important role in PHS resistance in Chinese landraces (Flintham, 2000; Warner et al., 2000; Himi et al., 2002). In all test environments conducted in this study, the germination level of white-grained accessions was significantly higher than red-grained accessions. While red-grained wheat is generally more resistant to PHS (Probert, 2000; Warner et al., 2000), some white-grained accessions have been reported to display high levels of resistance (Torada and Amano, 2002; Bi et al., 2014). In this study, nine white-grained accessions displayed high levels of PHS resistance and were selected for breeding and further genetic studies.

The main QTL positioned on Chr 5D (QTL3) in this study was considered a novel genomic region potentially harboring loci for PHS resistance. This region seems promising for introgression into white-grained wheat cultivars because it does not co-locate with known genes influencing grain color.

Separate GWAS analyses for white- and red-grained accessions were performed in search for GCR-QTL that may have been masked by main QTL. Although a small number of white-grained accessions displayed PHS resistance, no GCR-QTL was detected within this set. This could be due to population size, as this set only contained 77 accessions. Regardless, the genetic architecture of PHS resistance in the identified white-grained accessions should be subjected to further investigation. When GWAS was carried out for the red-grained accessions, a total of 32 GCR-QTL were detected. Of these regions, almost two-thirds (20 GCR-QTL) have been reported in previous mapping studies. Interestingly, *Tamyb10* in the B and D genomes were not identified, only *Tamyb10* (GCR-QTL13). Although grain color genes contribute to PHS resistance in wheat, there is evidence for genetic factors that are not affected by grain color (Lin et al., 2016). Apart from GCR-QTL13, the remaining 31 GCR-QTL did not co-locate with known genes influencing grain color, thus present good candidates to improve PHS resistance in white-grained wheat. Surprisingly, red-grained landraces were enriched with favorable haplotypes for the GCR-QTL and the number of favorable haplotypes was highly correlated with GR (**Figure 6**). This provided further evidence that GCR-QTL significantly contribute to levels of PHS resistance in red-grained wheat accessions. Further, this highlights the genetic complexity of PHS resistance and the challenge plant breeders face to assemble genotypes incorporating adequate levels of resistance.

Certainly, the process of wheat domestication affected many traits, including SD (Huang et al., 2010a). But following domestication, wheat landraces were cultivated for 1000s of years under diverse eco-geographical conditions prior to modern breeding (Dwivedi et al., 2016; Riaz et al., 2016). Interesting links between the origin and spread of haplotypes associated with agro-climatic traits have been found in sorghum (Morris et al., 2013), rice (Weng et al., 2008; Huang et al., 2010b), and soybean (Zhou et al., 2015). PHS resistance traits and their underlying genes may have been subject to natural and artificial selection performed by farmers in specific environments. In this study, the frequency of favorable haplotypes for PHS resistance QTL varied among landraces originating from the 10 wheat grown zones of China. Favorable haplotypes occurred at high frequencies (92.8–97.0%) in landrace accessions sourced from mesic zones III-YTS, IV-SAS, and V-SWAS (**Figure 4**). Notably, PHS occurs more frequently in these zones compared to zones in northern and north-western China (Jin, 1996; He et al., 2000; Xiao et al., 2002; Yuan et al., 2003; Liu L. et al., 2013). Therefore, it seems PHS resistance was an important

trait for crop improvement in southern and eastern China where selective pressure for genes/loci controlling PHS resistance is apparent. The high frequency of favorable haplotypes in landraces originating from high rainfall environments highlights the importance of these haplotypes for future breeding efforts to develop cultivars incorporating PHS resistance.

AUTHOR CONTRIBUTIONS

YZ, HT, M-PC, and KD carried out experiments, analyzed the data, and contributed to writing; Z-XC, Z-YL, SG, Y-XL, Q-TJ, X-JL, Z-EP, Y-MW, and Y-LZ carried out experiments and analyzed the data. LH contributed to the analysis and writing for the association mapping; J-RW formulated the questions, designed and carried out experiments, analyzed the data and wrote the manuscript.

ACKNOWLEDGMENTS

The authors thank Drs. Lihui Li and Xiuquan Li (Chinese Academy of Agricultural Science) for plant materials (Chinese wheat landraces) support. This work was supported by the National Basic Research Program of China (2014CB147200), the National Natural Science Foundation of China (31571654 and 31171555). Dr. Jirui Wang thanks the National Supercomputer Centre in Guangzhou houses (SUN YAT-SEN University) for granting CPU-time on the Tianhe-2 (http://en.nscc-gz.cn/).

SUPPLEMENTARY MATERIAL

The Supplementary Material for this article can be found online at: http://journal.frontiersin.org/article/10.3389/fpls.2017.00401/full#supplementary-material

REFERENCES

Albrecht, T., Oberforster, M., Kempf, H., Ramgraber, L., Schacht, J., Kazman, E., et al. (2015). Genome-wide association mapping of preharvest sprouting resistance in a diversity panel of European winter wheats. *J. Appl. Genet.* 56, 277–285. doi: 10.1007/s13353-015-0286-5

Bandelt, H. J., Forster, P., and Röhl, A. (1999). Median-joining networks for inferring intraspecific phylogenies. *Mol. Biol. Evol.* 16, 37–48. doi: 10.1093/oxfordjournals.molbev.a026036

Barrero, J. M., Cavanagh, C., Verbyla, K. L., Tibbits, J. F., Verbyla, A. P., Huang, B. E., et al. (2015). Transcriptomic analysis of wheat near-isogenic lines identifies PM19-A1 and A2 as candidates for a major dormancy QTL. *Genome Biol.* 16, 93. doi: 10.1186/s13059-015-0665-6

Bewley, J. D., and Black, M. (1982). "Viability and longevity," in *Physiology and Biochemistry of Seeds in Relation to Germination*, eds J. D. Bewley and M. Black (Berlin: Springer), 1–59. doi: 10.1007/978-3-642-68643-6_1

Bi, H. H., Sun, Y. W., Xiao, Y. G., and Xia, L. Q. (2014). Characterization of DFR allelic variations and their associations with pre-harvest sprouting resistance in a set of red-grained Chinese wheat germplasm. *Euphytica* 195, 197–207. doi: 10.1007/s10681-013-0986-z

Bradbury, P. J., Zhang, Z., Kroon, D. E., Casstevens, T. M., Ramdoss, Y., and Buckler, E. S. (2007). TASSEL: software for association mapping of complex traits in diverse samples. *Bioinformatics* 23, 2633–2635. doi: 10.1093/bioinformatics/btm308

Cabral, A. L., Jordan, M. C., McCartney, C. A., You, F. M., Humphreys, D. G., MacLachlan, R., et al. (2014). Identification of candidate genes, regions and markers for pre-harvest sprouting resistance in wheat (*Triticum aestivum* L.). *BMC Plant Biol.* 14:340. doi: 10.1186/s12870-014-0340-1

Cao, L., Hayashi, K., Tokui, M., Mori, M., Miura, H., and Onishi, K. (2016). Detection of QTLs for traits associated with pre-harvest sprouting resistance in bread wheat (*Triticum aestivum* L.). *Breed. Sci.* 66, 260–270. doi: 10.1270/jsbbs.66.260

Chang, C., Feng, J. M., Si, H. Q., Yin, B., Zhang, H. P., and Ma, C. X. (2010). Validating a novel allele of viviparous-1 (Vp-1Bf) associated with high seed dormancy of Chinese wheat landrace, Wanxianbaimaizi. *Mol. Breed.* 25, 517–525. doi: 10.1007/s11032-009-9350-3

Chang, C., Zhang, H. P., Zhao, Q. X., Feng, J. M., Si, H. Q., Lu, J., et al. (2011). Rich allelic variations of Viviparous-1A and their associations with seed dormancy/pre-harvest sprouting of common wheat. *Euphytica* 179, 343–353. doi: 10.1007/s10681-011-0348-7

Chen, C. X., Cai, S. B., and Bai, G. H. (2008). A major QTL controlling seed dormancy and pre-harvest sprouting resistance on chromosome 4A in a Chinese wheat landrace. *Mol. Breed.* 21, 351–358. doi: 10.1007/s11032-007-9135-5

Dong, Z. D., Chen, J., Li, T., Chen, F., and Cui, D. Q. (2015). Molecular survey of *Tamyb10-1* genes and their association with grain colour and germinability in Chinese wheat and *Aegilops tauschii*. *J. Genet.* 94, 453–459. doi: 10.1007/s12041-015-0559-0

Dwivedi, S. L., Ceccarelli, S., Blair, M. W., Upadhyaya, H. D., Are, A. K., and Ortiz, R. (2016). Landrace germplasm for improving yield and abiotic stress adaptation. *Trends Plant Sci.* 21, 31–42. doi: 10.1016/j.tplants.2015.10.012

Earl, D. A., and vonHoldt, B. M. (2012). STRUCTURE HARVESTER: a website and program for visualizing STRUCTURE output and implementing the Evanno method. *Conserv. Genet. Resour.* 4, 359–361. doi: 10.1007/s12686-011-9548-7

Fakthongphan, J., Graybosch, R. A., and Baenziger, P. S. (2016). Combining ability for tolerance to pre-harvest sprouting in common wheat (*Triticum aestivum* L.). *Crop Sci.* 56, 1025–1035. doi: 10.2135/cropsci2015.08.0490

Falush, D., Stephens, M., and Pritchard, J. K. (2003). Inference of population structure using multilocus genotype data: linked loci and correlated allele frequencies. *Genetics* 164, 1567–1587..

Fieller, E. C., Hartley, H. O., and Pearson, E. S. (1957). Tests for rank correlation coefficients I. *Biometrika* 44, 470–481. doi: 10.1093/biomet/44.3-4.470

Finch-Savage, W. E., and Leubner-Metzger, G. (2006). Seed dormancy and the control of germination. *New Phytol.* 171, 501–523. doi: 10.1111/j.1469-8137.2006.01787.x

Flintham, J. E. (2000). Different genetic components control coat-imposed and embryo-imposeddormancy in wheat. *Seed Sci. Res.* 10, 43–50. doi: 10.1017/S0960258500000052

Fofana, B., Humphreys, D. G., Rasul, G., Cloutier, S., Brûlé-Babel, A., Woods, S., et al. (2009). Mapping quantitative trait loci controlling pre-harvest sprouting resistance in a red × white seeded spring wheat cross. *Euphytica* 165, 509–521. doi: 10.1007/s10681-008-9766-6

Groos, C., Gay, G., Perretant, M. R., Gervais, L., Bernard, M., Dedryver, F., et al. (2002). Study of the relationship between pre-harvest sprouting and grain color by quantitative trait loci analysis in a white × red grain bread-wheat cross. *Theor. Appl. Genet.* 104, 39–47. doi: 10.1007/s001220200004

He, Z. H., Rajaram, S., Xin, Z. Y., and Huang, G. Z. (2001). *A History of Wheat Breeding in China*. Texcoco: CIMMYT. Available at: libcatalog.cimmyt.org/download/cim/74633.pdf

He, Z. T., Chen, X. N., and Han, Y. P. (2000). Progress on preharvest sprouting resistance in white wheat. *J. Triticeae Crops* 20, 84–87.

Himi, E., Maekawa, M., Miura, H., and Noda, K. (2011). Development of PCR markers for *Tamyb10* related to R-1, red grain color gene in wheat. *Theor. Appl. Genet.* 122, 1561–1576. doi: 10.1007/s00122-011-1555-2

Himi, E., Mares, D. J., Yanagisawa, A., and Noda, K. (2002). Effect of grain colour gene (R) on grain dormancy and sensitivity of the embryo to abscisic acid (ABA) in wheat. *J. Exp. Bot.* 53, 1569–1574. doi: 10.1093/jxb/erf005

Himi, E., and Noda, K. (2005). Red grain colour gene (R) of wheat is a Myb-type transcription factor. *Euphytica* 143, 239–242. doi: 10.1007/s10681-005-7854-4

Huang, X., Schmitt, J., Dorn, L., Griffith, C., Effgen, S., Takao, S., et al. (2010a). The earliest stages of adaptation in an experimental plant population: strong

selection on QTLS for seed dormancy. *Mol. Ecol.* 19, 1335–1351. doi: 10.1111/j.1365-294X.2010.04557.x

Huang, X., Wei, X., Sang, T., Zhao, Q., Feng, Q., Zhao, Y., et al. (2010b). Genome-wide association studies of 14 agronomic traits in rice landraces. *Nat. Genet.* 42, 961–967. doi: 10.1038/ng.695

Hubisz, M. J., Falush, D., Stephens, M., and Pritchard, J. K. (2009). Inferring weak population structure with the assistance of sample group information. *Mol. Ecol. Resour.* 9, 1322–1332. doi: 10.1111/j.1755-0998.2009.02591.x

Imtiaz, M., Ogbonnaya, F. C., Oman, J., and van Ginkel, M. (2008). Characterization of quantitative trait loci controlling genetic variation for preharvest sprouting in synthetic backcross-derived wheat lines. *Genetics* 178, 1725–1736. doi: 10.1534/genetics.107.084939

Jaiswal, V., Mir, R. R., Mohan, A., Balyan, H. S., and Gupta, P. K. (2012). Association mapping for pre-harvest sprouting tolerance in common wheat (*Triticum aestivum* L.). *Euphytica* 188, 89–102. doi: 10.1007/s10681-012-0713-1

Jakobsson, M., and Rosenberg, N. A. (2007). CLUMPP: a cluster matching and permutation program for dealing with label switching and multimodality in analysis of population structure. *Bioinformatics* 23, 1801–1806. doi: 10.1093/bioinformatics/btm233

Jin, S. B. (1996). *Wheat in China*. Beijing: Chinese agricultural publisher.

Kato, K., Nakamura, W., Tabiki, T., Miura, H., and Sawada, S. (2001). Detection of loci controlling seed dormancy on group 4 chromosomes of wheat and comparative mapping with rice and barley genomes. *Theor. Appl. Genet.* 102, 980–985. doi: 10.1007/s001220000494

Kulwal, P., Ishikawa, G., Benscher, D., Feng, Z., Yu, L. X., Jadhav, A., et al. (2012). Association mapping for pre-harvest sprouting resistance in white winter wheat. *Theor. Appl. Genet.* 125, 793–805. doi: 10.1007/s00122-012-1872-0

Kulwal, P. L., Singh, R., Balyan, H. S., and Gupta, P. K. (2004). Genetic basis of pre-harvest sprouting tolerance using single-locus and two-locus QTL analyses in bread wheat. *Funct. Integr. Genom.* 4, 94–101. doi: 10.1007/s10142-004-0105-2

Kumar, A., Kumar, J., Singh, R., Garg, T., Chhuneja, P., and Gupta, P. K. (2009). QTL analysis for grain colour and pre-harvest sprouting in bread wheat. *Plant Sci.* 177, 114–122. doi: 10.1016/j.plantsci.2009.04.004

Leigh, J. W., and Bryant, D. (2015). Popart: full-feature software for haplotype network construction. *Methods Ecol. Evol.* 6, 1110–1116. doi: 10.1111/2041-210X.12410

Li, H., Peng, Z., Yang, X., Wang, W., Fu, J., and Wang, J. (2013). Genome-wide association study dissects the genetic architecture of oil biosynthesis in maize kernels. *Nat. Genet.* 45, 43–50. doi: 10.1038/ng.2484

Lin, M., Cai, S., Wang, S., Liu, S., Zhang, G., and Bai, G. (2015). Genotyping-by-sequencing (GBS) identified SNP tightly linked to QTL for pre-harvest sprouting resistance. *Theor. Appl. Genet.* 128, 1385–1395. doi: 10.1007/s00122-015-2513-1

Lin, M., Zhang, D., Liu, S., Zhang, G., Yu, J., Fritz, A. K., et al. (2016). Genome-wide association analysis on pre-harvest sprouting resistance and grain color in U.S. winter wheat. *BMC Genomics* 17:794. doi: 10.1186/s12864-016-3148-6

Liu, L., Wang, H. Q., and Chen, Z. G. (2013). Advances on Resistance to Pre-Harvest Sprouting in Wheat. *Crops* 4, 6–10.

Liu, S., and Bai, G. (2010). Dissection and fine mapping of a major QTL for preharvest sprouting resistance in white wheat Rio Blanco. *Theor. Appl. Genet.* 121, 1395–1404. doi: 10.1007/s00122-010-1396-4

Liu, S., Bai, G., Cai, S., and Chen, C. (2011). Dissection of genetic components of preharvest sprouting resistance in white wheat. *Mol. Breed.* 27, 511–523. doi: 10.1007/s11032-010-9448-7

Liu, S., Li, J., and Wang, Q. (2014). Germplasm screening for resistance to pre-harvest sprouting in southwest China. *Southw. China J. Agric. Sci.* 27, 931–937.

Liu, S., Sehgal, S. K., Li, J., Lin, M., Trick, H. N., Yu, J., et al. (2013). Cloning and characterization of a critical regulator for preharvest sprouting in wheat. *Genetics* 195, 263–273. doi: 10.1534/genetics.113.152330

Liu, S., Sehgal, S. K., Lin, M., Li, J., Trick, H. N., and Gill, B. S. (2015). Independent mis-splicing mutations in TaPHS1 causing loss of preharvest sprouting (PHS) resistance during wheat domestication. *New Phytol.* 208, 928–935. doi: 10.1111/nph.13489

Mares, D., Rathjen, J., Mrva, K., and Cheong, J. (2009). Genetic and environmental control of dormancy in white-grained wheat (*Triticum aestivum* L.). *Euphytica* 168, 311–318. doi: 10.1007/s10681-009-9927-2

Mares, D. J. (1983). Preservation of dormancy in freshly harvested wheat grain. *Crop Pasture Sci.* 34, 33–38. doi: 10.1071/AR9830033

Mares, D. J., and Mrva, K. (2001). Mapping quantitative trait loci associated with variation in grain dormancy in Australian wheat. *Crop Pasture Sci.* 52, 1257–1265. doi: 10.1071/AR01049

Mares, D. J., Mrva, K., Cheong, J., Williams, K., Watson, B., Storlie, E., et al. (2005). A QTL located on chromosome 4A associated with dormancy in white- and red-grained wheats of diverse origin. *Theor. Appl. Genet.* 111, 1357–1364. doi: 10.1007/s00122-005-0065-5

Medina-Puche, L., Cumplido-Laso, G., Amil-Ruiz, F., Hoffmann, T., Ring, L., Rodríguez-Franco, A., et al. (2014). MYB10 plays a major role in the regulation of flavonoid/phenylpropanoid metabolism during ripening of *Fragaria* × *ananassa* fruits. *J. Exp. Bot.* 65, 401–417. doi: 10.1093/jxb/ert377

Mohan, A., Kulwal, P., Singh, R., Kumar, V., Mir, R. R., Kumar, J., et al. (2009). Genome-wide QTL analysis for pre-harvest sprouting tolerance in bread wheat. *Euphytica* 168, 319–329. doi: 10.1007/s10681-009-9935-2

Mori, M., Uchino, N., Chono, M., Kato, K., and Miura, H. (2005). Mapping QTLs for grain dormancy on wheat chromosome 3A and the group 4 chromosomes, and their combined effect. *Theor. Appl. Genet.* 110, 1315–1323. doi: 10.1007/s00122-005-1972-1

Morris, G. P., Ramu, P., Deshpande, S. P., Hash, C. T., Shah, T., Upadhyaya, H. D., et al. (2013). Population genomic and genome-wide association studies of agroclimatic traits in sorghum. *Proc. Natl. Acad. Sci. U.S.A.* 110, 453–458. doi: 10.1073/pnas.1215985110

Nakamura, S., Abe, F., Kawahigashi, H., Nakazono, K., Tagiri, A., Matsumoto, T., et al. (2011). A wheat homolog of MOTHER OF FT AND TFL1 acts in the regulation of germination. *Plant Cell* 23, 3215–3229. doi: 10.1105/tpc.111.088492

Nakamura, S., and Toyama, T. (2001). Isolation of a VP1 homologue from wheat and analysis of its expression in embryos of dormant and non-dormant cultivars. *J. Exp. Bot.* 52, 875–876. doi: 10.1093/jexbot/52.357.875

Nyachiro, J. M. (2012). Pre-harvest sprouting in cereals. *Euphytica* 188, 1–5. doi: 10.1007/s10681-012-0779-9

Ogbonnaya, F. C., Imtiaz, M., Ye, G., Hearnden, P. R., Hernandez, E., and Eastwood, R. F. (2008). Genetic and QTL analyses of seed dormancy and preharvest sprouting resistance in the wheat germplasm CN10955. *Theor. Appl. Genet.* 116, 891–902. doi: 10.1007/s00122-008-0712-8

Osa, M., Kato, K., Mori, M., Shindo, C., Torada, A., and Miura, H. (2003). Mapping QTLs for seed dormancy and the Vp1 homologue on chromosome 3A in wheat. *Theor. Appl. Genet.* 106, 1491–1496. doi: 10.1007/s00122-003-1208-1

Pritchard, J. K., Stephens, M., and Donnelly, P. (2000). Inference of population structure using multilocus genotype data. *Genetics* 155, 945–959..

Probert, R. J. (2000). The role of temperature in the regulation of seed dormancy and germination. *Seeds* 261, 292. doi: 10.1079/9780851994321.0261

R Core Team (2014). *R: A Language and Environment for Statistical Computing*. Vienna: R Foundation for Statistical Computing.

Rajjou, L., Duval, M., Gallardo, K., Catusse, J., Bally, J., and Job, D. (2012). Seed germination and vigor. *Annu. Rev. Plant Biol.* 63, 507–533. doi: 10.1146/annurev-arplant-042811-105550

Rasheed, A., Wen, W., Gao, F., Zhai, S., Jin, H., and He, Z. (2016). Development and validation of KASP assays for genes underpinning key economic traits in bread wheat. *Theor. Appl. Genet.* 129, 1843–1860. doi: 10.1007/s00122-016-2743-x

Rasul, G., Humphreys, D. G., Brule-Babel, A., McCartney, C. A., Knox, R. E., and DePauw, R. M. (2009). Mapping QTLs for pre-harvest sprouting traits in the spring wheat cross 'RL4452/AC Domain'. *Euphytica* 168, 363–378. doi: 10.1007/s10681-009-9934-3

Rehman Arif, M. A., Neumann, K., Nagel, M., Kobiljski, B., Lohwasser, U., and Börner, A. (2012). An association mapping analysis of dormancy and pre-harvest sprouting in wheat. *Euphytica* 188, 409–417. doi: 10.1007/s10681-012-0705-1

Riaz, A., Hathorn, A., Dinglasan, E., Ziems, L., Richard, C., and Hickey, L. (2016). Into the vault of the Vavilov wheats: old diversity for new alleles. *Genet. Resour. Crop Evol.* 64, 531–544. doi: 10.1007/s10722-016-0380-5

Singh, R., Matus-Cádiz, M., Båga, M., Hucl, P., and Chibbar, R. N. (2010). Identification of genomic regions associated with seed dormancy in white-grained wheat. *Euphytica* 174, 391–408. doi: 10.1007/s10681-010-0137-8

Somyong, S., Ishikawa, G., Munkvold, J. D., Tanaka, J., Benscher, D., Sorrells, M. E., et al. (2014). Fine mapping of a preharvest sprouting QTL interval on chromosome 2B in white wheat. *Theor. Appl. Genet.* 127, 1843–1855. doi: 10.1007/s00122-014-2345-4

Su, J., Fan, S., Li, L., Wei, H., Wang, C., and Wang, H. (2016). Detection of favorable QTL alleles and candidate genes for lint percentage by GWAS in Chinese upland cotton. *Front. Plant Sci.* 7:1576. doi: 10.3389/fpls.2016.01576

Tan, M. K., Sharp, P. J., Lu, M. Q., and Howes, N. (2006). Genetics of grain dormancy in a white wheat. *Crop Pasture Sci.* 57, 1157–1165. doi: 10.1071/AR06101

Torada, A., and Amano, Y. (2002). Effect of seed coat color on seed dormancy in different environments. *Euphytica* 126, 99–105. doi: 10.1023/A:1019603201883

Torada, A., Ikeguchi, S., and Koike, M. (2005). Mapping and validation of PCR-based markers associated with a major QTL for seed dormancy in wheat. *Euphytica* 143, 251–255. doi: 10.1007/s10681-005-7872-2

Torada, A., Koike, M., Ogawa, T., Takenouchi, Y., Tadamura, K., Wu, J., et al. (2016). A causal gene for seed dormancy on wheat chromosome 4A encodes a MAP kinase kinase. *Curr. Biol.* 26, 782–787. doi: 10.1016/j.cub.2016.01.063

Turner, S. D. (2014). qqman: an R package for visualizing GWAS results using Q-Q and manhattan plots. *bioRxiv*. doi: 10.1101/005165

Wang, J., Liu, Y., Wang, Y., Chen, Z., Dai, S., Cao, W., et al. (2011). Genetic variation of Vp1 in Sichuan wheat accessions and its association with pre-harvest sprouting response. *Genes Genomics* 33, 139–146. doi: 10.1007/s13258-010-0125-3

Wang, W. Y., Barratt, B. J., Clayton, D. G., and Todd, J. A. (2005). Genome-wide association studies: theoretical and practical concerns. *Nat. Rev. Genet.* 6, 109–118. doi: 10.1038/nrg1522

Wang, Y., Wang, X. L., Meng, J. Y., Zhang, Y. J., He, Z. H., and Yang, Y. (2016). Characterization of Tamyb10 allelic variants and development of STS marker for pre-harvest sprouting resistance in Chinese bread wheat. *Mol. Breed.* 36:148. doi: 10.1007/s11032-016-0573-9

Warner, R. L., Kudrna, D. A., Spaeth, S. C., and Jones, S. S. (2000). Dormancy in white-grain mutants of Chinese Spring wheat (*Triticum aestivum* L.). *Seed Sci. Res.* 10, 51–60.

Weisstein, E. W. (2004). *Bonferroni Correction*. Available at: http://mathworld.wolfram.com/BonferroniCorrection.html.

Weng, J., Gu, S., Wan, X., Gao, H., Guo, T., and Su, N. (2008). Isolation and initial characterization of GW5, a major QTL associated with rice grain width and weight. *Cell Res.* 18, 1199–1209. doi: 10.1038/cr.2008.307

Xiao, S. H., Zhang, X. Y., Yan, C. S., and Lin, H. (2002). Germplasm improvement for preharvest sprouting resistance in Chinese white-grained wheat: an overview of the current strategy. *Euphytica* 126, 35–38. doi: 10.1023/A:1019679924173

Yuan, Y. P., Chen, X., and Xiao, S. H. (2003). Advances in the study on wheat pre-harvest sprouting. *Acta Tritical Crops* 3, 31.

Zhang, H. F., and Liu, R. Z. C. (1989). Studies on preharvest sprouting resistance in winter wheat and its determination. *Acta Agron. Sin.* 15, 116–122. doi: 10.1007/s13353-015-0286-5

Zhang, H. P., Chang, C., Xia, G. Y., Zhang, X. Y., Yan, C. S., Xiao, S. H., et al. (2010). Identification of molecular markers associated with seed dormancy in micro-core collections of Chinese wheat and landraces. *Acta Agron. Sin.* 36, 1649–1656. doi: 10.1016/S1875-2780(09)60077-8

Zhang, Y., Miao, X., Xia, X., and He, Z. (2014). Cloning of seed dormancy genes (TaSdr) associated with tolerance to pre-harvest sprouting in common wheat and development of a functional marker. *Theor. Appl. Genet.* 127, 855–866. doi: 10.1007/s00122-014-2262-6

Zhang, Y., Xia, X., and He, Z. (2017). The seed dormancy allele TaSdr-A1a associated with pre-harvest sprouting tolerance is mainly present in Chinese wheat landraces. *Theor. Appl. Genet.* 130, 81–89. doi: 10.1007/s00122-016-2793-0

Zhang, Z., Ersoz, E., Lai, C. Q., Todhunter, R. J., Tiwari, H. K., Gore, M. A., et al. (2010). Mixed linear model approach adapted for genome-wide association studies. *Nat. Genet.* 42, 355–360. doi: 10.1038/ng.546

Zhou, Z., Jiang, Y., Wang, Z., Gou, Z., Lyu, J., Li, W., et al. (2015). Resequencing 302 wild and cultivated accessions identifies genes related to domestication and improvement in soybean. *Nat. Biotechnol.* 33, 408–414. doi: 10.1038/nbt.3096

Conflict of Interest Statement: The authors declare that the research was conducted in the absence of any commercial or financial relationships that could be construed as a potential conflict of interest.

frontiers in Plant Science

ORIGINAL RESEARCH
published: 14 February 2018
doi: 10.3389/fpls.2018.00141

Genome-Wide Association Mapping for Tolerance to Preharvest Sprouting and Low Falling Numbers in Wheat

Shantel A. Martinez[1,2], Jayfred Godoy[2], Meng Huang[2], Zhiwu Zhang[1,2], Arron H. Carter[1,2], Kimberly A. Garland Campbell[1,2,3†] and Camille M. Steber[1,2,3*†]*

[1] Molecular Plant Sciences, Washington State University, Pullman, WA, United States, [2] Department of Crop and Soil Sciences, Washington State University, Pullman, WA, United States, [3] USDA-ARS Wheat Health, Genetics, and Quality Research Unit, Washington State University, Pullman, WA, United States

OPEN ACCESS

Edited by:
Jose Maria Barrero, Commonwealth Scientific and Industrial Research Organisation (CSIRO), Australia

Reviewed by:
Daryl John Mares, University of Adelaide, Australia
María Verónica Rodríguez, Instituto de Investigaciones Fisiológicas y Ecologicas Vinculadas a la Agricultura (IFEVA)—CONICET, Argentina

***Correspondence:**
Kimberly A. Garland Campbell
Kim.Garland-Campbell@ars.usda.gov
Camille M. Steber
camille.steber@ars.usda.gov

† These authors have contributed equally to this work.

Specialty section:
This article was submitted to Plant Breeding, a section of the journal Frontiers in Plant Science

Received: *31 October 2017*
Accepted: *25 January 2018*
Published: *14 February 2018*

Citation:
Martinez SA, Godoy J, Huang M, Zhang Z, Carter AH, Garland Campbell KA and Steber CM (2018) Genome-Wide Association Mapping for Tolerance to Preharvest Sprouting and Low Falling Numbers in Wheat. Front. Plant Sci. 9:141. doi: 10.3389/fpls.2018.00141

Preharvest sprouting (PHS), the germination of grain on the mother plant under cool and wet conditions, is a recurring problem for wheat farmers worldwide. α-amylase enzyme produced during PHS degrades starch resulting in baked good with poor end-use quality. The Hagberg-Perten Falling Number (FN) test is used to measure this problem in the wheat industry, and determines how much a farmer's wheat is discounted for PHS damage. PHS tolerance is associated with higher grain dormancy. Thus, breeding programs use germination-based assays such as the spike-wetting test to measure PHS susceptibility. Association mapping identified loci associated with PHS tolerance in U.S. Pacific Northwest germplasm based both on FN and on spike-wetting test data. The study was performed using a panel of 469 white winter wheat cultivars and elite breeding lines grown in six Washington state environments, and genotyped for 15,229 polymorphic markers using the 90k SNP Illumina iSelect array. Marker-trait associations were identified using the FarmCPU R package. Principal component analysis was directly and a kinship matrix was indirectly used to account for population structure. Nine loci were associated with FN and 34 loci associated with PHS based on sprouting scores. None of the *QFN.wsu* loci were detected in multiple environments, whereas six of the 34 *QPHS.wsu* loci were detected in two of the five environments. There was no overlap between the QTN detected based on FN and PHS, and there was little correlation between the two traits. However, both traits appear to be PHS-related since 19 of the 34 *QPHS.wsu* loci and four of the nine *QFN.wsu* loci co-localized with previously published dormancy and PHS QTL. Identification of these loci will lead to a better understanding of the genetic architecture of PHS and will help with the future development of genomic selection models.

Keywords: preharvest sprouting, falling number, seed dormancy, wheat, association mapping

INTRODUCTION

Rainy conditions before harvest can cause mature grain to initiate germination while still on the mother plant (Rodríguez et al., 2015). This problem, called preharvest sprouting (PHS), occurs in many cereal crops such as wheat (*Triticum aestivum* L.), barley (*Hordeum vulgare* L.), and sorghum (*Sorghum bicolor*) (Paterson and Sorrells, 1990; Gualano et al., 2007; Ullrich et al., 2009).

Germination is associated with α-amylase enzyme induction in order to mobilize starch reserves for use by the growing embryo (Clarke et al., 1984). This α-amylase induction during PHS in wheat grain leads to problems with poor end-use quality due to starch degradation. Thus, sprouted wheat grain is discounted in the marketplace.

The degree of PHS tolerance is associated with multiple environmental and genetic factors. Grain dormancy can account for up to 60% of variation in PHS tolerance, although spike morphology and epicuticular waxes are also associated with PHS response (King, 1984; King and Richards, 1984; DePauw and McCaig, 1991; King and von Wettstein-Knowles, 2000). Dormant seeds cannot germinate under favorable environmental conditions (light, moisture, and temperature) (Bewley and Black, 1994). Seeds are most dormant at physiological maturity, and then lose dormancy through a period of dry storage called after-ripening (Finkelstein et al., 2008). Dormancy can also be broken by moist chilling (called cold stratification) or seed coat scarification (Paterson et al., 1989; Finkelstein et al., 2008). The degree of wheat grain dormancy and PHS tolerance depends on environmental conditions both before and after the grain reaches physiological maturity. Grain dormancy is higher when the mother plant is exposed to cooler conditions during the maturation phase of grain development (Nakamura et al., 2011). Conversely, cold stratification of mature grain breaks dormancy. If rain and cold temperatures occur after physiological maturity, seed dormancy can be broken through cold stratification and grain is more likely to sprout. Thus, cold temperatures have opposite effects depending on whether they occur prior to or after the maturation date. Because seed dormancy is also broken through dry after-ripening, wheat also becomes more likely to sprout the longer unharvested mature grain stands dry in the field before it rains (Gerjets et al., 2010). Thus, variation in PHS tolerance also depends on when the rain occurred relative to maturation date. Higher PHS tolerance is associated with genetic loci that increase grain dormancy including red kernel color and the synthesis or response to the dormancy-inducing hormone ABA (abscisic acid) (Walker-Simmons, 1987; Flintham, 2000; Warner et al., 2000; Schramm et al., 2010; Himi et al., 2011; Jaiswal et al., 2012; Kulwal et al., 2012; Martinez et al., 2016). Since lack of red kernel color reduces dormancy, other genetic mechanisms supporting PHS tolerance must be identified and selected in wheat with white kernels.

The spike-wetting test is often used to assess PHS tolerance in breeding programs because it examines multiple variables affecting PHS (Paterson et al., 1989). In order to control for variation due to maturity date, intact spikes are harvested from the field at physiological maturity and allowed to dry after-ripen for the same number of days (5–14 days) before placing them under a greenhouse misting system. The use of intact spikes takes into account the effect of awns, erectness of the spike, gloom tightness, and head type (Pool and Patterson, 1958; Ibrahim, 1966; Hong, 1979; King and Richards, 1984). Spikes are assigned a sprouting score using a scale based on visible germination and post-germinative growth throughout the spike (McMaster and Derera, 1976). The sprouting scores of McMaster and Derera (1976) actually reflect three biological stages: (1) initial germination or the first appearance of roots (scores 1-5), (2) coleoptile emergence (scores 6-8), and (3) seedling growth (scores 9-10). Other methods for assessing PHS tolerance include plating assays to assess degree of seed dormancy, the Falling Numbers test (see below), and variations on the spike-wetting test (Paterson et al., 1989; Kumar et al., 2009; Zhang et al., 2014; Jiménez et al., 2016; Zhou et al., 2017).

Damage due to α-amylase induction from PHS is measured in the wheat industry using the Hagberg-Perten Falling Numbers (FN) test (Perten, 1964). During the FN test, a slurry of wheat meal and water is mixed while being heated to 100°C. Then the FN machine measures the time in seconds (sec) that it takes for a stirrer to fall through the slurry. The higher the α-amylase level, the thinner the slurry, allowing the stirrer to fall faster resulting in a lower FN. If the FN is below 300 s, then the farmer receives significantly less money for his/her grain. Because some studies have shown a significant correlation between FN and sprouting scores, one might expect spike-wetting tests and FN to map similar PHS tolerance loci (reviewed by DePauw et al., 2012). However, this has not been directly tested.

Here we present a genome-wide association mapping study (GWAS) for PHS tolerance in white wheat based on sprouting scores and FN. A large panel of 469 white wheat lines representing six northwestern U.S. breeding programs was examined over multiple environments in order to characterize the genetic architecture of PHS tolerance/susceptibility. The goal was to identify quantitative trait nucleotides (QTN) associated with PHS tolerance in white wheat breeding programs, while examining the phenotypic connection between FN and spike-wetting test scores.

MATERIALS AND METHODS

Plant Materials

This study used a mapping panel of 469 winter wheat accessions, consisting of advanced soft white breeding lines and cultivars from US Pacific Northwest breeding programs (Supplementary Table 1; Supplementary Figure 1). The accessions included 36% club (*T. aestivum* ssp *compactum*) genotypes with compact spike morphology and 64% soft white genotypes with lax spike morphology. The same panel was recently analyzed for soil acidity, aluminum tolerance, Cephalosporium stripe resistance, and stripe rust resistance (Froese and Carter, 2016; Froese et al., 2016; Liu et al., 2017).

Field Research Environments

The mapping panel was grown as 1.5 m long headrows at Central Ferry, WA in 2014, 2015, and 2016 (C14, C15, C16), or as 8 m^2 plots at the Washington State University Spillman Agronomy Farm in Pullman, WA in 2014, 2015, and 2016 (P14, P15, P16) using recommended agronomic practices for those locations. The panel was also grown as headrows in Pullman, WA in 2013 (P13). Heading dates from the Pullman 2014 environment were determined after 50% of the plot reached full spike emergence from the boot. **Table 1** lists the planting dates and harvest dates for each environment. Spikes were harvested at physiological maturity, right after the peduncle turned yellow,

TABLE 1 | Environments tested for preharvest sprouting traits. For the **(A)** Falling Numbers test (seconds) and the **(B)** spike-wetting test (sprouting score), planting dates, harvest dates, and general statistics are reported.

Location[a]	Year	Planting Date	Harvest date[b]		Rain event precipitation	Rain event temperature	n[c]	t rep[d]	Mean ± SD[e]	Range (min/max)
			PM	HM	cm	°C				
(A)										
Pullman	2013	–[f]	–	Aug 15, 2013	0.43	22 ± 3	459	1	379 ± 55	88/504
Central Ferry	**2014**	Oct 2, 2013	–	Aug 6, 2014	1.91	26 ± 5	458	2	331 ± 39	202/538
Pullman	**2015**	Oct 8, 2014	–	Aug 1, 2015	0.00	–	464	2	326 ± 31	187/410
Central Ferry	**2015**	Oct 1, 2014	–	Jul 31, 2015	3.80	31 ± 2	397	2	389 ± 55	111/537
Central Ferry	2016	Oct 13, 2015	–	Jul 14, 2016	1.80	71 ± 2	426	2	347 ± 54	154/538
(B)										
Pullman	2014	Oct 10, 2013	Jul 11–18, 2014	–	–	–	427	5	3.9 ± 1.9	1/10
Central Ferry	**2014**	Oct 2, 2013	Jun 30–Jul 8, 2014	–	–	–	230	5	4.2 ± 1.7	1/9
Pullman	**2015**	Oct 8, 2014	Jul 1–10, 2015	–	–	–	416	5	4.05 ± 2.2	1/10
Central Ferry	**2015**	Oct 1, 2014	Jun 15–25, 2015	–	–	–	275	5	5.8 ± 2.3	1/10
Pullman	2016	Oct 12, 2015	Jul 15–22, 2016	–	–	–	437	5	6.5 ± 1.9	1/10

[a] *Pullman, WA and Central Ferry, WA. Bold environments had both the FN and spike-wetting test conducted whereas the other environments had either the FN or spike-wetting test conducted.*

[b] *FN samples were harvested at harvest maturity (HM) whereas spike-wetting test samples were harvested at physiological maturity (PM).*

[c] *Number (n) of accessions harvested and conducted in the FN and sprouting tests.*

[d] *Technical (t) replicates used for each test and environment.*

[e] *Mean and standard deviation (SD) were calculated; Sprouting scores from Day 5 are reported.*

[f] *Planting date was not recorded.*

for the spike-wetting test (see below) only in Pullman 2014, 2015, and 2016 and Central 2014 and 2015.

Reduced FN was examined in field-grown material after PHS induced either by natural or artificial rain events. PHS-inducing natural rain events occurred after physiological maturity in Pullman 2013 and Central Ferry 2016. Therefore, these two environments were not used for spike-wetting tests, since the material was already sprouted. In Pullman 2013, rain occurred over 3 consecutive days with precipitation amounts of 0.38, 0.025, and 0.025 cm, and high temperatures of 22.8, 18.2, and 23.8°C, respectively (AgWeatherNet, 2016 weather.wsu.edu). Central Ferry 2016 received 1.8 cm of precipitation over 4 days with an average maximum temperature of 17°C. Artificial rain was used to induce PHS in Central Ferry 2014 and 2015 using overhead sprinkler irrigation at 2 weeks past the average physiological maturity date of the trial (precipitation = 1.91, 3.8 cm, average maximum temperature = 26 and 31°C, respectively). Approximately, 0.64 cm was applied daily over 3 days in order to induce mild sprouting. Pullman 2015 was included in the analysis as a "no event" control because there was no natural or artificial rain event after physiological maturity. Grain was harvested from plots 2–3 weeks after physiological maturity for FN tests (see below) when grain moisture was <12%. In Pullman, single plot replicates were harvested using a Wintersteiger Classic small plot combine (Wintersteiger Ag, Ried im Innkreis, Austria). In Central Ferry, one headrow was hand-harvested with a sickle per accession and machine threshed using the Vogel headrow thresher (Bill's Welding, Pullman, WA). All harvested grain was cleaned of chaff using a gravity cleaner.

Preharvest Sprouting Evaluation

Spike-wetting tests were used to evaluate preharvest sprouting tolerance of field samples (Anderson et al., 1993). Intact spikes were hand-harvested from the field at physiological maturity, and allowed to dry after-ripen for the 5 days before storing at −15°C to maintain dormancy until tests were conducted (within 2–4 months). A representative set of spikes were tested for moisture content at physiological maturity, following 5 d of after-ripening, and after storage at −15°C, and found to be an average of 31, 14, and 10%, respectively. Spike-wetting tests were conducted in a greenhouse with a 16 h day/8 h night photoperiod and 22–25°C day and 16°C night temperature. Supplemental lighting was used to maintain the photoperiod with a light intensity of 300–400 $\mu mol/m^2/s$. Spikes were misted for 6 s every minute. The rare moldy spikes were thrown out of the experiment. Sprouting scores based on the McMaster and Derera (1976) 1–10 scale were determined every 24 h for 7 days, except that the "11" value was not used. Note that no sprouting was observed until day 3 of each experiment. Since the greenhouse misting system could test a maximum of 194 genotypes at a time, each environment had to be tested over multiple weeks. Two PHS tolerant controls, "Brevor" and "Clark's Cream," and two PHS susceptible controls, "Greer" and "Bruneau," were included in every experiment as a check for consistency (Walker-Simmons, 1987; Tuttle et al., 2015). Spikes were arranged in a randomized order, including five technical replicates (i.e., five spikes) for each genotype.

Analyses of the spike-wetting tests were performed using sprouting scores and a sprouting index designed to give more weight to earlier than later sprouting. Sprouting index (SI) was calculated as $(7 \times s_{day1} + 6 \times s_{day2} \ldots + 1 \times s_{day7})/(7 \times n)$

where s is the sprouting score on each day and n is the maximum sprouting score. SI ranged from 0 to 1, where an SI of 1 indicated that the spike reached 100% highly sprouted by day 1 of misting. For the day 3, 4, 5, 6, and 7 sprouting scores and for the SI of each accession, best linear unbiased predictors (BLUPs) were calculated within each environment over the five technical replicates using the MIXED procedure in SAS/STAT v9.4 (Piepho et al., 2008). Furthermore, the week the accession was tested and the tray location in the misting system were used as covariates in the model and accessions were treated as random effects.

Falling Number Evaluation

The Hagberg-Perten FN test was conducted using cleaned machine-threshed grain from Central Ferry, WA in 2014, 2015, and 2016 and from Pullman, WA in 2013 and 2015 (**Table 1**). FN can gradually increase during storage at higher temperatures (Ji and Baik, 2016). Grain was stored in sealed containers at −15°C to reduce problems with increasing FN. The FN test was conducted according to the ICC standard No. 107/1 (1995) and the AACC Method 56-81.03A (1999) expect that a 25 g sample was used to represent a plot or headrow rather than a 250 g sample used to represent a field. Twenty-five grams of grain was ground to meal using a Udy Cyclone Sample Mill with a 0.5 mm screen, and stored in air-tight 2 oz jars. Meal moisture content was averaged over four random samples, and applied to a subset of 48 samples. The sample weight used for the test was adjusted for moisture in order to be equivalent to 7 g of meal at 14% moisture. After 25 mL of distilled water was added to a sample, it was placed in a shaker for 5 s, then placed in a Perten Falling Number machine (Model 1600 or 1700). The FN machine determines the time needed for a stirrer to fall to the bottom of the tube after stirring and heating the samples for 60 s (minimum FN is 60 s). A lower FN is indicative of more α-amylase digestion, leading to lower gelling capacity. The FN was corrected for an altitude of 2500 ft (762 m) using FGIS Directive 9180.3 (2009). The material was examined using two technical replicates per accession with the exception of Pullman 2013, which only had one technical replicate. Each technical replicate was run on different days in 2014, within 5 min of one another in 2015, and side-by-side in 2016.

BLUPs for FN were also calculated over the artificial rain environments, the natural rain environments, and the no-rain event environment. Due to each year and environment having a different rain or no-rain event, we did not analyze BLUPs over all years or all environments (Supplementary Figure 2). An analysis of variance between accessions was performed using the MIXED procedure in SAS/STAT v9.4. Covariates were added to the analysis when relevant and included the individual who ran the test, the FN Machine used, and the seed-moisture sample subset (sets of 48 milled and tested together).

Spearman's significant rank correlations between the FN and the sprouting scores were conducted using the CORR procedure in SAS/STAT v9.4 (Supplementary Table 2). Since this is an association panel, the genotypic repeatability (R^2), rather than the heritability (H^2), was calculated using the lme4 package v1.1-13 in R (Campbell and Lipps, 1998; Bates et al., 2015). For the repeatability calculations, genotypes and covariates were considered to be random effects, whereas FN, sprouting score, or SI was used as the dependent variable.

Genotyping

DNA was harvested and extracted as described in Froese and Carter (2016). Extracted DNA was genotyped using the Illumina Infinium iSelect 90K SNP array, and polymorphic markers were identified and curated using GenomeStudio v2011.1 (Illumina) (Wang et al., 2014). Monomorphic markers were filtered out based on the criteria of only having 0 or 1 accession with an alternate allele (out of 469). Markers with 20% or more missing data and minor allele frequency (MAF) <5% were excluded from the analysis. A consensus map consisting of SNP markers were used to align chromosome locations of polymorphic markers (Wang et al., 2014). Genetic locations of unmapped (unk for unknown) markers were cross referenced with the GrainGenes database and are reported, without reference to a cM position on a chromosome (www.graingenes.org). Missing values for markers with published locations were imputed using default parameters in BEAGLE v3.3.2 (Browning and Browning, 2016). This resulted in a total of 15,229 polymorphic markers, of which 12,681 had known locations covering all chromosomes.

Genome-Wide Association Study

The GAPIT R package identified three principal component sub-groups associated with market class and breeding program of origin in the mapping panel (Tang et al., 2016). Variances captured by the first three principal components (PCs) accounted for 29.6% of the total variance among the genotypes (Liu et al., 2017). In order to account for the presence of population structure, the top three PCs were fitted into the model as fixed effects (Supplementary Figure 1).

A portion of the data were analyzed using multiple statistical models, and the best statistical method selected based on how the observed *p*-values exceeded the null expectation on the Q-Q plot from GAPIT and FarmCPU (Lipka et al., 2012; Liu et al., 2016; Tang et al., 2016). Using the Pullman 2014 FN and sprouting score phenotypic data, a general linear model (GLM), mixed linear model (MLM), compressed mixed linear model (CMLM), SUPER model, and FarmCPU model were compared (Zhang et al., 2010; Wang et al., 2014; Liu et al., 2016; Supplementary Figure 3). The results indicated that the FarmCPU model performed better than the other models. All subsequent genome-wide association analyses used only the FarmCPU model.

FarmCPU default parameters were used except that the "optimum" bin method with default range and interval parameters was used instead of the "static" method. The FN trait least squares means (LSMeans) and the sprouting score BLUPs were used as dependent variables in this GWAS (Supplementary Figure 3). Markers were identified as significantly associated with the trait after a 1% Bonferroni multiple test correction ($p < 2.85\text{E-}07$; $-\log_{10}(p) > 6.55$).

The proportion of explained phenotypic variance was calculated as follows:

$$r^2 = \frac{\sum_{i=1}^{n} (\hat{y}_i - \hat{y})^2}{\sum_{i=1}^{n} (y_i - y)^2}$$

where y_i is observed phenotype value, $\hat{y}_i$ is the estimated phenotype value from a multiple linear regression model that was fitted to all significant SNPs as an independent variable with fixed effect.

Linkage disequilibrium (LD) was calculated using JMP software v6.0 (SAS, Cary, NC). LD of significant markers were used to estimate boundaries of potential quantitative trait loci (QTL) using the criteria of LD ($R^2 > 0.2$), chromosome location (cM) based on Wang et al. (2014), correlation between markers, and marker-trait information among the significant markers. For each designated QTL, the marker with the strongest association with either FN or sprouting scores was reported. Criteria for a strong association include: (a) phenotypic variation explained by the marker (r^2); (b) allelic effect; and (c) marker p value.

Tolerant nucleotides of each significant marker were used to determine the pyramiding effect of PHS tolerant loci. A linear model regression was applied to the phenotypic estimates and number of favorable loci per accession. "Favorable" loci nucleotides were those that lowered the sprouting score or increased the FN. Pearson's correlation coefficients were calculated between the trait and number of favorable loci using the "cor" function in R v.3.2.5.

Comparison of QTN Locations with Previously Reported PHS Genes and QTL

A comparison of identified QTN with previous studies was performed using the integrated map of Maccaferri et al. (2015) that includes SSR markers, 9k SNP markers, 90k SNP markers, Synthetic × Opata DH GBS markers, and the Diversity Array Technology markers (Supplementary Table 3; Akbari et al., 2006; Cavanagh et al., 2013; Saintenac et al., 2013; Wang et al., 2014). Maccaferri et al. (2015) converted distances in cM into relative % length distances by dividing them by total chromosome length. The approximate relative positions of QTN were estimated based on known marker positions. Note that the LD of QTL from other studies were not recalculated.

RESULTS

Environmental Response of PHS-Related Traits in Soft White Wheat

A panel of 469 soft white wheat accessions was evaluated for PHS tolerance based on spike-wetting tests and FN following rain in the field. FN was examined in five environments over 4 years and at two locations. The mean FN ranged from 326 to 389 s for all environments (**Table 1**). Increasing α-amylase activity tends to correlate with decreasing FN below 325 s (Perten, 1964; Yu et al., 2015). All environments had multiple accessions below the 325 s threshold (ranging from 36 to 234 accessions; **Figure 1**; Supplementary Figure 2). Natural sprout-inducing rain events occurred in Pullman 2013 and Central Ferry 2016. Artificial rain was applied to induce sprouting in Central Ferry in 2014 and 2015. Pullman 2013, and Central Ferry 2015 and 2016 had wide variation for FN, but Central Ferry 2015 had very few accessions below 325 s. The Pullman 2015 data was included in the analysis as a "no-rain-event" control in an attempt to differentiate PHS-induced differences in FN from differences in FN due to starch or protein composition (AgWeatherNet, 2016 weather.wsu.edu). Pullman 2015 had 234 accessions below 325 s but had lower variation than other environments. This is likely due to poor grain filling since that season had unusually high summer temperatures. QTN mapped based on FN data will be referred to as *QFN.wsu*.

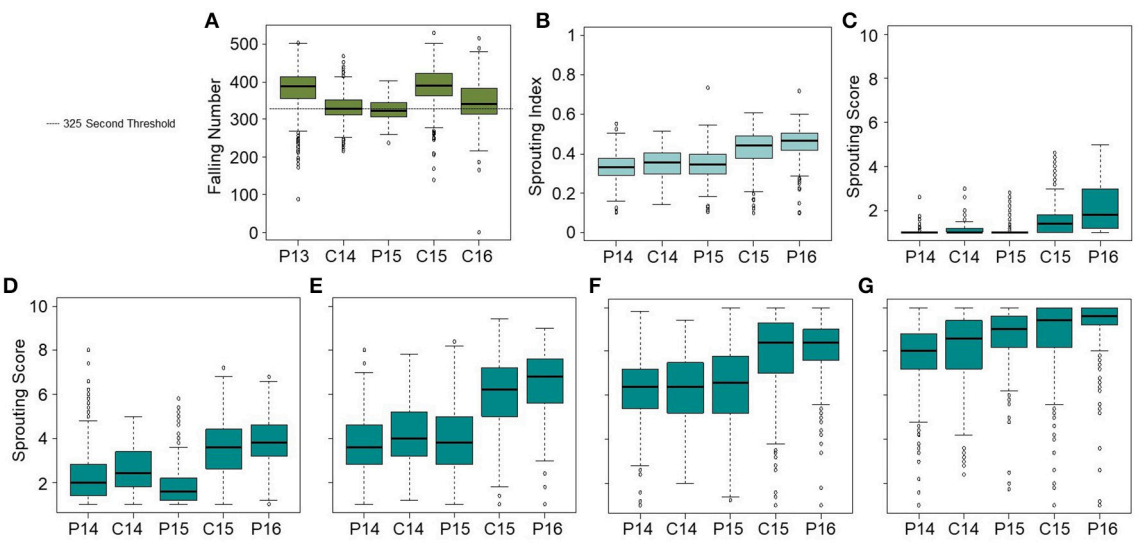

FIGURE 1 | FN and PHS distributions. **(A)** FN distributions across environments including the natural rain events in Pullman 2013 (P13) and Central Ferry 2016 (C16), an artificial rain event in Central Ferry 2014 (C14) and 2015 (C15), and an environment without rain in Pullman 2015 (P15). Spike-wetting tests were performed for Pullman 2014 (P14) as well as C14, P15, C15, and Pullman 2016 (P16). **(B)** Sprouting index was calculated over all 7 days of misting. Sprouting scores after **(C)** 3, **(D)** 4, **(E)** 5, **(F)** 6, and **(G)** 7 days of misting were based on a 1-10 scale.

In spike-wetting tests, environments had similar effects on results regardless of whether we examined sprouting scores or the sprouting index. For example, Central Ferry 2015 and Pullman 2016 consistently showed the highest level of sprouting (**Figure 1**; **Table 1**). BLUP analysis was performed in order to reduce environmental variation in sprouting scores prior to mapping (Supplementary Figure 2). BLUPs calculated over all environments were highly correlated over days of sprouting and with the sprouting index (SI) (Supplementary Table 2A). Based on the range of values, we expected to have enough variation to map QTN associated with PHS tolerance due to reduced germination or slower post-germinative growth. For ease of communication, QTN identified based on sprouting scores or SI will be referred to collectively as PHS loci or *QPHS.wsu*.

PHS Trait Correlations

Correlations were used to examine whether genotypic differences in FN or sprouting scores were consistent between environments, and to examine whether FN and sprouting scores were related. The FN values showed a weak but significant positive correlation between environments, ranging from 0.23 to 0.46 ($p < 0.001$; **Table 2**). Sprouting scores were positively correlated between environments, but not always significantly (Supplementary Tables 2B–G). Day 3 sprouting scores showed the least significant correlation between environments, whereas day 5 and day 6 sprouting scores showed significant positive correlations between environments. SI had the strongest and most significant correlation between environments. The genotypic repeatability of FN ($R^2 = 0.50$) was greater than sprouting scores ($R^2 < 0.31$), especially when covariates like operator, machine, subset, and replicate, were taken into account (**Table 3**). When repeatability was calculated on a line mean basis, both traits had similar repeatability in our experiments (FN $R^2 = 0.67$; SI $R^2 = 0.70$). The genotypic repeatability of sprouting was highest when spikes were misted longer or when all measurements were integrated in the SI (**Table 3**). Because seed germination induces α-amylase, which in turn lowers FN, we expected higher sprouting scores to negatively correlate with lower FN, but this was not the case (**Table 2**). BLUPs for SI generated over all days scored showed the strongest and most significant negative correlation with FN in years when natural sprouting events occurred (**Table 2B**). In Central Ferry 2015, the FN did not correlate to the sprouting scores and SI. Overall, 4 days of misting had the highest correlation across all FN environments.

Association Analysis for Falling Numbers

GWAS for FN was performed using FarmCPU within each environment because environments varied drastically. All environments fit the FarmCPU association mapping model (Supplementary Figure 4). However, Central Ferry 2015 showed no significant marker-trait associations, regardless of which model was used for GWAS (Supplementary Figure 3D). Nine significant QTN associated with FN were mapped on chromosomes 4A, 5A, 5D, 7A, and 7B (**Table 4**). The three QTN identified without rain in Pullman 2015 likely represent grain characteristics that are independent of PHS. The remaining QTN were identified in natural rain events. The QTN detected on chromosomes 6D ($-\log_{10}(p) = 5.88$) and 7A ($-\log_{10}(p) = 6.17$) in Central Ferry 2014 were just below the stringent threshold for significance ($-\log_{10}(p) = 6.55$). *QFN.wsu-7A.1* and *QFN.wsu-7B.2* had the largest effects, increasing FN by 26 and 27 s, respectively. *QFN.wsu-7A.2* had the highest significance ($-\log_{10}(p) = 12.36$) and had an 8 s effect. In order to reduce the effect of loci unrelated to PHS tolerance on the GWAS, the data were re-analyzed with 400 s set as the maximum possible FN. When this was done, none of the nine *QFN.wsu* were detected and two unique significant QTN, *QFN.wsu-6A* and *QFN.wsu-7A.3* were identified in Central Ferry 2016 (Supplementary Table 4). These two QTN had large effects, increasing FN by 17 and 13 s, respectively, but only explained 1% of the phenotypic variation. A GWAS was also conducted for heading date from Pullman

TABLE 2 | Rank correlation coefficients for **(A)** FN LSMeans across environments and **(B)** PHS score BLUPs compared to FN environments.

(A)	FN:	P13[a]	C14	P15	C15		
FN	C14	0.29**					
	P15	0.23**	0.42**				
	C15	0.23**	0.29**	0.29**			
	C16	0.33**	0.46**	0.30**	0.34**		
(B)	**PHS:**	**3 days**	**4 days**	**5 days**	**6 days**	**7 days**	**SI**
FN	P13	−0.16**	−0.24**	−0.17**	−0.18**	−0.20**	−0.21**
	C14	−0.07	−0.09*	−0.06	−0.09	−0.10*	−0.10*
	P15	−0.07	−0.13*	−0.12*	−0.12*	−0.17**	−0.15**
	C15	−0.09	−0.04	0.00	0.01	0.00	−0.01
	C16	−0.17**	−0.19**	−0.18**	−0.17**	−0.17**	−0.19**

*Represents a p-value ≤ 0.05 and **represents a p-value ≤ 0.001.
[a]Environments Pullman (P) and Central Ferry (C).

TABLE 3 | Genotypic repeatability (R^2) of FN, spouting scores, and SI across all environments.

Trait	Simple R^{2a}	Covariate R^{2b}	Line mean basis R^{2c}
FN	0.197	0.500	0.667
PHS d3 [d]	0.109	0.145	0.459
PHS d4	0.163	0.240	0.612
PHS d5	0.151	0.214	0.577
PHS d6	0.229	0.276	0.656
PHS d7	0.218	0.230	0.599
SI	0.228	0.315	0.697

[a]*Genetic and environmental variances were calculated using a simple y ∼ x model with x (genotypes) as a fixed effect and repeatability* $R^2 = V_g / (V_g - V_e)$ *was calculated.*
[b]*Genetic and environmental variances were calculated using a simple y ∼ x + covariates model with x (genotypes) and covariates (time, machine, operator, etc.) as a fixed effect.*
[c]*Repeatability* $R^2 = V_g/(V_g - (V_e/n))$ *was expressed by a line mean basis by dividing the environmental variance* (V_e, *residuals*) *with the number of technical reps (n; FN = 2 and spike-wetting test = 5).*
[d]*Sprouting score (PHS) on days (d) 3 through 7.*

TABLE 4 | Loci significantly associated with Falling Numbers (FN), early preharvest sprouting (PHS) scores (days 3–4), 5 days of misting, late PHS scores (days 6–7), and PHS sprouting index (SI).

QTL[a]	Marker	Chr[b]	cM[b]	–log10(*p*)	maf	Effect[c]	r^2	Environment	Favorable Allele[d]
*QFN.wsu-4A**	IWB1884	4A	152	6.63	0.48	10.28	0.00	C16 FN	**A**/C
*QFN.wsu-5A.1**	IWB60191	5A	23	7.27	0.27	7.53	0.00	P15 FN	**A**/G
QFN.wsu-5A.2	IWB9800	5A	141	7.77	0.20	7.43	0.00	P15 FN	**A**/G
QFN.wsu-5D	IWB36060	5D	202	6.11	0.35	11.70	0.08	P13 FN	A/**C**
QFN.wsu-7A.1	IWB22966	7A	35	8.34	0.06	26.09	000	P13 FN	A/**G**
QFN.wsu-7A.2	IWA334	7A	126	12.36	0.41	7.99	0.01	P15 FN	A/**C**
QFN.wsu-7B.1	IWB39063	7B	162	7.91	0.48	10.88	0.01	C16 FN	A/**G**
QFN.wsu-7B.2	IWB75387	7B	–	6.15	0.09	27.35	0.00	P13 FN	A/**C**
QFN.wsu-unk	IWB37658	unk	–	6.82	0.09	15.49	0.00	C16 FN	T/**C**
QPHS.wsu-1A.1	IWB2320	1A	82	6.73	0.15	−0.04	0.00	P14 d3	**T**/C
QPHS.wsu-1A.2	IWB6759	1A	155	11.70	0.47	−0.31	0.15	P14 d3	**A**/G
	IWB77968	1A	155	12.72	0.47	−0.02	0.10	P14 d3	**A**/G
QPHS.wsu-1B.2	IWB64868	1B	135	9.00	0.15	−0.40	0.17	C14 d4	**A**/G
	IWB31676	1B	137	8.18	0.08	−0.37	0.00	P16 d3	**A**/G
QPHS.wsu-2A.1	IWB42693	2A	25	6.87	0.22	−0.16	0.02	C15 d3	**T**/G
QPHS.wsu-2D	IWB7652	2D	52	10.03	0.37	−0.46	0.00	C14 d4	T/**C**
	IWA8544	2D	50	8.73	0.46	−0.28	0.01	P16 d3	**A**/G
	IWA8544	2D	50	9.12	0.46	−0.32	0.07	P16 d4	**A**/G
QPHS.wsu-3A.2	IWB50719	3A	68	6.71	0.14	−0.29	0.04	C14 d4	A/**G**
QPHS.wsu-4A.1	IWA7535	4A	58	8.57	0.05	−0.07	0.03	P14 d3	A/**G**
QPHS.wsu-4B.2	IWB21707	4B	75	8.93	0.10	−0.42	0.07	P14 d4	A/**G**
*QPHS.wsu-4B.3**	IWB22055	4B	101	6.57	0.08	−0.37	0.00	P16 d3	A/**G**
QPHS.wsu-5B.1	IWB31067	5B	26	8.75	0.08	−0.06	0.01	P14 d3	T/**G**
QPHS.wsu-7B.1	IWB54418	7B	3	7.46	0.03	−0.26	0.01	P16 d3	A/**G**
*QPHS.wsu-1B.1**	IWB22868	1B	31	7.88	0.18	−0.30	0.01	P14 d5	**T**/C
QPHS.wsu-2D	IWB46396	2D	54	9.63	0.39	−0.49	0.02	C14 d5	**A**/G
QPHS.wsu-3B.2	IWA6185	3B	62	6.55	0.44	−0.23	0.01	P14 d5	A/**G**
QPHS.wsu-4A.2	IWB54609	4A	66	7.30	0.17	−0.35	0.01	P16 d5	**A**/G
*QPHS.wsu-5A.2**	IWB10250	5A	70	9.13	0.32	−0.44	0.03	P15 d5	**T**/C
QPHS.wsu-5B.3	IWB73511	5B	129	6.73	0.30	−0.28	0.01	P16 d5	A/**G**
*QPHS.wsu-6B**	IWA1838	6B	65	10.53	0.07	−0.29	0.05	P14 d5	**A**/G
*QPHS.wsu-7B.2**	IWB7099	7B	133	9.00	0.00	−0.34	0.00	C14 d5	A/**G**
*QPHS.wsu-1D**	IWB71680	1D	163	7.61	0.06	−0.60	0.09	P14, P16 d6	**A**/G
*QPHS.wsu-2A.2**	IWB17580	2A	53	9.02	0.07	−0.69	0.02	C15 d7	T/**C**
QPHS.wsu-2A.3	IWB79387	2A	–	6.88	0.01	−0.31	0.00	C14 d6	A/**G**
QPHS.wsu-2D	IWB7652	2D	52	12.69	0.37	−0.85	0.12	C14 d6, d7	T/**C**
QPHS.wsu-3A.1	IWB32631	3A	15	6.63	0.26	−0.31	0.02	C14 d7	A/**G**
*QPHS.wsu-3B.1**	IWB6430	3B	11	8.92	0.08	−0.38	0.01	P14 d7	T/**C**
QPHS.wsu-3B.3	IWB9902	3B	–	7.76	0.07	−0.59	0.06	P14 d7	**T**/C
QPHS.wsu-4A.2	IWB46089	4A	73	6.83	0.16	−0.33	0.04	P16 d6	A/**G**
QPHS.wsu-4A.3	IWB1389	4A	151	7.51	0.23	−0.45	0.02	C14 d7	**T**/G
QPHS.wsu-4B.1	IWB72936	4B	60	7.92	0.25	−0.46	0.02	C14 d7	**A**/G
QPHS.wsu-4B.2	IWA1382	4B	73	8.04	0.06	−0.53	0.00	P15 d7	A/**G**
QPHS.wsu-5A.2	IWB60303	5A	70	7.56	0.34	−0.39	0.01	C15 d7	A/**G**
*QPHS.wsu-5A.3**	IWB6049	5A	84	9.92	0.19	−0.31	0.00	P16 d6	**A**/G
QPHS.wsu-6A	IWB6726	6A	77	7.52	0.07	−0.48	0.03	P14 d7	**T**/G
QPHS.wsu-6B	IWB76583	6B	65	9.76	0.05	−0.33	0.03	P14 d6	**A**/G
*QPHS.wsu-6D**	IWB49280	6D	153	7.17	0.03	−0.39	0.00	P15 d7	**A**/G
*QPHS.wsu-7A**	IWB51129	7A	152	6.64	0.00	−0.27	0.06	P16 d6	A/**G**
QPHS.wsu-7B.3	IWB10815	7B	171	10.62	0.05	−0.41	0.00	P14 d7	T/**C**
QPHS.wsu-1D*	IWB71680	1D	163	7.22	0.06	−0.03	0.10	P16 SI	**A**/G

(Continued)

TABLE 4 | Continued

QTL[a]	Marker	Chr[b]	cM[b]	–log10(*p*)	maf	Effect[c]	r^2	Environment	Favorable Allele[d]
QPHS.wsu-2B	IWB30853	2B	87	7.59	0.21	−0.02	0.00	C14 SI	A/**G**
QPHS.wsu-2D	IWB46396	2D	54	11.97	0.39	−0.03	0.07	C14 SI	**A**/G
QPHS.wsu-3B.3	IWB9902	3B	–	7.31	0.07	−0.03	0.00	P14 SI	**T**/C
QPHS.wsu-5A.1	IWB10998	5A	53	8.70	0.41	−0.02	0.25	C14 SI	T/**C**
QPHS.wsu-6B	IWB57747	6B	64	6.85	0.07	−0.02	0.07	P16 SI	**A**/G
	IWB76583	6B	65	6.57	0.02	−0.01	0.00	P14 SI	**A**/G
*QPHS.wsu-7B.2**	IWB7099	7B	133	8.63	0.00	−0.02	0.01	C14 SI	A/**G**
	IWB7099	7B	133	7.58	0.01	−0.02	0.00	P16 SI	A/**G**

[a] *QTL in bold explained 10% (r^2 > 0.1) or more of the phenotypic variation. QTL underlined were significant in 2 environments. Loci more than 10 cM away from previously published QTL were considered to be novel and are indicated with an*.*

[b] *Chromosome and position according to Wang et al. (2014). Positions are not reported if the location was identified on the GrainGenes database.*

[c] *The allelic effect is shown in FN seconds or sprouting score BLUPs.*

[d] *The significant allele is favorable (in bold) if it decreases sprouting scores in the spike-wetting tests or increases Falling Numbers.*

2014 and there were no heading date QTN discovered that overlapped with QTNs for either FN or PHS (Supplementary Table 5).

Association Analysis for Sprouting Score and Sprouting Index

For the spike-wetting tests, 34 significant *QPHS.wsu* were detected based on sprouting scores or on SI (**Table 4**). There were 12 *QPHS.wsu* associated with early germination and root emergence (3–4 days of misting) (**Figure 1**; **Table 4**; McMaster and Derera, 1976). Seven *QPHS.wsu* were identified after 5 days of misting, only one of which was also seen with 3–4 days of misting. There were 16 significant *QPHS.wsu* associated with coleoptile emergence and elongation at 6–7 days of misting, 13 of which were unique to 6–7 days of misting. There were 3 additional *QPHS.wsu* uniquely detected by SI (**Figure 2B**). An association at the *QPHS.wsu-2D* locus was detected over all days of scoring, suggesting that it is not unique to any one sprouting stage (**Figure 2A**). The *QPHS.wsu-1B.2* and *QPHS.wsu-6B* were detected on two of the scoring days. Of the 34 total QTN found in the spike-wetting tests, only 6 *QPHS.wsu* on chromosomes 1B, 1D, 2D, 5A, 6B, and 7B were significant in two environments (**Figure 2C**). No *QPHS.wsu* were detected in more than 2 environments. Five *QPHS.wsu* on chromosomes 1A, 1B, 1D, 2D, and 5A explained more than 10% of the phenotypic variation. In Central Ferry 2015, only sprouting scores on days 3 and 7 fit the expected −log(*p*), whereas days 4, 5, 6, and SI did not (Supplementary Figure 4). Therefore, very few significant *QPHS.wsu* were identified in this environment.

In order to reduce the effect of post-germinative growth versus germination *per se*, the GWAS was repeated with the maximum sprouting score set at 5 and referred to as *QPHSg.wsu* (Supplementary Table 4). Out of 46 QTN detected, 32 QTN were unique to this analysis and 21 were no longer significant (Supplementary Figure 5). The major QTN, *QPHS.wsu-1D*, *QPHS.wsu-2D*, *QPHS.wsu-5A.2*, and *QPHS.wsu-7B.2* were also detected in this germination-based analysis. The *QPHSg.wsu-2D* locus was highly significant in this GWAS ($7.64 < -\log_{10}(p) < 37.13$), and had strong effects (0.02 to 0.72).

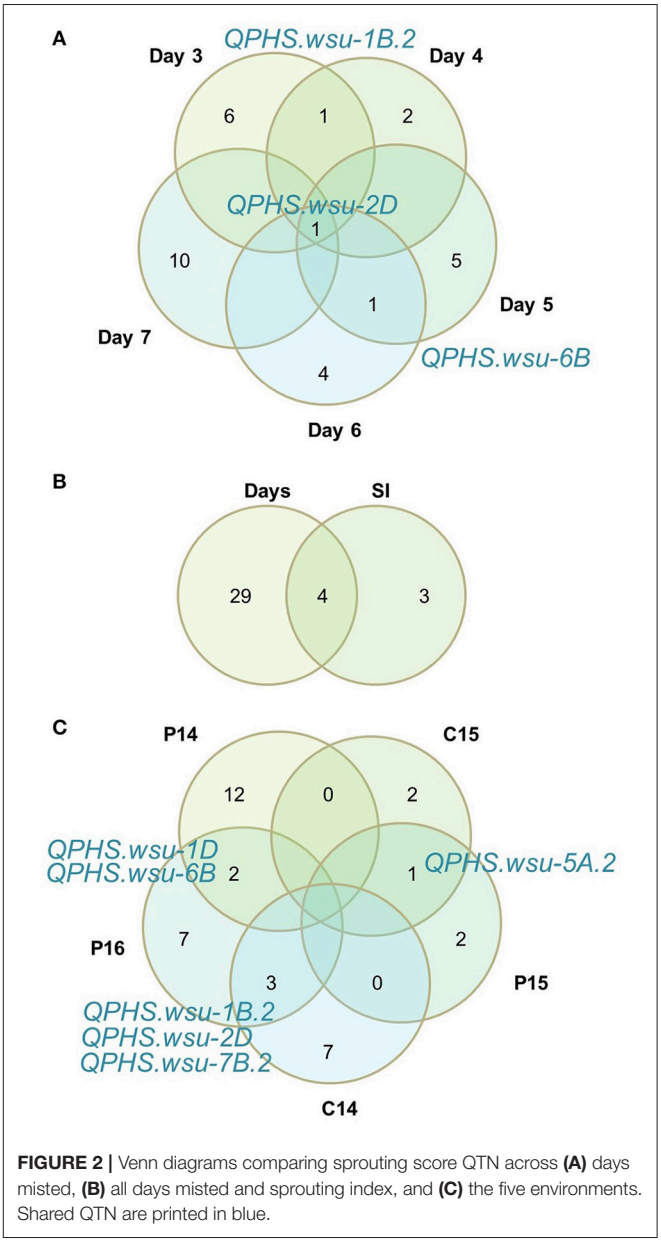

FIGURE 2 | Venn diagrams comparing sprouting score QTN across **(A)** days misted, **(B)** all days misted and sprouting index, and **(C)** the five environments. Shared QTN are printed in blue.

Association Analysis without Using the Club Wheat Breeding Program as a Covariate

Based on the fact that the strong *QPHS.wsu-2D* locus was near the *C* locus region for compact spike morphology, we examined whether the club wheat breeding program contributed more PHS tolerance to the GWAS than the lax wheat breeding programs (**Figure 3**). In Central Ferry 2014, when the tolerant and susceptible loci from the strongest marker within *QPHS.wsu-2D* were compared, 98% of the tolerant loci were club (**Figure 3A**). When the BLUPs were compared across all environments, the same trend was observed (**Figure 3B**). In fact, the club wheat breeding program generally contributed more PHS tolerance in the GWAS than the other programs (**Figure 3C**). Thus, it is possible that using the principle components as a covariate in the GWAS may artifactually remove some of the PHS loci contributed by the club wheat breeding program. To test this hypothesis, the GWAS was repeated without incorporating the principle components into the model (Supplementary Table 6). The *QPHS.wsu-2D* QTN became stronger in this analysis, increasing to a $-\log_{10}(p)$ of up to 30.03 and an effect of 1.08. An additional 32 *QPHSnPC.wsu* and 2 *QFNnPC.wsu* were detected, whereas 15 *QPHS.wsu* and 2 *QFN.wsu* were found in common (Supplementary Figure 5).

Pyramiding Effects of FN and PHS QTN

Next, we examined whether an increasing number of favorable QTN were associated with increasing FN or PHS tolerance. The number of favorable *QFN.wsu* loci within accessions ranged from 2 to 9 (**Figures 4A–C**). An increasing number of *QFN.wsu* loci was only weakly correlated to higher FN. The correlation was actually stronger when there was no rain event than when there was a natural or artificial rain event ($r = 0.23, 0.19, 0.09$, respectively). The number of *QPHS.wsu* loci varied more widely within the accessions (8 to 26), making it easier to assess the effects of pyramiding multiple tolerance loci (**Figures 4D–I**). An increasing number of tolerance loci was negatively correlated with sprouting scores ranging from $r = -0.47$ to $r = -0.55$ (Supplementary Figure 6). Thus, having more *QPHS.wsu* loci was associated with more PHS tolerance. Tolerant FN loci only slightly correlated with the increasing sprouting scores, and vice versa ($r < 0.20$; Supplementary Figure 6).

Within the mapping panel, there was only one accession, "A00154," with all 9 *QFN.wsu* that had an average FN of 461 s across natural rain events. The accession "6J020288-1" had the highest number of favorable alleles, including 26 out of 34 *QPHS.wsu* and 6 of 9 *QFN.wsu*. This was reflected in the phenotype since 6J020288-1 had an average FN of 380 s across natural rain events and a sprouting score of 1 after 5 days of misting from all environments. In contrast, the accession "J950409-10-2" had only 9 out of 34 *QPHS.wsu* and 5 of 9 *QFN.wsu*, associated with an average FN of 272 s and a high sprouting score of 7 after 5 days of misting. Interestingly, "Lewjain" had only 8 of the 34 *QPHS.wsu* and 5 of the 9 *QFN.wsu* but had an average FN of 401 s and a sprouting score of 4 after 5 days. Thus, these QTN do not always behave in an additive fashion, suggesting that there are epistatic effects. For example, some of the few favorable QTN in Lewjain may have a stronger effect on the phenotype than the unfavorable alleles.

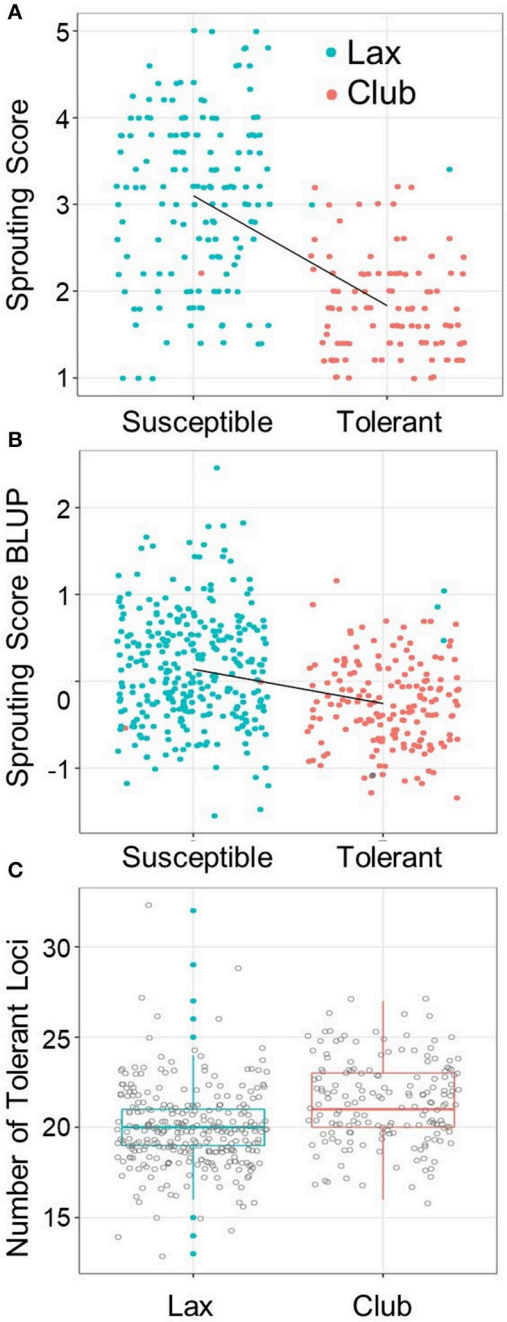

FIGURE 3 | *QPHS.wsu-2D* in club versus lax mapping lines. Scatter plot of sprouting score **(A)** raw means over the environment, Central Ferry 2014, that *QPHS.wsu-2D* had the strongest effect and **(B)** Sprouting score BLUPs across all five environments after 4 days of misting versus the presence of the *QPHS.wsu-2D* susceptible (S) or tolerant (T) allele. Club genotypes are in red and lax in blue. **(C)** Total number of favorable loci are compared to club versus lax spike morphology.

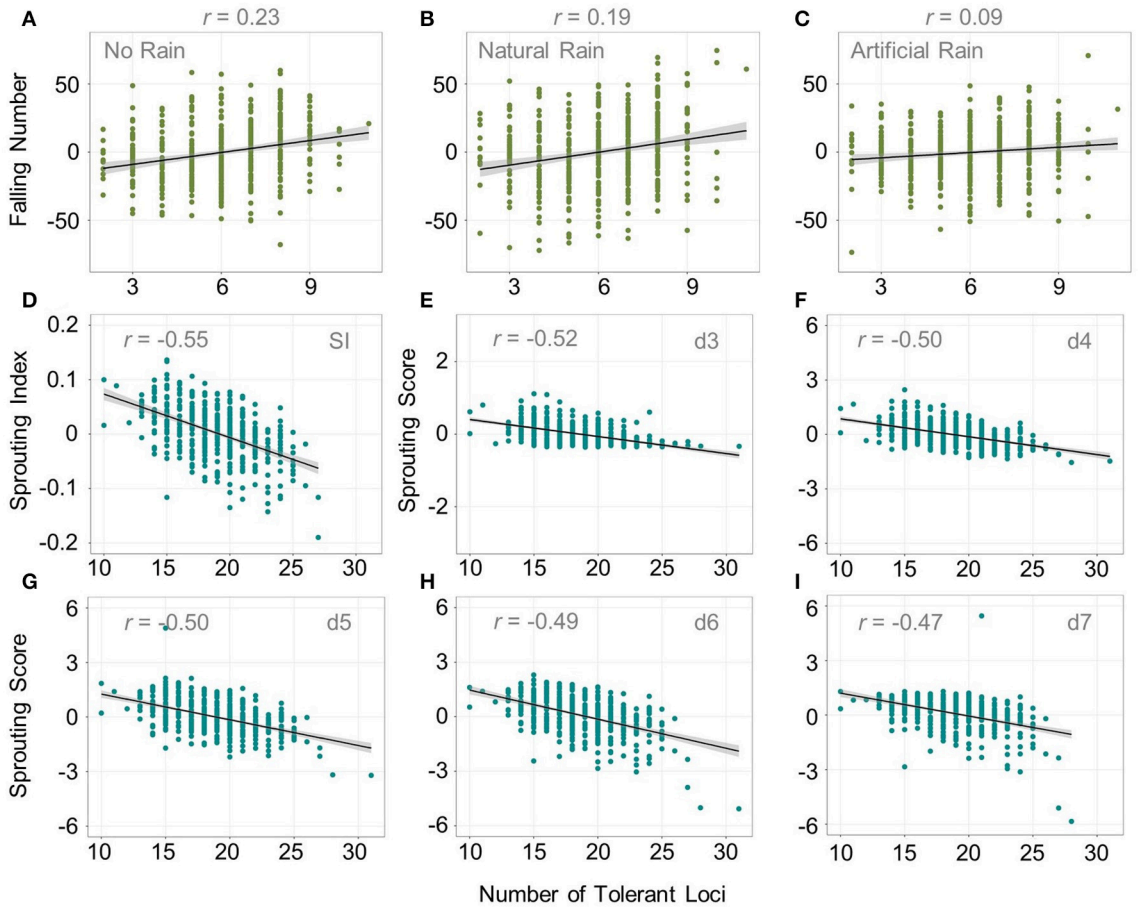

FIGURE 4 | The effect of pyramiding multiple *QFN.wsu* and *QPHS.wsu* loci. Scatter plots of the number of favorable *QFN.wsu* loci versus FN BLUPs across: **(A)** in the absence of rain, **(B)** both natural rain environments combined, and **(C)** both artificial rain environments combined. Scatter plots of the number of favorable *QPHS.wsu* loci versus BLUPs calculated across all environments for **(D)** sprouting index, and sprouting scores on days **(E)** 3, **(F)** 4, **(G)** 5, **(H)** 6, and **(I)** 7 of misting. *r* is the Pearson correlation coefficient between the trait and number of tolerant loci.

Comparative Mapping for PHS

The location of QTN for FN and sprouting scores were compared to locations of PHS-related loci identified in 54 previous studies (**Figure 5**). This was done using the comparative map of commonly used wheat markers created by Maccaferri et al. (2015). The studies used in the comparison are shown in Supplementary Table 3. Mapped traits that are related to FN and end-use quality included FN, starch content, protein content, and α-amylase activity. Mapped traits related to sprouting and dormancy included germination assays, kernel color, and sprouting scores from spike-wetting tests. There is currently no experimental standard for the spike-wetting test, and methods vary from misting of intact spike to spike immersion to the use of wet sand (McMaster and Derera, 1976; Paterson et al., 1989; Anderson et al., 1993; Humphreys and Noll, 2002; Rehman Arif et al., 2012). Even within each method, the number of days of after-ripening, the duration of spikes wetting, and the day scored vary between studies. Only a few studies score PHS after 4–6 days of misting (Anderson et al., 1993; Munkvold et al., 2009; Kulwal et al., 2012; Somyong et al., 2014). This inconsistency across studies led us to ask whether or not our assay could map previously published cloned genes and QTL. Nineteen of the 34 sprouting QTN detected in this study co-localized with known major PHS QTL and cloned genes such as *TaMFT* on chromosome 3A (**Figure 5**; Nakamura et al., 2011). Interestingly, 14 of the 34 sprouting QTN were identified near known FN or quality QTL. Three of 9 FN QTN were identified near known FN and quality QTL, whereas 4 of 9 FN QTN were identified near dormancy or PHS QTL. Of these FN QTN, 2 co-localized with both PHS and FN/quality QTL. A total of 2 QTN for FN and 10 QTN for sprouting score appeared to be unique to this study (marked with a star in **Table 4**).

DISCUSSION

This genome-wide association study was, to our knowledge, the first to map preharvest sprouting loci based both on sprouting scores from the spike-wetting test (*QPHS.wsu*) and

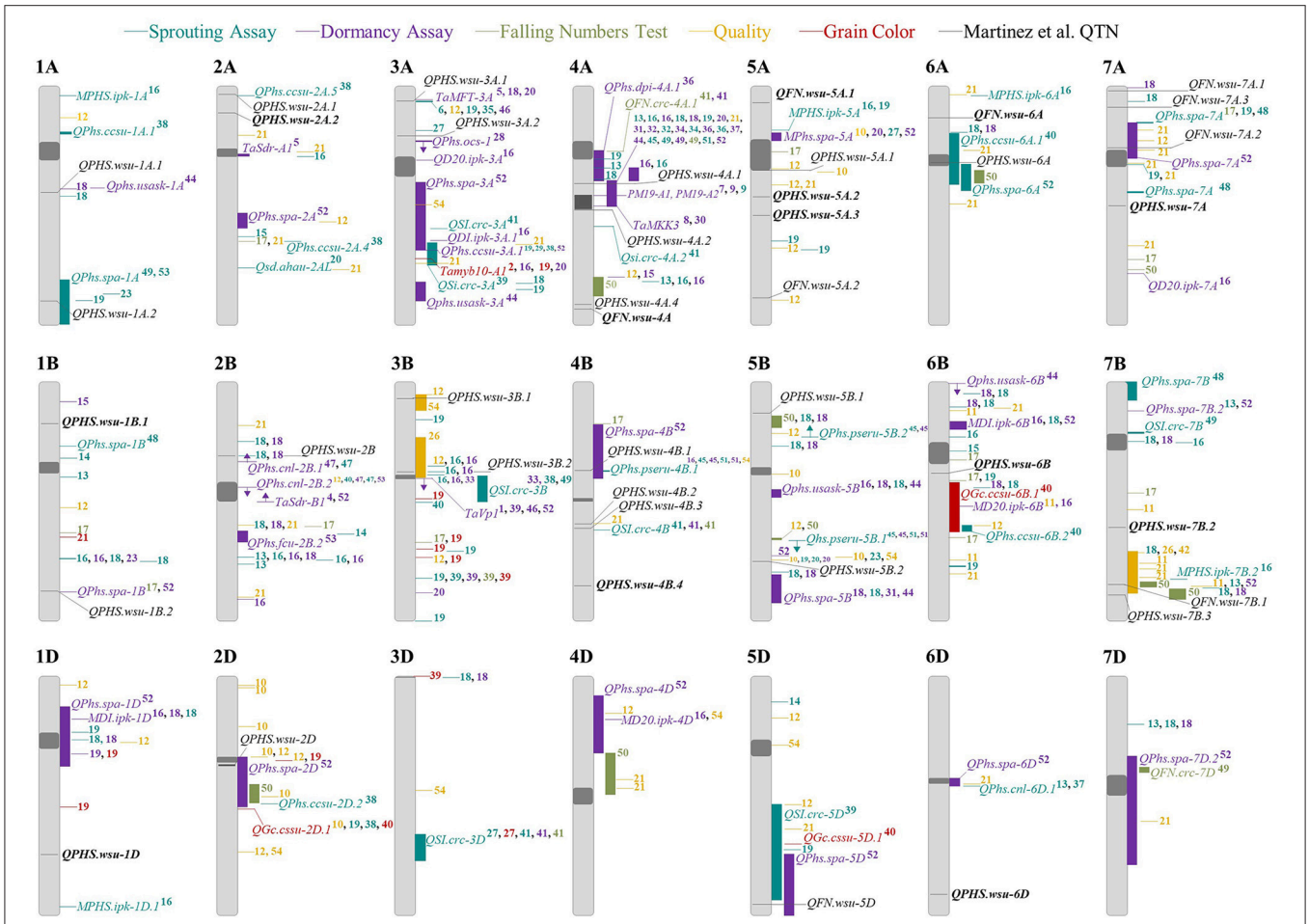

FIGURE 5 | Chromosome positions of PHS-related loci. Comparative mapping of quantitative trait nucleotides identified in this study (black), and previously published quantitative trait loci (QTL) for PHS tolerance (blue), dormancy (purple), Falling Number (green), grain color (red), and quality (orange). Potentially novel *QPHS.wsu* or *QFN.wsu* QTN are in bold. Published QTL were aligned to the Maccaferri et al. (2015) comparative map using the flanking markers or significant associated markers. Chromosomes are presented as a standardized relative length. An arrow along a QTL indicates the QTL direction when only one flanking marker was found in the comparative map. The centromeric region is a dark gray oval. ID numbers to the right of the QTL correspond to the references found in Supplementary Table 3. Illumina 9 or 90 k SNP markers were not reported on chromosome 3D, resulting in an incomplete map.

FN (*QFN.wsu*). FN is an important and complex trait that determines the value of the grain in the wheat industry. While there were 34 significant *QPHS.wsu* loci across the five different sprouting time points and sprouting index, only nine significant *QFN.wsu* loci were identified. We expected FN and sprouting scores to identify some of the same QTN because the α-amylase expression that lowers FN is a consequence of germination. However, none of the identified significant FN and PHS loci were linked (**Table 4**). While *QFN.wsu-4A* and *QPHS.wsu-4A.3* appeared to be close to one another (1 cM apart), they were not in the same linkage group (p between 0.05 and 0.01), and had only a −0.13 correlation to one another. Moreover, we failed to find a strong correlation between FN and sprouting scores. This result contrasts with previous studies showing a correlation of up to −0.8 between spike-wetting tests and FN in Canadian and Chilean breeding lines (Rasul et al., 2009; Jiménez et al., 2016).

The lack of a strong correlation between FN and sprouting score in our study has multiple likely causes: our association panel was larger and sampled more variability for FN related traits; our environments were more variable; or the causes of low FN were not solely due to PHS. Eastern Washington is a semi-arid environment where grain is planted deeply to reach moisture and selection for emergence may have led to early and strong induction of α-amylase to fuel seedling growth. This, in turn, may have resulted in lower FN than would be expected for a given sprouting score. Future work may investigate this by determining if a propensity for low FN is associated with earlier expression of α-amylase during germination. The *QFN.wsu* loci identified, however, did appear to be related to preharvest sprouting because they co-localized with PHS-related loci identified in other studies. Thus, while sprouting scores were not predictive of FN in this study, both traits appeared to be useful for identifying PHS-related loci.

Comparison to Previously Published PHS QTL and Genes

Based on comparative mapping, 12 potentially novel PHS tolerance loci were identified (**Figure 5**). With the exception of *QPHS.wsu-4B.3*, the QTN identified during early sprouting (3–4 days misted) were near published QTL (**Table 4**). In contrast, six novel loci were identified during late sprouting (6–7 days misted). Previous PHS mapping studies mostly used spike-wetting test data collected after 4–6 days of misting (Anderson et al., 1993; Munkvold et al., 2009; Kulwal et al., 2012; Somyong et al., 2014).

Multiple *QFN.wsu* were located near published QTL or cloned genes governing PHS-related traits (**Figure 5**; Supplementary Table 3). Three of the six *QFN.wsu* identified in the presence of natural rain were near known preharvest sprouting and dormancy QTL (Fofana et al., 2009; Kumar et al., 2009, 2015; Kulwal et al., 2012; Albrecht et al., 2015). Previous work has shown FN samples after a rainfall negatively correlate with dormancy which may be another explanation as to why we see FN QTN near dormancy QTL (Biddulph et al., 2008). *QFN.wsu-7A.1* had the largest effect on FN, and was near PHS and dormancy QTN found in a European winter wheat GWAS (Albrecht et al., 2015). *QFN.wsu-7B.1* localized in a region containing known QTL mapped based on spike-wetting tests, spike immersion, dormancy, and FN (Kulwal et al., 2012; Mohler et al., 2014; Albrecht et al., 2015; Kumar et al., 2015). Given that these QTN were detected after a natural rainfall event, it is curious that they were not detected in any of our spike-wetting test environments. This suggests that either these *QFN.wsu* loci resulted in higher FN due to PHS tolerance, or that the co-localization of these FN QTN with sprouting QTLs was a coincidence. FN is also controlled by grain starch characteristics. Consistent with this, the *QFN.wsu-5A.2* and *QFN.wsu-7A.2* loci identified in the absence of rain were located near starch content and starch granule size QTL (Reif et al., 2011; Li et al., 2017).

Many *QPHS.wsu* were found near published QTL or cloned genes associated with seed dormancy and PHS tolerance (**Figure 5**). *QPHS.wsu-2A.1* was located near a preharvest sprouting QTL, *QPhs.ccsu-2A.5*, found in the dormant accession "SPR8198" (Mohan et al., 2009). *QPHS.wsu-2B* was located near the locus providing dormancy and PHS tolerance in the soft white wheat cultivar "Cayuga" and in a European winter wheat QTL (Somyong et al., 2014; Albrecht et al., 2015). The *QPHS.wsu-2D* QTN had the strongest effect, and co-localized with the *QPhs.spa-2D* locus identified in Canadian wheat (Kumar et al., 2015). *QPHS.wsu-3A.1* was within 1 cM of the major dormancy and PHS tolerance gene *MOTHER OF FT AND TFL1* (*TaMFT*), identified by map-based cloning in both Japanese and U.S. wheat (Nakamura et al., 2011; Liu et al., 2013). *QPHS.wsu-4A.1* and *QPHS.wsu-4A.2* are within the *Phs-A1* region associated with dormancy and PHS tolerance in mapping studies world-wide (Mares and Mrva, 2014; Barrero et al., 2015; Shorinola et al., 2016, 2017; Torada et al., 2016). A polymorphism in the *MITOGEN-ACTIVATED PROTEIN KINASE KINASE 3* (*TaMKK3-A*) gene likely accounts for the seed dormancy providing PHS tolerance on chromosome 4A. Future work will need to examine if the PHS tolerance loci mapped in the current study are associated with the known dormancy-associated polymorphisms in *TaMFT* and *TaMKK3*. If so, then these perfect markers can be used for selecting PHS tolerance within the breeding programs represented in this GWAS. Identifying QTL near regions of known PHS QTL validates the GWAS and suggests that breeding programs in the northwestern U.S. have historically used multiple sources of PHS tolerance.

The strong *QPHS.wsu-2D* locus co-localized both with a known PHS locus and with the *C* locus that determines club head type (Supplementary Table 3; Johnson et al., 2008). The strong *QPHS.wsu-2D* locus associated with the *C* locus may partly be an artifact because the club wheat breeding program was the dominant source of this PHS tolerance locus in the mapping panel. Since *QPHS.wsu-2D* is <1 cM from the *C* locus flanking marker wmc144, this invited the question as to whether the *C* locus itself provided PHS tolerance or whether there was another PHS-tolerance locus in tight linkage with the *C* locus. The latter seemed more likely because previous studies found that the club head type took up more water during rain events and was sometimes associated with higher preharvest sprouting in near-isogenic lines (Hong, 1979; King and Richards, 1984; R.E. Allan, personal comm.). Interestingly, there were three PHS tolerant lax wheat lines that carried the *QPHS.wsu-2D* locus (J950409-10-4, J950409-10-5, and ID581), and there were two PHS susceptible club wheat lines (J970057-5 and ARS00226) that did not carry the *QPHS.wsu-2D* locus. While these counter-examples suggest that there was a PHS QTL strongly linked to the *C* locus, they are not proof because these PHS phenotypes may have resulted from variation at other loci. Future work will need to examine this question using near-isogenic lines that differ only for the *C* locus and for the *QPHS.wsu-2D* locus.

Breeding for PHS Tolerance Based on Spike-Wetting Tests and FN

Sprouting scores for this population did not correlate strongly with FN (**Table 2**). While increasing number of *QPHS.wsu* loci correlated to increasing sprouting index and sprouting scores, we observed little or no correlation to increasing FN in natural rain, artificial rain, or no-rain environments (**Figure 4**; Supplementary Figure 6). Moreover, there was no strong association between increasing *QFN.wsu* loci and sprouting scores. In fact, sprouting scores and FN provided complementary information. It is possible that the tendency toward low FN is dependent more on the timing and strength of α-amylase induction during seed imbibition, then on the timing of visible sprout/germination *per se*. For example, there may be varieties that induce α-amylase earlier in the germination program, prior to germination *per se*. Such varieties would be prone to higher α-amylase/lower FN than expected based on the timing of visible sprout.

Breeding for FN is complicated by the fact that it is a complex trait governed by multiple factors. Although the intention was to map preharvest sprouting QTL, our FN field environments may have also experienced conditions that induced late maturity α-amylase (LMA). During LMA, α-amylase is induced in response to large temperature fluctuations during late grain filling (Farrell and Kettlewell, 2008; Mares and Mrva, 2014). While four of the

five environments experienced either natural or artificial rain events, we cannot rule out the possibility that the wheat also experienced LMA. Indeed, the *QFN.wsu-7B.1* locus co-localized with a large LMA QTL (**Figure 5**; Mrva and Mares, 2001; McNeil et al., 2009; Emebiri et al., 2010). In the environment without rain, differences in FN likely resulted from differences in properties of grain starch and protein (Graybosch et al., 2000; Guo et al., 2003; Ross et al., 2012). Such properties likely also impact FN over 300 s when there is a rain event. The FN test has a fairly high standard deviation within technical replicates (Supplementary Figure 7). The genotypic repeatability (R^2) of FN increased when we took experimental covariates (such as machine and operator) and technical replicates into account (**Table 3**). The FN test has other limitations for breeding such as the need for an expensive instrument, and the fact that it is more time-consuming to run FN than spike-wetting tests. Future research should examine whether α-amylase enzyme assays (Phadebas™ or Megazyme) or ELISA assays may serve as a faster, cheaper, or less variable proxy to FN (Mares and Mrva, 2008; Barrero et al., 2013). Environmental factors also caused variation in FN, resulting in only moderate correlations between environments in the current study (**Table 2A**). While the Zhang et al. (2014) study had higher correlations between FN in different environments ($0.43 > r > 0.80$), it had fewer samples below 300 s suggesting that less sprouting occurred in their environments. Breeders cannot rely on natural rain occurring when they want to screen for low FN due to PHS, making the use of artificial rain necessary. Other differences in the environment, such as temperature during maturation or temperature during the sprout-inducing rainfall, can impact grain dormancy, PHS susceptibility, and FN. Future artificial rain experiments may be improved by applying the artificial rain during lower evening temperatures or letting the wheat after-ripen longer in the field prior to misting.

The spike-wetting test has long been favored for selecting preharvest sprouting tolerance because the experimental design takes into account after-ripening time, spike morphology, and grain dormancy/germinability (Paterson et al., 1989). A limitation of FN testing of field-harvested grain is that differences in maturation date can be a major covariate, since early maturing varieties may have lost more dormancy through after-ripening than late maturing varieties. The spike-wetting test reduces this problem by harvesting spikes at physiological maturity and then after-ripening for the same number of days before conducting the test. When screening large numbers of breeding lines, it would be convenient to avoid scoring daily over 3 to 7 days of misting. Based on the correlations between spike-wetting test and all FN environments (with and without rain), scoring after 4 days of misting should provide breeders with both adequate variation and higher correlation to FN (**Table 2B**). Scoring after 4 days misting also provides good insight into initial germination capacity (scores 1-5) rather than speed of seedling growth (scores 6-10) (**Figure 1**). However, it should be noted that the day 6 sprouting score had the highest genotypic repeatability in this study. One drawback of selecting for PHS tolerance based on seed dormancy, is that too much dormancy may result in poor seedling emergence of winter wheat when grain is planted ∼8 weeks after harvest (Rodríguez et al., 2015). Future work will need to develop a genomic selection model for breeding wheat with sufficient seed dormancy to prevent preharvest sprouting without compromising seedling emergence.

Seed dormancy and PHS tolerance are stronger if temperatures are cool during grain maturation (Nakamura et al., 2011). One could remove temperature during grain development as a variable in spike-wetting tests by growing plants in a controlled environment instead of in the field. We might have also seen better correlations if spike-wetting tests had been performed for the entire trial in the 2 years with natural rain events. However, when spike-wetting tests were performed on 162 accessions in Pullman 2013, only a −0.26 correlation was observed. A more likely explanation is that FN in these environments was impacted by multiple factors in addition to preharvest sprouting, including LMA, starch, and protein characteristics. Thus, within this study, FN and spike-wetting tests were not two ways to measure the same trait.

PHS tolerance is profoundly impacted by environmental conditions during grain maturation and during the sprout-inducing rain event (Cao et al., 2016; Kashiwakura et al., 2016; Martinez et al., 2016). Thus, it is not uncommon to find lack of agreement between environments in PHS tolerance association studies based on spike-wetting tests (Ogbonnaya et al., 2008; Jaiswal et al., 2012; Kulwal et al., 2012; Zhou et al., 2017). A total of 6 out of 34 *QPHS.wsu* were identified in at least two of the five environments. In fact, the correlations between our environments were as good as those in other spike-wetting test studies (Jaiswal et al., 2012; Kulwal et al., 2012). The fact that this study identified some QTN in multiple environments and that many of the QTN identified agreed with previous studies, suggests that this association study will lay a strong foundation for future efforts to develop genomic selection for PHS tolerance in northwestern U.S. wheat.

AUTHOR CONTRIBUTIONS

SM, KG, and CS: Designed the experiments; SM: Conducted the experiments, analyzed the phenotypic data, performed the statistical analysis and GWAS, and constructed the visualizations; JG: Curated and filtered the genotypic data and performed the LD analysis; MH: Calculated the phenotypic variation; MH and ZZ: Provided expert guidance on performing the GWAS; KG and AC: Provided field resources; CS, KG, AC, and ZZ: Obtained funding; SM and CS: Wrote the manuscript.

FUNDING

This work was funded by the NIFA projects 2015-05798 and 2016-68004-24770, the USDA-ARS project 424575, and the WA Grain Commission projects 7599, 5389, and 126593.

ACKNOWLEDGMENTS

The authors wish to thank Rehana Parveen, Tracy Harris, Patricia DeMacon, Gary Shelton, and Xavian Thompson for expert technical assistance. The authors sincerely thank Dan Dreesman

for constructing the greenhouse misting system. Thanks are due to members of the KG, AC, and CS labs for assistance with planting, sampling, and harvesting. Special thanks go to the KG and CS labs for helpful feedback on the research and manuscript.

SUPPLEMENTARY MATERIAL

The Supplementary Material for this article can be found online at: https://www.frontiersin.org/articles/10.3389/fpls.2018.00141/full#supplementary-material

REFERENCES

AgWeatherNet (2016). *Station Details: Pullman*. Avaliable online at: https://weather.wsu.edu/?p=90150&UNIT_ID=300029 (Accessed October 2, 2017).

Akbari, M., Wenzl, P., Caig, V., Carling, J., Xia, L., Yang, S., et al. (2006). Diversity arrays technology (DArT) for high-throughput profiling of the hexaploid wheat genome. *Theor. Appl. Genet.* 113, 1409–1420. doi: 10.1007/s00122-006-0365-4

Albrecht, T., Oberforster, M., Kempf, H., Ramgraber, L., Schacht, J., Kazman, E., et al. (2015). Genome-wide association mapping of preharvest sprouting resistance in a diversity panel of European winter wheats. *J. Appl. Genet.* 56, 277–285. doi: 10.1007/s13353-015-0286-5

Anderson, J. A., Sorrells, M. E., and Tanksley, S. D. (1993). RFLP analysis of genomic regions associated with resistance to preharvest sprouting in wheat. *Crop Sci.* 33, 453–459. doi: 10.2135/cropsci1993.0011183X003300030008x

Barrero, J. M., Cavanagh, C., Verbyla, K. L., Tibbits, J. F. G., Verbyla, A. P., Huang, B. E., et al. (2015). Transcriptomic analysis of wheat near-isogenic lines identifies PM19-A1 and A2 as candidates for a major dormancy QTL. *Genome Biol.* 16, 93. doi: 10.1186/s13059-015-0665-6

Barrero, J. M., Mrva, K., Talbot, M. J., White, R. G., Taylor, J., Gubler, F., et al. (2013). Genetic, hormonal, and physiological analysis of late maturity α-amylase in wheat. *Plant Physiol.* 161, 1265–1277. doi: 10.1104/pp.112.209502

Bates, D., Maechler, M., Bolker, B., and Walker, S. (2015). Fitting linear mixed-effects models using lme4. *J. Stat. Softw.* 67, 1–48. doi: 10.18637/jss.v067.i01

Bewley, J. D., and Black, M. (1994). *Seeds: Physiology of Development and Germination, 2nd Edn*. New York, NY: Plenum Publishing Corporation.

Biddulph, T. B., Plummer, J. A., Setter, T. L., and Mares, D. J. (2008). Seasonal conditions influence dormancy and preharvest sprouting tolerance of wheat (*Triticum aestivum* L.) in the field. *Field Crops Res.* 107, 116–128. doi: 10.1016/j.fcr.2008.01.003

Browning, B. L., and Browning, S. R. (2016). Genotype imputation with millions of reference samples. *Am. J. Hum. Genet.* 98, 116–126. doi: 10.1016/j.ajhg.2015.11.020

Campbell, K. A. G., and Lipps, P. E. (1998). Allocation of resources: sources of variation in fusarium head blight screening nurseries. *Phytopathology* 88, 1078–1086. doi: 10.1094/PHYTO.1998.88.10.1078

Cao, L., Hayashi, K., Tokui, M., Mori, M., Miura, H., and Onishi, K. (2016). Detection of QTLs for traits associated with pre-harvest sprouting resistance in bread wheat (*Triticum aestivum* L.). *Breed Sci.* 66, 260–270. doi: 10.1270/jsbbs.66.260

Cavanagh, C. R., Chao, S., Wang, S., Huang, B. E., Stephen, S., Kiani, S., et al. (2013). Genome-wide comparative diversity uncovers multiple targets of selection for improvement in hexaploid wheat landraces and cultivars. *Proc. Natl. Acad. Sci. U.S.A.* 110, 8057–8062. doi: 10.1073/pnas.1217133110

Clarke, J. M., Ronald, M., De, P., and Christensen, J. V. (1984). Effect of weathering on falling numbers of standing and windrowed wheat. *Can. J. Plant Sci.* 64, 457–463. doi: 10.4141/cjps84-068

DePauw, R. M., and McCaig, T. N. (1991). Components of variation, heritabilities and correlations for indices of sprouting tolerance and seed dormancy in *Triticum* spp. *Euphytica* 52, 221–229. doi: 10.1007/BF00029399

DePauw, R. M., Knox, R. E., Singh, A. K., Fox, S. L., Humphreys, D. G., and Hucl, P. (2012). Developing standardized methods for breeding preharvest sprouting resistant wheat, challenges and successes in Canadian wheat. *Euphytica* 188, 7–14. doi: 10.1007/s10681-011-0611-y

Emebiri, L. C., Oliver, J. R., Mrva, K., and Mares, D. (2010). Association mapping of late maturity α-amylase (LMA) activity in a collection of synthetic hexaploid wheat. *Mol. Breed.* 26, 39–49. doi: 10.1007/s11032-009-9375-7

Farrell, A. D., and Kettlewell, P. S. (2008). The effect of temperature shock and grain morphology on alpha-amylase in developing wheat grain. *Ann. Bot.* 102, 287–293. doi: 10.1093/aob/mcn091

Finkelstein, R. R., Reeves, W., Ariizumi, T., and Steber, C. M. (2008). Molecular aspects of seed dormancy. *Annu. Rev. Plant Biol.* 59, 387–415. doi: 10.1146/annurev.arplant.59.032607.092740

Flintham, J. E. (2000). Different genetic components control coat-imposed and embryo-imposed dormancy in wheat. *Seed Sci. Res.* 10, 43–50. doi: 10.1017/S0960258500000052

Fofana, B., Humphreys, D. G., Rasul, G., Cloutier, S., Brûlé-Babel, A., Woods, S., et al. (2009). Mapping quantitative trait loci controlling pre-harvest sprouting resistance in a red × white seeded spring wheat cross. *Euphytica* 165, 509–521. doi: 10.1007/s10681-008-9766-6

Froese, P. S., and Carter, A. H. (2016). Single nucleotide polymorphisms in the wheat genome associated with tolerance of acidic soils and aluminum toxicity. *Crop Sci.* 56, 1662–1677. doi: 10.2135/cropsci2015.10.0629

Froese, P. S., Murray, T. D., and Carter, A. H. (2016). Quantitative Cephalosporium stripe disease resistance mapped in the wheat genome. *Crop Sci.* 56, 1586–1601. doi: 10.2135/cropsci2015.09.0568

Gerjets, T., Scholefield, D., Foulkes, M. J., Lenton, J. R., and Holdsworth, M. J. (2010). An analysis of dormancy, ABA responsiveness, after-ripening and pre-harvest sprouting in hexaploid wheat (*Triticum aestivum* L.) caryopses. *J. Exp. Bot.* 61, 597–607. doi: 10.1093/jxb/erp329

Graybosch, R. A., Guo, G., and Shelton, D. R. (2000). Aberrant falling numbers of waxy wheats independent of α-amylase activity. *Cereal Chem. J.* 77, 1–3. doi: 10.1094/CCHEM.2000.77.1.1

Gualano, N., Carrari, F., Rodriguez, M. V., Perez-Flores, L., Sanchez, R., Iusem, N., et al. (2007). Reduced embryo sensitivity to abscisic acid in a sprouting-susceptible sorghum (*Sorghum bicolor*) variety is associated with altered ABA signalling. *Seed Sci. Res.* 17, 81–90. doi: 10.1017/S0960258507708115

Guo, G., Jackson, D., Graybosch, R., and Parkhurst, A. (2003). Asian salted noodle quality: impact of amylose content adjustments using waxy wheat flour. *Faculty Publications Food Sci. Technol.* 80, 437–445. doi: 10.1094/CCHEM.2003.80.4.437

Himi, E., Maekawa, M., Miura, H., and Noda, K. (2011). Development of PCR markers for Tamyb10 related to R-1, red grain color gene in wheat. *Theor. Appl. Genet.* 122, 1561–1576. doi: 10.1007/s00122-011-1555-2

Hong, B. H. (1979). *Genetic and Environmental Aspects of Preharvest Sprouting and Related Traits in Triticum aestivum L.* em Thell, Ph.D. dissertation, Washington State University, Pullman, WA.

Humphreys, D. G., and Noll, J. (2002). Methods for characterization of preharvest sprouting resistance in a wheat breeding program. *Euphytica* 126, 61–65. doi: 10.1023/A:1019671622356

Ibrahim, H. A. (1966). *Studies on the Sprouting Problem in Soft White Wheats*. Ph.D. dissertation Cornell University, Ithaca, NY.

Jaiswal, V., Mir, R. R., Mohan, A., Balyan, H. S., and Gupta, P. K. (2012). Association mapping for pre-harvest sprouting tolerance in common wheat (*Triticum aestivum* L.). *Euphytica* 188, 89–102. doi: 10.1007/s10681-012-0713-1

Ji, T., and Baik, B.-K. (2016). Storage conditions affecting increase in falling number of soft red winter wheat grain. *Cereal Chem. J.* 93, 263–267. doi: 10.1094/CCHEM-08-15-0167-R

Jiménez, N., Mares, D., Mrva, K., Lizana, C., Contreras, S., and Schwember, A. R. (2016). Susceptibility to preharvest sprouting of Chilean and Australian elite cultivars of common wheat. *Crop Sci.* 57, 462–474. doi: 10.2135/cropsci2016.02.0138

Johnson, E. B., Nalam, V. J., Zemetra, R. S., and Riera-Lizarazu, O. (2008). Mapping the compactum locus in wheat (*Triticum aestivum* L.) and its relationship to other spike morphology genes of the Triticeae. *Euphytica* 163, 193–201. doi: 10.1007/s10681-007-9628-7

Kashiwakura, Y., Kobayashi, D., Jikumaru, Y., Takebayashi, Y., Nambara, E., Seo, M., et al. (2016). Highly sprouting-tolerant wheat grain exhibits extreme dormancy and cold imbibition-resistant accumulation of abscisic acid. *Plant Cell Physiol.* 57, 715–732. doi: 10.1093/pcp/pcw051

King, R. W. (1984). Water uptake in relation to pre-harvest sprouting damage in wheat: grain characteristics. *Aust. J. Agric. Res.* 35, 337–345. doi: 10.1071/AR9840337

King, R. W., and Richards, R. A. (1984). Water uptake in relation to pre-harvest sprouting damage in wheat: ear characteristics. *Aust. J. Agric. Res.* 35, 327–336. doi: 10.1071/AR9840327

King, R. W., and von Wettstein-Knowles, P. (2000). Epicuticular waxes and regulation of ear wetting and pre-harvest sprouting in barley and wheat. *Euphytica* 112, 157–166. doi: 10.1023/A:1003832031695

Kulwal, P., Ishikawa, G., Benscher, D., Feng, Z., Yu, L.-X., Jadhav, A., et al. (2012). Association mapping for pre-harvest sprouting resistance in white winter wheat. *Theor. Appl. Genet.* 125, 793–805. doi: 10.1007/s00122-012-1872-0

Kumar, A., Kumar, J., Singh, R., Garg, T., Chhuneja, P., Balyan, H. S., et al. (2009). QTL analysis for grain colour and pre-harvest sprouting in bread wheat. *Plant Sci.* 177, 114–122. doi: 10.1016/j.plantsci.2009.04.004

Kumar, S., Knox, R. E., Clarke, F. R., Pozniak, C. J., DePauw, R. M., Cuthbert, R. D., et al. (2015). Maximizing the identification of QTL for pre-harvest sprouting resistance using seed dormancy measures in a white-grained hexaploid wheat population. *Euphytica* 205, 287–309. doi: 10.1007/s10681-015-1460-x

Li, J., Rasheed, A., Guo, Q., Dong, Y., Liu, J., Xia, X., et al. (2017). Genome-wide association mapping of starch granule size distribution in common wheat. *J. Cereal Sci.* 77, 211–218. doi: 10.1016/j.jcs.2017.08.016

Lipka, A. E., Tian, F., Wang, Q., Peiffer, J., Li, M., Bradbury, P. J., et al. (2012). GAPIT: Genome Association and Prediction Integrated Tool. *Bioinformatics* 28, 2397–2399. doi: 10.1093/bioinformatics/bts444

Liu, S., Sehgal, S. K., Li, J., Lin, M., Trick, H. N., Yu, J., et al. (2013). Cloning and characterization of a critical regulator for preharvest sprouting in wheat. *Genetics* 195, 263–273. doi: 10.1534/genetics.113.152330

Liu, W., Naruoka, Y., Miller, K., Garland-Campbell, K. A., and Carter, A. H. (2017). Characterizing and validating stripe rust resistance loci in US Pacific Northwest winter wheat accessions *(Triticum aestivum L.)* by genome-wide association and linkage mapping. *Plant Genome.* 11. doi: 10.3835/plantgenome2017.10.0087

Liu, X., Huang, M., Fan, B., Buckler, E. S., and Zhang, Z. (2016). Iterative usage of fixed and random effect models for powerful and efficient genome-wide association studies. *PLoS Genet.* 12:e1005767. doi: 10.1371/journal.pgen.1005767

Maccaferri, M., Zhang, J., Bulli, P., Abate, Z., Chao, S., Cantu, D., et al. (2015). A genome-wide association study of resistance to stripe rust (*Puccinia striiformis* f. sp. *tritici*) in a worldwide collection of hexaploid spring wheat (*Triticum aestivum* L.). *G3* 5, 449–465. doi: 10.1534/g3.114.014563

Mares, D. J., and Mrva, K. (2014). Wheat grain preharvest sprouting and late maturity alpha-amylase. *Planta* 240, 1167–1178. doi: 10.1007/s00425-014-2172-5

Mares, D., and Mrva, K. (2008). Late-maturity α-amylase: low falling number in wheat in the absence of preharvest sprouting. *J. Cereal Sci.* 47, 6–17. doi: 10.1016/j.jcs.2007.01.005

Martinez, S. A., Tuttle, K. M., Takebayashi, Y., Seo, M., Campbell, K. G., and Steber, C. M. (2016). The wheat ABA hypersensitive ERA8 mutant is associated with increased preharvest sprouting tolerance and altered hormone accumulation. *Euphytica* 212, 229–245. doi: 10.1007/s10681-016-1763-6

McMaster, G. J., and Derera, N. F. (1976). Methodology and sample preparation when screening for sprouting damage in cereals. *Cereal Res. Commun.* 4, 251–254.

McNeil, M. D., Diepeveen, D., Wilson, R., Barclay, I., McLean, R., Chalhoub, B., et al. (2009). Haplotype analyses in wheat for complex traits: tracking the chromosome 3B and 7B regions associated with late maturity alpha amylase (LMA) in breeding programs. *Crop Pasture Sci.* 60, 463–471. doi: 10.1071/CP08340

Mohan, A., Kulwal, P., Singh, R., Kumar, V., Mir, R. R., Kumar, J., et al. (2009). Genome-wide QTL analysis for pre-harvest sprouting tolerance in bread wheat. *Euphytica* 168, 319–329. doi: 10.1007/s10681-009-9935-2

Mohler, V., Albrecht, T., Mrva, K., Schweizer, G., and Hartl, L. (2014). Genetic analysis of falling number in three bi-parental common winter wheat populations. *Plant Breed.* 133, 448–453. doi: 10.1111/pbr.12177

Mrva, K., and Mares, D. J. (2001). Quantitative trait locus analysis of late maturity α-amylase in wheat using the doubled haploid population Cranbrook Halberd. *Aust. J. Agric. Res.* 52, 1267–1273. doi: 10.1071/AR01047

Munkvold, J. D., Tanaka, J., Benscher, D., and Sorrells, M. E. (2009). Mapping quantitative trait loci for preharvest sprouting resistance in white wheat. *Theor. Appl. Genet.* 119, 1223–1235. doi: 10.1007/s00122-009-1123-1

Nakamura, S., Abe, F., Kawahigashi, H., Nakazono, K., Tagiri, A., Matsumoto, T., et al. (2011). A wheat homolog of MOTHER OF FT AND TFL1 acts in the regulation of germination. *Plant Cell* 23, 3215–3229. doi: 10.1105/tpc.111.088492

Ogbonnaya, F. C., Imtiaz, M., Ye, G., Hearnden, P. R., Hernandez, E., Eastwood, R. F., et al. (2008). Genetic and QTL analyses of seed dormancy and preharvest sprouting resistance in the wheat germplasm CN10955. *Theor. Appl. Genet.* 116, 891–902. doi: 10.1007/s00122-008-0712-8

Paterson, A. H., and Sorrells, M. E. (1990). Inheritance of grain dormancy in white-kernelled wheat. *Crop Sci.* 30, 25–30. doi: 10.2135/cropsci1990.0011183X003000010006x

Paterson, A. H., Sorrells, M. E., and Obendorf, R. L. (1989). Methods of evaluation for preharvest sprouting resistance in wheat breeding programs. *Can. J. Plant Sci.* 69, 681–689. doi: 10.4141/cjps89-084

Perten, H. (1964). Application of the falling number method for evaluating α-amylase activity. *Cereal Chem.* 41, 127–140.

Piepho, H. P., Möhring, J., Melchinger, A. E., and Büchse, A. (2008). BLUP for phenotypic selection in plant breeding and variety testing. *Euphytica* 161, 209–228. doi: 10.1007/s10681-007-9449-8

Pool, M., and Patterson, F. L. (1958). Moisture relations in soft red winter wheats. II. Awned versus Awnless and Waxy versus Nonwaxy Glumes. *Agron. J.* 50, 158–160. doi: 10.2134/agronj1958.00021962005000030013x

Rasul, G., Humphreys, D. G., Brûlé-Babel, A., McCartney, C. A., Knox, R. E., DePauw, R. M., et al. (2009). Mapping QTLs for pre-harvest sprouting traits in the spring wheat cross 'RL4452/AC Domain.' *Euphytica* 168, 363–378. doi: 10.1007/s10681-009-9934-3

Rehman Arif, M. A., Neumann, K., Nagel, M., Kobiljski, B., Lohwasser, U., and Börner, A. (2012). An association mapping analysis of dormancy and pre-harvest sprouting in wheat. *Euphytica* 188, 409–417. doi: 10.1007/s10681-012-0705-1

Reif, J. C., Gowda, M., Maurer, H. P., Longin, C. F. H., Korzun, V., Ebmeyer, E., et al. (2011). Association mapping for quality traits in soft winter wheat. *Theor. Appl. Genet.* 122, 961–970. doi: 10.1007/s00122-010-1502-7

Rodríguez, M. V., Barrero, J. M., Corbineau, F., Gubler, F., and Benech-Arnold, R. L. (2015). Dormancy in cereals (not too much, not so little): about the mechanisms behind this trait. *Seed Sci. Res.* 25, 99–119. doi: 10.1017/S0960258515000021

Ross, A. S., Flowers, M. D., Zemetra, R. S., and Kongraksawech, T. (2012). Effect of grain protein concentration on falling number of ungerminated soft white winter wheat. *Cereal Chem. J.* 89, 307–310. doi: 10.1094/CCHEM-07-12-0085-RC

Saintenac, C., Jiang, D., Wang, S., and Akhunov, E. (2013). Sequence-based mapping of the polyploid wheat genome. *G3* 3, 1105–1114. doi: 10.1534/g3.113.005819

Schramm, E. C., Abellera, J. C., Strader, L. C., Campbell, K. G., and Steber, C. M. (2010). Isolation of ABA-responsive mutants in allohexaploid bread wheat (*Triticum aestivum* L.): drawing connections to grain dormancy, preharvest sprouting, and drought tolerance. *Plant Sci.* 179, 620–629. doi: 10.1016/j.plantsci.2010.06.004

Shorinola, O., Balcárková, B., Hyles, J., Tibbits, J. F. G., Hayden, M. J., Holušova, K., et al. (2017). Haplotype ANalysis of the pre-harvest sprouting resistance locus Phs-A1 reveals a causal role of TaMKK3-A in global germplasm. *Front. Plant Sci.* 8:1555. doi: 10.3389/fpls.2017.01555

Shorinola, O., Bird, N., Simmonds, J., Berry, S., Henriksson, T., Jack, P., et al. (2016). The wheat Phs-A1 pre-harvest sprouting resistance locus delays the rate of seed dormancy loss and maps 0.3 cM distal to the PM19 genes in UK germplasm. *J. Exp. Bot.* 67, 4169–4178. doi: 10.1093/jxb/erw194

Somyong, S., Ishikawa, G., Munkvold, J. D., Tanaka, J., Benscher, D., Cho, Y.-G., et al. (2014). Fine mapping of a preharvest sprouting QTL interval

on chromosome 2B in white wheat. *Theor. Appl. Genet*. 127, 1843–1855. doi: 10.1007/s00122-014-2345-4

Tang, Y., Liu, X., Wang, J., Li, M., Wang, Q., Tian, F., et al. (2016). GAPIT Version 2: an enhanced integrated tool for genomic association and prediction. *Plant Genome* 9, 1–9. doi: 10.3835/plantgenome2015.11.0120

Torada, A., Koike, M., Ogawa, T., Takenouchi, Y., Tadamura, K., Wu, J., et al. (2016). A causal gene for seed dormancy on wheat chromosome 4A encodes a MAP kinase kinase. *Curr. Biol*. 26, 782–787. doi: 10.1016/j.cub.2016.01.063

Tuttle, K. M., Martinez, S. A., Schramm, E. C., Takebayashi, Y., Seo, M., and Steber, C. M. (2015). Grain dormancy loss is associated with changes in ABA and GA sensitivity and hormone accumulation in bread wheat, *Triticum aestivum* (L.). *Seed Sci. Res.* 25, 179–193. doi: 10.1017/S0960258515000057

Ullrich, S. E., Lee, H., Clancy, J. A., del Blanco, I. A., Jitkov, V. A., Kleinhofs, A., et al. (2009). Genetic relationships between preharvest sprouting and dormancy in barley. *Euphytica* 168, 331–345. doi: 10.1007/s10681-009-9936-1

Walker-Simmons, M. (1987). ABA Levels and sensitivity in developing wheat embryos of sprouting resistant and susceptible cultivars. *Plant Physiol.* 84, 61–66. doi: 10.1104/pp.84.1.61

Wang, S., Wong, D., Forrest, K., Allen, A., Chao, S., Huang, B. E., et al. (2014). Characterization of polyploid wheat genomic diversity using a high-density 90 000 single nucleotide polymorphism array. *Plant Biotechnol. J.* 12, 787–796. doi: 10.1111/pbi.12183

Warner, R. L., Kudrna, D. A., Spaeth, S. C., and Jones, S. S. (2000). Dormancy in white-grain mutants of Chinese Spring wheat (*Triticum aestivum* L.). *Seed Sci. Res*. 10, 51–60. doi: 10.1017/S0960258500000064

Yu, N., Laurenz, R., Siler, L., Ng, P. K. W., Souza, E., and Lewis, J. M. (2015). Evaluation of α-amylase activity and falling number around maturity for soft white and soft red wheat varieties in Michigan. *Cereal Res. Commun.* 43, 1–10. doi: 10.1556/0806.43.2015.026

Zhang, J., Chen, J., Bowman, B. C., O'Brien, K., Marshall, J. M., and Bonman, J. M. (2014). Association mapping of hagberg falling number in hard white spring wheat. *Crop Sci*. 54:1243. doi: 10.2135/cropsci2013.08.0551

Zhang, Z., Ersoz, E., Lai, C.-Q., Todhunter, R. J., Tiwari, H. K., Gore, M. A., et al. (2010). Mixed linear model approach adapted for genome-wide association studies. *Nat. Genet*. 42, 355–360. doi: 10.1038/ng.546

Zhou, Y., Tang, H., Cheng, M.-P., Dankwa, K. O., Chen, Z.-X., Li, Z.-Y., et al. (2017). Genome-wide association study for pre-harvest sprouting resistance in a large germplasm collection of chinese wheat landraces. *Front. Plant Sci.* 8:401. doi: 10.3389/fpls.2017.00401

Conflict of Interest Statement: The authors declare that the research was conducted in the absence of any commercial or financial relationships that could be construed as a potential conflict of interest.

frontiers in Plant Science

ORIGINAL RESEARCH
published: 08 August 2017
doi: 10.3389/fpls.2017.01393

New Genetic Loci Associated with Preharvest Sprouting and Its Evaluation Based on the Model Equation in Rice

*Gi-An Lee[1,2], Young-Ah Jeon[1], Ho-Sun Lee[3], Do Yoon Hyun[1], Jung-Ro Lee[1], Myung-Chul Lee[1], Sok-Young Lee[1], Kyung-Ho Ma[1] and Hee-Jong Koh[2]**

[1] National Agrobiodiversity Center, National Institute of Agricultural Sciences, Jeonju, South Korea, [2] Department of Plant Science, Plant Genomics and Breeding Institute, and Research Institute of Agriculture and Life Sciences, Seoul National University, Seoul, South Korea, [3] International Technology Cooperation Center, Jeonju, South Korea

Preharvest sprouting (PHS) in rice panicles is an important quantitative trait that causes both yield losses and the deterioration of grain quality under unpredictable moisture conditions at the ripening stage. However, the molecular mechanism underlying PHS has not yet been elucidated. Here, we explored the genetic loci associated with PHS in rice and formulated a model regression equation for rapid screening for use in breeding programs. After re-sequencing 21 representative accessions for PHS and performing enrichment analysis, we found that approximately 20,000 SNPs revealed distinct allelic distributions between PHS resistant and susceptible accessions. Of these, 39 candidate SNP loci were selected, including previously reported QTLs. We analyzed the genotypes of 144 rice accessions to determine the association between PHS and the 39 candidate SNP loci, 10 of which were identified as significantly affecting PHS based on allele type. Based on the allele types of the SNP loci, we constructed a regression equation for evaluating PHS, accounting for an R^2 value of 0.401 in *japonica* rice. We validated this equation using additional accessions, which exhibited a significant R^2 value of 0.430 between the predicted values and actual measurements. The newly detected SNP loci and the model equation could facilitate marker-assisted selection to predict PHS in rice germplasm and breeding lines.

Keywords: rice, genetic resources, preharvest sprouting (PHS), dormancy, regression model

OPEN ACCESS

Edited by:
Chengdao Li,
Murdoch University, Australia

Reviewed by:
Yongzhong Xing,
Huazhong Agricultural University, China
Laura Toppino,
Unità di Ricerca per l'Orticoltura (CREA-ORL), Italy

***Correspondence:**
Hee-Jong Koh
heejkoh@snu.ac.kr

Specialty section:
This article was submitted to Crop Science and Horticulture, a section of the journal Frontiers in Plant Science

Received: *10 May 2017*
Accepted: *26 July 2017*
Published: *08 August 2017*

Citation:
Lee G-A, Jeon Y-A, Lee H-S, Hyun DY, Lee J-R, Lee M-C, Lee S-Y, Ma K-H and Koh H-J (2017) New Genetic Loci Associated with Preharvest Sprouting and Its Evaluation Based on the Model Equation in Rice. Front. Plant Sci. 8:1393. doi: 10.3389/fpls.2017.01393

INTRODUCTION

Rice, possessing a relatively small genome size of approximately 370 Mb, is widely used in genomic studies as a model cereal crop plant. Identifying important genes in rice is an excellent approach for finding functional genes in grass-family crops such as wheat (hexaploid) and barley by comparative genomics (He et al., 2007; Liu et al., 2012). Next generation sequencing (NGS) was recently used to detect candidate genes associated with complex traits in diverse genetic backgrounds, and genome-wide associated studies based on haplotype maps have revealed several candidate genes for various agronomic traits in rice (Huang et al., 2010).

Preharvest sprouting (PHS) in rice panicles is caused by the breakage of adequate seed dormancy, while, under normal seed dormancy, the maturation status of the seed is arrested

for various periods of time to allow it to germinate under favorable conditions (Gubler et al., 2005). PHS is an important trait in cereal crops, as it reduces grain yields and grain quality under unpredictable moisture conditions (Bewley and Black, 1982; Bailey et al., 1999; Li et al., 2004). Therefore, improving PHS resistance is a major breeding target for cereal crops worldwide (Zhang et al., 2014), and understanding of the genetic basis of seed dormancy and its breakage is important for regulating PHS in cereal crops.

The major genes associated with seed dormancy and germination reported to date are related to the biosynthesis, catabolism, perception, and signal transduction of abscisic acid (ABA), revealing its central role in controlling seed dormancy. Arabidopsis *AtABI3* plays a role in the initial ABA-dependent check point for seed dormancy, and its orthologous genes *ZmVP-1* in maize, *OsVP1* in rice and *TaVp-1* in wheat are global regulators of seed maturation in these crops (Hattori et al., 1994; Nakamura and Toyama, 2001; Lopez-Molina et al., 2002; De Laethauwer et al., 2012; Huang et al., 2012).

In rice, *Sdr4* is positively regulated by *OsVP1*, which acts as an intermediate regulator in the genetic regulation of seed dormancy (Sugimoto et al., 2010), and Zhang et al. (2014) isolated *TaSdr*, which is associated with tolerance to PHS, and developed a functional marker in wheat in a comparative study based on rice *Sdr4* (Zhang et al., 2014). Mutations in genes that participate in the biosynthesis of the carotenoid precursors of ABA cause PHS in rice (Fang et al., 2008). The dormancy QTL *qSD12*, which was delimited to a 75 kb region of chromosome 12, includes two candidate underlying genes: *PIL5* (phytochrome-interacting factor3-like 5) and *bHLH* (basic helix-loop-helix) (Gu et al., 2010). *qSD7-1/qPC7* (*Rc* locus) is a pleiotropic gene that promotes the expression of key genes for ABA biosynthesis and seed pigmentation (Gu et al., 2011). Although several QTLs associated with seed dormancy and PHS caused by the breakage of adequate dormancy have been reported (Dong et al., 2003; Gao et al., 2008; Hori et al., 2010) and both fine mapping analysis based on QTLs and mutant studies have been conducted to unveil the genetic basis of seed dormancy and PHS (Dong et al., 2003; Fang et al., 2008; Gao et al., 2008; Gu et al., 2010, 2011; Hori et al., 2010; Sugimoto et al., 2010), the molecular mechanism of dormancy release and PHS has been unclear. Therefore, many more genes and alleles associated with seed dormancy and PHS must be identified to help breeders overcome the problem of PHS in cereal crops under unpredictable climate conditions. Magwa et al. (2016) reported genome-wide 16 loci significantly associated with seed germination in diverse rice germplasm by association mapping.

We previously analyzed the variation in PHS and seed germination among various rice genetic resources to increase the number of available alleles for PHS, as most studies of PHS and seed dormancy have been performed using limited resources and alleles from some well-known accessions (Lee et al., 2016); In this study, wide variations in PHS degree were discovered and the increase in germination of detached seeds from the panicle was detected among diverse rice genetic resources. Interestingly, PHS-susceptible accessions maintained higher or similar ABA levels compared with PHS-resistant accessions, suggesting that the key factors for seed dormancy and its breakage could be ABA perception and signal transduction.

The seed germination test after cultivation in Korean middle and southern region for 2 years revealed similar variation of seed germinability (data not shown), and these reflected that some genetic factors artificially selected during rice domestication might affect the diversity of seed germination besides environmental effects. In the current study, we searched for SNPs showing distinct allelic distribution between PHS resistant and susceptible accessions based on genome re-sequencing of representative accessions. We then genotyped the putative PHS-associated SNPs in rice germplasm and constructed a regression equation for the quantitative trait PHS, which could facilitate breeding for PHS resistance in rice.

MATERIALS AND METHODS

Characterization of PHS and GI

The flowering date were tagged by panicles of each accession, and seeds and panicles having same flowering date (**Table 1** and Supplementary Tables 1, 7) were harvested at 42 days after flowering (DAF) in the various rice accessions. The moisture content was adjusted by drying at 15°C (RH 10%) during a 7 days period, as previously described (Lee et al., 2016). The susceptibility for PHS (PHS value) was surveyed using three panicles per each accession, which were incubated at 25°C (RH 100%) for 7 days, after which the number of germinated seeds on each panicle was recorded and expressed as a percentage of the total grain number per panicle. The lower the PHS value, the lower the susceptibility to PHS and the higher the resistance. Seed germination at harvesting time (GHT) was determined by threshing the panicles and planting three replications of 50 seeds (fruits in hulls) onto moistened Whatman filter paper (10 mL of distilled water) in Petri dishes. The seeds were incubated at 25°C (RH 100%) based on International Seed Testing Association (ISTA) guidelines, and germinated seeds (radicle and coleoptile emerged from the hull) were counted daily for a period of 10 days. The cumulative number of germinated seeds was expressed as the percentage of seeds planted. Germination index (GI) was calculated as described by Basra et al. (2005).

DNA Re-sequencing and Detection of Divergent SNPs by PHS Group

Twenty-one samples (*japonica*, 14; *indica/tongil*, 7; **Table 1**), revealing similar flowering times (early August), were selected as representatives by PHS resistance (PHS resistant representatives: PHS $< 20\%$, PHS susceptible representatives: PHS $> 40\%$) at 42 DAF among the diverse rice genetic resources (Lee et al., 2016) in that environmental noises might reduce the resolution for the detection of PHS associated genetic loci in the field condition test. The samples were re-sequenced using the Illumina HiSeq 2500 platform to identify genome-wide variations and to detect genetic signals associated with PHS.

Genomic DNA was extracted from the 21 rice samples using a Gentra Puregene Cell Kit for Plants (Qiagen, Hilden,

TABLE 1 | Accessions used for the detection of divergent SNPs based on the PHS trait using re-sequencing and enrichment analysis.

Ecotype	Group	N	Accessions
japonica	PHS susceptible	8	Hyangjeomdo_IT204516(CHN), Janggyeong 1_IT204522(CHN), white rice_IT246754(KGZ), GIZA 159_IT001447(EGY), Gopum_Var-1(KOR), Migwang_Var-2(KOR), Woonbong 40_Var-3(KOR), Hwayoung_Var-4(KOR)
	PHS resistant	6	Share-192-1-B_IT213660(KOR), Chungseungjaerae_IT214294(JPN), Koshihikari_IT226904(JPN), Xiaozhanjiangmidao_IT225135(CHN), Jowoon_Var-5(KOR), Joongsaenggold_Var-6(KOR)
indica	PHS susceptible	3	CHACHME_IT679(TWN), Tianshangu_IT223668(CHN), KULU_IT2805(AUS)
	PHS resistant	4	Aswina_IT251140(BGD), KELEE_IT259863(BGD), DaccA14_IT259940(IND), Dasan_Var-7(KOR)

Germany). Library construction and sequencing data collection were conducted using Illumina's official protocol with a 101 bp paired-end read length. Trimmomatic-0.33 (Bolger et al., 2014) was used to remove adapters and low-quality reads. The adapter-free trimmed reads were mapped against the reference genome of *Oryza sativa* L. (IRGSP-1.0.27) using Bowtie2 with default parameters (Langmead and Salzberg, 2012). The mapped reads were assigned to read groups and sorted using Picard version 1.138.[1] Picard was also used to remove potential PCR duplicates and to repair mismatches between each read and its mate pair. For the subsequent local realignment, base quality recalibration, and variant calling steps, Genome Analysis Toolkit (GATK) version 3.4.46 (McKenna et al., 2010) was used. Local realignment of reads was carried out to correct misalignments caused by the presence of InDels. Base quality recalibration was performed to compensate for base quality errors from empirical measurements. For variant calling, arguments including "UnifiedGenotyper" and "SelectVariants" were used. Finally, the identified variants were filtered using the "VariantFiltration" argument based on the following criteria: (1) Reads with a mapping quality of zero, MQ0 higher than 4, and MQ0/(1.0*DP) higher than 0.1, where DP is the unfiltered read depth, (2) FS higher than 200 to reduce false positives, and (3) Phred-scaled quality score lower than 30.

To identify specific SNPs in the PHS groups (PHS resistant and susceptible group), Fisher's exact test implemented in SNPSift was conducted to analyze the resulting genotype count data (Cingolani et al., 2012) contrary to the linear or mixed model generally used for genome-wide association studies (GWAS) (Korte and Farlow, 2013). Information about PHS-specific groups and the genotype data assigned to the dominant and recessive models of the 2×2 contingency tables were used in this statistical test. To minimize the rate of false positives, multiple Bonferroni correction was conducted. SNPs were considered significant when the *p*-value of the total number of tests was below 0.05. Significantly enriched SNPs were annotated with SNPeff.

Genotyping of Candidate SNPs in Diverse Rice Germplasm

Thirty-nine candidate SNP loci (for genotyping diverse rice genetic resources) were selected, including SNPs in germination-related genes with hormonal action, such as ABA perception and signal transduction, as well as SNPs in genes expressed specifically in florets and grains (Supplementary Table 8). A total of 144 accessions (80 *japonica* accessions and 64 *indica* accessions) showing PHS variations (Supplementary Table 7) were used to genotype the candidate SNPs, and an additional 56 *japonica* accessions (mainly Korean landraces) were used to validate the regression model.

Genotyping was performed using Fluidigm 192.24 Dynamic Array integrated fluid circuits (Fluidigm Incorporated, San Francisco, CA, United States). The IFC Controller utilizes pressure to control the valves in the chips and to the load samples and genotyping assay reagents into the reaction chambers. The EP-1 system was used as an endpoint image reader. Specific target amplification (STA) reactions were performed in a GeneAmp PCR System 9700 from Applied Biosystems.

For SNP genotyping, 5 μL of STA mix was prepared for each sample, containing 1 × Qiagen Multiplex PCR Master Mix (Qiagen, PN 206143) and 50–60 ng of genomic DNA. After diluting the STA mix, an allele-specific SNP genotyping assay was carried out with the SNPtype assays protocol in the Fluidigm 192.24 Dynamic Array IFC User's Guide (PN 68000098 N1). After PCR amplification, the endpoint fluorescent image data were acquired on the EP-1 System. Data were analyzed using Fluidigm SNP Genotyping Analysis software to obtain genotype calls.

Since the *japonica* and *indica* ecotypes have different genetic constitutions, the accessions were separately analyzed based on ecotype (Morishima and Oka, 1981; Sun et al., 2002, 2015). Despite the scarcity of suitable molecular markers for seed germinability, some reported markers were available, such as InDel and SNP loci in *qLTG3-1* controlling low-temperature germinability in rice (Fujino et al., 2008; Fujino and Sekiguchi, 2011); these markers (and modified markers) were used to elaborate the regression equation for PHS.

Data Analysis

One-way analysis of variance (ANOVA), Duncan's multiple range test (DMRT), correlation analysis, and regression analysis were conducted using R software (ver. 3.2.3)[2], and differences were considered significant when $p\text{-}value < 0.05$. The spatio-temporal expression patterns of genes in various tissues throughout plant growth were surveyed using the Rice Expression Profile Database (RiceXPro)[3].

[1] http://picard.sourceforge.net

[2] http://www.r-project.org/

[3] http://ricexpro.dna.affrc.go.jp

RESULTS

Sequencing of Representative Rice Accessions to Detect Genome-Wide Variation

A total of 21 accessions with similar heading dates were sequenced using an Illumina HiSeq 2500 sequencer to identify polymorphisms between PHS resistant and susceptible accessions (**Table 1**). The genomes of these selected accessions were sequenced at an average of ∼25.7 × coverage, with an average of 9.59 Gb total bases (8.01–10.82) and 94.9 million reads (Supplementary Table 1). The sequences were aligned against the reference genome of *Oryza sativa* L. (IRGSP-1.0.27) using Bowtie2 with default parameters (Langmead and Salzberg, 2012). The alignment rate ranged from 92.8% (IT226904, Koshihikari) to 98.7% (IT 259863, KELEE), with a mean alignment rate of 96.8%. After filtering of potential PCR duplicates and correction of misalignments due to the presence of InDels, the genome-wide SNPs were detected using GATK (McKenna et al., 2010). To minimize the number of false-positive calls, we used several filtering steps before subjecting the candidate SNPs to further analyses based on the following: Phred-scaled quality score, mapping quality, quality depth, and Phred-scaled *p*-value. We ultimately acquired approximately 4.27 million genome-wide SNPs, with an average ratio of one SNP per 87 bp (Supplementary Table 2).

Distribution of SNPs Showing Allelic Differentiation between PHS Resistant and Susceptible Accessions

We conducted enrichment analysis using Fisher's exact test implemented in SNPSift (Cingolani et al., 2012) to detect allelic differentiation between PHS resistant and susceptible accessions and annotated significantly enriched SNPs in each PHS grou2.p using SNPef. Among the 4.27 million SNPs detected genome-wide, approximately 21,000 and 18,000 SNP loci showed distinguished allelic distribution between PHS resistant and susceptible accessions (21 accessions, including 14 *japonica* and 7 *indica/tongil*) based on dominant and recessive models (*p-value* < 0.05), respectively, and the common SNPs detected in both model were 16,753 loci (**Table 2** and Supplementary Tables 3, 4). Among the 14 *japonica* accessions, approximately 5,600 and 4,300 SNPs were detected based on dominant and recessive models, respectively, and the common SNPs detected in both models were 4,115 loci (**Table 2** and Supplementary Tables 5, 6).

Among the SNPs showing allelic differentiation between PHS resistant and susceptible accessions, the number of SNPs in genic regions was approximately 4,100 and 1,000 among the 21 total accessions (*japonica*, 14; *indica*, 6; *tongil*, 1) and the 14 *japonica* accessions, respectively (Supplementary Tables 3, 5), based on the dominant model and approximately 3,700 and 800 among the 21 and 14 accessions, respectively, based on the recessive model (Supplementary Tables 4, 6). Among the genic SNPs, intron variants were most prevalent among the 21 accessions (dominant model: 48.3% and recessive model: 48.0%), followed by exon variants (34.0 and 34.3%), 3′ UTR variants (11.4 and 11.3%), and 5′ UTR variants (6.4 and 6.4%). Among the 14 *japonica* accessions, exon variants were most prevalent (dominant model: 43.4% and recessive model: 44.6%), followed by intron variants (31.1 and 28.9%), 3′ UTR variants (16.5 and 16.9%), and 5′ UTR variants (9.1 and 9.5%).

TABLE 2 | Summary of PHS-associated SNPs based on enrichment analysis.

Fisher's exact test	No. of accessions	Total no. of detected SNPs (Common SNPs ¶)	No. of SNPs in genic reg. (Common SNPs ¶)
Dominant model	21 accessions	21,032 (16,753)	4,119 (3,520)
	14 *japonica* accessions	5,644 (4,115)	1,038 (844)
Recessive model	21 accessions	17,988 (16,753)	3,707 (3,520)
	14 *japonica* accessions	4,309 (4,115)	874 (844)

¶ Common SNPs: detected SNPs in both dominant and recessive model.

Chromosomal Distribution of SNPs in Different Alleles Based on PHS Group

We constructed a density plot of SNPs in PHS resistant versus susceptible accessions using a 1 Mb bin size along the rice genome (**Figure 1**). Among the SNPs detected genome-wide, an average of 55 SNPs per bin revealed allelic differentiation between PHS resistant and susceptible accessions. Chromosome-1 has the highest number of SNPs, with an average of 142 per bin, followed by chromosome-11 (78 per bin) and chromosome-12 (69 per bin). Chromosome-8 has the fewest SNPs (12 per bin). Among the *japonica* accessions, only an average of 13 SNPs per bin revealed allelic differentiation between the PHS resistant and susceptible groups. Chromosome-11 has the highest number of SNPs, averaging 36 per bin, followed by chromosome-12 (34 per bin) and chromosome-4 (16 per bin). The fewest SNPs were found on chromosome-10 (three per bin). We compared the locations of the SNPs with publicly reported QTLs related to PHS and dormancy along the rice chromosome, finding that some chromosomal regions contain high numbers of these SNP loci. Region-1 (Chr.1: ∼1–5 Mb, 71 genic SNPs / 184 common SNPs) has a high density of SNPs overlapping with QTL *Sdr6* (Marzougui et al., 2012), *qSD-1* (Miura et al., 2002), *qSD1* (Gu et al., 2004, 2006) and *qDEG1* (Li et al., 2011). Region-2 (Chr.1: ∼31–33 Mb, 140 genic SNPs/787 common SNPs) contains the QTL *qSdn-1* (Lu et al., 2011), while Region-3 (Chr.3: ∼3–11 Mb) contains the QTLs *Sdr1* (Takeuchi et al., 2003), *qDT-SGC3.1* (Jiang et al., 2011) and *qSD-3* (Guo et al., 2004). Region-6 (Chr.7: ∼22–25 Mb, 91 genic SNPs / 787 common SNPs) harbors QTLs overlapping with *qSD-7-2* (Gu et al., 2004), *qMT-SGC7.2* (Jiang et al., 2011), *qPHS-7* (Dong et al., 2003) and fine-mapped *Sdr4* gene (Sugimoto et al., 2010). Region-7 (Chr.12: ∼21–27 Mb, 386 genic SNPs/1,391 common SNPs) harbors the QTL *qSD-12* (Gu et al., 2004) and fine mapped *qSD-12* gene (Gu et al., 2010). Although several studies reported QTLs in Region-4 (Chr.5: ∼24–28 Mb, 1 genic SNPs/5 common

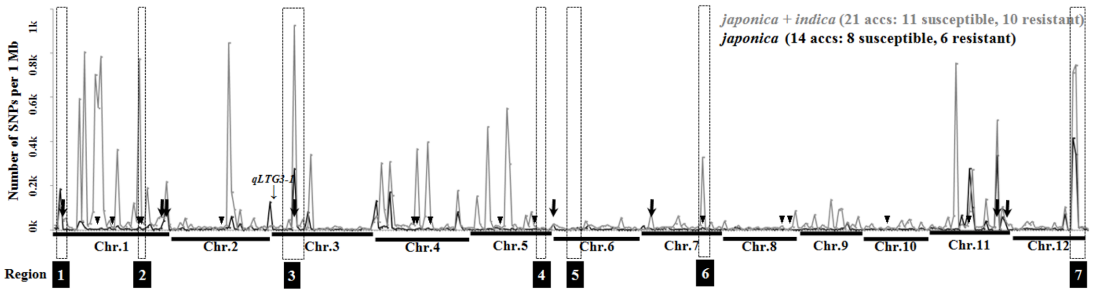

No	QTLs/Genes	Reference	No	QTLs/Genes	Reference
1	*Sdr6,*	(Marzougui et al., 2012)	5	*Sdr9*	(Marzougui et al., 2012)
	qSD-1	(Miura et al., 2002)		*qDOR6-2*	(Cai and Morishima, 2000)
	qSD1	(Gu et al., 2004; Gu et al., 2006)		*qSD6*	(Gu et al., 2004; Gu et al., 2006)
	qDEG1	(Li et al., 2011)	6	*SDR4*	(Sugimoto et al., 2010)
2	*qSdn-1*	(Lu et al., 2011)		*qMT-SGC7.2*	(Jiang et al., 2011)
3	*Sdr1*	(Takeuchi et al., 2003)		*qSD-7-2*	(Gu et al., 2004)
	qDT-SGC3.1	(Jiang et al., 2011)		*qPHS-7*	(Dong et al., 2003)
	qSD-3	(Guo et al., 2004)	7	*qSD12*	(Gu et al., 2004, 2010)
4	*qSdn-5*	(Lu et al., 2011)	►: Germination associated loci (Magwa et al. 2016)		
	qMT-SGC5.1	(Jiang et al., 2011)	→: New significant genetic loci for PHS and GI in this study		

FIGURE 1 | SNP Density plot of SNPs between PHS resistant and susceptible accessions and the locations of reported QTLs; SNP loci associated with PHS and GI in tested accessions are presented.

SNPs) and Region-5 (Chr.6: ∼6–12 Mb, 0 genic SNPs/4 common SNPs), we detected few SNPs in these regions in the current study. Other chromosomal regions revealing high density of SNPs without overlapping with reported QTLs included several germination associated loci by GWAS study (Magwa et al., 2016).

Genotyping of Candidate SNPs and Their Association with PHS in Various Rice Germplasm

Among the approximately 20,000 SNP loci revealing distinct allelic distribution between PHS resistant and susceptible accessions, we genotyped 144 rice germplasm (80 *japonica* accessions and 64 *indica* accessions, Supplementary Table 7) using the 39 SNPs mainly located in genic or promoter region of candidate genes (Supplementary Table 8). We analyzed the differences in PHS and GI values according to genotype. Six and seven loci, including *qLTG3-1* (Fujino et al., 2008; Fujino and Sekiguchi, 2011) revealed significant differences in PHS and GI values according to allele type in 80 *japonica* accessions (p-*value* < 0.05 and p-*value* < 0.01), respectively (**Table 3**). Furthermore, the existence of an awn was also significantly associated with PHS and GI values. Three significant SNP loci were associated with PHS and GI values in 64 *indica* accessions. Specifically, among significant SNPs associated with PHS in *japonica* and *indica* rice, V2 is a significant variant in an upstream region of the rice homolog ortholog of *AtBG1*, which functions in ABA conjugation in Arabidopsis. V5 is a variant in the intron region of a *ROS* homeostasis gene, and the S4 locus is located in the upstream region of *OsVP1*. S13 and S21 are missense variations in the *BRCT domain-containing protein* gene and the *Guanine nucleotide-binding protein* gene, respectively. S3 and S9 are located in a *Dynamin family protein* gene, representing a missense variation and an extra stop codon, respectively. S16 and S19 are missense variations in *CINNAMYL ALCOHOL DEHYDROGENASE 4*. Finally, S1, which is significant only in the *indica* group, is a missense variation in a *hypothetical protein* gene.

Seven new PHS- and GI-associated loci (V2, S4, V5, S13, S21, S16, and S19) in the *japonica* group are not included among previously reported QTLs, whereas the *Dynamin family protein* gene (OS03G0260000), containing the S3 and S9 variations associated with GI, overlaps with reported QTLs including *Sdr1* (Takeuchi et al., 2003), *qDT-SGC3.1* (Jiang et al., 2011) and *qSD-3* (Guo et al., 2004). Among the three loci that are significantly associated with PHS in the *indica* group, S1, located on the short arm of chromosome-1, overlaps with reported QTLs including *Sdr6* (Marzougui et al., 2012), *qSD-1* (Miura et al., 2002), *qSD1* (Gu et al., 2004, 2006), *qDEG1* (Li et al., 2011). We investigated the spatio-temporal expression patterns of genes harboring significant PHS- and GI-associated SNPs by surveying a publically available expression database (RiceXPro).[4] *OsVP1* (S4 variation), *BRCT domain containing protein* (S13 variation), and *Hypothetical protein* (S1 variation) are highly expressed in embryos and endosperm compared with other tissues, whereas *G-protein* (S21 variation) is expressed at low levels in embryos and endosperm during seed maturation (data not shown). *Dynamin family protein* (S3 and S9 variation), *THIOREDOXIN H-TYPE* (V5 variation), and *OsCAD4* (S16 and S19 variation) are more highly expressed in endosperm than in

[4]http://ricexpro.dna.affrc.go.jp/

TABLE 3 | Information about significant SNP loci and PHS and GI distribution by genotype in 80 *japonica* and 64 *indica* accessions.

Ecotype	Group	Name	Loci	Type	*N*	*F*-value	PHS	*F*-value	GI
japonica	Genotype	*qLTG3-1* [27,37]	Chr3 (220067-220621)	normal	67	7.01**	38.4 ± 26.1 b	15.83**	8.6 ± 4.7 b
				72 bp del	13		16.1 ± 23.4 a		3.2 ± 2.7 a
		V2	Chr11_27656171	AA	49	10.66**	42.3 ± 28.4 a	8.225*	8.9 ± 5 a
			(OS11G0683500, *Os11bglu36*)	GG	31		23 ± 18.5 b		5.8 ± 3.9 b
		S4	Chr1_39719385	CC	73	6.071*	37.1 ± 26.6 a	5.268*	8.1 ± 4.8 a
			(OS01G0911700, *OsVP1*)	GG	7		10.4 ± 11.2 b		3.8 ± 2.8 b
		V5	Chr7_4576008	CC	26	5.713*	44.4 ± 27.9 a	2.225	8.8 ± 4.2
			(OS07G0186000, *OsTRXh1*)	AA	54		30.2 ± 24.8 b		7.1 ± 5
		S13	Chr1_41233179	CC	55	5.9*	29.9 ± 25.3 b	3.446	7 ± 5
			(OS01G0939300,	TT	25		45.6 ± 26.5 a		9.2 ± 4.1
			BRCT domain containing protein)						
		S21	Chr6_637769	GG	72	4.414*	32.8 ± 25.6 b	0.002	7.7 ± 4.9
			(OS06G0111400, G-protein)	AA	8		52.9 ± 29.8 a		7.6 ± 3.5
		S3, S9	Chr3_8434986, Chr3_8435901	CC	27	1.416	27.4 ± 28	4.406*	6 ± 4.3 ab
			(OS03G0260000,	CT	1		26.3 ± 0		0.3 ± 0 b
			Dynamin family protein)	TT	52		38.8 ± 25.4		8.7 ± 4.7 a
		S16, S19	Chr11_24303075,	TT	54	1.715	32.2 ± 25.4	8.483**	6.6 ± 4.3 b
			Chr11_24307321	AA	26		40.2 ± 28.6		9.9 ± 5.2 a
			(OS11G0622800, *OsCAD4*)						
	Phenotype		Awn	None	44	4.759*	29.1 ± 24.5 b	6.103*	6.5 ± 4.4 b
				Present	36		41.8 ± 27.6 a		9.1 ± 4.9 a
indica	Genotype	S1	Chr1_3283359	GG	39	10.67**	15 ± 22.3 b	8.894**	4 ± 4.3 b
			(OS01G0162900,	GC	18		24.2 ± 30.1 b		5.3 ± 5.5 b
			Hypothetical protein)	CC	7		63 ± 25.1 a		12.5 ± 5.1 a
		S13	Chr1_41233179	CC	63	5.42*	21.9 ± 28.1 b	4.413*	5.1 ± 5.3 b
			(OS01G0939300,	TT	1		84.5 ± 0 a		16.4 ± 0 a
			BRCT domain containing protein)						
		V2	Chr11_27656171	AA	60	3.14	21.2 ± 28.1	4.81*	4.9 ± 5.3 b
			(OS11G0683500, *Os11bglu36*)	GG	4		48.3 ± 30.6		11 ± 3.8 a

*P-value: ** and * indicate significance at the 1 and 5% level, respectively.*

embryo tissue, while *BETA-GLUCOSIDASE 36* (V2 variation) is expressed at lower levels in endosperm than in embryo tissue.

Development and Validation of a Regression Model for PHS in *japonica* Rice

We conducted regression analysis based on the genotypes of 11 significant loci including *qLTG3-1* and PHS values among 80 *japonica* accessions. The genotypes of significant loci and the presence/absence of awns were converted into binary data (Supplementary Table 9): the reference genotype was coded as "0," while alternative types were coded as "1"; the absence of awns was coded as "0," and their presence was coded as "1." We performed regression analysis using this data set and calculated parameter estimates, *p*-values, and adjusted R^2 values accordingly. The regression model revealing the highest adjusted R^2 value was adopted for PHS estimation, with an adjusted R^2 value of 0.401 [PHS predicted value = 33.082 − 12.171(qLTG3.1) − 14.479(V2) − 11.629(V5) − 20.62(S4) + 22.544(S21) + 12.209(S3) + 10.864(S13) + 11.767(Awn)] (**Table 4**). The regression model is composed of eight factors, including six SNP loci (five loci – significant in PHS, one locus – significant in GI), one InDel locus of *qLTG3-1*, and the awn character.

TABLE 4 | Regression equation for PHS in *japonica*.

Name	Loci	Parameter estimate	*P*-value
qLTG3-1	qLTG3-1	−12.171	*
V2	Chr11_27656171	−14.479	***
V5	Chr7_4576008	−11.629	**
S4	Chr_1_39719385	−20.62	**
S21	Chr_6_637769	22.544	**
S3	Chr_3_8434986	12.209	**
S13	Chr_1_41233179	10.864	**
	Awn	11.767	*
	Intercept	33.082	***
	Adjusted R^2	0.401	

*P-value: ***, **, and * indicate significance at the 1%, 5%, and 10% level, respectively.*

To validate the estimation model for PHS, we genotyped 56 additional Korean *japonica* accessions and measured the PHS value at 42 DAF (Supplementary Table 10). The estimated PHS values derived from the PHS regression equation were

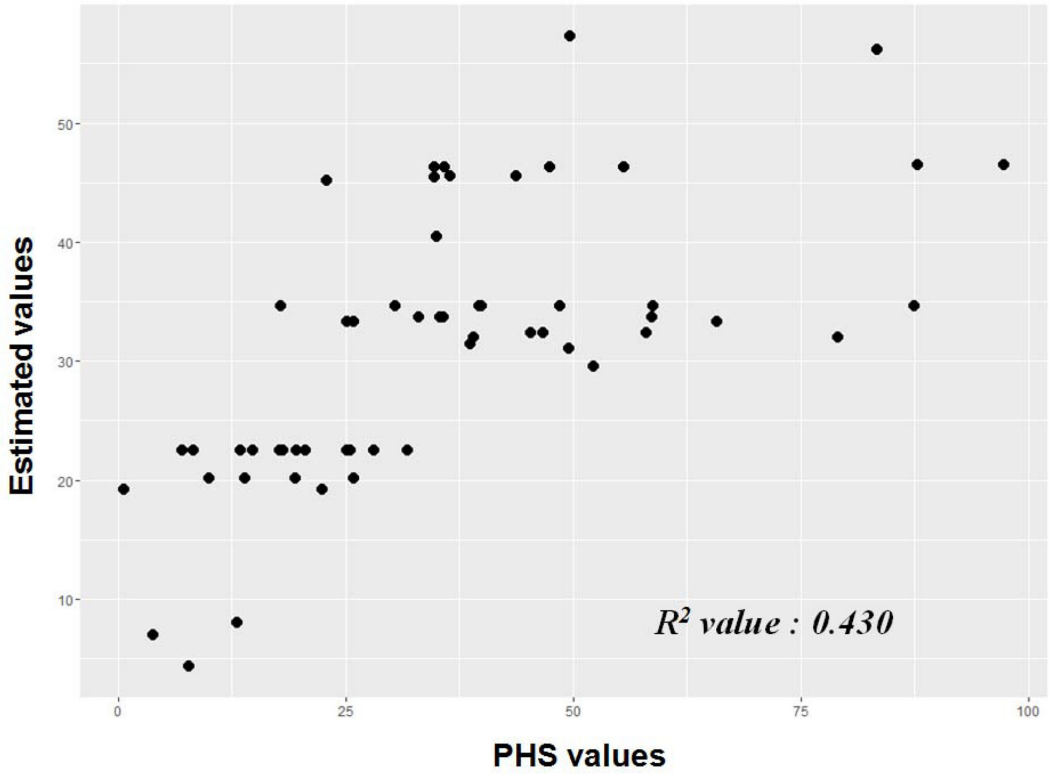

FIGURE 2 | Validation of regression equation model for PHS; 56 *japonica* accessions. * [PHS predicted value = 33.082 − 12.171(qLTG3.1) − 14.479(V2) − 11.629(V5) − 20.62(S4) + 22.544(S21) + 12.209(S3) + 10.864(S13) + 11.767(Awn)]

calculated and compared to actual PHS measurements (**Figure 2**). The R^2 (coefficient of determination) value between the predicted PHS estimates and the actual measurements was 0.430 (*p-values* < 0.001).

DISCUSSION

The regulation of PHS has become a crucial issue due to global climate change, as unpredictable moisture conditions can lead to PHS, which reduces both the quality and quantity of usable grain. Several studies investigated the molecular mechanism underlying PHS caused by the breakage of adequate dormancy, including the identification and fine-mapping of QTLs related to seed dormancy and PHS (Hattori et al., 1994; Bentsink et al., 2006; Fang et al., 2008; Fujino et al., 2008; Gu et al., 2010; Sugimoto et al., 2010; Gu et al., 2011; De Laethauwer et al., 2012). While GWAS using 350 worldwide accessions revealed germination associated 16 loci (Magwa et al., 2016), most studies investigating PHS and seed dormancy in rice have been limited to a few genetic resources. Therefore, in the current study, we surveyed naturally occurring alleles in rice, a model cereal crop, to expand the available alleles for PHS based on phenotypic variations in PHS among diverse rice genetic resources (Lee et al., 2016).

We conducted enrichment analysis using Fisher's exact test to identify differential SNPs between PHS resistant and susceptible accessions to find effective genic SNPs while a linear or mixed model generally have been used for GWAS in plant population (Korte and Farlow, 2013). These SNPs, which reveal increased allelic frequency in either PHS resistant or susceptible rice, might be associated with PHS. While the loss of positive loci or the inclusion of negative loci for PHS might be possible due to the small analyzed samples (21 accessions), these loci could serve as the basis for finding candidate genes affecting the quantitative trait, PHS. We detected approximately 21,000 and 18,000 SNPs revealing distinct allelic distribution between PHS resistant and susceptible accessions (*p-value* < 0.05), respectively, including approximately 4,100 and 3,700 variations in genic regions based on dominant and recessive models, respectively. We constructed a density plot of SNPs showing allelic differentiation between PHS resistant and susceptible accessions, finding different densities in different chromosomal regions. Some regions containing high numbers of these SNPs overlap with previously reported QTLs associated with PHS and seed dormancy; Region-1 and Region-2 of Chromosome-1, Region-3 of Chromosome-3, Region-6 of Chromosome-7, and Region-7 of Chromosome-12 overlap with previously reported QTLs and fine-mapped genes (Miura et al., 2002; Dong et al., 2003; Takeuchi et al., 2003; Gu et al., 2004, 2006, 2010; Sugimoto et al., 2010; Jiang et al., 2011; Li et al., 2011; Lu et al., 2011; Marzougui et al., 2012). The most genome-wide germination associated loci reported by GWAS in rice germplasm (Magwa et al., 2016) were included in the

regions revealing high number of differential SNPs between PHS resistant and susceptible accessions. In this regard, these chromosomal regions might include several genes that are strongly associated with PHS, which could serve as the basis for finding valuable alleles for PHS regulation.

Weedy rice is characterized by seed shattering, higher dormancy, and the presence of awns compared with cultivated rice (Oka, 1988; Cao et al., 2006). Gu et al. (2003) reported that the presence of an awn was negatively correlated with seed germination in F_2 populations derived from a weedy rice strain. In the current study, although the presence of an awn was not significantly correlated with PHS and GI in the *indica* accessions examined, *japonica* accessions with awns showed higher PHS and GI than those lacking awns. Therefore, the presence of an awn might be associated PHS in domesticated *japonica* accessions, which might reflect the different genetic constitutions between *japonica* and *indica* ecotype (Morishima and Oka, 1981; Sun et al., 2002; Sun et al., 2015). We ultimately acquired six and seven SNP loci that were significantly associated with PHS and GI, respectively, in *japonica* rice. Among these loci, the S3 and S9 loci in the *Dynamin family protein* gene (OS03G0260000) are included in the chromosomal region harboring germination-related QTLs such as *Sdr1* (Takeuchi et al., 2003) *Hd8* (QTL for heading date), *qDT-SGC3.1* (Jiang et al., 2011), and *qSD-3* (Guo et al., 2004). S1, which is significant only in *indica* rice, is a variant in the *Hypothetical protein* gene (OS01G0162900). This locus is included in the chromosomal region of germination-related QTLs *Sdr6* (Marzougui et al., 2012), *qSD-1* (Miura et al., 2002), *qSD1* (Gu et al., 2004, 2006), and *qDEG1* (Li et al., 2011). Genes containing these significant SNP loci and overlapping with reported QTL regions might be functional genes for the regulation of PHS. The other genes possessing significant SNP loci are not located in reported major QTL regions. However, these genes might be associated with PHS, as these loci might represent new alleles in natural populations that were difficult to detect in previous general QTL studies using restricted sets of parents.

Using the genotypes of significant SNP loci, we constructed a regression equation for PHS in *japonica* rice. The regression equation showing the highest adjusted R^2 value (0.401) included seven genetic factors and one phenotypic factor (absence or presence of an awn). We validated the regression equation model, finding that the R^2 value between the predicted and actual values was 0.430 ($p\text{-}values < 0.001$). As PHS is a quantitative trait that is regulated by complex factors, it is reasonable to expect that the adjusted R^2 value and the correlation between actual and predicted values would be low.

Several QTLs and significant SNPs have been reported for seed dormancy and PHS, and finding additional factors associated with PHS might increase the resolving power of our equation. Based on this study, we will try to elaborate the regression equation for PHS including previously reported high quality SNPs, and this might be valuable for the molecular breeding for PHS resistance.

AUTHOR CONTRIBUTIONS

G-AL: performed research, analyzed data, wrote the paper. Y-AJ: phenotyped samples, analyzed data. H-SL: performed research, wrote the paper. DH: performed research, analyzed data. J-RL: performed research, analyzed data. M-CL: performed research, analyzed data. S-YL: designed research, performed research. K-HM: designed research, performed research. H-JK: designed research, performed research, wrote the paper.

ACKNOWLEDGMENTS

This work was supported by a grant from the Next-Generation BioGreen 21 Program (Plant Molecular Breeding Center, no. PJ01102401) and was carried out with the support of the Research Program for Agricultural Science & Technology Development (Project No. PJ010898), National Institute of Agricultural Sciences, Rural Development Administration, Republic of Korea

SUPPLEMENTARY MATERIAL

The Supplementary Material for this article can be found online at: http://journal.frontiersin.org/article/10.3389/fpls.2017.01393/full#supplementary-material

REFERENCES

Bailey, P., Mckibbin, R., Lenton, J., Holdsworth, M., Flintham, J., and Gale, M. (1999). Genetic map locations for orthologous *Vp1* genes in wheat and rice. *Theor. Appl. Genet.* 98, 281–284. doi: 10.1007/s001220051069

Basra, S., Farooq, M., Tabassam, R., and Ahmad, N. (2005). Physiological and biochemical aspects of pre-sowing seed treatments in fine rice (*Oryza sativa* L.). *Seed Sci. Technol.* 33, 623–628. doi: 10.15258/sst.2005.33.3.09

Bentsink, L., Jowett, J., Hanhart, C. J., and Koornneef, M. (2006). Cloning of *DOG1*, a quantitative trait locus controlling seed dormancy in *Arabidopsis*. *Proc. Natl. Acad. Sci. U.S.A.* 103, 17042–17047. doi: 10.1073/pnas.0607877103

Bewley, J. D., and Black, M. (1982). *Physiology and Biochemistry of Seeds in Relation to Germination: Viability, Dormancy and Environmental Control*, Vol. 2. Berlin: Springer-Verlag. doi: 10.1007/978-3-642-68643-6

Bolger, A. M., Lohse, M., and Usadel, B. (2014). Trimmomatic: a flexible trimmer for Illumina sequence data. *Bioinformatics* 30, 2114–2120. doi: 10.1093/bioinformatics/btu170

Cao, Q., Lu, B.-R., Xia, H., Rong, J., Sala, F., Spada, A., et al. (2006). Genetic diversity and origin of weedy rice (*Oryza sativa* f. *spontanea*) populations found in north-eastern China revealed by simple sequence repeat (SSR) markers. *Ann. Bot.* 98, 1241–1252. doi: 10.1093/aob/mcl210

Cingolani, P., Patel, V. M., Coon, M., Nguyen, T., Land, S. J., Ruden, D. M., et al. (2012). Using *Drosophila melanogaster* as a model for genotoxic chemical mutational studies with a new program, SnpSift. *Front. Genet.* 3:35. doi: 10.3389/fgene.2012.00035

De Laethauwer, S., Reheul, D., De Riek, J., and Haesaert, G. (2012). *Vp1* expression profiles during kernel development in six genotypes of wheat, triticale and rye. *Euphytica* 188, 61–70. doi: 10.1007/s10681-011-0613-9

Dong, Y., Tsuzuki, E., Kamiunten, H., Terao, H., Lin, D., Matsuo, M., et al. (2003). Identification of quantitative trait loci associated with pre-harvest sprouting resistance in rice (*Oryza sativa* L.). *Field Crops Res.* 81, 133–139. doi: 10.1186/s12870-014-0340-1

Fang, J., Chai, C., Qian, Q., Li, C., Tang, J., Sun, L., et al. (2008). Mutations of genes in synthesis of the carotenoid precursors of ABA lead to pre-harvest sprouting

and photo-oxidation in rice. *Plant J.* 54, 177–189. doi: 10.1111/j.1365-313X.2008.03411.x

Fujino, K., and Sekiguchi, H. (2011). Origins of functional nucleotide polymorphisms in a major quantitative trait locus, qLTG3-1, controlling low-temperature germinability in rice. *Plant Mol. Biol.* 75, 1–10. doi: 10.1007/s11103-010-9697-1

Fujino, K., Sekiguchi, H., Matsuda, Y., Sugimoto, K., Ono, K., and Yano, M. (2008). Molecular identification of a major quantitative trait locus, *qLTG3–1*, controlling low-temperature germinability in rice. *Proc. Natl. Acad. Sci. U.S.A.* 105, 12623–12628. doi: 10.1073/pnas.0805303105

Gao, F., Ren, G., Lu, X., Sun, S., Li, H., Gao, Y., et al. (2008). QTL analysis for resistance to preharvest sprouting in rice (*Oryza sativa*). *Plant Breed.* 127, 268–273. doi: 10.1111/j.1439-0523.2007.01450.x

Gu, X., Kianian, S., and Foley, M. (2006). Isolation of three dormancy QTLs as Mendelian factors in rice. *Heredity* 96, 93–99.

Gu, X.-Y., Chen, Z.-X., and Foley, M. E. (2003). Inheritance of seed dormancy in weedy rice. *Crop Sci.* 43, 835–843. doi: 10.2135/cropsci2003.8350

Gu, X.-Y., Foley, M. E., Horvath, D. P., Anderson, J. V., Feng, J., Zhang, L., et al. (2011). Association between seed dormancy and pericarp color is controlled by a pleiotropic gene that regulates abscisic acid and flavonoid synthesis in weedy red rice. *Genetics* 189, 1515–1524. doi: 10.1534/genetics.111.131169

Gu, X.-Y., Kianian, S. F., and Foley, M. E. (2004). Multiple loci and epistases control genetic variation for seed dormancy in weedy rice (*Oryza sativa*). *Genetics* 166, 1503–1516. doi: 10.1534/genetics.166.3.1503

Gu, X.-Y., Liu, T., Feng, J., Suttle, J. C., and Gibbons, J. (2010). The *qSD12* underlying gene promotes abscisic acid accumulation in early developing seeds to induce primary dormancy in rice. *Plant Mol. Biol.* 73, 97–104. doi: 10.1007/s11103-009-9555-1

Gubler, F., Millar, A. A., and Jacobsen, J. V. (2005). Dormancy release, ABA and pre-harvest sprouting. *Curr. Opin. Plant Biol.* 8, 183–187. doi: 10.1016/j.pbi.2005.01.011

Guo, L., Zhu, L., Xu, Y., Zeng, D., Wu, P., and Qian, Q. (2004). QTL analysis of seed dormancy in rice (*Oryza sativa* L.). *Euphytica* 140, 155–162. doi: 10.1007/s10681-004-2293-1

Hattori, T., Terada, T., and Hamasuna, S. T. (1994). Sequence and functional analyses of the rice gene homologous to the maize *Vp1*. *Plant Mol. Biol.* 24, 805–810. doi: 10.1007/BF00029862

He, X., He, Z., Zhang, L., Sun, D., Morris, C., Fuerst, E., et al. (2007). Allelic variation of polyphenol oxidase (PPO) genes located on chromosomes 2A and 2D and development of functional markers for the PPO genes in common wheat. *Theor. Appl. Genet.* 115, 47–58. doi: 10.1007/s00122-007-0539-8

Hori, K., Sugimoto, K., Nonoue, Y., Ono, N., Matsubara, K., Yamanouchi, U., et al. (2010). Detection of quantitative trait loci controlling pre-harvest sprouting resistance by using backcrossed populations of japonica rice cultivars. *Theor. Appl. Genet.* 120, 1547–1557. doi: 10.1007/s00122-010-1275-z

Huang, T., Qu, B., Li, H.-P., Zuo, D.-Y., Zhao, Z.-X., and Liao, Y.-C. (2012). A maize viviparous 1 gene increases seed dormancy and preharvest sprouting tolerance in transgenic wheat. *J. Cereal Sci.* 55, 166–173. doi: 10.1016/j.jcs.2011.11.003

Huang, X., Wei, X., Sang, T., Zhao, Q., Feng, Q., Zhao, Y., et al. (2010). Genome-wide association studies of 14 agronomic traits in rice landraces. *Nat. Genet.* 42, 961–967. doi: 10.1038/ng.695

Jiang, W., Lee, J., Jin, Y.-M., Qiao, Y., Piao, R., Jang, S. M., et al. (2011). Identification of QTLs for seed germination capability after various storage periods using two RIL populations in rice. *Mol. Cells* 31, 385–392. doi: 10.1007/s10059-011-0049-z

Korte, A., and Farlow, A. (2013). The advantages and limitations of trait analysis with GWAS: a review. *Plant Methods* 9:29. doi: 10.1186/1746-4811-9-29

Langmead, B., and Salzberg, S. L. (2012). Fast gapped-read alignment with Bowtie 2. *Nat. Methods* 9, 357–359. doi: 10.1038/nmeth.1923

Lee, G.-A., Jeon, Y.-A., Lee, H.-S., Hyun, D.-Y., Lee, J.-R., Lee, M.-C., et al. (2016). Variation in pre-harvest sprouting resistance, seed germination and changes in abscisic acid levels during grain development in diverse rice genetic resources. *Plant Genet. Resour.* doi: 10.1017/S1479262116000319 [Epub ahead of print].

Li, C., Ni, P., Francki, M., Hunter, A., Zhang, Y., Schibeci, D., et al. (2004). Genes controlling seed dormancy and pre-harvest sprouting in a rice-wheat-barley comparison. *Funct. Integr. Genomics* 4, 84–93. doi: 10.1007/s10142-004-0104-3

Li, W., Xu, L., Bai, X., and Xing, Y. (2011). Quantitative trait loci for seed dormancy in rice. *Euphytica* 178, 427–435. doi: 10.1007/s10681-010-0327-4

Liu, Y., He, Z., Appels, R., and Xia, X. (2012). Functional markers in wheat: current status and future prospects. *Theor. Appl. Genet.* 125, 1–10. doi: 10.1007/s00122-012-1829-3

Lopez-Molina, L., Mongrand, S., Mclachlin, D. T., Chait, B. T., and Chua, N. H. (2002). ABI5 acts downstream of ABI3 to execute an ABA-dependent growth arrest during germination. *Plant J.* 32, 317–328. doi: 10.1046/j.1365-313X.2002.01430.x

Lu, B., Xie, K., Yang, C., Wang, S., Liu, X., Zhang, L., et al. (2011). Mapping two major effect grain dormancy QTL in rice. *Mol. Breed.* 28, 453–462. doi: 10.1007/s11032-010-9495-0

Magwa, R. A., Zhao, H., and Xing, Y. (2016). Genome-wide association mapping revealed a diverse genetic basis of seed dormancy across subpopulations in rice (*Oryza sativa* L.). *BMC Genet.* 17:28. doi: 10.1186/s12863-016-0340-2

Marzougui, S., Sugimoto, K., Yamanouchi, U., Shimono, M., Hoshino, T., Hori, K., et al. (2012). Mapping and characterization of seed dormancy QTLs using chromosome segment substitution lines in rice. *Theor. Appl. Genet.* 124, 893–902. doi: 10.1007/s00122-011-1753-y

McKenna, A., Hanna, M., Banks, E., Sivachenko, A., Cibulskis, K., Kernytsky, A., et al. (2010). The Genome Analysis Toolkit: a MapReduce framework for analyzing next-generation DNA sequencing data. *Genome Res.* 20, 1297–1303. doi: 10.1101/gr.107524.110

Miura, K., Lin, S., Yano, M., and Nagamine, T. (2002). Mapping quantitative trait loci controlling seed longevity in rice (*Oryza sativa* L.). *Theor. Appl. Genet.* 104, 981–986. doi: 10.1007/s00122-002-0872-x

Morishima, H., and Oka, H. I. (1981). Phylogenetic differentiation of cultivated rice, XXII. Numerical evaluation of the indica-japonica differentiation. *Jpn. J. Breed.* 31, 402–413. doi: 10.1270/jsbbs1951.31.402

Nakamura, S., and Toyama, T. (2001). Isolation of a VP1 homologue from wheat and analysis of its expression in embryos of dormant and non-dormant cultivars. *J. Exp. Bot.* 52, 875–876. doi: 10.1093/jexbot/52.357.875

Oka, H. (1988). *Origin of Cultivated Rice*. Amsterdam: Elsevier.

Sugimoto, K., Takeuchi, Y., Ebana, K., Miyao, A., Hirochika, H., Hara, N., et al. (2010). Molecular cloning of *Sdr4*, a regulator involved in seed dormancy and domestication of rice. *Proc. Natl. Acad. Sci. U.S.A.* 107, 5792–5797. doi: 10.1073/pnas.0911965107

Sun, C., Wang, X., Yoshimura, A., and Doi, K. (2002). Genetic differentiation for nuclear, mitochondrial and chloroplast genomes in common wild rice (*Oryza rufipogon* Griff.) and cultivated rice (*Oryza sativa* L.). *Theor. Appl. Genet.* 104, 1335–1345. doi: 10.1007/s00122-002-0878-4

Sun, X., Jia, Q., Guo, Y., Zheng, X., and Liang, K. (2015). Whole-genome analysis revealed the positively selected genes during the differentiation of indica and temperate japonica rice. *PLoS ONE* 10:e0119239. doi: 10.1371/journal.pone.0119239

Takeuchi, Y., Lin, S., Sasaki, T., and Yano, M. (2003). Fine linkage mapping enables dissection of closely linked quantitative trait loci for seed dormancy and heading in rice. *Theor. Appl. Genet.* 107, 1174–1180. doi: 10.1007/s00122-003-1364-3

Zhang, Y., Miao, X., Xia, X., and He, Z. (2014). Cloning of seed dormancy genes (*TaSdr*) associated with tolerance to pre-harvest sprouting in common wheat and development of a functional marker. *Theor. Appl. Genet.* 127, 855–866. doi: 10.1007/s00122-014-2262-6

Conflict of Interest Statement: The authors declare that the research was conducted in the absence of any commercial or financial relationships that could be construed as a potential conflict of interest.

frontiers in Plant Science

ORIGINAL RESEARCH
published: 13 December 2017
doi: 10.3389/fpls.2017.02123

An Advanced Backcross Population through Synthetic Octaploid Wheat as a "Bridge": Development and QTL Detection for Seed Dormancy

Zhang Dale[1,2†], *He Jie*[1†], *Huang Luyu*[1], *Zhang Cancan*[1], *Zhou Yun*[1,2], *Su Yarui*[1] and *Li Suoping*[1,2*]

[1] School of Life Science, Henan University, Kaifeng, China, [2] Institute of Plant Stress Biology, Henan University, Kaifeng, China

The seed dormancy characteristic is regarded as one of the most critical factors for pre-harvest sprouting (PHS) resistance. As a wild wheat relative species, *Aegilops tauschii* is a potential genetic resource for improving common wheat. In this study, an advanced backcross population (201 strains) containing only *Ae. tauschii* segments was developed by means of synthetic octaploid wheat (hexaploid wheat Zhoumai 18 × *Ae. tauschii* T093). Subsequently, seed dormancy rate (Dor) in the advanced backcross population was evaluated on the day 3, 5 and 7, in which 2 major QTLs (*QDor-2D* and *QDor-3D*) were observed on chromosomes 2D and 3D with phenotypic variance explained values (PVEs) of 10.25 and 20.40%, respectively. Further investigation revealed significant correlation between *QDor-3D* and *Tamyb10* gene, while no association was found between the former and *TaVp1* gene, implying that *QDor-3D* site could be of closer position to *Tamyb10.* The obtained quantitative trait locus sites (QTLs) in this work could be applied to develop wheat cultivars with PHS resistance.

Keywords: quantitative trait locus (QTL), *Aegilops tauschii*, pre-harvest sprouting, seed dormancy, synthetic octaploid wheat

OPEN ACCESS

Edited by:
Jose Maria Barrero, Commonwealth Scientific and Industrial Research Organisation (CSIRO), Australia

Reviewed by:
Marion S. Röder, Leibniz-Institut für Pflanzengenetik und Kulturpflanzenforschung (IPK), Germany
Jirui Wang, Sichuan Agricultural University, China

***Correspondence:**
Li Suoping
hedawheat@163.com;
lisuoping@henu.edu.cn

[†] *These authors have contributed equally to this work.*

Specialty section:
This article was submitted to Plant Breeding, a section of the journal Frontiers in Plant Science

Received: *12 October 2017*
Accepted: *29 November 2017*
Published: *13 December 2017*

Citation:
Dale Z, Jie H, Luyu H, Cancan Z, Yun Z, Yarui S and Suoping L (2017) An Advanced Backcross Population through Synthetic Octaploid Wheat as a "Bridge": Development and QTL Detection for Seed Dormancy. Front. Plant Sci. 8:2123. doi: 10.3389/fpls.2017.02123

INTRODUCTION

As a serious natural disaster, pre-harvest sprouting (PHS) is featured by seed germination occurring in spikes before wheat harvest (Sharma et al., 1994), leading to consumption of seed storage material, reduction of grain weight as well as degradation of nutrition and processing quality (Groos et al., 2002). In China, PHS has caused severe damage in many areas including the middle and lower reaches of the Yangtze river, southwest winter wheat and northeast spring wheat regions, due to conventional abundant rains in harvest season (Xiao et al., 2002). Unexpectedly, this situation has occasionally happened in the Huanghuai and north winter wheat regions in recent years. Therefore, breeding PHS resistant varieties has emerged as one of the major objectives to overcome this challenge, particularly for the wet and humid regions in harvest season (Liu et al., 2016).

Resistance to PHS is known to be linked to multi-factors including seed coat color, seed dormancy time, spike characteristics (spikelet density and awn length), germination inhibition substances of glume, alpha amylase activity, abscisic acid (ABA), and gibberellic acid (GA), etc., among which seed dormancy characteristic is regarded as one of the most critical factors for PHS resistance (Mares and Mrva, 2001; Gatford et al., 2002; Kottearachchi et al., 2006; Tan et al., 2006; Munkvold et al., 2009; Liu et al., 2017). Seed dormancy is a complex trait, as it can be affected by

genetic background/gene combinations, as well as environmental conditions (Jaiswal et al., 2012; Kulwal et al., 2012). Therefore, a single major gene or quantitative trait locus (QTL) for seed dormancy cannot comprehensively explain the genetic diversity of wheat varieties. Up to now, QTLs for seed dormancy have been identified on each of the 21 chromosomes of wheat genome utilizing various mapping populations (Mares and Mrva, 2014). Most major QTLs are located on chromosomes 2B (Munkvold et al., 2009; Chao et al., 2010; Somyong et al., 2014), 3A (Mori et al., 2005; Liu et al., 2013), and 4A (Mares et al., 2005; Chen et al., 2008; Ogbonnaya et al., 2008; Torada et al., 2008; Mohan et al., 2009; Rasul et al., 2009; Cao et al., 2016). Major QTLs for PHS were also detected on chromosome 3D of red kernels wheat and 2D of synthetic hexaploid wheat (Groos et al., 2002; Ren et al., 2008). In addition, *TaVp1* and *Tamyb10* genes for PHS resistance have been identified in bread wheat, which are located on the long arms of chromosomes 3A, 3B, and 3D, respectively (Xia et al., 2009; Himi et al., 2011; Sun et al., 2012). *TaVp1* gene also performs the multi-functions of advancing embryo dormancy and repressing germination, besides promoting embryo maturation (McCarty et al., 1991). *Tamyb10* gene is found to be a transcription factor to regulate the flavonoid biosynthetic pathway, controlling proanthocyanidin synthesis in testa. PHS resistance is closely related with the red pigmentation, which could be possibly attributed to the pleiotropic effect of this gene (Himi et al., 2002).

Aegilops tauschii Cosson (DD, 2n = 2x = 14), the diploid progenitor of common wheat, is an annual, self-pollinated plant with high level of genetic variability for disease-resistance, productivity traits and abiotic stress resistance (Sukhwinder et al., 2012). It has a wide natural distribution in central Eurasia, spreading from northern Syria and Turkey to western China. In China, this species mainly distributes in Yili area of Xinjiang and middle reaches of the Yellow River (including Shanxi and Henan provinces) (Wei et al., 2008). The genetic variation of *Ae. tauschii* is more abundant than that of wheat D genome since only *Ae. tauschii* in certain distribution areas are involved in the origin of common wheat (Wang et al., 2013). Therefore, analogous to other wild crop progenitors, *Ae. tauschii* is considered as a prospective gene donor for improving common wheat (Kilian et al., 2011).

Many superior genes of *Ae. tauschii* have been transferred into common wheat by taking synthetic hexaploid wheat (tetraploid wheat × *Ae. tauschii*) as a "bridge" (Miranda et al., 2007). Actually, previous studies indicated that lots of QTLs from synthetic hexaploid wheat had been identified and some were found located on the D genome by utilizing advanced backcross population or introgression lines (Pestsova et al., 2006; Kunert et al., 2007; Naz et al., 2008; Yu et al., 2014). Alternatively, desirable traits may also be transferred from *Ae. tauschii* to common wheat via direct crossing (Miranda et al., 2007). Gill and Raupp (1987) proposed the first systematic direct gene transfer protocol. Though wheat genomes A, B, and D could be improved concurrently through hybridization of synthetic hexaploid wheat with common wheat, the interesting target alleles in *Ae. tauschii* could be transferred into common wheat through direct crossing, avoiding interference of adaptive allelic combinations from the other A and B genomes. However, only a few studies focused on this strategy due to its high sterility in hybrid F_1 from distant hybridization and extremely low ripening rates in backcross between hybrid F_1 and recurrent parent (Cox et al., 1990; Fritz et al., 1995; Olson et al., 2013). As a feature of this work, synthetic octaploid wheat (AABBDDDD, 2n = 8x = 56) was proposed as a "bridge" to overcome the above challenge through chromosome doubling of hybrid F_1 obtained from the cross of *Ae. tauschii* and common wheat. In this study, an advanced backcross population containing only *Ae. tauschii* segments was developed through backcross of synthetic octaploid wheat with recurrent parent, which could effectively broaden the genetic background of common wheat. Meanwhile, QTLs for seed dormancy from *Ae. tauschii* were located in the population, and the obtained strains with seed dormancy characteristics could also provide novel genetic resource for PHS-resistance in wheat breeding.

MATERIALS AND METHODS

Plant Material

The diploid *Ae. tauschii* ssp. *tauschii* accession T093 was originally derived from Henan province, which is resistant to PHS with long seed dormancy time after harvest. Zhoumai 18, a typical white-grain wheat with high susceptibility to PHS, was applied as recurrent parent in this work. Hybrid F_1 plants were obtained through hybridization of *Ae. tauschii* accession T093 as female parents with Zhoumai 18, which were then treated with colchicine to generate synthetic octaploid wheat (AABBDDDD, 2n = 8x = 56). The next year, emasculated florets of Zhoumai 18 were pollinated by synthetic octaploid wheat to generate BC_1F_1 seeds. Afterwards, the BC_1F_1 plants, as female parents, were successively backcrossed two times by Zhoumai 18 and then selfed four generations to produce advanced backcross population (BC_3F_4 population) (**Figure 1**). Phenotypic traits of strains within the group were stabilized after several generations of backcross and selfing, demonstrating consistent ripening rates with the recurrent parent Zhoumai 18. The mapping population and Zhoumai 18 were cultivated on the 2014–2015 crop season in the wheat breeding farm of Plant Germplasm Resources and Genetic Engineering Laboratory, Henan University. Seeds were sown with 10 cm distance between plants and 30 cm row gap, which were grown under consistent field conditions.

Map Construction and QTL Analysis

DNA was extracted from the fresh leaves of advanced backcross population and Zhoumai 18 in 2014 according to the method described previously (Olson et al., 2013). The genetic map was constructed based on the physical positions of simple sequence repeat (SSR) markers from wheat D genome (http://wheat.pw.usda.gov/cgi-bin/GG3/), in which the S19676-2 marker (F: CACTCAGCCAACCCAGGAAA, R: CAAATAGTTCTATCACTTGGTCTCCC) was exploited by utilizing the *Ae. tauschii* genome sequences (Jia et al., 2013). PCR reactions for SSR were performed using the method described by Röder et al. (1998). SSR markers were anchored and grouped to the seven *Ae. tauschii* chromosomes through sequence alignment

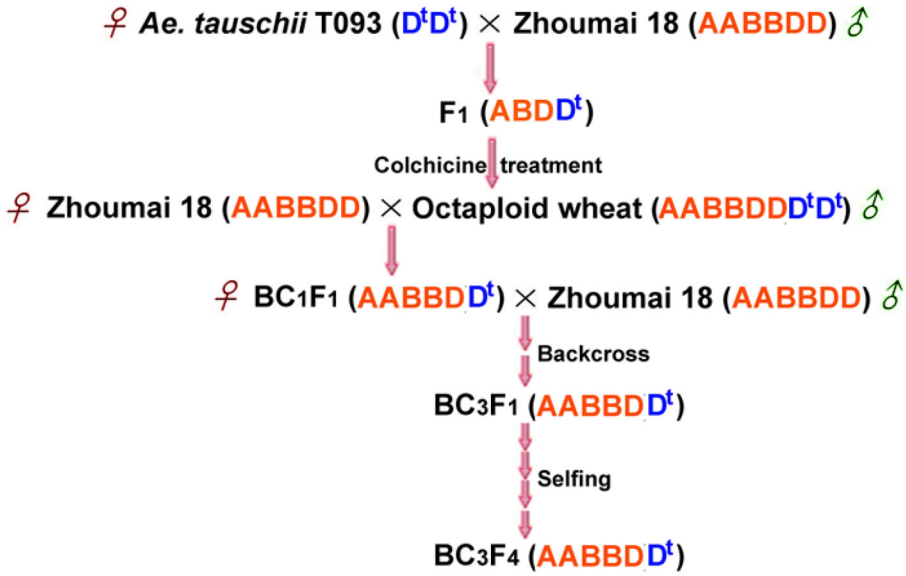

FIGURE 1 | A crossing scheme for obtaining advanced backcross population through the "bridge" of synthetic octaploid wheat. D^t highlighted in blue designates the genome of *Ae. tauschii*.

between the primers and reference genome. The calculation of segment lengths and genome ratios was referred to the method described by Liu et al. (2006). The QTLs for seed dormancy were identified utilizing QTL IciMapping Ver 4.0 (Meng et al., 2015). RSTEP-LRT-ADD mapping (stepwise regression-based likelihood ratio test for additive QTL) was adopted and a significant threshold of likelihood of odds (LOD) was estimated by running 1,000 permutations with a type I error of 0.05.

Amplification and Analysis of *TaVp1* and *Tamyb10* Genes

Two pairs of primers, *TaVp1-4-F1* (5′-TCTTGGTTCACTCG TTAGCATC-3′) + *Vp1-4-R1* (5′- CATTCTGCTCTTGTT GTT GGG-3′) and *Tamyb10-5-F1* (5′-AAGGAATGCGGCAAGAG TGA-3′) + *Tamyb10-5-R1* (5′-TCCTCCACGACCAAAGACCC-3′), were designed from the available sequences of *TaVp1D* (Genbank ID: AJ400714) and *Tamyb10-D1* (Genbank ID: KP279637), respectively. PCR reactions were performed using the method described by Röder et al. (1998). The physical positions of *TaVp1D* and *Tamyb10-D1* were determined based on the sequence alignment with *Ae. tauschii* reference genome. QTLs for seed dormancy of the former were checked in the advanced backcross population utilizing QTL IciMapping Ver 4.0. The correlation between PCR fragments from the latter and seed dormancy was analyzed by Wilcoxon rank sum test.

Phenotypic Evaluation

Five spikes from each line were harvested at day-40 post anthesis (40-dpa), and dried indoors for 5 days at ambient humidity and temperature, which were then manually threshed and placed at −20°C to preserve dormancy for 2 weeks due to slight differences in maturity. Fifty seeds were placed on moistened filter paper in a petri dish (150 mm diameter) and incubated in the dark. The Dor values were evaluated by germination test under room temperature (25°C) on the 3, 5, and 7 days, respectively, based on the method described by Cao et al. (2016) [Dor (%) = 100–GR (%) (GR: germination rate)]. The experiment was conducted with two replicates and the Dor was presented as the arithmetic mean values. The GR of each treatment was calculated using the following formula: GR = G/N, in which G and N stand for the numbers of germinated seeds and the total seeds in a given petri dish, respectively. With regard to lines with rather low germination rate value (≤5%), the remaining seeds were treated with 1 mL of 10 mM gibberellic acid and were then placed at 4°C for 3 days to break dormancy. Afterwards, they were transferred back at room temperature (25°C) and assessed for germination 10 days later. Lines which had not germinated were considered inviable and excluded for further calculation.

Statistical Analysis

Statistical analysis was performed on IBM® statistics 19 (SPSS Inc.,), including Friedman test, Wilcoxon rank sum test, and correlation coefficient (Pearson correlation). The significant difference of seed dormancy rate among correlated samples on the three detections was assessed by Friedman test, while that between two independent samples based on amplified fragments from *Tamyb10-5F1/Tamyb10-5R1* was evaluated by Wilcoxon rank sum test.

RESULTS

Polymorphism Marker on the D Genome and Number of Introgressed Segments

Two hundred and one BC_3F_4 lines were successfully genotyped by SSR markers. Altogether 1114 SSR markers were used to detect polymorphism between the donor parent *Ae. tauschii* T093 and

TABLE 1 | The size of introgressed segments detected in the advanced backcross population and cumulative proportion in the donor genome.

Chr.	Polymorphic markers	Homozygous segments		Heterozygous segments		Maximum chromosome coverage (%)
		No. of segments	Average length (Mb)	No. of segments	Average length (Mb)	
1D	6	23	27.5	12	21.9	31.2
2D	15	82	7.6	30	9.3	31.2
3D	16	212	11.3	33	8.1	32.5
4D	6	21	20.1	6	19.8	17.6
5D	36	686	8.4	27	7.3	75.6
6D	9	106	17.0	15	21.1	39.0
7D	16	233	16.1	36	6.7	44.3
Total	104	1363	15.4	159	13.5	37.0

the recurrent parent Zhuomai 18. Among them, polymorphism between the two parents was detected in 374 SSR markers, in which 104 of them were confirmed to be polymorphic in the advanced backcross population, accounting for 27.8%, with an average of 14.9 markers for each chromosome (**Table 1**). Most of the polymorphic markers were observed on chromosome 5D with the total number of 36, whereas the least was found on chromosome 1D and 4D with the total number of only 6. Besides the unidentified 70 markers, a physical map was constructed based on the 304 polymorphic SSR markers between parents (**Figure 2**), which displayed heterogeneous distribution on 7 linkage groups of D genome, with a total length of 4004.5 Mb. The physical map illustrates an average interval of 36.2 Mb among 104 polymorphic markers in the population, while these markers also exhibit inhomogeneous distribution in different chromosome regions. Specifically, some markers concentrate in the same region with a very short distance, demonstrating a minimum gap of only 0.8 Mb or even no recombination events between them. However, huge long distances were also found for some other markers. For instance, the distance between markers *Xgdm72* and *Xbarc42* on chromosome 3D is determined to be 416.1 Mb.

Altogether 1,522 chromosome segments from *Ae. tauschii* were detected in the advanced backcross population (201 lines). Specifically, no segment was found in 39 lines (19.4%). While the remaining 162 lines (80.6%) contain 1363 homozygous and 159 heterozygous segments, with an average of 8.41 homozygous and 0.98 heterozygous segments in each line (Table S1, Figure S1). Only a single introgressed segment was observed in 34 lines, and 2 segments were identified in 19 lines. According to the physical positions of SSR markers, the size of each introgressed segment in the lines and ratios accounting for the whole donor genome were estimated (**Table 1**). The introgressed segments range from 1.0 to 60.5 Mb, with an average size of 15.4 Mb in homozygous and 13.5 Mb in heterozygous. In addition, the distribution of chromosome segment from *Ae. tauschii* exhibited a significant difference in wheat D genome (Figure S2). Typically, the introgression fragments from 4D of *Ae. tauschii* contain the least 27 fragments, only accounting for 1.8%. Whereas those from 5D occupy the most 713 fragments, accounting for 46.8%. The results herein clearly confirm that the chromosome segments of *Ae. tauschii* have been transferred into common wheat by means of synthetic octaploid wheat (*Ae. tauschii* T093 × Zhoumai18), which effectively broadens the genetic background of common wheat.

Evaluation of Seed Dormancy Rate

Seed dormancy rate (Dor) from 201 lines in the advanced backcross population was examined on the day 3, 5, and 7 (Table S2). Similar frequency distribution of Dor from 201 lines could be observed in the three detections (**Figure 3**), in which the most intensive distribution consistently located at rather low value (Dor $\leq$ 5%). For the long seed dormancy (Dor $>$ 90%), the proportions were determined to be 10.9, 8.9, and 6.9%, respectively, for the day 3, 5, and 7. While as marked by the black arrows, the respective seed dormancy rates of the recurrent parent Zhoumai 18 were 44, 28, and 20% in the parallel experiment, indicating that the PHS-resistance strains are contained in the advanced backcross population. Phenotypic correlations among the obtained seed dormancy rates for the three detections were further analyzed through Pearson coefficient. As shown in **Table 2**, each pair of Dor exhibits high positive correlation with coefficient no $<$0.98. The correlation coefficients for 2 replicates were shown in Table S3. The higher positive correlation coefficient, the less Dor is affected by the external environment factors in this experiment. Additionally, Friedman test of Dor among the lines show highly significant difference ($P < 0.01$) for the three detections, implying minor phenotypic detection error for the obtained phenotype data.

QTL Analysis of Seed Dormancy Rate

To elucidate the genetic control for seed dormancy traits associated with PHS resistance, two major QTLs (*QDor-2D* and *QDor-3D*) were located on Xwmc503 of 2D and Xcfd223 of 3D by QTL IciMapping software in three detections under the single environment (**Figure 4**, **Table 3**). As listed in **Table 3**, the positive alleles of additive effect are derived from *Ae. tauschii*, further underscoring the valuable genes in *Ae. tauschii* as wheat wild resource (Sukhwinder et al., 2012). The *QDor-2D* displays the phenotypic variance explained values (PVEs) of 6.59, 6.02, and 5.64% in the three detections, respectively, corresponding to the additive effect values of 25.13, 23.50, and 22.02. As for *QDor-3D*, the PVE demonstrates prominently enhanced values of 13.83, 12.58, and 11.77%, with the additive effect values of

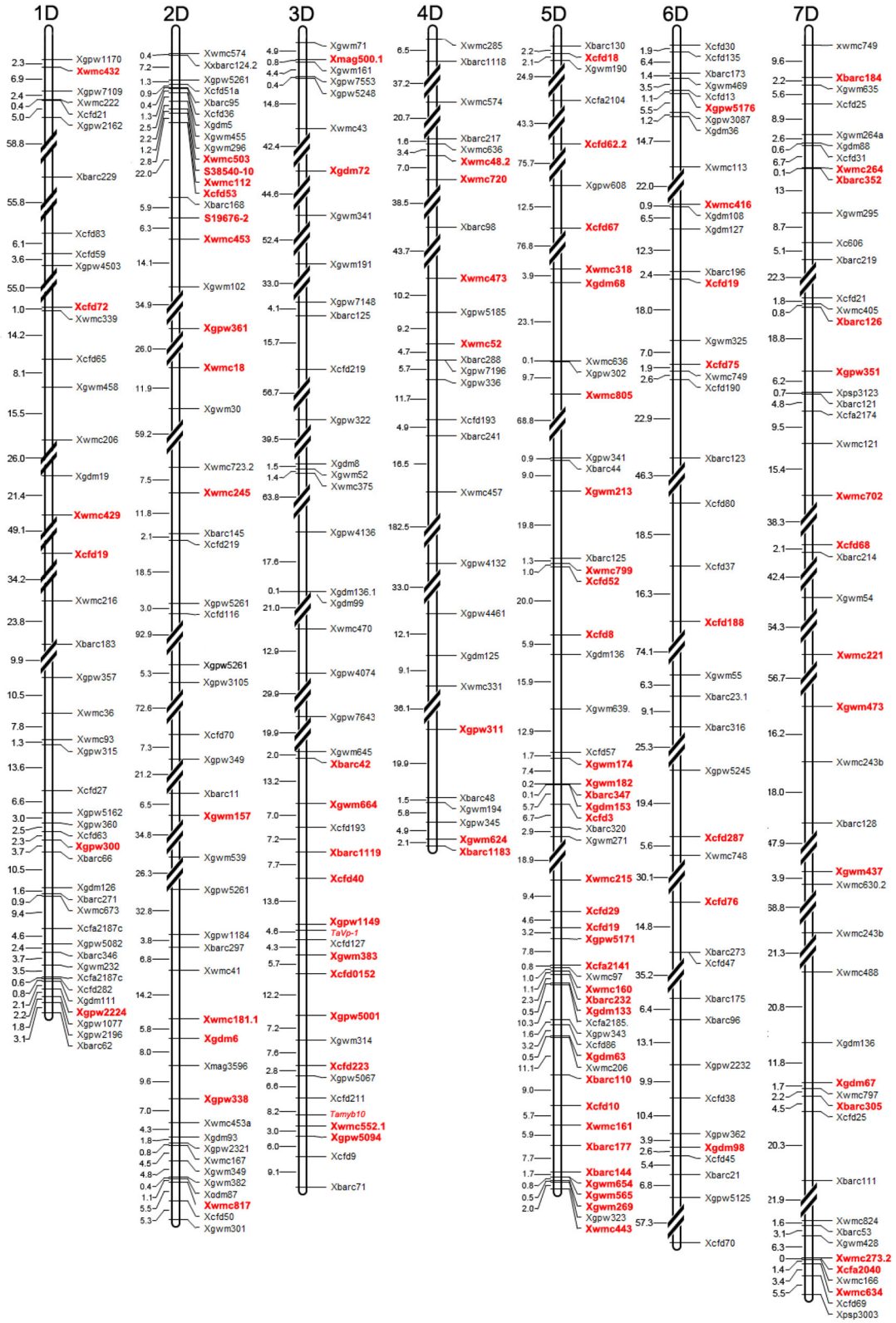

FIGURE 2 | Physical map constructed based on the 304 polymorphic SSR markers between parents. Polymorphic markers in the advanced backcross population are highlighted in red. The unit of distance is megabasepairs (Mb).

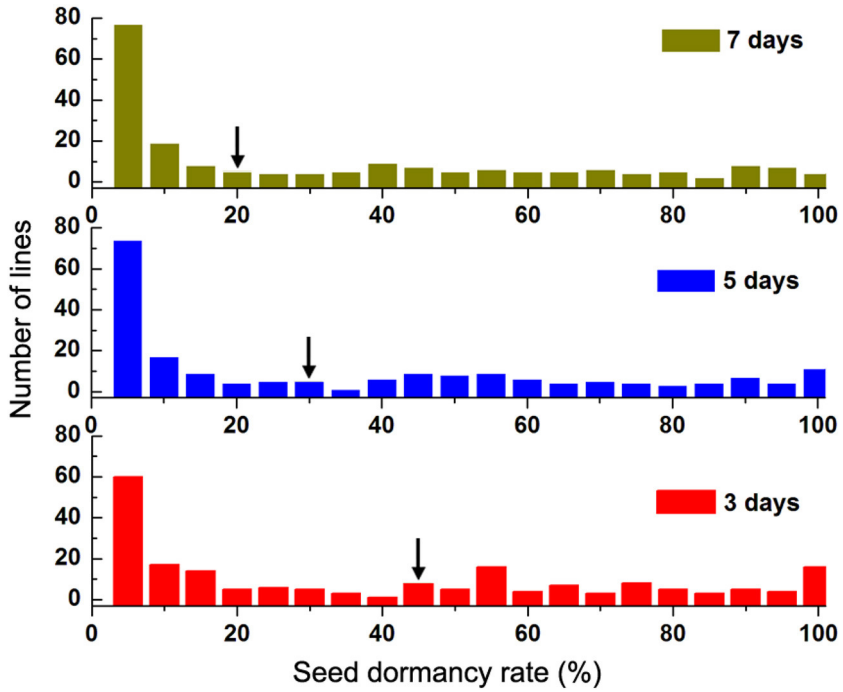

FIGURE 3 | Frequency distributions of seed dormancy rate (Dor) of the advanced backcross population on the day 3, 5, and 7. Red: seed dormancy rate on the day 3; Blue: seed dormancy rate on the day 5; Green: seed dormancy rate on the day 7. Black arrows indicate the mean values of Dor from Zhoumai 18.

TABLE 2 | Correlation coefficients among three time periods associated with Dor in the advanced backcross population.

	Dor 5	Dor 7
Dor 3	0.989**	0.982**
Dor 5	-	0.996**

*Dor 3, seed dormancy rate on the day 3; Dor 5, seed dormancy rate on the day 5; Dor 7, seed dormancy rate on the day 7; **,correlation is significant at the 0.01 level (2-tailed).*

20.91, 19.50, and 18.27. Apparently, QTL detection for Dor could explain more phenotypic variance on the 3rd day compared with the other two measurements, implying the most prominent difference in the seed dormancy among lines in this detection.

Correlation Analysis of *TaVp1*, *Tamyb10* Genes and Seed Dormancy

The genotypes of 201 strains in the advanced backcross population were analyzed through *TaVp1-4F1/TaVp1-4R1* and *Tamyb10-5F1/Tamyb10-5R1* primers (**Figure 5**). The former displayed co-dominant marker with two amplified fragments (282 bp from *Ae. tauschii* and 423 bp from Zhoumai 18), which was afterwards located on chromosome 3D by *Ae. tauschii* genome map (**Figure 2**). The LOD value of this site was found to be <3.0 (**Table 3**), demonstrating little correlation of *TaVp1* with seed dormancy traits. As could be observed in **Figure 5**, 389 bp fragment was amplified only from *Ae. tauschii* in the advanced backcross population by the dominant markers *Tamyb10-5F1/Tamyb10-5R1* since *Tamyb10-D1* gene in white-grained wheat varieties might be deleted. (Himi et al., 2011). Therefore, Wilcoxon rank sum test of two genotypes (0, 1) in the advanced backcross population was performed, revealing significant differences ($p < 0.01$) in seed dormancy between the two genotypes. This result implied that *Tamyb10-D1* gene may have prominent correlation with seed dormancy in the advanced backcross population.

DISCUSSION

Exploration and utilization of fine genes from *Ae. tauschii* is an effective approach to improve the resistance of common wheat, especially in view of the drastic reduction in genetic diversity due to modern breeding (Sukhwinder et al., 2012). Meanwhile, it is convenient to transfer *Ae. tauschii* genes into common wheat by recombination between homologous chromosomes, and most possibly, undesirable gene linkages could be easily broken by repeated backcross with common wheat. Direct crossing from diploid species into hexaploid wheat has been applied as a possible plant breeding technique for rapid introgression of useful traits. Gill and Raupp (1987) provided the first systematic direct gene transfer protocol. Based on this perspective, BC_2F_1 population was constructed through direct crossing of Ug99-resistant *Ae. tauschii* with rust-susceptible wheat (Olson et al., 2013). Another work of direct crossing was reported by Sehgal et al. (2011), who constructed BC_1F_4 population derived from the cross of three heat-tolerant *Ae. tauschii* with bread wheat. In this work, advanced backcross population of BC_3F_4 was constructed through synthetic octaploid wheat as a "bridge," which was obtained from chromosome doubling of hybrid F_1 through direct crossing of *Ae. tauschii* T093 with common wheat

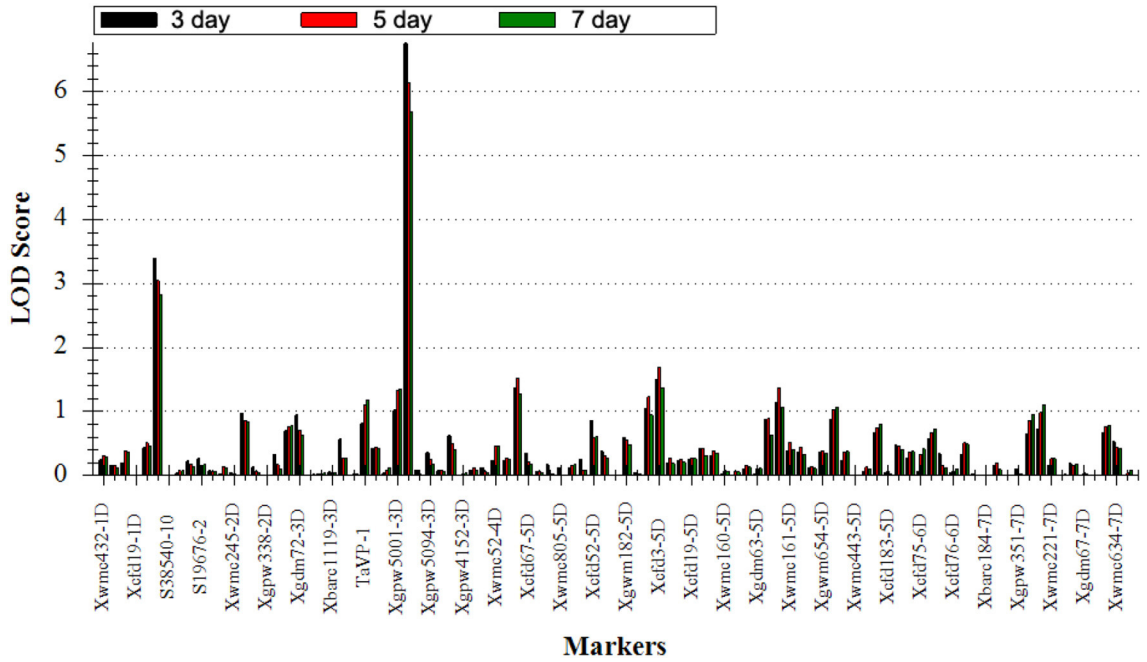

FIGURE 4 | Positions of putative QTLs detected on the day 3, 5, and 7 in the advanced backcross population. Black: LOD of *QTLs* on the day 3; Red: LOD of *QTLs* on the day 5; Green: LOD of *QTLs* on the day 7.

TABLE 3 | Analysis of putative QTLs for seed dormancy traits in the advanced backcross population.

QTL	Detections	Position	Markers	LOD	PVE (%)	Add
QDor-2D	3 day	2D (22.2 Mb)	Xwmc503	3.40	6.59	25.13
	5 day			3.04	6.02	23.50
	7 day			2.82	5.64	22.02
QDor-3D	3 day	3D (576.5 Mb)	Xcfd223	6.76	13.83	20.91
	5 day			6.13	12.58	19.50
	7 day			5.69	11.77	18.27
TaVp-1	3 day	3D (536.8 Mb)	Vp1-4	0.81	1.62	7.90
	5 day			1.10	2.20	9.00
	7 day			1.18	2.37	9.04

LOD, likelihood of odds; PVE, phenotypic variance explained by each QTL; Add, additive effect. Positive values of Add indicate the effects increasing trait values by Ae. tauschii alleles, respectively.

Zhoumai 18. Meanwhile, many strains with poor comprehensive traits could be eliminated in the process of multigenerational backcross and selfing. Therefore, only 27.8% SSR markers were detected in the advanced backcross population, though 374 SSR markers between *Ae. tauschii* accession T093 and Zhoumai 18 were determined to be polymorphic. While in another aspect, the reserved strains may possess better agronomic traits, and no phenotype segregation was found in each line, indicating that these lines are cytogenetically stable, which could be utilized more easily through further breeding.

Seed dormancy is widely regarded as one of the most critical factors for PHS resistance in common wheat, which is greatly influenced by temperature in seed germination stage. Specially, high temperature (>26°C) has negative influence on seed dormancy in late development stage (Ueno, 2002). In this work, the experiment was conducted at ∼25°C, very close to that proposed in the previous literature (Ueno, 2002). The strains with high Dor values could still be detected in this case, revealing the strong additive effect of QTL for seed dormancy in the advanced backcross population. These strains containing desirable seed dormancy characterization herein could provide valuable genes for PHS-resistance breeding.

It is well known that wheat grain color (GC) is linked to PHS-resistance, and red-grained wheat is of more PHS resistance than the white-grained one (Flintham, 2000; Warner et al., 2000; Himi et al., 2002). Early cytogenetic study suggested that GC was controlled by three genes, *R-A1*, *R-B1*, and *R-D1*, locating on homoeologous group 3 chromosomes (Metzger and Silbaugh, 1970). Groos et al. (2002) detected 3 QTLs for PHS locating on the long arm of chromosomes 3A, 3B, and 3D in a bi-parental population, closing to the loci of genes *R* and *TaVp1*, with boundary from *Xgwm314* to *Xcfd9* on chromosome 3D and marker interval of 37.9 cM. The additive effect of QTLs was attributed to the wheat variety "'Renan" with red kernels. Lin et al. (2016) also found 3 QTLs for GC on chromosome 3A, 3B, and 3D in 185 wheat cultivars by genome-wide association study (GWAS). Among the 3 sites, *Tamyb10-D1* demonstrated the highest effect on GC (R^2 = 0.23) in the association mapping panel. Moreover, the corresponding *Qphs.hwwgr-3DL* for PHS-resistance was also observed on chromosome 3D, explaining PVE of 8.3%, which suggests the pleiotropic effects of *Tamyb10-D1* on PHS resistance under the field conditions. In this study, the additive effect of *QDor-3D* origins from *Ae. tauschii*, with the highest value of 20.91 and PVE of 13.83%

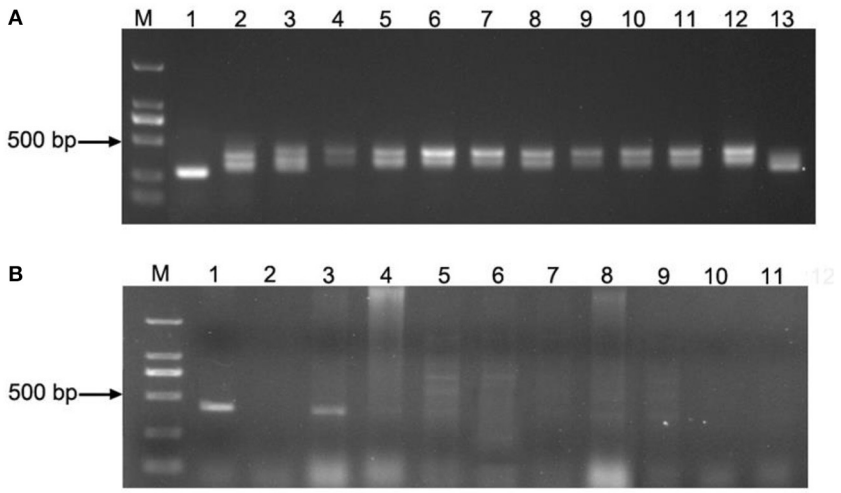

FIGURE 5 | PCR amplification of *TaVp1* and *Tamyb10* sites in partial strains: *TaVp1* **(A)** (M: DL2000 marker; 1: *Ae. tauschii* (282 bp); 2: Zhoumai 18 (423 bp); 3–13: partial strains of advanced backcross population.); *Tamyb10* **(B)** (M: DL2000 marker; 1: *Ae. tauschii* (389 bp); 2: Zhoumai 18; 3–11: partial strains of advanced backcross population).

(higher than the PVE of *Qphs.hwwgr-3DL*). Further analysis indicates that *Tamyb10-D1* from *Ae. tauschii* is highly related with seed dormancy ($p < 0.01$), while no correlation was found between *TaVp1* and seed dormancy. A novel candidate gene is thus speculated to exist between *QDor-3D* (576.5 Mb) and *Tamyb10-D1* (583.9 Mb) for rather large distance (7.4 Mb) in physical position and the little difference in testa color (yellow) among the lines.

QTLs for PHS on chromosome 2D have been identified in recent years. Through a DH population from cross of wheat Cascades with AUS1408, Tan et al. (2006) found a major QTL locating on chromosome 2D (marker interval *Xwmc112-Xgwm102*), with enhanced dormancy from the allele of Cascades. Ren et al. (2008) detected a major QTL (*Qphs.sau-2D*) for PHS-resistance on the short arm of chromosome 2D in 140 F_2 plants. The *Qphs.sau-2D* was identified within the marker interval of *Xwmc261-Xgwm484*, with genetic distance of 15.4 cM, whose additive effect was established to be derived from the D genome of synthetic hexaploid wheat cultivar "RSP." In this study, the additive effect of *QDor-2D* originates from *Ae. tauschii*, with the highest value of 25.19 and PVE of 20.40 %, which was located on Xwmc503 of 2D, which was completely included in Xgwm261-Xgwm484 based on the *Ae. tauschii* reference genome. Specifically, the physical positions of Xwmc503 and Xgwm261 are respectively located in 22226966 ∼ 22227188 bp and 22218627 ∼ 22218480 bp, with a strikingly close distance of 8 Kb. QTLs for PHS-resistance could be found at analogous positions on 2D by utilizing different mapping populations, providing a strong evidence of the existence of candidate genes for PHS-resistance nearby. From this point of view, the *QDor-2D* identified in this study is suitable for marker-assisted breeding to trace the *Ae. tauschii* segment with seed dormancy characterization.

In conclusion, an advanced backcross population containing only *Ae. tauschii* segments was established through the synthetic octaploid wheat (hexaploid wheat Zhoumai 18 × *Ae. tauschii* T093) as a "bridge." Meanwhile, 2 major QTLs (*QDor-2D* and *QDor-3D*) for seed dormancy from *Ae. tauschii* were located on Xwmc503 of 2D and Xcfd223 of 3D through the advanced backcross population, respectively. These QTLs could provide valuable information for marker-assisted breeding, and the obtained strains with long seed dormancy may also provide novel genetic resource for PHS-resistance in wheat breeding.

AUTHOR CONTRIBUTIONS

Conceived and designed the study: LS. Generated the data and performed the analysis: ZD, HJ, HL, ZC, and LS. Contributed reagents, materials, analysis tools: ZY and SY. Wrote the paper: ZD and LS. All authors read and approved the final manuscript.

ACKNOWLEDGMENTS

This work was supported by National Natural Science Foundation of China (Grant Nos. 31401379, 31571649 and 31601297) and Project of Young Teachers in Henan Province (Grant No. 2015GGJS-019) and Project of Major Science and Technology in Henan Province (Grant No. 161100110400), and Project of Science and Technology Department of Henan Province (Grant No. 1721021100048).

SUPPLEMENTARY MATERIAL

The Supplementary Material for this article can be found online at: https://www.frontiersin.org/articles/10.3389/fpls.2017.02123/full#supplementary-material

REFERENCES

Cao, L., Hayashi, K., Tokui, M., Mori, M., Miura, H., and Onishi, K. (2016). Detection of QTLs for traits associated with pre-harvest sprouting resistance in bread wheat (*Triticum aestivum* L.). *Breed. Sci.* 66, 260–270. doi: 10.1270/jsbbs.66.260

Chao, S., Xu, S. S., Elias, E. M., Faris, J. D., and Sorrells, M. E. (2010). Identification of chromosome locations of genes affecting preharvest sprouting and seed dormancy using chromosome substitution lines in tetraploid wheat (*Triticum turgidum* L.). *Crop Sci.* 50, 1180–1187. doi: 10.2135/cropsci2009.10.0589

Chen, C. X., Cai, S. B., and Bai, G. H. (2008). A major QTL controlling seed dormancy and pre-harvest sprouting resistance on chromosome 4A in a Chinese wheat landrace. *Mol. Breed.* 21, 351–358. doi: 10.1007/s11032-007-9135-5

Cox, T. S., Hatcher, J. H., Gill, B. S., Raupp, W. J., and Sears, R. G. (1990). Agronomic performance of hexaploid wheat lines derived from direct crosses between wheat and *Aegilops squarrosa*. *Plant Breed.* 105, 271–277. doi: 10.1111/j.1439-0523.1990.tb01285.x

Flintham, J. E. (2000). Different genetic components control coat-imposed and embryo-imposed dormancy in wheat. *Seed Sci. Res.* 10, 43–50. doi: 10.1017/S0960258500000052

Fritz, A. K., Cox, T. S., Gill, B. S., and Sears, R. G. (1995). Molecular marker-facilitated analysis of introgression in winter wheat × *Triticum tauschii* populations. *Crop Sci.* 35, 1691–1695. doi: 10.2135/cropsci1995.0011183X003500060030x

Gatford, K. T., Eastwood, R. F., and Halloran, G. M. (2002). Germination inhibitors in bracts surrounding the grain of *Triticum tauschii*. *Funct. Plant Biol.* 29, 881–890. doi: 10.1071/PP01011

Gill, B. S., and Raupp, W. J. (1987). Direct genetic transfers from *Aegilops squarrosa* L. to hexaploid wheat. *Crop Sci.* 27, 445–450. doi: 10.2135/cropsci1987.0011183X002700030004x

Groos, C., Gay, G., Perretant, M. R., Bernard, G. M., Dedryver, F., and Charmet, G. (2002). Study of the relationship between pre-harvest sprouting and grain color by quantitative trait loci analysis in a white×red grain bread-wheat cross. *Theor. Appl. Genet.* 104, 39–47. doi: 10.1007/s001220200004

Himi, E., Maekawa, M., Miura, H., and Noda, K. (2011). Development of PCR markers for *Tamyb10* related to R-1, red grain color gene in wheat. *Theor. Appl. Genet.* 122, 1561–1576. doi: 10.1007/s00122-011-1555-2

Himi, E., Mares, D. J., Yanagisawa, A., and Noda, K. (2002). Effect of grain colour gene (R) on grain dormancy and sensitivity of the embryo to abscisic acid (ABA) in wheat. *J. Exp. Bot.* 53, 1569–1574. doi: 10.1093/jxb/erf005

Jaiswal, V., Mir, R. R., Mohan, A., Balyan, H. S., and Gupta, P. K. (2012). Association mapping for pre-harvest sprouting tolerance in common wheat (*Triticum aestivum* L.). *Euphytica* 188, 89–102. doi: 10.1007/s10681-012-0713-1

Jia, J. Z., Zhao, S. C., Kong, X. Y., Li, Y. R., Zhao, G. Y., He, W. M., et al. (2013). *Aegilops tauschii* draft genome sequence reveals a gene repertoire for wheat adaptation. *Nature* 496, 91–95. doi: 10.1038/nature12028

Kilian, B., Mammen, K., Millet, E., Sharma, R., Graner, A., Salamini, F., et al. (2011). "Aegilops," in *Wild Crop Relatives: Genomic and Breeding Resources Cereals*, ed C. Kole (Berlin: Springer), 1–76.

Kottearachchi, N. S., Uchino, N., Kato, K., and Miura, H. (2006). Increased grain dormancy in white-grained wheat by introgression of pre-harvest sprouting tolerance QTLs. *Euphytica* 152, 421–428. doi: 10.1007/s10681-006-9231-3

Kulwal, P., Ishikawa, G., Benscher, D., Feng, Z., Yu, L. X., Jadhav, A., et al. (2012). Association mapping for pre-harvest sprouting resistance in white winter wheat. *Theor. Appl. Genet.* 125, 793–805. doi: 10.1007/s00122-012-1872-0

Kunert, A., Naz, A. A., Dedeck, O., Pillen, K., and Léon, J. (2007). AB-QTL analysis in winter wheat: I. Synthetic hexaploid wheat (*T. turgidum* ssp. *dicoccoides* × *T. tauschii*) as a source of favourable alleles for milling and baking quality traits. *Theor. Appl. Genet.* 115, 683–695. doi: 10.1007/s00122-007-0600-7

Lin, M., Zhang, D. D., Liu, S. B., Zhang, G. R., Yu, J. M., Fritz, A. K., et al. (2016). Genome-wide association analysis on pre-harvest sprouting resistance and grain color in U.S. winter wheat. *BMC Genomics* 17:794. doi: 10.1186/s12864-016-3148-6

Liu, C. X., Ding, F., Hao, F. H., Yu, M., Lei, H. H., Wu, X. Y., et al. (2016). Reprogramming of seed metabolism facilitates pre-harvest sprouting resistance of wheat. *Sci. Rep.* 6:20593. doi: 10.1038/srep20593

Liu, S. B., Sehgal, S. K., Li, J. R., Lin, M., Trick, H. N., Yu, J. M., et al. (2013). Cloning and characterization of a critical regulator for pre-harvest sprouting in wheat. *Genetics* 195, 263–273. doi: 10.1534/genetics.113.152330

Liu, S., Zhou, R., Dong, Y., Li, P., and Jia, J. (2006). Development, utilization of introgression lines using a synthetic wheat as donor. *Theor. Appl. Genet.* 112, 1360–1373. doi: 10.1007/s00122-006-0238-x

Liu, Y., Liu, Y., Zhou, Y., Wight, C., Pu, Z., Qi, P., et al. (2017). Conferring resistance to pre-harvest sprouting in durum wheat by a QTL identified in *Triticum spelta*. *Euphytica* 213, 19. doi: 10.1007/s10681-016-1796-x

Mares, D. J., and Mrva, K. (2001). Mapping quantitative trait loci associated with variation in grain dormancy in Australian wheat. *Aust. J. Agric. Res.* 52, 1257–1265. doi: 10.1071/AR01049

Mares, D. J., and Mrva, K. (2014). Wheat grain pre-harvest sprouting and late maturity alpha-amylase. *Planta* 240, 1167–1178. doi: 10.1007/s00425-014-2172-5

Mares, D. J., Mrva, K., Cheong, J., Williams, K., Watson, B., Storlie, E., et al. (2005). A QTL located on chromosome 4A associated with dormancy in white and red grained wheat of diverse origin. *Theor. Appl. Genet.* 111, 1357–1364. doi: 10.1007/s00122-005-0065-5

McCarty, D. R., Hattori, T., Carson, C. B., Vasil, V., Lazar, M., and Vasil, I. K. (1991). The viviparous-1 developmental gene of maize encodes a novel transcriptional activator. *Cell* 66, 895–905. doi: 10.1016/0092-8674(91)90436-3

Meng, L., Li, H. H., Zhang, L. Y., and Wang, J. K. (2015). QTL IciMapping: Integrated software for genetic linkage map construction and quantitative trait locus mapping in biparental populations. *Crop J.* 3, 269–283. doi: 10.1016/j.cj.2015.01.001

Metzger, R. J., and Silbaugh, B. A. (1970). Location of genes for seed coat color in hexaploid wheat, *Triticum aestivum* L. *Crop Sci.* 10, 495–496. doi: 10.2135/cropsci1970.0011183X001000050012x

Miranda, L. M., Murphy, J. P., Marshall, D., Cowger, C., and Leath, S. (2007). Chromosomal location of Pm35, a novel *Aegilops tauschii* derived powdery mildew resistance gene introgressed into common wheat (*Triticum aestivum* L.). *Theor. Appl. Genet.* 114, 1451–1456. doi: 10.1007/s00122-007-0530-4

Mohan, A., Kulwal, P., Singh, R., Kumar, V., Mir, R. R., Kumar, J., et al. (2009). Genome-wide QTL analysis for pre-harvest sprouting tolerance in bread wheat. *Euphytica* 168, 319–329. doi: 10.1007/s10681-009-9935-2

Mori, M., Uchino, N., Chono, M., Kato, K., and Miura, H. (2005). Mapping QTLs for grain dormancy on wheat chromosome 3A and group 4 chromosomes, and their combined effect. *Theor. Appl. Genet.* 110, 1315–1323. doi: 10.1007/s00122-005-1972-1

Munkvold, J. D., Tanaka, J., Benscher, D., and Sorrells, M. E. (2009). Mapping quantitative trait loci for preharvest sprouting resistance in white wheat. *Theor. Appl. Genet.* 119, 1223–1235. doi: 10.1007/s00122-009-1123-1

Naz, A. A., Kunert, A., Lind, V., Pillen, K., and Léon, J. (2008). AB-QTL analysis in winter wheat: II. Genetic analysis of seedling and field resistance against leaf rust in a wheat advanced backcross population. *Theor. Appl. Genet.* 116, 1095–1104. doi: 10.1007/s00122-008-0738-y

Ogbonnaya, F. C., Imtiaz, M., Ye, G., Hearnden, P. R., Hernandez, E., Eastwood, R. F., et al. (2008). Genetic and QTL analyses of seed dormancy and preharvest sprouting resistance in the wheat germplasm CN10955. *Theor. Appl. Genet.* 116, 891–902. doi: 10.1007/s00122-008-0712-8

Olson, E. L., Rouse, M. N., Pumphrey, M. O., Bowden, R. L., Gill, B. S., and Poland, J. A. (2013). Simultaneous transfer, introgression, and genomic localization of genes for resistance to stem rust race TTKSK (Ug99) from *Aegilops tauschii* to wheat. *Theor. Appl. Genet.* 126, 1179–1188. doi: 10.1007/s00122-013-2045-5

Pestsova, E. G., Börner, A., and Röder, M. S. (2006). Development and QTL assessment of *Triticum aestivum-Aegilops tauschii* introgression lines. *Theor. Appl. Genet.* 112, 634–647. doi: 10.1007/s00122-005-0166-1

Rasul, G., Humphreys, D. G., Brûlé-Babel, A., McCartney, C. A., Knox, R. E., DePauw, R. M., et al. (2009). Mapping QTLs for pre-harvest sprouting traits in the spring wheat cross "RL4452/AC Domain". *Euphytica* 168, 363–378. doi: 10.1007/s10681-009-9934-3

Ren, X. B., Lan, X. J., Liu, D. C., Wang, J. L., and Zheng, Y. L. (2008). Mapping QTLs for pre-harvest sprouting tolerance on chromosome 2D in a synthetic hexaploid wheat×common wheat cross. *J. Appl. Genet.* 49, 333–341. doi: 10.1007/BF03195631

Röder, M. S., Korzun, V., Wendehake, K., Plaschke, J., Tixier, M. H., Leroy, P., et al. (1998). A microsatellite map of wheat. *Genetics* 149, 2007–2023.

Sehgal, S. K., Kaur, S., Gupta, S., Sharma, A., Kaur, R., and Bains, N. S. (2011). A direct hybridization approach to gene transfer from *Aegilops tauschii* Coss. to *Triticum aestivum* L. *Plant Breed.* 130, 98–100. doi: 10.1111/j.1439-0523.2010.01817.x

Sharma, S. K., Dhaliwal, H. S., Multani, D. S., and Bains, S. S. (1994). Inheritance of pre-harvest sprouting tolerance in *Triticum aestivum* and its transfer to an amber-grained cultivar. *J. Hered.* 85, 312–314. doi: 10.1093/oxfordjournals.jhered.a111466

Sukhwinder, S., Chahal, G. S., Singh, P. K., and Gill, B. S. (2012). Discovery of desirable genes in the germplasm pool of *Aegilops tauschii* Coss. *Indian J Genet.* 72, 271–277.

Somyong, S., Ishikawa, G., Munkvold, J. D., Tanaka, J., Benscher, D., Cho, Y. G., et al. (2014). Fine mapping of a preharvest sprouting QTL interval on chromosome 2B in white wheat. *Theor. Appl. Genet.* 127, 1843–1855. doi: 10.1007/s00122-014-2345-4

Sun, Y. W., Yang, Y., Shewry, P. R., Jones, H. D., and Xia, L. Q. (2012). Isolation and characterization of *Viviparous-1* haplotypes in wheat related species. *Euphytica* 188, 71–84. doi: 10.1007/s10681-012-0659-3

Tan, M. K., Sharp, P. J., Lu, M. Q., and Howes, N. (2006). Genetics of grain dormancy in a white wheat. *Aust. J. Agri. Res.* 57, 1157–1165. doi: 10.1071/AR06101

Torada, A., Koike, M., Ikeguchi, S., and Tsutsui, I. (2008). Mapping of a major locus controlling seed dormancy using backcrossed progenies in wheat (*Triticum aestivum* L.). *Genome* 51, 426–432. doi: 10.1139/G08-007

Ueno, K. (2002). Effects of desiccation and a change in temperature on germination of immature grains of wheat (*Triticum aestivum* L.). *Euphytica* 126, 107–113. doi: 10.1023/A:1019655218722

Wang, J. R., Luo, M. C., Chen, Z. X., You, F. M., Wei, Y. M., Zheng, Y. L., et al. (2013). *Aegilops tauschii* single nucleotide polymorphisms shed light on the origins of wheat D-genome genetic diversity and pinpoint the geographic origin of hexaploid wheat. *New Phytol.* 198, 925–937. doi: 10.1111/nph.12164

Warner, R. L., Kudrna, D. A., Spaeth, S. C., and Jones, S. S. (2000). Dormancy in white-grain mutants of Chinese Spring wheat (*Triticum aestivum* L.). *Seed Sci. Res.* 10, 51–60. doi: 10.1017/S0960258500000064

Wei, H. T., Li, J., Peng, Z. S., Lu, B. R., Zhao, Z. J., and Yang, W. Y. (2008). Relationships of *Aegilops tauschii* revealed by DNA fingerprints: The evidence for agriculture exchange between China and the West. *Prog. Nat. Sci.* 18, 1525–1531. doi: 10.1016/j.pnsc.2008.05.022

Xia, L. Q., Yang, Y., Ma, Y. Z., Chen, X. M., He, Z. H., Röder, M. S., et al. (2009). What can the *Viviparous-1* gene tell us about wheat pre-harvest sprouting? *Euphytica* 168, 385–394. doi: 10.1007/s10681-009-9928-1

Xiao, S. H., Zhang, X. Y., Yan, C. S., and Lin, H. (2002). Germplasm improvement for preharvest sprouting resistance in Chinese white-grained wheat: An overview of the current strategy. *Euphytica* 126, 35–38. doi: 10.1023/A:1019679924173

Yu, M., Chen, G. Y., Zhang, L. Q., Liu, Y. X., Liu, D. C., Wang, J. R., et al. (2014). QTL Mapping for important agronomic traits in synthetic hexaploid wheat derived from *Aegiliops tauschii* ssp. *tauschii*. *J. Integr. Agric.* 13, 1835–1844. doi: 10.1016/S2095-3119(13)60655-3

Conflict of Interest Statement: The authors declare that the research was conducted in the absence of any commercial or financial relationships that could be construed as a potential conflict of interest.

frontiers in Plant Science

ORIGINAL RESEARCH
published: 30 October 2017
doi: 10.3389/fpls.2017.01840

Quantitative Trait Loci and Maternal Effects Affecting the Strong Grain Dormancy of Wild Barley (*Hordeum vulgare* ssp. *spontaneum*)

Shingo Nakamura[1]‡, Mohammad Pourkheirandish[1,2‡], Hiromi Morishige[1], Mohammad Sameri[1†], Kazuhiro Sato[3] and Takao Komatsuda[1]*

[1] Institute of Crop Science, National Agriculture and Food Research Organization, Tsukuba, Japan, [2] Plant Breeding Institute, The University of Sydney, Sydney, NSW, Australia, [3] Institute of Plant Science and Resources, Okayama University, Kurashiki, Japan

OPEN ACCESS

Edited by:
Chengdao Li,
Murdoch University, Australia

Reviewed by:
Xiaoli Jin,
Zhejiang University, China
Francesca Sparvoli,
Consiglio Nazionale delle Ricerche (CNR), Italy

***Correspondence:**
Shingo Nakamura
shingo@affrc.go.jp

†Present address:
Mohammad Sameri,
Department of Plant Biology, Swedish University of Agricultural Sciences, Uppsala, Sweden

‡These authors have contributed equally to this work.

Specialty section:
This article was submitted to Plant Breeding, a section of the journal Frontiers in Plant Science

Received: 09 August 2017
Accepted: 10 October 2017
Published: 30 October 2017

Citation:
Nakamura S, Pourkheirandish M, Morishige H, Sameri M, Sato K and Komatsuda T (2017) Quantitative Trait Loci and Maternal Effects Affecting the Strong Grain Dormancy of Wild Barley (Hordeum vulgare ssp. spontaneum). Front. Plant Sci. 8:1840. doi: 10.3389/fpls.2017.01840

Wild barley (*Hordeum vulgare* ssp. *spontaneum*) has strong grain dormancy, a trait that may enhance its survival in non-cultivated environments; by contrast, cultivated barley (*Hordeum vulgare* ssp. *vulgare*) has weaker dormancy, allowing uniform germination in cultivation. Malting barley cultivars have been bred for especially weak dormancy to optimize their use in malt production. Here, we analyzed the genetic mechanism of this difference in seed dormancy, using recombinant inbred lines (RILs) derived from a cross between the wild barley accession 'H602' and the malting barley cultivar 'Kanto Nakate Gold (KNG)'. Grains of H602 and KNG harvested at physiological maturity and dried at 30°C for 7 days had germination of approximately 0 and 100%, respectively. Analysis of quantitative trait loci (QTL) affecting grain dormancy identified the well-known major dormancy QTL *SD1* and *SD2* (located near the centromeric region and at the distal end of the long arm of chromosome 5H, respectively), and QTL at the end of the long arm of chromosome 4H and in the middle of the long arm of chromosome 5H. We designated these four QTL *Qsd1-OK*, *Qsd2-OK*, *Qsdw-4H*, and *Qsdw-5H*, and they explained approximately 6, 38, 3, and 13% of the total phenotypic variation, respectively. RILs carrying H602 alleles showed increased dormancy levels for all QTL. The QTL acted additively and did not show epistasis or QTL–environment interactions. Comparison of QTL locations indicated that all QTL except *Qsdw-5H* are likely the same as the QTL previously detected in the doubled haploid population from a cross between the malting cultivar 'Haruna Nijo' and 'H602.' We further examined *Qsd2-OK* and *Qsdw-5H* by analyzing the segregation of phenotypes and genotypes of F_2 progenies derived from crosses between RILs carrying specific segments of chromosome 5H from H602 in the KNG background. This analysis confirmed that the two genomic regions corresponding to these QTL are involved in the regulation of grain dormancy. Germination tests of F_1 grains derived from reciprocal crosses between H602 and KNG revealed that the H602 strong dormancy phenotype shows maternal inheritance with incomplete dominance. These results provide new insight into the mechanisms regulating grain dormancy in barley.

Keywords: dormancy, germination, QTL, wild barley, maturing temperature, maternal inheritance, domestication, pre-harvest sprouting

INTRODUCTION

The timing of germination plays a key role in plant survival. Many plants have evolved the ability to suppress germination, even under favorable conditions, a phenomenon termed seed (grain) dormancy (Finkelstein et al., 2008; Nonogaki, 2014; Rodríguez et al., 2015). Having some seeds remain dormant in case conditions turn unfavorable may have adaptive advantages for wild plants. By contrast, many cultivated plants have been selected for weak dormancy. For example, barley (*Hordeum vulgare* ssp. *vulgare*) is a major cereal crop in the Triticeae and has a wide range of grain dormancy levels (Takeda and Hori, 2007). In general, the wild progenitor of cultivated barley (*H. vulgare* ssp. *spontaneum*) has very strong grain dormancy, enabling it to survive various adverse environmental conditions. By contrast, malting barley cultivars have very low levels of grain dormancy, as they have been bred for simultaneous, rapid germination upon imbibition for malt production.

Many genetic and environmental factors affect seed dormancy and examining the genetic mechanisms governing the large difference in grain dormancy between wild and malting barley can identify natural mutations for dormancy that will enhance our understanding of the mechanisms by which dormancy decreased during and after domestication. This approach will also improve the development of barley cultivars with higher levels of tolerance to pre-harvest sprouting (PHS), which can cause devastating damage to yield and grain quality.

A number of grain dormancy quantitative trait loci (QTL) analyses in barley have been carried out, mainly using populations from various combinations of barley cultivars. These analyses have detected dormancy QTL on all seven chromosomes, and revealed two major dormancy QTL, *SD1* and *SD2*, located on chromosome 5H near the centromeric region and at the distal end of the long arm, respectively (Ullrich et al., 1992; Oberthur et al., 1995; Han et al., 1996; Thomas et al., 1996; Li et al., 2003; Edney and Mather, 2004; Prada et al., 2004; Zhang et al., 2005; Vanhala and Stam, 2006; Hori et al., 2007; Bonnardeaux et al., 2008; Ullrich et al., 2009; Hickey et al., 2012; Gong et al., 2014). To examine the genetic mechanisms underlying the striking difference in grain dormancy between wild and malting barley, a QTL analysis of grain dormancy was previously carried out using doubled haploid lines derived from a cross between the Japanese malting barley cultivar Haruna Nijo (HN) and the wild barley accession H602 (Hori et al., 2007). This analysis detected dormancy QTL on chromosomes 1H, 4H, and at the *SD1* (*Qsd1*) and *SD2* (*Qsd2*) loci on chromosome 5H; these QTL explained approximately 5, 5, 70, and 6% of the phenotypic variation, respectively (Hori et al., 2007).

Previous work indicated that *SD1* is a major regulator of dormancy in wild barley, and a recent study used map-based cloning to identify the causal gene of *Qsd1*, which encodes an alanine aminotransferase (AlaAT; Sato et al., 2016). The main cause for *Qsd1* was found to be a substitution at amino acid 214 of AlaAT, from a leucine (L) in the dormant allele to a phenylalanine (F) in the non-dormant allele. This substitution is caused by a single-nucleotide polymorphism (SNP) in exon 9 and is highly correlated with the dormancy phenotypes. Therefore, the naturally occurring L214F substitution seems to have been an important mutation that occurred in wild barley to produce the transition from the strong dormancy in wild barley to the weak dormancy in cultivated barley.

By contrast, another dormancy QTL may have been selected in cultivated barley to prevent PHS. *Qsd2-AK*, a major dormancy QTL located at the *SD2* locus was found using recombinant inbred lines (RILs) derived from a cross between the dormant Japanese cultivar Azumamugi (Az) and the Japanese malting barley Kanto Nakate Gold (KNG) (Nakamura et al., 2016). The causal gene of *Qsd2-AK* was identified as *MITOGEN-ACTIVATED PROTEIN KINASE KINASE 3* (*MKK3*) by map-based cloning (Nakamura et al., 2016). The causal sequence polymorphism, thought to be a naturally occurring mutation in the Az dormant allele, causes a non-synonymous substitution from Asparagine (N) to Threonine (T) at the 260th amino acid, and reduces MKK3 kinase activity. After cultivated barley reached East Asia from the Fertile Crescent several 1000 years ago, the N260T mutation may have improved barley adaptation to the climate in East Asia by preventing PHS, because in this region, the harvest season tends to overlap with the rainy season in the Asian monsoon. Therefore, this mutation seems not to be related to the transition from wild to cultivated barley. In fact, the wild barley H602 does not have N260T mutation, as it has the evolutionarily conserved N260. Therefore, we do not know whether *SD2* is also involved in the regulation of the strong dormancy in wild barley.

To understand the complex, multigenic mechanism that regulates dormancy, we need to study minor and major QTL. The resulting knowledge will provide useful information for fine-tuning the level of dormancy in cultivars to balance germination at a level that prevents PHS and allows simultaneous germination at sowing and/or malting. Moreover, the identification of other causal genes for dormancy QTL in barley could also aid in the reduction of PHS in related grain crops. For example, *MKK3*, the causal gene for *Qsd2-AK* in barley, is also the causal gene for the major dormancy QTL *Phs1* in wheat (*Triticum aestivum*; Torada et al., 2016).

In this study, we examined the dormancy of barley using a QTL analysis of RILs derived from a cross between wild barley H602 and cultivated barley KNG. We found that four QTLs including *SD2* and a novel QTL on chromosome 5H acted as the major factors determining the strong dormancy of H602. In addition, the strong dormancy seems to be maternally inherited. These results identify novel targets for future studies of the mechanisms that regulate dormancy in barley and wheat.

MATERIALS AND METHODS

Plant Materials

A total of 94 F_9 RILs were derived from a cross between H602 and KNG using a single-seed descent approach. H602 is wild barley (*Hordeum vulgare* ssp. *spontaneum*) accession. Kanto Nakate Gold (KNG) is a Japanese two-row malting barley cultivar (*H. vulgare* ssp. *vulgare*). A total of 93 near isogenic lines (NILs; BC_3F_2) were also developed from crosses between

H602 (donor parent) and KNG (recurrent parent). To break the strong dormancy of H602 or its derivatives for planting, the grains were treated with 1% (v/v) hydrogen peroxide overnight at room temperature before sowing. Barley plants were grown in an experimental field in Tsukuba, Japan.

Germination Tests

Germination percentages were estimated using grains manually threshed from spikes harvested at physiological maturity, dried at 30°C for 7 days, then stored at −30°C. Grains from a harvested spike were sown onto two sheets of No. 2 filter paper (ADVANTEC) in 9-cm Petri dishes containing 4.5 mL distilled water with fungicide (0.0125% (w/v) iminoctadine-triacetate). The dishes were incubated in the dark for 7 days at 15°C in a chamber with 100% relative humidity, after which the germinated and ungerminated seeds were counted and germination percentages were calculated. All germination tests were performed on at least three independent biological replicates (approximately 20–30 grains per spike for each biological replicate).

Genomic DNA Extraction, PCR, and Sequencing

Genomic DNA was isolated from shoots or leaves using the DNeasy Plant Mini Kit (Qiagen), following the manufacturer's protocol. The genomic DNA sequences were amplified by PCR using TaKaRa Ex Taq or PrimeSTAR GXL DNA polymerase (Takara), according to the manufacturer's protocol. The PCR conditions and primer sequences are described in Supplementary Table S1. The amplified fragments were purified using a QIAquick Gel Extraction Kit (Qiagen), then sequenced using a 3730xl-Avant DNA Analyzer (Applied Biosystems) and BigDye Terminator version 3.1 reagents (Thermo Fisher Scientific). The sequences were analyzed using Sequencher version 5.2.4 (Gene Codes Corporation) and the DNASIS Pro sequence analysis software (version 2.1; Hitachi Solutions). The genomic sequence of *Qsd1* from KNG was determined as described in Sato et al. (2016).

Genotyping and Linkage Map Construction

Frozen extracted genomic DNA samples were sent to the Southern California Genotyping Consortium, Illumina BeadLab, at the University of California, Los Angeles, where they were subjected to an oligonucleotide pooled assay (OPA)-single nucleotide polymorphism (SNP) assay using the 1,536-plex barley OPA1 (BOPA1) detection platform developed by Dr. Tim Close, University of California (Close et al., 2009; Sato and Takeda, 2009). OPA genotyping was performed on the 94 RILs and 93 NILs using the Illumina GoldenGate BeadArray. The seven expressed sequence tag (EST) markers used in this study were selected from a set of 384 core markers from the high-density EST marker map (Sato and Takeda, 2009). Genomic sequence information for the known causal genes (Nakamura et al., 2016; Sato et al., 2016) was used for the marker construction of the two major seed dormancy QTL, *Qsd1* and *Qsd2*. These markers were also used to genotype the RILs and NILs. Detailed information about the EST, *Qsd1*, and *Qsd2* markers is provided in Supplementary Table S1. Genetic maps were constructed using JoinMap 4.1 software (Kyazma[1]; Van Ooijen, 2006) with Kosambi mapping function (Kosambi, 1943).

QTL Analysis

Germination percentages were measured in 2010, 2011, and 2013 for the 94 RILs derived from a cross between H602 and KNG. QTL analysis was carried out using the simple interval mapping (SIM) method with the linkage map and MapQTL 6 software (Van Ooijen, 2009). To detect QTL, the significant logarithm of odds (LOD) threshold of 2.3 was determined using a permutation test (1,000 repetitions, $p < 0.05$). QTL analysis was also performed with mixed model-based composite interval mapping (MCIM) method using QTLNetwork ver. 2.1 (Yang et al., 2008) to identify the main QTL, and to evaluate epistatic interactions and QTL-by-environment interactions across all tested environments. Threshold *F*-values for an experiment-wise significance level of 0.05 were determined by performing 1000 permutations. Tests to detect QTL were conducted at 1-cM intervals with a window size of 10 cM. A Monte Carlo Markov Chain approach was used to estimate the main and epistatic QTL effects.

Association Analysis between Phenotypes and Genotypes in the F_2 Progenies

To evaluate the effect of the chromosome segments corresponding to the dormancy QTL regions, F_1 plants were made from crosses between three RILs with different H602 chromosome 5H segments in the KNG background. The segregation of chromosome segments was determined for approximately 96 F_2 plants derived from the F_1 plants using DNA markers. The germination percentages of the resulting F_3 grains produced from the F_2 plants with homozygous H602 or KNG genotypes at these markers were determined. The germination percentages of the H602- and KNG-homozygous F_2 plants were statistically analyzed using a Student's *t*-test in Microsoft Excel. If a significant difference was detected, the association between germination percentages and the H602 or KNG genotypes at the DNA markers was assessed to determine whether the segregating chromosome segments of the F_2 plants contain the grain dormancy QTL.

RESULTS

Frequency Distribution of Germination Percentage in RILs

To examine the distribution and year-to-year variation in germination, we first examined the distribution of germination frequencies in the RIL population grown in three different years. We performed germination tests for the H602 × KNG RILs in

[1]http://www.kyazma.nl/

2010, 2011, and 2013 (Supplementary Table S2). The frequency distributions of the RIL germination percentages are shown in **Figure 1**. As expected, the H602 grains showed almost 0% germination in all 3 years while nearly 100% of the KNG grains germinated in 2010 and 2013, which decreased to 90% in 2011. The frequency distributions showed continuous patterns and the overall distributions fluctuated yearly. The mean germination percentages of the RILs were 43, 30, and 51% in 2010, 2011, and 2013, respectively (**Figure 1**). This indicated that the RILs showed the strongest dormancy in 2011, moderate dormancy in 2010, and the lowest dormancy in 2013 (**Figure 1**).

The observed year-to-year variation in the dormancy levels of the RILs might be explained by fluctuations in temperature during grain development, which is thought to be a major factor determining the level of grain dormancy in barley (Benech-Arnold, 2001; Rodríguez et al., 2015). In general, lower temperatures lead to higher levels of dormancy in barley. In our field, the flowering season of the H602 × KNG RILs started around the end of April and the harvest season began at the end of May; therefore, grain developed in the RILs during May. The weather conditions around our fields are monitored and recorded by the Weather Data Acquisition System[2], and the data from May 2010, 2011, and 2013 are shown in Supplementary Table S3. These data show that the fields had more rainy and cloudy days in May in 2011 compared with 2010 and 2013. In addition, the mean air temperature in May in 2011 was 0.4°C lower than the 17.5°C observed in 2010 and 2013. The mean daily solar radiation was 18.8 MJ/m^2, 16.2 MJ/m^2, and 22.1 MJ/m^2 in 2010, 2011, and 2013, respectively. Therefore, we can estimate that the mean temperature of the spikes during grain development was highest in 2013, intermediate in 2010, and lowest in 2011. This corresponds well with the dormancy levels observed in the RILs; therefore, our results agree with the general rule that lower temperatures during grain development lead to higher acquired levels of dormancy in barley.

Genetic Map Construction and Analysis of Grain Dormancy QTL

To identify QTL affecting dormancy in this population, we first constructed a genetic map using known markers that are polymorphic in the parents, then used this map to find QTL by two methods, SIM and MCIM. Among the 1,536 SNP markers incorporated in the BOPA1 system, 629 (41%) showed polymorphisms between H602 and KNG. Using genotyping data from the SNP markers, the seven EST markers, and the two major grain dormancy QTL markers (*Qsd1* and *Qsd2*), we constructed a genetic linkage map of the H602 × KNG RILs (Supplementary Tables S4, S5).

Simple Interval Mapping

Using the genetic map and the 3 years of germination data, we identified grain dormancy QTL by SIM. The LOD curve patterns for 3 years looked very similar (Supplementary Figure S1). Two QTL were detected above the determined LOD threshold of 2.3, and were designated *Qsd2-OK* and *Qsdw-5H*. An additional LOD peak was observed at the locus of the *Qsd1* marker, and although it was not above the threshold, we designated it *Qsd1-OK*. The calculated parameters of each QTL are summarized in **Table 1**.

Qsd1-OK was detected at the same location (57 cM) as the causal gene (*AlaAT*) for *Qsd1*, a major dormancy QTL. *Qsd1-OK* explained 11% of the phenotypic variation, and the H602 allele was associated with higher levels of dormancy. Its LOD score is 2.3, just at the determined threshold, and it was detected only in 2010.

Qsd2-OK was detected at the *SD2* locus in all 3 years and is flanked by the SNP markers *1509* and *Qsd2*, which are located at 197 cM on chromosome 5H, within a 0.85-cM interval. *Qsd2-OK* explained about 29%, 43%, and 47% of the phenotypic variation

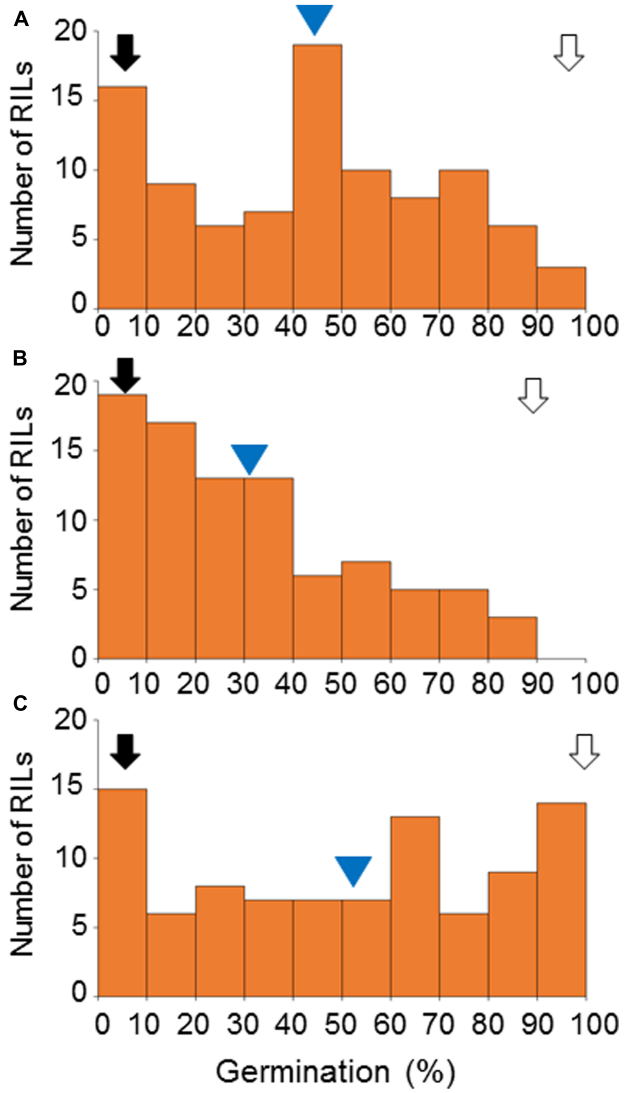

FIGURE 1 | Frequency distribution of the germination percentages of the RILs. Germination percentages for 94, 88, and 92 RILs were measured in 2010 **(A)**, 2011 **(B)**, and 2013 **(C)**, respectively. Black and white arrows indicate germination of H602 and KNG, respectively. Blue triangles indicate mean germination percentage of the RILs.

[2]http://www.naro.affrc.go.jp/org/niaes/aws/weatherdata.html

in 2010, 2011, and 2013, respectively, and the H602 allele was associated with higher levels of dormancy.

Qsdw-5H was detected in the middle of the long arm of chromosome 5H in 2010 and 2013 and is flanked by the SNP markers *1202* and *1168*, which map at 121 and 127 cM, respectively. *Qsdw-5H* explained about 20% of the phenotypic variation in both years, and the H602 allele was responsible for higher dormancy.

Mixed-Model-Based Composite Interval Mapping

In addition to the three QTL detected by SIM, we identified another QTL near the end of the long arm of chromosome 4H by MCIM (**Figure 2** and **Table 2**). This QTL, designated *Qsdw-4H*, is flanked by the SNP markers *79* and *792*, which map at 136 and 138 cM, respectively. *Qsdw-4H* explained about 3% of the phenotypic variation and the H602 allele conferred dormancy at *Qsdw-4H*. The phenotypic variation explained by the QTL and the estimated additive effect values calculated by MCIM (**Table 2**) were a little smaller than the values determined by SIM (**Table 1**). We detected no epistatic interactions between QTL and no additive by environment interactions, indicating that QTL effects were relatively constant through the 3 years.

Association Analysis of Phenotypes and Genotypes in the F_2 Progenies

To confirm the genomic regions responsible for the QTL, we carried out association analysis using F_2 plants segregating H602 chromosome segments at the QTL region. The causal gene for *Qsd1* was already identified (Sato et al., 2016) and the effect of *Qsdw-4H* appears to be too small for us to conduct association analysis. For the remaining two QTL, *Qsdw-5H* and *Qsd2-OK*, we used F_2 plants derived from three crosses: cross I between KNG and RIL4078, cross II between RIL4078 and RIL4013, and cross III between RIL4013 and RIL4058 (**Figure 3A**). To estimate the phenotypic effect of *Qsdw-5H* alone, we also carried out a germination test for NIL6072. RIL4078, RIL4013, RIL4058, and NIL6072 have approximately 7-, 29-, 106-, and 68-cM chromosome segments from H602 on the long arm of chromosome 5H, respectively (**Figure 3A**). H602 and KNG showed about 0 and 90% germination, respectively; RIL4078, RIL4013, and NIL6072 showed similar germination percentages of around 80%; RIL4058 had a germination rate of around 40% (**Figure 3B**).

We compared the mean germination percentages of F_2 plants with H602- and KNG-homozygous genotypes, determined by the markers *Qsd2*, *K00894,* and *K03272*, which correspond to the segregating chromosome segments in crosses I, II, and III, respectively. We detected a significant difference ($p < 0.003$) in the mean germination percentages of the cross I F_2 plants with H602- and KNG-homozygous genotypes at the *Qsd2* marker (**Figure 3C**, Supplementary Table S6). This indicates that the 7-cM genomic segment from the *153* marker to the end of long arm of chromosome 5H is involved in the regulation of grain dormancy. This genomic region corresponds to *Qsd2-OK*.

We did not detect a significant difference in the mean germination percentages of F_2 plants derived from cross II (**Figure 3C**, Supplementary Table S6). This indicates that the approximately 22-cM genomic region between markers *153* and *1070* is not relevant to the regulation of grain dormancy. However, we did detect a strong, significant difference ($p < 0.001$) in the mean germination percentages of the cross III F_2 plants with H602- and KNG-homozygous genotypes at the *K03272* marker (**Figure 3C**, Supplementary Table S6). This indicates that the 77-cM genomic segment between markers *1070* and *685* is involved in the regulation of grain dormancy. This genomic region corresponds to *Qsdw-5H*.

Germination of F_1 Grains

To test for maternal or paternal effects on germination, we tested the germination of F_1 grains derived from reciprocal crosses between H602 and KNG (**Figure 4**). As the parents H602 and KNG always show strong and weak dormancy, respectively, the F_1 grains derived from crosses of H602 × H602, and KNG × KNG showed 0 and 88% germination, respectively. However, we detected a large difference in the germinations of the reciprocal crosses. The F_1 grains derived from a cross with H602 as the female parent and KNG as the male showed 8% germination, which is close to the germination of H602 × H602. By contrast, the F_1 grains derived from crosses with KNG as the female parent and H602 as the male showed 54% germination, which is an intermediate phenotype between the germinations of the H602 × H602 and KNG × KNG parental crosses. These results indicated the involvement of maternal inheritance in the H602 strong dormancy phenotype.

Sequence Analysis of *Qsd1* and *Qsd2* in H602 and KNG

To examine whether the known dormancy gene *Qsd1* could be affecting the difference in dormancy between H602 and KNG, we determined the 3787-bp genomic DNA sequence of the *Qsd1* gene in KNG from the start codon to the stop codon (accession no. LC314597). The genomic sequence of *Qsd1* in H602 was reported in a previous study (Sato et al., 2016), which proposed that the amino acid substitution L214F in Qsd1 is the primary cause for the difference between the dormant allele and the less-dormant allele (Sato et al., 2016). Comparison of the deduced amino acid sequences of H602 and KNG showed that both cultivars have an L as the 214th amino acid residue of Qsd1, an allele producing strong dormancy (Sato et al., 2016). This could explain the small effect of *Qsd1-OK* in the H602 × KNG cross. The predicted amino acid sequences of Qsd1 in H602 and KNG differed at positions 288, 371, and 433 (Supplementary Table S7), indicating that these amino acids might contribute to the small effect of *Qsd1-OK*. Comparison of the deduced amino acid sequences of KNG and the malting barley cultivar HN showed that only the 214th amino acid residue was different; HN has F and KNG has an L (Supplementary Table S7). This is consistent with previous results that showing the L214F substitution is a major determinant for the effect of *Qsd1*.

TABLE 1 | Grain dormancy QTL identified by SIM.

QTL	Year	Flanking marker	Chr.	Peak position (cM)	LOD	PVE (%)	Additive effect (%)
Qsd1-OK	2010	*Qsd1*	5H	56.9	2.3	10.9	−9.0
Qsdw-5H	2010	*1202*	5H	123.3	3.8	17.3	−12.0
	2013	*1202*	5H	124.3	4.3	19.9	−15.6
Qsd2-OK	2010	*Qsd2*	5H	197.5	6.7	28.6	−14.4
	2011	*1509*	5H	196.6	10.3	42.7	−15.5
	2013	*1509*	5H	196.6	12.6	47.4	−22.3

LOD, logarithm of odds. PVE, phenotypic variation explained by the QTL.

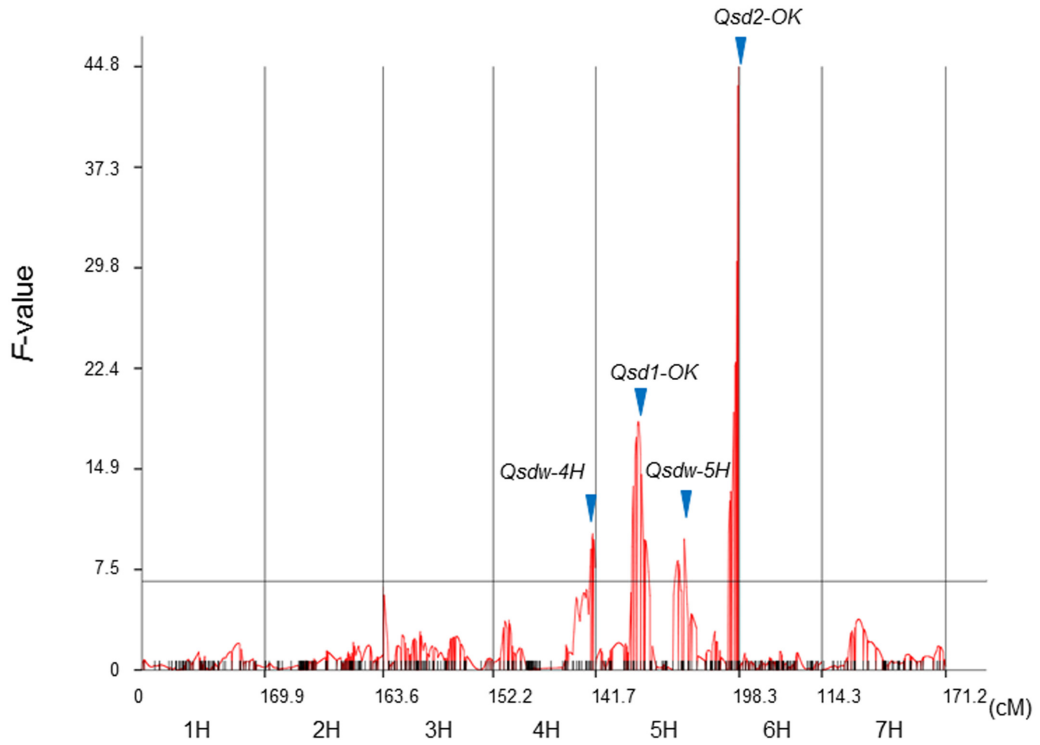

FIGURE 2 | Quantitative trait loci (QTL)-likelihood curves generated by QTLNetwork. Germination data of the RILs with three replications in 3 years, 2010, 2011, and 2013, were used for data processing. Blue arrows indicate the detected QTL locations. The horizontal black line indicates the QTL threshold equivalent to a critical *F*-value of 6.58 ($p < 0.05$). cM: centiMorgan.

The genomic sequences of *Qsd2* (*MKK3* gene) of H602 and KNG were previously reported (Nakamura et al., 2016). The deduced amino acid sequences of H602 and KNG differed at positions 232, 350, and 383 (Supplementary Table S8). These amino acid substitutions might be related to the large effect of *Qsd2-OK*. However, H602 has the same amino acid residues as Az at these three positions and previous research (Nakamura et al., 2016) revealed that these amino acid substitutions are not the primary cause for *Qsd2-AK*; rather, the N260T substitution is the primary cause for *Qsd2-AK*.

TABLE 2 | Grain dormancy QTL identified by MCIM.

QTL	Chr.	Position (cM)	Flanking markers	Position (cM)	Marker Range (cM)	*F*	PVE (%)	Additive effect (%)	Dormant allele
Qsdw-4H	4H	137.7	*79-792*	137.7	135.7–138.0	10.1	3.4	−4.4	H602
Qsd1-OK	5H	58.9	*Qsd1-1489*	58.9	56.9–61.9	18.4	6.3	−7.4	H602
Qsdw-5H	5H	122.3	*1202-1168*	122.3	121.3–124.3	9.7	13.3	−9.0	H602
Qsd2-OK	5H	197.5	*Qsd2-117*	197.5	196.6–197.5	44.8	37.9	−16.7	H602

QTL, QTL name; Chr., chromosome; Flanking markers, QTL flanking markers; F, maximum QTL F-value; PVE, phenotypic variation explained by the QTL.

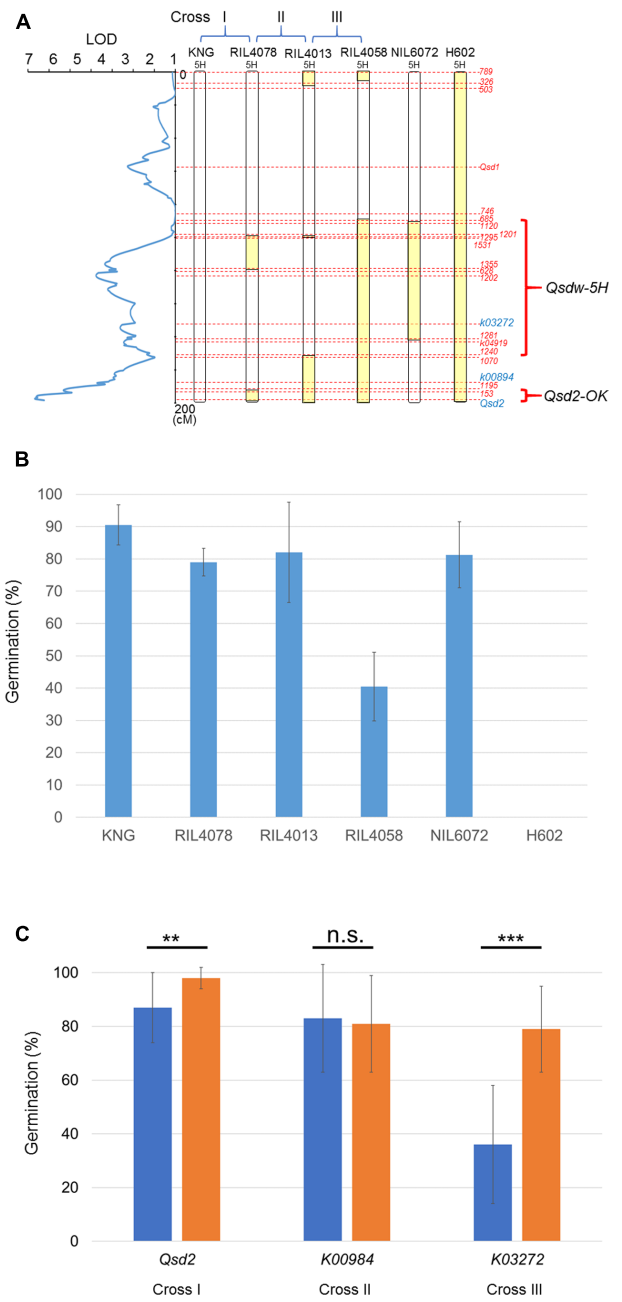

FIGURE 3 | Association analysis between phenotypes and genotypes in the F_2 progenies. **(A)** Genotypes of the parental lines. Graphical genotypes of chromosome 5H. The results of QTL analysis in 2010 using SIM are displayed on the left. LOD, logarithm of odds. cM, centiMorgan. Yellow bars: H602-homozygous genomic region. Open bars: KNG-homozygous genomic region. Blue letters: DNA markers names used for association analysis. Red letters: DNA marker names. The QTL regions estimated from the association analysis are shown on the right. **(B)** Phenotypes of the parental lines. Germination percentages. The germination test was performed using samples harvested in 2015. Blue bars: mean germination percentages. Vertical bars: standard deviation. $n = 3$ spikes. **(C)** Analysis of the mean germination percentages of F_3 grains derived from F_2 plants with homozygous H602 or KNG genotypes at the DNA markers. The germination test was performed using samples harvested in 2015. The F_2 plants were derived from

(Continued)

FIGURE 3 | Continued
each cross, Cross I: RIL4078 × KNG, Cross II: RIL4013 × RIL4078, Cross III: RIL4058 × RIL4013. Blue and orange bars show mean germination percentages for F_2 plants with homozygous H602 or KNG genotypes at the DNA markers, respectively. Vertical bars: standard deviation. $n = 3$ spikes. Italic letters: DNA marker names. Data were analyzed using a Student's *t*-test. Two asterisks: significant difference at $p < 0.01$. Three asterisks: significant difference at $p < 0.001$. n.s., no significant difference.

DISCUSSION

Dormancy QTL between Wild Barley H602 and the KNG Cultivar

Here, we identified *Qsd2-OK* at the *SD2* locus as a major dormancy QTL for wild barley. *Qsd2-OK* and *Qsd2-AK* appear to be located at the same genetic position, suggesting that both QTL could have the same causal gene. The causal gene for *Qsd2-AK* was already identified as *MKK3* (Nakamura et al., 2016). MKK3 transmits signals by phosphorylation in mitogen-activated protein kinase cascades (Ichimura et al., 2002) and participates in abscisic acid signal transduction (Danquah et al., 2015; Matsuoka et al., 2015), which plays important roles in many developmental and physiological processes, including dormancy (Finkelstein et al., 2008; Nonogaki, 2014; Rodríguez et al., 2015). A single-nucleotide substitution in exon 7 of *MKK3*, which replaces an adenine (A) in the non-dormant allele with a cytosine (C) in the dormant allele (A779C), was found to be the causal sequence polymorphism of *Qsd2-AK* (Nakamura et al., 2016). This SNP results in a non-synonymous amino acid substitution at the evolutionarily conserved 260th amino acid [asparagine (N) to threonine (T)], reducing the kinase activity of MKK3. Therefore, the mutated MKK3 likely cannot efficiently transmit signals for germination and the mutation delays germination and confers the dormant phenotype. The *MKK3* allele of H602 does not have this mutation (Supplementary Table S8, Nakamura et al., 2016), demonstrating that *Qsd2-OK* and *Qsd2-AK* have different causal sequence polymorphisms. Similarly, the dormant lines in which *SD2* was previously detected (Steptoe, Triumph, and TR306) do not have the A779C SNP, again suggesting a different causal sequence polymorphism (Nakamura et al., 2016). Comparison of the predicted amino acid sequences of MKK3 found three amino acid residues that differ in H602 and KNG: V232L, G350R, and D383N in H602 and KNG, respectively (Supplementary Table S8, Nakamura et al., 2016). However, none of these amino acids is evolutionally conserved. Dormant and non-dormant cultivars have the V232, G350, and D383 found in H602, indicating no correlation to the strong dormancy phenotype of H602. In the same way, because dormant and non-dormant cultivars have the R350 and N383 alleles also found in KNG, these changes seem not to be related to the non-dormancy phenotype of KNG. The L232 in the kinase domain is specific to KNG; however, previous kinase assays showed that MKK3 with L232V (as well as R350G and N383D) have similar kinase activities to the KNG MKK3, indicating that L232 has no effect on MKK3 kinase activity in KNG (Nakamura et al., 2016). These results suggest the amino acid differences in MKK3 between

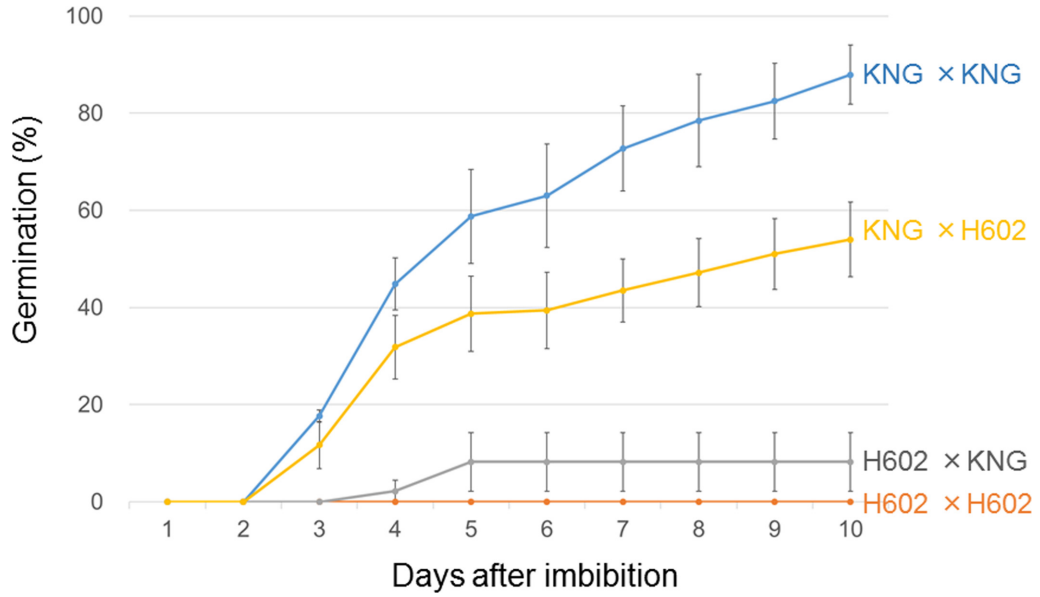

FIGURE 4 | Germination of F_1 progenies derived from reciprocal crosses between H602 and KNG. Orange line: H602 × H602. Gray line: H602 (as female) × KNG (as male). Yellow line: KNG (as female) × H602 (as male). Blue line: KNG × KNG. Circles: mean germination percentages. Vertical bars: standard deviation. $n = 3$ spikes.

H602 and KNG cannot explain the effect of *Qsd2-OK*. Therefore, we need to consider other possibilities for the explanation, such as a potential difference in *MKK3* gene expression or other causal genes that might be located at the vicinity of *MKK3*, such as barley homologs of *PM19-A1* and *A2*, the abscisic acid-induced Wheat Plasma Membrane 19 family genes, which have been proposed as causal genes for *SD2* (Barrero et al., 2015). In this study, we narrowed down the genomic region containing *Qsd2-OK* to a 7-cM sequence. Further narrowing of the genomic region could lead to the identification of the causal gene for *Qsd2-OK*, and will help elucidate the complex regulatory mechanisms involved.

Previously, analyses of dormancy QTL in barley revealed an interesting relationship between *SD1* and *SD2*; either *SD1* or *SD2* is always detected as the major dormancy QTL; in other words, if one is detected, then the other is either not detected or detected as a minor QTL (Gong et al., 2014). This is also true in the case of wild barley H602, although *Qsd1* is thought to be a principal determinant of the differences in dormancy between wild and cultivated barley, and within cultivated barley (Sato et al., 2009). In this study, the effect of *Qsd1-OK* was much smaller than the effect of *Qsd1* previously detected using the HN and H602 DH population. The H602 *Qsd1* allele is common between the two populations and therefore, this difference must be due to a difference in the genetic background between HN and KNG. The genomic sequence of KNG *Qsd1* revealed that KNG Qsd1 and H602 Qsd1 have the same L214 allele, indicating that KNG *Qsd1* might have a similar effect on dormancy to H602 *Qsd1*, but a different effect from HN *Qsd1*. This could explain why the effect of *Qsd1-OK* is smaller than the effect of *Qsd1* from the HN and H602 population. Qsd1 has three more amino acid polymorphisms, in addition to L214F, between H602 and KNG: C288Y, T371I, and M422V (T371I and M422V are polymorphic in KNG and HN; Supplementary Table S7). Sato et al. (2016) mentioned that difference at these three amino acid residues might affect the dormancy level; thus, these differences might result in the small effect observed for *Qsd1-OK*.

We detected another QTL, *Qsdw-5H*, in the middle of the long arm of chromosome 5H. This QTL was not reported in the previous analysis using the HN and H602 population (Hori et al., 2007). Previous studies reported another QTL adjacent to the *SD2* locus (Ullrich et al., 2009; Hickey et al., 2012; Gong et al., 2014); however, *Qsdw-5H* is likely to be located farther from *SD2* than the previously identified QTL. *Qsdw-5H* therefore seems to be a novel dormancy QTL. Our association analysis of Cross III showed that the phenotypes of F_2 plants that have *Qsdw-5H* and *Qsd2-OK* H602 dormant alleles can clearly be distinguished from the phenotypes of F_2 plants that have the *Qsdw-5H* KNG non-dormant allele and the *Qsd2-OK* H602 dormant allele (**Figure 3C**, Supplementary Table S6), indicating that we may be able to narrow down the region further to identify the causal sequence polymorphism of *Qsdw-5H*.

Previously, a study using the HN and H602 population detected a dormancy QTL near the end of the long arm of chromosome 4H (Hori et al., 2007). The LOD score was 4.7, the phenotypic variation explained was 5.1%, and its position was between the EST markers *k03067* and *k00136*. We compared the position of the QTL with that of *Qsdw-4H* using the HN/H602 linkage map that was constructed from data of BOPA1 and EST markers (Sato and Takeda, 2009). In the linkage map, *k03067* and *k00136* are located at 112.2 and 129.7 cM, and the flanking markers *79* and *792* for *Qsdw-4H* are at 129.6 and 136.4 cM (Supplementary Table S9).

Thus, the *Qsdw-4H* region seems to overlap with the region of the previously identified QTL, suggesting that these two QTL might be the same. This indicates that, although they explained only a small amount of the phenotypic variation, they are real QTL. Therefore, among the four QTL we detected in this study, three of them likely were commonly detected in the HN and H602 population and the H602 and KNG population.

Qsdw-4H and *Qsdw-5H* seemed to not be detected within the germplasm from cultivated barley used in the QTL analysis previously reported. Since genetic variation has continued to be reduced by domestication and modern plant breeding (Tanksley and McCouch, 1997), the *Qsdw-4H* and *Qsdw-5H* H602 dormant alleles might have been lost from modern cultivars through bottlenecks imposed by these processes, but could be identified by comparing malting barley with a wild barley accession.

Maternal Inheritance of the H602 Strong Dormancy Phenotype

The germination test of F_1 plants derived from the reciprocal crosses showed that the strong dormancy of H602 was maternally inherited. If the cytoplasmic inheritance of organelles were responsible, their DNA should be involved in the inheritance of the strong dormancy trait in H602. The RILs we used all have H602 cytoplasm (Senthil and Komatsuda, 2005), but since not all the RILs displayed the strong dormancy of H602, cytoplasmic inheritance cannot explain the maternal effect of dormancy inheritance. The following three possibilities can explain the maternal inheritance:

(1) The involvement of maternal tissues, such as the testa (seed coat) and pericarp, of grains in the regulation of dormancy. Seed color/pigmentation has been suggested to affect dormancy (Debeaujon et al., 2000; Flintham, 2000). For example, a transcription factor gene, *Hvmyb10* maps to chromosome 3H, regulates proanthocyanidin accumulation in the testa of developing grains, and was reported to affect grain dormancy in barley (Himi et al., 2012).
(2) Genomic imprinting leading to the preferential expression of either maternal or paternal alleles. The expression of maternal-specific alleles leads to maternal inheritance. In plants, expression of imprinted genes occurs primarily in the endosperm (Gehring, 2013; Pires and Grossniklaus, 2014), which is an important tissue for the regulation of germination and dormancy. In cereals, for example, following the release of the hormone gibberellin from germinated embryos, the outermost layer of the endosperm, the aleurone, synthesizes and secretes hydrolytic enzymes that degrade the starch reserves in the endosperm to nourish the growing seedling (Sun and Gubler, 2004). In Arabidopsis, the endosperm directly regulates dormancy; the endosperm of dormant seeds continuously synthesizes and releases abscisic acid toward the embryo to prevent embryonic growth (Lee et al., 2010). Moreover, a recent study reported that several genes related to germination are maternally expressed in Arabidopsis, suggesting that imprinted genes could implement the maternal inheritance of dormancy levels (Piskurewicz et al., 2016).
(3) A gene expression dosage effect resulting from the different numbers of parental genomes in the endosperm tissue, which contains two maternal genomes and one paternal genome.

From the results of the present study, it is not possible to determine which of these possibilities, or which combination of possibilities, causes this maternal inheritance. The future identification of the causal genes for the four QTL might allow us to address this question.

The F_1 grains from the reciprocal cross KNG × H602 showed 54% germination, which is intermediate between those of the parental crosses KNG × KNG and H602 × H602 (88 and 0%, respectively). Thus, the germination of the F_1 heterozygote was 10% higher than the average germination (44%) of the two homozygous parental crosses. Finding the explanation for this is also difficult because it does not result from the simple bi-allelic segregation of a gene locus; we need to consider four QTL and the maternal effect involved in regulating the germination of the F_1 grains. Previous studies showed the dormant alleles of H602 and Az are recessive and the non-dormant alleles of HN and KNG are incompletely dominant in *Qsd1* and *Qsd2-AK* (Sato et al., 2009; Nakamura et al., 2016). Taking these results into account, and if we do not consider the maternal effect for the KNG × H602 cross, the simplest explanation could be that the four QTL might be incompletely dominant with dominance that skews toward non-dormancy or no dominance, and thus the F_1 grains showed intermediate germination percentages; however, further work is needed to analyze the dominance effect of each QTL.

Future Perspective

Recently, a high-quality reference genome assembly for barley was released (Mascher et al., 2017), which will accelerate the map-based cloning of QTL genes, including *Qsd2-OK* and *Qsdw-5H*. As demonstrated in this study, we could narrow down the genomic regions for the QTL with an association analysis; further advances may enable us to identify the causal genes for the QTL. The identification of these genes will contribute to basic and applied science, enhancing our understanding of the genetic regulatory mechanisms of seed dormancy, and can be expected to offer opportunities for crop improvement, both in barley and its close relatives, to confer the appropriate level of grain dormancy and avoid pre-harvest sprouting.

AUTHOR CONTRIBUTIONS

HM, MS, and KS performed the research and analyzed the data. TK designed the research. MP and SN designed the research, performed research, analyzed the data, and wrote the article.

FUNDING

This research was financially supported by grants from the Japanese Ministry of Agriculture, Forestry and Fisheries

(Genomics for Agricultural Innovation, TRC-1002 and TRG-1002, and Genomics-Based Technology for Agriculture Improvement, TRS-1001).

ACKNOWLEDGMENTS

We thank Robbie Waugh, James Hutton Institute, for kindly providing us with the array for the BOPA1 analysis. The H602 seed samples were provided through the National Bioresource Project of Barley, MEXT of Japan.

SUPPLEMENTARY MATERIAL

The Supplementary Material for this article can be found online at: https://www.frontiersin.org/articles/10.3389/fpls.2017.01840/full#supplementary-material

REFERENCES

Barrero, J. M., Cavanagh, C., Verbyla, K. L., Tibbits, J. F. G., Verbyla, A. P., Huang, B. E., et al. (2015). Transcriptomic analysis of wheat near-isogenic lines identifies PM19-A1 and A2 as candidates for a major dormancy QTL. *Genome Biol.* 16, 93–110. doi: 10.1186/s13059-015-0665-6

Benech-Arnold, R. L. (2001). "Bases of pre-harvest sprouting resistance in barley: physiology, molecular biology and environmental control of dormancy in the barley grain," in *Barley Science. Recent Advances from Molecular Biology to Agronomy of Yield and Quality*, eds G. A. Slafer, J. L. Molina-Cano, R. Savin, J. L. Araus, and I. Romagosa (New York, NY: Food Product Press), 481–502.

Bonnardeaux, Y., Li, C., Lance, R., Zhang, X. Q., Sivasithamparam, K., and Appels, R. (2008). Seed dormancy in barley: identifying superior genotypes through incorporating epistatic interactions. *Aust. J. Agric. Res.* 59, 517–526. doi: 10.1071/AR07345

Close, T., Bhat, P. R., Lonardi, S., Wu, Y., Rostoks, N., Ramsay, L., et al. (2009). Development and implementation of high-throughput SNP genotyping in barley. *BMC Genomics* 10:582. doi: 10.1186/1471-2164-10-582

Danquah, A., Zélicourt, A., Boudsocq, M., Neubauer, J., Frey, N. F., Leonhardt, N., et al. (2015). Identification and characterization of an ABA-activated MAP kinase cascade in *Arabidopsis thaliana*. *Plant J.* 82, 232–244. doi: 10.1111/tpj.12808

Debeaujon, I., León-Kloosterziel, K. M., and Koornneef, M. (2000). Influence of the testa on seed dormancy, germination, and longevity in *Arabidopsis*. *Plant Physiol.* 122, 403–413. doi: 10.1104/pp.122.2.403

Edney, M. J., and Mather, D. E. (2004). Quantitative trait loci affecting germination traits and malt friability in a two-rowed by six-rowed barley cross. *J. Cereal Sci.* 39, 283–290. doi: 10.1016/j.jcs.2003.10.008

Finkelstein, R., Reeves, W., Ariizumi, T., and Steber, C. (2008). Molecular aspects of seed dormancy. *Annu. Rev. Plant Biol.* 59, 387–415. doi: 10.1146/annurev.arplant.59.032607.092740

Flintham, J. E. (2000). Different genetic components control coat-imposed and embryo-imposed dormancy in wheat. *Seed Sci. Res.* 10, 43–50. doi: 10.1017/S0960258500000052

Gehring, M. (2013). Genomic imprinting: insights from plants. *Annu. Rev. Genet.* 47, 187–208. doi: 10.1146/annurev-genet-110711-155527

Gong, X., Li, C., Zhou, M., Bonnardeaux, Y., and Yan, G. (2014). Seed dormancy in barley is dictated by genetics, environments and their interactions. *Euphytica* 197, 355–368. doi: 10.1007/s10681-014-1072-x

Han, F., Ullrich, S. E., Clancy, J. A., Jitkov, V., Kilian, A., and Romagosa, I. (1996). Verification of barely seed dormancy loci via linked molecular markers. *Theor. Appl. Genet.* 92, 87–91. doi: 10.1007/BF00222956

Hickey, L. T., Lawson, W., Arief, V. N., Fox, G., Franckowiak, J., and Dieters, M. J. (2012). Grain dormancy QTL identified in a doubled haploid barley population derived from two non-dormant parents. *Eyphytica* 188, 113–122. doi: 10.1007/s10681-011-0577-9

Himi, E., Yamashita, Y., Haruyama, N., Yanagisawa, T., Maekawa, M., and Taketa, S. (2012). Ant28 gene for proanthocyanidin synthesis encoding the R2R3 MYB domain protein (Hvmyb10) highly affects grain dormancy in barley. *Euphytica* 188, 141–151. doi: 10.1007/s10681-011-0552-5

Hori, K., Sato, K., and Takeda, K. (2007). Detection of seed dormancy QTL in multiple mapping populations derived from crosses involving novel barley germplasm. *Theor. Appl. Genet.* 115, 869–876. doi: 10.1007/s00122-007-0620-3

Ichimura, K., Shinozaki, K., Tena, G., Sheen, J., Henry, Y., Champion, A., et al. (2002). Mitogen-activated protein kinase cascades in plants: a new nomenclature. *Trends Plant Sci.* 7, 301–308. doi: 10.1016/S1360-1385(02)02302-6

Kosambi, D. D. (1943). The estimation of map distances from recombination values. *Ann. Eugen.* 12, 172–175. doi: 10.1111/j.1469-1809.1943.tb02321.x

Lee, K. P., Piskurewicz, U., Tureèková, V., Strnad, M., and Lopez-Molina, L. (2010). A seed coat bedding assay shows that RGL2-dependent release of abscisic acid by the endosperm controls embryo growth in Arabidopsis dormant seeds. *Proc. Natl. Acad. Sci. U.S.A.* 107, 19108–19113. doi: 10.1073/pnas.1012896107

Li, C. D., Tarr, A., Lance, R. C. M., Harasymow, S., Uhlmann, J., Westcot, S., et al. (2003). A major QTL controlling seed dormancy and pre-harvest sprouting/grain alpha-amylase in two-rowed barley (*Hordeum vulgare* L.) Aust. *J. Agric. Res.* 54, 1303–1313. doi: 10.1071/AR02210

Mascher, M., Gundlach, H., Himmelbach, A., Beier, S., Twardziok, S. O., Wicker, T., et al. (2017). A chromosome conformation capture ordered sequence of the barley genome. *Nature* 544, 427–433. doi: 10.1038/nature22043

Matsuoka, D., Yasufuku, T., Furuya, T., and Nanmori, T. (2015). An abscisic acid inducible *Arabidopsis* MAPKKK, MAPKKK18 regulates leaf senescence via its kinase activity. *Plant Mol. Biol.* 87, 565–575. doi: 10.1007/s11103-015-0295-0

Nakamura, S., Pourkheirandish, M., Morishige, H., Kubo, Y., Nakamura, M., Ichimura, K., et al. (2016). Mitogen-activated protein kinase kinase 3 regulates seed dormancy in barley. *Curr. Biol.* 26, 775–781. doi: 10.1016/j.cub.2016.01.024

Nonogaki, H. (2014). Seed dormancy and germination-emerging mechanisms and new hypotheses. *Front. Plant Sci.* 5:233. doi: 10.3389/fpls.2014.00233

Oberthur, L., Blake, T. K., Dyer, W. E., and Ullrich, S. E. (1995). Genetic analysis of seed dormancy in barley (*Hordeum vulgare* L.). *J. Quant. Trait Loci* 1, 5.

Pires, N. D., and Grossniklaus, U. (2014). Different yet similar: evolution of imprinting in flowering plants and mammals. *F1000Prime Rep.* 6:63. doi: 10.12703/P6-63

Piskurewicz, U., Iwasaki, M., Susaki, D., Megies, C., Kinoshita, T., and Lopez-Molina, L. (2016). Dormancy-specific imprinting underlies maternal inheritance of seed dormancy in *Arabidopsis thaliana*. *eLife* 5:e19573. doi: 10.7554/eLife.19573

Prada, D., Ullrich, S. E., Molina-Cano, J. L., Cisture, L., Clancy, J. A., and Romagosa, I. (2004). Genetic control of dormancy in a Triumph/Morex cross in barley. *Theor. Appl. Genet.* 109, 62–70. doi: 10.1007/s00122-004-1608-x

Rodríguez, M. V., Barrero, J. M., Corbineau, F., Gubler, F., and Benech-Arnold, R. L. (2015). Dormancy in cereals (not too much, not so little): about the mechanisms behind this trait. *Seed Sci. Res.* 25, 99–119. doi: 10.1017/S0960258515000021

Sato, K., Matsumoto, T., Ooe, N., and Takeda, K. (2009). Genetic Analysis of seed dormancy QTL in barley. *Breed. Sci.* 59, 645–650. doi: 10.1270/jsbbs.59.645

Sato, K., and Takeda, K. (2009). An application of high-throughput SNP genotyping for barley genome mapping and characterization of recombinant chromosome substitution lines. *Theor. Appl. Genet.* 119, 613–619. doi: 10.1007/s00122-009-1071-9

Sato, K., Yamane, M., Yamaji, N., Kanamori, H., Tagiri, A., Schwerdt, J. G., et al. (2016). Alanine aminotransferase controls seed dormancy in barley. *Nat. Commun.* 7:11625. doi: 10.1038/ncomms11625

Senthil, N., and Komatsuda, T. (2005). Inter-subspecific maps of non-brittle rachis genes btr1/btr2 using occidental, oriental and wild barley lines. *Euphytica* 145, 215–220. doi: 10.1007/s10681-005-1166-6

Sun, T.-P., and Gubler, F. (2004). Molecular mechanism of gibberellin signaling in plants. *Annu. Rev. Plant Biol.* 55, 197–223. doi: 10.1146/annurev.arplant.55.031903.141753

Takeda, K., and Hori, K. (2007). Geographical differentiation and diallel analysis of seed dormancy in barley. *Euphytica* 153, 249–256. doi: 10.1007/s10681-006-9260-y

Tanksley, S. D., and McCouch, S. R. (1997). Seed banks and molecular maps: unlocking genetic potential from the wild. *Science* 277, 1063–1066. doi: 10.1126/science.277.5329.1063

Thomas, W. T. B., Powell, W., Swanston, J. S., Ellis, R., Chalmers, K. J., Barua, U. M., et al. (1996). Quantitative trait loci for germination and malting quality characters in a spring barley cross. *Crop Sci.* 36, 265–273. doi: 10.2135/cropsci1996.0011183X003600020009x

Torada, A., Koike, M., Ogawa, T., Takenouchi, Y., Tadamura, K., Wu, J., et al. (2016). A causal gene for seed dormancy on wheat chromosome 4A encodes a MAP kinase kinase. *Curr. Biol.* 26, 782–787. doi: 10.1016/j.cub.2016.01.063

Ullrich, S. E., Hayes, P. M., Dyer, W. E., Blake, T. K., and Clancy, J. A. (1992). "Quantitative trait locus analysis of seed dormancy in 'Steptoe' barley," in *Preharvest Sprouting in Cereals 1992*, eds M. K. Walker-Simons and J. L. Ried (St Paul, MN: American Association of Cereal Chemistry), 136–145.

Ullrich, S. E., Lee, H., Clancy, J. A., Blanco, I. A., Jitkov, V. A., Kleinhofs, A., et al. (2009). Genetic relationships between preharvest sprouting and dormancy in barley. *Euphytica* 168, 331–345. doi: 10.1007/s10681-009-9936-1

Van Ooijen, J. W. (2006). *JoinMap 4, Software for the Calculation of Genetic Linkage Maps in Experimental Populations*. Wageningen: Kyazma B.V.

Van Ooijen, J. W. (2009). *MapQTL 6, Software for the Mapping of Quantitative Trait Loci in Experimental Populations of Diploid Species*. Wageningen: Kyazma B.V.

Vanhala, T. K., and Stam, P. (2006). Quantitative trait loci for seed dormancy in wild barley (*Hordeum spontaneum* C. Koch). *Genet. Resour. Crop Evol.* 53, 1013–1019. doi: 10.1007/s10722-004-7368-2

Yang, J., Hu, C., Hu, H., Yu, R., Xia, Z., Ye, X., et al. (2008). QTLNetwork: mapping and visualizing genetic architecture of complex traits in experimental populations. *Bioinformatics* 24, 721–723. doi: 10.1093/bioinformatics/btm494

Zhang, F., Chen, G., Huang, Q., Orion, O., Krugman, T., Fahima, T., et al. (2005). Genetic basis of barley caryopsis dormancy and seedling desiccation tolerance at the germination stage. *Theor. Appl. Genet.* 110, 445–453. doi: 10.1007/s00122.004-1851-1

Conflict of Interest Statement: The authors declare that the research was conducted in the absence of any commercial or financial relationships that could be construed as a potential conflict of interest.

frontiers in Plant Science

ORIGINAL RESEARCH
published: 31 January 2018
doi: 10.3389/fpls.2018.00065

QTL Mapping in Three Connected Populations Reveals a Set of Consensus Genomic Regions for Low Temperature Germination Ability in *Zea mays* L.

Xuhui Li[1], Guihua Wang[1], Junjie Fu[2], Li Li[1], Guangyao Jia[1], Lisha Ren[1], Thomas Lubberstedt[3], Guoying Wang[2], Jianhua Wang[1] and Riliang Gu[1]**

[1] Center of Seed Science and Technology, Beijing Key Laboratory of Crop Genetics and Breeding, Innovation Center for Seed Technology (Ministry of Agriculture), China Agricultural University, Beijing, China, [2] Institute of Crop Sciences, Chinese Academy of Agricultural Sciences, Beijing, China, [3] Department of Agronomy, Iowa State University, Ames, IA, United States

OPEN ACCESS

Edited by:
Chengdao Li,
Murdoch University, Australia

Reviewed by:
Elisabetta Frascaroli,
Università di Bologna, Italy
Hongjun Liu,
Shandong Agricultural University, China

***Correspondence:**
Jianhua Wang
wangjh63@cau.edu.cn
Riliang Gu
rilianggu@cau.edu.cn

Specialty section:
This article was submitted to Plant Breeding, a section of the journal Frontiers in Plant Science

Received: *09 November 2017*
Accepted: *12 January 2018*
Published: *31 January 2018*

Citation:
Li X, Wang G, Fu J, Li L, Jia G, Ren L, Lubberstedt T, Wang G, Wang J and Gu R (2018) QTL Mapping in Three Connected Populations Reveals a Set of Consensus Genomic Regions for Low Temperature Germination Ability in Zea mays L. Front. Plant Sci. 9:65. doi: 10.3389/fpls.2018.00065

Improving seed vigor in response to cold stress is an important breeding objective in maize that allows early sowing. Using two cold tolerant inbred lines 220 and P9-10 and two susceptible lines Y1518 and PH4CV, three connected $F_{2:3}$ populations were generated for detecting quantitative trait locus (QTL) related to seed low-temperature germination ability. At 10°C, two germination traits (emergence rate and germination index) were collected from a sand bed and three seedling traits (seedling root length, shoot length, and total length) were extracted from paper rolls. Significant correlations were found among all traits in all populations. Via single-population analysis, 43 QTL were detected with explained phenotypic variance of 0.62%∼39.44%. Seventeen QTL explained more than 10% phenotypic variance; of them sixteen (94.12%) inherited favorable alleles from the tolerant lines. After constructing a consensus map, three meta-QTL (mQTL) were identified to include at least two initial QTL from different populations. *mQTL1-1* included seven initial QTL for both germination and seedling traits; with three explaining more than 30% phenotypic variance. *mQTL2-1* and *mQTL9-1* covered two to three initial QTL. The favorable alleles of the QTL within these three mQTL regions were all inherited from the tolerant line 220 and P9-10. These results provided a basis for cloning of genes underlying the mQTL regions to uncover the molecular mechanisms of maize cold tolerance during germination.

Keywords: low temperature, seed vigor, germination, QTL mapping, maize

INTRODUCTION

Vigorous and uniform seedlings are necessary for achieving a high yield in crop production. However, various abiotic stresses occurring after sowing impair seedling establishment (Basnet et al., 2015; Liu et al., 2017). Maize (*Zea mays* L.) is one of the most important crops, accounting for 40% of the world's cereal food production (Bouis and Welch, 2010). As maize originated from tropical and subtropical regions, it is sensitive to low temperature, particularly during early growth stages, where a relatively high temperature threshold for germination is required (Greaves, 1996;

Verheul et al., 1996; Rodriguez et al., 2008; He et al., 2017; Pandit et al., 2017). Although global warming increases Earth surface temperature by 0.6–0.9°C in the past decades, low temperature stress still occurs in anytime of early spring at high-latitude regions, which results in failure of maize seedling establishment and yield loss (Stirling et al., 1991; Leipner et al., 1999; Hansen et al., 2000; Hu et al., 2016). Thus, improving a maize cultivar's low-temperature germination ability (LTGA) is vital for maize yield production and global food security. Moreover, low temperature is one of the main ecological factor limiting maize distribution. High LTGA seed could be not only sown at high latitudes to extend the maize planting area, but also sown in early spring to extend crop growing season with benefit to crop rotation and annual yield output (Leipner et al., 2008; Frascaroli and Landi, 2017).

Plant low-temperature acclimation is a complex inherited quantitative trait controlled by several minor genes, and easily influenced by environment. Quantitative trait locus (QTL) mapping is a powerful approach to study and manipulate complex traits important in agriculture. QTL for low-temperature acclimation has been conducted in rice, wheat and bean (Fujino et al., 2004; Baga et al., 2007; Lu et al., 2014; Sallam et al., 2016; Zhang W.B. et al., 2017). In rice, dozens of QTL of cold adaption were identified, and two major QTL were successfully used for enhancing low-temperature acclimation in breeding programs (Fujino et al., 2008; Zhang Z. et al., 2017). In maize, traits at germination and seedling stages were conducted for mapping of QTL associated with low temperature using different populations under different temperatures. Using an $F_{2:3}$ population, Rodriguez et al. (2014) identified three important genomic regions controlling seedling development under 15°C. Hund et al. (2004) found a large number of independently inherited loci for controlling seedling development at 15/13°C (day/night). Using recombinant inbred line (RIL) populations, Shi et al. (2016) identified 5 meta-QTL (mQTL) from 26 initial seed vigor related QTL at 18°C. Hu et al. (2016) detected 6 QTL for LTGA at 18/12°C (day/night). In addition, QTL related to leaf traits of seedling, such as photosynthesis related parameters, leaf area and weight, and nitrogen content had been investigated to reflect seed vigor under cold conditions (Fracheboud et al., 2002; Jompuk et al., 2005; Guerra-Peraza et al., 2011; Allam et al., 2016). Of these identified QTL, few were common in the same genomic regions across experiments, suggesting that QTL for maize cold tolerance are mainly determined by the specific genetic backgrounds and environmental conditions. Therefore, analysis of QTL using different genetic resources is necessary to enrich number of QTL and extract promising QTL for further fine-mapping or molecular breeding of LTGA in maize.

In this study, we employed three $F_{2:3}$ populations, derived from four inbred lines, two tolerant and two susceptible to cold stress, to detect the QTL related to maize LTGA under sand bed and paper roll germination conditions. The objectives of this study were: (1) to analyze low temperature seed emergence and seedling performance of the three $F_{2:3}$ populations and the four parental lines; (2) to identify QTL for LGTA from each population; (3) to integrate QTL from different populations and pinpoint mQTL for further fine-mapping or molecular breeding.

MATERIALS AND METHODS

Plant Materials

Based on a germplasm screening program targeting at seed vigor, inbred lines 220 and P9-10 were selected as cold tolerant lines, whereas PH4CV and Y1518 were susceptible. PH4CV was the paternal parent of XY335, a widely cultivated hybrid generated by the Pioneer Technology Co., Tieling, Jilin Province, China (Gu et al., 2017). The P9-10 was derived from the hybrid PN78599 (also called P78599) by using bicyclic breeding strategy (Wang et al., 2017). Another elite inbred line Y1518, a perfect material for maize transformation, was also applied in this study (Zhou et al., 1999). Besides that, an inbred line 220, which the pedigree was untraceable was collected from northeast China. Among that, 220 and P9-10 are flint-type maize, while PH4CV and Y1518 belong to dent-type. Three $F_{2:3}$ populations, 220 × PH4CV, 220 × Y1518 and P9-10 × PH4CV, were generated by crossing a tolerant to a susceptible line (**Figure 1A**). F_2 plant was grown in Shunyi, Beijing, China (116°.65'E longitude, 40'.13'N latitude) in 2014. After self-pollination, the $F_{2:3}$ seed was harvested and used for vigor tests. By standard germination test (at 25°C) according to the International Seed Testing Association [ISTA] protocol (International Seed Testing Association [ISTA], 2015), 650 $F_{2:3}$ family lines had initial germination percentages higher than 98%, representing 223, 212, and 215 lines for 220 × PH4CV, 220 × Y1518 and P9-10 × PH4CV, respectively. These lines were used for phenotypic evaluation and QTL mapping.

Phenotype Evaluation

Germination experiments were performed in both sand bed and paper roll experiments in a dark chamber at 10°C. In sand bed, after sieving and washing to remove soil, nutrient and other contaminations, sand was dried at 130°C for 5 h, moistened using distilled water to 16% content, and then sprayed in a plastic box to form a 2 cm thick bed (**Figure 2A**). After sterilizing with 1% sodium hypochlorite (NaClO) for 5 min and washing with distilled water, 30 seeds from each line were sown in the bed with the embryo side up, and then covered with additional 1 cm sand.

Once a shoot broke through the sand and became visible, it was counted as emerged plant. Emergence of plants was counted from 17 to 25 days after sowing (DAS) at 2-day intervals (in total five records). Emergence rate (ER) was expressed as percentage of emerged plants at 25th DAS to the total seed used. The germination index (GI) was calculated as

$$\mathrm{GI} = \sum \frac{Gt}{Dt},$$

where Gt is the number of emerged plant at a given day (Dt, the days after sowing).

In paper rolls, 10 sterilized seeds were sown in a moist brown germination paper (Anchor Ltd., St. Paul, MN, United States) and another sheet of humid paper was used as a cover. Then the germination paper was rolled and put erectly in a sealed plastic bag (**Figure 2D**). After incubation at 10°C for 25 days, total length (TL), root length (RL), and shoot length (SL) of germinated seedlings was measured by a ruler. Both sand bed and paper roll

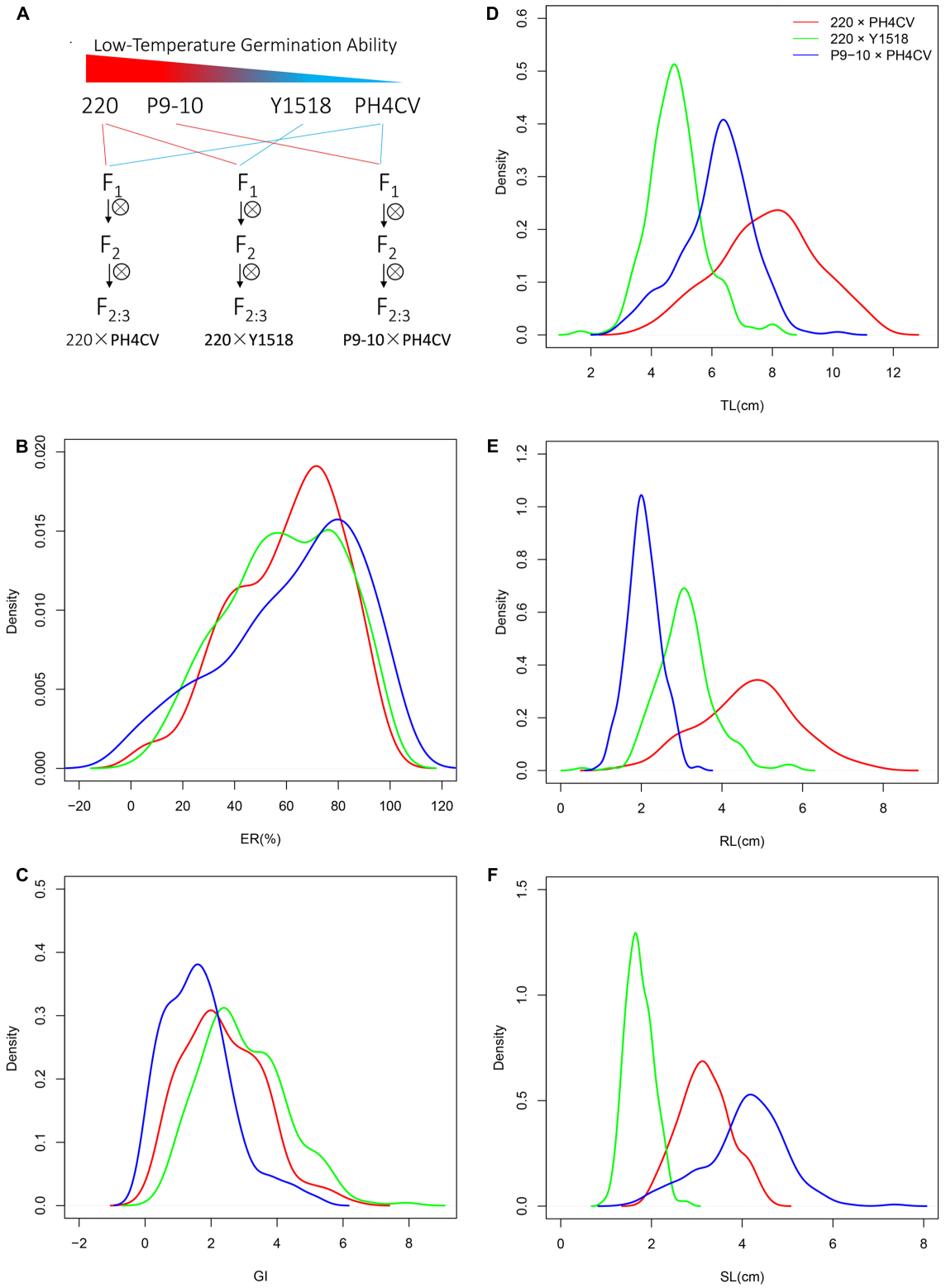

FIGURE 1 | The density of frequency distribution of cold germination related traits in populations. **(A)** Strategy for constructing the three connected populations 220 × PH4CV, 220 × Y1518, and P9-10 × PH4CV. Traits emergence rate (ER, **B**) and germination index (GI, **C**) were collected from sand bed experiment, and total length (TL, **D**), root length (RL, **E**) and shoot length (SL, **F**) were collected from paper rolls experiment. Line in red, green, and blue represented trait performance in population 220 × PH4CV, 220 × Y1518, and P9-10 × PH4CV, respectively.

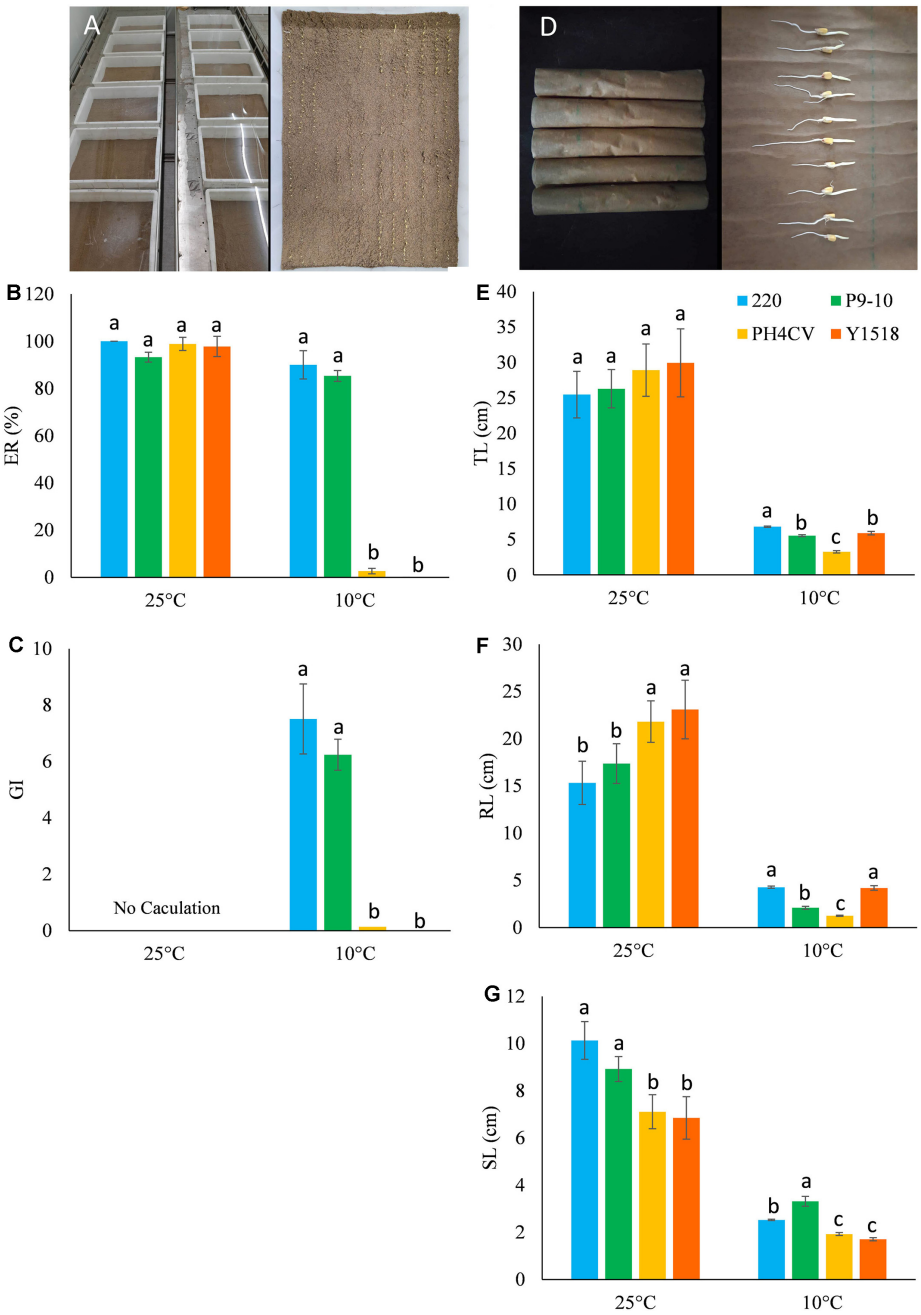

FIGURE 2 | Phenotypic performance of the four parental lines (220, P9-10, PH4CV, and Y1518) germinated under low (10°C) and normal (25°C) temperature in two germination systems of sand bed and paper rolls. **(A–C)** Plant germinated in sand bed. **(A)** Picture of sand bed; **(B)** ER; **(C)** GI. **(D–G)** Plant germinated in paper rolls. **(D)** Picture of paper rolls; **(E)** TL; **(F)** RL; **(G)** SL. Different small letters within a temperature treatment indicated significant differences among genotypes.

tests were conducted in three independent experiments for each line.

Data Analysis, QTL Detection, and Meta-QTL Analysis

The data were analyzed using the IBM Corp (2011) SPSS20.0 (IBM corp., Armonk, NY, United States) and the R statistical package (R Core Team, 2016). Mean of replicates was used for analysis of variance (ANOVA) and QTL mapping. Broad-sense heritability was calculated from an ANOVA fitting effect of genotype (G) and environment (E), as $H^2(\%) = \sigma^2_G/(\sigma^2_G+\sigma^2_E/r) \times 100\%$, where H^2 is broad sense heritability, σ^2_G is genotypic variance, σ^2_E is error variance, r is the number of replications (Nyquist, 1991). The coefficients of variation (CV, %) were calculated as follows: $CV = s/x$, where s is the standard deviation and x is the mean of each trait within

a population. The phenotypic correlation coefficients (Pearson's) were determined by linear regressions at significant level $p = 0.05$.

Shoots from 30 plants for each line were sampled for genomic DNA extraction following the cetyltrimethylammonium bromide (CTAB) method (Murray and Thompson, 1980). Genotyping was undertaken by using a 6K SNP chip (Illumina Inc., San Diego, CA, United States). Polymorphic makers between each parental pair were used for genetic linkage map construction and QTL mapping using the software QTL IciMapping 4.1. Inclusive composite interval mapping (ICIM) algorithm was conducted for QTL mapping by scanning the genome every 1 cM (Li et al., 2007). The threshold likelihood of odds (LOD) value was determined with 1,000 permutations at a $P = 0.05$ level (Churchill and Doerge, 1994). The resulting LOD values were 3.70–6.83 for all trials (Supplementary Table S1).

Based on the SNP markers shared by different populations, an integrated map was built according to the user manual of QTL IciMapping software (Chardon et al., 2004; Meng et al., 2015). In brief, SNP makers overlapped on at least two genetic maps were selected as anchor markers and used to integrate corresponding linkage groups on individual linkage maps. The marker order and marker positions were calculated after calculating the order and the relative position (within each genetic map) of the anchored markers, followed by integrating of all the detected markers into one map. Then all QTL identified from the three populations were projected onto the integrated map based on their confidence interval. If QTL confidence intervals overlapped, they were considered as mQTL (Blanc et al., 2006; Cui et al., 2014; Han et al., 2014).

Candidate-Gene Selection, RNA Extraction, and Quantification

Genes with well annotation involving in low-temperature adaption were collected from *Oryza sativa, Arabidopsis thaliana*, and *Sorghum bicolor*, and performed BLAST analysis in MaizeGDB[1]. Six genes located in our confident QTL interval were selected for quantitative PCR (qPCR) validation.

Two groups of seedlings growing in paper rolls were cultivated under 10°C and 25°C germination conditions, respectively, shoots were collected for RNA isolation once they have similar seedling length at 15 DAS (grown under 10°C) and 3 DAS (grown under 25°C), respectively. Ten shoots in each replication were pooled and grinded in liquid nitrogen for total RNA extraction using RNAprep pure Plant Kit [Tiangen Biotech (Beijing)]. RNA samples were treated with RNase-free DNase Kit (Invitrogen) to remove DNA contamination. Followed by reverse transcription reaction of cDNA with RT MasterMix (Applied Biological Materials Inc.), qPCR analysis was performed on Applied Biosystems QuantStudio 6 (Thermo Fisher) using qPCR MasterMix solution (Applied Biological Materials Inc.). The primers used in qPCR were listed in Supplementary Table S2. The maize *ZmGAPDH* gene was used as an internal control (Gu et al., 2013). The mean value from three replications was used as final gene expression.

[1]http://maizegdb.org/

RESULTS

Low-Temperature Germination Ability in the Parental Lines

Germination (ER and GI) and seedling (TL, RL, and SL) performance of the four parental lines was evaluated in sand bed and paper rolls, respectively (**Figure 2**). At optimal temperature, the four parents had similar TL (25.46–29.95 cm) and ER (>95.0%), while genotypes 220 and P9-10 had significantly higher SL, but lower RL than PH4CV and Y1518. At low temperature, 220 and P9-10 showed increased ER and GI, and 1.5–2 times elevated SL compared to Y1518 and PH4CV. Genotypes 220 and Y1518 had similar RL (4.19–4.28 cm), which was significantly higher than RL (1.26–2.10 cm) of P9-10 and PH4CV. Genotype 220 displayed the longest TL (6.80 cm), followed by P9-10 (5.53 cm), Y1518 (5.90 cm), and PH4CV (3.26 cm). Taken together, 220 and P9-10 are cold tolerant, and Y1518 and PH4CV are cold susceptible lines.

Low-Temperature Germination Ability in $F_{2:3}$ Populations

The average values of ER among the three populations were similar, while those of the other four traits showed differences (**Figure 1**). Average GI in P9-10 × PH4CV was lower than that in 220 × PH4CV and 220 × Y1518. Average TL in 220 × PH4CV was higher than that in the other two populations, which was consistent with the respective parent means (**Figures 1D**, **2E**).

Coefficients of variation (CV) and broad-sense heritabilities (H^2) were similar among these three populations for all traits (**Table 1**). CV for ER (35.5–42.15%) and GI (37.7–65.76%) were higher than for TL (19.03–21.05%), RL (19.46–25.71%) and SL (17.72–22.03%). H^2 estimates for ER and GI were lower (0.81–0.84) than for TL, RL, and SL (0.91–0.94). Higher CV and lower H^2 in ER and GI suggested that germination traits collected from sand bed might be more susceptible to environmental factors than seedling traits obtained from paper rolls.

Within a population, the phenotypic distribution of all five traits were approximately consistent with normal distributions based on low values of skewness and kurtosis (below 1, except for kurtosis for TL and RL in 220 × Y1518; **Table 1** and **Figure 1**). Pairwise correlation coefficients among the five traits were significant and positive for all three populations, with closer correlations between traits within an assay (sand-bed versus paper-roll experiment, $r = 0.78$–0.97) than across those assays ($r = 0.32$–0.64) (**Table 2**).

QTL Identification within Populations

A total of 5,179 SNP markers were scanned and resulted in 1,382, 1,500, and 1,419 markers that fit the expected 1:2:1 distribution ratio in $F_{2:3}$ lines, and were polymorphic between

TABLE 1 | Mean and heritability (H^2) estimates for traits related to low-temperature germination in population 220 × PH4CV, 220 × Y1518, and P9-10 × PH4CV.

Population	Trait[a]	Mean ± SD	CV (%)	Range	Kurtosis	Skewness	H^{2b}
220 × PH4CV	ER (%)	60.48	34.50	4.00–98.00	−0.38	−0.50	0.84
	GI	2.38	51.08	0.07–6.29	0.00	0.50	0.83
	TL (cm)	7.84	21.05	3.73–11.37	−0.41	−0.13	0.93
	RL (cm)	4.66	25.71	1.58–7.78	−0.17	−0.05	0.94
	SL (cm)	3.18	17.69	1.87–4.55	−0.43	0.12	0.91
220 × Y1518	ER (%)	59.65	37.70	4.44–97.78	−0.86	−0.27	0.85
	GI	2.98	42.70	0.48–6.72	−0.42	0.39	0.82
	TL (cm)	4.82	19.15	1.66–8.08	1.64	0.55	0.93
	RL (cm)	3.09	23.17	0.53–5.78	1.95	0.53	0.92
	SL (cm)	1.73	17.72	0.96–2.80	0.13	0.40	0.94
P9-10 × PH4CV	ER (%)	62.67	42.15	0–100.00	−0.50	−0.62	0.82
	GI	1.61	65.76	0–5.23	0.88	0.87	0.81
	TL (cm)	6.16	19.03	2.96–10.16	0.45	−0.32	0.94
	RL (cm)	2.06	19.46	0.97–3.40	0.11	0.17	0.94
	SL (cm)	4.06	22.03	1.53–7.36	0.66	−0.23	0.93

[a]Trait ER, GI, TL, RL, and SL represented emergence rate, germination index, total length, root length, and shoot length, respectively. ER and GI were evaluated in sand bed experiment, and TL, RL, and SL were evaluated in paper rolls experiment. [b]H^2 represented broad-sense heritability.

TABLE 2 | Phenotypic correlation between emergence rate (ER), germination index (GI), total length (TL), root length (RL), and shoot length (SL) in population 220 × PH4CV, 220 × Y1518 and P9-10 × PH4CV.

Populations	Traits	ER	GI	TL	RL	SL
220 × PH4CV	ER	1				
	GI	0.85 *	1			
	TL	0.55 *	0.49 *	1		
	RL	0.46 *	0.39 *	0.97 *	1	
	SL	0.64 *	0.59 *	0.86 *	0.72 *	1
220 × Y1518	ER	1				
	GI	0.93 *	1			
	TL	0.41 *	0.47 *	1		
	RL	0.32 *	0.36 *	0.96 *	1	
	SL	0.51 *	0.58 *	0.77 *	0.57 *	1
P9-10 × PH4CV	ER	1				
	GI	0.87 *	1			
	TL	0.52 *	0.48 *	1		
	RL	0.54 *	0.53 *	0.78 *	1	
	SL	0.42 *	0.39 *	0.95 *	0.56 *	1

*ER and GI were evaluated in sand bed experiment, and TL, RL, and SL were evaluated in paper rolls experiment. *Indicated significant difference at $p < 0.05$.*

the two parents of the population 220 × PH4CV, 220 × Y1518 and P9-10 × PH4CV, respectively (Supplementary Table S3). Based on these markers, three linkage maps were constructed with TLs of 1,689.8, 1,741.2, and 1,880.0 cM, and average interval sizes of 1.3, 1.3 and 1.5 cM for 220 × PH4CV, 220 × Y1518 and P9-10 × PH4CV, respectively (Supplementary Table S4).

A total of 43 QTL were identified to be associated with LTGA with 19, 13, and 11 from 220 × PH4CV, 220 × Y1518 and P9-10 × PH4CV, respectively (**Figure 3** and Supplementary Table S5). The number of QTL identified for each trait ranged from 1 to 5 within a population. LOD values for individual QTL ranged from 3.82 to 36.28, and the explained phenotype variances varied from 0.62 to 39.44%. Three QTL (*qp1TL1-1*, *qp3TL1-2,* and *qp3SL1-2*) explained phenotypic variance of more than 30% and had LOD values exceeding 22. The other 13 QTL explained 10–30% of phenotype variance (Supplementary Table S5).

QTL Analysis across Different Populations

Taking advantage of the same SNP chip used for genotyping, we integrated the three maps into a consensus linkage map (cMap) based on the markers shared by populations (**Figure 3** and Supplementary Table S5). The final cMap consisted of 2,693 SNP makers with a TL of 1,814.47 cM and an average marker interval length of 1.05 cM.

After projecting the 43 initial QTL on the cMap, 12 QTL (27.9%) overlapped, resulting in 3 mQTL (**Table 3**). *mQTL1-1* is located within the physical interval 175–184 Mb (base on B73 RefGen_v2) on chromosome 1, containing one and six QTL for germination and seedling traits, respectively, from population 220 × PH4CV and P9-10 × PH4CV. Like *mQTL1-1*, the *mQTL9-1* region (position 149–151 Mb on chromosome 9) harbored initial QTL from population 220 × PH4CV and P9-10 × PH4CV. This region only harbored three seedling specific QTL (one for TL and two for SL). The favorable alleles for QTL located in *mQTL1-1* and *mQTL9-1* were all inherited from the tolerant lines 220 or P9-10. The explained phenotypic variance for QTL in *mQTL1-1* was high (10.18–39.44%); while that for QTL in *mQTL9-1* was relatively low (3.02–5.04%).

mQTL2-1 region (position 194–199 Mb on chromosome 2) contained two germination specific QTL with a GI QTL from 220 × PH4CV and an ER QTL from 220 × Y1518 (**Table 3**). The favorable alleles for both QTL were inherited from the tolerant line 220. However, the

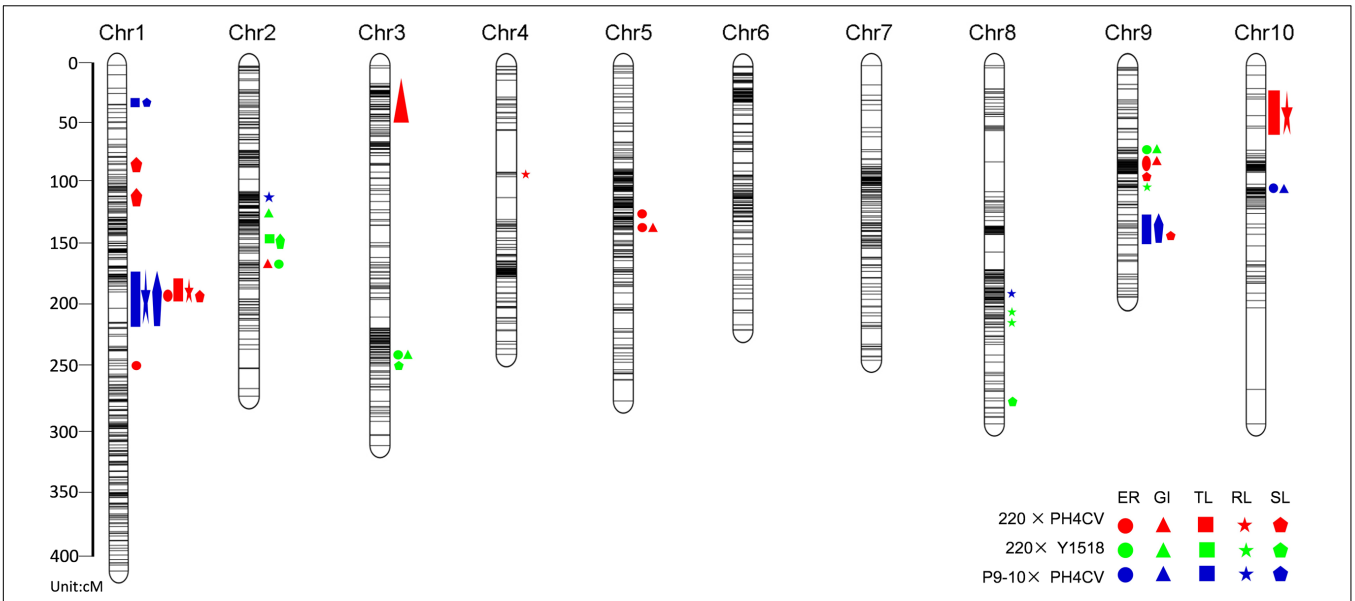

FIGURE 3 | QTL for low temperature germination related traits represented in the consensus linkage map of the three populations of 220 × PH4CV, 220 × Y1518, and P9-10 × PH4CV. The circle, triangle, square, star and pentagon represented traits of ER, GI, TL, RL, and SL. ER and GI were collected from sand bed experiment, and TL, RL, and SL were collected from paper rolls experiment. Color red, green and blue indicated QTL detected from population 220 × PH4CV, 220 × Y1518, and P9-10 × PH4CV, respectively.

TABLE 3 | Meta-QTL (mQTL) detected from the consensus linkage map.

Name	Flanking Makers	CI (cM)	Initail QTL[b]	Favorable Allele	Reference[c]
mQTL1-1[a]	M1c174799835–M1c184012303	164.57–223.23	*qp1ER1-1, qp1TL1-1, qp1RL1-1 qp1SL1-3, qp3TL1-2, qp3RL1-1, qp3SL1-2*	220 or P9-10	Fracheboud et al., 2002; Hund et al., 2004; Allam et al., 2016
mQTL2-1	M2c193833217–M2c199180638	163.75–165.86	*qp1GI2-1, qp2ER2-1*	220	Huang et al., 2013
mQTL9-1	M9c149041431–M9c151277505	129.89–146.48	*qp1SL9-2, qp3TL9-1, qp3SL9-1*	220 or P9-10	Jompuk et al., 2005; Allam et al., 2016; Hu et al., 2016

[a]*A mQTL included at least two initial QTL from different populations of 220 × PH4CV, 220 × Y1518, and P9-10 × PH4CV in the consensus linkage map.* [b]*Names of initial QTL were referred to Supplementary Table S3. P1, p2, and p3 represented initial QTL from population 220 × PH4CV, 220 × Y1518, and P9-10 × PH4CV, respectively.* [c]*Reference indicted that the mQTL overlapped with QTL identified in this study.*

explained phenotypic variance differed substantially with 18.21% (GI) and 4.81% (ER) explained phenotype variance, respectively.

Quantitative PCR Validation for Candidate Genes

The six candidate genes within the above detected QTL were homologous to published low-temperature adaption genes by BLAST analysis (Supplementary Tables S2, S5). Among that, three genes (GRMZM2G124011, GRMZM2G380561, and GRMZM2G125032) showed significant higher expression levels in 220 than in PH4CV in any conditions (both optimal- and low-temperatures), with that two genes (GRMZM2G124011 and GRMZM2G380561) in 220 were induced by cold stress, while in PH4CV, gene GRMZM2G125032 was induced (**Figures 4B,D,F**). Interestingly, gene GRMZM2G030167 showed significant higher expression in 220 than in PH4CV only under low-temperature condition, while showed similar expression level under optimal temperature (**Figure 4G**). There is no expression difference of the gene GRMZM2G050193 across the two parents and at the two germination conditions (**Figure 4C**). The last gene GRMZM2G065585 was a possible non-functional gene during seed germination since its expression level is 1/1,000 less than its homolog GRMZM2G125032 in the investigated tissues (**Figure 4E**).

A

Gene ID	Position in chromosome (B73 FefGen_V2)	QTL region	Gene anotation
GRMZM2G124011	chr2:194485273-194486255	*mQTL2-1 (qp1GI2-1, qp2ER2-1)*	C-repeat bonding factor 3/dehydration response element B1A (CBF3/DREB1A)
GRMZM2G050193	chr2:196329725-196336472	*mQTL2-1 (qp1GI2-1, qp2ER2-1)*	synaptotagmin A
GRMZM2G125032	chr3:151819389-151821475	*qp1GI3-1*	Glycosyl hydrolase 17
GRMZM2G065585	chr3:151971037-151972416	*qp1GI3-1*	Glycosyl hydrolase 17
GRMZM2G380561	chr8:120768105-120771539	*qp3RL8-1*	β-1,3-glucanase 1
GRMZM2G030167	chr8:148264071-148273363	*qp2RL8-1*	vacuolar ATP synthase subunit E1
GRMZM2G157760	chr9:128121880-128127627	*qp1ER9-1*	phospholipase C1

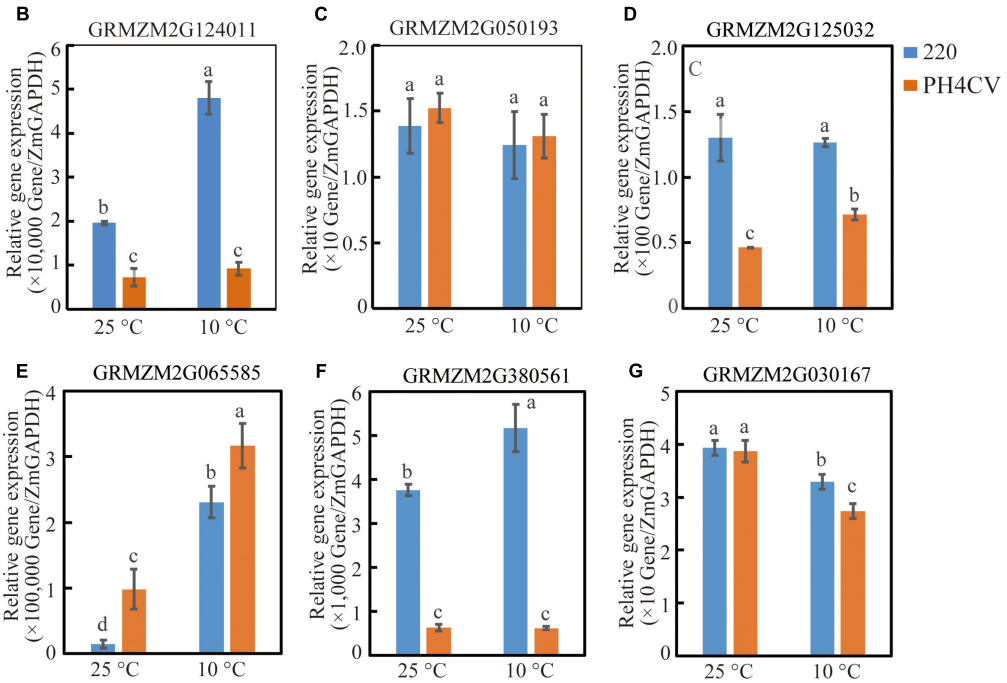

FIGURE 4 | Expressions of six candidate genes in parent lines 220 and PH4CV. Expression were conducted on shoots that were collected at 15 days after sowing (DAS) and 3 DAS under low (10°C) and normal (25°C) temperature, respectively. **(A)** Candidate genes and their chromosome locations. **(B–G)** Expression for different gene.

DISCUSSION

Important mQTL for Controlling Low-Temperature Germination Ability in Maize

Improvement of maize LTGA could help farmers to sow early, which has advantages in earlier harvest and longer plant life cycle: earlier harvest could extend maize growth region to higher altitudes and longer life cycle increases biomass accumulation and yield output (Frascaroli and Landi, 2017). Although seed LTGA could be improved by agronomic practices, such as seed priming or plastic sheeting (Li et al., 2017; Sheteiwy et al., 2017), the most economical and reliable method is to breed low-temperature tolerance cultivars aided by marker assisted selection (MAS). Recently, researchers identified various QTL associated with low temperature tolerance in maize (Fracheboud et al., 2004; Presterl et al., 2007; Rodriguez et al., 2008; Hu et al., 2016; Shi et al., 2016), but little is known about germination stage. Up to know, no LTGA QTL has been fine-mapped or cloned in maize. The major aim of this study is try to detect the most promising mQTL for further gene cloning and MAS.

To evaluate the reliability of QTL detected in this work, we compared our identified 43 QTL to the previous QTL released from several cold related publications in maize. According to the physical position of QTL on B73 RefGen_v2, we found that 29 QTL (67.4%) overlapped with published QTL (Supplementary Table S5). Among them six QTL (*qp3TL9-1*, *qp3SL9-1*, *qp2ER2-1*, *qp1GI2-1*, *qp1ER9-1*, and *qp1GI3-1*) overlapped with previous QTL at germination and seedling stage (Huang et al., 2013; Hu et al., 2016; Revilla et al., 2016). These results suggest that QTL detected in our study are highly reliable when used for gene cloning and MAS. In addition, a high frequency of germination QTL associated with QTL for other growth stages in diverse genetic backgrounds indicates that maize has

a relatively conservative mechanism to adapt to suboptimal temperatures.

Three mQTL were found to locate in chromosome regions that have been mentioned to harbor cold related QTL in previous reports (**Table 3**). The region of *mQTL1-1* included seven initial QTL associated with four traits (ER, TL, RL, and SL) in population 220 × PH4CV and P9-10 × PH4CV, with three QTL explaining more than 30% of phenotypic variance (Supplementary Table S5). In previous studies, some QTL have also been identified in this region for cold related traits by using different populations. Fracheboud et al. (2002) identified a QTL for CO_2 fixation and PSII of leaves at 15°C from a RIL population; Allam et al. (2016) identified a QTL associated ear height of mature plant under low temperature from another RIL population; and Hund et al. (2004) identified a root trait QTL using maize seedlings grown at low temperatures. These results indicate that this region might harbor a major gene or several effective genes with pleiotropic effect on maize low temperature response at different growth stages.

mQTL9-1 harbored three initial QTL for seedling traits. Although the explained phenotypic variances of QTL within *mQTL9-1* were low (3.02–5.04%), this region was confirmed to harbor consistently expressed QTL at low temperatures during germination, seedling and maturity stage (Supplementary Table S5). Hu et al. (2016) found two QTL controlling seed germination rate and seedling primary RL from the B73 × Mo17 population, with favor alleles inherited from cold tolerant line Mo17. Besides germination traits, Allam et al. (2016) identified two QTL to control plant height and 100 kernel weight from populations B73 × P39 and B73 × IL14h under low temperature, with trait-increasing alleles inherited from cold tolerant line P39 and IL14h, respectively. Jompuk et al. (2005) detected a QTL in this region controlling PSII content of plant under early sowing (low temperature during early spring). The explained phenotypic variance of QTL in *mQTL9-1* region varied from moderate in Allam et al. (2016) (13.8–18.6%) and in Jompuk et al. (2005) (3.6–24.8%) to low in Hu et al. (2016) (5.25–8.41%). These results suggest that *mQTL9-1* region also contain an important QTL for cold response, which might function at multiple growth stage and exist in multiple genetic background in maize.

mQTL2-1 harbored two initial QTL detected from populations 220 × PH4CV and 220 × Y1518 for germination traits. Trait-increasing alleles were both inherited from 220, suggesting that *mQTL2-1* allele from 220 could function in different genetic background. Although in this region there is no cold related QTL reported from bi-parental population, an SNP marker linked with a cold associated QTL (response for relative TL, the ratio of total seedling length measured under chilling stress and normal condition) was revealed from a genome wide associate study (GWAS, Huang et al., 2013). Moreover, a cold induced CBF3/DREB1A transcript factor, GRMZM2G124011, was identified to locate in this region (Maruyama et al., 2004; Chinnusamy et al., 2007). This gene showed higher expression level in tolerant line 220 than in susceptible line PH4CV, suggesting that GRMZM2G124011 might be a candidate gene in *mQTL2-1* region responding for the different cold tolerance between 220 and PH4CV (**Figure 4B**).

Quantitative trait locus with higher effect are generally easier for gene cloning or more efficient for MAS (Moreau et al., 2004; Stromberg et al., 1994; Asea et al., 2012). In this work, 16 QTL had phenotypic variance higher than 10% (Supplementary Table S5). Of them, eight belonged to single-population that located in chromosome regions other than the mQTL intervals. *qp2RL8-1* and *qp2RL8-2* explained 10.44–17.97% phenotype variations, and located in a neighboring region on Chr 8: 146.99–153.79 Mb, a region overlapped by the previously reported QTL which associated to maize seedling photosynthesis at chill condition (Jompuk et al., 2005). In addition, the gene GRMZM2G030167, encoding a vacuolar ATP synthase subunit E1, located in this QTL interval and showed higher expression in 220 than in PH4CV (**Figure 4** and Schulze et al., 2012; Zhang Z. et al., 2017). And the expression of GRMZM2G030167 in both parents decreased under cold stress (**Figure 4G**). Comparing to PH4CV, the slower decrease of *GRMZM2G030167* expression in 220 might be a reason responding for its higher cold tolerance that was achieved by maintaining a higher ATP metabolism level in 220 under cold stress. *qp2ER9-1* and *qp2GI9-1* were overlapping on Chr 9: 94.81–96.00 Mb, and explained phenotype variation of 13.72 and 21.46%, respectively (Supplementary Table S5). Of which QTL region, Leipner et al. (2008) detected a QTL responding for dry weight of ear that were subjected to chill stress during seedling stage. *qp2SL2-1* explained 12.31% phenotypic variance, and located on Chr 2: 190.93–191.82 Mb. This QTL region was overlapped with an identified QTL of controlling fresh weight grown in chill environment (Presterl et al., 2007). The last three QTL (*qp1ER5-2*, *qp2SL3-1,* and *qp3ER10-1*) with high-effect were new discovered QTL where no genes or QTL was reported in previously works (Supplementary Table S5).

Prospects for Gene Cloning and Marker-Assisted Selection for Low-Temperature Germination Ability in Maize

The reliability of QTL analysis depends on population size, phenotypic variance, phenotyping methods and marker density, etc. In this study, we addressed some of these obstacles and detected the most promising mQTL for further gene cloning and MAS. First, we applied two different methods (sand bed and paper rolls) for germination trait evaluation at low temperature, in contrast to previous studies that only used one of the methods of sand bed, peat bed, paper rolls or field evaluation at early spring (Hund et al., 2004; Rodriguez et al., 2014; Hu et al., 2016; Shi et al., 2016). We found significant correlations between traits collected from different methods, suggesting that QTL repeatedly detected by two methods might be more reliable for further gene cloning and MAS.

Second, use of three populations for phenotyping and genotyping enabled us to identify mQTL across populations. Although a number of QTL associated with cold acclimation have been identified, only few were consistent across diverse genetic backgrounds. In this work, three mQTL were identified to contain initial QTL from two populations. Furthermore, two of the identified mQTL (*mQTL1-1* and *mQTL2-1*) included

initial QTL with high explained phenotypic variance, making these mQTL attractive for gene cloning and MAS.

Third, outstanding parental lines with contrasting cold tolerance were selected for generating populations, which contributed to efficient identification of major QTL. Of the 43 initial QTL, 3 explained more than 30% and 14 explained 10–30% phenotypic variance. Cold tolerance increasing alleles were all inherited from the tolerant lines 220 or P9-10, further supporting the efficacy of selection of suitable parental lines. In contrast, phenotypic variance of QTL identified in previous reports were generally lower than 20% (Hund et al., 2004; Leipner et al., 2008; Rodriguez et al., 2014; Hu et al., 2016; Shi et al., 2016).

CONCLUSION

We identified 43 QTL responsible for maize LTGA using three connected populations germinated in a sand bed and paper rolls. By constructing a consensus linkage map, three mQTL were suggested to include initial QTL that detected from different populations. In future, it is of great interest to clone genes underlying mQTL regions and uncover the molecular mechanisms of maize cold tolerance during germination.

AUTHOR CONTRIBUTIONS

GyW, JW, and RG designed the study; XL, GhW, GJ, LR, and LL performed the experiments; XL and JF analyzed the data; XL drafted the manuscript; TL, JW, and RG advised on data analysis and revised the manuscript.

ACKNOWLEDGMENTS

This research was supported by the National Basic Research Program of China (2014CB138200), the China Agriculture Research System (CARS-08), the special fund for Agro-Scientific Research in the Public Interest (201303002), the National Science Foundation of China (31771891), the National Key Research and Development Program of China (2016YFD0101803).

SUPPLEMENTARY MATERIAL

The Supplementary Material for this article can be found online at: https://www.frontiersin.org/articles/10.3389/fpls.2018.00065/full#supplementary-material

REFERENCES

Allam, M., Revilla, P., Djemel, A., Tracy, W. F., and Ordas, B. (2016). Identification of QTLs involved in cold tolerance in sweet × field corn. *Euphytica* 208, 353–365. doi: 10.1007/s10681-015-1609-7

Asea, G., Vivek, B. S., Lipps, P. E., and Pratt, R. C. (2012). Genetic gain and cost efficiency of marker-assisted selection of maize for improved resistance to multiple foliar pathogens. *Mol. Breed.* 29, 515–527. doi: 10.1007/s11032-011-9568-8

Baga, M., Chodaparambil, S. V., Limin, A. E., Pecar, M., Fowler, D. B., and Chibbar, R. N. (2007). Identification of quantitative trait loci and associated candidate genes for low-temperature tolerance in cold-hardy winter wheat. *Funct. Integr. Genomics* 7, 53–68. doi: 10.1007/s10142-006-0030-7

Basnet, R. K., Duwal, A., Tiwari, D. N., Xiao, D., Monakhos, S., Bucher, J., et al. (2015). Quantitative trait locus analysis of seed germination and seedling vigor in *Brassica rapa* reveals QTL hotspots and epistatic interactions. *Front. Plant Sci.* 6:1032. doi: 10.3389/fpls.2015.01032

Blanc, G., Charcosset, A., Mangin, B., Gallais, A., and Moreau, L. (2006). Connected populations for detecting quantitative trait loci and testing for epistasis: an application in maize. *Theor. Appl. Genet.* 113, 206–224. doi: 10.1007/s00122-006-0287-1

Bouis, H. E., and Welch, R. M. (2010). Biofortification - a sustainable agricultural strategy for reducing micronutrient malnutrition in the global south. *Crop Sci.* 50, S20–S32. doi: 10.2135/cropsci2009.09.0531

Chardon, F., Virlon, B., Moreau, L., Falque, M., Joets, J., Decousset, L., et al. (2004). Genetic architecture of flowering time in maize as inferred from quantitative trait loci meta-analysis and synteny conservation with the rice genome. *Genetics* 168, 2169–2185. doi: 10.1534/genetics.104.032375

Chinnusamy, V., Zhu, J., and Zhu, J. K. (2007). Cold stress regulation of gene expression in plants. *Trends Plant Sci.* 12, 444–451. doi: 10.1016/j.tplants.2007.07.002

Churchill, G. A., and Doerge, R. W. (1994). Empirical threshold values for quantitative trait mapping. *Genetics* 138, 963–971.

Cui, F., Zhao, C., Ding, A., Li, J., Wang, L., Li, X., et al. (2014). Construction of an integrative linkage map and QTL mapping of grain yield-related traits using three related wheat RIL populations. *Theor. Appl. Genet.* 127, 659–675. doi: 10.1007/s00122-013-2249-8

Fracheboud, Y., Jompuk, C., Ribaut, J. M., Stamp, P., and Leipner, J. (2004). Genetic analysis of cold-tolerance of photosynthesis in maize. *Plant Mol. Biol.* 56, 241–253. doi: 10.1007/s11103-004-3353-6

Fracheboud, Y., Ribaut, J. M., Vargas, M., Messmer, R., and Stamp, P. (2002). Identification of quantitative trait loci for cold-tolerance of photosynthesis in maize (*Zea mays* L.). *J. Exp. Bot.* 53, 1967–1977. doi: 10.1093/jxb/erf040

Frascaroli, E., and Landi, P. (2017). Registration of maize inbred line Bo23 with high cold tolerance and agronomic performance for early sowing. *J. Plant Regist.* 11, 172–177. doi: 10.3198/jpr2016.05.0029

Fujino, K., Sekiguchi, H., Matsuda, Y., Sugimoto, K., Ono, K., and Yano, M. (2008). Molecular identification of a major quantitative trait locus, qLTG3-1 controlling low-temperature germinability in rice. *Proc. Natl. Acad. Sci. U.S.A.* 105, 12623–12628. doi: 10.1073/pnas.0805303105

Fujino, K., Sekiguchi, H., Sato, T., Kiuchi, H., Nonoue, Y., Takeuchi, Y., et al. (2004). Mapping of quantitative trait loci controlling low-temperature germinability in rice (*Oryza sativa* L.). *Theor. Appl. Genet.* 108, 794–799. doi: 10.1007/s00122-003-1509-4

Greaves, J. A. (1996). Improving suboptimal temperature tolerance in maize - the search for variation. *J. Exp. Bot.* 47, 307–323. doi: 10.1093/jxb/47.3.307

Gu, R., Duan, F., An, X., Zhang, S., von Wiren, N., and Yuan, L. (2013). Characterization of AMT-mediated high-affinity ammonium uptake in roots of maize (*Zea mays* L.). *Plant Cell Physiol.* 54, 1515–1524. doi: 10.1093/pcp/pct099

Gu, R., Li, L., Liang, X., Wang, Y., Fan, T., Wang, Y., et al. (2017). The ideal harvest time for seeds of hybrid maize (*Zea mays* L.) XY335 and ZD958 produced in multiple environments. *Sci. Rep.* 7:17537. doi: 10.1038/s41598-017-16071-4

Guerra-Peraza, O., Leipner, J., Reimer, R., Nguyen, H. T., Stamp, P., and Fracheboud, Y. (2011). Temperature at night affects the genetic control of acclimation to cold in maize seedlings. *Maydica* 56, 367–377. doi: 10.3929/ethz-a-005794605

Han, Z., Ku, L., Zhang, Z., Zhang, J., Guo, S. L., Liu, H., et al. (2014). QTLs for seed vigor-related traits identified in maize seeds germinated under artificial aging conditions. *PLOS ONE* 9:e92535. doi: 10.1371/journal.pone.0092535

Hansen, J., Sato, M., Ruedy, R., Lacis, A., and Oinas, V. (2000). Global warming in the twenty-first century: an alternative scenario. *Proc. Natl. Acad. Sci. U.S.A.* 97, 9875–9880. doi: 10.1073/pnas.170278997

He, F., Shen, H., Lin, C., Fu, H., Sheteiwy, M. S., Guan, Y., et al. (2017). Transcriptome analysis of chilling-imbibed embryo revealed membrane

recovery related genes in maize. *Front. Plant Sci.* 7:1978. doi: 10.3389/fpls.2016.01978

Hu, S., Lubberstedt, T., Zhao, G., and Lee, M. (2016). QTL mapping of lLow-temperature germination ability in the maize IBM syn4 RIL population. *PLOS ONE* 11:e152795. doi: 10.1371/journal.pone.0152795

Huang, J., Zhang, J., Li, W., Hu, W., Duan, L., Feng, Y., et al. (2013). Genome-wide association analysis of ten chilling tolerance indices at the germination and seedling stages in maize. *J. Integr. Plant Biol.* 55, 735–744. doi: 10.1111/jipb.12051

Hund, A., Fracheboud, Y., Soldati, A., Frascaroli, E., Salvi, S., and Stamp, P. (2004). QTL controlling root and shoot traits of maize seedlings under cold stress. *Theor. Appl. Genet.* 109, 618–629. doi: 10.1007/s00122-004-1665-1

IBM Corp (2011). *IBM SPSS Statistics for Windows, Version 20.0*. Armonk, NY: IBM Corp.

International Seed Testing Association [ISTA] (2015). *International Rules for Seed Test*. Zurich: International Seed Testing Association.

Jompuk, C., Fracheboud, Y., Stamp, P., and Leipner, J. (2005). Mapping of quantitative trait loci associated with chilling tolerance in maize (*Zea mays* L.) seedlings grown under field conditions. *J. Exp. Bot.* 56, 1153–1163. doi: 10.1093/jxb/eri108

Leipner, J., Fracheboud, Y., and Stamp, P. (1999). Effect of growing season on the photosynthetic apparatus and leaf antioxidative defenses in two maize genotypes of different chilling tolerance. *Environ. Exp. Bot.* 42, 129–139. doi: 10.1016/S0098-8472(99)00026-X

Leipner, J., Jompuk, C., Camp, K., Stamp, P., and Fracheboud, Y. (2008). QTL studies reveal little relevance of chilling-related seedling traits for yield in maize. *Theor. Appl. Genet.* 116, 555–562. doi: 10.1007/s00122-007-0690-2

Li, H., Ye, G., and Wang, J. (2007). A modified algorithm for the improvement of composite interval mapping. *Genetics* 175, 361–374. doi: 10.1534/genetics.106.066811

Li, Z., Xu, J., Gao, Y., Wang, C., Guo, G., Luo, Y., et al. (2017). The synergistic priming effect of exogenous salicylic acid and H_2O_2 on chilling tolerance enhancement during maize (*Zea mays* L.) seed germination. *Front. Plant Sci.* 8:1153. doi: 10.3389/fpls.2017.01153

Liu, H., Zhang, L., Wang, J., Li, C., Zeng, X., Xie, S., et al. (2017). Quantitative trait locus analysis for deep-sowing germination ability in the maize IBM syn10 DH population. *Front. Plant Sci.* 8:813. doi: 10.3389/fpls.2017.00813

Lu, G., Wu, F. Q., Wu, W., Wang, H. J., Zheng, X. M., Zhang, Y., et al. (2014). Rice LTG1 is involved in adaptive growth and fitness under low ambient temperature. *Plant J.* 78, 468–480. doi: 10.1111/tpj.12487

Maruyama, K., Sakuma, Y., Kasuga, M., Ito, Y., Seki, M., et al. (2004). Identification of cold-inducible downstream genes of the arabidopsis dreb1a/cbf3 transcriptional factor using two microarray systems. *Plant J. Cell Mol. Biol.* 38, 982–993. doi: 10.1111/j.1365-313X.2004.02100.x

Meng, L., Li, H., Zhang, L., and Wang, J. (2015). QTL IciMapping: Integrated software for genetic linkage map construction and quantitative trait locus mapping in biparental populations. *Crop J.* 3, 269–283. doi: 10.1016/j.cj.2015.01.001

Moreau, L., Charcosset, A., and Gallais, A. (2004). Experimental evaluation of several cycles of marker-assisted selection in maize. *Euphytica* 137, 111–118. doi: 10.1023/B:EUPH.0000040508.01402.21

Murray, M. G., and Thompson, W. F. (1980). Rapid isolation of high molecular weight plant DNA. *Nucleic Acids Res.* 8, 4321–4325. doi: 10.1093/nar/8.19.4321

Nyquist, W. E. (1991). Estimation of heritability and prediction of selection response in plant populations. *Crit. Rev. Plant Sci.* 10, 235–322. doi: 10.1080/07352689109382313

Pandit, E., Tasleem, S., Barik, S. R., Mohanty, D. P., Nayak, D. K., Mohanty, S. P., et al. (2017). Genome-wide association mapping reveals multiple QTLs governing tolerance response for seedling stage chilling stress in indica rice. *Front. Plant Sci.* 8:552. doi: 10.3389/fpls.2017.00552

Presterl, T., Ouzunova, M., Schmidt, W., Möller, E. M., Röber, F. K., Knaak, C., et al. (2007). Quantitative trait loci for early plant vigour of maize grown in chilly environments. *Theor. Appl. Genet.* 114, 1059–1070. doi: 10.1007/s00122-006-0499-4

R Core Team (2016). *R: A Language and Environment for Statistical Computing*. Vienna: R Foundation for Statistical Computing.

Revilla, P., Rodríguez, V. M., Ordás, A., Rincent, R., Charcosset, A., Giauffret, C., et al. (2016). Association mapping for cold tolerance in two large maize inbred panels. *BMC Plant Biol.* 16:127. doi: 10.1186/s12870-016-0816-2

Rodriguez, V. M., Butron, A., Rady, M. O. A., Soengas, P., and Revilla, P. (2008). Quantitative trait loci for cold tolerance in the maize IBM population. *Int. J. Plant Sci.* 169, 551–556. doi: 10.1086/528755

Rodriguez, V. M., Butron, A., Rady, M. O. A., Soengas, P., and Revilla, P. (2014). Identification of quantitative trait loci involved in the response to cold stress in maize (*Zea mays* L.). *Mol. Breed.* 33, 363–371. doi: 10.1007/s11032-013-9955-4

Sallam, A., Arbaoui, M., El-Esawi, M., Abshire, N., and Martsch, R. (2016). Identification and verification of QTL associated with frost tolerance using linkage mapping and GWAS in winter Faba Bean. *Front. Plant Sci.* 7:1098. doi: 10.3389/fpls.2016.01098

Schulze, W. X., Schneider, T., Starck, S., Martinoia, E., and Trentmann, O. (2012). Cold acclimation induces changes in Arabidopsis tonoplast protein abundance and activity and alters phosphorylation of tonoplast monosaccharide transporters. *Plant J.* 69, 529–541. doi: 10.1111/j.1365-313X.2011.04812.x

Sheteiwy, M., Shen, H., Xu, J., Guan, Y., Song, W., and Hu, J. (2017). Seed polyamines metabolism induced by seed priming with spermidine and 5-aminolevulinic acid for chilling tolerance improvement in rice (*Oryza sativa* L.) seedlings. *Environ. Exp. Bot.* 137, 58–72. doi: 10.1016/j.envexpbot.2017.02.007

Shi, Y., Li, G., Tian, Z., Wang, Z., Wang, X., Zhu, Y., et al. (2016). Genetic dissection of seed vigour traits in maize (*Zea mays* L.) under low-temperature conditions. *J. Genet.* 95, 1017–1022. doi: 10.1007/s12041-016-0714-2

Stirling, C. M., Nie, G. Y., Aguilera, C., Nugawela, A., Long, S. P., and Baker, N. R. (1991). Photosynthetic productivity of an immature maize crop: changes in quantum yield of CO_2 assimilation, conversion efficiency and thylakoid proteins. *Plant Cell Environ.* 14, 947–954. doi: 10.1111/j.1365-3040.1991.tb00964.x

Stromberg, L. D., Dudley, J. W., and Rufener, G. K. (1994). Comparing conventional early generation selection with molecular marker assisted selection in maize. *Crop Sci.* 34, 1221–1225. doi: 10.2135/cropsci1994.0011183X003400050014x

Verheul, M. J., Picatto, C., and Stamp, P. (1996). Growth and development of maize (*Zea mays* L.) seedlings under chilling conditions in the field. *Eur. J. Agron.* 5, 31–43. doi: 10.1016/S1161-0301(96)02007-2

Wang, H., Xu, C., Liu, X., Guo, Z., Xu, X., Wang, S., et al. (2017). Development of a multiple-hybrid population for genome-wide association studies: theoretical consideration and genetic mapping of flowering traits in maize. *Sci. Rep.* 6:40239. doi: 10.1038/srep40239

Zhang, W. B., Jiang, H. W., Qiu, P. C., Liu, C. Y., Chen, F. L., Xin, D. W., et al. (2017). Genetic overlap of QTL associated with low-temperature tolerance at germination and seedling stage using BILs in soybean. *Can. J. Plant Sci.* 92, 1381–1388. doi: 10.4141/CJPS2011-098

Zhang, Z., Li, J., Pan, Y., Li, J., Zhou, L., Shi, H., et al. (2017). Natural variation in CTB4a enhances rice adaptation to cold habitats. *Nat. Commun.* 8:14788. doi: 10.1038/ncomms14788

Zhou, F., Wang, G., Xie, Y., Cui, H., Guo, S., and Dai, J. (1999). Establishment of a genetic transformation system for maize inbred P9-10. *Chin. Sci. Bull.* 44, 624–627.

Conflict of Interest Statement: The authors declare that the research was conducted in the absence of any commercial or financial relationships that could be construed as a potential conflict of interest.

frontiers in Plant Science

ORIGINAL RESEARCH
published: 28 June 2017
doi: 10.3389/fpls.2017.01133

Functional Characterization of TaFUSCA3, a B3-Superfamily Transcription Factor Gene in the Wheat

Fusheng Sun†, Xiyan Liu†, Qiuhui Wei, Jiannan Liu, Tianxiang Yang, Liyang Jia, Yuesheng Wang, Guangxiao Yang and Guangyuan He**

The Genetic Engineering International Cooperation Base of Chinese Ministry of Science and Technology, Key Laboratory of Molecular Biophysics of Chinese Ministry of Education, College of Life Science and Technology, Huazhong University of Science and Technology, Wuhan, China

The end-use quality of wheat, including its unique rheology and viscoelastic properties, is predominantly determined by the composition and concentration of gluten proteins. While, the mechanism regulating expression of the seed storage protein (SSP) genes and other related genes in wheat remains unclear. In this study, we report on the cloning and functional identification of *TaFUSCA3*, a B3-superfamily transcription factor (TF) gene in wheat. Sequence alignment indicated that wheat and barley *FUSCA3* genes are highly conserved. Quantitative reverse-transcription (qRT)-PCR analysis showed that the transcript of *TaFUSCA3* was accumulated mostly in the stamens and the endosperms of immature wheat seeds. Yeast-one-hybrid results proved that the full-length TaFUSCA3 and its C-terminal region had transcriptional activities. Yeast-two-hybrid and bimolecular fluorescence complementation assays indicated that TaFUSCA3 could activate the expression of the high molecular weight glutenin subunit gene *Glu-1Bx7* and interact with the seed-specific bZIP protein TaSPA. DNA-protein-interaction enzyme-linked immunosorbent assay demonstrated that TaFUSCA3 specifically recognizes the RY-box of the *Glu-1Bx7* promoter region. Transient expression results showed that TaFUSCA3 could *trans*-activate the *Glu-1Bx7* promoter, which contains eight RY-box sequences. TaFUSCA3 was unable to activate the downstream transcription when the RY-box was fully mutated. TaFUSCA3 could activate the transcription of the *At2S3* gene promoter in a complementation of loss-of-function experiment using the *Arabidopsis thaliana* line *fus3-3*, which is a *FUSCA3* mutant, demonstrating the evolutionary conservation of the *TaFUSCA3* gene. In conclusion, the wheat B3-type TF, TaFUSCA3, is functional conserved between monocot and dicot, and could regulate SSP gene expression by interacting specifically with TaSPA.

Keywords: TaFUSCA3, TaSPA, seed storage protein, complementation of the loss-of-function, wheat

OPEN ACCESS

Edited by:
Chengdao Li,
Murdoch University, Australia

Reviewed by:
Karl Kunert,
University of Pretoria, South Africa
Chuang Ma,
Northwest A&F University, China

****Correspondence:***
Guangyuan He
hegy@hust.edu.cn
Guangxiao Yang
ygx@hust.edu.cn

† These authors have contributed equally to this work.

Specialty section:
This article was submitted to Crop Science and Horticulture, a section of the journal Frontiers in Plant Science

Received: *16 March 2017*
Accepted: *13 June 2017*
Published: *28 June 2017*

Citation:
Sun F, Liu X, Wei Q, Liu J, Yang T, Jia L, Wang Y, Yang G and He G (2017) Functional Characterization of TaFUSCA3, a B3-Superfamily Transcription Factor Gene in the Wheat. Front. Plant Sci. 8:1133. doi: 10.3389/fpls.2017.01133

Abbreviations: BiFC, bimolecular fluorescence complementation; DAP, days after pollination; DPI-ELISA, DNA-protein-interaction enzyme-linked immunosorbent assay; GFP, green fluorescent protein; GST, glutathione *S*-transferase; GUS, β-glucuronidase; HMW-GS, high molecular weight glutenin subunit; O2, opaque2; ORF, open reading frame; qRT, quantitative reverse-transcription; SSPs, seed storage proteins; TFs, transcription factors; Y1H, yeast one-hybrid; Y2H, yeast two-hybrid.

INTRODUCTION

Wheat (*Triticum aestivum* L.) is a very important cereal crop throughout the world, which can be made into diverse edible products for human beings because of the distinct viscoelastic characteristics of its cohesive dough conferred by the SSPs in the endosperm (Shewry, 2009). The HMW-GSs of SSPs play important roles in wheat gluten as the skeletal network that determines its structure and formation (Shewry and Tatham, 1990). The formation and accumulation of SSPs is controlled by various essential TFs at different developmental stages both in monocotyledons and dicotyledons (Plessis et al., 2013; González-Calle et al., 2014; Zhang et al., 2015). A group of important TFs, the AFL subfamily containing a plant-specific B3 DNA binding domain that takes part in this process, has been identified. Members of this family include ABSCISIC ACID-INSENSITIVE3 (ABI3), FUSCA3 (FUS3), LEAFY COTYLEDON1 (LEC1), and LEAFY COTYLEDON1 (LEC2), which regulate the desiccation tolerance and dormancy of the maturation stage of *Arabidopsis thaliana* (Stone et al., 2001; Swaminathan et al., 2008; Roscoe et al., 2015). The AFL subfamily genes are able to affect the biosynthesis of hormones and regulate the expression activity of downstream genes via protein–protein interactions (Carbonero et al., 2016). If any of the members including ABI3, FUS3, LEC1, and LEC2 are mutated, it will result in the reduced accumulation of endosperm-specific storage proteins. Besides, the TFs are interlocked in an intricate stratified reticular regulatory network by virtue of mutual interconnections (To et al., 2006).

The expression of SSP genes is regulated under strict organ-specific and temporal order during the seed development process (Kawagoe and Murai, 1992; Onodera et al., 2001), in which *cis*-acting elements of relevant promoters play an important role. The various accurate *cis*-acting elements, containing the B-box (5′-CAAACACC-3′), the RY-box (5′-CATGCA-3′), and the G-box (5′-CACGTG-3′) in the promoter of the gene encoding NapA, have been authenticated in *Brassica napus* (Ezcurra et al., 1999; Fauteux and Strömvik, 2009). The above-mentioned elements are functionally conserved and correlative in other species, such as the promoters of 2S albumins from *A. thaliana* (Kroj et al., 2003). Studies have revealed the significance of B3-type TFs and RY boxes (Mönke et al., 2004). FUSCA3 may directly regulate *At2S3* and *napA* by specifically recognizing the specific RY-box element in their promoters (Reidt et al., 2000). However, FUSCA3 could also indirectly control seed filling and the accumulation of seed storage reserves through an additional regulatory factor, such as TRANSPARENT TESTA GLABRA 1 (TTG1) (Chen et al., 2015), and the functional protein AtFUSCA3 with a conserved B3 domain has been shown to regulate late embryogenesis and seed maturation in *A. thaliana* (Luerssen et al., 1998). The seeds in the *FUSCA3* mutant of *A. thaliana* cannot process dormancy and they are further distinguished by the reduced accumulation of multiple storage substances and abundant production of anthocyanin (Roscoe et al., 2015).

Reserve substances consisting of starches, SSPs, and fatty acids are primarily accumulated in the endosperm of seeds in monocotyledons (Olsen and Becraft, 2013). Regulation of SSPs' expression depends on the interactions between *cis*-acting elements and *trans*-activating TFs (Mena et al., 2002; Shewry and Halford, 2002; Juhász et al., 2011). A diverse array of *cis*-acting elements in the promoters of these proteins has been verified. The DOF recognition site (PB-box, 5′-TGTAAAG-3′), LAV recognition site (RY-box, 5′-CATGCA-3′), bZIP recognition sites (GLM-box, 5′-ATGAG/CTCAT-3′ and G-box, 5′-TTACGTGG-3′), R2R3MYB recognition site (5′-AACAAC-3′), and other essential motifs are conserved in the promoters of genes encoding cereal SSPs (Wu et al., 2000; Geng et al., 2014).

In maize, opaque2 (O2) heterodimerizing proteins (OHP) and DOF proteins (MPBF) can synergistically activate the expression of the *γ-Zeins* 27 gene encoding an alcohol soluble protein through the O2-like box (Pysh et al., 1993; Zhang et al., 2015). In barley, HvFUSCA3, binding to the RY motif of *Itr1* and *Hor2* promoters, activates the transcription of these genes by interacting with BLZ2 (Moreno-Risueno et al., 2008). In wheat, TaSPA, the O2-like bZIP factor, recognizes the GLM (GCN4-like motif) in the bi-factorial endosperm box to regulate expression of the low molecular weight glutenin subunit (LMW-GS) gene (Albani et al., 1997). TaGAMyb, which attaches to the R2R3MYB family, has been identified to interact with the histone acetyltransferase TaGCN5 to activate the expression of *TaGLU-1Dy*, a HMW-GS gene in wheat (Guo et al., 2015). Regulation of the expression of SSPs is accomplished by the integrated action of multitudinous TFs (Shekhar et al., 2016). A previous study showed that the seed-specific storage protein genes in *A. thaliana* had a distinctly lower expression level in a *FUSCA3* mutant line (Bäumlein et al., 1994).

The RY motif is conserved among the promoters of the monocot prolamin and the dicot SSP genes. Whether or not the RY motif could be directly recognized by a B3 transcriptional factor, which plays an important part in the regulation of SSP expression, and the downstream target of regulation have not been documented previously in wheat. In order to evaluate whether the FUSCA3-like homologous gene in wheat could regulate the expression of SSP genes, we cloned and characterized *TaFUSCA3* in wheat and confirmed its function in the regulation of expression of the SSP Ta1Bx7 in this study. Our results showed that TaFUSCA3 is able to bind to and activate the *Ta1Bx7* gene specifically through the RY-box in the promoter region. Moreover, it was shown that TaFUSCA3 interacts with the seed-specific bZIP protein TaSPA *in vivo*. Complementation of the loss-of-function *FUSCA3* mutant in the *A. thaliana* mutant line *fus3-3* by TaFUSCA3 resulted in SSP gene expression in seeds.

MATERIALS AND METHODS

Plant Materials

Seeds of Bobwhite wheat (*T. aestivum* cv. Bobwhite), a model wheat cultivar, were germinated in sterile water for 1 week and then transplanted into a climate-controlled chamber (16 h light/8 h dark cycle at 26°C). Different organs including roots, young stems and young leaves were collected from young seedlings, while stamens, mature stems, mature leaves, flag leaves,

endosperms, and pistils were collected from mature wheat plants for organ-specific gene expression analysis. The endosperms were harvested from the seeds at 4, 8, 12, 16, 20, 24, 28, and 32 DAP, respectively, and stored at −80°C.

Cloning and Bioinformatic Analysis of *TaFUSCA3*

Total RNA extracted from young wheat seeds (20 DAP) was used to synthesize first-strand cDNAs and to amplify the cDNA of *TaFUSCA3*. To identify the putative *TaFUSCA3* gene in wheat, the sequence of the *HvFUSCA3* gene (GenBank No.: AM418838) from *Hordeum vulgare* was used as a query probe to blast the data library of wheat[1] (Moreno-Risueno et al., 2008). A *T. aestivum* gene sequence with high identity to the ORF of *HvFUSCA3* was identified. The sequence analysis showed that it included a complete ORF sequence, which was detected by ORF Finder[2]. This gene was then amplified from cDNA by the use of degenerate primers (Supplementary Table S1). The PCR product was purified and ligated into pMD18-T simple vector (Takara, Dalian, China), which was sequenced to confirm its veracity.

The FUSCA3 sequences from seven plant species were searched for and compared at the NCBI[3] and were used for phylogenetic analysis. The alignment of different sequences was performed by using the software DNAMAN, MEGA (version 5.1), and ClustalX2.0, and the neighbor-joining method was used to construct a phylogenetic tree (Saitou and Nei, 1987).

Subcellular Localization and Bimolecular Fluorescence Complementation (BiFC) of TaFUSCA3 and TaSPA

The coding sequences of *TaFUSCA3* and *TaSPA* (excluding the termination codon) were amplified using primers described in Supplementary Table S1 for transient expression in onion epidermal cells. The PCR-amplified products were then subcloned into the pCAMBIA1303-35S-*GFP* expression vector and pSPYNE-35S/pUC-SPYNE and pSPYCE-35S/pUC-SPYCE vectors for BiFC. The experiment was performed as described by Walter et al. (2004). Information on the vectors used in our study is listed in Supplementary Table S2.

Trans-activation and Binding Activity Analysis of TaFUSCA3 in Yeast

The assay for analysis of transcription activation properties of TaFUSCA3 was conducted in the *AH109* yeast strain. The complete coding sequences of *TaTAFUS3* (full-length ORF), and N-terminal (*TaFUSCA3-N*), B_3 domain (*TaFUSCA3-B*$_3$), and C-terminal (*TaFUSCA-C*) fragments were amplified by PCR using specific primers P17-P20, respectively (Supplementary Table S1).

Binding activity between FUSCA3 and the RY-box of both the *At2S3* and *Ta1Bx7* gene promoter regions was assayed by using the yeast one-hybrid (Y1H) system (Ouwerkerk and Meijer, 2001). RY-boxes of *At2S3* and *Ta1Bx7*, and mutant RY-boxes of *Ta1Bx7** containing two repeat copies were subcloned into the vector pHis2.0 subsequently. The particular process of the experiment was described by Wang et al. (2015).

Yeast Two-Hybrid (Y2H) Assay

The ORFs of *TaFUSCA3*, *TaFUSCA3**, *TaSPA*, *TaPBF*, and *TaGAMYB* were ligated into the pGADT7 and pGBKT7 vectors, respectively, to create the recombined plasmids (Supplementary Table S2). Of the five ORFs, *TaFUSCA3** is a mutated version in which the seventh to the 46th amino acids were removed. For yeast mating, various combinations of different plasmids were transformed into yeast strain *Y187* by the PEG/LiAc method.

DNA-Protein-Interaction Enzyme-Linked Immunosorbent Assay (DPI-ELISA)

The DNA-protein-interaction enzyme-linked immunosorbent assay (DPI-ELISA) assay is a versatile and effective method that was used to analyze plant TF-specific binding to DNA *in vitro*. The target protein TaFUSCA3, which was recombined with GST protein, was expressed in prokaryotic expressive *Escherichia coli* strain *BL21*. The short complementary primer sequences of biotinylation and non-biotinylation were synthesized by AuGCT DNA-SYNBiotech, Co., Ltd. (Wuhan, China) (Brand et al., 2010).

Plant Transformation and Generation of Transgenic Plants

The intact expression cassette of *TaFUSCA3* containing the 35S promoter of cauliflower mosaic virus and the NOS terminator was amplified by reverse-transcription (RT)-PCR and cloned into the eukaryotic expression vector pBI121 to get the recombinant plasmid pBI121-*TaFUSCA3*. Subsequently, the original promoter of the *GFP* gene was replaced by the promoter of the *At2S3* gene (GenBank No.: At4g27160) that encodes the 2S albumin storage protein in *A. thaliana*. The primers are listed in Supplementary Table S1. The wild-type *A. thaliana* line *Col* and the mutant line *fus3-3* were transformed by using the *A. tumefaciens* floral dipping technique (Clough and Bent, 1998). The transgenic lines were screened on MS medium containing 50 mg/L kanamycin to generate homozygous lines. PCR and qRT-PCR analyses were performed for molecular identification and to assess transgene expression in each generation of transgenic lines.

qRT-PCR Analysis of *TaFUSCA3*

Expression patterns of *TaFUSCA3* in different organs in wheat were analyzed by qRT-PCR (Bio-Rad, Hercules, CA, United States) using the fluorescent DNA intercalating dye SYBR Green I Master Mix. The first-strand cDNAs were synthesized from the total Poly(A)$^+$ mRNA using a FastQuant RT Kit (Tiangen, Beijing, China). The gene-specific oligonucleotide primers for the gene expression analysis were designed in the 3′-UTR region of the gene excluding the B_3 conserved domain and other highly conserved domains. To examine the efficiency and specificity, the primers were used for PCR and the products obtained were verified by sequencing as well as a melting curve analysis from

[1]http://plants.ensembl.org/Triticum_aestivum/Info/Index

[2]https://www.ncbi.nlm.nih.gov/orffinder

[3]https://www.ncbi.nlm.nih.gov

55 to 99°C. It was confirmed that a single band and peak was obtained for each primer pair. Different concentrations of various templates and primers were used to determine the optimum concentrations, and a control set of reactions was performed without template and with primer pair.

For each sample, three biological replicates were performed. The expression of *TaFUSCA3* was normalized to that of *Ta*β-*actin* as an internal control, and the data were analyzed based on the comparative $2^{-\Delta\Delta CT}$ formula (Livak and Schmittgen, 2001).

β-Glucuronidase (GUS) Histochemical Assay

β-Glucuronidase histochemical assay was performed with the plant tissues following the protocol of Gui et al. (2011). The samples were incubated at 37°C overnight in GUS staining buffer [100 mM sodium phosphate, 0.5 mM $K_3Fe(CN)_6$, 0.5 mM $K_4Fe(CN)_6$, 0.1% Triton X-100, 10 mM Na_2EDTA and 1 mg/mL X-Gluc] for blue color development. After staining, the sections were rinsed with 70% ethanol for at least 1 h. Photographs were taken under fluorescence microscopy (OLYMPUS DP72, Japan).

Western Blotting

Protein samples were electrophoresed on 12% SDS polyacrylamide gels and transferred onto nitrocellulose membranes (Millipore) for detection of the target proteins. The membranes were subsequently blocked by incubation in Tris-buffered saline plus Tween 20 (TBST: 25 mM Tris-HCl, 80 mM NaCl, 0.1% Tween 20) containing 6% fat-free milk overnight at 4°C. The membranes were incubated with the primary antibody (diluted 1:4000, 2 h), washed (10 min × 4 times), and treated with the appropriate secondary antibody for 1 h. After washing the membranes again four times with TBST, immunoreactive bands were visualized by using a chemiluminescence detection system (UVP ChemiDoc-It, Upland, CA, United States). The housekeeping β-actin protein was detected as a control (Li et al., 2012).

Statistical Analysis

All experiments in our study were carried out in triplicate. The statistical software program ORIGIN for Windows version 8.1 was used for statistical analysis of the experimental data. Analysis of variance was used to contrast the statistically significant difference by employing the Student's *t*-test procedure. The 5% significant differences ($P < 0.05$) and 1% remarkably significant differences ($P < 0.01$) were evaluated. Data are the means ± SD in three independent replicates ($n = 3$).

RESULTS

Cloning and Sequence Analysis of the *TaFUSCA3* Gene

The cDNA of *TaFUSCA3* containing 1,071 bp was obtained from common wheat by use of an *in silico* cloning method. The *FUSCA* gene was designated *TaFUSCA3* as it had high sequence homology to *FUSCA3* (GenBank No.: AM 418838) from *H. vulgare*. The ORF of *TaFUSCA3* encoded a polypeptide of 288 amino acid residues with a predicted relative molecular mass of 32.3 kDa containing a B3 DNA binding domain. The *TaFUSCA3* gene was localized on chromosomes 3B, 3DL, and 3AL, which was also validated by the latest URGI Blast database[4].

Multiple sequence alignment analysis indicated that TaFUSCA3 had a high sequence identity with the FUSCA3 proteins from some cereal crops (89.3% with HvFUSCA3 from *H. vulgare*, 76.3% with BdFUSCA3 from *Brachypodium distachyon*, and 68.47% with OsFUSCA3 from *Oryza sativa*), while it had lower sequence identity with FUSCA3 proteins from other monocots, such as *Triticum urartu*, *Aegilops tauschii*, and *Zea mays* (64.8, 64.2, and 61.8%, respectively) (**Figure 1A**). The protein sequences used to perform the multiple sequence alignment are shown in Supplementary Table S3. According to the Multiple EM for Motif Elicitation tool[5], TaFUSCA3 had seven motifs, including a typical conserved B3 domain (amino acids 64–174), which could recognize and bind to the specific sequence (RY-boxes), and a transcription activating domain (TAD) containing 115 amino acid resides in the C-terminal region.

In order to further confirm the evolutionary relationships between TaFUSCA3 and FUSCA3 proteins from seven other plant species, a phylogenic tree was generated to analyze the historical evolution based on amino acid sequence alignment (**Figure 1B**). This analysis provided a further indication that FUSCA3 proteins are very highly conserved evolutionarily, and TaFUSCA3 presented the closest genetic relationship with HvFUSCA3. These results showed that *TaFUSCA3* from common wheat was a member of the FUS3 family.

TaFUSCA3 and TaSPA Are Localized in Nucleus

In order to analyze the subcellular localizations of TaFUSCA3 and TaSPA, the full-length ORFs of these proteins were fused to GFP and were transiently expressed in onion epidermal cells. As shown in **Figure 2**, both TaFUSCA3 and TaSPA were localized in the nucleus under the dark field for green fluorescence and the bright field, whereas the GFP alone was distributed throughout the cytoplasm and nucleus.

TaFUSCA3 are Predominantly Expressed in Stamen and Endosperm

To define possible functions of TaFUSCA3, organ-specific expression analysis was performed by using qRT-PCR with RNA extracted from different organs including roots, young stems, young leaves, endosperms, mature stems, mature leaves, flag leaves, stamens, and pistils. The expression levels of the *TaFUSCA3* gene in different organs revealed a distinctive expression pattern, and the results showed that *TaFUSCA3* was expressed in all of the organs and had higher expression in the stamen, followed by the endosperm and pistil (**Figure 3**). This indicated that TaFUSCA3 could participate in the growth

[4]https://urgi.versailles.inra.fr/blast/blast.php

[5]http://meme-suite.org

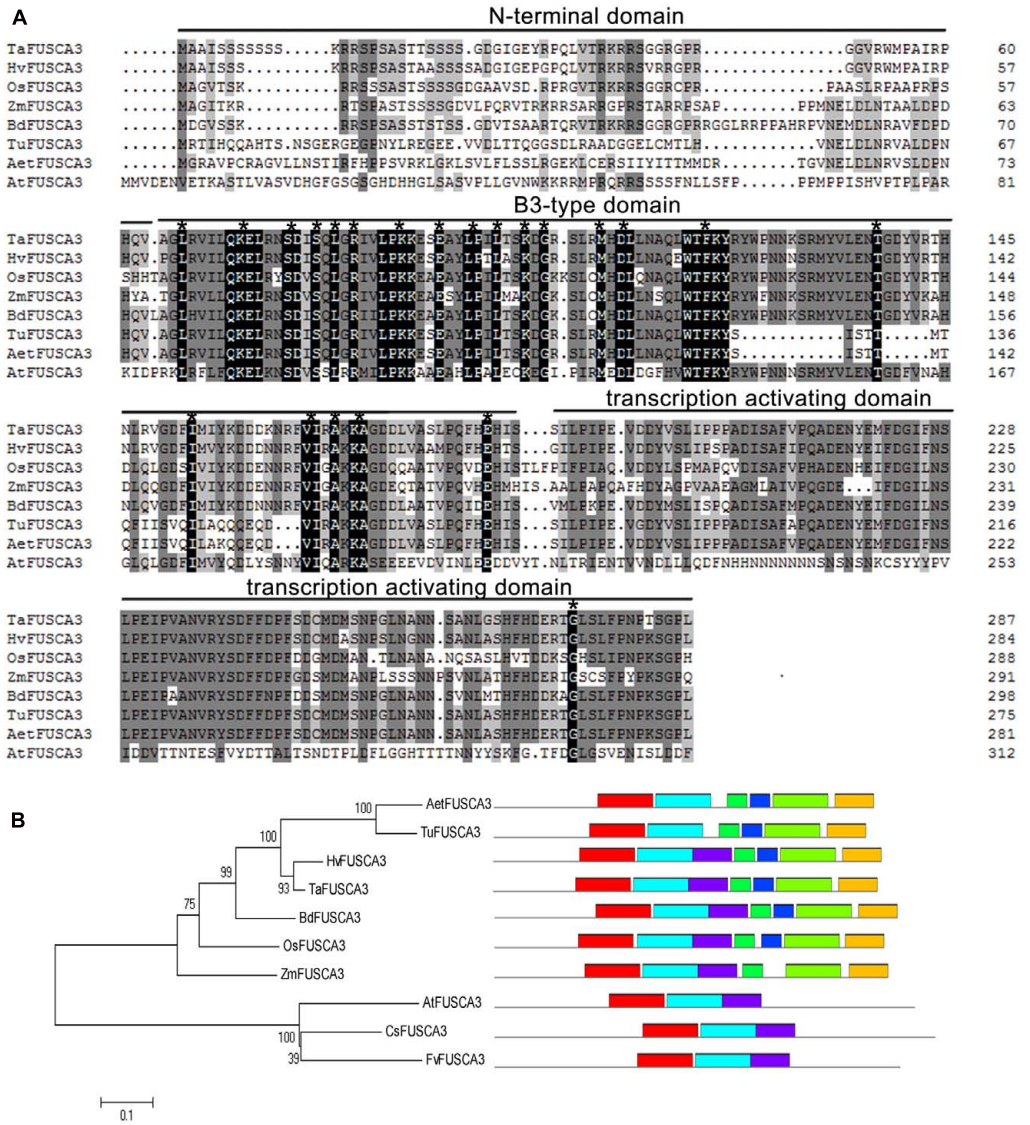

FIGURE 1 | Multiple sequence alignment and phylogenetic tree analysis of TaFUSCA3. **(A)** The multiple sequence alignment was performed by use of the software DNAMAN. The extremely conserved amino acid residues in all sequences are marked with asterisks. The FUSCA3 sequences from different plant species are shown as Ta: *T. aestivum*; Hv: *H. vulgare*; Os: *O. sativa*; Zm: *Z. mays*; Bd: *B. distachyon*; Tu: *T. urartu*; Aet: *Ae. tauschii*; At: *A. thaliana*. **(B)** The phylogenetic tree was established by using the software ClustalX2.0 and MEGA5.1, which employs the minimum-evolution test and default parameters.

and development of wheat and in endosperm development. In addition, significantly low expression was detected in roots, stems, mature stems, and flag leaves.

In order to further investigate the expression pattern of *TaFUSCA3* in the wheat endosperm, real-time qRT-PCR was performed with RNAs obtained from endosperms, which were isolated from the grains at different DAP (4, 8, 12, 16, 20, 24, 28, and 32). As presented in **Figure 4A**, the transcript level of *TaFUSCA3* was increased gradually from 4 DAP and peaked (sixfold) at 20 DAP, then decreased.

The expression of *TaFUSCA3* was similar to that of *TaSPA* (GenBank No.: D78609, a storage protein activator), which encodes a wheat bZIP TF of the O2-like type (Albani et al., 1997). The Pearson correlation coefficient between the expression level of *TaFUSCA3* and *TaSPA* was 0.8670, which indicated that the expression of *TaFUSCA3* was correlated positively and significantly with that of *TaSPA*. The expression pattern of *TaFUSCA3* was consistent with that of *TaSPA*, indicating that TaFUSCA3 might be a regulator of the glutenin in the developing endosperm.

The expression level of the HMW-GS gene (*Glu-1Bx*) *Ta1Bx7* was also examined by real-time qRT-PCR (**Figure 4B**). Its expression level reached a peak at 16 DAP and then reduced gradually. Wheat grain development has three growth stages: grain enlargement (10–14 days after flowering), grain fill (15–35 days after flowering), and physiological maturity. The

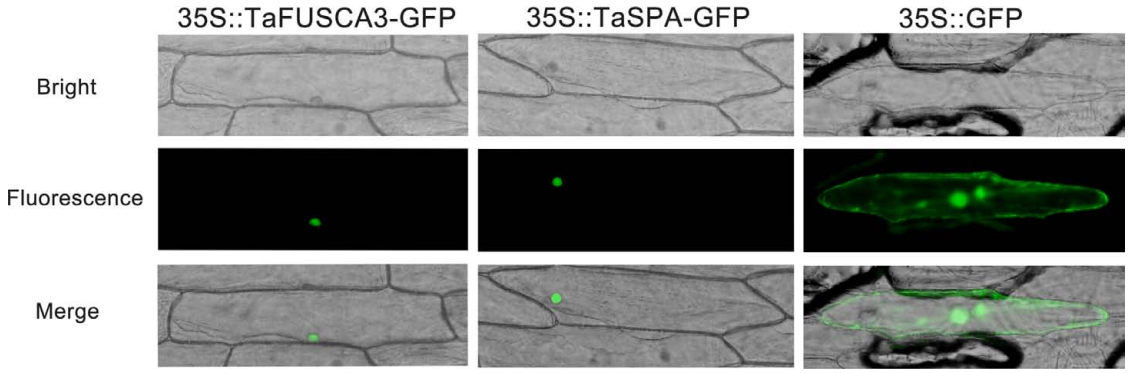

FIGURE 2 | Subcellular localizations of TaFUSCA3 and TaSPA. The fusion proteins 35S::FUSCA3-GFP (pCAMBIA1303-*FUSCA3-GFP*), 35S::SPA-GFP (pCAMBIA1303-*SPA-GFP*), and 35S::GFP (pCAMBIA1303-*GFP*, control) were transiently expressed in onion epidermal cells and visualized with fluorescence microscopy 24 h after bombardment.

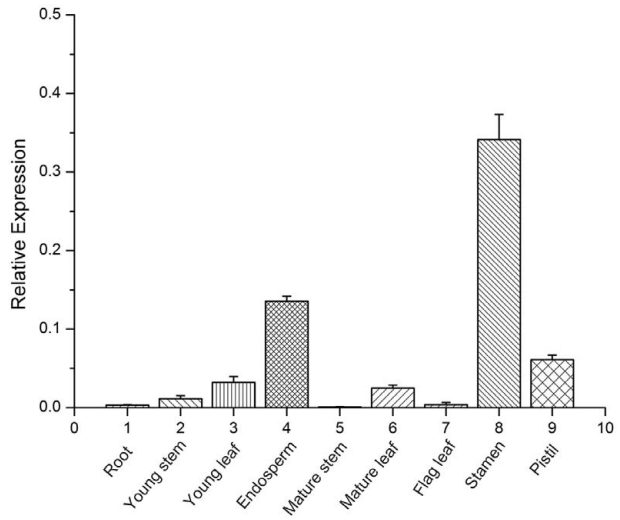

FIGURE 3 | Organ-specific expression assay of *TaFUSCA3* in wheat by real-time qRT-PCR. The organs include roots, young stems, young leaves, endosperms, mature stems, mature leaves, flag leaves, stamens, and pistils. Data are means ± SD (n = 3) in the organ-specific expression assays. Three biological experiments showed the same results.

seed increases rapidly in size as the cells that enclose the embryo sac divide and amplify during the grain enlargement stage. The grain weight increases at a constant rate as carbohydrate and protein are deposited into the grain during the grain fill stage. The SSP genes are transcribed at peak levels in the early grain fill stage in order to prepare enough mRNA templates for the next stages of carbohydrate and protein accumulation. Transcription of SSP genes is then reduced as grain development gradually comes to an end into the physiological maturity stage. The observation that *TaFUSCA3*, *TaSPA*, and *Ta1Bx7* presented almost identical expression patterns at each developmental stage suggested that *TaFUSCA3* and *TaSPA* could regulate the gene expression of the HMW-GS *Ta1Bx7* in wheat (Shewry and Halford, 2002; White and Edwards, 2008).

TaFUSCA3 Could Specifically Recognize the RY-Box of Promoters from *Ta1Bx7* and *At2S3*

TaFUSCA3 could activate the expression of the albumin *At2S3* gene in *A. thaliana* and the glutenin *Ta1Bx7* gene in wheat by binding the *cis*-acting RY-box element (CATGCA) in the promoter specifically (**Figure 6**). To determine whether it could activate the storage protein promoter, we compared four promoter sequences of SSPs, including *At2S3*, *1Dx5*, *1Bx7*, and *1Bx13* and the sequences of them were listed in the Supplementary Table S5. The promoters of albumin *At2S3* (GenBank No.: At4g27160) in *A. thaliana* and the HMW-GS *Ta1Bx7* that have eight RY-boxes were isolated and putative control elements were screened by using PLACE[6] (Geng et al., 2014). Yeast strains transformed with TaFUSCA3 and the RY-box from the promoters of *At2S3* and *Ta1Bx7* grew well on selective media (**Figure 6A**), which indicated that TaFUSCA3 could interact with the promoters of *At2S3* and *Ta1Bx7*.

In addition, a DPI-ELISA was performed to confirm the interaction between TaFUSCA3 and the RY-box in the promoter of *Ta1Bx7*. Firstly, we successfully obtained the TaFUSCA3-GST fusion protein by use of the prokaryotic expressive assay (**Figure 5**). As presented in **Figure 6B**, TaFUSCA3 with the RY-box produced a stronger absorption signal than that with the RYm-box, which had remarkably significant difference in absorption ($P < 0.01$). The competition experiment by DPI-ELISA was performed to verify the interaction by appending different concentrations of non-biotinylated RY-probe to the binding reaction (**Figure 6B**). The increasing concentrations of non-biotinylated RY-probes competed with the binding of TaFUSCA3 to the biotinylated RY-probe successfully. The absorption signal was significantly decreased with the addition of 10 pmol non-biotinylated RY-probe

[6]http://www.dna.affrc.go.jp/PLACE/signalup.html

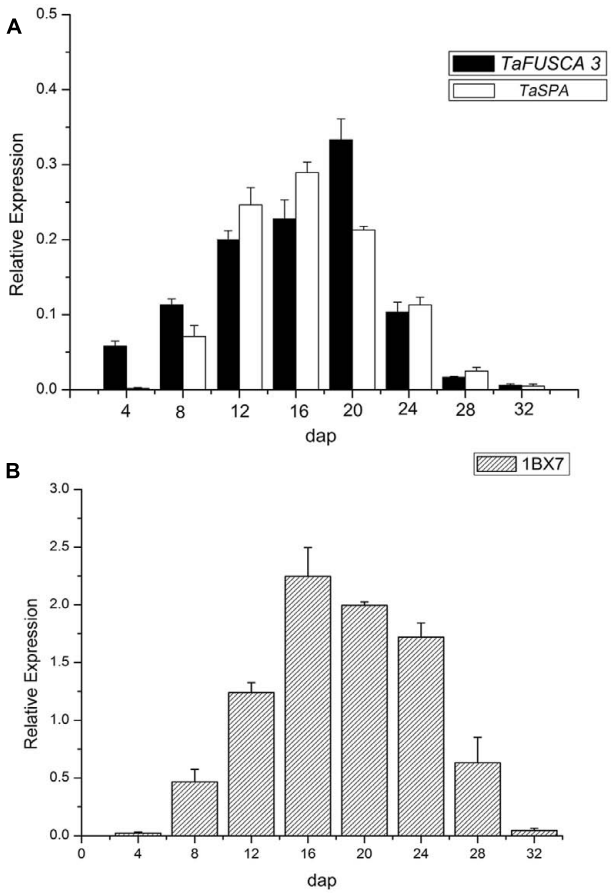

FIGURE 4 | Expression analyses of the *TaFUSCA3* gene by real-time qRT-PCR. **(A)** mRNA relative expression index of *TaFUSCA3* and *TaSPA* TFs. **(B)** Expression levels of the *Ta1Bx7* gene encoding the SSP in developing endosperms from 4 to 32 DAP are shown, respectively. The *Taβ-actin* gene was used as an internal control for standardization. Error bars represent the SD for three technical replicates. Three biological experiments gave the same results. The Pearson correlation coefficient between the expression levels of *TaFUSCA3* and *TaSPA* was 0.8670 and that between *TaFUSCA3* and *Ta1Bx7* was 0.8038.

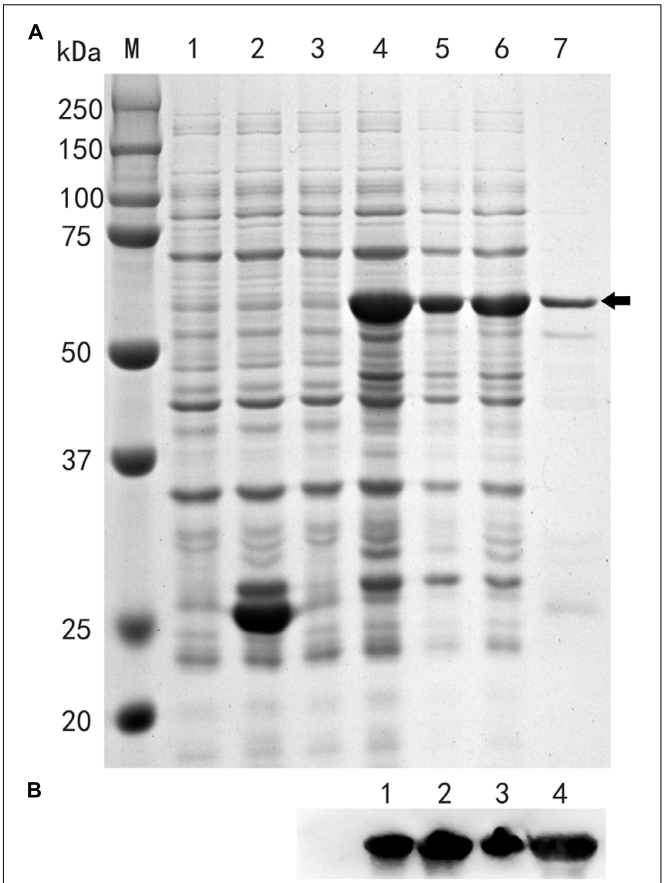

FIGURE 5 | TaFUSCA3 recombined with GST protein was expressed in prokaryotic expressive *E. coli* strain BL21. **(A)** SDS-PAGE of fusion proteins isolated from the prokaryotic expression system. (1) Total proteins of strain BL21 with GST before isopropyl β-D-1-thiogalactopyranoside (IPTG) induction. (2) Total proteins of strain BL21 with GST after IPTG induction. (3) Total proteins of strain BL21 with fusion protein TaFUSCA3-GST before IPTG induction. (4) Total proteins of strain BL21 with fusion protein TaFUSCA3-GST after IPTG induction. (5) Total supernatant fluid proteins of strain BL21 with fusion protein TaFUSCA3-GST after IPTG induction. (6) Total precipitated proteins of strain BL21 with fusion protein TaFUSCA3-GST after IPTG induction. (7) Purified proteins of strain BL21 with fusion protein TaFUSCA3-GST after IPTG induction. Arrow represents the fusion protein TaFUSCA3-GST. **(B)** Western blotting verified the results of fusion protein TaFUSCA3-GST isolated from the prokaryotic expression system. (1) Total proteins of strain BL21 with fusion protein TaFUSCA3-GST after IPTG induction. (2) Total supernatant fluid proteins of strain BL21 with fusion protein TaFUSCA3-GST after IPTG induction. (3) Total precipitated proteins of strain BL21 with fusion protein TaFUSCA3-GST after IPTG induction. (4) Purified proteins of strain BL21 with fusion protein TaFUSCA3-GST after IPTG induction.

($P < 0.05$) and it was remarkably significantly reduced when the concentration of non-biotinylated RY-probe was increased up to 50 pmol ($P < 0.01$). However, the mutated RYm-probe rarely competed with the recognition of TaFUSCA3 to the biotinylated RY-probe, even at increased concentrations. Hence, specific recognition between TaFUSCA3 and the RY-box of the promoter of *Ta1Bx7* was confirmed by the Y1H and DPI-ELISA assays.

C-Terminal Domain of TaFUSCA3 Shows Transcriptional Activity

Transcriptional activity of the TaFUSCA3 protein was analyzed by using the Y1H system. In order to verify which domain determines the activation capacity, yeast strain *Y187* was transformed with the recombinant plasmids containing full-length TaFUSCA3, the N-terminal region (1st to 60th amino acids), the C-terminal region (172th to 288th amino acids), and the B3 domain (61th to 171th amino acids) combined with the GAL4 binding domain, respectively. The growth status of the strain was observed on selective medium (**Figure 7A**). The yeast cells transformed with the BD-TaFUSCA3 and BD-C-terminal constructs grew well on SD medium without tryptophan, adenine, or histidine, demonstrating that TaFUSCA3 acted as a transcriptional activator. In β-galactosidase activity assay, the

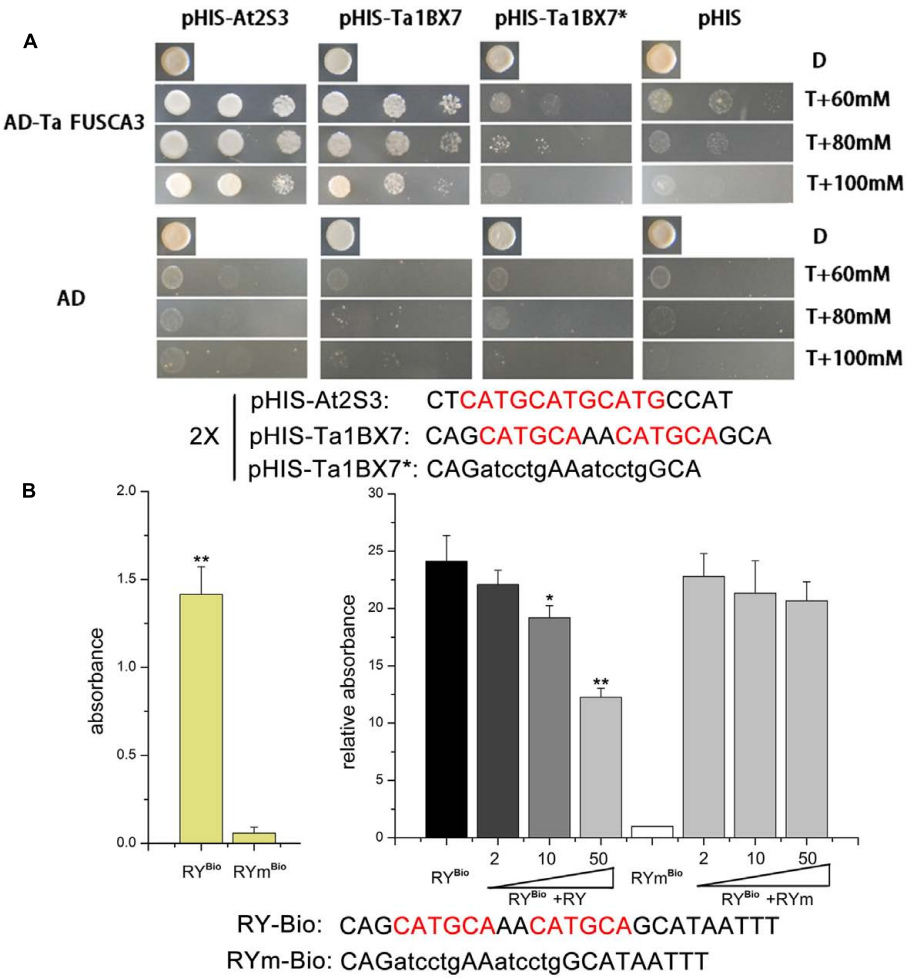

FIGURE 6 | TaFUSCA3 interacts with the RY-box from the promoter of *Ta1Bx7*. **(A)** Analysis of the RY-box binding activity of TaFUSCA3 by use of the yeast one-hybrid (Y1H) assay. The effector vectors were pGAD-TaFUSCA3 and pGADT7 and reporter vectors were pHIS-At2S3, pHIS-Ta1Bx7, pHIS-Ta1Bx7*, and pHIS, which was used for the Y1H system. The culture medium lacked Trp, Leu, and His with 3-amino-1,2,4-triazole (3-AT) added at a concentration of 60, 80, or 100 mM. **(B)** The specific binding property of the recombinant TF TaFUSCA3 to 5′-biotinylated dsDNA probes and competition experiment by DPI-ELISA. The RY-box probe from the promoter of *Ta1Bx7* was biotinylated at 5′ end. ELISA plates were coated with 2 pmol of double-stranded biotinylated RY Bio-probe. The specific binding of TaFUSCA3 to RY-probes was competed with non-biotinylated dsDNA in the competition experiment. Different concentrations of RY-probe or RYm-probe (0, 2, 10, 50 pmol) were added into the crude extract immediately before incubation. The biotinylated dsDNA RYmBio-probe incubated with the extract was regarded as a control. Data are means ± SD ($n = 3$) in the specific binding and competition assays. Asterisks represent statistically significant differences from the RYm-probe (0 pmol) (*$P < 0.05$, **$P < 0.01$).

β-galactosidase activity of the C-terminal region was 1.4 times that of the whole protein; the other domains did not grow on the selective medium (**Figure 7B**). These results indicated that the full TaFUSCA3 and its C-terminal region had transcriptional activities.

TaFUSCA3 Interacts with TaSPA in the Y2H System and BiFC Assay

To define the interaction of the TFs related to the regulation of wheat storage protein expression, additional cDNAs of *TaSPA* and *TaPBF* and *TaGAMYB* were cloned (Supplementary Table S4) and the Y2H assay was performed (Hu et al., 2013). For this purpose, we constructed plasmids AD-FUSCA3, AD-FUSCA3*, and AD-SPA. In the meantime, we constructed effector plasmids BD-FUSCA3, BD-SPA, BD-PBF, and BD-GAMYB, in which the TFs were fused to the binding domain of the Gal4 TF. Co-transfections into the *Y187* yeast strain were performed, and the resulting transformants were tested on SD/-Lea-Trp. As shown in **Figure 8A**, yeast cells harboring AD-FUSCA3, BD, or plasmids without inserts (pGBKT7 and pGADT7) did not show β-galactosidase enzyme activity. While the β-galactosidase enzyme activity of the combination of AD-FUSCA3 and BD-SPA was remarkably significantly increased compared with that of AD-FUSCA3 with BD-PBF and AD-FUSCA3 with BD-GAMYB ($P < 0.01$). Growth was not found in the mutant *FUSCA3** (**Figure 8B**). Co-expression of *AD-SPA* with *BD-FUSCA3* resulted in very high levels of β-galactosidase, and the enzyme activity of the combination of AD-FUSCA3 and

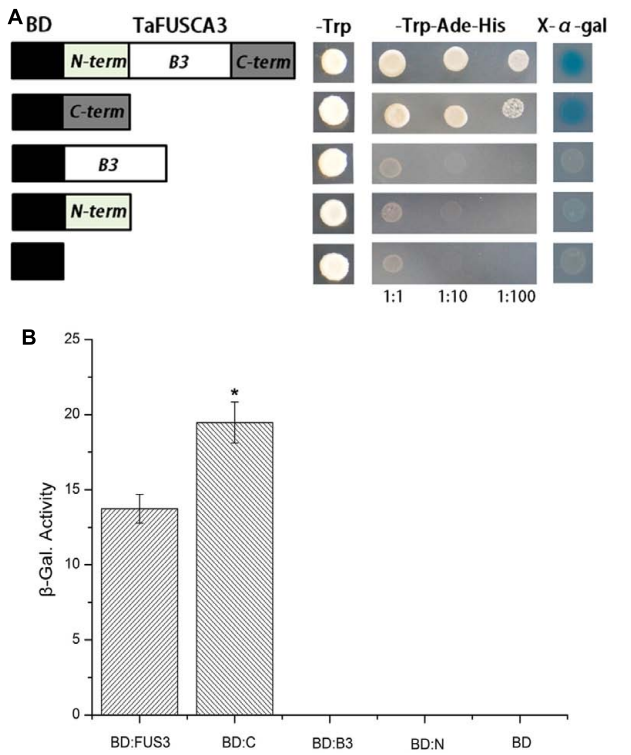

FIGURE 7 | Analysis of transcriptional activity of TaFUSCA3. **(A)** The growth status of yeast strains in the Y1H assay was observed on selective medium. **(B)** The recombinant constructs including the ORF of *TaFUSCA3* and intersected fragments were transformed into the yeast strain *Y187* to analyze the transcriptional activity. *LacZ* induction was employed to evaluate activation domains within TaFUSCA3. Data are means ± SD ($n = 3$) in the Y1H system assays. Asterisks represent statistically significant differences from BD:FUS ($^*P < 0.05$).

BD-SPA was roughly twofold higher than that of the group for AD-FUSCA3* and BD-SPA ($P < 0.01$), which implied that there exists an interaction between FUSCA3 and SPA.

The β-galactosidase activity assay further confirmed interactions between SPA and the N-terminal domain of FUSCA3 in yeast (**Figure 8C**). TaSPA was used as prey to interact with the N-terminal domain, B3 domain, and C-terminal domain from TaFUSCA3. For the N-terminal domain, the interaction with SPA was roughly fourfold greater than that of the B3 domain ($P < 0.01$). Because the C-terminal domain had a transcriptional activation activity, it showed a higher β-galactosidase activity when used as bait. But it presented a lower enzyme activity when used as prey.

To further confirm the interaction between TaFUSCA3 and TaSPA, a BiFC assay was performed in epidermal cells of onions. The C-terminal fragment of yellow fluorescent protein (YFP) fused with TaFUSCA3 was able to interact with the N-terminal fragment of YFP fused with TaSPA in the nucleus (**Figure 8D**). The fluorescence signal was found only in the nucleus. These results indicated that TaFUSCA3 interacts with TaSPA and the complex is colocalized in the nucleus.

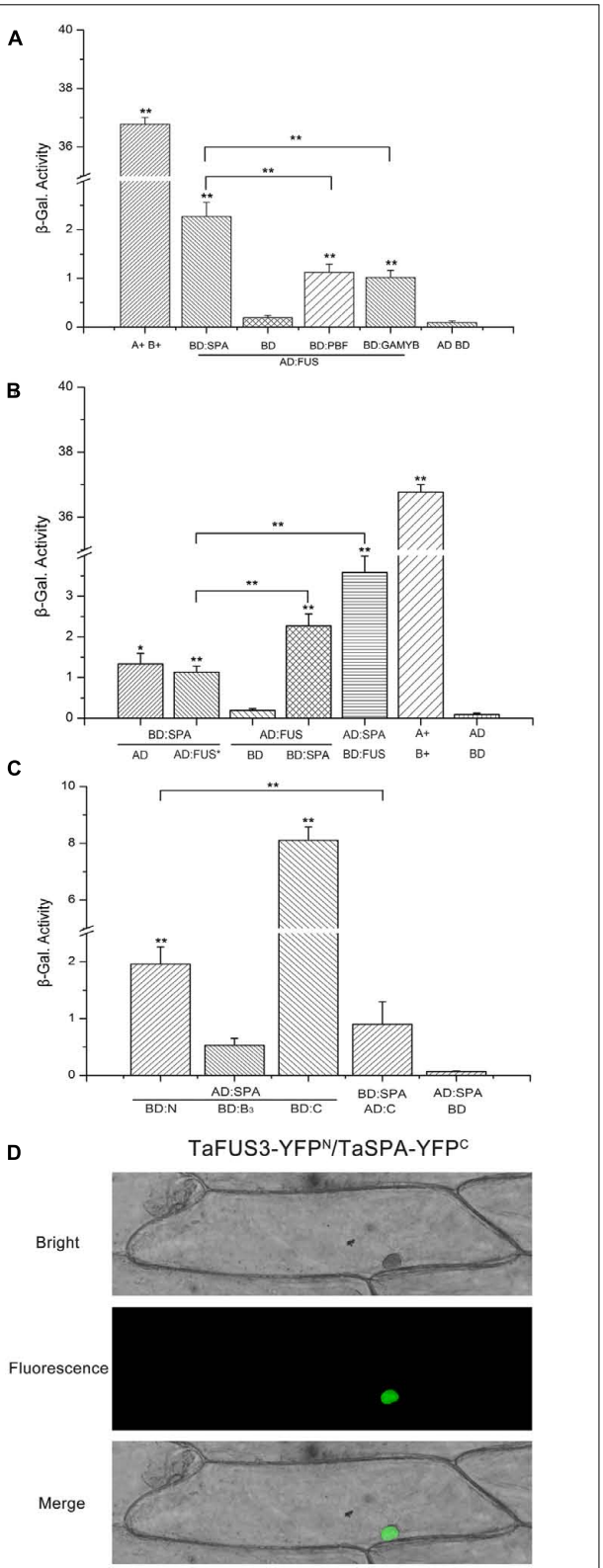

FIGURE 8 | Analysis of interactions between TaFUSCA3 and TFs related to wheat storage protein expression. **(A)** Interactions of TaFUSCA3 and TaSPA, TaPBF, and TaGAMYB in the Y2H system. The indicated effector constructs

(Continued)

FIGURE 8 | Continued
were used to transform yeast strain *Y187*. *LacZ* induction was employed to evaluate the interaction between intersected fragments TaSPA, TaPBF, or TaGAMYB and TaFUSCA3, and β-galactosidase activity was counted from three replicates. Asterisks represent statistically significant differences from AD:FUS and BD. **(B)** Interaction of TaFUSCA3 and TaSPA in the Y2H system. The indicated effector constructs were used to transform yeast strain *Y187* containing the reporter gene *LacZ* whose promoter was Gal4. *LacZ* induction was employed to evaluate the interaction between TaFUSCA3 or TaFUSCA3* and TaSPA, and β-galactosidase activity was counted from three replicates. The positive control presented the interaction between SV40 large T-antigen and murine p53. Asterisks represent statistically significant differences from AD:FUS and BD. **(C)** Interaction of TaFUSCA3′ intersected fragments and TaSPA in the Y2H system. The indicated effector constructs were used to transform yeast strain *Y187*. *LacZ* induction was employed to evaluate the interaction between intersected fragments N-term, B3, or C-term and TaSPA, and β-galactosidase activity was counted from three replicates. Three biological experiments showed the same results. Asterisks represent statistically significant differences from AD:SPA and BD:B_3. Data are means ± SD (n = 3) in the Y2H system assays (*$P < 0.05$, **$P < 0.01$). **(D)** BiFC assay of TaFUSCA3. The vectors pSPYNE-*TaFUSCA3* and pSPYCE-*TaSPA* were transiently expressed in onion epidermal cells and observed by fluorescence inversion microscopy (OLYMPUS DP72, Japan) after incubation at 25°C for 24 h on MS medium in the dark.

TaFUSCA3 Activates Transcription of the *At2S3* and *Ta1Bx7* Genes

To verify the inference about conservation of function between TaFUSCA3 and AtFUSCA3, the *A. thaliana* wild-type *Col* and mutant type *fus3-3* were transformed with *TaFUSCA3* (Keith et al., 1994). The expression cassette including CDS (coding sequence) of *TaFUSCA3*, 35S promoter, and NOS terminator was inserted into pBI121 in which the *GFP* gene was driven by the promoter of *At2S3*. The results of PCR and qRT-PCR for the molecular identification and detection of transgene expression in the transgenic lines are shown in **Supplementary Figures S1**, **S2**. The expression level of albumin 2S had been confirmed to be strongly decreased in the grains of the *FUSCA3* mutant line (Luerssen et al., 1998). The mature seeds of wild-type *Col* and mutant type *fus3-3* transformed respectively with the *GFP* gene under the control of the *At2S3* promoter and TaFUSCA3 were observed by fluorescence inversion microscopy (OLYMPUS DP72, Japan). As shown in **Figure 9A**, fluorescence intensity of GFP, which was weakened intensively in the *fus3-3* lines, was recovered to nearly the same level as that of the wild-type in the grains expressing *TaFUSCA3* constitutively.

The transient expression of *TaFUSCA3* in onion epidermal cells was used to confirm the transcription activation of the *Ta1Bx7* gene promoter (**Figure 9B**). The GUS staining of the onion epidermal cells revealed that expression level of *GUS* driven by the *Ta1Bx7* promoter was obviously increased following co-transformation with the *TaFUSCA3* gene. It could be inferred that TaFUSCA3 activated the transcription of the *Ta1Bx7* promoter, which led to the increase of expression of *GUS*.

DISCUSSION

FUSCA3 is a master regulator for seed growth, including lipid accumulation, establishment of developmental timing, and identity development of lateral organs, as well as playing a role in the formation of SSPs and seed maturation (Reidt et al., 2001; Gazzarrini et al., 2004; Tsai and Gazzarrini, 2012). Both the quantity and quality of SSPs can affect flour quality in

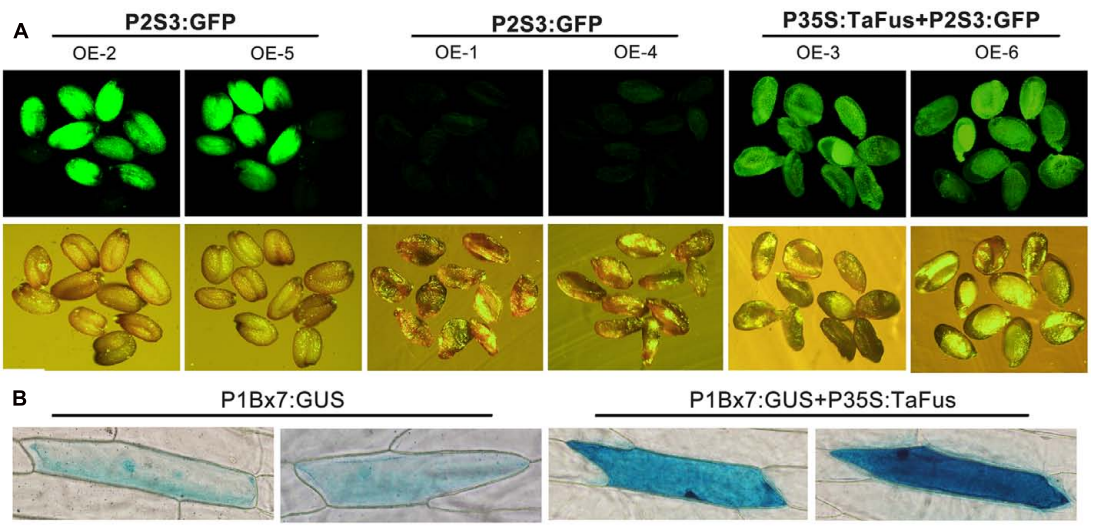

FIGURE 9 | Complementation of TaFUSCA3 in the *A. thaliana FUSCA3* mutant line *fus3-3* and transcriptional regulation of the promoter of Ta1Bx7 in a transient expression system. **(A)** The *GFP* gene under the control of the *At2S3* promoter and the *TaFUSCA3* gene driven by the *CaMV 35S* promoter were transformed into wild-type and *fus3-3* lines of *A. thaliana*, respectively. The genetic background of OE-2 and OE-5 was wild-type; that of OE-1, OE-4, OE-3, and OE-6 was the *FUSCA3* mutant line *fus3-3.* The seeds of transgenic lines were observed under a fluorescence microscope to evaluate the expression level of the *At2S3* promoter. **(B)** The *GUS* gene under the control of the *Ta1Bx7* promoter and the *TaFUSCA3* gene driven by the *CaMV 35S* promoter, respectively, were transformed into onion epidermal cells in a transient expression system.

wheat. Higher dough strength usually predicts better-quality bread in the process of wheat breeding (Cooper et al., 2016). Although the functional importance of FUSCA3 has been studied in *A. thaliana* and other model plants, the structural and functional characteristics of FUSCA3 in wheat, especially in the transcriptional regulation of SSPs, have not yet been explored.

We cloned a FUS3CA-like transcriptional factor gene designated *TaFUS3CA3* from *T. aestivum* in this study. Our results show that *TaFUS3CA3* is the putative paralogous gene of *HvFUSCA3* from barely. Both genes not only have high homology phylogenetically, but also can exert analogous functions. *TaFUSCA3* was expressed in different tissues, but it had highest expression in the endosperm. We compared three promoter sequences of wheat storage proteins, including *1Dx5*, *1Bx7*, and *1Bx13* and the sequences of them were listed in the Supplementary Table S5. It is confirmed that TaFUSCA3 can activate the promotion of the HMW-GS gene *Ta1Bx7*. Our results showed that expression patterns of *TaFUSCA3* and the storage protein gene *Ta1Bx7* were similar in the wheat endosperm. The Pearson correlation coefficient between the expression levels of *TaFUSCA3* and *Ta1Bx7* was 0.8038, which indicated that the expression of *TaFUSCA3* was correlated significantly with that of *Ta1Bx7*. The SSPs of cereals are accumulated in the endosperms, whereas those of *A. thaliana* are accumulated in the cotyledons (Santos-Mendoza et al., 2008). Therefore, the distinct functions of FUSCA3 in the two different species should be explored further.

Expressional regulation of target genes is usually manifested by the synergistic effects of various TFs. The expression level of a gene could be attributed to the regulating effects of multiple TFs by recognizing a specific promoter cooperatively. Many significant interactions (such as O2-PBF, BLZ2-BLZ1, SAD-GAMYB, AKIN10-FUSCA3, and GAMYB-VP1) have been identified in the regulation of target genes in some species (Nakamura et al., 2001; Diaz et al., 2005; Tsai and Gazzarrini, 2012; Abraham et al., 2016). Further studies are still necessary to explore the interactions between TaFUSCA3 and other relevant TFs in wheat.

In order to define the TFs that interacts with TaFUSCA3, the TFs related to the regulation of wheat storage protein expression including TaSPA, TaPBF, and TaGAMYB were screened (**Figure 8A**). Our data revealed that TaFUSCA3 can interact with TaSPA (**Figure 8B**), and the protein–protein interactions between TaFUSCA3 and TaSPA increased the β-galactosidase activity remarkably significantly in the Y2H assay ($P < 0.01$). Furthermore, the mutated type TaFUSCA3* was not able to interact with TaSPA (**Figure 8B**), and TaFUSCA3 could interact with TaSPA through the N-terminal domain (**Figure 8C**). The BiFC assay further provided evidence for the interaction between TaFUSCA3 and TaSPA (**Figure 8D**). The expression level of TaFUSCA3 was consistent with that of TaSPA, indicating that TaFUSCA3 was a regulator of the glutenin in the developing endosperm (**Figure 4**). TaFUSCA3 could activate the expression of the albumin *At2S3* gene in *A. thaliana* and the glutenin *Ta1Bx7* gene in wheat by specifically binding the *cis*-acting RY-box element (CATGCA) from their promoters in the Y1H and DPI-ELISA assays (**Figure 6**). The interactions between TaFUSCA3 and TaSPA TFs shown in our study propose the further exploration of the regulatory mechanism of SSPs in wheat. It is apparent that the regulation of expression of stored energy substances in wheat can be attributed to complicated interactions of TFs.

It was reported that AtFUSCA3 can activate transcription by recognizing the sequence 5′-CATGCA-3′ (RY-box) of SSP gene promoters (Wang and Perry, 2013). Furthermore, other reports suggest that FUSCA3 indirectly modulates the expression of seed storage reserve genes through suppressing formation of TTG1, which is related to epidermal morphogenesis (Tsuchiya et al., 2004; Wang et al., 2014; Chen et al., 2015). Here, we showed that TaFUSCA3 could specifically recognize and combine with the RY-box (5′-CATGCA-3′), which comes from the promoters of the *Ta1Bx7* and *At2S3* genes, through the B3 domain and activate expression of these genes through the C domain (**Figures 6**, **7**). We also carried out the reciprocal assay in which the RY-box was mutated, which prevented TaFUSCA3 from recognizing the promoter of the *Ta1Bx7* gene and destroyed the TaFUSCA3-mediated activity of transcriptional activation (**Figure 6**). Our results indicated that transcriptional activation of *Ta1Bx7* and *At2S3* resulted from the immediate recognition and binding of the RY motif of promoters by TaFUSCA3.

The objective of our research was to clone the *FUSCA3* gene in wheat and to identify its function in the control of expression of wheat SSP. A wheat cDNA was cloned, which was the homologous gene to *HvFUSCA3*. When the ORF of *TaFUSCA3* was transformed into *A. thaliana* line *fus3-3* with *AtFUSCSA3* mutated, we found that characteristics were recovered in transgenic plants, such as activated expression of the promoter from the SSP gene *At2S3* (**Figure 9A**). TaFUSCA3 could restore the mutant feature of *fus3-3*, which indicates that it possibly takes part in the same regulatory pathways of the SSPs by acting in the same role as AtFUSCA3. It might perform these functions by combining with the other regulatory factors and forming a transcription initiation complex.

The composition and quantity of SSPs can dramatically affect dough quality in wheat, and the regulation of expression is important to control in the formation of SSPs (Wieser, 2000). TaFUSCA3 was able to activate transcription of At2S3, which suggested to us to consider whether the *FUSCA3* gene from wheat was also related to the transcriptional regulation of SSP in wheat. We explored the inference by analyzing the promoters of storage proteins in wheat that include conserved base sequences (RY-box) for TaFUSCA3 (*1Dx5*, *1Bx7*, and *1Bx13*). We found that TaFUSCA3 could *trans*-activate the promoter of the *Ta1Bx7* gene encoding the HMW-GS by recognizing a necessary RY motif component in the storage protein gene (**Figures 6**, **9**), which suggested that we might be able to improve the SSP content by overexpressing *TaFUSCA3* and *TaSPA* in grains. Regulation of the wheat storage protein gene by TaFUSCA3 and its compensatory effect in the mutant line *fus3-3* in *A. thaliana* reflect the conservation of the evolution of this gene between the dicotyledonous and monocotyledonous SSP. The conservation not only is reflected in the structure of proteins but also in the *cis*-action and *trans*-action regulation (Lara et al., 2003).

CONCLUSION

TaFUSCA3 was identified and cloned in wheat. The structure and functional characteristics of wheat B3-type TF TaFUSCA3 were explored in the aspects of sequence alignment and expression pattern, as well as the protein interactions and transcriptional regulation in wheat SSPs. TaFUSCA3 can specifically recognize and combine with the RY-box (5′-CATGCA-3′) of the promoters from the *Ta1Bx7* and *At2S3* genes through the B3 domain and activate expression of these genes through the C domain. Moreover, it was shown that TaFUSCA3 interacted with the seed-specific bZIP protein TaSPA through the N domain. TaFUSCA3 can complement loss-of-function in the *A. thaliana FUSCA3* mutant line *fus3-3* by regulating SSP gene expression in seeds. The structure and functional characteristics of wheat B3-type TF TaFUSCA3 were explored in the aspects of sequence alignment and expression pattern, as well as the protein interactions and transcriptional regulation in wheat SSPs. Although the function of *TaFUSCA3* was not verified in transgenic wheat, the findings of this study shed light on the regulatory mechanism and increased abundance of SSP in wheat.

AUTHOR CONTRIBUTIONS

GH, GY, and FS designed the experiments and wrote the paper. FS and XL performed all experiments and analyzed the data. TY and LJ helped to construct the relevant vectors. QW and JL helped to conduct the experiments. YW participated in partial experiments.

ACKNOWLEDGMENTS

The work was supported by National Genetically Modified New Varieties of Major Projects of China (2016ZX08010004-004) and the National Natural Science Foundation of China (No. 31570261, 31601995).

SUPPLEMENTARY MATERIAL

The Supplementary Material for this article can be found online at: http://journal.frontiersin.org/article/10.3389/fpls.2017.01133/full#supplementary-material

FIGURE S1 | The molecular identification by PCR for transgenic lines in *A. thaliana*. **(A)** The transgenic lines with *GFP* gene under the control of the *At2S3* promoter and genetic background was wild type. WT: wild type. The primer used was GFP1 listed in the Supplementary Table S1. **(B)** The transgenic lines with *GFP* gene under the control of the *At2S3* promoter and genetic background was *AtFUSCA3* mutant line *fus3-3*. MT: non-transgenic mutant type. The primer used was GFP1 listed in the Supplementary Table S1. **(C)** Transgenic lines with the *GFP* gene under the control of the *At2S3* promoter and the *TaFUSCA3* gene driven by the *CaMV 35S* promoter; the genetic background was the *AtFUSCA3* mutant line *fus3-3*. MT: non-transgenic mutant type. The primer used was GFP1 listed in the Supplementary Table S1. **(D)** Transgenic lines with the *GFP* gene under the control of the *At2S3* promoter and the *TaFUSCA3* gene driven by the *CaMV 35S* promoter; the genetic background was the *AtFUSCA3* mutant line *fus3-3*. MT: non-transgenic mutant type. The primer used was JDfusca3 listed in Supplementary Table S1.

FIGURE S2 | The expression analyses of GFP and TaFUSCA3 by qRT-PCR in transgenic *A. thaliana*. The 14 DAP seeds were collected for the cDNA of qRT-PCR. **(A)** Relative expression levels of GFP in the transgenic lines with *GFP* gene; the genetic background was wild type. WT: wild type. **(B)** Relative expression levels of GFP in the transgenic lines with *GFP* gene; the genetic background were *AtFUSCA3* mutant line *fus3-3*. MT: non-transgenic mutant type. **(C)** Relative expression levels of GFP in the transgenic lines with GFP and TaFUSCA3; the genetic background were *AtFUSCA3* mutant line *fus3-3*. MT: non-transgenic mutant type. **(D)** Relative expression levels of TaFUSCA3 in the transgenic lines with GFP and TaFUSCA3; the genetic background was the *AtFUSCA3* mutant line *fus3-3*. MT: non-transgenic mutant type. Data are means ± SD ($n = 3$). Three independent experiments were performed.

REFERENCES

Abraham, Z., Fernández, R. I., Martínez, M., Diaz, I., Carbonero, P., and Vicente-Carbajosa, J. (2016). A developmental switch of gene expression in the barley seed mediated by HvVP1 (Viviparous1) and HvGAMYB interactions. *Plant Physiol.* 170, 2146–2158. doi: 10.1104/pp.16.00092

Albani, D., Hammond-Kosack, M., Smith, C., Conlan, S., Colot, V., Holdsworth, M., et al. (1997). The wheat transcriptional activator SPA: a seed-specific bZIP protein that recognizes the GCN4-like motif in the bifactorial endosperm box of prolamin genes. *Plant Cell* 9, 171–184. doi: 10.1105/tpc.9.2.171

Bäumlein, H., Miséra, S., Luerßen, H., Kölle, K., Horstmann, C., Wobus, U., et al. (1994). The FUS3 gene of *Arabidopsis thaliana* is a regulator of gene expression during late embryogenesis. *Plant J.* 6, 379–387. doi: 10.1046/j.1365-313X.1994.06030379.x

Brand, L. H., Kirchler, T., Hummel, S., Chaban, C., and Wanke, D. (2010). DPI-ELISA: a fast and versatile method to specify the binding of plant transcription factors to DNA *in vitro*. *Plant Methods* 6:25. doi: 10.1186/1746-4811-6-25

Carbonero, P., Iglesias-Fernández, R., and Vicente-Carbajosa, J. (2016). The AFL subfamily of B3 transcription factors: evolution and function in angiosperm seeds. *J. Exp. Bot.* 68, 871–880. doi: 10.1093/jxb/erw458

Chen, M., Zhang, B., Li, C., Kulaveerasingam, H., Chew, F. T., and Yu, H. (2015). *TRANSPARENT TESTA GLABRA 1* regulates the accumulation of seed storage reserves in Arabidopsis. *Plant Physiol.* 169, 391–402. doi: 10.1104/pp.15.00943

Clough, S. J., and Bent, A. F. (1998). Floral dip: a simplified method for *Agrobacterium*-mediated transformation of *Arabidopsis thaliana*. *Plant J.* 16, 735–743. doi: 10.1046/j.1365-313x.1998.00343.x

Cooper, J. K., Stromberger, J. A., Morris, C. F., Bai, G., and Haley, S. D. (2016). End-use quality and agronomic characteristics associated with the high-molecular-weight glutenin allele in U.S. Hard winter wheat. *Crop Sci.* 56, 1–6. doi: 10.2135/cropsci2015.10.0610

Diaz, I., Martinez, M., Isabel-LaMoneda, I., Rubio-Somoza, I., and Carbonero, P. (2005). The DOF protein, SAD, interacts with GAMYB in plant nuclei and activates transcription of endosperm-specific genes during barley seed development. *Plant J.* 42, 652–662. doi: 10.1111/j.1365-313X.2005.02402.x

Ezcurra, I., Ellerström, M., Wycliffe, P., Stålberg, K., and Rask, L. (1999). Interaction between composite elements in the napA promoter: both the B-box ABA-responsive complex and the RY/G complex are necessary for seed-specific expression. *Plant Mol. Biol.* 40, 699–709. doi: 10.1023/a:1006206124512

Fauteux, F., and Strömvik, M. V. (2009). Seed storage protein gene promoters contain conserved DNA motifs in Brassicaceae. Fabaceae and Poaceae. *BMC Plant Biol.* 9:126. doi: 10.1186/1471-2229-9-126

Gazzarrini, S., Tsuchiya, Y., Lumba, S., Okamoto, M., and McCourt, P. (2004). The transcription factor *FUSCA3* controls developmental timing in *Arabidopsis* through the hormones gibberellin and abscisic acid. *Dev. Cell* 7, 373–385. doi: 10.1016/j.devcel.2004.06.017

Geng, Y., Pang, B., Hao, C., Tang, S., Zhang, X., and Li, T. (2014). Expression of wheat high molecular weight glutenin subunit 1Bx is affected by large insertions

and deletions located in the upstream flanking sequences. *PLoS ONE* 9:e105363. doi: 10.1371/journal.pone.0105363

González-Calle, V., Iglesias-Fernández, R., Carbonero, P., and Barrero-Sicilia, C. (2014). The BdGAMYB protein from *Brachypodium distachyon* interacts with BdDOF24 and regulates transcription of the *BdCathB* gene upon seed germination. *Planta* 240, 539–552. doi: 10.1007/s00425-014-2105-3

Gui, J., Shen, J., and Li, L. (2011). Functional characterization of evolutionarily divergent 4-coumarate: coenzyme A ligases in rice. *Plant Physiol.* 157, 574–586. doi: 10.1104/pp.111.178301

Guo, W., Yang, H., Liu, Y., Gao, Y., Ni, Z., Peng, H., et al. (2015). The wheat transcription factor TaGAMyb recruits histone acetyltransferase and activates the expression of a high molecular weight glutenin subunit gene. *Plant J.* 84, 347–359. doi: 10.1111/tpj.13003

Hu, W., Huang, C., Deng, X., Zhou, S., Chen, L., Li, Y., et al. (2013). TaASR1, a transcription factor gene in wheat, confers drought stress tolerance in transgenic tobacco. *Plant Cell Environ.* 36, 1449–1464. doi: 10.1111/pce.12074

Juhász, A., Makai, S., Sebestyén, E., Tamás, L., and Balázs, E. (2011). Role of conserved non-coding regulatory elements in LMW glutenin gene expression. *PLoS ONE* 6:e29501. doi: 10.1371/journal.pone.0029501

Kawagoe, Y., and Murai, N. (1992). Four distinct nuclear proteins recognize in vitro the proximal promoter of the bean seed storage protein beta-phaseolin gene conferring spatial and temporal control. *Plant J. Cell Mol. Biol.* 2, 927–936. doi: 10.1046/j.1365-313X.1992.t01-6-00999.x

Keith, K., Kraml, M., Dengler, N. G., and Mccourt, P. (1994). fusca3: a heterochronic mutation affecting late embryo development in Arabidopsis. *Plant Cell* 6:589. doi: 10.1105/tpc.6.5.589

Kroj, T., Savino, G., Valon, C., Giraudat, J., and Parcy, F. (2003). Regulation of storage protein gene expression in *Arabidopsis*. *Development* 130, 6065–6073. doi: 10.1242/dev.00814

Lara, P., Oñate-Sánchez, L., Abraham, Z., Ferrándiz, C., Díaz, I., Carbonero, P., et al. (2003). Synergistic activation of seed storage protein gene expression in *Arabidopsis* by ABI3 and two bZIPs related to OPAQUE2. *J. Biol. Chem.* 278, 21003–21011. doi: 10.1074/jbc.M210538200

Li, Y., Wang, Q., Li, X., Xiao, X., Sun, F., Wang, C., et al. (2012). Coexpression of the high molecular weight glutenin subunit 1Ax1 and puroindoline improves dough mixing properties in durum wheat (*Triticum turgidum* L. ssp. *durum*). *PLoS ONE* 7:e50057. doi: 10.1371/journal.pone.0050057

Livak, K. J., and Schmittgen, T. D. (2001). Analysis of relative gene expression data using real-time quantitative PCR and the $2^{-\Delta\Delta\ C}$T method. *Methods* 25, 402–408. doi: 10.1006/meth.2001.1262

Luerssen, H., Kirik, V., Herrmann, P., and Misera, S. (1998). FUSCA3 encodes a protein with a conserved VP1/ABI3-like B3 domain which is of functional importance for the regulation of seed maturation in *Arabidopsis thaliana*. *Plant J.* 15, 755–764. doi: 10.1046/j.1365-313X.1998.00259.x

Mena, M., Cejudo, F. J., Isabellamoneda, I., and Carbonero, P. (2002). A role for the DOF transcription factor BPBF in the regulation of gibberellin-responsive genes in barley aleurone. *Plant Physiol.* 130, 111–119. doi: 10.1104/pp.005561

Mönke, G., Altschmied, L., Tewes, A., Reidt, W., Mock, H. P., Bäumlein, H., et al. (2004). Seed-specific transcription factors ABI3 and FUS3: molecular interaction with DNA. *Planta* 219, 158–166. doi: 10.1007/s00425-004-1206-9

Moreno-Risueno, M. Á., Gonzalez, N., Díaz, I., Parcy, F., Carbonero, P., and Vicente-Carbajosa, J. (2008). FUSCA3 from barley unveils a common transcriptional regulation of seed-specific genes between cereals and Arabidopsis. *Plant J.* 53, 882–894. doi: 10.1111/j.1365-313X.2007.03382.x

Nakamura, S., Lynch, T. J., and Finkelstein, R. R. (2001). Physical interactions between ABA response loci of *Arabidopsis*. *Plant J.* 26, 627–635. doi: 10.1046/j.1365-313x.2001.01069.x

Olsen, O., and Becraft, P. W. (2013). "Endosperm development," in *The Seed Genomics*, ed. P. Becraft (Hoboken, NJ: John Wiley & Sons, Inc.), 43–60. doi: 10.1002/9781118525524.ch3

Onodera, Y., Suzuki, A., Wu, C. Y., Washida, H., and Takaiwa, F. (2001). A rice functional transcriptional activator, RISBZ1, responsible for endosperm-specific expression of storage protein genes through GCN4 motif. *J. Biol. Chem.* 276, 14139–14152. doi: 10.1074/jbc.M007405200

Ouwerkerk, P. B., and Meijer, A. H. (2001). Yeast one-hybrid screening for DNA-protein interactions. *Curr. Protoc. Mol. Biol.* 55, 12.12.1–12.12.12. doi: 10.1002/0471142727.mb1212s55

Plessis, A., Ravel, C., Bordes, J., Balfourier, F., and Martre, P. (2013). Association study of wheat grain protein composition reveals that gliadin and glutenin composition are trans-regulated by different chromosome regions. *J. Exp. Bot.* 64, 3627–3644. doi: 10.1093/jxb/ert188

Pysh, L. D., Aukerman, M. J., and Schmidt, R. J. (1993). OHP1: a maize basic domain/leucine zipper protein that interacts with opaque2. *Plant Cell* 5, 227–236. doi: 10.1105/tpc.5.2.227

Reidt, W., Ellerström, M., Kölle, K., Tewes, A., Tiedemann, J., Altschmied, L., et al. (2001). FUS3-dependent gene regulation during late embryogenesis. *J. Plant Physiol.* 158, 411–418. doi: 10.1078/0176-1617-00352

Reidt, W., Wohlfarth, T., Ellerström, M., Czihal, A., Tewes, A., Ezcurra, I., et al. (2000). Gene regulation during late embryogenesis: the RY motif of maturation-specific gene promoters is a direct target of the FUS3 gene product. *Plant J.* 21, 401–408. doi: 10.1046/j.1365-313x.2000.00686.x

Roscoe, T. T., Guilleminot, J., Bessoule, J.-J., Berger, F., and Devic, M. (2015). Complementation of seed maturation phenotypes by ectopic expression of *ABSCISIC ACID INSENSITIVE3, FUSCA3* and *LEAFY COTYLEDON2* in Arabidopsis. *Plant Cell Physiol.* 56, 1215–1228. doi: 10.1093/pcp/pcv049

Saitou, N., and Nei, M. (1987). The neighbor-joining method: a new method for reconstructing phylogenetic trees. *Mol. Biol. Evol.* 4, 406–425. doi: 10.1093/oxfordjournals.molbev.a040454

Santos-Mendoza, M., Dubreucq, B., Baud, S., Parcy, F., Caboche, M., and Lepiniec, L. (2008). Deciphering gene regulatory networks that control seed development and maturation in Arabidopsis. *Plant J.* 54, 608–620. doi: 10.1111/j.1365-313X.2008.03461.x

Shekhar, S., Agrawal, L., Mishra, D., Buragohain, A. K., Unnikrishnan, M., Mohan, C., et al. (2016). Ectopic expression of amaranth seed storage albumin modulates photoassimilate transport and nutrient acquisition in sweetpotato. *Sci. Rep.* 6:25384. doi: 10.1038/srep25384

Shewry, P. R. (2009). Wheat. *J. Exp. Bot.* 60, 1537–1553. doi: 10.1093/jxb/erp058

Shewry, P. R., and Halford, N. G. (2002). Cereal seed storage proteins: structures, properties and role in grain utilization. *J. Exp. Bot.* 53, 947–958. doi: 10.1093/jexbot/53.370.947

Shewry, P. R., and Tatham, A. S. (1990). The prolamin storage proteins of cereal seeds: structure and evolution. *Biochem. J.* 267, 1–12. doi: 10.1042/bj2670001

Stone, S. L., Kwong, L. W., Yee, K. M., Pelletier, J., Lepiniec, L., Fischer, R. L., et al. (2001). LEAFY COTYLEDON2 encodes a B3 domain transcription factor that induces embryo development. *Proc. Natl. Acad. Sci. U.S.A.* 98, 11806–11811. doi: 10.1073/pnas.201413498

Swaminathan, K., Peterson, K., and Jack, T. (2008). The plant B3 superfamily. *Trends Plant Sci.* 13, 647–655. doi: 10.1016/j.tplants.2008.09.006

To, A., Valon, C., Savino, G., Guilleminot, J., Devic, M., Giraudat, J., et al. (2006). A network of local and redundant gene regulation governs *Arabidopsis* seed maturation. *Plant Cell* 18, 1642–1651. doi: 10.1105/tpc.105.039925

Tsai, A. Y. L., and Gazzarrini, S. (2012). AKIN10 and FUSCA3 interact to control lateral organ development and phase transitions in Arabidopsis. *Plant J.* 69, 809–821. doi: 10.1111/j.1365-313X.2011.04832.x

Tsuchiya, Y., Nambara, E., Naito, S., and McCourt, P. (2004). The *FUS3* transcription factor functions through the epidermal regulator *TTG1* during embryogenesis in *Arabidopsis*. *Plant J.* 37, 73–81. doi: 10.1046/j.1365-313X.2003.01939.x

Walter, M., Chaban, C., Schütze, K., Batistic, O., Weckermann, K., Näke, C., et al. (2004). Visualization of protein interactions in living plant cells using bimolecular fluorescence complementation. *Plant J.* 40, 428–438. doi: 10.1111/j.1365-313X.2004.02219.x

Wang, F., and Perry, S. E. (2013). Identification of direct targets of FUSCA3, a key regulator of Arabidopsis seed development. *Plant Physiol.* 161, 1251–1264. doi: 10.1104/pp.112.212282

Wang, X., Zeng, J., Li, Y., Rong, X., Sun, J., Sun, T., et al. (2015). Expression of *TaWRKY44*, a wheat WRKY gene, in transgenic tobacco confers multiple abiotic stress tolerances. *Front. Plant Sci.* 6:615. doi: 10.3389/fpls.2015.00615

Wang, Z., Chen, M., Chen, T., Xuan, L., Li, Z., Du, X., et al. (2014). *TRANSPARENT TESTA2* regulates embryonic fatty acid biosynthesis by targeting *FUSCA3* during the early developmental stage of Arabidopsis seeds. *Plant J.* 77, 757–769. doi: 10.1111/tpj.12426

White, J., and Edwards, J. (2008). *Wheat Growth and Development*. Orange, NSW: Department of Primary Industries.

Wieser, H. (2000). Comparative investigations of gluten proteins from different wheat species I. Qualitative and quantitative composition of gluten protein types. *Eur. Food Res. Technol.* 211, 262–268. doi: 10.1007/s00217-003-0748-6

Wu, C. Y., Washida, H., Onodera, Y., Harada, K., and Takaiwa, F. (2000). Quantitative nature of the prolamin-box, ACGT and AACA motifs in a rice glutelin gene promoter: minimal cis-element requirements for endosperm-specific gene expression. *Plant J.* 23, 415–421. doi: 10.1046/j.1365-313x.2000.00797.x

Zhang, Z., Yang, J., and Wu, Y. (2015). Transcriptional regulation of zein gene expression in maize through the additive and synergistic action of opaque2, prolamine-box binding factor, and O2 heterodimerizing proteins. *Plant Cell* 27, 1162–1172. doi: 10.1105/tpc.15.00035

Conflict of Interest Statement: The authors declare that the research was conducted in the absence of any commercial or financial relationships that could be construed as a potential conflict of interest.

frontiers in Plant Science

ORIGINAL RESEARCH
published: 01 February 2018
doi: 10.3389/fpls.2018.00063

Targeted Haplotype Comparisons between South African Wheat Cultivars Appear Predictive of Pre-harvest Sprouting Tolerance

Scott L. Sydenham and Annelie Barnard*

Agricultural Research Council-Small Grain, Bethlehem, South Africa

Pre-harvest sprouting (PHS) has been a serious production constraint for over two decades, especially in the summer rainfall wheat production regions of South Africa. It is a complex genetic trait controlled by multiple genes, which are significantly influenced by environmental conditions. This complicates the accurate prediction of a cultivar's stability in terms of PHS tolerance. A number of reports have documented the presence of major QTL on chromosomes 3A and 4A of modern bread wheat cultivars, which confer PHS tolerance. In this study, the SSR marker haplotype combination of chromosomes 3A and 4A of former and current South African cultivars were compared with the aim to select for improved PHS tolerance levels in future cultivars. A total of 101 wheat cultivars, including a susceptible cultivar and five international tolerant sources, were used in this study. These cultivars and donors were evaluated for their PHS tolerance by making use of a rain simulator. In addition, five seeds of each entry were planted out into seedling trays and leaf material harvested for DNA isolation. A modified CTAB extraction method was used before progressing to downstream PCR applications. Eight SSR markers targeted from the well-characterized 3A and 4A QTL regions associated with PHS tolerance, were used to conduct targeted haplotype analysis. Additionally, recently published KASP SNP markers, which identify the casual SNP mutations within the *TaPHS1* gene, were used to genotype the germplasm. The haplotype marker data and phenotypic PHS data were compared across all cultivars and different production regions. A relative change in observed phenotypic variation percentage was obtained per marker allele and across marker haplotype combinations when compared to the PHS susceptible cultivar, Tugela-DN. Clear favorable haplotypes, contributing 40–60% of the variation for PHS tolerance, were identified for QTL 3A and 4A. Initial analyses show haplotype data appear to be predictive of PHS tolerance status and germplasm can now be selected to improve PHS tolerance. These haplotype data are the first of its kind for PHS genotyping in South Africa. In future, this can be used as a tool to predict the possible PHS tolerance range of a new cultivar.

Keywords: haplotype, pre-harvest sprouting, *TaPHS1*, *Phs1-A1*, QTL, SSRs, wheat

OPEN ACCESS

Edited by:
Jose Maria Barrero, Commonwealth Scientific and Industrial Research Organisation (CSIRO), Australia

Reviewed by:
Lee Hickey, The University of Queensland, Australia
Frank Gubler, Commonwealth Scientific and Industrial Research Organisation (CSIRO), Australia

****Correspondence:***
Scott L. Sydenham
sydenhams@arc.agric.za

Specialty section:
This article was submitted to Plant Breeding, a section of the journal Frontiers in Plant Science

Received: *29 August 2017*
Accepted: *12 January 2018*
Published: *01 February 2018*

Citation:
Sydenham SL and Barnard A (2018) Targeted Haplotype Comparisons between South African Wheat Cultivars Appear Predictive of Pre-harvest Sprouting Tolerance. Front. Plant Sci. 9:63. doi: 10.3389/fpls.2018.00063

INTRODUCTION

Pre-harvest sprouting (PHS) is a common phenomenon in the wheat (*Triticum aestivum* L.) producing areas of South Africa and has been well-documented over the past two decades (Barnard et al., 1997; Barnard, 2001; Barnard and Bona, 2004; Barnard and Smith, 2009). It has been a serious production constraint especially in the summer rainfall regions where rain occurs frequently just prior to or during harvest time. It is well-documented that PHS negatively affects the grain quality and ultimately flour quality. As a result, the price that farmers can get for their crop at harvest is severely affected (Barnard, 2001; Liu et al., 2008).

Research has shown that extensive genotypic variation exists for PHS in South African cultivars, indicating that progress in the development of cultivars with improved sprouting tolerance is feasible (Barnard et al., 1997, 2005; Barnard, 2001). The PHS tolerance levels in South African wheat cultivars has improved significantly over the years as a result of successful breeding (Smit et al., 2010). These winter wheat cultivars can be categorized into three major groups, namely cultivars that are highly tolerant to PHS, cultivars that are highly susceptible to PHS and a third moderate group that includes cultivars that are strongly influenced by the environment (Barnard and Smith, 2009). According to Biddulph et al. (2005) environment, and specifically moisture stress, can have a large effect on dormancy expression. Drought conditions combined with high temperatures during grain filling, tend to increase dormancy in wheat (Mares and Mrva, 2014).

PHS is a complex trait controlled by multiple genes or QTL (Bailey et al., 1999; Mares et al., 2005; Yang et al., 2007) where trait expression is significantly influenced by environmental conditions (Trethowan et al., 1996; Johansson, 2002). This complicates the accurate prediction of the stability of a cultivar in terms of PHS tolerance.

In the past decade, a number of QTL for PHS tolerance have been identified and mapped across all 21 wheat chromosomes in a number of wheat cultivars from different parts of the world (Mori et al., 2005; Ogbonnaya et al., 2007; Chen et al., 2008; Mohan et al., 2009; Jaiswal et al., 2012; Singh et al., 2012; Graybosch et al., 2013). These QTL analyses in wheat led to the identification of markers linked closely with desirable alleles of different QTL (Mares et al., 2005; Chen et al., 2008; Liu et al., 2008; Fofana et al., 2009; Kulwal et al., 2010, 2012). The chromosomes containing the most common and stable major QTL for PHS tolerance are 3A (Kulwal et al., 2005) and 4A (Mares et al., 2005; Mori et al., 2005; Ogbonnaya et al., 2007; Chen et al., 2008; Imtiaz et al., 2008; Zhang et al., 2008). A number of robust reliable simple-sequence repeat (SSR) markers have been associated to a number of these specific QTL for PHS tolerance in specific cultivar backgrounds. However, the characterization and validation of the true phenotypic effects of these QTL individually or in combination in diverse germplasm remains a challenge due to the genetic complexity of the PHS tolerance trait.

The major QTL on chromosome 4A was identified and mapped in 2000 (Flintham, 2000), which is now referred to as the *Phs1-A1* locus (Shorinola et al., 2016). Recently, the *Phs1-A1* region was fine mapped and new tightly molecular markers with MAS potential were identified. However, the causal gene underpinning the *Ph1-A1* locus is still unclear (Barrero et al., 2015; Shorinola et al., 2016). In 2008, a major QTL on chromosome 3A, named *Qphs.pseru-3AS*, was characterized and mapped from the white wheat cultivar Rio Blanco (Liu et al., 2008). In recent years, some important candidate genes which control PHS tolerance at these (3A and 4A) loci and others have been identified (Liu et al., 2013; Cabral et al., 2014; Barrero et al., 2015; Shorinola et al., 2016; Zhou et al., 2017). Importantly, the TaPHS1 gene, which forms an integral part of the major QTL on chromosome 3A (*Qphs.pseru-3AS*), which confers PHS tolerance, was cloned and characterized further. Two important, functional SNP mutations within the third and fourth exons of the *TaPHS1* gene-coding region, were identified. Both SNP mutations occurred together in all PHS susceptible cultivars covering a set of diverse genetic backgrounds and are considered critical for future PHS tolerant cultivar development (Liu et al., 2013).

The aim of this study was to characterize a collection of South African wheat cultivars for their known PHS tolerance QTL on chromosomes 3A and 4A and to compare marker haplotype combinations observed with the original PHS cultivar scoring averages. In this study, we aim to validate whether these markers could be used during MAS to select for better PHS tolerant cultivars and to determine if it would be possible to predict a cultivar's potential PHS tolerant class based solely on marker haplotypes.

MATERIALS AND METHODS

Wheat Cultivars and Trials

A total of 96 red wheat cultivars (**Table 1**) were included in this study and evaluated for their PHS tolerance or susceptibility over a 20 year-period and across six environments per year. These cultivars from three different seed companies (ARC-Small Grain, Pannar and Sensako), were commonly grown under dryland conditions in the summer rainfall dryland area, as well as under irrigation conditions in the central wheat producing areas of South Africa. Tugela-DN was used as a susceptible check, while Elands was included as a tolerant check (Barnard et al., 2005). The cultivars were planted according to a randomized complete block design (RCBD) with four replicates and accessed annually for the period that they were commercially available. Five sources of PHS tolerance namely AC Domain (Fofana et al., 2009) RL4137 (DePauw et al., 2009), Renan (Groos et al., 2002), Transvaal (Morris and DeMacon, 1994) and Rio Blanco (Liu et al., 2008), were also evaluated for their PHS characteristics over the last 3 years.

Assessment of PHS

During anthesis 48 ears per cultivar were labeled to ensure that all the ears were at the same physiological stage. These ears were hand-harvested at physiological maturity and air dried at room temperature for a week. The ears were then subjected to simulated rainfall for 72 h in a rain simulator at 15°C/25°C day/night temperature with 98% humidity as described by

TABLE 1 | The PHS phenotypic data of 96 wheat cultivars commonly grown in South Africa over multiple years and seasons.

	Dryland cultivars				Irrigation cultivars		
	Year released	**# years evaluated**	**Mean PHS score ± SD**		**Year released**	**# years evaluated**	**Mean PHS score ± SD**
Betta	1969	4	1.5 ± 0.33	Adam Tas	1989	3	5.8 ± 0.50
Betta-DN	1993	13	2.1 ± 0.92	Baviaans	2000	11	2.9 ± 0.43
Caledon	1996	15	2.7 ± 0.69	Biedou	2001	1	2.9
Elands	1998	17	2.0 ± 0.71	Buffels	2007	6	2.5 ± 0.26
Flamink	1979	1	6.8	Chokka	1989	2	4.6 ± 0.77
Gariep	1994	18	3.5 ± 0.48	CRN 826	2002	10	4.4 ± 0.59
Hugenoot	1989	9	4.8 ± 1.49	Dias	1988	1	5.4
Karee	1982	8	2.1 ± 0.69	Duzi	2004	11	3.7 ± 0.38
Komati	2002	6	2.0 ± 0.41	Gamtoos	1985	4	3.9 ± 0.99
Koonap	2010	4	3.9 ± 0.53	Inia	1970	9	4.1 ± 0.55
Letaba	1987	3	3.2 ± 1.06	Kariega	1993	17	2.5 ± 0.70
Limpopo	1994	11	3.1 ± 0.94	Krokodil	2004	11	4.1 ± 0.55
Matlabas	2004	11	2.7 ± 0.56	Marico	1993	12	3.1 ± 1.14
Molen	1986	5	5.4 ± 0.97	Nantes	1990	3	3.9 ± 0.89
Molopo	1988	3	3.2 ± 1.94	Olifants	2001	11	4.9 ± 0.93
Oom Charl	1987	3	1.9 ± 0.81	Palmiet	1985	6	4.4 ± 1.12
PAN 3111	2012	2	4.4 ± 0.57	PAN 3400	2011	3	4.2 ± 1.05
PAN 3118	2001	12	3.8 ± 0.81	PAN 3434	2004	7	3.5 ± 0.55
PAN 3120	2002	11	2.6 ± 0.56	PAN 3471	2008	7	4.9 ± 0.69
PAN 3122	2002	2	4.5 ± 0.42	PAN 3478	2008	6	3.3 ± 0.30
PAN 3144	2005	6	2.7 ± 0.48	PAN 3489	2011	3	4.8 ± 0.68
PAN 3161	2007	7	4.5 ± 0.58	PAN 3497	2011	3	3.4 ± 0.35
PAN 3191	1999	6	3.8 ± 1.44	PAN 3515	2013	1	3.2
PAN 3195	2011	3	5.4 ± 0.46	PAN 3623	2013	1	2.5
PAN 3198	2012	2	4.5 ± 0.71	Sabie	2010	6	2.8 ± 0.56
PAN 3355	2006	6	3.0 ± 0.49	SST 38	1993	6	2.9 ± 0.61
PAN 3364	1996	7	2.3 ± 0.82	SST 806	2000	13	4.8 ± 0.55
PAN 3368	2007	7	2.4 ± 0.54	SST 822	1992	18	3.8 ± 0.91
PAN 3377	1997	9	3.3 ± 1.03	SST 825	1992	9	5.4 ± 0.49
PAN 3379	2007	7	3.6 ± 0.33	SST 835	2003	10	4.6 ± 0.61
Scheepers 69	1969	2	2.0 ± 0.28	SST 843	2008	7	4.5 ± 0.60
Senqu	2010	4	2.7 ± 0.15	SST 866	2011	5	4.0 ± 0.58
SST 124	1987	10	3.7 ± 1.65	SST 867	2009	5	2.5 ± 0.44
SST 316	2013	3	3.8 ± 0.67	SST 875	2012	5	4.3 ± 0.72
SST 317	2013	3	2.8 ± 0.06	SST 876	1997	14	5.6 ± 0.62
SST 322	2002	4	2.4 ± 0.54	SST 877	2010	5	2.3 ± 0.28
SST 347	2004	7	2.7 ± 0.60	SST 884	2013	4	4.7 ± 0.91
SST 356	2005	8	3.5 ± 0.36	SST 895	2014	4	3.2 ± 0.71
SST 374	2011	2	3.0 ± 0.85	SST 896	2014	1	5.0
SST 387	2012	5	3.8 ± 0.54	SST 16	1988	3	5.7 ± 1.25
SST 398	2010	4	2.7 ± 1.04	SST 33	1988	3	4.5 ± 1.54
SST 399	1999	7	2.8 ± 0.44	SST 44	1988	1	6.1
SST 935	2003	2	4.7 ± 0.07	SST 66	1988	4	6.0 ± 0.56
SST 936	1994	4	3.5 ± 0.39	SST 86	1988	2	3.3 ± 0.25
SST 946	2004	1	3.6	Steenbras	1999	10	4.9 ± 0.57
Tugela	1986	5	7.2 ± 0.16	T4	1965	6	2.3 ± 0.80
Tugela-DN	1992	25	6.4 ± 0.89	Tamboti	2011	3	3.4 ± 0.32
				Timbavati	2011	3	3.3 ± 0.85
				Umlazi	2010	3	3.3 ± 0.23

Barnard et al. (1997). According to this technique, individual ears were evaluated on a scale from 1 to 8, where 1 represents total tolerance to PHS and 8 represents total susceptibility (**Figure 1**). The PHS phenotypic data collected, were averaged per cultivar.

DNA Isolation

Five seeds of each entry were planted out into seedling trays. Seven days post seedling emergence, fresh leaf material was harvested for DNA isolation. The leaf tissue was homogenized finely within 750 µl of extraction buffer for 1 min at 30 r/s with the Qiagen TissueLyser II. Genomic DNA was isolated according to a modified cetyltrimethylammonium bromide (CTAB) DNA extraction protocol by Saghai-Maroof et al. (1994) and treated with 2 µl RNase A enzyme (Inqaba Biotechnology). The quality, purity and concentration of each DNA sample was determined at 260/280 nm with a Nanodrop 2000 Spectrophotometer (Thermo Scientific Pty Ltd, USA). The DNA samples were then diluted with 1x TE (Tris-EDTA) buffer to 50 ng/µl before progressing to downstream PCR applications.

Markers Used

All SSR marker primer pairs were synthesized by Integrated DNA Technologies (www.IDTDNA.com) and ordered through Whitehead Scientific PTY (Ltd) (www.whitesci.co.za). Initially, 31 different SSR marker primer sequences and relevant PCR conditions were obtained either from Röder et al. (1998) and/or the grain genes 2.0 website (https://wheat.pw.usda.gov/GG2/). These 31 SSR markers were screened on seven local cultivars and the five international sources to identify informative polymorphic markers. **Table 2** lists these SSR markers, as well as the targeted PHST QTL per chromosome, and describes whether these markers were informative or not. From the initial screening, four polymorphic SSR markers were identified for potential targeted haplotype combination analysis. These markers, namely *Barc57* and *Barc12* (3A QTL) and *DuPw004* and *Wmc650* (4A QTL) were targeted from the well-characterized 3A and 4A QTL regions associated with PHS tolerance. The 96 cultivars, as well as the five international PHS tolerant donors were genotyped with the four SSR markers.

Simple Sequence Repeat Analysis

Extracted genomic DNA, totalling a 200 ng (4 µl) concentration was used as template DNA per sample in a 20 µl final volume PCR reaction. Reaction conditions recommended for the KAPA 2X Ready Mix PCR Kit (KAPA Biosystems, Cape Town, South Africa, www.kapabiosystems.com were applied. Each PCR reaction consisted of 10 µl (1x) KAPATaq 2X Ready Mix, 0.5 µl (10 µM) per SSR primer and the remaining volume (5.0 µl) of DNAse Free water. The PCR reactions were performed in a MyCyclerTM Thermal Cycler (www.bio-rad.com) with the following cycling conditions: 3 min at 95°C, 40 cycles of 30 s at 95°C, 30 s at Tm°C, 30 s at 72°C and a final extension step of 5 min at 72°C. After amplification each specific SSR marker PCR amplicons were separated on a 3.0–3.5% (w/v) Certified Low Range Ultra Agarose high-resolution gel (Bio-Rad Laboratories, Inc. www.bio-rad.com), made up in 1x TBE with 1x GRGreen Nucleic Acid gel stain solution (Inqaba Biotechnology, www.labsupplymall.com) and run at 100–125 V for 1–4 h. SSR product sizes were determined according to 100 bp and/or 20 bp (Lonza SimplyLoad®, Lonza Rockland Inc. USA) DNA ladders. A digital gel picture under UV light exposure was taken with the Bio-Rad Molecular Imager Gel Doc™ XR Instrument. Observed SSR marker alleles were sized, recorded and analyzed per cultivar both visually and with image Lab™ gel analysis software.

KASPR Marker Genotyping

Two KASP assays, namely *TaPHS1-646* (TaPHS1-SNP1 marker) and *TaPHS1-666* (TaPHS1-SNP2 marker), designed during the study of Liu et al. (2013), are considered the functional SNP mutations in and around the *TaPHS1* gene region on chromosome 3A. These two KASP assays were screened on the 64 cultivars that were assigned haplotypes based on SSR markers, and the five international tolerant sources. The primer sequences of each assay and PCR condition were obtained from the MAS Wheat Website (http://maswheat.ucdavis.edu/protocols/TaPHS1/index.htm). The PCR reactions and fluorescence detection were performed in an Agilent Technologies Mx3500P Real-time Thermal Cycler as recommended by LGC (http://www.kbioscience.co.uk).

The specific SNP allele for each KASP marker was recorded per cultivar. When one of the unfavorable alleles for either SNP marker was present, a cultivar was predicted as susceptible. When the allele that was present was favorable, but the other allele was missing, a cultivar was treated as unknown. When both alleles were missing, a cultivar was also treated as unknown.

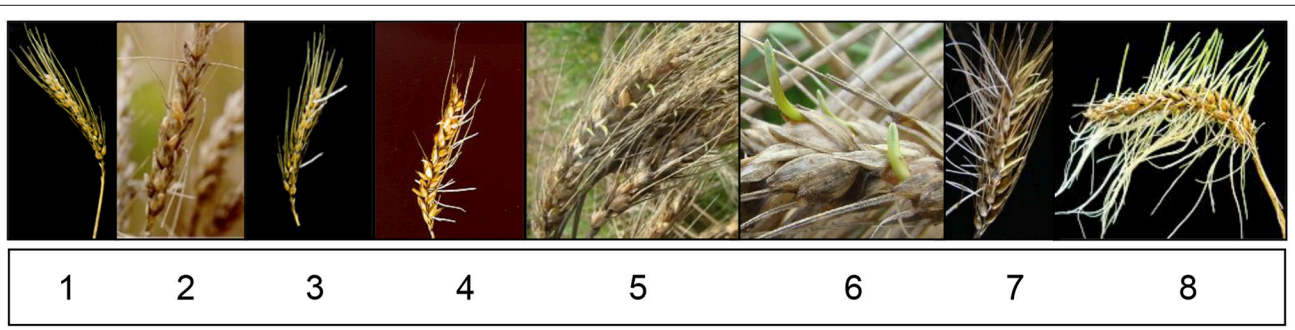

FIGURE 1 | Evaluation scale to determine the PHS tolerant or susceptibility of cultivars.

TABLE 2 | List of the SSR markers that were used during the initial screening phase of this study, together with their targeted chromosomes.

SSR Marker	Target QTL	Status	Comments
Wmc650	Major PHS 4A QTL	Polymorphic	Informative
Barc170		Polymorphic	Mostly informative
DuPw004		Polymorphic	Informative
Gwm397		Polymorphic	Mostly informative
Xgwm269			
Wmc48	4AL	Polymorphic	Informative certain tolerant material
Wmc491	4AL	Polymorphic	Not reliable
Wmc680	4AL	Polymorphic	Mostly informative
Wmc707	4AL	Polymorphic	Mostly informative
gwm494	4AL	Monomorphic	Not Informative
Barc57	Major PHS 3A QTL	Polymorphic	Informative
Barc12		Polymorphic	Informative
Barc321		Polymorphic	Not informative
Gwm403	3AL	Polymorphic	Mostly informative
Wmc428	3AL	Monomorphic	Not Informative
Wmc96	3AL	Monomorphic	Not Informative
gdm99	3AL	Monomorphic	Not Informative
Wwmc664	3AS	Unreliable	Not Informative
Gwm32	3AS	Monomorphic	Not Informative
Gwm4	3AS	Monomorphic	Not Informative
Gwm5	2D/3AS	Polymorphic	Not informative
Wmc492	3DS	Polymorphic	Not Informative
Wmc656	3DL	Unreliable	Not Informative
Gwm456	3DL	Polymorphic	Informative on certain tolerant material
Gwm3	3D	Polymorphic	Not Informative
Wmc349	4BS	Monomorphic	Not Informative
Wmc413	4BS	Monomorphic	Not Informative
Xgwm6	4BS	Did not work	Not Informative
Wmc657	4BL	Polymorphic	Informative on certain tolerant material
gwm63	7AL	Unreliable	Not Informative
Gwm37	7DL	Unreliable	Not Informative

Data Analyses

Four SSR markers, namely *Barc57* and *Barc12* (3A QTL) and *DuPw004* and *Wmc650* (4A QTL), were used in the final haplotype analyses of the 3A and 4A QTL. Additive allele identification was performed based on average PHS data for a particular marker haplotype combination on the comparison of mean PHS scores of the susceptible check, Tugela-DN. Mean PHS scores per SSR allele were used to calculate the percentage change in observed phenotypic variation in PHS tolerance from the susceptible check. This was done regardless of genetic background to attempt to reduce the effect that different genetic backgrounds might have on observed PHS tolerance levels. Tugela-DN was used as the susceptible check as a point of reference in the observed phenotypic variation analysis. The average PHS score per marker allele containing multiple genotypes was deducted from the average PHS score of the susceptible cultivar (Tugela-DN) and then divided by the Tugela-DN average to get an observed phenotypic variation percentage. The alleles were then classed as tolerant, moderate or susceptible based on these PHS averages.

Example: Marker 1, Allele 1 = **6.4** (Tugela-DN)–**2.9** (Marker 1/Allele 1) = 3.5/6.4 = 54.7% relative observed phenotypic variation (OPV).

RESULTS

PHS Characterization

The 96 cultivars used in this study are listed alphabetically in **Table 1**. These cultivars released from the late 1960's onwards were evaluated over a period of 25 years. Since new cultivars were released each year and older cultivars withdrawn from the market, it was difficult to evaluate these cultivars for similar periods of time. The number of years that the cultivars were evaluated for their PHS tolerance is therefore also shown in **Table 1**. Tugela-DN was released as a commercial cultivar in 1992 and has been the susceptible check since, with an average PHS value of 6.4. Elands, released in 1998, has an average PHS value of 2.0 and has been the tolerant check for the last 20 years.

The five international sources, namely AC Domain, RL4137, Rio Blanco, Transvaal and Renan, all had low PHS scores, namely 1.1, 1.2, 1.2, 1.6, and 1.1, respectively. This indicates excellent PHS tolerance.

The PHS tolerance levels of the cultivars in the study varied from excellent (scores lower than 3.0) to moderate (scores between 3.0 and 4.5) to highly susceptible (scores higher than 4.5). The cultivars adapted to dryland conditions were more tolerant to PHS with 43% of the entries having excellent tolerance to PHS, compared to the 20% of excellent tolerance in irrigation cultivars. The number of cultivars with moderate tolerance was similar in both groupings (43 and 47%, respectively, for dryland and irrigation cultivars).

Figure 2 shows the cumulative PHS data over the past 25 years. From these data in it is clear that the older cultivars (released in the previous millennium) had poorer tolerance than cultivars released after 2002. This was especially true for the dryland cultivars. The higher number of susceptible cultivars released in 2006, 2007, 2011, and 2012, were mainly irrigation cultivars.

Favorable Marker Allele Identification

Alleles were considered favorable for PHS tolerance when representative cultivars had PHS average scores of 3.0 or lower. An allele was classified as moderate if the average PHS scores ranged from 3.1 to 4.4. Finally, a marker allele was considered unfavorable for PHS tolerance if the average PHS scores of the representative cultivars were 4.5 or higher.

In **Table 3** the single marker alleles for markers flanking the 3A QTL, *Barc57* and *Barc12,* and their relative observed phenotypic variation percentage are shown.

Barc57

SSR marker *Barc57* amplified five different alleles across the cultivars studied (**Table 3**). Allele $Barc57^{220/240}$ contributed

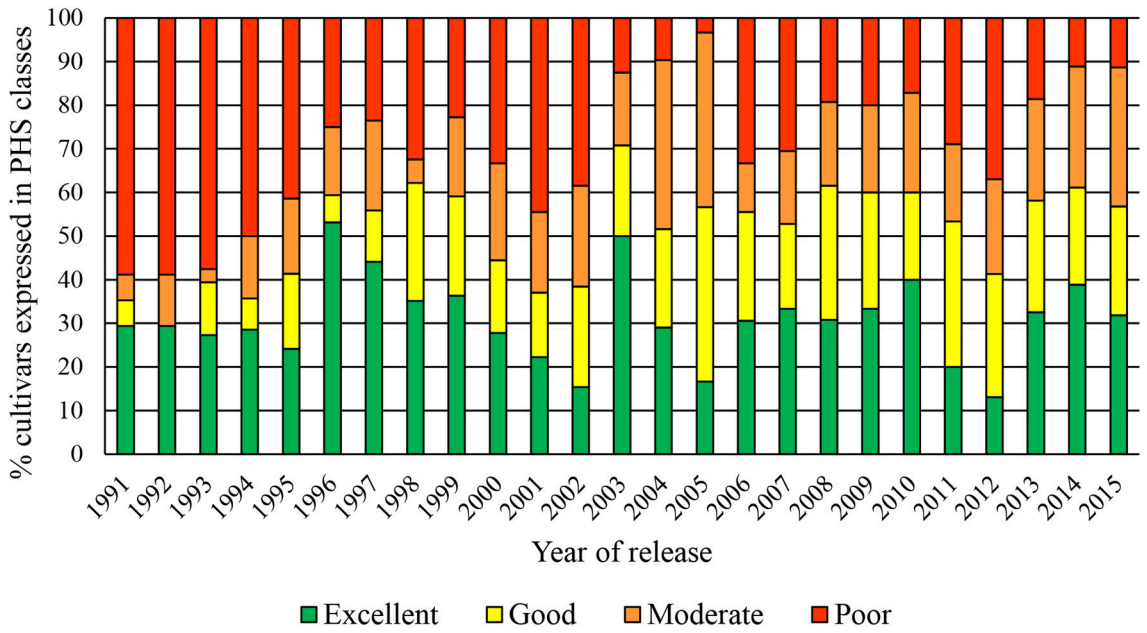

FIGURE 2 | Evaluation scale to determine the PHS tolerant or susceptibility of cultivars.

TABLE 3 | Analysis of markers *Barc57* and *Barc12* that flank the 3A QTL to identify favorable alleles for PHS tolerance and the relative observed phenotypic variation (%) based on rain simulator screening of 96 wheat cultivars.

Barc57				*Barc12*			
Allele	**Mean PHS score***	**OPV%****	**Range**	**Allele**	**Mean PHS score**	**OPV%**	**Range**
220	3.2	50.0	1.5–7.2	220	3.3	48.4	1.5–4.9
210	3.6	43.8	2.4–4.9	200	3.6	43.8	2.0–5.4
210/240	4.1	35.9	2.0–5.4	160	3.8	40.6	1.9–6.1
220/240	4.1	35.9	2.3–6.4	180	3.9	39.1	2.8–5.0
				210	3.9	39.1	2.6–4.6
				240	4.8	25.0	2.3–6.4

**PHS, Pre-harvest sprouting.*
***OPV, Observed phenotypic variation.*

53.1% to the observed phenotypic variation (OPV), with an average PHS score of 3.0 and appears to be more favorable for PHS tolerance than alleles *Barc57*$^{210/240}$ and *Barc57*^{210}. The *Barc57*^{220} allele, with a 40.6% contribution to the OPV (%), was moderate in its contribution. The *Barc57*^{240} allele, with a 20.3% OPV across cultivars, is not favorable for PHS tolerance. *Barc57*$^{220/240}$ and *Barc57*^{240} should, therefore, be considered for positive and negative MAS, respectively.

Barc12

SSR marker *Barc12* amplified six different alleles across the cultivars studied (**Table 3**). Two favorable alleles for PHS tolerance, namely *Barc12*^{240} and *Barc12*^{220}, were identified with 59.4 and 54.7% OVP contributions, and average PHS values of 2.6 and 2.9, respectively. The four other alleles (*Barc12*^{200}, *Barc12*^{160}, *Barc12*^{180}, and *Barc12*^{210}) are moderate contributing alleles with an OPV range of 32.8–40.6% and average PHS scores of 3.8, 3.9, 4.3, and 4.3, respectively. SSR *Barc12* alleles 240 and 220 should be considered more favorable for MAS to improve PHS tolerance.

Seven and four alleles, respectively, were amplified for the respective flanking 4A QTL SSR markers *Wmc650* and *DuPw004* (**Table 4**). No clear favorable single alleles below the 3.0 PHS threshold could be identified for any of these markers.

Wmc650

Three alleles, namely *Wmc650*^{210}, *Wmc650*^{220}, *Wmc650*^{235} are more favorable than the other four alleles that amplified (**Table 4**). These three alleles contributed between 48.4 and 51.6% to the OPV and had PHS averages of 3.3, 3.1, and 3.2, respectively. *Wmc650*^{260} contributed 12.5% OPV and cultivars with this allele present had an average PHS score of 5.6. *Wmc650*^{260} is unfavorable for PHS tolerance. *Wmc650*^{170}, *Wmc650*^{200}, and *Wmc650*^{null} reacted moderately with PHS averages of 4.3, 3.9,

TABLE 4 | Analysis of markers *Wmc650* and *DuPw004* that flank the 4A QTL to identify favorable alleles for PHS tolerance and the relative observed phenotypic variation (%) based on rain simulator screening of 96 wheat cultivars.

Wmc650				*DuPw004*			
Allele	**Mean PHS score***	**OPV%****	**Range**	**Allele**	**Mean PHS score**	**OPV%**	**Range**
220	2.6	59.4	2.3–3.2	190	3.6	43.8	1.5–7.2
200	3.2	50.0	2.3–4.3	280	3.8	40.6	2.0–6.8
235	3.5	45.3	1.5–7.2	190/280	4.5	29.7	3.6–5.4
170	3.7	40.3	1.9–5.4				
Null	4.0	37.5	2.7–5.4				
210	4.1	35.9	2.4–5.6				
260	5.6	12.5	5.4–5.8				

*PHS, Pre-harvest sprouting.
**OPV, Observed phenotypic variation.

and 3.6, respectively. MAS $Wmc650^{260}$ should be avoided when breeding for cultivars with PHS tolerance.

DuPw004

Allele $DuPw004^{190}$ is more favorable than the other three alleles of *DuPw004* with an OPV contribution of 48.4% and a PHS average of 3.3 (**Table 4**). Alleles $DuPw004^{280}$, $DuPw004^{190/280}$, and $DuPw004^{null}$ contributed 34.4–37.5% to the OPV with PHS scores of 4.2, 4.2 and 4.0, respectively. These three alleles are not favorable for the improvement of PHS tolerance in South African germplasm.

Favorable Haplotype Identification

For the whole haplotype analysis, the particular haplotypes were classed in the same manner than the single marker alleles based on the phenotypic PHS evaluation scale (Tolerant $\leq$3.0, Moderate 3.1–4.5 and Susceptible $\geq$4.6). The moderate class still remains difficult to define with a relevant score threshold as environmental effects might have a bigger influence on this group of cultivars than the other two classes. Cultivars from the moderate class can, depending on season and environment, move between classes.

Favorable Haplotype Identification for the 3A QTL

After the analyses of the allelic SSR marker data across the 3A QTL region, a total of 13 different haplotypes were observed (**Table 5**). Haplotypes 1 and 2 are considered favorable for PHS tolerance, both with PHS averages of 3.0 and an OPV (%) range of 53.1, respectively. The moderately favorable alleles from single SSR allele analysis, namely $Barc57^{220}$, $Barc12^{220}$, and $Barc12^{160}$, are the contributors to favorable haplotypes 1 and 2. These marker alleles contribute additively to haplotypes 1 and 2 with overall improvements in the PHS averages.

Haplotypes 3 to 11 are considered moderate contributing haplotypes toward PHS tolerance in South African cultivars for the 3A QTL region (**Table 5**). Haplotype 3 is a favorable moderate haplotype with a PHS average of 3.2, consisting of two moderate marker alleles $Barc57^{220}$ and less favorable moderate marker allele $Barc12^{210}$, suggesting additive allele interactions. Haplotype 4 is a combination of the moderate $Barc57^{210}$ allele with the moderate $Barc12^{200}$ allele, while haplotype 5 is a combination of the more favorable moderate $Barc57^{220}$ allele and the less favorable $Barc12^{180}$ moderate allele. Haplotype 6 is a combination of the less favorable moderate $Barc57^{210/240}$ and the more favorable moderate $Barc12^{200}$ allele combination. Haplotypes 4, 5, and 6 had average PHS scores of 3.4 with 46.9% OVP (%). Haplotype 5, with PHS score of 3.5 and OVP (%) of 45.3% is comprised of two moderate alleles, namely the less favorable $Barc57^{220/240}$ and the more favorable $Barc12^{220}$ allele. Haplotypes 8 to 11 are classed as less favorable moderate haplotypes with PHS averages of 3.8, 3.8, 4.3, and 4.3, respectively. These four haplotypes are all different combinations of less favorable moderate alleles from both flanking markers.

Haplotypes 12 and 13 are susceptible haplotypes both with 4.8 PHS averages. These two haplotypes are made up of the less favorable moderate marker allele combinations $Barc57^{220/240}$ and $Barc12^{160}$ and $Barc12^{180}$. These SSR allele combinations of haplotypes 12 and 13 appear to have negative interactions or

TABLE 5 | Analyses of the haplotype combinations for the 3A QTL across markers *Barc57* and *Barc12* to determine favorable haplotypes for PHS tolerance and the relative observed phenotypic variation (%) based on rain simulator screening of 96 wheat cultivars.

Haplotype	***Barc57***	***Barc12***	**Mean PHS score***	**OPV%****
1	220	220	3.0	53.1
2	220	160	3.0	53.1
3	220	210	3.2	50.0
4	210	200	3.4	46.9
5	220	180	3.4	46.9
6	210/240	200	3.4	43.8
7	220/240	220	3.5	45.3
8	210	160	3.8	40.6
9	220/240	200	3.8	40.6
10	210/240	210	4.3	39.1
11	220/240	240	4.3	39.1
12	220/240	160	4.8	37.5
13	220/240	180	4.8	34.4

*PHS, Pre-harvest sprouting.
**OPV, Observed phenotypic variation.

contribute susceptibility factors as the PHS score averages are higher (indicating more susceptibility) than the single moderate contributing SSR marker alleles.

For the 3A QTL region, haplotypes 1, 2, and 3 can be considered for potential MAS to improve PHS tolerance. Haplotypes 12 and 13 can be targeted negatively in MAS and should strictly be avoided during germplasm development.

Favorable Haplotype Identification for the 4A QTL

Analyses of the allelic SSR marker data across the 4A QTL region, identified ten different haplotypes (**Table 6**). Haplotypes 1 and 2 are considered highly favorable tolerant haplotypes for PHS tolerance with PHS average scores of 2.2 and 2.6, respectively. Haplotype 1 is a unique combination of two strong moderate alleles *Wmc650*^{170} and *DuPw004*^{190}, working additively to confer a tolerant haplotype. The change of two moderately favorable marker alleles to a favorable haplotype elucidates to strong additive effects in this 4A QTL region or across both QTL regions. Haplotype 2 is a combination of tolerant marker allele *Wmc650*^{220} and moderate allele *DuPw004*^{190} with negating contributing effects to the haplotype PHS average. Allele *Wmc650*^{220} (**Table 4**) shows a dominant effect on haplotype 2 with a mean PHS score of 2.6.

Haplotypes 3 and 4, with PHS mean values of 3.2 and 3.5, respectively (**Table 6**), are less favorable than haplotypes 1 and 2 for the 4A QTL region and as a result are classified as moderate haplotypes. Both these haplotypes are combinations of moderate contributing alleles for both markers *Wmc650* and *DuPw004*. Haplotypes 5 (PHS = 3.7), 6 (PHS = 3.8), 7 (PHS = 4.1), and 8 (PHS = 4.3) are less favorable moderate haplotypes. These four haplotypes consist of combinations of less favorable moderate marker alleles and contribute less favorably to PHS tolerance than haplotypes 1, 2, 3, or 4.

Haplotypes 9 and 10 are unfavorable for PHS tolerance with mean PHS scores of 4.5 and 5.6, respectively. Haplotype 9 consists of two strong moderate alleles namely *Wmc650*^{170} and *DuPw004*$^{190/280}$ (**Table 4**), while haplotype 10 contains the moderately favorable *DuPw004*^{190} allele and the susceptible *Wmc650*^{260} allele.

Haplotypes 1, 2, and 3 should be considered for potential use in MAS for PHS tolerance, while haplotypes 4, 5, 6, 7, and 8 should be avoided if possible to eliminate the potential moderate PHS class as the moderate class tends to be strongly influenced by environmental factors. Haplotypes 9 and 10 can be targeted negatively for MAS when trying to improve PHS tolerance in new germplasm.

Additive Haplotype Combination Identification across 3A and 4A QTL

When haplotype combinations for both the 3A and 4A QTL regions combined were considered, 13 different haplotypes were observed after analyses (**Table 7**). The majority of the cultivars (58%) were classed into haplotype combinations 1, 2, 5, 7, and 8. Two clear favorable additive (tolerant) haplotypes for PHS tolerance, namely haplotypes 1 and 2 both with PHS average scores of 2.7 and OVP (%) contributions of 57.8%, were identified. Haplotype 1 (**Table 7**) is comprised of the favorable 3A QTL haplotype 1 (**Table 5**) and the moderately favorable 4A QTL haplotype 4 (**Table 6**). Haplotype 2 (**Table 7**) is an additive combination of the 3A QTL haplotype 2 (**Table 5**) and 4A QTL haplotype 5 (**Table 6**).

Haplotypes 3, 4, and 5 are moderately favorable for PHS tolerance with PHS averages of 3.1, 3.4, and 3.5, respectively. These three haplotypes consist of different combinations of favorable and moderately favorable haplotypes. Haplotypes 3, 4 and 5 with OPV (%) in the range of 45.3–51.6% still contributed significantly to the observed phenotypic variation for PHS tolerance. Haplotypes 3, 4, and 5 (**Table 7**) consist of different combinations of moderate haplotypes from 3A and 4A QTL.

TABLE 6 | Analyses of the haplotype combinations for the 4A QTL across markers *Wmc650* and *DuPw004* to determine favorable haplotypes for PHS tolerance and the relative observed phenotypic variation (%) based on rain simulator screening of 96 wheat cultivars.

Haplotype	*Wmc650*	*DuPw004*	Mean PHS score*	OPV%**
1	170	190	2.2	65.6
2	220	190	2.6	59.4
3	200	190	3.2	50.0
4	235	190	3.5	45.3
5	170	280	3.7	42.2
6	Null	280	3.8	40.6
7	210	190	4.1	35.9
8	Null	190	4.3	32.8
9	170	190/280	4.5	29.7
10	260	190	5.6	12.5

*PHS, Pre-harvest sprouting.
**OPV, Observed phenotypic variation.

TABLE 7 | Analyses across both 3A and 4A QTL to identify additive haplotype combinations for PHS tolerance and the relative observed phenotypic variation (%) based on rain simulator screening of 96 wheat cultivars.

Haplotype combination	Number of cultivars	*Barc57*	*Barc12*	*Wmc650*	*DuPw004*	Mean PHS score*	OPV%**
1	8	220	220	235	190	2.7	57.8
2	7	220	160	170	280	2.7	57.8
3	3	210/240	200	170	280	3.1	51.6
4	4	220	180	235	190	3.4	46.9
5	8	220/240	220	235	190	3.5	45.3
6	2	210	200	Null	280	3.7	42.2
7	6	210	160	210	190	3.8	40.6
8	8	220/240	200	170	280	3.8	40.6
9	3	220/240	220	Null	190	4.0	37.5
10	2	220/240	200	Null	280	4.0	37.5
11	5	220/240	240	235	190	4.0	37.5
12	5	210/240	210	170	280	4.3	29.7
13	3	220/240	160	260	190	5.6	12.5

*PHS, Pre-harvest sprouting.
**OPV, Observed phenotypic variation.

Haplotypes 6, 7, and 8 (**Table 7**) are shown to be less favorable moderate haplotypes across both the 3A and 4A QTL regions, with average PHS scores of 3.7, 3.8, and 3.8, respectively. Haplotypes 9, 10, 11, and 12 are strong moderate haplotypes with average PHS scores of 4.0, 4.0, 4.0, and 4.3, which are less favorable for PHS tolerance. The OPV (%) contribution range of 29.7–37.5%, resulted from different combinations of moderate haplotypes from both the 3A QTL and 4A QTL.

It is important to note that the susceptible haplotype 13 (**Table 5**) of the 3A QTL region and the strong moderate haplotype 9 (**Table 6**) for the 4A QTL region, did not appear regularly in any haplotype combinations across the 3A and 4A QTL region (**Table 7**).

The highly unfavorable susceptible haplotype 13 (**Table 7**) with an average PHS value of 5.6 contributed a low 12.5% toward the PHS tolerance observed. It is comprised of the susceptible haplotype combination of haplotype 12 (**Table 5**) for the 3A QTL and haplotype 10 (**Table 6**) for 4A QTL region.

PHS Class Prediction Based on SSR Marker Data

Only haplotype combinations that were present in two or more of the cultivars were considered for analysis. Haplotypes were considered unique when different combinations of the representative haplotypes in 3A and 4A QTL analysis only appeared once, or when a totally unique single SSR marker allele was present in the genotype. The results of the PHS prediction based on marker haplotypes are shown in **Table 8A** for dryland cultivars and **Table 8B** for irrigation cultivars. In these tables the cultivars with unique haplotypes were removed and were not used in the prediction. In the end, 64 cultivars of the original 96 were used in the prediction of PHS.

Dryland Cultivar Predictions

Thirty of the 47 dryland cultivars could be assigned to a specific haplotype combination (**Table 8A**). Seventeen cultivars had unique haplotypes and were removed from the analyses. Of the 30 cultivars that were haplotyped, only seven did not predict the correct PHS class. In 76.7% of the time, the haplotype combinations were able to predict the correct PHS class overall for the dryland cultivars. The 30 cultivars that were haplotyped, could be divided into true PHS classes, where 13 cultivars were tolerant, 15 were moderate and two cultivars were susceptible. Within the tolerant class, 10 out of the 13 cultivars (76.9%) were predicted correctly. Within the moderate class, 12 of the 15 cultivars (80.0%) were predicted correctly. Both susceptible cultivars were incorrectly predicted as moderate.

Irrigation Cultivar Predictions

Thirty-four of the 49 irrigation cultivars could be assigned to a haplotype combination (**Table 8B**). Fifteen cultivars have unique or unassignable haplotype combinations based on the SSR data across both the 3A and 4A QTL and were removed. The haplotype analysis on irrigation cultivars was able to predict the correct PHS class of 67.6% of the irrigation cultivars after comparison with the actual PHS average scores. Of the 34 cultivars haplotyped, seven were classed as tolerant, 18 as moderate and nine as susceptible based on the actual PHS score averages. Two of the seven tolerant cultivars (28.6%) and three of the nine (33.3%) susceptible cultivars were predicted correctly. Of the moderate classed cultivars all 18 (100%) were predicted correctly based on the relative haplotype combination analysis. This mixture of prediction accuracy could be a result of the different environmental conditions and more complex gene interactions at play under irrigation production.

TABLE 8A | PHS tolerance class prediction based on molecular marker haplotype combinations across 3A and 4A QTL on the dryland cultivars used in this study.

Dryland cultivar	Haplotype combination	PHS* score prediction	Predicted PHS class	Actual mean PHS score	Actual PHS class
Betta	1	2.7	Tolerant	1.5	Tolerant
Betta-DN	1	2.7	Tolerant	2.1	Tolerant
Elands	2	2.7	Tolerant	2.0	Tolerant
Gariep	5	3.5	Moderate	3.5	Moderate
Karee	2	2.7	Tolerant	2.1	Tolerant
Komati	5	3.1	Moderate	2.0	Tolerant
Koonap	2	2.7	Tolerant	3.9	Moderate
Letaba	7	3.8	Moderate	3.2	Moderate
Limpopo	3	3.1	Moderate	3.1	Moderate
Matlabas	2	2.7	Tolerant	2.7	Tolerant
Molopo	2	2.7	Tolerant	3.2	Moderate
PAN 3111	9	4.0	Moderate	4.4	Moderate
PAN 3118	7	3.8	Moderate	3.8	Moderate
PAN 3122	8	3.8	Moderate	4.5	Moderate
PAN 3144	1	2.7	Tolerant	2.7	Tolerant
PAN 3161	6	3.7	Moderate	4.5	Moderate
PAN 3198	8	3.8	Moderate	4.5	Moderate
PAN 3355	2	2.7	Tolerant	3.0	Tolerant
PAN 3377	4	3.4	Moderate	3.3	Moderate
PAN 3379	1	2.7	Tolerant	3.6	Moderate
Senqu	1	2.7	Tolerant	2.7	Tolerant
SST 316	4	3.4	Moderate	3.8	Moderate
SST 356	4	3.4	Moderate	3.5	Moderate
SST 374	2	2.7	Tolerant	3.0	Tolerant
SST 387	7	3.3	Moderate	3.8	Moderate
SST 398	9	4.0	Moderate	2.7	Tolerant
SST 399	6	3.7	Moderate	2.8	Tolerant
SST 936	1	2.7	Tolerant	3.5	Tolerant
Tugela	11	4.0	Moderate	7.2	Susceptible
Tugela-DN	11	4.0	Moderate	6.4	Susceptible

**PHS, Pre-harvest sprouting.*

TaPHS1 SNP Genotyping

The two diagnostic causal SNP mutation markers of the *TaPHS1* gene region, *TaPHS1-646* and *TaPHS1-666*, were screened on the 64 cultivars, which were successfully assigned a SSR haplotype combination across the 3A and 4A QTL regions (**Tables 9A,B**). Thirty-two cultivars were not considered for SNP genotyping based on the unique SSR haplotype combinations observed in

TABLE 8B | PHS tolerance class prediction based on molecular marker haplotype combinations across 3A and 4A QTL on the irrigation cultivars used in this study.

Irrigation cultivar	Haplotype combination	PHS* score prediction	Predicted PHS class	Actual mean PHS score	Actual PHS class
Adam Tas	13	5.6	Susceptible	5.8	Susceptible
Biedou	8	3.8	Moderate	2.9	Tolerant
Chokka	12	4.3	Moderate	4.6	Susceptible
CRN 826	12	4.3	Moderate	4.4	Moderate
Duzi	5	3.5	Moderate	3.7	Moderate
Gamtoos	10	4.0	Moderate	3.9	Moderate
Inia	10	4.0	Moderate	4.1	Moderate
Kariega	11	4.0	Moderate	2.5	Tolerant
Marico	7	3.8	Moderate	3.1	Moderate
Nantes	8	3.8	Moderate	3.9	Moderate
Olifants	7	3.8	Moderate	4.9	Susceptible
Palmiet	12	4.3	Moderate	4.4	Moderate
PAN 3434	5	3.5	Moderate	3.5	Moderate
PAN 3471	9	4.0	Moderate	4.9	Susceptible
PAN 3478	5	3.5	Moderate	3.3	Moderate
PAN 3489	8	3.8	Moderate	4.8	Susceptible
PAN 3497	5	3.5	Moderate	3.4	Moderate
PAN 3515	8	3.8	Moderate	3.2	Moderate
Sabie	1	2.7	Tolerant	2.8	Tolerant
SST 38	3	3.1	Moderate	2.9	Tolerant
SST 806	11	4.0	Moderate	4.8	Susceptible
SST 822	12	4.3	Moderate	3.8	Moderate
SST 825	13	5.6	Susceptible	5.4	Susceptible
SST 866	8	3.8	Moderate	4.0	Moderate
SST 867	7	3.8	Moderate	2.5	Tolerant
SST 876	13	5.6	Susceptible	5.6	Susceptible
SST 877	4	3.4	Moderate	2.3	Tolerant
SST 884	11	4.0	Moderate	4.7	Susceptible
SST 33	12	4.3	Moderate	4.5	Moderate
SST 86	3	3.1	Moderate	3.3	Moderate
T4	1	2.7	Tolerant	2.3	Tolerant
Tamboti	8	3.8	Moderate	3.4	Moderate
Timbavati	5	3.5	Moderate	3.3	Moderate
Umlazi	5	3.5	Moderate	3.3	Moderate

PHS, Pre-harvest sprouting.

TABLE 9A | PHS tolerance class prediction based on KASP SNP marker analyses on the dryland cultivars used in this study.

Dryland cultivar	KASP Marker		Prediction according to marker analyses	Mean PHS* Score	Actual PHS class**
	TaPHS1-646	*TaPHS1-666*			
Betta	G	A	Tolerant	1.5	Tolerant
Betta-DN	G	A	Tolerant	2.1	Tolerant
Elands	G	A	Tolerant	2.0	Tolerant
Gariep	–	A	Unknown	3.5	Susceptible
Karee	G	A	Tolerant	2.1	Tolerant
Komati	G	A	Tolerant	2.0	Tolerant
Koonap	A	A	Susceptible	3.9	Susceptible
Letaba	A/G	T	Susceptible	3.5	Susceptible
Limpopo	G	A	Tolerant	3.1	Tolerant
Matlabas	G	A	Tolerant	2.7	Tolerant
Molopo	G	A	Tolerant	3.2	Tolerant
PAN 3111	–	–	Unknown	4.4	Susceptible
PAN 3118	A	T	Susceptible	3.8	Susceptible
PAN 3122	A/G	A	Susceptible	4.5	Susceptible
PAN 3144	A	A	Susceptible	2.7	Tolerant
PAN 3161	–	T	Susceptible	4.5	Susceptible
PAN 3198	A	T	Susceptible	4.5	Susceptible
PAN 3355	G	A	Tolerant	3.0	Tolerant
PAN 3377	G/A	A	Susceptible	3.3	Tolerant
PAN 3379	A	T	Susceptible	3.6	Susceptible
Senqu	G	A	Tolerant	2.7	Tolerant
SST 316	G	T	Susceptible	3.8	Susceptible
SST 356	G	T	Susceptible	3.5	Susceptible
SST 374	A/G	T	Susceptible	3.0	Tolerant
SST 387	A	A	Susceptible	3.8	Susceptible
SST 398	G	A	Tolerant	2.7	Tolerant
SST 399	G	A	Tolerant	2.8	Tolerant
SST 936	A/G	T	Susceptible	3.5	Tolerant
Tugela	A	T	Susceptible	7.2	Susceptible
Tugela-DN	A	T	Susceptible	6.4	Susceptible

PHS, Pre-harvest sprouting.
**Class category at a cut-off value of 3.5.*

those cultivars. With the nature of the SNP data only being able to reliably distinguish between tolerant and susceptible classes, an adjustment in prediction methodology was needed. For this SNP data analyses an actual PHS average score of 3.5 was considered a threshold between tolerant and susceptible classes. For the purpose of these analyses, a cultivar was considered tolerant with a PHS value $\leq$3.4 and susceptible with a PHS value $\geq$3.5.

PHS susceptibility is based on the presence of one or both of the unfavorable alleles A (for the *TaPHS1-646* marker) and T (for the *TaPHS1-666* marker).

The international tolerant sources AC Domain, RL4137, Rio Blanco and Renan all amplified the favorable SNP alleles for PHS tolerance, namely the G allele for *TaPHS1-646* and the A allele for *TaPHS1-666*. The tolerant source, Transvaal, had a mixed haplotype with the favorable SNP allele at *Ta-PHS1-646,* but is heterozygous with a T/A SNP allele at the *TaPHS1-666*. The local tolerant cultivar, Elands, contained both favorable SNP alleles for PHS tolerance. Tugela-DN, which is the local susceptible check, contained the complete susceptible haplotype across the *TaPHS1* gene region, with the A allele and T allele present for *TaPHS1-646* and *TaPHS1-666*, respectively.

Dryland Cultivar Predictions Based on TaPHS1 SNP Genotyping

Thirty dryland cultivars were screened with both SNP markers *TaPHS1-646* and *TaPHS1-666* (**Table 9A**). Some cultivars gave reliability difficulties on each of the markers. After several reaction and procedural repeats, two cultivars (Gariep and PAN 3111) still had missing data and were referred to as unknown

TABLE 9B | PHS tolerance class prediction based on KASP SNP marker analyses on the irrigation cultivars used in this study.

Dryland cultivar	KASP Marker		Prediction according to marker analyses	Mean PHS* score	Actual PHS class**
	TaPHS1-646	*TaPHS1-666*			
Adam Tas	G/A	A	Susceptible	5.8	Susceptible
Biedou	G	A	Tolerant	2.9	Tolerant
Chokka	G	A	Tolerant	4.6	Susceptible
CRN 826	G	T	Susceptible	4.4	Susceptible
Duzi	G	A	Tolerant	3.7	Susceptible
Gamtoos	G	T	Susceptible	3.9	Susceptible
Inia	A	A	Susceptible	4.1	Susceptible
Kariega	G	A	Tolerant	2.5	Tolerant
Marico	A	A	Susceptible	3.1	Tolerant
Nantes	G	T	Susceptible	3.9	Susceptible
Olifants	A	T	Susceptible	4.9	Susceptible
Palmiet	G	A/T	Susceptible	4.4	Susceptible
PAN 3434	G	T	Susceptible	3.5	Susceptible
PAN 3471	A	T	Susceptible	4.9	Susceptible
PAN 3478	A/G	T	Susceptible	3.3	Tolerant
PAN 3489	A/G	T	Susceptible	4.8	Susceptible
PAN 3497	A/G	T	Susceptible	3.4	Tolerant
PAN 3515	G	A	Tolerant	3.2	Tolerant
Sabie	G	A	Tolerant	2.8	Tolerant
SST 38	G	A	Tolerant	2.9	Tolerant
SST 806	–	T	Susceptible	4.8	Susceptible
SST 822	A	T	Susceptible	3.8	Susceptible
SST 825	A	T	Susceptible	5.4	Susceptible
SST 866	A	T	Susceptible	4.0	Susceptible
SST 867	G	A	Tolerant	2.5	Tolerant
SST 876	A	A	Susceptible	5.6	Susceptible
SST 877	A	A	Susceptible	2.3	Tolerant
SST 884	A	T	Susceptible	4.7	Susceptible
SST33	G	T	Susceptible	4.5	Susceptible
SST86	G	A	Tolerant	3.3	Tolerant
T4	G	A	Tolerant	2.3	Tolerant
Tamboti	A	A	Susceptible	3.4	Tolerant
Timbavati	G	A	Tolerant	3.3	Tolerant
Umlazi	–	A	Unknown	3.3	Tolerant

*PHS, Pre-harvest sprouting.
**Class category at a cut-off value of 3.5.

in terms of a prediction as explained in section KASPR Marker Genotyping. According to this methodology, the cultivar PAN 3161 was predicted as susceptible based on the presence of one unfavorable allele.

From the joint SNP data of markers *TaPHS1-646* and *TaPHS1-666*, 24 of the 28 (85.7%) cultivars were predicted into the correct PHS classes based on this analysis. This equates to a 9% improvement in prediction accuracy from the SSR haplotype predictions on the same dryland cultivars (**Table 8A**). Twelve of the 16 tolerant dryland cultivars were accurately predicted (75.0%) and all 12 susceptible cultivars were correctly predicted as susceptible (100%).

Irrigation Cultivar Predictions Based on TaPHS1 SNP Genotyping

The genotypic SNP data and PHS class prediction of the 34 irrigation cultivars is presented in **Table 9B**. These predictions are based solely on the SNP data. The cultivar Umlazi was treated as unknown in the prediction class because of unreliable and missing SNP data as discussed in section KASPR Marker Genotyping. The cultivar SST 806 was predicted as susceptible based on the presence of the unfavorable allele for the *TaPHS1-666* marker according to the methodology explained previously.

Twenty-six of the remaining 33 cultivars (78.8%) were predicted correctly into tolerant or susceptible classes after comparison with the actual PHS scores. This is an 11% percent accuracy improvement from the 67.6% class prediction accuracy achieved with SSR haplotype data analysis. Nine of the 14 tolerant cultivars (64.3%) were predicted correctly and 17 of the 19 susceptible cultivars (89.5%) were accurately predicted as susceptible.

Across all cultivars, the *TaPHS1* SNP data predicted 70% of the tolerant cultivars and 94% of susceptible cultivars correctly, based on the 3.5 PHS average threshold.

DISCUSSION

The cultivars that were assessed in this study were released by three different seed companies and represented diverse genetic backgrounds and growth types. All wheat cultivars grown in South Africa are red wheat types with exceptional bread making quality characteristics (Smit et al., 2010).

The PHS tolerance levels in South African wheat cultivars has steadily improved directly or indirectly through wheat breeding over the past 25 years (Barnard et al., 2005; Smit et al., 2010). As a result of continuous evaluations and adaptations to the respective breeding programmes, the PHS tolerance of cultivars improved to such an extent that only three of the dryland cultivars that are currently commercially available, have poor PHS tolerance compared to the almost 60% of cultivars with poor PHS tolerance in 1991 (Barnard et al., 1997). It is well-known that environmental conditions during grain filling can have a large effect on the expression of dormancy (Biddulph et al., 2007). Research by Biddulph et al. (2005, 2007) has shown that drought conditions during grain filling might increase dormancy in certain cultivars (Mares and Mrva, 2014). These phenomena could explain the high variation in the PHS levels of the moderate group of cultivars, especially in the dryland production regions where sporadic periods of moisture stress and high temperatures are experienced. Opposed to the higher PHS levels in dryland cultivars, it has been shown over many years that cultivars grown under irrigated conditions in South Africa do not display the same levels of tolerance. However, in these irrigated production areas moisture stress is not a factor. Previous research by Biddulph et al. (2007) has shown that a reduction in dormancy can occur when the water supply was high during the later stages of grain filling. Therefore, the sufficient supply of water at critical growth stages might reduce dormancy, possibly

explaining the lower levels of PHS observed in irrigation cultivars in South Africa.

This study was the first to investigate the distribution and effect of known major QTL for PHS tolerance in South African wheat cultivars. The well-documented 3A and 4A QTL (Kulwal et al., 2005, 2012; Mares et al., 2005; Chao et al., 2010; Cao et al., 2016) were targeted for further investigation after initial screenings with several SSR markers.

According to the data from this study, the South African PHS tolerant check, Elands, compares favorably with the international sources. Based on pedigree comparisons there are no known PHS tolerance donor to confer tolerance. Data from this study are the first indication of the underlining genetic basis of the PHS tolerance in this cultivar to be predominantly as a result of the *TaPHS1* gene and other additive QTL combinations. From SSR haplotying it appears that different alleles of the contributing genes of the *Phs1-A1* locus (4A QTL) might be different from the international PHS tolerant donors.

According to previous research the 3A *Qphs.pseru-3AS* (Kulwal et al., 2005; Liu et al., 2008, 2011) and 4A QTL regions (Flintham, 2000; Mares et al., 2005; Ogbonnaya et al., 2007; Chen et al., 2008; Zhang et al., 2008; Graybosch et al., 2013; Cabral et al., 2014) contribute significantly to the partial PHS tolerance conferred by multiple genes. Additional common and stable QTL for PHS tolerance are 2A (Mohan et al., 2009), 2B (Chao et al., 2016; Fakthongphan et al., 2016), 3B, 3D (Kulwal et al., 2004; Ogbonnaya et al., 2007; Fofana et al., 2009; Jaiswal et al., 2012), 4B (Kulwal et al., 2012; Cao et al., 2016), 5A (Groos et al., 2002), 6B and 7D (Roy et al., 1999). Similar to other genetic studies that suggest that genes linked with PHS tolerance are mostly located on chromosome 3A and 4A (Graybosch et al., 2013; Cabral et al., 2014), it became clear from the current study that the effects of the 3A and 4A QTL on the phenotypic variation of PHS of South African cultivars are most important.

The four SSR markers, *Barc57*, *Barc12*, *Wmc650,* and *DuPw004* used to haplotype the studied material, identified clear single favorable marker alleles across diverse genetic backgrounds, which can be considered for MAS. The same markers for the 3A QTL region were used during the fine mapping and cloning of candidate gene *TaPHS1* (Liu et al., 2013). These markers have also been used successfully during the positional mapping of these QTL in previous studies (Singh et al., 2012; Tyagi and Gupta, 2012; Cao et al., 2016). The allelic variation identified with the four SSR markers strongly suggests the presence of different allelic versions of candidate genes or presence of novel mutations at the 3A and 4A QTL regions. The 13 haplotypes identified for the 3A QTL, as well as the 10 haplotypes for the 4A QTL, represented cultivars from all three PHS tolerance classes (tolerant, moderate and susceptible). In other mapping studies, an explained phenotypic variation for a single allele linked to PHS tolerance ranged between 15 and 45% (Hori et al., 2010; Chang et al., 2011; Liu et al., 2011). In the current study the OPV (%) range (higher than 40%) which was calculated in nine out of the 13 haplotypes for the 3A QTL and six out of the 10 haplotypes for the 4A QTL, indicated significant contributions by favorable haplotypes toward PHS tolerance. This OPV (%) range of up to almost 60% suggests the additive effect of the contribution of candidate genes within both the 3A and 4A QTL regions. From these combined analyses, it is therefore clear that additive haplotype combinations can be targeted during MAS.

Based on SSR haplotyping, cultivars were predicted to have a certain PHS tolerance. This is the first attempt to predict PHS tolerance based on molecular data in commercially available cultivars. In the case of dryland cultivars, this methodology predicted the correct PHS class in almost 77% of the time and 68% in the irrigation cultivars. Although some of the predictions based on SSR haplotyping classed cultivars incorrectly, in these cases cultivars were always classed in the group directly following or directly prior to that specific grouping and never two groupings apart. At no stage was a susceptible cultivar wrongly classed as tolerant or a tolerant cultivar wrongly classed as susceptible. The cultivars were always wrongly grouped between moderate and tolerant or moderate and susceptible classes.

Analyses based on SNP haplotyping were different, because only two PHS classing groups (tolerant and susceptible) were considered. In this case, cultivars that were phenotypically tolerant could be predicted through SNP haplotyping as susceptible or *vice versa*. Importantly, the SNP predictions were based solely on the contributions made by the *TaPHS1* gene of the 3A QTL. The contributions of the 4A QTL, *Phs1-A1* (Barrero et al., 2015; Shorinola et al., 2016), are unknown for these predictions and warrant further investigation on this germplasm. Predictions made with SNP data were more accurate than the SSR data with an improvement of almost 10% in both dryland and irrigation cultivars. Dryland cultivars were predicted correctly in 86% of the cases, while the irrigation cultivars were correct in 78% of cases. However, markers *TaPHS1-646* and *TaPHS1-666* were not completely diagnostic as mentioned by Liu et al. (2013), possibly due to the fact that South African cultivars might have novel mutations in and around the *TaPHS1* gene.

With the SNP data it was harder to correctly predict tolerant cultivars than susceptible cultivars, possibly due to the masking effect of moderate cultivars, as well as the unknown effects of the 4A QTL and potential susceptibility factors. The accurate predictions of moderately tolerant cultivars remains a challenge. However, the data from this study has given more insight into the genetic variation within the moderate class, further emphasizing the complexity of the PHS traits influenced by the environment (Kulwal et al., 2012; Liu et al., 2013; Mares and Mrva, 2014). The high success rate of predicted values of almost 82% on average are indicative of the possible application of this methodology in future PHS screenings. It appears that these data could be a preliminary indication of a cultivar's potential PHS class. However, the lack of a universal PHS evaluation scale, as well as the theoretical cut-off PHS score between classes, might influence the prediction outcomes.

In future, the SNP markers (*TaPHS1-646* and *TaPHS1-666*) specific to the 3A QTL can be used to select for better PHS tolerance cultivars. The newly published diagnostic markers for the *Phs1-A1* locus need to be validated on this set of

cultivars. Potentially the combination of using targeted MAS for *TaPHS1* (3A) and *Phs1-A1* (4A) with true diagnostic markers, may improve PHS class prediction accuracy in the future. It is envisaged that this methodology will be further fine-tuned and validated with in-season phenotyping screenings and leaf material sampling to assist with PHS tolerance classification and recommendations.

The fact that the phenotypic PHS screenings of the 96 cultivars were conducted over a 25-year period and at several wheat producing localities throughout the wheat production areas of South Africa, could also have influenced the outcome of the data. It has been reported that environmental effects play a significant role in the PHS tolerance or susceptibility of certain cultivars (Barnard, 2001; Barnard et al., 2005; Barnard and Smith, 2009).

The methodology explained in this study has the potential to be applied in a MAS approach to predict the PHS tolerance class during the development of germplasm, enabling breeders to select for and release cultivars with improved PHS tolerance.

AUTHOR CONTRIBUTIONS

Both authors have contributed to the work and agreed to be in the author list. SS is the molecular scientist and contributed molecular data and the interpretation thereof. AB, as the plant physiologist, contributed phenological PHS data and the interpretation thereof. Both authors contributed to the writing of the manuscript and preparing it for publication.

FUNDING

Funding for this research was made possible by the Winter Cereal Trust (WCT/W/2014/01) and the Agricultural Research Council (000903-Y5).

ACKNOWLEDGMENTS

Ms Shunay Human and Ms Bongiwe Nhlapho are acknowledged for technical support.

REFERENCES

Bailey, P. C., McKibbin, R. S., and Lenton, J. R. (1999). Genetic map location for orthoilogous VP1 genes in wheat and rice. *Theor. Appl. Genet.* 98, 281–284. doi: 10.1007/s001220051069

Barnard, A., and Smith, M. F. (2009). The effect of rainfall and temperature on the preharvest sprouting tolerance of winter wheat in the dryland production areas of the free state province. *Field Crops Res.* 112, 158–164. doi: 10.1016/j.fcr.2009.02.011

Barnard, A., Van Deventer, C. S., and Maartens, H. (2005). Genetic variability of preharvest sproutingthe south african situation. *Euphytica* 143, 291–296. doi: 10.1007/s10681-005-7885-x

Barnard, A. (2001). The genetic diversity of South African winter wheat cultivars in relation to their preharvest sprouting resistance and falling number. *Euphytica* 119, 109–112. doi: 10.1023/A:1017571212607

Barnard, A., and Bona, L. (2004). Sprout damage and falling number in South African and Hungarian wheats. *Cer. Res. Commun*. 32, 259–264.

Barnard, A., Purchase, J. L., Smith, M. F., and Van Lill, D. (1997). Determination of the preharvest sprouting resistance of South African winter wheat (*Triticum aestivum* L) cultivars. *S. A. J. Plant Soil* 14, 4–8. doi: 10.1080/02571862.1997.10635073

Barrero, J. M., Cavanagh, C., Verbyla, K. L., Tibbits, J. F. G., Verbyla, A. P., Huang, B. E., et al. (2015). Transcriptomic analysis of wheat near-isogenic lines identifies PM19-A1 and A2 as candidates for a major dormancy QTL. *Genome Biol.* 16, 93–111. doi: 10.1186/s13059-015-0665-6

Biddulph, T. B., Mares, D. J., Plummer, J. A., and Setter, T. L. (2005). Drought and high temperature increases preharvest sprouting tolerance in a genotype without grain dormancy. *Euphytica* 143, 277–283. doi: 10.1007/s10681-005-7882-0

Biddulph, T. B., Plummer, J. A., Setter, T. L., and Mares, D. J. (2007). Influence of high temperature and terminal moisture stress on dormancy in wheat (*Triticum aestivum* L). *Field Crops Res.* 103, 139–153. doi: 10.1016/j.fcr.2007.05.005

Cabral, A. L., Jordan, M. C., McCartney, C. A., You, F. M., Humphreys, D. G., MacLachlan, R., et al. (2014). Identification of candidate genes, regions and markers for pre-harvest sprouting resistance in wheat (*Triticum aestivum* L). *BMC Plant Biol.* 14, 340–352. doi: 10.1186/s12870-014-0340-1

Cao, L., Hayashi, K., Tokui, M., Mori, M., Miura, H., and Onishi, K. (2016). Detection of QTLs for traits associated with pre-harvest sprouting resistance in bread wheat (*Triticum aestivum* L.). *Breed. Sci.* 66, 260–270. doi: 10.1270/jsbbs.66.260

Chang, C., Zhang, H. P., Zhao, Q. X., Feng, J. M., Si, H. Q., Lu, J. et al. (2011). Rich allelic variations of Viviparous-1A and their associations with seed dormancy/pre-harvest sprouting of common wheat. *Euphytica* 179, 343–353. doi: 10.1007/s10681-011-0348-7

Chao, S., Elias, E., Benscher, D. Ishikawa, G., Huang, Y.-F., Saito, M., et al. (2016). Genetic mapping of major-effect seed dormancy quantitative trait loci on chromosome 2B using recombinant substitution lines in tetraploid wheat*Crop Sci.* 56, 59–72. doi: 10.2135/cropsci2015.05.0315

Chao, S., Xu, S. S., Elias, E. M., Faris, J. D., and Sorrells, M. E. (2010). Identification of chromosome locations of genes affecting preharvest sprouting and seed dormancy using chromosome substitution lines in tetraploid wheat (*Triticum turgidum* L.). *Crop Sci.* 50, 1180–1187. doi: 10.2135/cropsci2009.10.0589

Chen, C.-X., Cai, S.-B., and Bai, G.-H. (2008). A major QTL controlling seed dormancy and pre-harvest sprouting resistance on chromosome 4A in a Chinese wheat landrace. *Mol. Breed.* 21, 351–358. doi: 10.1007/s11032-007-9135-5

DePauw, R. M., Clarke, F. R., Fofana, B., Knox, R., Humphreys, G., and Cloutier, S. (2009). RL4137 contributes preharvest sprouting resistance to Canadian wheats. *Euphytica* 168, 347–361. doi: 10.1007/s10681-009-9933-4

Fakthongphan, J., Bai, G., St Amand, P., Graybosch, R. A., and Baenziger, P. S. (2016). Identification of markers linked to genes for sprouting tolerance (independent of grain color) in hard white winter wheat (HWWW). *Theor. Appl. Genet.* 129, 419–430. doi: 10.1007/s00122-015-2636-4

Flintham, J. E. (2000). Different genetic components control coat-imposed and embryo-imposed dormancy in wheat. *Seed Sci. Res.* 10, 43–50. doi: 10.1017/S0960258500000052

Fofana, B., Humphreys, D. G., Rasul, G., Cloutier, S., Brule-Babel, A., Woods, S., et al. (2009). Mapping quantitative trait loci controlling pre-harvest sprouting resistance in a red x white seeded spring wheat cross. *Euphytica* 165, 509–521. doi: 10.1007/s10681-008-9766-6

Graybosch, R. A., St Amand, P., and Bai, G. (2013). Evaluation of genetic markers for prediction of preharvest sprouting tolerance in hard white winter wheats. *Plant Breedi.* 132, 359–366. doi: 10.1111/pbr.12071

Groos, C., Gay, G., Perretant, M.-R., Gervais, L., Bernard, M., Dedryver, F., and Charmet, G. (2002). Study of the relationship between pre-harvest sprouting and grain color by quantitative trait loci analysis in a white x red grain bread-wheat cross. *Theor. Appl. Genet.* 104, 39–47. doi: 10.1007/s001220200004

Hori, K., Sugimoto, K., Nonoue, Y., Ono, N., Matsubara, K., Yamanouchi, U., et al. (2010). Detection of quantitative trait loci controlling pre-harvest sprouting resistance by using backcrossed populations of japonica rice cultivars. *Theor. Appl. Genet.* 120, 1547–1557. doi: 10.1007/s00122-010-1275-z

Imtiaz, M., Ogbonnaya, F. C., Oman, J., and Van Ginkel, M. (2008). Characterization of quantitative trait loci controlling genetic variation for preharvest sprouting in synthetic backcross-derived wheat lines. *Genetics* 178, 1725–1736. doi: 10.1534/genetics.107.084939

Jaiswal, V., Mir, R. R., Mohan, A., Balyan, H. S., and Gupta, P. K. (2012). Association mapping for pre-harvest sprouting tolerance in common wheat (*Triticum aestivum* L.) *Euphytica* 188, 89–102. doi: 10.1007/s10681-012-0713-1

Johansson, E. (2002). Effect of two genotypes and Swedish environment on falling number, amylase activities, and protein concentration and composition. *Euphytica* 126, 143–149. doi: 10.1023/A:1019646916905

Kulwal, P. L., Ishikawa, G., Benscher D., Feng Z., Yu, L.-X., Jadhav A., et al. (2012). Association mapping for pre-harvest sprouting resistance in white winter wheat. *Theor. Appl. Genet.* 125, 793–805. doi: 10.1007/s00122-012-1872-0

Kulwal, P. L., Kumar, N., Gaur, A., Khurana, P., Khurana, J. P., Tyagi, A. K., et al. (2005). Mapping of a major QTL for pre-harvest sprouting tolerance on chromosome 3A in bread wheat. *Theor. Appl. Genet*. 111, 1052–1059. doi: 10.1007/s00122-005-0021-4

Kulwal, P. L., Mir, R. R., Kumar, S., and Gupta, P. L. (2010). QTL Analysis and molecular breeding for seed dormancy and pre-harvest sprouting tolerance in bread wheat. *J. Plant Biol.* 37, 59–74.

Kulwal, P. L., Singh, R., Balyan, H. S., and Gupta, P. K. (2004). Genetic basis of pre-harvest sprouting tolerance using single-locus and two-locus QTL analyses in bread wheat. *Funct. Integr. Genomics* 4, 94–101. doi: 10.1007/s10142-004-0105-2

Liu, S., Bai, G., Cai, S., and Chen, C. (2011). Dissection of genetic components of preharvest sprouting resistance in white wheat. *Mol. breed.* 27, 511–523. doi: 10.1007/s11032-010-9448-7

Liu, S., Cai, S., Graybosch, R. A., Chen, C., and Bai, G. (2008). Quantitative trait loci for resistance to pre-harvest sprouting in US hard white winter wheat Rio Blanco. *Theor. Appl. Genet.* 117, 691–699. doi: 10.1007/s00122-008-0810-7

Liu, S., Sehgal, K., Li, J., Lin, M. Tjrick, H. N., Yu, J., et al. (2013). Cloning and Characterization of a critical regulator for preharvest sprouting in wheat. *Genetics* 195, 263–273. doi: 10.1534/genetics.113.152330

Mares, D. J., and Mrva, K. (2014). Wheat grain preharvest sprouting and late maturity alpha-amylase. *Planta* 240, 1167–1178. doi: 10.1007/s00425-014-2172-5

Mares, D., Mrva, K., Cheong, J., Williams, K., Watson, B., Storlie, E., et al. (2005). A QTL located on chromosome 4A associated with dormancy in white and red- grained wheat of diverse origin. *Theor. Appl. Genet.* 111, 1357–1364. doi: 10.1007/s00122-005-0065-5

Mohan, A., Kulwal, P., Singh, R., Kumar, V., Mir, R. R., Kuman, J., et al. (2009). Genome-wide QTl analysis for pre-harvest sprouting tolerance in bread wheat. *Euphytica* 168, 319–329. doi: 10.1007/s10681-009-9935-2

Mori, M., Uchino, N., Chono, M., Kato, K., and Miura, H. (2005). Mapping QTLs for grain dormancy on wheat chromosome 3A and the group 4 chromosomes, and their combined effect. *Theor. Appl. Genet.* 110, 1315–1323. doi: 10.1007/s00122-005-1972-1

Morris, G. F., and DeMacon, V. L. (1994). Seed dormancy and tissue culture response in wheat. *Crop Sci.* 34, 1324–1329. doi: 10.2135/cropsci1994.0011183X003400050034x

Ogbonnaya, F. C., Imtiaz, M., and Depauw, R. M. (2007). Haplotype diversity of preharvest sprouting QTLs in wheat. *Genome* 50, 107–118. doi: 10.1139/g06-142

Röder, M. S., Korzun, V., Wendehake, K. Plaschke, J., Tixier, M.-H., Leroy, P., et al. (1998). A Microsatellite map of wheat. *Genetics* 149, 2007–2023.

Roy, J. K., Prasad, M., Varshney, R. K., Balyan, H. S., Blake, T. K., Dhaliwal, H. S., et al. (1999). Identification of a microsatellite on chromosomes 6B and a STS on 7D of bread wheat showing an association with preharvest sprouting tolerance. *Theor. Appl. Genet*. 99, 336–340. doi: 10.1007/s001220051241

Saghai-Maroof, M. A., Biyashev, R. M., Yang, G. P., Zhang, Q., and Allard, R. W. (1994). Extraordinary polymorphic microsatellite DNA in Barley: species diversity, chromosomal locations and population dynamics. *Proc. Natl. Acad. Sci. U.S.A.* 91, 5466–5470.

Shorinola, O., Bird, N., Simmonds, J., Berry, S., Henriksson, T., Jack, P., et al. (2016). The wheat Phs-A1 pre-harvest sprouting resistance locus delays the rate of seed dormancy loss and maps 0.3 cM distal to the PM19 genes in UK germplasm. *J. Exp. Bot.* 67, 4169–4178. doi: 10.1093/jxb/erw194

Singh, R., Hucl, P., Aga, M. B., and Chibbar, R. N. (2012). Validation of molecular markers for pre-harvest sprouting resistance in bread wheat. *Cer. Res. Commun*. 40, 194–204. doi: 10.1556/CRC.40.2012.2.3

Smit, H. A., Tolmay, V. L., Barnard, A., Jordaan, J. P., Koekemoer, F. P., Otto, W. M., et al. (2010). An overview of the context and scope of wheat (*Triticum aestivum*) research in South Africa from 1983 to 2008. *S. A. J. Plant Soil* 27, 81–96. doi: 10.1080/02571862.2010.10639973

Trethowan, R. M., Rajaram, S., and Ellison, F. W. (1996). Preharvest sprouting tolerance in wheat in the field and under rain simulation. *Aust. J. Agric. Res*. 47, 705–716. doi: 10.1071/AR9960705

Tyagi, S., and Gupta, P. K. (2012). Meta-analysis of QTLs involved in Pre-harvest sprouting tolerance and dormancy in bread wheat. *Triticeae Genom. Genet.* 3, 9–24. doi: 10.5376/tgg.2012.03.0002

Yang, Y., Zhao, X. L., Xia, L. Q., Chen, X. M., Xia, X. C., Yu, Z., et al. (2007). Development and validation of a viviparous-1 STS marker for pre-harvest sprouting tolerance in Chinese wheats. *Theor. Appl. Genet.* 115, 971–980. doi: 10.1007/s00122-007-0624-z

Zhang, X.-Q., Li, C., Tay, A., Lance, R., Mares, D., Cheong, J., et al. (2008). A new PCR-based marker on chromosome 4AL for resistance to pre-harvest sprouting in wheat (*Triticum aestivum* L.) *Mol. Breed.* 22, 227–236. doi: 10.1007/s11032-008-9169-3

Zhou, K., Yang, J., Wang, Z.-X., and Wang, J.-R. (2017). Sequence analysis and expression profiles of TaABI5, a pre-harvest sprouting resistance gene in wheat. *Genes Genom.* 39, 161–171. doi: 10.1007/s13258-016-0483-6

Conflict of Interest Statement: The authors declare that the research was conducted in the absence of any commercial or financial relationships that could be construed as a potential conflict of interest.

The reviewer FG and handling Editor declared their shared affiliation.

frontiers in Plant Science

ORIGINAL RESEARCH
published: 13 September 2017
doi: 10.3389/fpls.2017.01555

Haplotype Analysis of the Pre-harvest Sprouting Resistance Locus *Phs-A1* Reveals a Causal Role of *TaMKK3-A* in Global Germplasm

*Oluwaseyi Shorinola[1], Barbara Balcárková[2], Jessica Hyles[3], Josquin F. G. Tibbits[4], Matthew J. Hayden[4], Katarina Holušova[2], Miroslav Valárik[2], Assaf Distelfeld[5], Atsushi Torada[6], Jose M. Barrero[3] and Cristobal Uauy[1]**

[1] John Innes Centre, Norwich, United Kingdom, [2] Institute of Experimental Botany, Centre of the Region Haná for Biotechnological and Agricultural Research, Olomouc, Czechia, [3] Commonwealth Scientific and Industrial Research Organisation (CSIRO), Agriculture and Food, Canberra, ACT, Australia, [4] Department of Economic Development, Jobs, Transport and Resources, Centre for AgriBioscience, Bundoora, VIC, Australia, [5] The Institute for Cereal Crop Improvement, Tel Aviv University, Tel Aviv, Israel, [6] HOKUREN Agricultural Research Institute, Naganuma, Japan

OPEN ACCESS

Edited by:
Hikmet Budak,
Montana State University,
United States

Reviewed by:
Alessandro Tondelli,
Consiglio per la Ricerca in Agricoltura e l'Analisi dell'Economia Agraria (CREA), Italy
Marco Maccaferri,
Consiglio per la Ricerca in Agricoltura e l'Analisi dell'Economia Agraria (CREA), Italy
Mike Giroux,
Montana State University,
United States

***Correspondence:**
Cristobal Uauy
cristobal.uauy@jic.ac.uk

Specialty section:
This article was submitted to Crop Science and Horticulture, a section of the journal Frontiers in Plant Science

Received: 25 May 2017
Accepted: 25 August 2017
Published: 13 September 2017

Citation:
Shorinola O, Balcárková B, Hyles J, Tibbits JFG, Hayden MJ, Holušova K, Valárik M, Distelfeld A, Torada A, Barrero JM and Uauy C (2017) Haplotype Analysis of the Pre-harvest Sprouting Resistance Locus Phs-A1 Reveals a Causal Role of TaMKK3-A in Global Germplasm. Front. Plant Sci. 8:1555. doi: 10.3389/fpls.2017.01555

Pre-harvest sprouting (PHS) is an important cause of quality loss in many cereal crops and is particularly prevalent and damaging in wheat. Resistance to PHS is therefore a valuable target trait in many breeding programs. The *Phs-A1* locus on wheat chromosome arm 4AL has been consistently shown to account for a significant proportion of natural variation to PHS in diverse mapping populations. However, the deployment of sprouting resistance is confounded by the fact that different candidate genes, including the tandem duplicated *Plasma Membrane 19* (*PM19*) genes and the *mitogen-activated protein kinase kinase 3* (*TaMKK3-A)* gene, have been proposed to underlie *Phs-A1*. To further define the *Phs-A1* locus, we constructed a physical map across this interval in hexaploid and tetraploid wheat. We established close proximity of the proposed candidate genes which are located within a 1.2 Mb interval. Genetic characterization of diverse germplasm used in previous genetic mapping studies suggests that *TaMKK3-A*, and not *PM19*, is the major gene underlying the *Phs-A1* effect in European, North American, Australian and Asian germplasm. We identified the non-dormant *TaMKK3-A* allele at low frequencies within the A-genome diploid progenitor *Triticum urartu* genepool, and show an increase in the allele frequency in modern varieties. In United Kingdom varieties, the frequency of the dormant *TaMKK3-A* allele was significantly higher in bread-making quality varieties compared to feed and biscuit-making cultivars. Analysis of exome capture data from 58 diverse hexaploid wheat accessions identified fourteen haplotypes across the extended *Phs-A1* locus and four haplotypes for *TaMKK3-A*. Analysis of these haplotypes in a collection of United Kingdom and Australian cultivars revealed distinct major dormant and non-dormant *Phs-A1* haplotypes in each country, which were either rare or absent in the opposing germplasm set. The diagnostic markers and haplotype information reported in the study will help inform the choice of germplasm and breeding strategies for the deployment of *Phs-A1* resistance into breeding germplasm.

Keywords: dormancy, seed, *PM19*, *TaMKK3-A*, pre-harvest sprouting, *Triticum aestivum*, haplotype

INTRODUCTION

Pre-harvest sprouting (PHS) refers to the too-early germination of physiologically matured grains while still on the ear, but before harvest. PHS is primarily caused by insufficient levels, or rapid loss, of seed dormancy and is an important cause of quality loss in many cereal crops (Li et al., 2004; Fang and Chu, 2008). This is particularly relevant in wheat due to its detrimental effects on bread-making potential which represents the most common use of wheat grains globally (Simsek et al., 2014). PHS is believed to be a modern phenomenon, as progenitor and wild wheat species generally display high levels of seed dormancy (Gatford et al., 2002; Lan et al., 2005). Selection for reduced seed dormancy during domestication and modern breeding programs allowed for more uniform seed germination and rapid crop establisment (Nave et al., 2016). However, this also resulted in higher level of susceptiblity to PHS in modern wheat varieties (Barrero et al., 2010). In addition to its detrimental effect on quality, PHS also reduces yield and affects seed viability, making resistance to PHS a high priority in many breeding programs.

Occurrence of PHS is heavily influenced by the environment. PHS is prevalent in wheat growing regions with high levels of rainfall during the period of grain maturation and after-ripening. Increased ambient temperature during this period can further increase the susceptibility of grains to sprouting (Barnard and Smith, 2009; Mares and Mrva, 2014). This enviromental dependency of PHS constitutes a constraint in selecting for PHS resistance in field conditions. In addition, resistance to PHS is highly quantitative and is controlled by numerous quantitative trait loci (QTL) located on all 21 chromosomes of bread wheat (Flintham et al., 2002; Kulwal et al., 2005; Mori et al., 2005; Kottearachchi et al., 2006; Ogbonnaya et al., 2007; Liu et al., 2008; Torada et al., 2008; Xiao-bo et al., 2008; Mohan et al., 2009; Munkvold et al., 2009; Knox et al., 2012; Kulwal et al., 2012; Gao et al., 2013; Lohwasser et al., 2013; Mares and Mrva, 2014; Kumar et al., 2015). This makes resistance to PHS one of the most multi-genic traits in wheat and further highlights the complexity in breeding for this trait.

Despite the multi-genic control of PHS resistance, a few major loci have been consistently shown to account for a significant proportion of natural variation to sprouting in diverse mapping populations. This include the homoeologous *R* (Red color) genes on the long arms of chromosome group 3 controlling seed coat color, *Qphs.pseru-3AS* (same as *QPhs.ocs-3A.1*) on chromosome 3AS and a locus on chromosome arm 4AL, designated as *Phs-A1* (Flintham, 2000; Himi and Noda, 2005; Mori et al., 2005; Liu et al., 2008; reviewed by Mares and Mrva, 2014). Consistent with its strong effect, *Phs-A1* has been identified in at least 11 bi-parental and multi-parent mapping populations derived from diverse germplasm from Australia, United Kingdom, Japan, China, Mexico, Canada and Europe (Torada et al., 2005; Ogbonnaya et al., 2007; Chen et al., 2008; Torada et al., 2008; Cabral et al., 2014; Albrecht et al., 2015; Barrero et al., 2015). Physiological evaluation of *Phs-A1* shows that it delays the rate of dormancy loss during seed after-ripening when plants are grown across a wide range of temperatures (13°C–22°C; Shorinola et al., 2016).

Unlike the *Qphs.pseru-3AS* and *R* loci, which have been unequivocally cloned to be wheat *Mother of Flowering Time* (*TaMFT; same as TaPHS1*) and *Myb10 transcription factor* (*TaMyb10*), respectively (Himi and Noda, 2005; Nakamura et al., 2011; Liu et al., 2013), two different candidate genes have been proposed to underlie the effect of *Phs-A1*. Recently, two independent studies by Barrero et al. (2015) and Torada et al. (2016) identified the tandem duplicated *Plasma Membrane 19* (*PM19-A1* and *PM19-A2*) genes and a *mitogen-activated protein kinase kinase 3* (*TaMKK3-A*) gene, respectively, as candidates for *Phs-A1*. The *PM19* genes were identified through a combined genetic approach using multi-parent mapping populations and transcriptomic analysis of near-isogenic recombinant inbred lines. The *TaMKK3-A* gene was identified through a more traditional positional cloning strategy using bi-parental mapping populations. Each study confirmed the effect of the gene(s) on dormancy through either down-regulation of transcript levels through RNA interference (*PM19*) or transgenic complementation of the susceptible parent with the resistant allele (*TaMKK3-A*).

It is presently unclear whether the sprouting variation associated with *Phs-A1* across diverse germplasm is due to allelic variation at *PM19* or *TaMKK3-A* alone, or if it's due to a combination of both genes (Torada et al., 2016). Fine-mapping studies (Shorinola et al., 2016) defined *Phs-A1* to a genetic interval distal to *PM19* for United Kingdom germplasm, consistent with the position of *TaMKK3-A*. However, a comprehensive understanding of *Phs-A1* diversity taking into account both *PM19* and *TaMKK3-A* genes across a wider set of germplasm is lacking.

In this study, we characterized the *Phs-A1* physical interval in both hexaploid and tetraploid emmer wheat to establish the physical proximity of *PM19* and *TaMKK3-A*. We developed markers for the candidate genes, and showed *TaMKK3-A* alleles to be diagnostic for sprouting resistance in a panel of parental lines from mapping populations in which *Phs-A1* was identified. We used diploid, tetraploid and hexaploid accessions to further trace the origin of the sprouting susceptible *TaMKK3-A* allele and used exome capture data from the wheat HapMap panel (Jordan et al., 2015) to examine the haplotype variation across the *Phs-A1* locus.

MATERIALS AND METHODS

Physical Map Sequence Assembly and Annotation

A fingerprinted Bacterial Artificial Chromosome (BAC) library of flow-sorted 4A chromosome was used for constructing the Chinese Spring *Phs-A1* physical map[1]. Using the high-throughput BAC screening approach described by Cvikova et al. (2015), a sequence database made from a three-dimensional pool of BAC clones comprising the Minimum Tilling Path (MTP) was searched for the sequences of *PM19-A1* and *TaMKK3-A*. This identified two positive clones for *PM19-A1* (TaaCsp4AL037H11

[1]https://urgi.versailles.inra.fr/gb2/gbrowse/wheat_phys_4AL_v2/

and TaaCsp4AL172K12) and three positive clones for *TaMKK3-A* (TaaCsp4AL032F12, TaaCsp4AL012P14 and TaaCsp4AL002F16; Supplementary Table S1). Using Linear Topology Contig (LTC; Frenkel et al., 2010) BAC clustering information for this library, we identified the BAC clusters (defined as a network of overlapping BACs forming a contiguous sequence) to which these BACs belong. The *PM19-A1*-containing BACs belong to BAC Cluster 16421 which has 20 BACs in its MTP while the *TaMKK3-A*-containing BACs belong to BAC Cluster 285 comprised of four MTP BACs (Supplementary Table S1).

DNA of the BACs was extracted using the Qiagen Plasmid Midi Kit (Qiagen, Cat. No. 12143). Eleven of the 20 MTP BACs containing and distal to *PM19-A1* in the physical map of Cluster 16421 and the four MTP BACs of Cluster 285 were sequenced on the Illumina MiSeq with 250 bp paired-end reads. An average of 2,105,488 and 2,752,220 paired-end reads per BAC were produced for Cluster 16421 and 285 BACs, respectively. Illumina reads for each BAC were separately assembled using the CLC Bio genomic software[2]. Before assembly, reads were filtered to remove contaminant sequences by mapping to the BAC vector (pIndigoBAC-5) sequence and the *Escherichia coli* genome. *De novo* assembly of reads after contaminant removal was done with the following assembly parameters: Word size: 64 bp; Bubble size: 250 bp; Mismatch cost: 2; Insertion cost: 3; Deletion cost 3; Length fraction: 90%; Similarity fraction: 95%.

The assembled contigs were repeat-masked by BLASTn analysis against the Triticeae Repeat Element Database (TREP[3]; Wicker et al., 2000). Gene annotation was performed using the wheat gene models described by Krasileva et al. (2013) and by BLASTX analysis to NBCI nr.[4] Gene models were also obtained by *ab initio* gene prediction with FGENESH (Solovyev et al., 2006). Only FGENESH gene models with protein sequence support from NCBI or *Ensembl* Plant protein databases[5] were used. Gene models with greater than 90% protein or nucleotide sequence identity and more than 75% sequence coverage to already annotated genes on NCBI or *Ensembl* databases were considered as high confidence genes. Gene models that did not meet these criteria were considered as low confidence genes, and were not analyzed further.

TaMKK3-A Genotyping

A Kompetitive Allele Specific PCR (KASP; Smith and Maughan, 2015) assay was developed for genotyping the C to A (C > A) causal *TaMKK3-A* mutation reported by Torada et al. (2016). For this, two allele-specific reverse primers (*TaMKK3-A-snp1-res*: TTTTTGCTTCGCCCTTAAGG and *TaMKK3-A-snpA1-sus:* TTTTTGCTTCGCCCTTAAGT) each containing the allele-specific SNP at the 3′ end, were used in combination with a common A-genome specific forward primer (GCATAGAGATCTAAAGCCAGCA). To distinguish the amplification signal produced from each allele specific primer, FAM and HEX fluorescence dye probes (Ramirez-Gonzalez et al., 2015) were added to the 5′ end of *TaMKK3-A-snpA1-res* and *TaMKK3-A-snpA1-sus,* respectively. KASP assays were performed as previously described (Shorinola et al., 2016).

In addition to the KASP assay, a genome-specific Cleavage Amplified Polymorphism Sequence (CAPS) assay (Konieczny and Ausubel, 1993), designated as *TaMKK3-A-caps,* was developed. This CAPS marker is associated with the presence/absence of an *Hpy*166II restriction site which co-localizes with the C > A causal polymorphism in the fourth exon of *TaMKK3-A*. Genome-specific primer pairs (Forward: CACCAAAGAATAGAAATGCTCTCT and Reverse: AGGAGTAGTTCTCATTGCGG) were designed to amplify an 887-bp sequence including the fourth exon. PCR was performed with Phusion High Fidelity polymerase (NEB, United Kingdom; Cat No: M0530S) in a 50 μL volume containing 20% buffer, 0.2 mM of dNTP, 5 μM each of *TaMKK3-A-cap* forward and reverse primers, 3% of DMSO, 200 – 400 ng of genomic DNA and 0.5 unit of Phusion polymerase (NEB, United Kingdom; Cat No: M0530S). Thermal cycling was done with Eppendorf Mastercycler® Pro Thermal Cyclers with the following program: initial denaturation at 98°C for 2 min; 35 cycles of denaturation at 98°C for 30 s; Annealing at 62°C for 30 s and extension at 72°C for 60 s; final extension at 72°C for 10 min. Following PCR amplification, a 25 μL restriction digest reaction containing 21.5 μL of the final PCR reaction, 2.5 μL of CutSmart® Buffer (NEB, United Kingdom; Cat No: B7204S) and 10 units of *Hpy*166II was incubated at 37°C for 1 h. Digest products were separated on a 1.5% agarose gel.

PM19-A1 Genotyping

Detection of an 18 bp deletion on the promoter region of *PM19-A1* was carried out using primers TaPM19-A1-5F (GAAACAGCTACCGTGTAAAGC) and TaPM19-A1-5R (TGGTGAAGTGGAGTGTAGTGG) reported by Barrero et al. (2015). PCR reaction mixture contained template DNA, 2.5 mM $MgCl_2$, 1.5 mM dNTP, 1.5 μM of each primer, and 1 unit of *Taq* polymerase (NEB). The reaction mixture was made up to a total volume of 10 μl. The PCR conditions were as follows: 3 min at 94°C, followed by 30 cycles of 40 s at 94°C, 40 s at 60°C, and 1 min at 72°C. The last step was incubation for 7 min at 72°C. The PCR products were resolved on a 4% agarose gel and visualized with SYBR green I (Cambrex Bio Science, Rockland, ME, United States).

Germplasm for Genetic Characterization of *TaMKK3* and *PM19*

We genotyped *PM19* and *TaMKK3-A* across 23 wheat varieties previously reported to segregate for *Phs-A1*, including United Kingdom (Alchemy, Robigus, Option, Claire, Boxer, Soleil), Australian (Yitpi, Baxter, Chara, Westonia, Cranbrook, Aus1408, Janz, Cunningham, Halberd), Japanese (Kitamoe, Haruyokoi, OS21-5), Mexican/CIMMYT (W7984, Opata M85), Canadian (Leader), Chinese (SW95-50213) and Swiss varieties (Münstertaler). We also genotyped *TaMKK3-A* in accessions from progenitor species *T. urartu* (41 accessions; A^u genome), *T. turgidum* ssp. *dicoccoides* (151 accessions; AABB genomes),

[2]www.clcbio.com

[3]wheat.pw.usda.gov/ITMI/Repeats

[4]https://blast.ncbi.nlm.nih.gov/

[5]https://plants.ensembl.org

804 hexaploid accessions from the Watkins landrace collection (Wingen et al., 2014), and 457 modern European bread wheat varieties from the Gediflux collection released between 1945 and 2000 (Reeves et al., 2004).

Variant Calling and Haplotype Analysis

We examined the haplotype structure around the *Phs-A1* locus in three different germplasm sets. These included 457 varieties in the Gediflux collection, a panel of 195 Australian varieties, and the wheat Haplotype Map (HapMap) panel consisting of 62 diverse global accessions (Jordan et al., 2015). For the HapMap panel, we selected polymorphic sites as follows. We extracted SNP information from published variant call files (VCF) produced from whole exome capture (WEC) resequencing dataset of the 62 HapMap lines[6]. For this, the corresponding IWGSC contig information for genes represented in the *Phs-A1* physical map were first obtained and used to filter the HapMap VCF for SNP sites located within these contigs. We kept SNP sites with allele frequencies of >5% and accessions with >80% homozygous calls across SNPs. Allele information at the selected SNP loci was reconstructed for each line using the reference, alternate and genotype field information obtained from the VCF. Haplotype cluster analysis was done with Network 5.0.0.0 (Fluxus Technology Limited, United Kingdom) using the Median Joining Network Algorithm. Haplotypes in the Gediflux and Australian germplasm were defined using a subset of the HapMap SNPs which were most informative in distinguishing between the HapMap haplotypes and with >30% allele frequency.

Pedigree Visualization

Pedigree information was obtained from the Genetic Resources Information System for Wheat and Triticale (GRIS[7]) and the International Crop Information System (ICIS[8]). Pedigree visualization was performed with Helium (Shaw et al., 2014). The coefficient of parentage (COP) analysis (i.e., the probability that alleles of two individuals are identical by descent) was calculated for all pairwise comparisons of lines within the most prevalent haplotypes (Australian: H1/H2 and H5/H7; United Kingdom: H3 and H12). For accuracy, landraces or cultivars with unknown or ambiguous pedigrees were not included in the COP analysis. Diversity within haplotype groups was estimated by the mean calculation of all COPs within each matrix.

RESULTS

TaMKK3-A and *PM19* Are Located within a 1.2 Mb Physical Interval

We constructed an extended physical map across the *Phs-A1* interval to investigate the physical proximity between the *TaMKK3-A* and *PM19* candidate genes. Using *PM19-A1* and *TaMKK3-A* sequences as queries, we screened *in silico* a BAC library of flow-sorted 4AL chromosome arm of the bread wheat cultivar Chinese Spring (CS). *PM19-A1* and *TaMKK3-A* were found on two independent non-overlapping BAC clone clusters which were anchored on the high resolution radiation hybrid map of chromosome 4A (Balcárková et al., 2016). The MTP of Cluster 16421 (*PM19*) was comprised of 20 BAC clones whereas the MTP of Cluster 285 (*TaMKK3-A*) included four BAC clones (**Figure 1A** and Supplementary Table S1).

Individual BACs were sequenced, assembled, repeat-masked and annotated for coding sequences. In eleven of the 20 MTP BACs of Cluster 16421 sequenced, nine high-confidence genes were found in addition to the *PM19-A1* and *PM19-A2*. These included *YUCCA3-like, Myosin-J Heavy Chain protein, Ubiquitin Conjugating Enzyme, Amino-Cyclopropane Carboxylate Oxidase 1 like (ACC Oxidase-1),* two *Leucine-Rich Repeat Kinases* (*LRR kinase 1 and LRR kinase 2*), *Agmatine Coumaroyl Transferase, Malonyl Coenzyme A:anthocyanin 3-O-glucoside-6″-O-malonyltransferase* and a gene encoding for a hypothetical protein. In addition to *TaMKK3-A*, Cluster 285 contained four additional genes including *Protein Phosphatase1-Like (PP1-Like), Activating Signal Co-integrator 1- Like* (*ASC1-Like*), *Ethylene Responsive Factor-1B-Like* (*ERF-1B-Like*) and a gene fragment showing high sequence similarity to *ERF-1B-Like* and as such designated as *ERF-C*. Together, this highlights the presence of at least 16 protein-coding genes across the *Phs-A1* interval in hexaploid bread wheat (**Figure 1**).

We also characterized the *Phs-A1* interval in the recently constructed assembly of a wild emmer wheat, Zavitan (**Figure 1B**; Hen-Avivi et al., 2016; Avni et al., 2017). This allowed comparative analysis of the *Phs-A1* interval in tetraploid and hexaploid wheat species. Fifteen of the 16 genes found in the CS physical map were located on two Zavitan scaffolds. Nine of these 15 genes were positioned across a 0.93 Mb interval on the Zavitan 4A pseudomolecule. These included 4 genes from BAC Cluster 285 and five genes from BAC Cluster 16421 (**Figure 1**). The remaining six genes spanned a 0.13 Mb interval on an unanchored scaffold. On average, the coding sequence identity between CS and Zavitan was 99.7% across the genes shared by both assemblies. We could not find sequence for *ERF-C* in the Zavitan assembly at similar identity. We annotated two genes encoding for disease resistance protein *RPM1* in the Zavitan sequence corresponding to the gap between the two CS BAC clusters. Combining the CS and Zavitan physical maps, the physical region between *TaMKK3-A* and the *PM19* genes was covered and estimated to be approximately 1.2 Mb (**Figure 1**).

TaMKK3-A Is Most Closely Associated with *Phs-A1*

Torada et al. (2016) reported a C > A mutation in position 660 of the *TaMKK3-A* coding sequence (C660A) as being causative of the *Phs-A1* effect. Using alignments of the three wheat genomes, we developed a genome-specific and co-dominant KASP assay for this SNP designated as *TaMKK3-A-snp1*. The *TaMKK3-A-snp1* assay is co-dominant as it distinguished between heterozygotes and homozygotes F_2 progenies in the Alchemy × Robigus population previously reported to segregate for *Phs-A1* (Shorinola et al., 2016; **Figure 2A**). We also developed

[6]https://wheat-urgi.versailles.inra.fr/Seq-Repository/Variations

[7]http://wheatpedigree.net/

[8]www.icis.cgiar.org

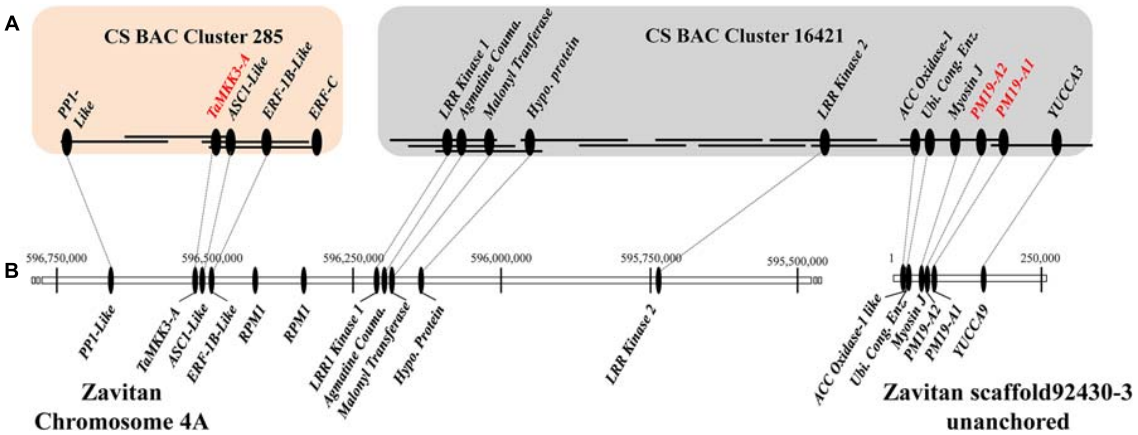

FIGURE 1 | Physical map of the *Phs-A1* interval in bread wheat Chinese Spring (CS) and wild emmer (Zavitan). **(A)** *Phs-A1* interval in CS is covered by two non-overlapping BAC clusters: Cluster 285 (4 BACs) and Cluster 16421 (11 of the 20 MTP BACs). BACs are represented by solid lines while genes found on the BAC are represented by filled ovals. The proposed candidate genes for *Phs-A1* are in red font. **(B)** Whole genome assembly of Zavitan wild emmer across the *Phs-A1* interval. Genes present in both assemblies are joined by dotted lines.

a CAPS marker (Konieczny and Ausubel, 1993) for *TaMKK3-A* to enable genotyping of *Phs-A1* using a gel-based assay. This marker, designated as *TaMKK3-A-cap*, amplifies a genome-specific 887 bp region and is designed to discriminate for the presence of an *Hpy*166II site (GTNNAC) which is lost by the C660A mutation. Dormant lines with the C allele maintain the *Hpy*166II site which leads to digestion of the 887 bp amplicon into fragments of 605 and 282 bp (**Figure 2B**). Conversely, non-dormant lines with the A allele lose the *Hpy*166II site and hence remain intact (887 bp) after digestion. As with the KASP assay, the CAPS marker was co-dominant when used to genotype F_2 progenies (**Figure 2B**).

Using the KASP assay, we genotyped a panel comprised of the parents of 11 bi-parental mapping populations and a MAGIC population in which *Phs-A1* had previously been reported (**Table 1**). The *TaMKK3-A-snp1* was polymorphic and diagnostic for *Phs-A1* in all parental lines. Consistent with Torada et al. (2016), non-dormant sprouting-susceptible parents carry the *TaMKK3-A* "A" allele while all the dormant sprouting-resistant parents carry the *TaMKK3-A-snp1* "C" allele (**Table 1**). We genotyped the same panel for the promoter deletion in *PM19-A1* previously proposed to be causal of PHS susceptibility (Barrero et al., 2015). We found the *PM19-A1* deletion to be linked with the non-dormant *TaMKK3-A* A allele in most, but not all, of these populations. The putative linkage was broken in the dormant Kitamoe, OS21-5 and SW95-50213 parents, whose dormancy phenotypes are not consistent with their *PM19-A1* promoter deletion status, but can be explained by their *TaMKK3-A* genotype (**Table 1**). This association was confirmed genetically in the SW95-50213 × AUS1408 cross. This population, which did not segregate for the dormancy phenotype in the original work by Mares et al. (2005), is monomorphic for the dormant C allele at *TaMKK3-A*, but segregates for the *PM19-A1* deletion. Similarly, parents of the two populations OS21-5 × Haruyokoi and Kitamoe × Münstertaler segregating for the dormancy phenotype in the work by Torada et al. (2005) are monophormic for the *PM19-A1* deletions, but segregate accordingly for the *TaMKK3-A* causal mutation. These results strongly support *TaMKK3-A* as the most likely causal gene for *Phs-A1* across this highly informative panel.

Origin and Distribution of the *TaMKK3-A* Alleles in Ancestral and Modern Germplasm

To examine the origin, distribution and allele frequencies of the causative *TaMKK3-A* C660A SNP, we genotyped a set of 41 *T. urartu* (diploid: AA genome) and 151 *T. turgidum* ssp. *dicoccoides* (tetraploid: AABB genome) accessions. These represent the diploid and tetraploid progenitors of the modern bread wheat A genome on which *Phs-A1* is located. Torada et al. (2016) previously suggested that the non-dormant A allele was the mutant form since the dormant C SNP was conserved across different species. Across *T. urartu* accessions, the C allele was predominant (39 accessions) while the non-dormant A allele was present in only two accessions (5% allele frequency; **Figure 2C**). Similarly, across *T. dicoccoides* accessions, the dormant C allele was found in 134 accessions while the non-dormant allele was found in 17 accessions (11% allele frequency; **Figure 2C**). Our results are consistent with Torada et al. (2016) in that the non-dormant A allele is derived from the wild type C allele. In addition, the presence of the A allele across both progenitor species suggests that the mutation predates the hybridization and domestication events that gave rise to modern bread wheat.

We also genotyped the Watkins Collection representing a set of global bread wheat landraces collected in the 1920s and 1930s (Wingen et al., 2014), as well as the Gediflux collection comprised of modern European bread wheat varieties released between 1945 and 2000 (Reeves et al., 2004). The allele frequency of the non-dormant A allele was 13% in the Watkins landrace collection (**Figure 2C** and Supplementary Table S2), comparable to that in *T. dicoccoides* (11%). However, the non-dormant A allele frequency in the Gediflux collection was 48% across 457

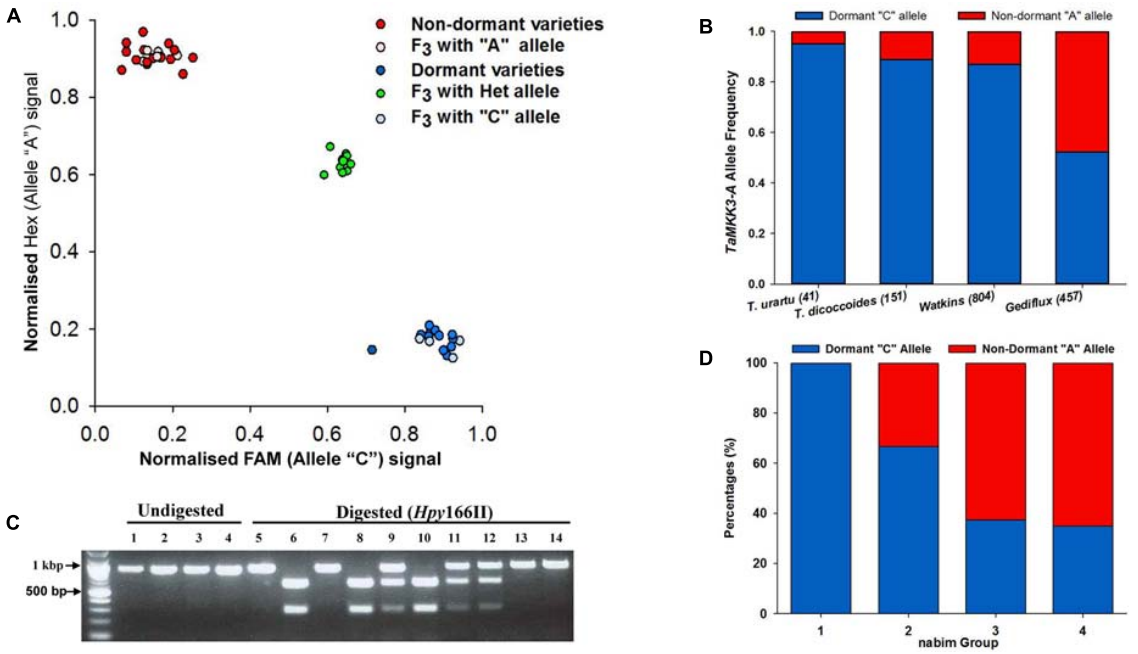

FIGURE 2 | Marker development and allele distribution of *MKK3-A* in ancestral and historic germplasm. **(A)** Genotype plot of varieties and a F_3 population segregating for *Phs-A1* using the *TaMKK3-A* KASP assay. **(B)** Development of co-dominant CAPS marker based on *Hpy*166II restriction digest of the C660A SNP. Lanes 1 - 4 contain undigested fragments of Robigus, Alchemy, Claire and Option, respectively, while Lanes 5 – 14 contain digested fragments of Robigus, Alchemy, Claire and Option (lanes 5–8) and six segregating F_3 plants from an Alchemy × Robigus cross (lanes 9–16). **(C)** Allele frequency of the causal C660A SNP in *T. urartu* and *T. turgidum* ssp. *dicoccoides* accessions and the Watkins and Gediflux collections. The number of lines genotyped in each germplasm set is in parenthesis. (D) *TaMKK3-A* allele distribution in the four wheat end-use groups (nabim 1–4) in the United Kingdom. The red and blue bars in **(C,D)** represents the non-dormant "A" allele" and dormant "C" allele, respectively.

varieties (**Figure 2C**). This represents a marked increase of the non-dormant allele in the more modern European collection when compared to the 15% A allele frequency of the European sub-population within the Watkins collection (Supplementary Table S2).

To determine if the *TaMKK3-A* dormant allele was associated with improved end-use quality, we genotyped 41 United Kingdom varieties representing the four United Kingdom market classes (**Figure 2D**, nabim groups 1–4; nabim, 2014). Of the 13 bread-making quality varieties (groups 1 and 2), 11 (85%) had the dormant *TaMKK3-A* allele. This frequency was significantly higher (Contingency table $\chi^2 = 8.497$; $P < 0.01$) than in the 28 biscuit and animal feed varieties (groups 3 and 4) in which the *TaMKK3-A* dormant allele was only present in 10 varieties (36%).

Phs-A1 Haplotypes in Global Germplasm

We next examined the allelic diversity across the extended *Phs-A1* interval (including *TaMKK3-A* and *PM19*) with the aim of elucidating the haplotype structure across this region. For this, we used the SNP Haplotype Map (HapMap) dataset obtained from WEC resequencing of 62 diverse germplasm (Jordan et al., 2015). From this SNP dataset, we obtained data for eight of the sixteen genes found in the *Phs-A1* interval (*PP1-like, TaMKK3-A, ASC1-like, ERF-C, LRR Kinase 1, LRR Kinase 2, PM19-A2* and *PM19-A1*) corresponding to 51 SNPs. To improve the accuracy of the haplotype analysis, we selected accessions with >80% homozygous calls across the selected genes and SNPs with >5% allele frequency. This filtering resulted in 39 SNPs across the eight genes in 58 accessions.

Across the *Phs-A1* interval (*PP1-like* to *PM19-A1*) we identified 14 distinct haplotypes (H1–14; **Figure 3A**). Haplotypes were comprised of a mix of cultivars, landrace, breeding lines and synthetic population in varying proportion (**Figure 3B** and Supplementary Table S3). H1 represented the major haplotype present in 33% of all accessions examined, whereas five haplotypes were relatively infrequent (<5%; H2, H5, H6, H9, H13). Six of the selected SNPs were found in *TaMKK3-A* including the causal C660A SNP in the fourth exon and five additional intron SNPs. These six SNPs defined four distinct *TaMKK3-A* haplotypes (**Figure 3C** and Supplementary Table S3; TaMKK3-A_HapA – D) in the HapMap collection with only one having the non-dormant A allele (TaMKK3-A_HapA). The non-dormant A allele was present in 50% of the HapMap population, consistent with the Gediflux collection (48%).

Haplotype Structure at the *Phs-A1* Interval in United Kingdom and Australian Germplasm

To characterize a larger set of European (Gediflux) and Australian germplasm, we selected seven informative

polymorphisms across seven genes from the HapMap dataset and developed KASP assays for these (Supplementary Table S4). Using these seven assays, we defined 16 haplotypes in the European Gediflux collection (Supplementary Table S5). This included eleven haplotypes previously identified in the global HapMap dataset and five haplotypes unique to this European germplasm set, although these were relatively infrequent (**Figure 4**). The United Kingdom subpopulation within the Gediflux collection comprised 176 varieties and contained 11 of the 15 haplotypes identified. Six haplotypes include the dormant *TaMKK3-A* C allele (63% of United Kingdom varieties), with the majority of these varieties sharing haplotype H12 (89 of 110 varieties), consistent with the wider Gediflux population (**Figure 4**). This suggests one main source of PHS resistance in United Kingdom and European germplasm.

By combining haplotype and pedigree information for these lines we could trace, to a reasonable degree of accuracy, the founder lines for the most common resistant haplotypes in United Kingdom germplasm (Supplementary Figure S1). We identified the origin of the major resistant haplotype in the United Kingdom germplasm (H12) as ViImorin-27, a French winter wheat variety released in the late 1920s (**Figure 5** and Supplementary Figure S2). Vilmorin-27 was a direct parent and the donor of haplotype H12 for Cappelle–Desprez, a major founder variety for wheat breeding programs in Northern France and the United Kingdom released in 1948. Haplotype H12 has since remained an important part of United Kingdom breeding programs through varieties such as Rendezvous and Riband (released between 1985 and 1987).

Within the 195 Australian varieties we identified 12 haplotypes including ten previously identified HapMap haplotypes, and two Australian-specific haplotypes at low frequency (<1%, Supplementary Table S6 and Figure S3). Eight haplotypes present in 88 varieties (45%) have the dormant *TaMKK3-A* C allele while the other four haplotypes present in 107 varieties (55%) have the non-dormant *TaMKK3-A* A allele (Supplementary Figure S4). This represents a near balanced distribution of both alleles in Australian germplasm. In this set, 71% of lines with the dormant *TaMKK3-A* C alleles were traced to Federation (or Purple Straw) ancestry. Across the entire set, the alternative, non-dormant allele was more associated with the presence of cv. Gabo or CIMMYT-derived material in the pedigree. These lines had a more recent

TABLE 1 | *TaMKK3-A* and *PM19* alleles in *Phs-A1* association panel.

Population	Variety	Origin	Status*	*TaMKK3-A* Allele	*PM19-A1* promoter InDel	Reference
Alchemy × Robigus	Alchemy	UK	Dormant	C	Insertion	Shorinola et al., 2016
	Robigus	UK	Non-dormant	A	Deletion	
Option × Claire	Option	UK	Dormant	C	Insertion	Shorinola et al., 2016
	Claire	UK	Non-dormant	A	Deletion	
MAGIC Population	Yitpi	AUS	Dormant	C	Insertion	Barrero et al., 2015
	Baxter	AUS	Non-dormant	A	Deletion	
	Chara	AUS	Non-dormant	A	Deletion	
	Westonia	AUS	Non-dormant	A	Deletion	
Opata × W7984	W7984	MEX	Dormant	C	Insertion	Lohwasser et al., 2013
	Opata	MEX	Non-dormant	A	Deletion	
OS21-5 × Haruyokoi	OS21-5	JPN	Dormant	C	Deletion	Torada et al., 2008
	Haruyokoi	JPN	Non-dormant	A	Deletion	
Leader × Haruyokoi	Leader	CAN	Dormant	C	Insertion	Torada et al., 2008
	Haruyokoi	JPN	Non-dormant	A	Deletion	
Kitamoe × Münstertaler	Kitamoe	JPN	Dormant	C	Deletion	Torada et al., 2005
	Münstertaler	SUI	Non-dormant	A	Deletion	
Cranbrook × Halberd	Halberd	AUS	Dormant	C	Insertion	Mares et al., 2005; Zhang et al., 2008
	Cranbrook	AUS	Non-dormant	A	Deletion	
Janz × AUS1408	Aus1408	AUS, SA	Dormant	C	Insertion	Mares et al., 2005; Ogbonnaya et al., 2007
	Janz	AUS	Non-dormant	A	Deletion	
SW95-50213 × Cunningham	SW95-50213	CHN	Dormant	C	Deletion	Mares et al., 2005
	Cunningham	AUS	Non-dormant	A	Deletion	
SW95-50213 × AUS1408#	SW95-50213	CHN	Dormant	C	Deletion	Mares et al., 2005
	Aus1408	AUS, SA	Dormant	C	Insertion	
Boxer × Soleil	Soleil	UK	Dormant	C	Insertion	Flintham, 2000
	Boxer	UK	Non-dormant	A	Deletion	

**Phenotypic classifications are based on comparisons between the parental varieties of each population through genetic studies. #Phs-A1 was not detected in this population as the DH lines were generally dormant. However, limited number of lines showed transgressive segregation relative to the dormant phenotypes of the two parents.*

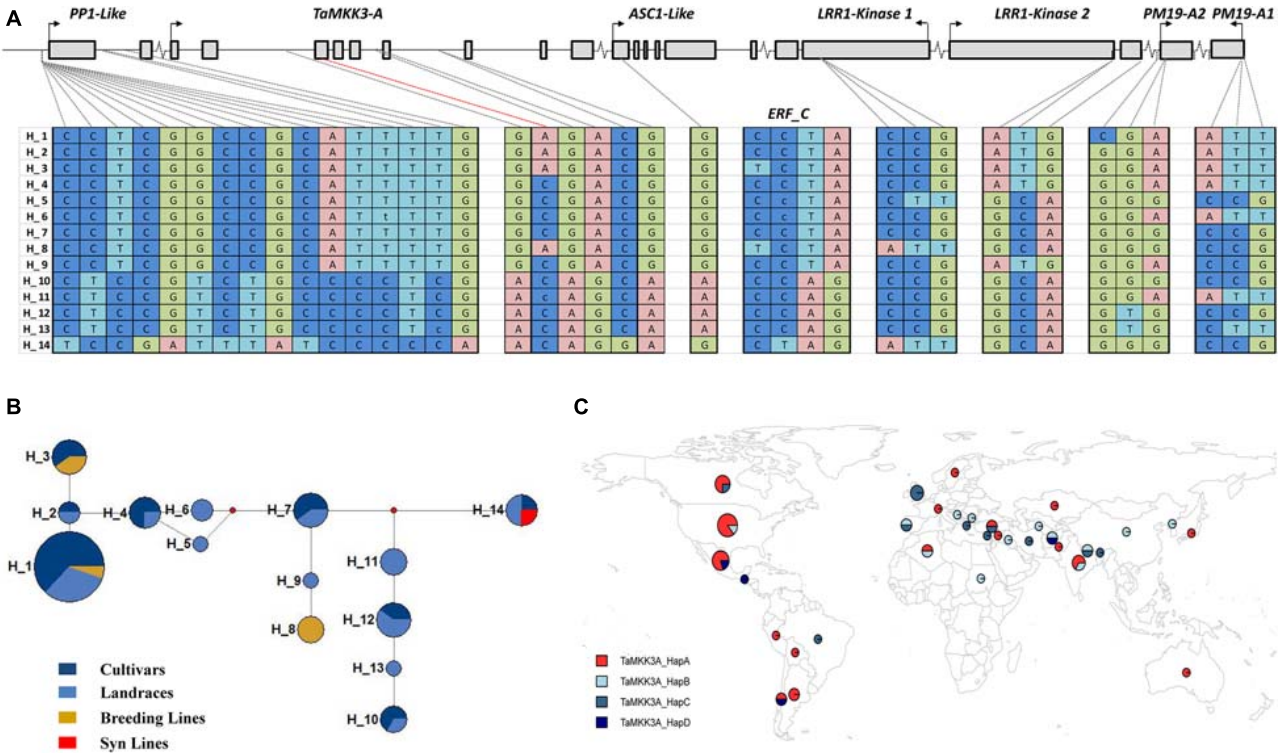

FIGURE 3 | *Phs-A1* haplotype analysis. **(A)** Structure of 14 haplotypes identified in the HapMap population across 39 SNP loci in the *Phs-A1* interval. SNP loci are ordered based on their physical position on the Zavitan assembly. Exons, intron and intergenic regions are represented by filled boxes, solid lines and breaks, respectively. Note that *ERF-C* is not on the Zavitan assembly. **(B)** Haplotype network of the 14 haplotypes. The size of each circle corresponds to the number of lines in each haplotype. Blue, light blue, amber and red represent cultivars, landraces, breeding and synthetic line in each haplotype, respectively. **(C)** Geographical distribution of the four *TaMKK3-A* haplotypes (Supplementary Table S3). The size of the circle represents the sample size obtained within each country while each section represents the proportion of the country sample size with the specified haplotype.

average release date of 1976 compared to the lines with the dormant allele (average release date 1941).

The mean COP for the Australian and United Kingdom Gediflux set of lines was 0.10 and 0.11 respectively (**Table 2**). Within each germplasm set, the lines with the most prevalent haplotypes had higher COP values, indicating a higher degree of relatedness amongst these lines relative to the entire collection (**Table 2**).

DISCUSSION

Physical Map

We characterized the *Phs-A1* interval by constructing a 1.5 Mb physical map spanning the *PM19* and *TaMKK3-A* candidate genes (Barrero et al., 2015; Torada et al., 2016) and including 16 protein-coding genes. We observed near perfect sequence and gene content conservation in the interval between hexaploid and tetraploid physical maps. A similar overall collinearity between bread wheat, barley and *Brachypodium* was also observed except for the interval between *ACC Oxidase-1* and *ERF-C* where the gene content in each species diverged (Supplementary Figure S5). The *PM19* candidates where conserved across these species, whereas *TaMKK3-A* was only present in barley and wheat.

Sequence information from the BAC-based CS assembly and the whole genome shotgun Zavitan assemblies was used in a complementary manner. Neither assembly was fully contiguous across the *Phs-A1* interval, but the gaps were different in the two assemblies allowing the spanning of the complete interval. This lack of contiguity was also present in the IWGSC WGA v0.4[9], TGAC (Clavijo et al., 2017) and Refeqv1.0 assemblies, where intervals covering *TaMKK3-A and ASC1-Like* were unanchored. While the new whole genome assemblies offer major improvements in contiguity, the available BAC physical maps will be of value to assign unanchored scaffolds or solve inconsistencies in regions were contiguity is broken.

TaMKK3-A Determines *Phs-A1* Effect across Diverse Germplasm

The 1.5 Mb physical interval which defines *Phs-A1* includes the proposed candidates *PM19* and *TaMKK3-A*, as well as other genes with potential roles in dormancy/germination regulation. For example, *ACC Oxidase-1* catalyzes the last steps in the biosynthesis of ethylene – a germination promoting hormone

[9]https://wheat-urgi.versailles.inra.fr/Seq-Repository/Assemblies

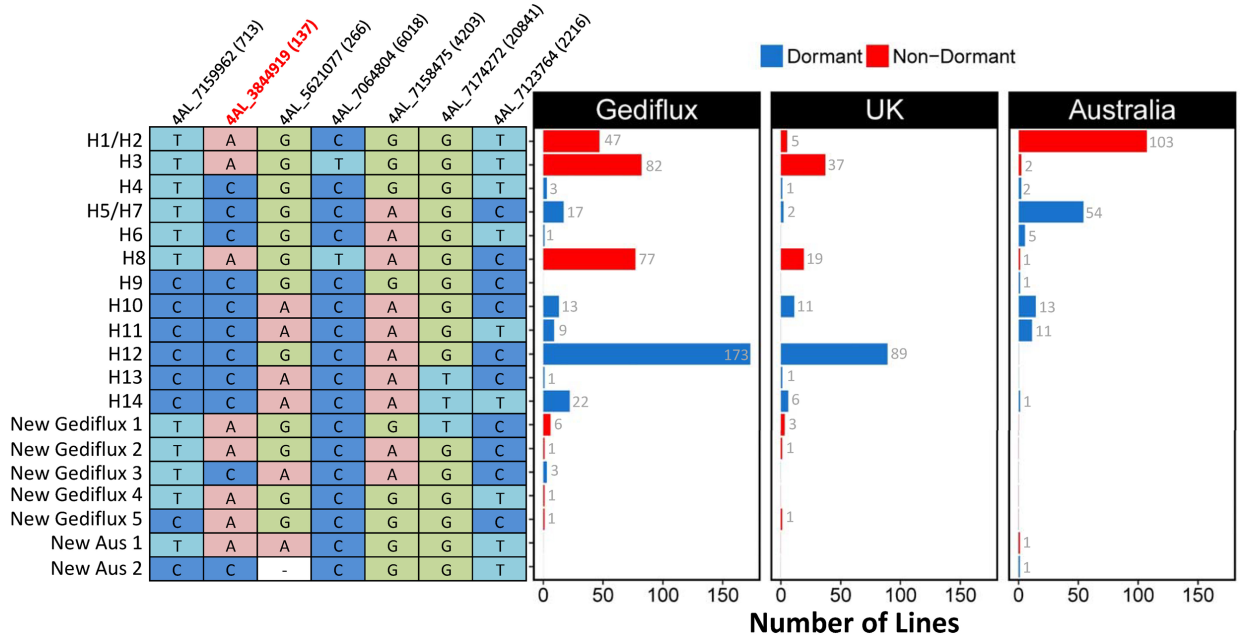

FIGURE 4 | Relationship between the European, United Kingdom, Australian and HapMap *Phs-A1* Haplotypes. The distribution (bar charts) of the HapMap and unique haplotypes found in the Gediflux (European), United Kingdom and Australian germplasm using genotype information of seven of the 39 HapMap SNPs within the *Phs-A1* interval. Red bars correspond to the non-dormant "A" allele, whereas blue bars correspond to the dormant "C" allele.

(Matilla and Matilla-Vázquez, 2008; Linkies and Leubner-Metzger, 2012; Corbineau et al., 2014). However, using two bi-parental mapping populations we showed linkage of *Phs-A1* to the interval between *PP1-Like – LRR Kinase 2* in United Kingdom populations, thereby excluding the *PM19* and *ACC Oxidase-1* loci as candidate genes (Shorinola et al., 2016). This was consistent with Torada et al. (2016) who identified *TaMKK3-A* as the causal gene in their mapping population and work in barley which identified the barley homolog (*MKK3*) as the causal gene for the seed dormancy QTL SD2 (Nakamura et al., 2016).

In support of this, the causal *TaMKK3-A* C660A SNP is perfectly associated with the phenotypes of 19 diverse parents of 11 mapping population in which *Phs-A1* had previously been identified. This was also the case for the parents of the MAGIC population (Yipti, Chara, Westonia, Baxter) previously used to propose the *PM19* loci as the causal gene (Barrero et al., 2015). Barrero et al. (2015) proposed a promoter deletion in *PM19-A1* affecting motifs important for ABA responsiveness as the cause of non-dormancy in sprouting susceptible genotypes. The *PM19-A1* deletion and the non-dormant *TaMKK3-A* A allele are in complete linkage in all the non-dormant parents from the multiple mapping populations. However, the *PM19-A1* promoter deletion did not account for the dormant phenotype of Kitamoe, OS21-5 and SW95-50213 (**Table 1**). These dormant varieties have the *PM19-A1* promoter deletion associated with low dormancy, but carries the dormant *TaMKK3-A* allele. These natural recombinants suggest that *TaMKK3-A* is the causal *Phs-A1* gene. SW95-50213 is a Chinese landrace which is an important source of *Phs-A1*-mediated dormancy in Australian breeding programs. When SW95-50213 was crossed to a line carrying both *TaMKK3-A* and *PM19* dormant alleles (AUS1408), no grain dormancy QTL could be identified (Mares et al., 2005). Despite the segregation of the *PM19-A1* promoter polymorphism in this population, all lines displayed dormant to intermediate dormancy phenotype consistent with the *TaMKK3-A* genotype of their parents. Taken together, this evidence confirms the tight linkage between *TaMKK3-A*, *PM19*, and the *Phs-A1* phenotype, and suggest that *TaMKK3-A*, but not *PM19*, is the causal gene underlying sprouting variation associated with *Phs-A1* in diverse European, North American, Australian, and Asian germplasm.

Breeding Implications

Given the identification of a number of *T. urartu* accessions with the non-dormant A allele, it is likely that the C660A mutation originates from this diploid ancestor and predates the domestication and hybridization events that gave rise to modern bread wheat. This is similar to the causal mutation in *TaPHS1*, the major gene controlling PHS resistance QTL on 3AS which was also found in diploid (*T. monococcum*) and hexaploid wheat species. However, unlike *TaMKK3-A*, it is believed that the diploid and hexaploid mutations in *TaPHS1* arose independently as these mutations could not be found in the diploid (*T. urartu*) and tetraploid (*T. dicoccoides*) A-genome progenitor of the modern bread wheat (Liu et al., 2015).

The non-dormant allele frequency was below 15% in accessions and landraces collected previous to 1920, but rose sharply to close to 50% in more modern germplasm. It is tempting to speculate that this could be due to selective pressure by breeders over the past 70 years for the non-dormant A allele in European and Australian environments. This pressure could be

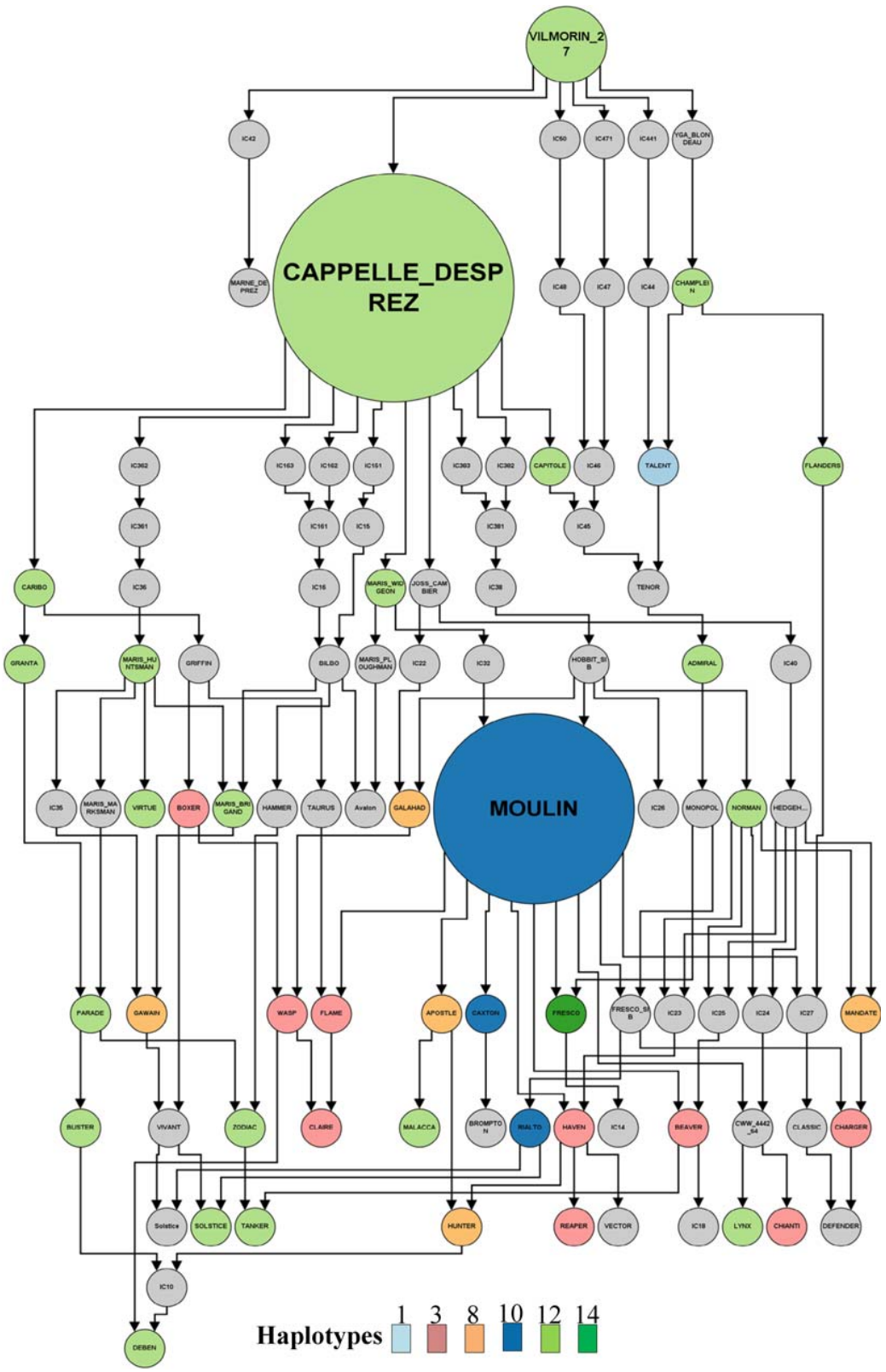

FIGURE 5 | Pedigree of selected United Kingdom and European varieties highlighting the origin of the major resistant haplotype (H12). Each circle represents a variety and colors represent the different haplotypes. Nodes are size based on the number of varieties derived from the node.

TABLE 2 | Mean Coefficient of Parentage (COP) within Australian and United Kingdom germplasm, and between groups of the most prevalent haplotypes containing dormant (C) and non-dormant (A) SNPs at *TaMKK3-A*.

Germplasm	Haplotype	*TaMKK3-A* SNP	Mean COP	Comparisons (n)
Australia	All	A/C	0.10	13530
Australia	H5/H7	C	0.17	350
Australia	H1/H2	A	0.15	2700
United Kingdom	All	A/C	0.11	1596
United Kingdom	H12	C	0.20	496
United Kingdom	H3	A	0.21	55

driven by selection for genotypes with more rapid and uniform germination that would be associated with the non-dormant allele. However, allele frequencies for both alleles have remained overall balanced given the improved end-use quality associated with the dormant allele. This hypothesis is supported by the fact that 85% of United Kingdom bread-making varieties carry the dormant allele, compared to only 35% of feed and biscuit-making varieties.

To facilitate breeding for PHS resistance, we developed co-dominant KASP and CAPS markers for the causal *TaMKK3-A* mutation, as well as KASP markers for the wider region. We identified 14 *Phs-A1* haplotypes in a global germplasm panel with four haplotypes for the *TaMKK3* gene itself, of which only one included the C660A non-dormant SNP. Comparison of Australian and United Kingdom haplotypes highlighted distinct frequencies in both sets with the most prevalent haplotypes containing the dormant *TaMKK3-A* allele differing in both countries. Haplotype H5/H7 is most frequent in Australian varieties, whereas haplotype H12 dominates in the United Kingdom. Interestingly, these haplotypes are either rare (<5% H5/H7 in United Kingdom) or absent (H12 not present in Australia) in the other country, suggesting distinct sources of PHS resistance in Australian and United Kingdom breeding programs. Understanding haplotypes structure across genes of agronomic interest is increasingly possible with the latest advances in wheat genomics (Clavijo et al., 2017; Uauy, 2017). It is also increasingly relevant given potential negative linkage drag associated with major phenology traits (Voss-Fels et al., 2017). The markers and knowledge generated in this study should facilitate the choice of parental genotypes for the deployment of *TaMKK3-A* in commercial cultivars.

The earliest line in the Australian set (Golden Drop, released 1840) carries the favorable TaMKK3-A 'C' SNP and also the most prevalent haplotype (H5/H7) at this locus. Golden Drop was derived from a Purple Straw/Yandilla cross and its sister line, Federation (released in 1901) became the foundation of many successful Australian cultivars due to earlier maturity and thus ability to avoid drought stress late in the growing season. Not only was Federation wheat better adapted to the Australian climate, it also had improved grain quality for milling, and so become widely adopted by breeders (Eagles et al., 2009).

The next major introduction of germplasm into Australia occurred in the 1970's, as CIMMYT material was deployed widely by breeders seeking traits affecting height, quality and disease resistance (Brennan and Fox, 1998). Important CIMMYT parents in Australian breeding include Sonora-64, Pitic, Pavon-76, WW15 and WW80. Pedigree analysis suggests that such material could be the source of the most prevalent haplotype in Australia (H1/H2) containing the non-favorable *TaMKK3-A* allele. A high proportion of modern Australian cultivars with the non-dormant haplotype suggests opportunities may exist for the incorporation of favorable alleles at the locus. In this context, current breeding programs in Australia are using SW95-50213 and also Aus1408 as a source of dormancy (Hickey et al., 2009), lines that carry the favourable allele at the *TaMKK3-A* locus.

Future Outlook

The dormant *TaMKK3-A* C allele is predominant in all the progenitor and historic germplasm evaluated in this study, suggesting that it represents the ancestral allele as proposed by Torada et al. (2016). The N220K amino acid substitution (C660A mutation) in the kinase domain results in a gain-of-function allele which reduces dormancy in wheat. This is in contrast with barley where the non-dormant *MKK3* allele is ancestral and the N260T substitution in the kinase domain results in a loss-of-function allele leading to increased seed dormancy (Nakamura et al., 2016). This provides an additional example of how for the same biological process, gain-of-function (dominant) mutations have been more readily selected in polyploid wheat compared to recessive variation in diploid barley (Borrill et al., 2015). The fact that the same gene has been selected in both species also suggests that the kinase activity of *TaMKK3-A* can be modulated to fine-tune the level of seed dormancy in temperate cereals. A better understanding of the activity and regulation of *TaMKK3-A* and its homoeologs could allow the identification of mutants (Krasileva et al., 2017) or the creating of gene edited alleles (Zong et al., 2017) with different levels of activity or the design of novel alleles with different degrees of dormancy.

In addition, the cloning of three of the major genes controlling PHS resistance (*TaMyb10, TaPHS1 and TaMKK3-A*) in wheat now offers a unique opportunity to examine how allelic combination of these genes can be used to modulate the levels of seed dormancy. Using a RIL population segregating for *Phs-A1* and *Qphs.pseru-3AS*, Mori et al. (2005) demonstrated the additive interaction between these loci. This suggests that the markers generated in this study and others (Himi et al., 2011; Liu et al., 2015) will be valuable in deploying different levels of seed dormancy across different agro-ecological zones.

AUTHOR CONTRIBUTIONS

OS led the genotype and pedigree analysis of the United Kingdom varieties, annotation of BAC sequences, developed the KASP and CAPS marker, and analyzed the HapMap data; JH performed pedigree analysis of Australian; JT and MH performed genotyping of Australian varieties; MV, BB, and KH constructed the 4AL physical map of

CS; AD constructed the physical map of tetraploid wheat Zavitan; AT performed genotyping of Japanese varieties; JB led the work on Australian varieties; OS, CU, JH, and JB contributed to the writing of the manuscript; OS and CU designed the experiments.

FUNDING

This work was supported by the United Kingdom Biotechnology and Biological Sciences Research Council (BBSRC), AHDB-HGCA, KWS, Lantmännen, Limagrain and RAGT (BB/I01800X/1, BB/J004588/1, BB/J004596/1, BB/P013511/1, BB/P016855/1). BB and MV were supported by grant LO1204 from the National Program of Sustainability I, by the Czech Science Foundation (14-07164S). OS was supported by the John Innes Foundation. The work performed in Australia was supported by the Grains and Research Development Corporation.

ACKNOWLEDGMENTS

We thank Chloe Riviere for help with plant husbandry and Dr. Sergio Galvez-Rojas for advice on data visualization. We also thank Katerina Viduka for the assistance in the genotyping, Dr. Ben Trevaskis and Dr. Howard Eagles for assistance in the pedigree analysis of the Australian collection, and Dr. Frank Gubler for the helpful discussions and support. We thank the International Wheat Genome Sequencing Consortium (IWGSC) for pre-publication access to the wheat genome RefSeq v0.4 and v1.0.

SUPPLEMENTARY MATERIAL

The Supplementary Material for this article can be found online at: http://journal.frontiersin.org/article/10.3389/fpls.2017.01555/full#supplementary-material

REFERENCES

Albrecht, T., Oberforster, M., Kempf, H., Ramgraber, L., Schacht, J., Kazman, E., et al. (2015). Genome-wide association mapping of preharvest sprouting resistance in a diversity panel of European winter wheats. *J. Appl. Genet.* 56, 277–285. doi: 10.1007/s13353-015-0286-5

Avni, R., Nave, M., Barad, O., Baruch, K., Twardziok, S. O., Gundlach, H., et al. (2017). Wild emmer genome architecture and diversity elucidate wheat evolution and domestication. *Science* 357, 93–97. doi: 10.1126/science.aan0032

Balcárková, B., Frenkel, Z., Škopová, M., Abrouk, M., Kumar, A., Chao, S., et al. (2016). A high resolution radiation hybrid map of wheat chromosome 4A. *Front. Plant Sci.* 7:2063. doi: 10.3389/fpls.2016.02063

Barnard, A., and Smith, M. F. (2009). The effect of rainfall and temperature on the preharvest sprouting tolerance of winter wheat in the dryland production areas of the Free State Province. *Field Crops Res.* 112, 158–164. doi: 10.1016/j.fcr.2009.02.011

Barrero, J. M., Cavanagh, C., Verbyla, K. L., Tibbits, J. F., Verbyla, A. P., Huang, B. E., et al. (2015). Transcriptomic analysis of wheat near-isogenic lines identifies *PM19-A1* and *A2* as candidates for a major dormancy QTL. *Genome Biol.* 16, 93. doi: 10.1186/s13059-015-0665-6

Barrero, J. M., Jacobsen, J., and Gubler, F. (2010). "Seed dormancy: approaches for finding new genes in cereals," in *Plant Developmental Biology - Biotechnological Perspectives*, Vol. 1, eds E. C. Pua and M. R. Davey (Berlin: Springer), 361–381. doi: 10.1007/978-3-642-02301-9_18

Borrill, P., Adamski, N., and Uauy, C. (2015). Genomics as the key to unlocking the polyploid potential of wheat. *New Phytol.* 208, 1008–1022. doi: 10.1111/nph.13533

Brennan, J. P., and Fox, P. N. (1998). Impact of CIMMYT varieties on the genetic diversity of wheat in Australia, 1973-1993. *Aust. J. Agric. Res.* 49, 175–178. doi: 10.1071/A97065

Cabral, A. L., Jordan, M. C., Mccartney, C. A., You, F. M., Humphreys, D. G., Maclachlan, R., et al. (2014). Identification of candidate genes, regions and markers for pre-harvest sprouting resistance in wheat (*Triticum aestivum* L.). *BMC Plant Biol.* 14:340. doi: 10.1186/s12870-014-0340-1

Chen, C. X., Cai, S. B., and Bai, G. H. (2008). A major QTL controlling seed dormancy and pre-harvest sprouting resistance on chromosome 4A in a Chinese wheat landrace. *Mol. Breed.* 21, 351–358. doi: 10.1007/s11032-007-9135-5

Clavijo, B. J., Venturini, L., Schudoma, C., Accinelli, G. G., Kaithakottil, G., Wright, J., et al. (2017). An improved assembly and annotation of the allohexaploid wheat genome identifies complete families of agronomic genes and provides genomic evidence for chromosomal translocations. *Genome Res.* 27, 885–896. doi: 10.1101/gr.217117.116

Corbineau, F., Xia, Q., Bailly, C., and El-Maarouf-Bouteau, H. (2014). Ethylene, a key factor in the regulation of seed dormancy. *Front. Plant Sci.* 5:539. doi: 10.3389/fpls.2014.00539

Cvikova, K., Cattonaro, F., Alaux, M., Stein, N., Mayer, K. F., Dolezel, J., et al. (2015). High-throughput physical map anchoring via BAC-pool sequencing. *BMC Plant Biol.* 15:99. doi: 10.1186/s12870-015-0429-1

Eagles, H. A., Cane, K., and Vallance, N. (2009). The flow of alleles of important photoperiod and vernalisation genes through Australian wheat. *Crop Pasture Sci.* 60, 646–657. doi: 10.1071/CP09014

Fang, J., and Chu, C. (2008). Abscisic acid and the pre-harvest sprouting in cereals. *Plant Signal. Behav.* 3, 1046–1048. doi: 10.4161/psb.3.12.6606

Flintham, J. (2000). Different genetic components control coat-imposed and embryo-imposeddormancy in wheat. *Seed Sci. Res.* 10, 43–50. doi: 10.1017/S0960258500000052

Flintham, J., Adlam, R., Bassoi, M., Holdsworth, M., and Gale, M. D. (2002). Mapping genes for resistance to sprouting damage in wheat. *Euphytica* 126, 39–45. doi: 10.1023/A:1019632008244

Frenkel, Z., Paux, E., Mester, D., Feuillet, C., and Korol, A. (2010). LTC: a novel algorithm to improve the efficiency of contig assembly for physical mapping in complex genomes. *BMC Bioinformatics* 11:584. doi: 10.1186/1471-2105-11-584

Gao, X., Hu, C. H., Li, H. Z., Yao, Y. J., Meng, M., Dong, L., et al. (2013). Factors affecting pre-harvest sprouting resistance in wheat (*Triticum aestivum* l.): a review. *J. Anim. Plant Sci.* 23, 556–565.

Gatford, K. T., Eastwood, R. F., and Halloran, G. M. (2002). Germination inhibitors in bracts surrounding the grain of *Triticum tauschii*. *Funct. Plant Biol.* 29, 881–890. doi: 10.1071/PP01011

Hen-Avivi, S., Savin, O., Racovita, R. C., Lee, W. S., Adamski, N. M., Malitsky, S., et al. (2016). A metabolic gene cluster in the wheat *W1* and the barley *cer-cqu* loci determines beta-diketone biosynthesis and glaucousness. *Plant Cell* 28, 1440–1460. doi: 10.1105/tpc.16.00197

Hickey, L. T., Dieters, M. J., Delacy, I. H., Kravchuk, O. Y., Mares, D. J., and Banks, P. M. (2009). Grain dormancy in fixed lines of white-grained wheat (*Triticum aestivum* L.) grown under controlled environmental conditions. *Euphytica* 168, 303–310. doi: 10.1007/s10681-009-9929-0

Himi, E., Maekawa, M., Miura, H., and Noda, K. (2011). Development of PCR markers for *Tamyb10* related to *R-1*, red grain color gene in wheat. *Theor. Appl. Genet.* 122, 1561–1576. doi: 10.1007/s00122-011-1555-2

Himi, E., and Noda, K. (2005). Red grain colour gene (*R*) of wheat is a Myb-type transcription factor. *Euphytica* 143, 239–242. doi: 10.1007/s10681-005-7854-4

Jordan, K. W., Wang, S., Lun, Y., Gardiner, L. J., Maclachlan, R., Hucl, P., et al. (2015). A haplotype map of allohexaploid wheat reveals distinct patterns of selection on homoeologous genomes. *Genome Biol.* 16, 48. doi: 10.1186/s13059-015-0606-4

Knox, R. E., Clarke, F. R., Clarke, J. M., Fox, S. L., Depauw, R. M., and Singh, A. K. (2012). Enhancing the identification of genetic loci and transgressive segregants for preharvest sprouting resistance in a durum wheat population. *Euphytica* 186, 193–206. doi: 10.1007/s10681-011-0557-0

Konieczny, A., and Ausubel, F. M. (1993). A procedure for mapping *Arabidopsis* mutations using co-dominant ecotype-specific PCR-based markers. *Plant J.* 4, 403–410. doi: 10.1046/j.1365-313X.1993.04020403.x

Kottearachchi, N. S., Uchino, N., Kato, K., and Miura, H. (2006). Increased grain dormancy in white-grained wheat by introgression of preharvest sprouting tolerance QTLs. *Euphytica* 152, 421–428. doi: 10.1007/s10681-006-9231-3

Krasileva, K., Buffalo, V., Bailey, P., Pearce, S., Ayling, S., Tabbita, F., et al. (2013). Separating homeologs by phasing in the tetraploid wheat transcriptome. *Genome Biol.* 14:R66. doi: 10.1186/gb-2013-14-6-r66

Krasileva, K. V., Vasquez-Gross, H. A., Howell, T., Bailey, P., Paraiso, F., Clissold, L., et al. (2017). Uncovering hidden variation in polyploid wheat. *Proc. Natl. Acad. Sci. U.S.A.* 114, E913–E921. doi: 10.1073/pnas.1619268114

Kulwal, P., Ishikawa, G., Benscher, D., Feng, Z., Yu, L.-X., Jadhav, A., et al. (2012). Association mapping for pre-harvest sprouting resistance in white winter wheat. *Theor. Appl. Genet.* 125, 793–805. doi: 10.1007/s00122-012-1872-0

Kulwal, P. L., Kumar, N., Gaur, A., Khurana, P., Khurana, J. P., Tyagi, A. K., et al. (2005). Mapping of a major QTL for pre-harvest sprouting tolerance on chromosome 3A in bread wheat. *Theor. Appl. Genet.* 111, 1052–1059. doi: 10.1007/s00122-005-0021-4

Kumar, S., Knox, R., Clarke, F., Pozniak, C., Depauw, R., Cuthbert, R., et al. (2015). Maximizing the identification of QTL for pre-harvest sprouting resistance using seed dormancy measures in a white-grained hexaploid wheat population. *Euphytica* 205, 287–309. doi: 10.1007/s10681-015-1460-x

Lan, X. J., Wei, Y. M., Liu, D. C., Yan, Z. H., and Zheng, Y. L. (2005). Inheritance of seed dormancy in Tibetan semi-wild wheat accession Q1028. *J. Appl. Genet.* 46, 133–138.

Li, C., Ni, P., Francki, M., Hunter, A., Zhang, Y., Schibeci, D., et al. (2004). Genes controlling seed dormancy and pre-harvest sprouting in a rice-wheat-barley comparison. *Funct. Integr. Genomics* 4, 84–93. doi: 10.1007/s10142-004-0104-3

Linkies, A., and Leubner-Metzger, G. (2012). Beyond gibberellins and abscisic acid: how ethylene and jasmonates control seed germination. *Plant Cell Rep.* 31, 253–270. doi: 10.1007/s00299-011-1180-1

Liu, S., Cai, S., Graybosch, R., Chen, C., and Bai, G. (2008). Quantitative trait loci for resistance to pre-harvest sprouting in US hard white winter wheat Rio Blanco. *Theor. Appl. Genet.* 117, 691–699. doi: 10.1007/s00122-008-0810-7

Liu, S., Sehgal, S. K., Li, J., Lin, M., Trick, H. N., Yu, J., et al. (2013). Cloning and characterization of a critical regulator for preharvest sprouting in wheat. *Genetics* 195, 263–273. doi: 10.1534/genetics.113.152330

Liu, S., Sehgal, S. K., Lin, M., Li, J., Trick, H. N., Gill, B. S., et al. (2015). Independent mis-splicing mutations in *TaPHS1* causing loss of preharvest sprouting (PHS) resistance during wheat domestication. *New Phytol.* 208, 928–935. doi: 10.1111/nph.13489

Lohwasser, U., Rehman Arif, M. A., and Börner, A. (2013). Discovery of loci determining pre-harvest sprouting and dormancy in wheat and barley applying segregation and association mapping. *Biol. Plant.* 57, 663–674. doi: 10.1007/s10535-013-0332-2

Mares, D., and Mrva, K. (2014). Wheat grain preharvest sprouting and late maturity alpha-amylase. *Planta* 240, 1167–1178. doi: 10.1007/s00425-014-2172-5

Mares, D., Mrva, K., Cheong, J., Williams, K., Watson, B., Storlie, E., et al. (2005). A QTL located on chromosome 4A associated with dormancy in white- and red-grained wheats of diverse origin. *Theor. Appl. Genet.* 111, 1357–1364. doi: 10.1007/s00122-005-0065-5

Matilla, A. J., and Matilla-Vázquez, M. A. (2008). Involvement of ethylene in seed physiology. *Plant Sci.* 175, 87–97. doi: 10.1016/j.plantsci.2008.01.014

Mohan, A., Kulwal, P., Singh, R., Kumar, V., Mir, R., Kumar, J., et al. (2009). Genome-wide QTL analysis for pre-harvest sprouting tolerance in bread wheat. *Euphytica* 168, 319–329. doi: 10.1007/s10681-009-9935-2

Mori, M., Uchino, N., Chono, M., Kato, K., and Miura, H. (2005). Mapping QTLs for grain dormancy on wheat chromosome 3A and the group 4 chromosomes, and their combined effect. *Theor. Appl. Genet.* 110, 1315–1323. doi: 10.1007/s00122-005-1972-1

Munkvold, J., Tanaka, J., Benscher, D., and Sorrells, M. (2009). Mapping quantitative trait loci for preharvest sprouting resistance in white wheat. *Theor. Appl. Genet.* 119, 1223–1235. doi: 10.1007/s00122-009-1123-1

nabim (2014). *Wheat Varieties*. Available at: http://www.nabim.org.uk/wheat/wheat-varieties [accessed April 19, 2017].

Nakamura, S., Abe, F., Kawahigashi, H., Nakazono, K., Tagiri, A., Matsumoto, T., et al. (2011). A wheat homolog of *MOTHER OF FT AND TFL1* acts in the regulation of germination. *Plant Cell* 23, 3215–3229. doi: 10.1105/tpc.111.088492

Nakamura, S., Pourkheirandish, M., Morishige, H., Kubo, Y., Nakamura, M., Ichimura, K., et al. (2016). Mitogen-activated protein kinase kinase 3 regulates seed dormancy in barley. *Curr. Biol.* 26, 775–781. doi: 10.1016/j.cub.2016.01.024

Nave, M., Avni, R., Ben-Zvi, B., Hale, I., and Distelfeld, A. (2016). QTLs for uniform grain dimensions and germination selected during wheat domestication are co-located on chromosome 4B. *Theor. Appl. Genet.* 129, 1303–1315. doi: 10.1007/s00122-016-2704-4

Ogbonnaya, F. C., Imtiaz, M., and Depauw, R. M. (2007). Haplotype diversity of preharvest sprouting QTLs in wheat. *Genome* 50, 107–118. doi: 10.1139/g06-142

Ramirez-Gonzalez, R. H., Segovia, V., Bird, N., Fenwick, P., Holdgate, S., Berry, S., et al. (2015). RNA-Seq bulked segregant analysis enables the identification of high-resolution genetic markers for breeding in hexaploid wheat. *Plant Biotechnol. J.* 13, 613–624. doi: 10.1111/pbi.12281

Reeves, J., Chiapparino, E., Donini, P., Ganal, M., Guiard, J., Hamrit, S., et al. (2004). "Changes over time in the genetic diversity of four major European crops: a report from the GEDIFLUX Framework 5 Project," in *Proceedings of the 17th EUCARPIA General Congress, Tulln, Austria, 8–11 September 2004*, eds J. Vollmann, H. Grausgruber, and P. Ruckenbauer (Vienna: University of Natural Resources and Applied Life Sciences), 3–7.

Shaw, P. D., Graham, M., Kennedy, J., Milne, I., and Marshall, D. F. (2014). Helium: visualization of large scale plant pedigrees. *BMC Bioinformatics* 15:259. doi: 10.1186/1471-2105-15-259

Shorinola, O., Bird, N., Simmonds, J., Berry, S., Henriksson, T., Jack, P., et al. (2016). The wheat *Phs-A1* pre-harvest sprouting resistance locus delays the rate of seed dormancy loss and maps 0.3 cM distal to the *PM19* genes in UK germplasm. *J. Exp. Bot.* 67, 4169–4178. doi: 10.1093/jxb/erw194

Simsek, S., Ohm, J.-B., Lu, H., Rugg, M., Berzonsky, W., Alamri, M. S., et al. (2014). Effect of pre-harvest sprouting on physicochemical properties of starch in wheat. *Foods* 3, 194–207. doi: 10.3390/foods3020194

Smith, S. M., and Maughan, P. J. (2015). SNP genotyping using KASPar assays. *Methods Mol. Biol.* 1245, 243–256. doi: 10.1007/978-1-4939-1966-6_18

Solovyev, V., Kosarev, P., Seledsov, I., and Vorobyev, D. (2006). Automatic annotation of eukaryotic genes, pseudogenes and promoters. *Genome Biol.* 7(Suppl. 1):S10. doi: 10.1186/gb-2006-7-s1-s10

Torada, A., Ikeguchi, S., and Koike, M. (2005). Mapping and validation of PCR-based markers associated with a major QTL for seed dormancy in wheat. *Euphytica* 143, 251–255. doi: 10.1007/s10681-005-7872-2

Torada, A., Koike, M., Ikeguchi, S., and Tsutsui, I. (2008). Mapping of a major locus controlling seed dormancy using backcrossed progenies in wheat (*Triticum aestivum* L.). *Genome* 51, 426–432. doi: 10.1139/G08-007

Torada, A., Koike, M., Ogawa, T., Takenouchi, Y., Tadamura, K., Wu, J., et al. (2016). A causal gene for seed dormancy on wheat chromosome 4A encodes a MAP kinase kinase. *Curr. Biol.* 26, 782–787. doi: 10.1016/j.cub.2016.01.063

Uauy, C. (2017). Wheat genomics comes of age. *Curr. Opin. Plant Biol.* 36, 142–148. doi: 10.1016/j.pbi.2017.01.007

Voss-Fels, K. P., Qian, L., Parra-Londono, S., Uptmoor, R., Frisch, M., Keeble-Gagnère, G., et al. (2017). Linkage drag constrains the roots of modern wheat. *Plant Cell Environ.* 40, 717–725. doi: 10.1111/pce.12888

Wicker, T., Matthews, D. E., and Keller, B. (2000). TREP: a database for Triticeae repetitive elements. *Trends Plant Sci.* 7, 561–562. doi: 10.1016/S1360-1385(02)02372-5

Wingen, L. U., Orford, S., Goram, R., Leverington-Waite, M., Bilham, L., Patsiou, T. S., et al. (2014). Establishing the A. E. Watkins landrace cultivar collection

as a resource for systematic gene discovery in bread wheat. *Theor. Appl. Genet.* 127, 1831–1842. doi: 10.1007/s00122-014-2344-5

Xiao-bo, R., Xiu-Jin, L., Deng-Cai, L., Jia-Li, W., and You-Liang, Z. (2008). Mapping QTLs for pre-harvest sprouting tolerance on chromosome 2D in a synthetic hexaploid wheat × common wheat cross. *J. Appl. Genet.* 49, 333–341. doi: 10.1007/BF03195631

Zhang, X. Q., Li, C., Tay, A., Lance, R., Mares, D., Cheong, J., et al. (2008). A new PCR-based marker on chromosome 4AL for resistance to pre-harvest sprouting in wheat (*Triticum aestivum* L.). *Mol. Breed.* 22, 227–236. doi: 10.1007/s11032-008-9169-3

Zong, Y., Wang, Y., Li, C., Zhang, R., Chen, K., Ran, Y., et al. (2017). Precise base editing in rice, wheat and maize with a Cas9- cytidine deaminase fusion. *Nat. Biotechnol.* 35, 438–440. doi: 10.1038/nbt.3811

Conflict of Interest Statement: The authors declare that the research was conducted in the absence of any commercial or financial relationships that could be construed as a potential conflict of interest.

The reviewer MG and handling editor declared their shared affiliation.

frontiers in Plant Science

PERSPECTIVE
published: 31 January 2017
doi: 10.3389/fpls.2017.00090

Prevention of Preharvest Sprouting through Hormone Engineering and Germination Recovery by Chemical Biology

*Mariko Nonogaki and Hiroyuki Nonogaki**

Department of Horticulture, Oregon State University, Corvallis, OR, USA

Vivipary, germination of seeds on the maternal plant, is observed in nature and provides ecological advantages in certain wild species, such as mangroves. However, precocious seed germination in agricultural species, such as preharvest sprouting (PHS) in cereals, is a serious issue for food security. PHS reduces grain quality and causes economical losses to farmers. PHS can be prevented by translating the basic knowledge of hormone biology in seeds into technologies. Biosynthesis of abscisic acid (ABA), which is an essential hormone for seed dormancy, can be engineered to enhance dormancy and prevent PHS. Enhancing nine-*cis*-epoxycarotenoid dioxygenase (NCED), a rate-limiting enzyme of ABA biosynthesis, through a chemically induced gene expression system, has successfully been used to suppress germination of Arabidopsis seeds. The more advanced system *NCED* positive-feedback system, which amplifies ABA biosynthesis in a seed-specific manner without chemical induction, has also been developed. The proofs of concept established in the model species are now ready to be applied to crops. A potential problem is recovery of germination from hyperdormant crop grains. Hyperdormancy induced by the *NCED* systems can be reversed by inducing counteracting genes, such as *NCED* RNA interference or gibberellin (GA) biosynthesis genes. Alternatively, seed sensitivity to ABA can be modified to rescue germination using the knowledge of chemical biology. ABA antagonists, which were developed recently, have great potential to recover germination from the hyperdormant seeds. Combination of the dormancy-imposing and -releasing approaches will establish a comprehensive technology for PHS prevention and germination recovery.

Keywords: chemical biology, germination, hormone, hyperdormancy, inducible gene expression, positive feedback

OPEN ACCESS

Edited by:
Alma Balestrazzi, University of Pavia, Italy

Reviewed by:
Xuming Huang, South China Agricultural University, China
Hak Soo Seo, Seoul National University, South Korea

****Correspondence:***
Hiroyuki Nonogaki
hiro.nonogaki@oregonstate.edu

Specialty section:
This article was submitted to Crop Science and Horticulture, a section of the journal Frontiers in Plant Science

Received: *23 November 2016*
Accepted: *16 January 2017*
Published: *31 January 2017*

Citation:
Nonogaki M and Nonogaki H (2017) Prevention of Preharvest Sprouting through Hormone Engineering and Germination Recovery by Chemical Biology. Front. Plant Sci. 8:90. doi: 10.3389/fpls.2017.00090

INTRODUCTION

Seed development and germination are not necessarily separate developmental programs in terms of timing (before or after seed dispersal) or location (on the maternal plant or soil). In some species, such as mangroves, these two developmental programs are observed continuously without a temporal or spatial intermission, which is referred to as vivipary (Bewley et al., 2013). However, in many other species, maturation drying, which is natural desiccation of seeds at the late developmental stage, interferes with continuous development of seeds into seedlings. There is

a more active mechanism, which suspends germination of developing seeds, that is, seed dormancy. Dormant seeds do not germinate even in the presence of water and under the conditions that are otherwise favorable for germination (Bewley et al., 2013).

Seed dormancy can be found in many wild species while agricultural crops tend to exhibit weak or little dormancy. Seed dormancy traits were present in the wild ancestors of agricultural crops, however, they have been lost over the course of domestication (Nakamura et al., 2016; Subburaj et al., 2016). The lack of dormancy could cause preharvest sprouting (PHS) from grains on the maternal plants in the fields when they are exposed to rain or high humidity.

Genetic research has identified genes associated with seed dormancy and PHS resistance, some of which are associated with grain color (Lin et al., 2016) while others are independent of that trait (Fakthongphan et al., 2016). The genes which play a fundamental role in cellular responses, such as mitogen-activated protein kinase kinase 3 (MKK3), have been identified as a causal gene of PHS in barley (*Hordeum vulgare*) (Nakamura et al., 2016) and wheat (*Triticum aestivum*) (Torada et al., 2016). Interestingly, ARGONAUTE4_9, a key regulator of the RNA-dependent DNA methylation (RdDM) pathway and epigenetic regulation, has also been suggested as a causal gene of PHS in barley (Singh and Singh, 2012) and wheat (Singh et al., 2013).

A variety of genes with different biochemical functions have been identified for PHS resistance or susceptibility. Many of them are associated with hormone signaling, particularly abscisic acid (ABA) signaling (Gao et al., 2012; Gao and Ayele, 2014). It is possible that MKK3 is also associated with ABA signal transduction and/or downstream. The wheat seed dormancy quantitative trait locus (QTL) *QPhs.ocs-3A.1* was found to be *MOTHER OF FT AND TFL1* (*MFT*), a key regulator of ABA signal transduction (Nakamura et al., 2011). An independent analysis of the wheat QTL *Qphs.pseru-3AS* also identified *MFT* as a PHS regulator (Liu et al., 2013). *MFT* has been used as a DNA marker for deep dormancy in wheat (Chono et al., 2015).

The potential of *MFT*, which was originally identified and characterized in the model plant Arabidopsis, for PHS prevention in wheat, suggests that the knowledge of ABA signal transduction obtained from the model plant can directly be translated into cereal crops. ABA insensitive mutations reduce seed dormancy also in wheat (Schramm et al., 2012). Therefore, wheat orthologs of the Arabidopsis genes, which causes ABA hypersensitivity, could enhance seed dormancy and confer PHS resistance to cereals. In fact, mutations in wheat *ENHANCED RESPONSE to ABA* (*ERA*) caused deep dormancy in wheat (Schramm et al., 2013; Martinez et al., 2014) and offer great potential for PHS prevention. Other genes involved in PHS through ABA signaling include ABA-induced *Plasma Membrane-associated protein 19* (*PM19*). *PM19* was suggested to be a seed dormancy regulator in barley (Ranford et al., 2002) and was identified as a dormancy QTL in wheat (Barrero et al., 2015).

Abscisic acid sensitivity has been considered the most critical factor for germination of mature wheat grains. However, there is evidence that ABA metabolism also significantly affect PHS susceptibility and resistance. The importance of ABA 8′-hydroxylase, an ABA deactivation enzyme, in the regulation of barley seed dormancy has been well established (Barrero et al., 2009), which is subject to the regulation by blue light through the CRYPTOCHROME (CRY1) receptor. Blue light inhibits barley seed germination by downregulating *ABA 8′-hydroxylase* and upregulating *nine-cis-epoxycarotenoid dioxygenase* (*NCED*), an ABA biosynthesis gene (Barrero et al., 2014). Wheat ABA biosynthesis and deactivation genes have also been characterized for their function in seed dormancy (Son et al., 2016). Mutations in ABA deactivation genes increased ABA levels in wheat grains and reduced germination (Chono et al., 2013), demonstrating the utility of this approach for PHS prevention. In *Sorghum bicolor*, *GA2ox*, a gibberellin deactivation gene, plays a critical role in PHS, although this gene is regulated also by the ABA pathway through sorghum ABI4 and ABI5 (Cantoro et al., 2013). These findings demonstrate the robustness of hormone metabolism in the regulation of seed dormancy and germination, which makes engineering of the hormone metabolism pathways in seeds as a logical target of modification in technology development for PHS prevention.

SWITCHING OFF GERMINATION IN THE FIELD

The recent advances of hormone biology in seeds provide an excellent foundation for translational biology to prevent PHS. Many genes associated with hormone metabolism in seeds are regulated at the transcriptional level while posttranslational modifications are more prevalent for hormone signal transduction. It is probably more straightforward to alter hormone metabolism through gene expression control, rather than manipulating a certain chemical property (e.g., phosphorylation) of a specific protein involved in ABA signaling.

Enhancing the expression of an ABA biosynthesis gene particularly has great potential to reinforce seed dormancy and prevent PHS. It is possible to spray ABA directly to plants, however, precise control of endogenous ABA is preferable and has been investigated. Expression of *Phaseolus vulgaris NCED* in *Nicotiana tabacum* seeds using the dexamethasone (DEX)-inducible system did not suppress germination adequately (Qin and Zeevaart, 1999). The negative result could be attributed to the experiments performed in the heterologous system or incomplete penetration of the inducible system (Martinez-Andujar et al., 2011). Evidence has been obtained that constitutive expression of *Solanum lycopersicum NCED1* in tomato itself enhances seed dormancy. However, constitutive expression causes undesirable phenotypes in other organs such as leaves (Thompson et al., 2000). It has also been suggested that enhanced levels of ABA could make plants more susceptible to disease (Fan et al., 2009). Therefore, conditional expression of *NCED* in a seed-specific manner is desirable for crops.

Chemically induced gene expression allows conditional expression of *NCED* in seeds, although a steroid hormone agonist like DEX cannot be used for applications in the filed. For agricultural applications, it is necessary to use an inducible system that employs a field-applicable ligand. The Plant Gene Switch System (PGSS), a chemically induced gene expression

system (Padidam, 2003; Koo et al., 2004; Tavva et al., 2007), uses methoxyfenozide (MOF), a non-steroid ecdysone agonist, as a ligand. Intrepid2F (Dow AgroSciences), which contains MOF, has been approved by the US Environmental Protection Agency (EPA) and applicable to crop production, making PGSS as a good candidate to be used for PHS prevention. An important question is whether a conditional induction of *NCED*, a single gene, alone would be sufficient to increase ABA levels in seeds and suppress PHS, because many enzymes are associated with the ABA biosynthesis pathway while NCED is believed to be a rate-limiting enzyme (Chernys and Zeevaart, 2000).

The potential of *NCED* induction by PGSS has been tested in Arabidopsis, which demonstrated that induction of *NCED* alone was robust enough to suspend germination in imbibed seeds. Precocious germination of developing Arabidopsis seeds from the siliques, which was experimentally induced to mimic PHS in cereals, was also prevented by *NCED* induction (Martinez-Andujar et al., 2011) (**Figure 1A**). These results suggest that switching on *NCED* alone is sufficient to switch off germination and maintain seeds dormant. It appears that the ABA biosynthesis pathway upstream of NCED is always running in seeds and constantly providing substrates for NCED. Thus, it is feasible to switch off germination of developing grains in the field and prevent PHS by ligand application if the *NCED*-inducible PGSS is introduced to cereal crops.

SPONTANEOUS HYPERDORMANCY IN DEVELOPING SEEDS

While a proof of concept has been obtained for the *NCED*-inducible system with an EPA-approved chemical (Martinez-Andujar et al., 2011), it is laborious to spray the ligand in large fields, which might also affect plant organs other than seeds at the last stage of crop production. It is preferable if *NCED* expression is enhanced specifically in seeds and at the maturation stage without chemical application.

A system that causes ABA increase specifically in maturing seeds in a spontaneous manner, without chemical application, has been sought for. To establish such system, *NCED* can be driven by a seed maturation-specific promoter. However, tissue- or organ-specific and stage-specific promoters may not be as robust as a constitutive promoter. A substantial level of *NCED* expression has to be reached in seeds so that ABA levels will exceed the threshold necessary for dormancy imposition. An idea to address this issue is to use an ABA-responsive promoter to drive *NCED*, which is expected to create a positive-feedback loop through *NCED* expression (**Figure 1B**). An initial increase of ABA caused by the native system in seeds will be enhanced by a positive-feedback mechanism, which will then stimulate the ABA-responsive promoter through activation of the ABA responsive element (ABRE)-binding factor (ABF). The consequence of each round of positive feedback is the further enhancement of *NCED* expression by ABF. Therefore, this mechanism is expected to amplify ABA production to an unusually high level in seeds and cause hyperdormancy spontaneously. Since this "ABA-responsive ABA biosynthesis"

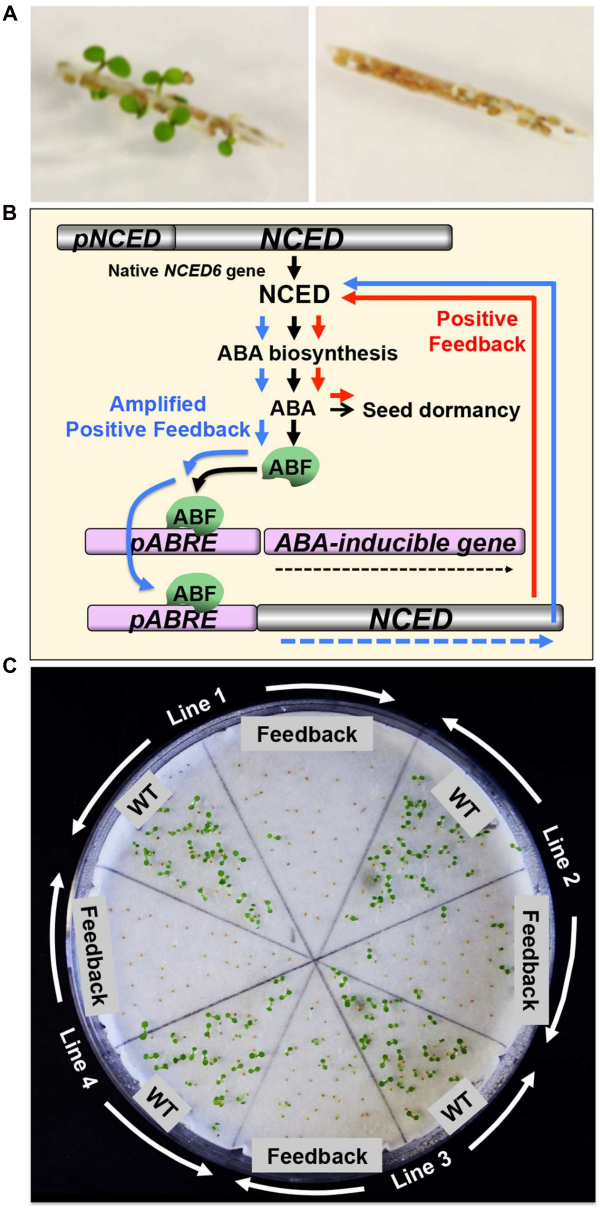

FIGURE 1 | Preharvest sprouting (PHS) prevention by inducible or spontaneous hyperdormancy through hormone engineering. **(A)** Precocious germination of developing Arabidopsis seeds, which was experimentally caused in the silique of the nine-*cis*-epoxycarotenoid dioxygenase (*NCED*)-inducible Plant Gene Switch System (PGSS) line (without *NCED* induction) (*left*). Precocious germination was suppressed by *NCED* induction in the same line (*right*). Modified from Martinez-Andujar et al. (2011). **(B)** Schematic representation of amplified *NCED* expression and enhanced abscisic acid (ABA) biosynthesis and signaling through a positive-feedback mechanism. In the native pathway in seeds (black arrows), *NCED* is expressed to synthesize ABA and induce dormancy. ABA also induces the ABA responsive element (ABRE)-binding factor (ABF), which binds to ABRE in the promoter region of the target genes to induce them. Introduction of the chimeric gene, which contains sorghum *NCED* under the wheat ABA-responsive and seed-specific *Early Methionine-labeled* promoter, into Arabidopsis (bottom), caused positive feedback regulation of *NCED* expression and enhanced dormancy (red arrows), which was further amplified

(*Continued*)

FIGURE 1 | Continued
through ABF (blue arrows). See text for details. Modified from Nonogaki et al. (2014). **(C)** Spontaneous hyperdormancy caused by amplified *NCED* expression and enhanced ABA biosynthesis and signaling through a positive-feedback mechanism. Germination of wild-type (WT) and positive-feedback (Feedback) seeds produced from each maternal plant in hemizygous status (Line 1, 2, 3, or 4) is shown. Modified from Nonogaki et al. (2014).

occurs in the only seed tissues that produces native ABA at the right timing, the positive-feedback system is devoid of pleiotropic effects.

This idea has been tested using the *Triticum aestivum Early Methionine-labeled* (*TaEM*) promoter, which is an ABA-responsive seed maturation-specific promoter, and *Sorghum bicolor NCED* (*SbNCED*) (Nonogaki et al., 2014). Introduction of this system (*pTaEM:SbNCED*) into Arabidopsis increased ABA levels in seeds up to ∼70-fold compared to those in wild-type (WT) seeds and caused unusually deep hyperdormancy (**Figure 1C**). These results suggest that the sorghum NCED functioned efficiently in the metabolic pathway in Arabidopsis and the Arabidopsis transcription factors were able to activate the wheat promoter. The basic mechanisms of hormonal regulation of seed dormancy seem to be conserved between monocot and dicot species. Since the chimeric gene was constructed using the cereal promoter and coding gene and functioned in Arabidopsis properly, it is anticipated to function equally in cereal crops if not better. The *NCED* positive-feedback system is currently introduced to cereal crops for further investigation.

SWITCHING ON GERMINATION AFTER SEED HARVEST

Hyperdormancy is desirable for PHS prevention during crop production. However, the extremely deep dormancy maintained in harvested grains could be problematic when they are used as seeds and need to germinate for the next round of crop production. It is essential to secure strategies for seed germination recovery from the PHS-resistant hyperdormant seeds. To this end, PGSS can be used to induce positive regulators of seed germination, such as GA biosynthesis genes. While ligand application in large fields during crop production may not be practical (see above), it is highly feasible to apply a chemical ligand to harvested seeds in a warehouse. Many seed companies use wet treatments for vegetable and flower seeds. Cereal grains, as starting materials for crop production, can also be treated by chemicals in a small scale. Thus, PGSS offers a suitable method for seed germination recovery if the induction of counteracting gene(s) is sufficient to reverse the suppression of germination caused by *NCED* expression.

A potential problem is the permeability of seed covering tissues, such as the testa and pericarps. In the basic experiments in Arabidopsis, the chemical ligand was able to reach the endosperm (and most likely through the embryo also) after testa rupture (Martinez-Andujar et al., 2011). However, testa rupture does not occur in dormant seeds, including cereal grains. If the pericarp and testa of cereal grains are impermeable to the ligand, a sufficient level of gene induction may not occur, which hinders dormancy release and germination recovery. Therefore, an inducible gene expression system that employs a testa-permeable chemical ligand needs to be developed for efficient recovery of seed germination from hyperdormant seeds.

Nitrate permeates through the testa and could serve as an efficient inducer of gene expression. The nitrate responsive *cis*-element (NRE) in the promoter region of *NITRITE REDUCTASE1* (*NIR1*), which is involved in nitrate-responsive gene expression, has been characterized (Konishi and Yanagisawa, 2010). Induction of a counteracting gene, such as anti-*NCED* or *NCED* RNA interference (RNAi), using the nitrate-inducible system, is expected to antagonize the enhanced *NCED* expression in the hyperdormant seeds and reduce ABA levels in seeds (**Figure 2A**). There is another advantage of using the nitrate-inducible gene expression system for seed germination recovery. Nitrate activates nodule inception (NIN)-like protein 8 (NLP8), which directly binds to the promoter of *CYP707A2*, an ABA deactivation gene, and releases seed dormancy in the native system of Arabidopsis seeds (Yan et al., 2016). Therefore, nitrate application could have dual effects of reducing ABA biosynthesis (*NCED* expression) and enhancing ABA deactivation (*CYP707A2*), both of which reduce ABA levels and promote germination (**Figure 2A**). Nitrate-inducible expression of germination-promoting genes using the *NIR1* promoter has not been tested yet. However, the potential of this promoter for gene induction in seeds has already been tested, which was demonstrated to be efficient for the induction of a test gene (long non-coding RNA) in seeds at the stage before testa rupture (Nonogaki et al., 2015). Thus, nitrate has potential to induce gene expression in seeds at the early imbibitional stages and switch on germination in PHS-resistant seeds.

CHEMICAL BIOLOGY TO RECOVER GERMINATION

It is possible that induction of counteracting genes by PGSS is still insufficient to reduce (in the case of anti-*NCED*) or antagonize (in the case of *GA3ox*) ABA levels in the PHS-resistant seeds, which prevents germination. A strategy to overcome this issue is to alter the sensitivity of seeds to ABA. Even when ABA levels in seeds are still higher than the threshold to maintain dormancy, if the ABA sensitivity of seeds is reduced, the biochemical events that are necessary to alleviate dormancy but are blocked by ABA signaling may be allowed to happen, which should results in seed germination.

Abscisic acid signaling is initiated by perception of ABA by its receptor, to which protein phosphatase 2C (PP2C) binds. As a consequence, SNF1-related protein kinase 2 (SnRK2), which was suppressed by PP2C, is activated and phosphorylates the downstream factor ABF (Cutler et al., 2010). ABF then binds to ABRE to induce downstream genes (**Figure 2B**). Since these sequential events in ABA signal transduction depends on PP2C binding to the receptor, if the initial interaction is blocked, ABA signaling can be inhibited efficiently. Based on this concept, ABA

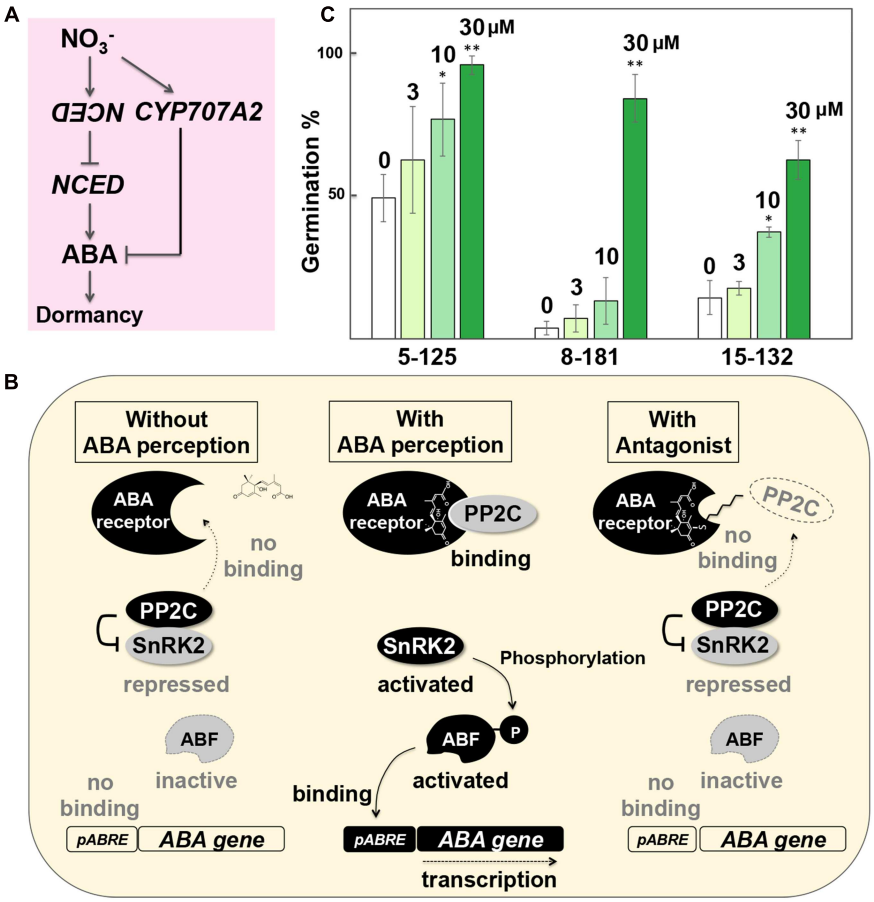

FIGURE 2 | Recovery of germination from PHS-resistant hyperdormant seeds. (A) Schematic representation illustrating the dual effects of antisense *NCED* or *NCED RNAi* induction in seeds by a nitrate-inducible gene expression system. Induction of anti-*NCED* genes using a nitrate-responsive promoter could counteract with enhanced *NCED* expression in the inducible or spontaneous hyperdormant seeds. At the same time, nitrate induces *CYP707A2*, an ABA deactivation gene, in the native system in seeds, which also reduces ABA. Therefore, nitrate-inducible anti-*NCED* gene expression could have dual effects to break dormancy and recover germination. **(B)** Schematic representation of germination recovery by a chemical biology approach. In the absence of ABA (*left*), protein phosphatase 2C (PP2C) suppresses the downstream events necessary for ABA signal transduction by binding to SNF1-related protein kinase 2 (SnRK2). In hyperdormant seeds (*middle*), ABA triggers PP2C binding to the receptor and causes ABA signal transduction, which suppresses germination. Application of 3′-hexylsulfanyl-ABA (AS6), an ABA antagonist (*right*), blocks PP2C binding due to the protruded *S*-hexyl chain and hinders ABA signaling, thereby making seeds insensitive to ABA. Based on Hayashi and Kinoshita (2014) and Takeuchi et al. (2014). **(C)** Recovery of germination by 3′-hexylsulfanyl-ABA (AS6), an ABA antagonist, from the *NCED*-induced hyperdormant seeds. Seeds of the three independent *NCED*-inducible lines (5-125, 8-181, 15-132) were treated with the chemical ligand Intrepid2F to suppress germination (0 μM [AS6]), from which germination was recovered by AS6 in a dose (3, 10, 30 μM)-dependent manner. $^{*}P < 0.05$, $^{**}P < 0.01$ (Student's *t*-test compared with 0 μM).

antagonists, which are capable of binding to the receptor but prevent its interaction with PP2C, have been developed. For instance, 3′-hexylsulfanyl-ABA (AS6) blocks PP2C binding to its receptor due to the protruded *S*-hexyl chain and hinders ABA signaling (Hayashi and Kinoshita, 2014; Takeuchi et al., 2014) (**Figure 2B**).

Although imbibed hyperdormant seeds maintain ABA biosynthesis at unusual levels (Nonogaki et al., 2014), if seeds become insensitive to ABA temporarily during early imbibition due to the presence of an ABA antagonist, they are expected to germinate. Application of AS6 has been tested with the *NCED*-inducible hyperdormant seeds. While the effects of AS6 differ among independent lines, AS6 application recovers germination from the *NCED*-induced seeds in a dose-dependent manner (**Figure 2C**), supporting the idea of seed germination recovery from PHS-resistant seeds by a chemical biology approach. There are occasions in which AS6 is not potent enough to affect dormant seeds, such as the WT accession of Arabidopsis seeds Cape Verde Islands (Cvi) (Rajagopalan et al., 2016). However, new antagonists, which are more potent than AS6 in terms of dormancy release, have also been developed recently (Takeuchi et al., 2015; Rajagopalan et al., 2016). It is possible that some antagonists do not permeate the testa and pericarp efficiently. Nonetheless, this issue also can be addressed by exploring and modifying ABA antagonists with different chemical properties. Thus, chemical biology also offers new strategies for seed germination recovery from PHS-resistant seeds.

CONCLUSION

Combination of hyperdormancy and seed germination recovery strategies will potentially establish a comprehensive technology for PHS prevention. Although this Perspective focused on hormone engineering, other strategies, such as manipulation of redox proteins, could also enhance seed dormancy and delay PHS (Li et al., 2009). In any case, all of these approaches require genetic engineering of cereal crops, which is subject to regulatory processes. The mutant and other genetic lines mentioned in Introduction can be used to confer PHS resistance to commercial varieties through traditional breeding. However, introduction of those genes and traits into the major varieties through crossings and selections will take a long time. Besides, the same varieties will need to go through another breeding program to transfer a seed germination recovery strategy, which will make further delays. Climate changes could cause unexpected and serious problems of PHS in various grain crops, which are food security issues. It is crucial to confer PHS resistance to the major crops used in global production. A possible game changer is the new technologies of crop modification, such as gene editing, which does not leave engineering tools in the final products and may not be subject to the regulations (Ledford, 2015; Waltz, 2016). These new methodologies could accelerate technology development for PHS prevention. Whether through genetic engineering or traditional breeding, progressive ideas to prevent PHS and recover germination need to be tested in the major crops so that new technologies will be established and can be utilized immediately when PHS issues become even more serious.

AUTHOR CONTRIBUTIONS

MN and HN designed and performed the research, analyzed the data, and wrote the paper.

FUNDING

This Perspective was funded by OSU Foundation Integrative Seed Biology.

ACKNOWLEDGMENTS

We are grateful to Roger Beachy, Washington University in St. Louis for his continuous support to us in translational biology and Chengdao Li, Dean Diepeveen, Deborah Boxall, Jose Barrero, and other organizers of the 13th International Symposium for Preharvest Sprouting in Cereals for inviting us to give presentations, which this Perspective was based on. We also thank Yasushi Todoroki, Shizuoka University for sharing AS6 for our experiments and Naoto Kawakami, Meiji University for providing guidance to MN for the completion of her Ph. D. program.

REFERENCES

Barrero, J. M., Cavanagh, C., Verbyla, K. L., Tibbits, J. F. G., Verbyla, A. P., Huang, B. E., et al. (2015). Transcriptomic analysis of wheat near-isogenic lines identifies PM19-A1 and A2 as candidates for a major dormancy QTL. *Genome Biol.* 16, 1–18. doi: 10.1186/s13059-015-0665-6

Barrero, J. M., Downie, A. B., Xu, Q., and Gubler, F. (2014). A role for barley CRYPTOCHROME1 in light regulation of grain dormancy and germination. *Plant Cell* 26, 1094–1104. doi: 10.1105/tpc.113.121830

Barrero, J. M., Talbot, M. J., White, R. G., Jacobsen, J. V., and Gubler, F. (2009). Anatomical and transcriptomic studies of the coleorhiza reveal the importance of this tissue in regulating dormancy in barley. *Plant Physiol.* 150, 1006–1021. doi: 10.1104/pp.109.137901

Bewley, J. D., Bradford, K. J., Hilhorst, H. W. M., and Nonogaki, H. (2013). *Seeds: Physiology of Development, Germination and Dormancy*. New York, NY: Springer. doi: 10.1007/978-1-4614-4693-4

Cantoro, R., Crocco, C. D., Benech-Arnold, R. L., and Rodríguez, M. V. (2013). In vitro binding of Sorghum bicolor transcription factors ABI4 and ABI5 to a conserved region of a GA 2-OXIDASE promoter: possible role of this interaction in the expression of seed dormancy. *J. Exp. Bot.* 64, 5721–5735. doi: 10.1093/jxb/ert347

Chernys, J. T., and Zeevaart, J. A. D. (2000). Characterization of the 9-cis-epoxycarotenoid dioxygenase gene family and the regulation of abscisic acid biosynthesis in avocado. *Plant Physiol.* 124, 343–354. doi: 10.1104/pp.124.1.343

Chono, M., Matsunaka, H., Seki, M., Fujita, M., Kiribuchi-Otobe, C., Oda, S., et al. (2013). Isolation of a wheat (*Triticum aestivum* L.) mutant in ABA 8'-hydroxylase gene: effect of reduced ABA catabolism on germination inhibition under field condition. *Breed. Sci.* 63, 104–115. doi: 10.1270/jsbbs.63.104

Chono, M., Matsunaka, H., Seki, M., Fujita, M., Kiribuchi-Otobe, C., Oda, S., et al. (2015). Molecular and genealogical analysis of grain dormancy in Japanese wheat varieties, with specific focus on MOTHER OF FT AND TFL1 on chromosome 3A. *Breed. Sci.* 65, 103–109. doi: 10.1270/jsbbs.65.103

Cutler, S. R., Rodriguez, P. L., Finkelstein, R. R., and Abrams, S. R. (2010). Abscisic acid: emergence of a core signaling network. *Annu. Rev. Plant Biol.* 61, 651–679. doi: 10.1146/annurev-arplant-042809-112122

Fakthongphan, J., Bai, G., St Amand, P., Graybosch, R. A., and Baenziger, P. S. (2016). Identification of markers linked to genes for sprouting tolerance (independent of grain color) in hard white winter wheat (HWWW). *Theor. Appl. Genet.* 129, 419–430. doi: 10.1007/s00122-015-2636-4

Fan, J., Hill, L., Crooks, C., Doerner, P., and Lamb, C. (2009). Abscisic acid has a key role in modulating diverse plant-pathogen interactions. *Plant Physiol.* 150, 1750–1761. doi: 10.1104/pp.109.137943

Gao, F., and Ayele, B. T. (2014). Functional genomics of seed dormancy in wheat: advances and prospects. *Front. Plant Sci.* 5:458. doi: 10.3389/fpls.2014.00458

Gao, F., Jordan, M. C., and Ayele, B. T. (2012). Transcriptional programs regulating seed dormancy and its release by after-ripening in common wheat (*Triticum aestivum* L.). *Plant Biotechnol. J.* 10, 465–476. doi: 10.1111/j.1467-7652.2012.00682.x

Hayashi, K.-I., and Kinoshita, T. (2014). Plant signaling: abscisic acid receptor hole-in-one. *Nat. Chem. Biol.* 10, 414–415. doi: 10.1038/nchembio.1529

Konishi, M., and Yanagisawa, S. (2010). Identification of a nitrate-responsive cis-element in the *Arabidopsis* NIR1 promoter defines the presence of multiple cis-regulatory elements for nitrogen response. *Plant J.* 63, 269–282. doi: 10.1111/j.1365-313X.2010.04239.x

Koo, J. C., Asurmendi, S., Bick, J., Woodford-Thomas, T., and Beachy, R. N. (2004). Ecdysone agonist-inducible expression of a coat protein gene from tobacco mosaic virus confers viral resistance in transgenic *Arabidopsis*. *Plant J.* 37, 439–448. doi: 10.1046/j.1365-313X.2003.01869.x

Ledford, H. (2015). Crispr, the disruptor. *Nature* 522, 20–24. doi: 10.1038/522020a

Li, Y.-C., Ren, J.-P., Cho, M.-J., Zhou, S.-M., Kim, Y.-B., Guo, H.-X., et al. (2009). The level of expression of thioredoxin is linked to fundamental properties and applications of wheat seeds. *Mol. Plant* 2, 430–441. doi: 10.1093/mp/ssp025

Lin, M., Zhang, D., Liu, S., Zhang, G., Yu, J., Fritz, A. K., et al. (2016). Genome-wide association analysis on pre-harvest sprouting resistance and grain color in U.S. winter wheat. *BMC Genomics* 17:794. doi: 10.1186/s12864-016-3148-6

Liu, S., Sehgal, S. K., Li, J., Lin, M., Trick, H. N., Yu, J., et al. (2013). Cloning and characterization of a critical regulator for preharvest sprouting in wheat. *Genetics* 195, 263–273. doi: 10.1534/genetics.113.152330

Martinez, S. A., Schramm, E. C., Harris, T. J., Kidwell, K. K., Garland-Campbell, K., and Steber, C. M. (2014). Registration of Zak ERA8 soft white spring wheat germplasm with enhanced response to ABA and increased seed dormancy. *J. Plant Regist.* 8, 217–220. doi: 10.3198/jpr2013.09.0060crg

Martinez-Andujar, C., Ordiz, M. I., Huang, Z., Nonogaki, M., Beachy, R. N., and Nonogaki, H. (2011). Induction of 9-cis-epoxycarotenoid dioxygenase in *Arabidopsis thaliana* seeds enhances seed dormancy. *Proc. Natl. Acad. Sci. U.S.A.* 108, 17225–17229. doi: 10.1073/pnas.1112151108

Nakamura, S., Abe, F., Kawahigashi, H., Nakazono, K., Tagiri, A., Matsumoto, T., et al. (2011). A wheat homolog of MOTHER OF FT AND TFL1 acts in the regulation of germination. *Plant Cell* 23, 3215–3229. doi: 10.1105/tpc.111.088492

Nakamura, S., Pourkheirandish, M., Morishige, H., Kubo, Y., Nakamura, M., Ichimura, K., et al. (2016). Mitogen-activated protein kinase kinase 3 regulates seed dormancy in barley. *Curr. Biol.* 26, 775–781. doi: 10.1016/j.cub.2016.01.024

Nonogaki, M., Sall, K., Nambara, E., and Nonogaki, H. (2014). Amplification of ABA biosynthesis and signaling through a positive feedback mechanism in seeds. *Plant J.* 78, 527–539. doi: 10.1111/tpj.12472

Nonogaki, M., Sekine, T., and Nonogaki, H. (2015). Chemically inducible gene expression in seeds before testa rupture. *Seed Sci. Res.* 25, 345–352. doi: 10.1017/S0960258515000240

Padidam, M. (2003). Chemically regulated gene expression in plants. *Curr. Opin. Plant Biol.* 6, 169–177. doi: 10.1016/S1369-5266(03)00005-0

Qin, X., and Zeevaart, J. (1999). The 9-cis-epoxycarotenoid cleavage reaction is the key regulatory step of abscisic acid biosynthesis in water-stressed bean. *Proc. Natl. Acad. Sci. U.S.A.* 96, 15354–15361. doi: 10.1073/pnas.96.26.15354

Rajagopalan, N., Nelson, K. M., Douglas, A. F., Jheengut, V., Alarcon, I. Q., McKenna, S. A., et al. (2016). Abscisic acid analogues that act as universal or selective antagonists of phytohormone receptors. *Biochemistry* 55, 5155–5164. doi: 10.1021/acs.biochem.6b00605

Ranford, J. C., Bryce, J. H., and Morris, P. C. (2002). PM19, a barley (*Hordeum vulgare* L.) gene encoding a putative plasma membrane protein, is expressed during embryo development and dormancy. *J. Exp. Bot.* 53, 147–148. doi: 10.1093/jexbot/53.366.147

Schramm, E., Nelson, S., Kidwell, K., and Steber, C. (2013). Increased ABA sensitivity results in higher seed dormancy in soft white spring wheat cultivar 'Zak'. *Theor. Appl. Genet.* 126, 791–803. doi: 10.1007/s00122-012-2018-0

Schramm, E. C., Nelson, S. K., and Steber, C. M. (2012). Wheat ABA-insensitive mutants result in reduced grain dormancy. *Euphytica* 188, 35–49. doi: 10.1007/s10681-012-0669-1

Singh, M., and Singh, J. (2012). Seed development-related expression of ARGONAUTE4_9 class of genes in barley: possible role in seed dormancy. *Euphytica* 188, 123–129. doi: 10.1007/s10681-012-0624-1

Singh, M., Singh, S., Randhawa, H., and Singh, J. (2013). Polymorphic homoeolog of key gene of RdDM Pathway, ARGONAUTE4_9 class is associated with pre-harvest sprouting in wheat (*Triticum aestivum* L.). *PloS ONE* 8:e77009. doi: 10.1371/journal.pone.0077009

Son, S., Chitnis, V. R., Liu, A., Gao, F., Nguyen, T. N., and Ayele, B. T. (2016). Abscisic acid metabolic genes of wheat (*Triticum aestivum* L.): identification and insights into their functionality in seed dormancy and dehydration tolerance. *Planta* 244, 429–447. doi: 10.1007/s00425-016-2518-2

Subburaj, S., Cao, S., Xia, X., and He, Z. (2016). Phylogenetic analysis, lineage-specific expansion and functional divergence of seed dormancy 4-like genes in plants. *PLoS ONE* 11:e0153717. doi: 10.1371/journal.pone.0153717

Takeuchi, J., Ohnishi, T., Okamoto, M., and Todoroki, Y. (2015). Conformationally restricted 3[prime or minute]-modified ABA analogs for controlling ABA receptors. *Org. Biomol. Chem.* 13, 4278–4288. doi: 10.1039/c4ob02662d

Takeuchi, J., Okamoto, M., Akiyama, T., Muto, T., Yajima, S., Sue, M., et al. (2014). Designed abscisic acid analogs as antagonists of PYL-PP2C receptor interactions. *Nat. Chem. Biol.* 10, 477–482. doi: 10.1038/nchembio.1524

Tavva, V., Dinkins, R., Palli, S., and Collins, G. (2007). Development of a tightly regulated and highly inducible ecdysone receptor gene switch for plants through the use of retinoid X receptor chimeras. *Transgenic Res.* 16, 599–612. doi: 10.1007/s11248-006-9054-y

Thompson, A. J., Jackson, A. C., Symonds, R. C., Mulholland, B. J., Dadswell, A. R., Blake, P. S., et al. (2000). Ectopic expression of a tomato 9-cis-epoxycarotenoid dioxygenase gene causes over-production of abscisic acid. *Plant J.* 23, 363–374. doi: 10.1046/j.1365-313x.2000.00789.x

Torada, A., Koike, M., Ogawa, T., Takenouchi, Y., Tadamura, K., Wu, J., et al. (2016). A causal gene for seed dormancy on wheat chromosome 4A encodes a MAP kinase kinase. *Curr. Biol.* 26, 782–787. doi: 10.1016/j.cub.2016.01.063

Waltz, E. (2016). Gene-edited CRISPR mushroom escapes US regulation. *Nature* 532, 293–293. doi: 10.1038/nature.2016.19754

Yan, D., Easwaran, V., Chau, V., Okamoto, M., Ierullo, M., Kimura, M., et al. (2016). NIN-like protein 8 is a master regulator of nitrate-promoted seed germination in *Arabidopsis*. *Nat. Commun.* 7, 13179. doi: 10.1038/ncomms13179

Conflict of Interest Statement: A patent application has been filed for a technology described in this article.

frontiers in Plant Science

PERSPECTIVE
published: 09 March 2018
doi: 10.3389/fpls.2018.00296

Nitric Oxide Enables Germination by a Four-Pronged Attack on ABA-Induced Seed Dormancy

Santiago Signorelli[1,2,3,4]* *and Michael J. Considine*[1,2,3,5,6]*

[1] The UWA Institute of Agriculture, The University of Western Australia, Perth, WA, Australia, [2] The School of Molecular and Chemical Sciences, The University of Western Australia, Perth, WA, Australia, [3] UWA School of Agriculture and Environment, The University of Western Australia, Perth, WA, Australia, [4] Departamento de Biología Vegetal, Universidad de la República, Montevideo, Uruguay, [5] Irrigated Agriculture, Department of Primary Industries and Regional Development, South Perth, WA, Australia, [6] Centre for Plant Sciences, School of Biology, University of Leeds, Leeds, United Kingdom

Nitric oxide (·NO) is known to attenuate dormancy and promote germination, a function that seemingly depends on crosstalk with the abscisic acid (ABA) signaling network. In the past 2 years, a number of independent studies have revealed that ·NO gates the ABA signaling network at multiple steps, ensuring redundant and effectively irreversible control of germination. Here we summarize the recent studies, and propose a model of the multiple functions of ·NO in seed dormancy.

Keywords: nitric oxide, dormancy, post-translational regulation, plant development, abscisic acid (ABA), phytohormone crosstalk

OPEN ACCESS

Edited by:
Jose Maria Barrero, Commonwealth Scientific and Industrial Research Organisation (CSIRO), Australia

Reviewed by:
Oscar Lorenzo, Universidad de Salamanca, Spain
Pablo Albertos, Technische Universität München, Germany

***Correspondence:**
Santiago Signorelli
ssignorelli@fagro.edu.uy
Michael J. Considine
michael.considine@uwa.edu.au

Specialty section:
This article was submitted to Plant Breeding, a section of the journal Frontiers in Plant Science

Received: *01 December 2017*
Accepted: *21 February 2018*
Published: *09 March 2018*

Citation:
Signorelli S and Considine MJ (2018) Nitric Oxide Enables Germination by a Four-Pronged Attack on ABA-Induced Seed Dormancy. Front. Plant Sci. 9:296. doi: 10.3389/fpls.2018.00296

INTRODUCTION

Elemental nitrogen is capable of a range of oxidation states (−3 to +5). The formation of reactive nitrogen species (RNS) is thus a necessary consequence of nitrogen metabolism. These RNS include peroxynitrite ($ONOO^-$), and the free radicals ·NO and nitrogen dioxide ($\cdot NO_2$). Due to their high reactivity, RNS can modify the structure and function of proteins through the nitration of tyrosine or nitrosylation of cysteine residues. These functions have been adopted as central modes of post-translational regulation, governing wide developmental, acclimation and stress response processes in plants. For example, root and shoot elongation, pollen and seed development, stomatal closure, and antioxidant defense (Prado et al., 2004; Lombardo et al., 2006).

Among the RNS, ·NO is the most well-studied, and several developmental and adaptive functions have been assigned. Distinct roles of ·NO in regulating seed dormancy and germination have been described, including the interaction with other plant growth regulators (Beligni and Lamattina, 2000; Batak et al., 2002; Bethke et al., 2006). Nevertheless, the collective influence of ·NO is pervasive, demonstrating function in tropic growth responses, root development and branching, nodule formation, cell wall lignification, xylem differentiation, cellulose biosynthesis, stomatal aperture, pollen tube growth, floral transitions, fruit maturation, and leaves senescence (reviewed by Sanz et al., 2014). Moreover, at physiological concentrations, ·NO is in the gas phase and able to diffuse across membranes, and may have relatively long half-life. These features make ·NO an important local and long-range signaling molecule and gasotransmitter (Lamattina and García Mata, 2016).

RNS EFFECT POST-TRANSLATIONAL CONTROL OF PHYTOHORMONE SIGNALING

Many of the developmental functions of RNS result from the interference with phytohormone signaling pathways, mainly by the *S*-nitrosylation of key intermediate signaling proteins.

For example, the *S*-nitrosylation of phosphotransfer proteins functions in the repression of cytokinin (CK) signaling (Feng et al., 2013). In a similar way, the *S*-nitrosylation of OPEN STOMATA1 (OST1) and SUCROSE NON-FERMENTING1 (SNF1)-RELATED PROTEIN KINASE2.6 (SnRK2.6) negatively regulates ABA signaling in guard cells (Wang et al., 2015a). Other SnRK2 proteins are also susceptible to *S*-nitrosylation, attenuating ABA control of seed germination (Wang et al., 2015b). In addition, ·NO was shown to increase the DELLA protein concentration, which negatively regulates gibberellic acid (GA) signal transduction (Lozano-Juste and Leon, 2011; Krasuska et al., 2016). Together, these observations demonstrate that ·NO can fine-tune phytohormone signaling at several levels, and is thus an important sensory medium.

INVOLVEMENT OF RNS IN THE ABA-MEDIATED DORMANCY CONTROL

The ABA network governing seed dormancy is well-described (Graeber et al., 2012). In this network, the binding of ABA to the ABA receptors, PYR/PYL/RCAR, results in the inactivation of type 2C protein phosphatases (PP2C). This inactivation triggers the action of the SnRK2 kinase, which promotes the activity of the basic leucine zipper transcription factor ABSCISIC ACID INSENSITIVE5 (ABI5) (**Figure 1**). In turn, ABI5 exerts considerable transcriptional control over dormancy (Skubacz et al., 2016). ABI5 is thus considered a key repressor of seed germination and post-germination development (Finkelstein and Lynch, 2000; Lopez-Molina et al., 2001).

Crosstalk between ·NO and ABA has been demonstrated by pharmacological and genetic approaches, for example the enhanced dormancy potential and ABA hypersensitivity of ·NO-deficient seeds of arabidopsis (*Arabidopsis thaliana*; Lozano-Juste and Leon, 2010), which was later explained by the hyperaccumulation of ABI5 (Albertos et al., 2015). However, on closer inspection it is clear that RNS can interfere with ABA signaling by four independent pathways (**Figure 1**).

Firstly, RNS can inactivate the PYR/PYL/RCAR receptor by tyrosine-nitration (Castillo et al., 2015), enabling the activity of PP2C, which inactivates SnRK2. Thus, the influence of ABI5 is attenuated (**Figure 1**, i). Secondly, different SnRK2 proteins (SnRK2.6, SnRK2.2, and SnRK2.3) were shown to be inactivated by *S*-nitrosylation (by ·NO), affecting ABA signaling not only in stomatal closure but also seed germination (Wang et al., 2015b). As mentioned above, in a nitrosative condition, most of the available SnRK2 would be dephosphorylated (inactive). It seems clear, however, that any remaining phosphorylated SnRK2 can be inactivated directly by ·NO, which nitrosylates a cysteine residue near the kinase catalytic site, blocking the kinase activity (**Figure 1**, ii; Wang et al., 2015a). Thirdly, ·NO assists the degradation of ABI5 by the *S*-nitrosylation at cysteine-153, targeting it to the proteasome by enhancing its interaction with CULLIN4-based and KEEP ON GOING E3 Ligases (**Figure 1**, iii; Albertos et al., 2015). Accordingly,

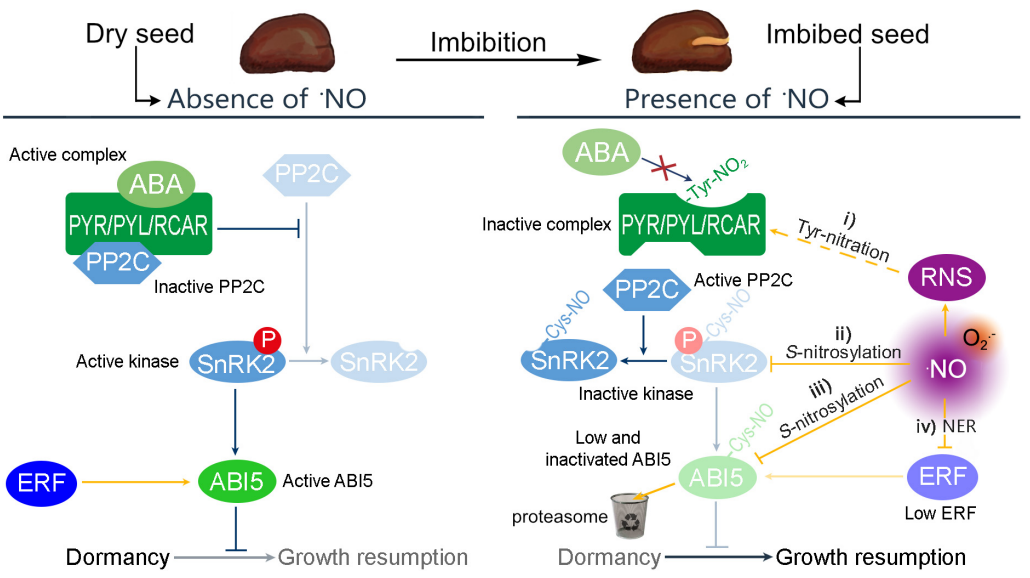

FIGURE 1 | Possible mechanisms by which RNS modulate the ABA regulation of dormancy. In absence of ·NO, the transcription factor ABI5 controls the expression of genes relevant to ensure the dormant state. The expression of *ABI5* is induced by the Group VII ETHYLENE RESPONSE FACTORS (ERF) and the activity of ABI5 is promoted by SnRK2 kinases. ABA binds to the PYR/PYL/RCAR receptor to complex PP2C and avoids the inactivation of SnRK2. However, seed imbibition produces an increase of ·NO levels, resulting in a potential increase of different RNS. In this situation, the ABA control of dormancy can be attenuated by four different pathways: (i) the PYR/PYL/RCAR complex can be *S*-nitrosylated avoiding the interaction with ABA; (ii) ·NO can *S*-nitrosylates SnRK2 kinases inactivating their kinase activity; (iii) ·NO can target ABI5 to the proteasome by *S*-nitrosylation affecting the expression of genes under its regulation; and (iv) ·NO also targets the Group VII ERF to the proteasome, via the N-end rule pathway of proteolysis.

the levels of ·NO and the amount of *S*-nitrosylated proteins increase in barley seed embryos during the first hours post-imbibition (Ma et al., 2016). Finally, ·NO promotes the degradation of the Group VII ETHYLENE RESPONSE FACTORS (ERF, **Figure 1**, iv) via the N-end rule pathway of proteolysis. These ERFs are positive regulators of the transcription of *ABI5,* and hence their degradation limits further synthesis (Gibbs et al., 2014).

PERSPECTIVES

- RNS can modulate a single signaling pathway at multiple levels. Here we have described the fine-tuning of ABA signaling by four independent mechanisms, all of which apparently negatively regulate the canonical ABA pathway. RNS crosstalks with other phytohormone pathways have been demonstrated. Due to the pervasive influence of RNS activities on enzyme functions, now we expect further detail to emerge on the redundancies of RNS signaling, positive, negative and conflicting influences.
- Although the crosstalk between RNS and ABA is well-developed, questions still remain. For example, whether the nitration of the PYR/PYL/RCAR complex does occur *in vivo*. The influence of ·NO is particularly dependent on spatial, temporal and concentration conditions.
- ·NO acts as a gasotransmitter affecting diverse biological processes. In plants, there are many pathways of ·NO synthesis. However, no ·NO synthase has been identified in plants yet. The potential finding of a plant ·NO synthase would be key to manage the ·NO homeostasis and thus the processes under its regulation.
- From a management point of view, and in particular for seed producers, it would be interesting to develop procedures to manage endogenous ·NO levels. This would lead to the possibility of producing seeds with prolonged or reduced dormancy, as desired.
- With the arising of genome editing techniques, it would be possible to replace susceptible residues to nitration and nitrosylation by amino acids with similar physicochemical characteristics in order to reduce the susceptibility of the enzymes to RNS but keeping their functionality.

CONCLUDING REMARKS

Nitric oxide participates in the regulation of the dormancy release by (i) the tyrosine nitration of ABA receptors, (ii) *S*-nitrosylation of SnRK2s, (iii) *S*-nitrosylation of ABI5, and (iv) the degradation of ERF. This evidence supports an inverse molecular link between ·NO and ABA hormone signaling in which ·NO acts upstream and downstream.

AUTHOR CONTRIBUTIONS

MC and SS jointly conceived and wrote the manuscript.

ACKNOWLEDGMENTS

SS and MC acknowledge research funding from the Australian Research Council (DP150103211).

REFERENCES

Albertos, P., Romero-Puertas, M. C., Tatematsu, K., Mateos, I., Sánchez-Vicente, I., Nambara, E., et al. (2015). S-nitrosylation triggers ABI5 degradation to promote seed germination and seedling growth. *Nat. Commun.* 6:8669. doi: 10.1038/ncomms9669

Batak, I., Dević, M., Gibal, Z., Grubišić, D., Poff, K. L., and Konjević, R. (2002). The effects of potassium nitrate and NO-donors on phytochrome A- and phytochrome B-specific induced germination of *Arabidopsis thaliana* seeds. *Seed Sci. Res.* 12, 253–259. doi: 10.1079/SSR2002118

Beligni, M. V., and Lamattina, L. (2000). Nitric oxide stimulates seed germination and de-etiolation, and inhibits hypocotyl elongation, three light-inducible responses in plants. *Planta* 210, 215–221. doi: 10.1007/PL00008128

Bethke, P. C., Libourel, I. G. L., and Jones, R. L. (2006). Nitric oxide reduces seed dormancy in *Arabidopsis*. *J. Exp. Bot.* 57, 517–526. doi: 10.1093/jxb/erj060

Castillo, M.-C., Lozano-Juste, J., Gonzalez-Guzman, M., Rodriguez, L., Rodriguez, P. L., and Leon, J. (2015). Inactivation of PYR/PYL/RCAR ABA receptors by tyrosine nitration may enable rapid inhibition of ABA signaling by nitric oxide in plants. *Sci. Signal.* 8:ra89. doi: 10.1126/scisignal.aaa7981

Feng, J., Wang, C., Chen, Q., Chen, H., Ren, B., Li, X., et al. (2013). S-nitrosylation of phosphotransfer proteins represses cytokinin signaling. *Nat. Commun.* 4:1529. doi: 10.1038/ncomms2541

Finkelstein, R. R., and Lynch, T. J. (2000). The *Arabidopsis* abscisic acid response gene *ABI5* encodes a basic leucine zipper transcription factor. *Plant Cell* 12, 599–610. doi: 10.1105/tpc.12.4.599

Gibbs, D. J., MdIsa, N., Movahedi, M., Lozano-Juste, J., Mendiondo, G. M., Berckhan, S., et al. (2014). Nitric oxide sensing in plants is mediated by proteolytic control of group VII ERF transcription factors. *Mol. Cell* 53, 369–379. doi: 10.1016/j.molcel.2013.12.020

Graeber, K., Nakabayashi, K., Miatton, E., Leubner-Metzger, G., and Soppe, W. J. J. (2012). Molecular mechanisms of seed dormancy. *Plant Cell Environ.* 35, 1769–1786. doi: 10.1111/j.1365-3040.2012.02542.x

Krasuska, U., Ciacka, K., Orzechowski, S., Fettke, J., Bogatek, R., and Gniazdowska, A. (2016). Modification of the endogenous NO level influences apple embryos dormancy by alterations of nitrated and biotinylated protein patterns. *Planta* 244, 877–891. doi: 10.1007/s00425-016-2553-z

Lamattina, L., and García Mata, C. (2016). *Gasotransmitters in Plants: The Rise of a New Paradigm in Cell Signaling*. Geneva: Springer International Publishing.

Lombardo, M. C., Graziano, M., Polacco, J. C., and Lamattina, L. (2006). Nitric oxide functions as a positive regulator of root hair development. *Plant Signal. Behav.* 1, 28–33. doi: 10.4161/psb.1.1.2398

Lopez-Molina, L., Mongrand, S., and Chua, N.-H. (2001). A postgermination developmental arrest checkpoint is mediated by abscisic acid and requires the ABI5 transcription factor in *Arabidopsis*. *Proc. Natl. Acad. Sci. U.S.A.* 98, 4782–4787. doi: 10.1073/pnas.081594298

Lozano-Juste, J., and Leon, J. (2010). Enhanced abscisic acid-mediated responses in nia1nia2noa1-2 triple mutant impaired in NIA/NR- and AtNOA1-dependent nitric oxide biosynthesis in Arabidopsis. *Plant Physiol.* 152, 891–903. doi: 10.1104/pp.109.148023

Lozano-Juste, J., and Leon, J. (2011). Nitric oxide regulates DELLA content and PIF expression to promote photomorphogenesis in Arabidopsis. *Plant Physiol.* 156, 1410–1423. doi: 10.1104/pp.111.177741

Ma, Z., Marsolais, F., Bykova, N. V., and Igamberdiev, A. U. (2016). Nitric oxide and reactive oxygen species mediate metabolic changes in barley seed

embryo during germination. *Front. Plant Sci.* 7:138. doi: 10.3389/fpls.2016.00138

Prado, A. M., Porterfield, D. M., and Feijó, J. A. (2004). Nitric oxide is involved in growth regulation and re-orientation of pollen tubes. *Development* 131, 2707–2714. doi: 10.1242/dev.01153

Sanz, L., Fernández-Marcos, M., Modrego, A., Lewis, D. R., Muday, G. K., Pollmann, S., et al. (2014). Nitric oxide plays a role in stem cell niche homeostasis through its interaction with auxin. *Plant Physiol.* 166, 1972–1984. doi: 10.1104/pp.114.247445

Skubacz, A., Daszkowska-Golec, A., and Szarejko, I. (2016). The role and regulation of ABI5 (ABA-Insensitive 5) in plant development, abiotic stress responses and phytohormone crosstalk. *Front. Plant Sci.* 7:1884. doi: 10.3389/fpls.2016.01884

Wang, P., Du, Y., Hou, Y.-J., Zhao, Y., Hsu, C.-C., Yuan, F., et al. (2015a). Nitric oxide negatively regulates abscisic acid signaling in guard cells by S-nitrosylation of OST1. *Proc. Natl. Acad. Sci. U.S.A.* 112, 613–618. doi: 10.1073/pnas.1423481112

Wang, P., Zhu, J. K., and Lang, Z. (2015b). Nitric oxide suppresses the inhibitory effect of abscisic acid on seed germination by S-nitrosylation of SnRK2 proteins. *Plant Signal. Behav.* 10:e1031939. doi: 10.1080/15592324.2015.1031939

Conflict of Interest Statement: The authors declare that the research was conducted in the absence of any commercial or financial relationships that could be construed as a potential conflict of interest.

frontiers in Plant Science

CORRECTION
published: 17 May 2018
doi: 10.3389/fpls.2018.00654

Corrigendum: Nitric Oxide Enables Germination by a Four-Pronged Attack on ABA-Induced Seed Dormancy

Santiago Signorelli [1,2,3,4]* *and Michael J. Considine* [1,2,3,5,6]*

[1] The UWA Institute of Agriculture, The University of Western Australia, Perth, WA, Australia, [2] The School of Molecular and Chemical Sciences, The University of Western Australia, Perth, WA, Australia, [3] UWA School of Agriculture and Environment, The University of Western Australia, Perth, WA, Australia, [4] Departamento de Biología Vegetal, Universidad de la República, Montevideo, Uruguay, [5] Irrigated Agriculture, Department of Primary Industries and Regional Development, South Perth, WA, Australia, [6] Centre for Plant Sciences, School of Biology, University of Leeds, Leeds, United Kingdom

Keywords: nitric oxide, dormancy, post-translational regulation, plant development, abscisic acid (ABA), phytohormone crosstalk

OPEN ACCESS

Edited and reviewed by:
Jose Maria Barrero, Commonwealth Scientific and Industrial Research Organisation (CSIRO), Australia

***Correspondence:**
Santiago Signorelli
ssignorelli@fagro.edu.uy
Michael J. Considine
michael.considine@uwa.edu.au

Specialty section:
This article was submitted to Plant Breeding, a section of the journal Frontiers in Plant Science

Received: *16 March 2018*
Accepted: *27 April 2018*
Published: *17 May 2018*

Citation:
Signorelli S and Considine MJ (2018) Corrigendum: Nitric Oxide Enables Germination by a Four-Pronged Attack on ABA-Induced Seed Dormancy. Front. Plant Sci. 9:654. doi: 10.3389/fpls.2018.00654

A corrigendum on

Nitric Oxide Enables Germination by a Four-Pronged Attack on ABA-Induced Seed Dormancy
by Signorelli, S., and Considine, M. J. (2018). Front. Plant Sci. 9:296. doi: 10.3389/fpls.2018.00296

There was an unnecessary arrow in Figure 1 as published. The correct version of **Figure 1** appears below. The author's apologies for the mistake, which may have led to misinterpretation. This error and correction does not affect the interpretation or intent of the figure with respect to the role of nitric oxide-dependent regulation of seed dormancy and germination.

The original article has been updated.

Conflict of Interest Statement: The authors declare that the research was conducted in the absence of any commercial or financial relationships that could be construed as a potential conflict of interest.

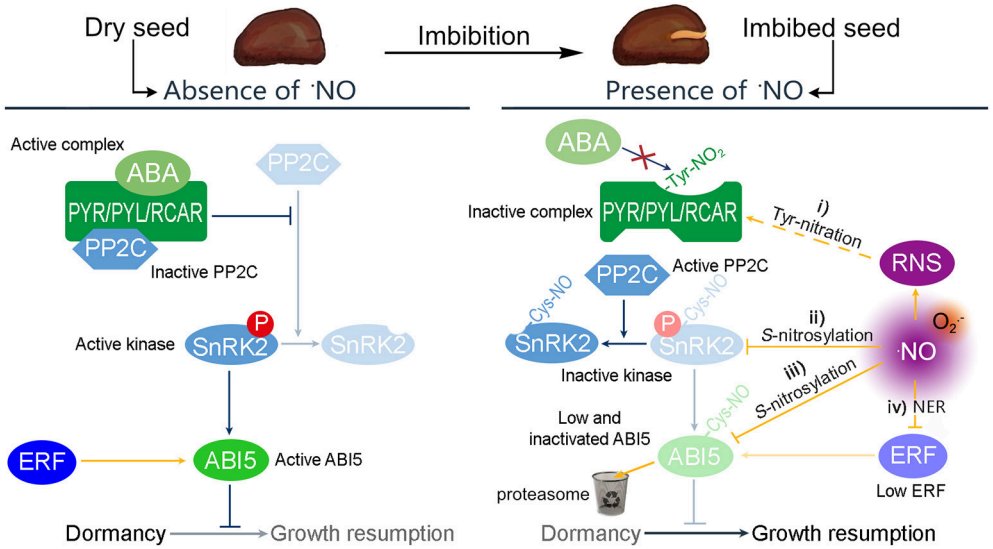

FIGURE 1 | Possible mechanisms by which RNS modulate the ABA regulation of dormancy. In absence of ·NO, the transcription factor ABI5 controls the expression of genes relevant to ensure the dormant state. The expression of *ABI5* is induced by the Group VII ETHYLENE RESPONSE FACTORS (ERF) and the activity of ABI5 is promoted by SnRK2 kinases. ABA binds to the PYR/PYL/RCAR receptor to complex PP2C and avoid the inactivation of SnRK2. However, seed imbibition produces an increase of ·NO levels, resulting in a potential increase of different RNS. In this situation, the ABA control of dormancy can be attenuated by four different pathways: (i) the PYR/PYL/RCAR complex can be *S*-nitrosylated avoiding the interaction with ABA; (ii) ·NO can *S*-nitrosylate SnRK2 kinases inactivating their kinase activity; (iii) ·NO can target ABI5 to the proteasome by *S*-nitrosylation affecting the expression of genes under its regulation; and (iv) ·NO also targets the Group VII ERF to the proteasome, via the N-end rule pathway of proteolysis.

frontiers in Plant Science

ORIGINAL RESEARCH
published: 05 October 2017
doi: 10.3389/fpls.2017.01727

Comparisons of Copy Number, Genomic Structure, and Conserved Motifs for α-Amylase Genes from Barley, Rice, and Wheat

*Qisen Zhang[1] and Chengdao Li[2]**

[1] Australian Export Grains Innovation Centre, South Perth, WA, Australia, [2] Western Barley Genetics Alliance, Murdoch University, Murdoch, WA, Australia

Barley is an important crop for the production of malt and beer. However, crops such as rice and wheat are rarely used for malting. α-amylase is the key enzyme that degrades starch during malting. In this study, we compared the genomic properties, gene copies, and conserved promoter motifs of α-amylase genes in barley, rice, and wheat. In all three crops, α-amylase consists of four subfamilies designated *amy1, amy2*, *amy3,* and *amy4*. In wheat and barley, members of *amy1* and *amy2* genes are localized on chromosomes 6 and 7, respectively. In rice, members of *amy1* genes are found on chromosomes 1 and 2, and *amy2* genes on chromosome 6. The barley genome has six *amy1* members and three *amy2* members. The wheat B genome contains four *amy1* members and three *amy2* members, while the rice genome has three *amy1* members and one *amy2* member. The B genome has mostly *amy1* and *amy2* members among the three wheat genomes. *Amy1* promoters from all three crop genomes contain a GA-responsive complex consisting of a GA-responsive element (CAATAAA), pyrimidine box (CCTTTT) and TATCCAT/C box. This study has shown that *amy1* and *amy2* from both wheat and barley have similar genomic properties, including exon/intron structures and GA-responsive elements on promoters, but these differ in rice. Like barley, wheat should have sufficient amy activity to degrade starch completely during malting. Other factors, such as high protein with haze issues and the lack of husk causing Lauting difficulty, may limit the use of wheat for brewing.

Keywords: α-amylase, barley, conserved motif, genome, gibberellin responsive complex, promoter

OPEN ACCESS

Edited by:
Jacqueline Batley, University of Western Australia, Australia

Reviewed by:
You-Liang Zheng, Sichuan Agricultural University, China
Marcelo Helguera, Instituto Nacional de Tecnología Agropecuaria (INTA), Argentina

****Correspondence:***
Chengdao Li
c.li@murdoch.edu.au

Specialty section:
This article was submitted to Crop Science and Horticulture, a section of the journal Frontiers in Plant Science

Received: *07 July 2017*
Accepted: *21 September 2017*
Published: *05 October 2017*

Citation:
Zhang Q and Li C (2017) Comparisons of Copy Number, Genomic Structure, and Conserved Motifs for α-Amylase Genes from Barley, Rice, and Wheat. Front. Plant Sci. 8:1727. doi: 10.3389/fpls.2017.01727

INTRODUCTION

The best quality barley grains are used predominantly for making malts and subsequently beer and whiskey. Malting consists of steeping, germination, and kilning (Gupta et al., 2010). Steeping and germination allow production of hydrolyzing enzymes including α-amylase (amy), β-amylase, limit dextrinase, and α-glucosidase for starch degradation (Bak-Jensen et al., 2007; Evans et al., 2010; Fincher, 2010; Shahpiri et al., 2015). Starch comprises an α-D-glucose homo-polymer amylose and branched amylopectin. The former is a linear molecule of α-1,4-linked glucose molecules, while the latter is a larger molecule with α-1,6 branching points (Bahaji et al., 2014). Amy [α-(1,4)-D-glucan glucanohydrolase, EC 3.2.1.1] cleaves α-(1,4) glycosidic linkage internally to produce

oligosaccharides and amylopectin. Amy is the most important enzyme for starch degradation during malting and mashing. Barley malts contain sufficient active amy enzymes to almost completely hydrolyze starch during malting and mashing.

Activation of amy expression is strictly controlled by the phytohormones gibberellin and ABA. During grain development, amy expression is repressed by ABA. However, in a genetic defect wheat, a high level of high pI amy genes could be expressed, resulting in poor grain quality during late grain development. This is normally referred to as late maturity α-amylase (LMA) (Barrero et al., 2013). During seed germination, amy expression is induced by elevated GA levels (Lanahan et al., 1992; Gómez-Cadenas et al., 2001; Woodger et al., 2010).

Genetic mapping associated barley malt amy activities with amy1 and amy2 loci on chromosomes 6H and 7H, respectively (Hayes et al., 1993; Oziel et al., 1996; Zale et al., 2000; Gao et al., 2004; Li et al., 2010). Isoelectric focusing electrophoresis identified low and high pI amy isoforms in barley aleurone extracts (Jacobsen and Higgins, 1982; Svensson et al., 1985). However, the number of amy isoforms in the barley genome is unknown but predicted to be from three to eight (Jacobsen and Higgins, 1982; Muthukrishnan et al., 1984; Svensson et al., 1985; Khursheed and Rogers, 1988; Evans et al., 2010). Nomenclatures of amys are complicated. Two families of amy, were named AMY1 and AMY2, referred to low and high pI enzymes, respectively (MacGregor et al., 1971; Jacobsen and Higgins, 1982; Svensson et al., 1985; Evans et al., 2010). A genomic clone and two cDNA clones coding for amy enzymes have been named amy32b, amy6-4, and amy46 (Rogers and Milliman, 1983; Whittier et al., 1987; Khursheed and Rogers, 1988). In a recently published barley genomic sequencing paper, new amy nomenclatures have been proposed. The barley genome contains at least 12 *amy* genes, grouped into four subfamilies *amy1*, *amy2*, *amy3,* and *amy4* (Mascher et al., 2017). Here, we compared gene copy numbers, genomic structures and promoter conserved motifs of *amy1* and *amy2* subfamilies from barley, wheat, and rice. We hypothesize that the expansion in *amy1* members combined with the presence of conserved regulatory motifs on promoters of *amy1* and *amy2* genes are important determinants for selecting barley as a malting crop.

MATERIALS AND METHODS

Genome sequences were downloaded to a local computer from ftp://ftp.ensemblgenomes.org/pub/plants/release-35/fasta/hordeum_vulgare/dna/ for barley; ftp://ftp.ensemblgenomes.org/pub/plants/release-35/fasta/oryza_sativa/dna/ for rice, and ftp://ftp.ensemblgenomes.org/pub/plants/release-35/fasta/triticum_aestivum/dna/ for wheat. The identification of barley, wheat, and rice amy genes are described in Mascher et al. (2017). *Amy* coding and promoter sequences (500 bp upstream of the translation start codon ATG) for all three crops were extracted after being blasted with the *amy* genes. Briefly, the *amy* genes were used to blast standalone blastable genomic databases to obtain *amy* gene nucleotide positions in pseudomolecules. According to these positions, the *amy* gene coding and promoter sequences were calculated and extracted with a Perl script. The promoter sequences were aligned with a ClustalW program[1] and conserved motifs were examined.

RESULTS AND DISCUSSION

Barley *amy* Copy Numbers – Historical and Genomic Evidence

Barley *amy* genes were initially mapped to chromosomes 6H and 7H with wheat–barley addition lines (Brown and Jacobsen, 1982; Muthukrishnan et al., 1984). Southern blot analysis of two different *amy* gene DNA probes detected at least six and three hybridization bands from addition lines containing barley chromosomes 6H and 7H, respectively (Muthukrishnan et al., 1984; Rogers and Milliman, 1984). There were multiple amy protein bands on SDS PAGE purified from the barley aleurone using cycloheptaamylose-sepharose affinity chromatography and at least four amy activity peaks separated by DEAE cellulose chromatography (Jacobsen and Higgins, 1982). These offered early experimental evidence of the *amy* multigene family. Isoelectric focusing (IEF) electrophoresis showed that purified amy proteins could be divided into two distinct groups, a low pI group with an isoelectric point of 4.5–5.1 and a high pI group with an isoelectric point of 5.0–6.6 (Jacobsen and Higgins, 1982). Due to its commercial and biological importance, a significant effort was made to clone *amy* genes. A genomic clone was identified as an *amy* gene (amy32b) and belongs to a low pI amy protein (Rogers and Milliman, 1983; Whittier et al., 1987). Two cDNA clones were also characterized as *amy* genes (amy6_4 and amy46) that belong to high pI enzymes (Khursheed and Rogers, 1988). Furthermore, 3D structures have been resolved for two barley amy proteins; one belonging to a low pI amy protein (1AMY) and the other to a high pI amy protein (1HT6) (Kadziola et al., 1994; Robert et al., 2003).

While experimental data has shown that amy proteins are coded by multigene families, the exact numbers of genes are unknown. Barley genome sequencing is a useful resource for identifying the number of amy genes and discovering their genomic features. The barley genome contained 12 *amy* genes (Mascher et al., 2017), which were grouped into four subfamilies (**Table 1**). Subfamily 1 consists of six members—four on chromosome 6H (533880485–542858990 bp) and two on the unsorted chromosome (195047130–196261798 bp, **Table 1**)—designated *amy1_1a* to *amy1_1e* and *amy1_2*. Four of which (*amy1_1a* to *amy1_1d*) have almost 100% sequence identity among members (Additional File 1: Supplementary Table S1A). One member (*amy1_1e*) is a truncated protein missing the carbohydrate-binding domain. Sequence identity analysis showed that the five *amy1_1* proteins matched the cloned gene *amy6_4* (Khursheed and Rogers, 1988), while the *amy1_2* protein, with 95% sequence identity with *amy1_1a*, matched the cloned gene amy46 in both promoter and coding regions (Khursheed and Rogers, 1988). All amy1 members belong to

[1]http://www.genome.jp/tools/clustalw/

TABLE 1 | Barley amy nomenclatures, gene ID, locations, and the association of old and new nomenclatures.

New names	IBSC gene ID	Chr	Genomic location	SF	Old nomenclatures
amy1_1a	HORVU6Hr1G078330	6H	533880485/533879015	1	*amy6_4, 1AMY, high pI*
amy1_1b	HORVU6Hr1G078360	6H	534112867/534114337	1	*amy6_4, 1AMY, high pI*
amy1_1c	HORVU6Hr1G078420	6H	534499529/534498059	1	*amy6_4, 1AMY, high pI*
amy1_1d	HORVU0Hr1G032700	0H	195047130/195048600	1	*amy6_4, 1AMY, high pI*
amy1_1e	HORVU0Hr1G032850	0H	196262594/196261798	1	*amy6_4, 1AMY, high pI*
amy1_2	HORVU6Hr1G080790	6H	542857506/542858990	1	*amy46, 1AMY, high pI*
amy2_1	HORVU7Hr1G091150	7H	556169683/556167920	2	low pI
amy2_2	HORVU7Hr1G091240	7H	557398785/557397068	2	low pI
amy2_3	HORVU7Hr1G091250	7H	557428810/557427021	2	*amy32b, 1HT6, low pI*
amy3	HORVU5Hr1G068350	5H	517452674/517454307	3	N/A
amy4_1	HORVU2Hr1G071710	2H	511664000/511667683	4	N/A
amy4_2	HORVU3Hr1G067620	3H	513498473/513485531	4	N/A

Chr, chromosome; SF, subfamily.

high pI enzymes (**Table 1**) and have high sequence identity with a 3D structure-resolved protein 1AMY (Kadziola et al., 1994). Subfamily *amy2* has three members on chromosome 7H (556169683–557427021 bp, **Table 1**), and are designated *amy2_1* to *amy2_3*. They have >92% sequence identity among the members, and >72% when compared to *amy1_1a*. *Amy2_3* had a high sequence identity with cloned gene *amy32b* (Rogers, 1985; Whittier et al., 1987) and 3D structure-resolved protein 1HT6 (Robert et al., 2003). They belong to genes coding for low pI enzymes (**Table 1**). *Amy3* has one member localized on chromosome 5H (designated *amy3*), while *amy4* has two members localized on chromosomes 2H and 3H (designated *amy4_1* and *amy4_2*). The *amy4* members have about 48% sequence identities compared between the members, or 43–46% sequence identity when compared to *amy1_1a* (Supplementary Table S1A).

Since *amy1* and *amy2* were located on chromosomes 6H and 7H, respectively, and many important malt quality QTLs were associated with these genetic loci, we believed that they were the most important members in relation to barley malt qualities (Hayes et al., 1993; Oziel et al., 1996; Zale et al., 2000; Gao et al., 2004; Li et al., 2010), we decided to investigate and compare gene and promoter structures for these two subfamilies in barley, rice, and wheat.

Barley amy Protein Secondary Structure

All amy proteins from amy1 and amy2 had the catalytic amino acid residues Asp_{203}, Glu_{228}, and Asp_{310} (*amy1_1a* positions), apart from *amy1_1e*, which was a truncated protein missing Asp_{310} (**Figure 1**). The near full-length proteins consisted of a central domain A forming $(\alpha/\beta)_8$ barrel, a structural loop domain B and a carbohydrate-binding domain C (**Figure 1**). Domain C formed five anti-parallel sheets (Kadziola et al., 1994; Robert et al., 2003). Barley amy proteins from amy3 and amy4 also contain the catalytic amino acids and a carbohydrate-binding module as discovered in the Domain Database at NCBI[2]. However, Asp_{310} on the active site was replaced with Glu_{310} for the two amy4 proteins (**Figure 1**).

[2]http://www.ncbi.nlm.nih.gov/Structure/bwrpsb/bwrpsb.cgi

Barley *amy* Gene Genomic Arrangement

Four barley *amy1* genes (*amy1_1a* to *amy1_1d*) had the same genomic arrangements as two introns and three exons. The nucleotide numbers for the introns and exons were the same as *amy1_1a* to *amy1_1d*, being 23 and 107 bp for the introns and 87, 1002, and 252 bp for the exons (Supplementary Table S2). While *amy1_2* had two introns and three exons, the nucleotide numbers differed from the *amy1_1a* to *amy1_1d* members, being 95 and 106 bp for the introns and 87, 945, and 252 bp for the exons. *Amy2-1* to *amy2_3* had three introns and four exons, but the nucleotide numbers for all introns and exons differed among the three *amy* genes (Supplementary Table S2). *Amy3* had three introns and four exons like *amy2*, but the nucleotide numbers differed from *amy2*. *Amy4* had more than five introns and six exons.

Barley *amy* Gene Promoter Conserved Motifs

Promoters of all barley *amy1* genes contained a conserved GA response complex (GARC) consisting of GARE (TAACAAA), pyrimidine (CCTTTT) and TATCCAC(T) boxes (Supplementary Table S3A and **Figure 2**) (Skriver et al., 1991; Gubler and Jacobsen, 1992; Rogers et al., 1994). There was also a cAMP-like response element (TGAGCTC) on *amy1* promoters (Gubler and Jacobsen, 1992), which represses gibberellin action. Pyrimidine and TATCCAC boxes enhanced the expression of amy1 proteins. The conserved motifs on subfamily 2 members differed from those on subfamily 1 genes and also among subfamily 2 members (Supplementary Table S3B and **Figure 3**). All three *amy2* genes had GARE (TAACAGAG) and pyrimidine (CCTTTT) boxes. The pyrimidine box was much closer to the translation start site (−17 bp) for *amy2_2*, but further away for *amy2_1*, and *amy2_3* at −211 and −236 bp, respectively. The original pyrimidine box of the *amy2_2* gene, at a similar position to *amy2_1*, and *amy2_3*, was mutated to CCATTT on *amy2_2* (**Figure 3**). A TATCCAT box was found in two *amy2* genes (*amy2_1* and *amy2_3*), but it was replaced with TACCCAT in the *amy2_2* gene. Furthermore, the *amy2_2* promoter had a conserved O2S box (CTTGxxTCATC) and cAMP-like box (TGAGCTC). Genomic

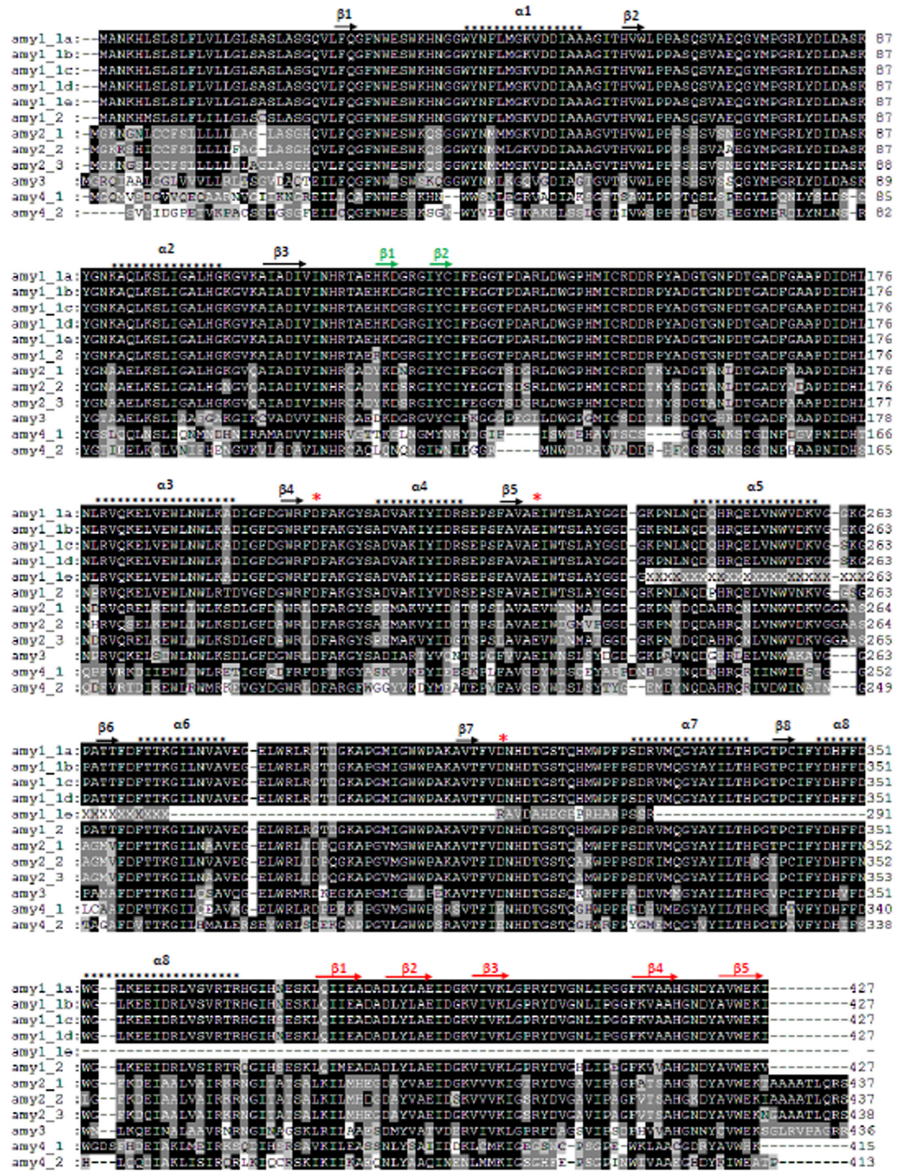

FIGURE 1 | Alignments and secondary structures of barley amy proteins. Barley amy1_1a and amy2_3 had 100% sequence identities with the two 3D structure-resolved barley amy proteins (1AMY and 1HT6), respectively (Kadziola et al., 1994; Robert et al., 2003). Their secondary structure features are shown on top of the alignments. There are three domains: domain A (black arrows and asterisks), domain B (green arrows), and domain C (red arrows). Domain A consists of a $(\alpha/\beta)_8$ barrel, while domain C has five β-sheets. The three catalytic amino acids Asp_{203}, Glu_{228}, and Asp_{310} are indicated by red asterisks (amy1_1a position).

sequence analysis showed that both *amy1* and *amy2* genes had a GARC, where GARE was required for GA induction of amy expression with pyrimidine and TA(T/C)CCAT box controlling gene expression levels (Lanahan et al., 1992).

When promoter regions (−500 bp) of subfamilies 1 and 2 were analyzed, the sequence identities were high (>99%) among *amy1_1a*, *amy1_1b,* and *amy1_1d* (Supplementary Table S4A). However, the *amy1_1e* promoter region was truncated to −151 bp, despite being 100% identical to the promoter sequence of *amy1_1a* gene. The promoter region of *amy1_1c* had high sequence identity within −350 bp, but low sequence identity beyond −350 bp, compared to *amy1_1a* (**Figure 2**). The sequence of the *amy1_2* promoter (−500 bp) was 64% identical to the *amy1_1a* promoter. The genomic locations of the conserved motifs in *amy1* were the same for all *amy1_1* members at −180, −199, −220, and −225 bp for TATCCA, GARE, cAMY-like and pyrimidine boxes, respectively (Supplementary Table S3A). However, the locations of these motifs from the *amy1_2* gene was a nucleotide closer to the ATG translation start site compared to the locations of *amy1_1* members (Supplementary Table S3A). The sequences of *amy2* promoters had low sequence identity (59–68%) compared to their members (Supplementary Table S4B).

FIGURE 2 | Barley *amy1* promoter sequence alignments and conserved motifs. ALL *amy1* promoters (except *amy1_1e*, which is truncated) contain a GA-responsive element (GARE) TAACAAA (red box). It requires for GA induction, They also contain a pyrimidine box (CCTTTT) and a TATCCA(C/T) box (blue boxes), which enhance gene expression after GA responses (Gubler and Jacobsen, 1992). A cAMP-like responsive element (TGAGCTC) is conserved (green box).

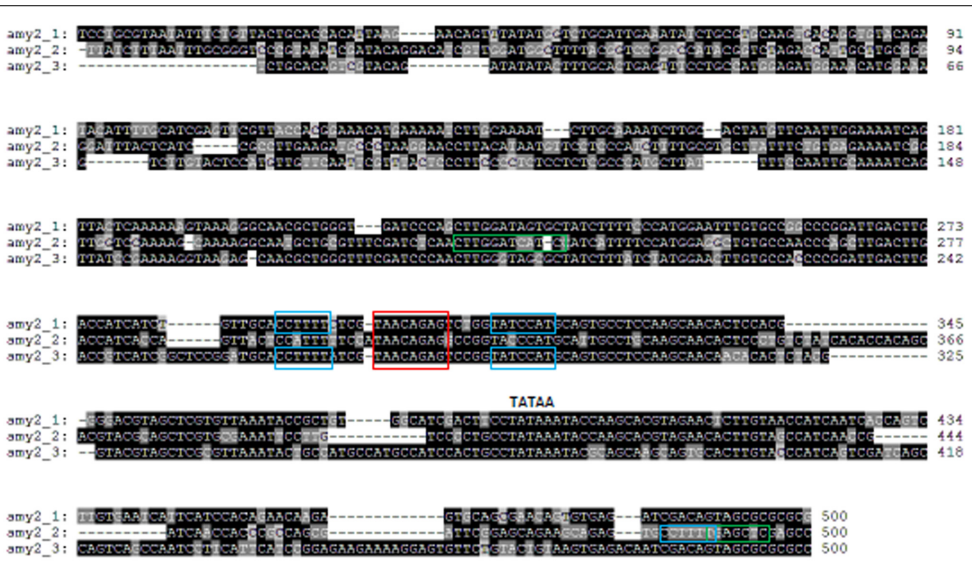

FIGURE 3 | Barley *amy2* promoter sequence alignments and conserved motif analysis. All three *amy2* promoters contain a GA-responsive element (GARE) TAACAGAG (red box) required for GA induction. Promoters of *amy2_1* and *amy2_3* contained a pyrimidine box (CCTTTT) and a TATCCA(C/T) box (blue boxes), which enhance gene expression (Gubler and Jacobsen, 1992). A pyrimidine box (blue box), a cAMP-like responsive element (TGAGCTC) (green box) and an O2S (CTTGXXTCATC) (green box) were present on *amy2_2* promoter.

Rice *amy* Gene Numbers and Conserved Motifs on Promoters

The rice genome contained 10 *amy* genes with three, one, four, and two members in subfamilies 1, 2, 3, and 4, respectively (**Table 2**). The number of *amy1* and *amy2* genes in rice was four, much less than the sum of *amy1* and *amy2* in barley. Rice *amy3* had the most gene members. Two of the *amy1* genes (LOC_Os02g52700 and LOC_OS02g52710) had three introns (Supplementary Table S2), unlike the barley *amy1* genes, which all had two introns. The other *amy1* gene (LOC_Os01g25510) had two introns. Alignment of the three amy1 protein sequences identified one protein (LOC_Os01g25510) with a very low sequence identity (24–30%) compared to the other two amy proteins (LOC_Os02g52700 and LOC_Os02g52710) (Supplementary Table S1B and **Figure S1**). The two amy1 proteins and one amy2 protein had similar secondary structures to the barley amy proteins. However, the amino acid compositions differed substantially on most of the β-strains and α-helices (**Supplementary Figure S1**). Rice had the same catalytic amino acids (Aps, Glu, and Asp) as barley. The promoters of the three rice *amy1* genes had >65% sequence identities (Supplementary Table S4C). They contained the GARE (TAACAAA), pyrimidine (CCTTTT) and TATCCAT boxes (Supplementary Table S3C and **Figure S2A**) but not the cAMY-like box. The rice amy2 protein (LOC_Os06g49970) had 72% sequence identity compared to the two amy1 proteins (LOC_OS02g527100 and LOC_Os02g52710). However, the promoter of the rice *amy2* gene only contained GARE (TAACAGAG), but not pyrimidine, TATCCAT or TATCCAC boxes (Supplementary Table S3C and **Figure S2B**).

Wheat *amy* Gene Numbers and Conserved Motifs on Promoters

The number of *amy* genes in the wheat A, B, and D genomes was 6, 10, and 8, respectively. The other four *amy* genes are located in unsorted chromosomes (**Table 2**). The wheat B genome had the most *amy* genes with four, three, one and two members in subfamilies *amy1*, *amy2*, *amy3,* and *amy4*, respectively. The number of *amy1* and *amy2* genes in each wheat genome did not exceed those in the barley genome (**Table 2**). All of the wheat *amy2* genes had the same genomic arrangement as the barley *amy2* genes with three introns and four exons (Supplementary Table S2). Most of the wheat *amy1* genes had two introns and three exons except for 6BL4, Un1 and Un2, which had three or four introns. The protein sequence identities were high within the wheat amy1 or amy2, being >80% (Supplementary Tables S1C,D and **Figures S3**, **S4**). The sequence identities for promoters of *amy1* genes were 50–100%, but much lower for *amy2* gene promoters (Supplementary Tables S4D,E). The promoters of all wheat *amy1* genes contained GARE (TAACAAA), pyrimidine, TATCCAT or TATCCAC boxes (**Supplementary Figure S5**). They also had a cAMP-like motif (TGAGCTC) box as per the barley *amy1* gene promoters. Five of the wheat *amy2* gene promoters contained a GARE (TAACAGAG) box, six contained pyrimidine and TATCCAT boxes, and seven had O2S motifs. The O2S motifs in the wheat genomes contained four variable nucleotides between the conserved CTTC and TCATC (**Supplementary Figure S6**), while the O2S in the barley *amy2* promoters had two variable nucleotides (**Figure 3**).

A Comparison of *amy* Gene Copy Numbers and Sequence Properties from Barley, Rice, and Wheat

Barley had the highest number of *amy1* genes (six), while wheat had four in the B genome and rice had three (**Table 2**). Both barley and wheat had the same number of *amy2* genes (B genome only), while rice had one. Rice contained the most *amy3* genes (four), while barley and wheat had one each. All the barley, wheat and rice genomes contained two *amy4* genes (**Table 2**). The intron numbers for *amy2* genes were the same for barley, wheat and rice, but differed for the *amy1* genes: barley had two, wheat had two or four, and rice had two or three (Supplementary Table S2). The intron numbers for *amy3* and *amy4* genes differed, ranging from two to nine (Supplementary Table S2). Barley *amy1* genes had high sequence identities with wheat *amy1* genes ranging from 83 to 97% (Supplementary Table S5). Barley *amy2* genes also had high sequence identities with wheat *amy2* genes (80–96%) (Supplementary Table S5). The barley and wheat *amy1* and *amy2* genes had similar promoter regions with sequence identities ranging from 50 to 76% (Supplementary Table S6). However, there was no similarity between barley and rice promoter sequences.

Expanded *amy1* and *amy2* Genes Are Important for Barley Malting Qualities

Barley amy proteins are grouped into four subfamilies according to their sequence properties (Mascher et al., 2017). The biological functions for each subfamily are unclear. Genetic mapping using molecular marker technologies showed that the regions associated with the genetic markers amy1 and amy2 on chromosomes 6 and 7 are important for malting qualities including amy enzyme activities and malt extracts (Hayes et al., 1993; Han and Ullrich, 1994; Oziel et al., 1996; Marquez-Cedillo et al., 2000; Emebiri et al., 2004). Thus, we conclude that *amy1* and *amy2* are the major genes responsible for starch degradation during seed germination. Other indirect evidence includes the induced expression of *amy1* and *amy2* genes during seed germination by GA (Khursheed and Rogers, 1988; Karrer et al., 1991). The abundance of mRNA levels ranks amy32b (*amy2_3*) > amy6-4 (*amy1_1a* to *amy1_1e,* possibly sum) > amy46 (*amy1_2*) about 24 h after GA induction (Khursheed and Rogers, 1988; Karrer et al., 1991). Barley *amy1* have expanded members due to genome duplication, which may play a key role in barley becoming a malting commodity. Furthermore, many amy genomic and cDNA clones had been deposited on Genbank. Their relationships for some of the clones with amy1 and amy2 was shown by a phylogenetic tree at **Supplementary Figure S7**.

There was no direct evidence for the function of amy3 and amy4 proteins in barley. In wheat, amy3 was highly expressed in developing grains, which affected carbon partitioning and diacylglycerol accumulation (Whan et al., 2014), while

TABLE 2 | Orthologs of rice and wheat α-amylase genes.

SF	Rice	Wheat			
		A	B	D	Unanchored
amy1	LOC_Os02g52700	6AL_amy1	6BL_amy2	6DL_amy1	
	LOC_Os02g52710	6AL_amy2	6BL_amy3	6DL_amy2	
	LOC_Os01g25510	6AL_amy3	6BL_amy4	6DL_amy3	
			6BL_amy5		
amy2	LOC_Os06g49970	7AL_amy1	7BL_amy1	7DL_amy1	Un_amy1
			7BL_amy2	7DL_amy2	Un_amy2
			7BL_amy3		Un_amy3
amy3	LOC_Os09g28400	5AL_amy1	5BL_amy1	5DL_amy1	
	LOC_Os09g28420				
	LOC_Os08g36900				
	LOC_Os08g36910				
amy4	LOC_Os04g33040	2AL_amy1	2BL_amy1	2DL_amy1	Un_amy4
	LOC_Os01g51754		3BL_amy1	3DL_amy1	

Rice and wheat amy protein sequences were downloaded from ftp://ftp.ensemblgenomes.org/pub/plants/release-35/fasta/oryza_sativa/dna/ and ftp://ftp.ensemblgenomes.org/pub/plants/release-35/fasta/triticum_aestivum/dna/, respectively. They were aligned with barley amy protein sequences using the clustalW program (http://www.genome.jp/tools/clustalw/). Sequences in the same clads were regarded as the same subfamily (SF) members. A, B, and D: wheat A, B, and D genomes.

the amy4 gene may be involved in starch degradation working in partnership with amy1 proteins (Mieog et al., 2017).

Significance of Conserved Motifs on Promoters of *amy1* and *amy2* in the Induction of *amy* Gene Expression

Barley amy enzymes are synthesized in barley aleurone layers induced by gibberellin (GA) (Chrispeels and Varner, 1967; Jacobsen et al., 1970). Two groups of proteins (A and B) were detected after GA induction. Their responses to GA induction differed in a time and GA concentration dependent manner (Jacobsen and Higgins, 1982). The group A proteins expressed earlier and required a low GA concentration, while the group B proteins were not detectable till 8 h after GA addition and required a higher GA concentration. However, the synthesis of group B proteins accelerated once expressed, and one of group B isoforms was most abundant at 24 h (Jacobsen and Higgins, 1982). The group A and B proteins were likely to be the products of *amy1* and *amy2* genes, respectively, as shown by changes in mRNA levels in response to GA (Khursheed and Rogers, 1988). Conserved motifs on *amy1* and *amy2* promoters played key roles in the induction of gene expression. A comparison of *amy1* with *amy2* promoters showed substantial differences in nucleotide composition of the conserved motifs. The GA-responsive element is TAACAAA on all *amy1* promoters, but TAACAGAG on all *amy2* promoters for all three crops. There is a cAMY-like responsive element close to the pyrimidine box on barley and wheat *amy1* promoters, but not *amy2* promoters. The difference in the conserved motifs may play a key role in GA-induced gene expression.

Gene expression induced by GA may have the same mechanism for all *amy1* members, since they contain extract same number of motifs with same nucleotide sequences except *Hvamy1_2* gene on which the TATCCAC box was replaced by TATCCAT. In contrast, barley *amy2* members may be differentially regulated, particularly for the *Hvamy2_2* gene, since the conserved motifs differed substantially from *amy1*, *amy2_1,* and *amy2_3*. Furthermore, no similar motifs were found in the promoters of *amy3* and *amy4*.

Genomic Properties of Wheat *amy* Genes Did Not Differ from Those of Barley *amy* Genes

Barley grains are often used for malting. Barley malts contain sufficient diastatic power (enzymatic hydrolytic activities) to completely convert starch to fermentable sugars. Extended numbers of *amy* genes and the presence of GA-regulatory motifs are important for barley to be used for malts (**Table 1** and **Figures 2**, **3**). However, wheat *amy* genes had similar genomic properties to barley *amy* genes with similar intron and exon structures (Supplementary Table S2). They also contained GA-regulatory motifs as in barley *amy* gene promoters (**Supplementary Figures S5**, **S6**). This could explain why wheat can also be used for malting (Fleming et al., 1960; Faltermaier et al., 2013). However, there are some problems with using wheat malts for brewing. Wheat grains lack husk, which is a problem for a brewing process called Lautering. Wheat also has higher protein (up to 20%). Wheat proteins promote foam formation, but also enhance haze issues (Faltermaier et al., 2015).

CONCLUSION

Subfamilies *amy1* and *amy2* have similar genomic properties in wheat and barley—including the number of exon/intron structures, localized on chromosomes 6 and 7, with

GA-responsive elements on promoters—but differ in rice. Interestingly, the barley genome contains at least three more *amy1* genes on chromosome 6H. Wheat should contain sufficient amy activity to completely degrade starch during malting. Other factors, such as high protein and the lack of husk, may limit the use of wheat for brewing.

AUTHOR CONTRIBUTIONS

All authors listed have made a substantial, direct and intellectual contribution to the work, and approved it for publication.

SUPPLEMENTARY MATERIAL

The Supplementary Material for this article can be found online at: https://www.frontiersin.org/articles/10.3389/fpls.2017.01727/full#supplementary-material

FIGURE S1 | Alignment of rice amy1 and amy2 proteins. Rice amy1 and amy2 proteins were aligned using ClustalW software (http://www.genome.jp/tools-bin/clustalw). The secondary structure features are shown on top of the alignments. There are three domains: domain A (black arrows and asterisks), domain B (green arrows) and domain C (red arrows). Domain A consists of a $(\alpha/\beta)_8$ barrel, while domain C has five β-sheets. The three catalytic amino acids Asp_{203}, Glu_{228}, and Asp_{310} are indicated by red asterisks.

FIGURE S2 | Rice *amy1* and *amy2* promoter alignments. **(A)** ALL *amy1* contain a GA-responsive element (GARE) TAACAAA (red box), a pyrimidine box (CCTTTT) and a TATCCA(C/T) box (blue boxes). **(B)** Rice amy2 promoter (LOC_Os06g49970) within 500 bp from translation start codon (ATG) contained GA-responsive element only. No pyrimidine and TATCCA(C/T) were found.

FIGURE S3 | Alignment of wheat amy1 proteins. Wheat amy1 proteins were aligned using ClustalW software (http://www.genome.jp/tools-bin/clustalw).

FIGURE S4 | Alignment of wheat amy2 proteins. Wheat amy2 proteins were aligned using ClustalW software (http://www.genome.jp/tools-bin/clustalw).

FIGURE S5 | Alignment of wheat amy1 promoter sequences. ALL wheat *amy1* contain a GA-responsive element (GARE) TAACAAA (red box), a pyrimidine box (CCTTTT), a TATCCA(C/T) box (blue boxes) and a cAMP-like motif (TGAGCTC) (green box).

FIGURE S6 | Alignment of wheat *amy2* promoter sequences. The GA-responsive element (GARE) TAACAAA (red), pyrimidine box (CCTTTT), TATCCA(C/T) box (blue), and OS2 motifs (green) are marked.

FIGURE S7 | A comparison of new and old amy nomenclatures. The phylogenetic tree was generated using the ClustalW program (http://www.genome.jp/tools-bin/clustalw). The nucleotide sequences were collected from GenBank with accession numbers M17125.1, M17126.1, M17127.1, and M17128.1 (Knox et al., 1987); X15226 and X15227 (Rahmatullah et al., 1989); J01236.1 (Rogers and Milliman, 1983); K02637 (Rogers, 1985); J04202 (Khursheed and Rogers, 1988), and X05166 (Whittier et al., 1987).

REFERENCES

Bahaji, A., Li, J., Sánchez-López, Á. M., Baroja-Fernández, E., Muñoz, F. J., Ovecka, M., et al. (2014). Starch biosynthesis, its regulation and biotechnological approaches to improve crop yields. *Biotechnol. Adv.* 32, 87–106. doi: 10.1016/j.biotechadv.2013.06.006

Bak-Jensen, K. S., Laugesen, S., Ostergaard, O., Finnie, C., Roepstorff, P., and Svensson, B. (2007). Spatio-temporal profiling and degradation of alpha-amylase isozymes during barley seed germination. *Febs J.* 274, 2552–2565. doi: 10.1111/j.1742-4658.2007.05790.x

Barrero, J. M., Mrva, K., Talbot, M. J., White, R. G., Taylor, J., Gubler, F., et al. (2013). Genetic, hormonal and physiological analysis of late maturity alpha-amylase (LMA) in wheat. *Plant Physiol.* 161, 1265–1277. doi: 10.1104/pp.112.209502

Brown, A. H. D., and Jacobsen, J. V. (1982). Genetic basis and natural variation of α-amylase isozymes in barley. *Genet. Res.* 40, 315–324. doi: 10.1017/s0016672300019182

Chrispeels, M. J., and Varner, J. E. (1967). Gibberellic acid-enhanced synthesis and release of α-amylase and ribonuclease by isolated barley and aleurone layers. *Plant Physiol.* 42, 398–406. doi: 10.1104/pp.42.3.398

Emebiri, L. C., Moody, D. B., Panozzo, J. F., and Read, B. J. (2004). Mapping of QTL for malting quality attributes in barley based on a cross of parents with low grain protein concentration. *Field Crop. Res.* 87, 195–205. doi: 10.1016/j.fcr.2003.11.002

Evans, D. E., Li, C., and Eglinton, J. K. (2010). "The properties and genetics of barley malt starch degrading enzymes," in *Genetics and Improvement of Barley Malt Quality*, eds G. Zhang and C. Li (Berlin: Springer), 143–189.

Faltermaier, A., Waters, D., Becker, T., Arendt, E., and Gastl, M. (2013). Protein modifications and metabolic changes taking place during the malting of common wheat (*Triticum aestivum* L.). *J. Am. Soc. Brew. Chem.* 71, 153–160.

Faltermaier, A., Zarnkow, M., Becker, T., Gastl, M., and Arendt, E. K. (2015). Common wheat (*Triticum aestivum* L.): evaluating microstructural changes during the malting process by using confocal laser scanning microscopy and scanning electron microscopy. *Eur. Food Res. Technol.* 241, 239–252. doi: 10.1007/s00217-015-2450-x

Fincher, G. B. (2010). "Biochemistry, physiology, and genetics of endosperm mobilization in germinated barley grain," in *Barley*, ed. S. Ullrich (Chichester: Wiley-Blackwell), 449–477. doi: 10.1002/9780470958636.ch14

Fleming, J. R., Johnson, J. A., and Miller, B. S. (1960). Effect of malting procedure and wheat storage conditions on alpha-amylase and protease activities. *Cereal Chem.* 37, 363–370.

Gao, W., Clancy, J. A., Han, F., Jones, B. L., Budde, A., Wesenberg, D. M., et al. (2004). Fine mapping of a malting-quality QTL complex near the chromosome 4H S telomere in barley. *Theor. Appl. Genet.* 109, 750–760. doi: 10.1007/s00122-004-1688-7

Gómez-Cadenas, A., Zentella, R., Walker-Simmons, M. K., and Ho, T.-H. D. (2001). Gibberellin/abscisic acid antagonism in barley aleurone cells: site of action of the protein kinase PKABA1 in relation to gibberellin signaling molecules. *Plant Cell* 13, 667–679. doi: 10.1105/tpc.13.3.667

Gubler, F., and Jacobsen, J. V. (1992). Gibberellin-responsive elements in the promoter of a barley high-pI alpha-amylase gene. *Plant Cell* 4, 1435–1441.

Gupta, M., Abu-Ghannam, N., and Gallaghar, E. (2010). Barley for brewing: Characteristic changes during malting, brewing and applications of its by-products. *Compr. Rev. Food Sci. F.* 9, 318–328. doi: 10.1111/j.1541-4337.2010.00112.x

Han, F., and Ullrich, S. E. (1994). Mapping of quantitative trait loci associated with malting quality in barley. *Barley Genet. Newsl.* 23, 84–97.

Hayes, P. M., Liu, B. H., Knapp, S. J., Chen, F., Jones, B., Blake, T., et al. (1993). Quantitative trait locus effects and environmental interaction in a sample of North American barley germ plasm. *Theor. Appl. Genet.* 87, 392–401. doi: 10.1007/bf01184929

Jacobsen, J. V., and Higgins, T. J. V. (1982). Characterization of the α-amylases synthesized by aleurone layers of Himalaya barley in response to gibberellic acid. *Plant Physiol.* 70, 1647–1653. doi: 10.1104/pp.70.6.1647

Jacobsen, J. V., Scandalios, J. G., and Varner, J. E. (1970). Multiple forms of amylase induced by gibberellic acid in isolated barley aleurone layers. *Plant Physiol.* 45, 367–371. doi: 10.1104/pp.45.4.367

Kadziola, A., Abe, J.-I., Svensson, B., and Haser, R. (1994). Crystal and molecular structure of barley α-amylase. *J. Mol. Biol.* 239, 104–121. doi: 10.1006/jmbi.1994.1354

Karrer, E. E., Litts, J. C., and Rodriguez, R. L. (1991). Differential expression of alpha-amylase genes in germinating rice and barley seeds. *Plant Mol. Biol.* 16, 797–805. doi: 10.1007/BF00015072

Khursheed, B., and Rogers, J. C. (1988). Barley alpha-amylase genes. Quantitative comparison of steady-state mRNA levels from individual members of the two different families expressed in aleurone cells. *J. Biol. Chem.* 263, 18953–18960.

Knox, C. A., Sonthayanon, B., Chandra, G. R., and Muthukrishnan, S. (1987). Structure and organization of two divergent alpha-amylase genes from barley. *Plant Mol. Biol.* 9, 3–17. doi: 10.1007/bf00017982

Lanahan, M. B., Ho, T. H., Rogers, S. W., and Rogers, J. C. (1992). A gibberellin response complex in cereal alpha-amylase gene promoters. *Plant Cell* 4, 203–211. doi: 10.1105/tpc.4.2.203

Li, C. D., Cakir, M., and Lance, R. (2010). "Genetic improvement of malting quality through conventional breeding and marker-assisted selection," in *Genetics and Improvement of Barley Malt Quality*, eds G. Zhang and C. Li (Berlin: Springer), 260–292.

MacGregor, A., LaBerge, D., and Meredith, W. (1971). Separation of α-and β-amylase enzymes from barley malt by ion-exchange chromatography. *Cereal Chem.* 48, 490–498.

Marquez-Cedillo, A. L., Hayes, M. P., Jones, L. B., Kleinhofs, A., Legge, G. W., Rossnagel, G. B., et al. (2000). QTL analysis of malting quality in barley based on the doubled-haploid progeny of two elite North American varieties representing different germplasm groups. *Theor. Appl. Genet.* 101, 173–184. doi: 10.1007/s001220051466

Mascher, M., Gundlach, H., Himmelbach, A., Beier, S., Twardziok, S. O., Wicker, T., et al. (2017). A chromosome conformation capture ordered sequence of the barley genome. *Nature* 544, 427–433. doi: 10.1038/nature22043

Mieog, J. C., Janeček, Š, and Ral, J.-P. (2017). New insight in cereal starch degradation: identification and structural characterization of four α-amylases in bread wheat. *Amylase* 1, 35–49. doi: 10.1515/amylase-2017-0004

Muthukrishnan, S., Gill, B. S., Swegle, M., and Chandra, G. R. (1984). Structural genes for alpha-amylases are located on barley chromosomes 1 and 6. *J. Biol. Chem.* 259, 13637–13639.

Oziel, A., Hayes, P. M., Chen, F. Q., and Jones, B. (1996). Application of quantitative trait locus mapping to the development of winter-habit malting barley. *Plant Breed.* 115, 43–51. doi: 10.1111/j.1439-0523.1996.tb00869.x

Rahmatullah, R. J., Huang, J. K., Clark, K. L., Reeck, G. R., Chandra, G. R., and Muthukrishnan, S. (1989). Nucleotide and predicted amino acid sequences of two different genes for high-pI alpha-amylases from barley. *Plant Mol. Biol.* 12, 119–121. doi: 10.1007/bf00017454

Robert, X., Haser, R., Gottschalk, T. E., Ratajczak, F., Driguez, H., Svensson, B., et al. (2003). The structure of barley α-amylase isozyme 1 reveals a novel role of domain C in substrate recognition and binding: a pair of sugar tongs. *Structure* 11, 973–984. doi: 10.1016/S0969-2126(03)00151-5

Rogers, J. C. (1985). Two barley alpha-amylase gene families are regulated differently in aleurone cells. *J. Biol. Chem.* 260, 3731–3738.

Rogers, J. C., Lanahan, M. B., and Rogers, S. W. (1994). The cis-acting gibberellin response complex in high-pl [alpha]-amylase gene promoters (requirement of a coupling element for high-level transcription). *Plant Physiol.* 105, 151–158. doi: 10.1104/pp.105.1.151

Rogers, J. C., and Milliman, C. (1983). Isolation and sequence analysis of a barley alpha-amylase cDNA clone. *J. Biol. Chem.* 258, 8169–8174.

Rogers, J. C., and Milliman, C. (1984). Coordinate increase in major transcripts from the high pI alpha-amylase multigene family in barley aleurone cells stimulated with gibberellic acid. *J. Biol. Chem.* 259, 12234–12240.

Shahpiri, A., Talaei, N., and Finnie, C. (2015). Spatio-temporal appearance of alpha-amylase and limit dextrinase in barley aleurone layer in response to gibberellic acid, abscisic acid and salicylic acid. *J. Sci. Food Agric.* 95, 141–147. doi: 10.1002/jsfa.6695

Skriver, K., Olsen, F. L., Rogers, J. C., and Mundy, J. (1991). Cis-acting DNA elements responsive to gibberellin and its antagonist abscisic acid. *Proc. Natl. Acad. Sci. U.S.A.* 88, 7266–7270. doi: 10.1073/pnas.88.16.7266

Svensson, B., Mundy, J., Gibson, R. M., and Svendsen, I. (1985). Partial amino acid sequences of α-amylase isozymes from barley malt. *Carlsberg Res. Commun.* 50, 15–22. doi: 10.1007/BF02910534

Whan, A., Dielen, A.-S., Mieog, J., Bowerman, A. F., Robinson, H. M., Byrne, K., et al. (2014). Engineering α-amylase levels in wheat grain suggests a highly sophisticated level of carbohydrate regulation during development. *J. Exp. Bot.* 65, 5443–5457. doi: 10.1093/jxb/eru299

Whittier, R. F., Dean, D. A., and Rogers, J. C. (1987). Nucleotide sequence analysis of alpha-amylase and thiol protease genes that are hormonally regulated in barley aleurone cells. *Nucleic Acids Res.* 15, 2515–2535. doi: 10.1093/nar/15.6.2515

Woodger, F., Jacobsen, J. V., and Gubler, F. (2010). "Gibberellin action in germinated cereal grains," in *Plant Hormones: Biosynthesis, Signal Transduction, Action!*, ed. P. J. Davies (Dordrecht: Springer), 221–240.

Zale, J. M., Clancy, J. A., Ullrich, S. E., Jones, B. L., and Hayes, P. M. (2000). North American barley genome project. Summary of barley malting-quality QTLs mapped in various populations. *Barley Genet. Newsl.* 30, 44–54.

Conflict of Interest Statement: The authors declare that the research was conducted in the absence of any commercial or financial relationships that could be construed as a potential conflict of interest.

frontiers in Plant Science

ORIGINAL RESEARCH
published: 07 September 2018
doi: 10.3389/fpls.2018.01356

Does Late Maturity Alpha-Amylase Impact Wheat Baking Quality?

*Marcus Newberry[1], Alexander B. Zwart[2], Alex Whan[1], Jos C. Mieog[1,2†], May Sun[1], Emmett Leyne[1], Jenifer Pritchard[1], Sergio Nicolas Daneri-Castro[1], Kutty Ibrahim[1], Dean Diepeveen[3], Crispin A. Howitt[1] and Jean-Philippe F. Ral[1]**

[1] Agriculture and Food, Commonwealth Scientific and Industrial Research Organisation, Canberra, ACT, Australia, [2] Data61, Commonwealth Scientific and Industrial Research Organisation, Canberra, ACT, Australia, [3] Department of Primary Industries and Regional Development, South Perth, WA, Australia

Late maturity α-amylase (LMA) and pre-harvest sprouting (PHS) are both recognized as environmentally induced grain quality defects resulting from abnormally high levels of α-amylase. LMA is a more recently identified quality issue that is now receiving increasing attention worldwide and whose prevalence is now seen as impeding the development of superior quality wheat varieties. LMA is a genetic defect present in specific wheat genotypes and is characterized by elevated levels of the high pI TaAMY1 α-amylase, triggered by environmental stress during wheat grain development. TaAMY1 remains present in the aleurone through the harvest, lowering Falling Number (FN) at receival, causing a down-grading of the grain, often to feed grade, thus reducing the farmers' income. This downgrading is based on the assumption within the grain industry that, as for PHS, a low FN represents poor quality grain. Consequently any wheat line possessing low FN or high α-amylase levels is automatically considered a poor bread wheat despite there being no published evidence to date, to show that LMA is detrimental to end product quality. To evaluate the validity of this assumption a comprehensive evaluation of baking properties was performed from LMA prone lines using a subset of tall non-Rht lines from a multi-parent advanced generation inter-cross (MAGIC) wheat population grown at three different sites. LMA levels were determined along with quality parameters including end product functionality such as oven spring, bread loaf volume and weight, slice area and brightness, gas cell number and crumb firmness. No consistent or significant phenotypic correlation was found between LMA related FN and any of the quality traits. This manuscript provides for the first time, compelling evidence that LMA has limited impact on bread baking end product functionality.

Keywords: late maturity alpha-amylase, baking, Falling Number, wheat, end product quality

OPEN ACCESS

Edited by:
Chengdao Li,
Murdoch University, Australia

Reviewed by:
Georg Langenkämper,
Max Rubner-Institut, Germany
Sladana Rakita,
University of Novi Sad, Serbia

****Correspondence:***
Jean-Philippe F. Ral
jean.ral@csiro.au

†Present address:
Jos C. Mieog,
Southern Cross Plant Science,
Southern Cross University, Lismore,
NSW, Australia

Specialty section:
This article was submitted to Plant Breeding, a section of the journal Frontiers in Plant Science

Received: *19 March 2018*
Accepted: *28 August 2018*
Published: *07 September 2018*

Citation:
Newberry M, Zwart AB, Whan A, Mieog JC, Sun M, Leyne E, Pritchard J, Daneri-Castro SN, Ibrahim K, Diepeveen D, Howitt CA and Ral J-PF (2018) Does Late Maturity Alpha-Amylase Impact Wheat Baking Quality? Front. Plant Sci. 9:1356. doi: 10.3389/fpls.2018.01356

INTRODUCTION

Alpha-amylases (EC 3.2.1.1) are endohydrolases that cleave α-1,4 glucosidic bonds breaking down starch macromolecules into smaller polysaccharides. Many biological and industrial processes, such as mammalian digestion, plant metabolism, biofuel production, baking, fermentation, and malting rely on the hydrolysis of native starch by α-amylase (Janecek et al., 2014).

Abbreviations: BLUP, best linear unbiased predictions; DW, dry weight; eFN, equivalent Falling Number; FN, Falling Number; LMA, late maturity alpha-amylase; MAGIC, multi-parent advanced generation inter-cross; PHS, pre-harvest sprouting; WT, wild-type.

Alpha-amylase is considered to be one of the primary enzymes responsible for starch degradation in cereals and particularly wheat. During grain germination, α-amylase initiates the conversion of starch into simple sugars to fuel embryo and coleoptile growth in the first few days of germination. At least four α-amylase isoforms have been described in wheat grain but only a subset of specific isoforms are involved either in grain development or in the germination process (Mieog et al., 2017).

Alpha-amylase has been consistently used by the baking industry to improve dough properties and end product quality (He and Hoseney, 1991). Several studies have demonstrated the beneficial effect of α-amylase on bread texture and elasticity (Patel et al., 2012; Barrera et al., 2016). However, detection of elevated levels of endogenous α-amylase in the grain has been considered as a serious grain quality defect due to its presumed effect on end-product quality (Buchanan and Nicholas, 1980). Premature production of α-amylase during grain development is the result of two different conditions that are considered quality defects by the wheat industry: (1) PHS and (2) LMA. Although PHS is considered an important issue by both wheat breeders and growers globally, it is only in Australia and the United Kingdom over several decades that LMA has been regarded as a significant grain quality defect, although more recently LMA has been considered an issue in other countries (for review Mares and Mrva, 2014).

Pre-harvest sprouting is a genetic condition that breaks grain dormancy when environmental triggers prior to harvest (usually heavy rainfall) cause the grain to germinate while still on the head (Gubler et al., 2005). Sprouted grain is unacceptable as milling wheat leading to it being downgraded to animal feed quality with a resulting decrease in value. Domestication and modern conventional breeding aims to reduce grain dormancy by encouraging rapid and uniform plant establishment, however, this has inadvertently favored PHS susceptibility and occurrence. Thus developing PHS resistance has become a high priority for breeders (Martinez et al., 2018).

Late maturity alpha-amylase is a genetic defect present in specific wheat genotypes and is characterized by abnormally elevated levels of a single α-amylase (TaAMY1) isoform in the aleurone layer during grain development through to harvest (Mares and Mrva, 2008). A recent study has also highlighted the potential involvement of TaAMY4 in the LMA phenotype (Mieog et al., 2017). This accumulation of α-amylase has no detrimental effect on grain composition, morphology, dormancy, or germination. Since the Green Revolution, which enhanced yield and reduced the height of wheat plants through the introduction of the semi-dwarf genes (Rht-D1), LMA has become a stochastically induced genetic defect triggered by environmental conditions (Gooding et al., 2012; Mieog et al., 2017). In Australia, a cold shock at a specific developmental stage induces LMA, while studies in the United Kingdom have described a similar phenotype following a heat shock (Farrell and Kettlewell, 2008).

Elevated levels of α-amylase in the grain reduce the value produced by the FN test. The FN test was developed by Hagberg (1960) as a rapid, high throughput method for determining α-amylase activity in grain and later adopted by industry as a test for sprout-damaged grain (Best and Muller, 1991). In Australia, if low FN is detected, there is a potential $AUS20–50/t penalty to growers due to downgrading superior milling wheat classes to feed grade (Kingwell and Carter, 2017). Therefore the premature production of α-amylase during grain development known as LMA has been considered the major quality problem affecting both growers and breeders in the Australian wheat industry (Lunn et al., 2001; Mares and Mrva, 2014). In the past few years the United States and France have encountered elevated α-amylase levels at harvest without signs of sprouting or starch damage, which suggests that LMA prone lines are present in all breeding programs worldwide. In the United States, the Pacific North West was severely impacted during the 2016 harvest, with losses estimated to be in the order of $US140 million (Bettge, 2018).

Despite the increasing importance and negative economic impacts of LMA to grain growers, to date only one study has been conducted to understand the mechanism underlying expression of LMA (Barrero et al., 2013). Unlike PHS with its widely acknowledged and clearly demonstrated detrimental effects on end-use quality, there is no direct evidence that elevated levels of α-amylase have negative effects on end-use quality (Ral et al., 2016, 2018b).

The current strategies to mitigate, and if possible eliminate LMA revolve around efforts to understand the genetic basis of LMA (Mrva and Mares, 2001; Mohler et al., 2014; Mieog et al., 2017; Milczarski et al., 2017; Borner et al., 2018). These LMA strategies have been put in place despite a clear knowledge gap around the real impact of LMA on wheat flour end product quality. One of the key issues that has impeded developing an understanding of the impact of LMA on end product quality has been the difficulty in inducing LMA under controlled conditions, on a scale large enough to produce sufficient grain for baking studies. The stochastic nature of LMA expression (combination of genetic, environmental conditions and plant developmental stage) makes the prediction of LMA occurence very cumbersome during LMA dedicated field trial (Mares and Mrva, 2014). To overcome this limitation we apply a novel approach focussed on the phenotypic aspects of LMA via exclusively studying the less economically significant constitutive LMA expressing non-Rht tall lines to assess the impact of LMA related elevated α-amylase on baking quality (Gooding et al., 2012).

This study involves a comprehensive assessment of LMA prone lines using a subset of LMA constitutive expressers from a MAGIC wheat population (Huang et al., 2012). LMA expression levels, FN test, total α-amylase activity and a LMA-specific antibody test available in Australia were determined, along with quality parameters including end product functionality such as bread loaf volume, bread slice gas cell number, size, and structure.

This study provides the first direct evaluation as to whether elevated levels of α-amylase caused by LMA impact baking quality.

MATERIALS AND METHODS

Biological Material and Design

Three sample sets were obtained from subsets of tall lines taken from a MAGIC 4-parent wheat population grown at three different site and year combinations: Yanco (34.6° S, 146.4° E) and Narrabri (30.3° S, 149.8° E) during growing season 2009 and 2010 (irrigated, very favorable conditions); and Wongan Hills (30.9° S, 116.7° E, low yielding conditions) during the growing season 2011. In this study and for the baking study, 72 non-Rht LMA prone genotypes were selected from Yanco, 101 genotypes from Narrabri and 67 genotypes from Wongan Hills. For each site, all genotypes were grown on similar size plots according to the local best practice. The LMA test comparison was performed on wholemeal samples from Yanco and included 84 lines for the Stirring Number (SN) test and 196 lines for the ELISA Test, total α-amylase activity assay and TaAMY1 expression level.

All three sites were planted according to partially replicated (*p*-rep) spatially optimized statistical designs and involved a range of 4-parent MAGIC population genotypes including both non-Rht (tall) and Rht (dwarf, semi dwarf) phenotypes. The original intent of these experiments was to utilize the genetic breadth of the MAGIC 4-parent population without any particular focus upon the influence of Rht lines on the quality traits. Consequently the tall non-Rht lines were randomly distributed throughout these experimental designs, including the milling, baking, and flour quality assessment designs. However, although the role of tall non-Rht lines on wheat and flour quality were not a specific objective of the original experimental designs, the ability to utilize quality data from these tall lines to aid in understanding the impact of LMA upon end-product quality was deemed sufficiently important to undertake an investigation using subsets of the 4-parent lines from the complete experimental designs.

Grain samples from Yanco 2009 were milled to produce wholemeal and white flour samples. Grain samples from Narrabri 2010 and Wongan Hills 2011 were milled to produce white flour samples. To reduce the time and cost of milling white flour samples from the three large field trials, a proportion of the white flour samples were milled from composites of grain from two plots growing the same genotypes (Ral et al., 2018a). Hence, a proportion of the white flour samples represent a blending of the environmental effects in the field.

Milling and Flour Preparation

White flour from grain (2 kg) samples from the three sites were milled at commercial testing laboratories using laboratory scale Bühler MLU-202 pneumatic laboratory mills (Bühler AG, Uzwil, Switzerland). Grain samples were conditioned to 14% moisture content, white flour was derived from blending the B1, B2, B3, R1, R2, and R3 mill fractions. The optimal water absorption levels of the flours were determined on small-scale 4 g micro-doughLAB z-arm mixers (Perten Instruments, Sydney, NSW, Australia).

For the Yanco site grain (4 g) was milled into wholemeal flour using an UDY Cyclone Sample Mill (UDY Corporation, Fort Collins, Co., United States) fitted with a 0.5 mm screen without any prior moisture conditioning.

Alpha-Amylase Assay

Alpha-amylase activity was determined in 10 mg samples using the CERALPHA kit (Megazyme International Ireland Ltd.), with the manufacturer's protocol adapted for 96-well format and with appropriate dilutions (Whan et al., 2014). Alpha-amylase activity is expressed in Ceralpha-unit per gram of flour as per the manufacturer's recommended methods.

ELISA Assay

Late maturity alpha-amylase testing was performed on protein extracted from 10 mg wholemeal flour according to the method described by (Verity et al., 1999; Barrero et al., 2013). All spectrophotometric measurements were performed using a Thermo Scientific Multiskan Spectrum plate reader.

RT-qPCR TaAMY1 Expression Level

RNA was extracted using the protocol described in Mieog et al. (2017). Amylase-isoform specific primers for real-time quantitative PCR (RT-qPCR) were developed for TaAMY1 as previously described for qPCR (Mieog et al., 2013). RT-qPCR runs were performed on the MyIQ real-time PCR system (Bio-Rad) using SensiFAST one-step RT-qPCR kits containing a mastermix, reverse transcriptase and RNAse inhibitor (Bioline). A typical reaction consisted of 10 μL mastermix, 4.6 μL primer premix (1.6 μM each), 0.2 μL reverse transcriptase and 0.4 μL RNAse inhibitor and 5 μL RNA sample. Primers, plasmids of TaAMY1 and TaActin, obtained during sequencing or from cloned RT-qPCR products, were mixed in equal copy numbers and used as a calibrator sample to be able to directly compare TaAMY1 expression levels according to Mieog et al. (2017).

Falling Number Determination

The eFN of the tall lines was determined using the RVA SN test (AACC International Approved Methods 22-08.01, 1995) on 4 g of wholemeal flour (for Yanco wholemeal samples) and 3.5 g of white flour for each of the three sites using a Rapid Visco Analyser RVA-4SA (Perten Instruments, Sydney, NSW, Australia). The eFN was estimated from the measured SN values as per the formula of Barnard et al. (2005).

Baking

The flour samples were subjected to a long fermentation straight dough bread-making process that is used internationally for determining the baking quality of wheats. The method was based upon AACC Approved Methods 10-09.01 and 10-10.03 (AACC International Approved Methods 10-09.01, 2008; AACC International Approved Methods 10-10.03, 2009). A doughLAB mixer with 300 g bowl (Perten Instruments, Sydney, NSW, Australia) was used to mix the doughs to peak dough consistency. The ingredients were added to 250 g of flour at the following percentages of flour weight: dried yeast 0.7% (Mauripan), vegetable fat 2% (Doveg Shortening), sugar 1%, salt 1%, baking improver 0.5% (Straight Dough Improver), and water at the

previously determined optimal water absorption level of less than 4%. The sugar and salt were domestic grade, while the dried yeast, vegetable fat and baking improver were all commercial baking ingredients with the latter two sourced from George Weston Foods (Sydney, NSW, Australia) and the yeast obtained from Mauri ANZ (Sydney, NSW, Australia). The doughs were mixed at 180 rpm to optimal dough development as determined by the baker, with mixing times ranging from 2.03 to 7.00 min. The doughLAB bowl temperature was maintained at 18.5–19°C to attain a final dough temperature of 26–28°C. Following mixing the dough was scaled into two 150 g pieces and placed into sealed containers and held at 28°C in a fermentation cabinet for 105 min. After passing the dough pieces through a bread molder (Mono Mini Moulder, MONO Equipment, Swansea, Queensway, United Kingdom) the dough pieces were returned to the sealed plastic container and fermented for a further 50 min at 28°C, after which they were again run through the bread molder, returned to the sealed container and subjected to another 28°C fermentation for a further 25 min. The dough pieces were then passed through the bread molder a final time before placing into baking tins and given a final proof at 35°C and 85% humidity for 50 min. The proofed doughs were baked at 230°C for 20 min. The baked loaves were cooled at room temperature for an hour then loaf volumes were determined using rapeseed displacement (AACC International Approved Methods 10-05.01, 2000), the weight of each loaf was also measured. Oven spring was determined from the difference in height of the baked loaf while still in the baking tin less the height of the proofed tinned dough measured immediately prior to placing into the oven. The crumb firmness and structure were measured 1 day after baking. To prevent drying out the loaves were stored in sealed plastic bags at room temperature immediately after loaf volume was measured. Immediately before measuring the firmness and structure of the loaves the breads were sliced into 14 mm thick slices. The crumb structure was determined on the middle two slices using image analysis (C-Cell Bread Image Analyser, Calibre Control International, Warrington, United Kingdom) immediately followed by crumb texture analysis. The Slice Area, Slice Brightness, and Number of Cells (number of gas bubbles per slice) measurement parameters for the two slices per loaf were extracted from the C-Cell data. Bread firmness was determined on the same two slices using TA.XTplus Texture Analyser instruments (Stable Micro Systems, Godalming, United Kingdom) utilizing a 0.5 inch diameter Delrin probe and the standard Texture Profile Analysis (TPA 1 method) double compression cycle was used (pre-test speed 1 $mm{\cdot}s^{-1}$, test and post-test speeds 5 $mm{\cdot}s^{-1}$, 10 mm compression distance, 5 g trigger force). The Crumb Firmness was determined from the maximum height of the second compression peak.

Statistical Analysis

The data obtained were collated into two datasets. The white flour dataset contained data for eFN and the bread quality parameters oven spring, loaf volume and weight, number of cells, slice area, crumb firmness and slice brightness. The wholemeal flour dataset contained data for eFN, LMA-ELISA test, and TaAMY1 expression level parameters. LMA-ELISA test, total α-amylase activity and TaAMY1 parameters were transformed by applying a base-2 logarithm prior to analysis.

For each parameter, there were field, milling and testing stages to the data collection process, with an associated statistical randomisation of the lines and grain/flour samples to the respective field/milling/testing layout. Bivariate linear mixed model (LMM) analyses were used to partition the effects at the milled grain sample level from other sources of variation produced by baking and testing stages, and hence estimate correlations between milled grain sample effects for relevant pairs of parameters. The LMM analyses also allowed us to account for possible extraneous effects in the analysis (such as "day of processing of sample" effects) in the milling and testing phases, effectively removing their influence from the estimation of effects and effect correlations. Models were fitted using the ASReml-R LMMs software (Butler et al., 2009). Milled samples were fitted as random effects, leading to BLUPs as estimates of the milled sample-level effects for each response, along with the estimated correlation and an associated *p*-value derived using the REML likelihood ratio test for assessing the statistical significance of the correlation estimate (Butler et al., 2009).

The interest here is in the correlations occurring at the level of the milled flour samples, hence the models used to estimate milled sample-level correlations in the white flour dataset did not model genotypic effects or account for environmental effects in the field trial, since these effects simply contribute to the variation observed between milled flour sample effects. An exception to the above analysis procedure was the estimation of correlations between eFN and LMA-ELISA, total α-amylase activity or TaAMY1 expression parameters in the wholemeal dataset. No replication of samples was performed when determining eFN in the wholemeal samples, hence only one eFN observation was obtained per milled sample. Consequently, milled sample-level effects cannot be completely isolated from other sources of variation introduced in the eFN testing process. Hence, reported correlations between eFN and LMA-ELISA, total α-amylase activity or TaAMY1 expression parameters are simple Pearson correlations between the eFN observations and milled sample level BLUPs, and the *p*-value is obtained from the standard *t*-test for a Pearson correlation rather than the REML likelihood test.

RESULTS

LMA Trait Measurements and Correlations

Subsets of tall non-Rht lines taken from a MAGIC 4-parent wheat population from the Yanco trial were selected to perform a complete LMA assessment including SN converted eFN, total α-amylase activity assay, ELISA based high pI α-amylase detection kit and RT-qPCR measurement of expression of the transcript expressed in LMA affected wheat, TaAMY1.

For this comparative LMA assessment population, eFN ranged from 193 to 294 s. Total α-amylase activity ranged from 0.002 to 1.977 Ceralpha unit per gram of flour. LMA values in the

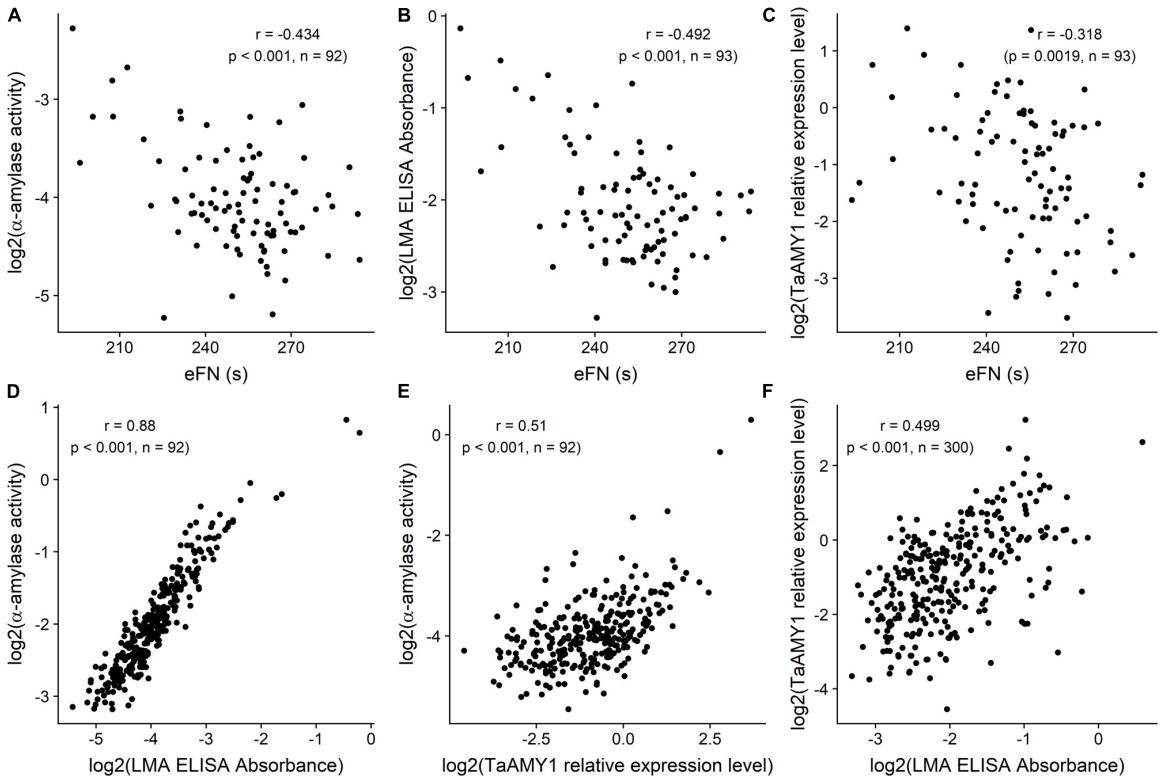

FIGURE 1 | Scatterplots and associated correlations (*r*) between equivalent Falling Number (eFN), and total a-amylase activity **(A)**, LMA ELISA Absorbance **(B)**, and TaAMY1 relative expression level **(C)** milled sample-level effects; between total a-amylase activity, and LMA ELISA Absorbance **(D)** and TaAMY1 relative expression level **(E)**; between TaAMY1 relative expression level and LMA ELISA Absorbance **(F)** for wholemeal flour samples from the Yanco site. Falling Number is expressed in seconds. LMA Elisa is expressed as absorbance according to Verity et al. (1999) and TaAMY1 is expressed as relative expression to Actin (Log2). Amylase assay responses were available for $n = 300$ milled samples, but only $n = 93$ samples were available for eFN assessment. Plotted amylase assay responses are milled sample-level Best Linear Unbiased Predictors (BLUPs) from linear mixed model analyses of the data, while eFN values are based on raw stirring number data only.

wholemeal flour ranged from 0.04 to 3.09 according to the ELISA test; and TaAMY1 relative expression to actin ranged from 0.03 to 11 (**Figure 1**; Ral et al., 2018a).

Among these samples, eFN was significantly negatively correlated with both total α-amylase activity (-0.434, $p < 0.001$), ELISA Test (-0.492, $p < 0.001$) and RT-qPCR (-0.318, $p = 0.00187$). Total α-amylase activity correlated highly with ELISA test (0.88, $p < 0.001$) and significantly with RT-qPCR (0.51, $p < 0.001$). ELISA and RT-qPCR were significantly positively correlated (0.499, $p < 0.001$) (**Figures 1A–F**).

These significant correlations between the four existing LMA tests confirmed the LMA nature of the tall population. For practical reasons and to reproduce the standard testing method for LMA the decision was made to focus on the most current and high throughput test, the effective FN as a surrogate for LMA identification in the white flour samples.

Baking Trait Measurements and Correlations

In this study 72 non-Rht LMA prone genotypes were selected from Yanco, 100 genotypes from Narrabri and 67 genotypes from Wongan Hills.

White flour baking performance including oven spring, bread loaf volume and weight, cell number, slice area and brightness and crumb firmness were assessed using an internationally approved AACCI methods.

The range of baking performance across the non-Rht population was compared to those from the MAGIC semi-dwarf genotypes and the set of elite cultivars included in the three site MAGIC trials (**Supplementary Figure S1**). The data show no statistical difference across the seven traits indicating that the baking performance of the tall lines did not differ from the semi-dwarf nor the commercial elite lines grown at the three sites.

The milled sample-level BLUP distributions of the baking traits for the three sites are presented as histograms in **Figure 2** and in the data repository (Ral et al., 2018a).

The baking traits were broadly similar across the three sites. Oven spring values, the increase in loaf volume during the baking stage, were similar for Narrabri and Wongan Hills, whereas the Yanco site exhibited a slightly larger oven spring. The loaf weights from the Yanco and Wongan Hills sites were similar, while those of the Narrabri site were slightly lighter and more variable. Loaf volumes could not be estimated for the Yanco site using the prediction model (see section "Materials and Methods") however, both the Narrabri and Wongan Hills sites displayed

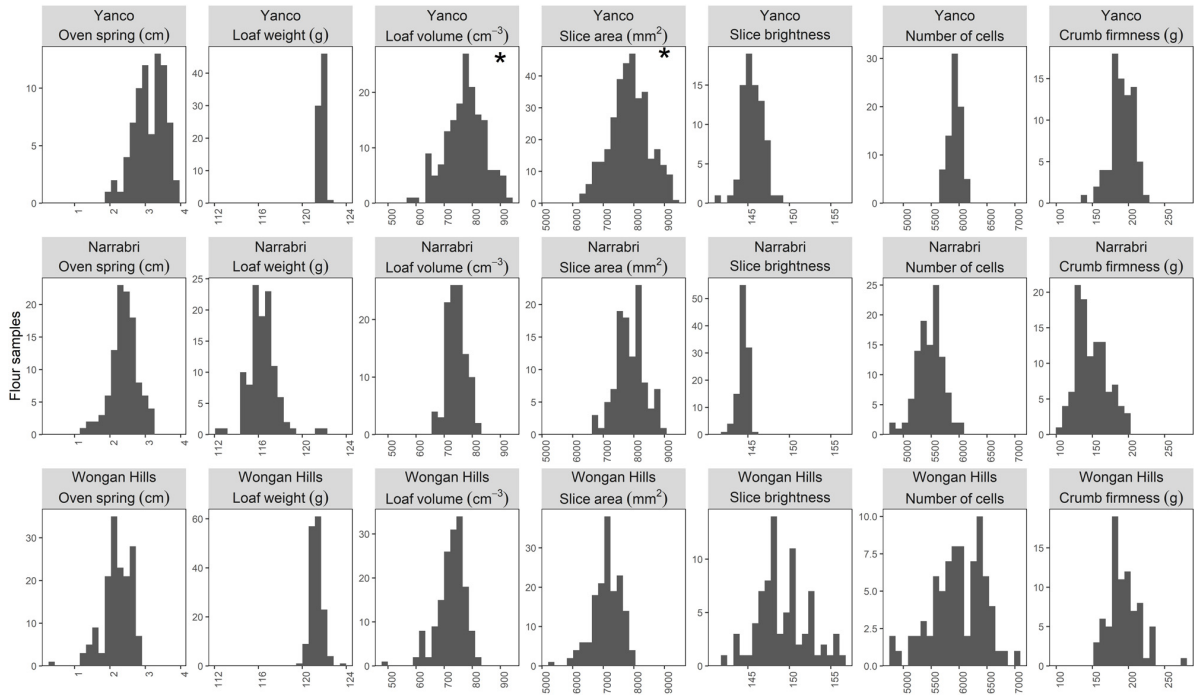

FIGURE 2 | Milled sample-level BLUP distributions for the baking quality traits for the Yanco, Narrabri, and Wongan Hills sites are presented as histogram. Subplots marked with an asterisk display raw trait data as the LMM analysis was unable to estimate any non-negligible variation between milled samples.

very similar loaf volumes. As with loaf volume the slice area of the bread could not be estimated for the Yanco site using prediction model, while the Narrabri and Wongan Hills sites had similar slice areas, although the Narrabri sites range extended to slightly larger slice areas. The slice brightness profiles were similar for the Narrabri and Yanco sites, while, the slice brightness measurements were more variable for Wongan Hills with the presence of much brighter slice values. The number of cells is a measure of the number of gas cells per bread slice and for the Straight Dough breadmaking method employed here greater numbers of small gas cells are preferable. Again the number of cells for the three sites was broadly similar, however, the Wongan Hills samples exhibited a much greater degree of variation with bread samples possessing gas cell numbers that were much greater than those observed at either the Yanco or Narrabri sites. The crumb firmness profiles were broadly similar across all three sites, although the Narrabri site did have some samples that were slightly less firm than the other two sites.

Among flour samples from tall lines at all three sites, eFN milled sample-level BLUPs ranged from ∼157 to ∼234 s with 250–300 s being the international average standard for FN of an acceptable grain sample.

Milled sample correlations between eFN and baking traits were not significantly different from zero at the $p < 0.05$ threshold, except for slice brightness at Wongan Hills (0.59, $p = 0.0014$), number of cells at Narrabri (0.34, $p = 0.0161$) and slice area at Narrabri (0.24, $p = 0.0308$), as summarized in **Figure 3** and data repository (Ral et al., 2018a). However, those correlations were not consistent across the three sites for those specific traits.

Quality responses in **Figure 3** exhibit small, though non-negligible, variation at the milled sample level, indicating that the variation in the phenotype was dominated by that introduced in the baking and quality testing steps.

For the parameters loaf volume and slice area in the Yanco 2009 trial, variation due to differences between milled samples (the milled sample-level effects) was negligible compared to variation introduced by the baking and quality testing steps of data collection process. Consequently, the LMM analysis could not estimate non-negligible variation between the milled samples, nor estimate the corresponding correlations with eFN. This is why, in **Figure 2**, the corresponding panels have been replaced by standard phenotypic correlation and no scatterplots are been presented in **Figure 3** for these two traits.

With the exception of the above mentioned traits, the correlations between baking traits and eFN were on average not significant across the three sites.

DISCUSSION

The original intent of this study was to utilize the genetic breadth of the MAGIC 4-parent population without any particular focus upon the influence of Rht lines on the quality traits.

Although the role of tall lines on wheat and flour quality was not a specific objective of these experimental designs, the ability to utilize quality data from these lines to aid in understanding

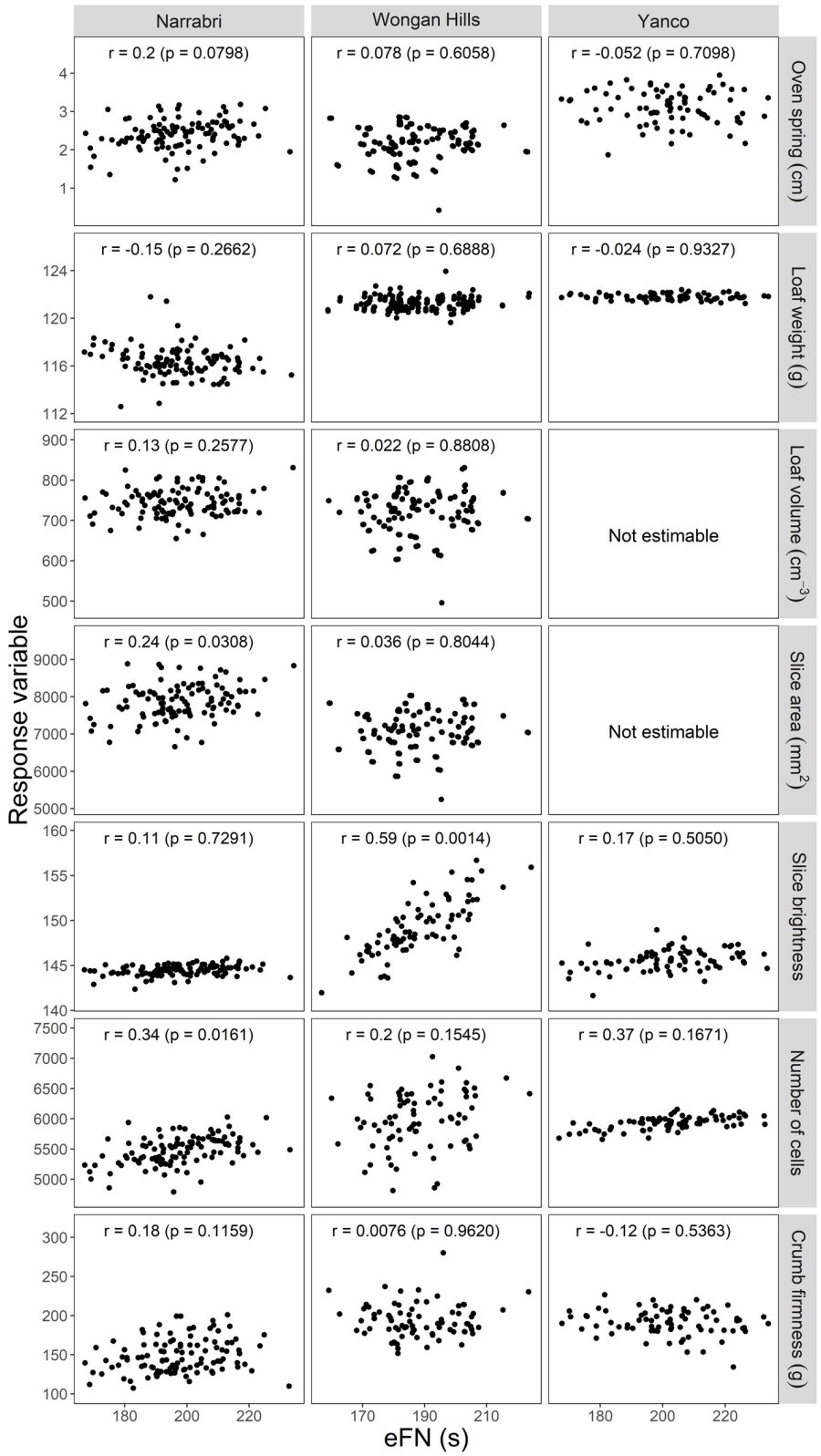

FIGURE 3 | Scatterplots of milled-sample level BLUPs and associated correlations (*r*) between equivalent Falling Number (eFN) and bread quality traits for the three sites, Yanco, Narrabri, and Wongan Hills, with associated REML likelihood ratio test *p*-values. Associated numbers of plotted observations are $n = 77$ (Yanco), $n = 108$ (Narrabri), and $n = 78$ (Wongan Hills). BLUPs for loaf volume and slice area at Yanco could not be estimated (see Section "Results").

the impact of LMA upon end-product quality was deemed sufficiently important to extract the data for this investigation.

With the selection of tall lines and in the absence of any evidence of sprouting, it was reasonable to assume that the reduced eFN was due to LMA rather than sprouting damage. However, we decided to confirm the LMA basis of the low eFN with LMA assessment methods (Mohler et al., 2014; Borner et al., 2018). Each reference test (including total α-amylase assay, ELISA test, RT-qPCR and SN), was performed on wholemeal flour to avoid any reduction of TaAMY1 protein or *TaAMY1* mRNA due to pearling (Chakraborty et al., 2003). In addition, Kweon et al. (2010) demonstrated the strong correlation between viscosity tests performed on wholemeal and related white flour samples.

For each of the alternative LMA assessment methods, clear correlations with eFN, demonstrating the involvement of TaAMY1 and LMA in the selected MAGIC lines were found. The correlation between the total α-amylase activity and the ELISA test, detecting TaAMY1 was strong confirming the sole involvement of TaAMY1 as active determining enzyme in the LMA phenotype. Mieog et al. (2017) has suggested the potential involvement of a newly discovered TaAMY4 in the LMA phenotype. This hypothesis was based on the significant co-expression of *TaAMY1* and *TaAMY4* in dry seed from LMA prone lines. While the mechanism through which TaAMY4 could be involved in the LMA phenotype remains to be elucidated, the result suggests that most of the total α-amylase activity in LMA affected dry grain is generated by TaAMY1. However, a role of an active TaAMY4 prior to grain maturation or during germination cannot be excluded.

The correlations involving *TaAMY1* expression level were the least convincing. Several factors could explain these weaker correlations. Determination of relative expression level required extraction of fragile total RNA that could introduce variation. In addition, Barrero et al. (2013) suggested a narrow window for TaAMY1 expression when LMA is triggered in an Rht background. Mieog et al. (2017) found elevated presence of TaAMY1 mRNA in LMA lines. The significant correlation found between RT-PCR and eFN clearly indicated that mRNA survives in dry grain but could be partially degraded during grain ripening.

The viscosity measurements performed on white flour (SN) gave a wide range of viscosities, corresponding to an eFN range of 157–234 s and 193–294 for the Yanco wholemeal flours. The result of lower eFN values for white flour compared to the Yanco wholemeal subsamples were unexpected. The milling process separates the bran from the flour and reduces the amount of aleurone specific enzymes thus increasing FN (Chakraborty et al., 2003). Therefore a higher FN is usually expected for white flour compared to wholemeal. However, several factors could explain this difference including a difference in the storage condition between white flour and grain. Brandolini et al. (2010) showed that storage temperature could impact the level of α-amylase activity. The difference in storage temperature between white flour and wholemeal in our experiment could explain the variation. The nature of the test sample could have also induced some variation. Viscosity test on white flour was based on 2 kg aliquots while wholemeal data was generated on samples of several grams. Because eFN and baking study were performed for the same low eFN white flour, this difference has no consequence on the study.

According to Mares and Mrva (2008), samples affected by LMA displayed a FN somewhere between 150 s and the acceptable threshold [from 250 to 350 s depending on the wheat grade and growing region, and country wheat quality receival standard according to Posner and Hibbs (2011)].

This study attempted to correlate eFN with seven baking quality attributes. However, no clear correlation could be found between any of the baking properties with the exception of slice brightness only for the Wongan Hills site (0.59). This strong correlation could illustrate what has been described as Maillard Reaction (Sanz-Penella et al., 2014; Ral et al., 2016; Marti et al., 2017). This reaction is directly related to the impact of α-amylase on starch conversion. Increased levels of α-amylase in flour accelerates soluble sugar release. These soluble sugars polymerise with amino acids toward the end of the baking process causing crumb browning. Another plausible explanation is that elevated α-amylase levels generated greater quantities of fermentable sugar leading to high CO_2 retention and altering gas cell formation due to enhanced yeast fermentation (Marti et al., 2017).

While association between eFN and slice brightness was expected, the lack of any strong and significant correlations was noteworthy. This result strongly suggested some limitation of the FN test in LMA detection. This limitation was also suggested by the correlation obtained with the wholemeal flour between FN and the other LMA tests available. Although the correlations between eFN and the other tests were highly significant, the correlations were not strong or at least not as strong as expected for a test that was created to detect α-amylase. While the FN test assesses viscosity of the flour slurry, it does not directly measure α-amylase activity. FN measures are affected by changes in the physical properties in the starch portion of the wheat grain during the test. However, in addition to α-amylase activity, several other factors can impact flour gelling properties, and therefore FN, including environment (Barnard and Smith, 2012) and starch structure. Starch composition, amylose-amylopectin ratio and chain structure can greatly affect the starch viscosity. Luo et al. (2015) have shown wide variations in starch viscosity among rice mutants affected by several starch metabolism enzymes. In potato, RNA interference of Glucan Water Dikinase caused reduction in tuber starch phosphate content associated with a clear reduction in viscosity (Viksø-Nielsen et al., 2001).

According to Lindahl and Eliasson (1992), protease and endopeptidase can also degrade the gluten matrix thus reducing wheat flour gelling properties. Gluten integrity is thus also affected during sprouting but as no proteases are expressed with LMA, gluten integrity remains unaffected (Simsek et al., 2014). The FN test is used to detect sprout damage where both α-amylase and protease are simultaneously expressed, but the presence of either α-amylases or proteases is sufficient to warrant a low FN especially in case of sprout damage (Edwards et al., 1989). The more significant role played by proteases over elevated α-amylases in decreasing end-product quality has been demonstrated a study comparing flours milled from

germinated grain and grain possessing transgenically elevated levels of α-amylases. This study on noodle quality revealed that germination does impact gluten integrity in wheat grain thus downgrading noodle quality; however, elevated levels of α-amylase alone did not show any detrimental effect (Ral et al., 2018b). This noodle research followed on from a previous study that showed even greatly elevated levels of a single α-amylase isoform had no detrimental effect on small scale baking quality (Ral et al., 2016).

To summarize, all flours with elevated levels of α-amylase will show a low FN as demonstrated in the wholemeal study with a significant negative correlation between LMA and eFN. However, not every low FN value is related to LMA or high α-amylase level. As LMA is characterized by the sole expression of single type of α-amylase (TaAMY1), this assumption that a decrease in flour paste viscosity measured by the FN test is associated with all the detrimental arsenal of degradative enzymes that typifies sprouting becomes problematic (Lunn et al., 2001).

Several alternative options to definitively identify LMA affected grains have been investigated over the years. Created with the aim of LMA detection, both the ELISA (Verity et al., 1999) and RT-qPCR relative α-amylase gene expression assays specifically target the main enzyme involved in LMA, TaAMY1 (Cheng et al., 2014). These approaches can be useful for breeding programs or wheat variety classification in quantifying the presence of TaAMY1 during grain development (Mares and Mrva, 2008), although the difficulties of triggering LMA in semi-dwarf breeding germplasm remains problematic. However, the methods are too slow and inappropriate for LMA detection at grain receival. During germination and sprouting, many α-amylases are expressed including TaAMY1 (Ainsworth et al., 1985) making the differentiation between LMA and sprouting cumbersome. Even in this study and despite the selection of constitutive LMA expressers, we cannot rule out the potential presence of some sprouted flour in the population.

The lack of correlation between the eFN LMA test and baking traits is particularly noteworthy. The overall total α-amylase activity present in flour samples ranged from near zero for the lowest to 2 Ceralpha unit per gram of flour for the highest. Although being significantly elevated and in accordance with an earlier LMA study (Mrva and Mares, 1999), this overall α-amylase activity remained very low compared to severely sprouted grains (Simsek et al., 2014). In germinated grain total α-amylase level can reach over 50 Ceralpha unit per gram of flour after 2 days (Ral et al., 2018b).

According to previous observations, a two to threefold increase of activity is sufficient to reduce the FN scores below the acceptable limit (300 s in Australia) (Mares and Mrva, 2008). Nevertheless there was no impact on baking. Transgenic wheat lines overexpressing wheat TaAMY3 specifically in the grain, have been shown not to have detrimental effects on either small scale baking quality or white salted noodle firmness despite having a FN close to 60 s (Ral et al., 2016, 2018b). These lines included some with a 30-fold increase in total α-amylase activity. An even greater increase in α-amylase activity results from the addition of commercial baking improver or malt (Marti et al., 2017). Recent studies showed that all four types of wheat α-amylase differ slightly in their protein structure including the presence of additional sugar binding domains suggesting different enzymatic properties (Cockburn et al., 2015; Mieog et al., 2017). While it is reasonable to assume that different types of α-amylase have different enzymatic properties, those differences are likely insignificant compared to the 1000-fold increase in α-amylase associated with the addition of baking improver.

If an elevated level of α-amylase due to LMA has the expected negative impact on baking quality then this would be evident from this large scale baking study involving LMA expressing lines.

Many factors can impact baking properties including genetic, phenotypic, or environmental (Cavanagh et al., 2010). However, if a strong correlation exists between two attributes, this correlation should be detected within the boundaries of the sampled population for 166 tall genotypes and three field sites. In this study there was a clear absence of correlation between LMA related eFN and any of the baking quality traits analyzed. Interestingly a recent study also highlighted the weak correlation between low FN in soft wheat and Japanese sponge cake volume (Kiszonas et al., 2018).

This pilot study further questions whether LMA is detrimental for baking quality. Because of the economic significance of this issue, further investigations are warranted with larger scale wheat flour based product quality testing using multisite dedicated trials including LMA constitutive, sensitive, and resistant varieties. With FN being one of the critical parameters upon which grain quality is assessed for trading wheat, it is understandable that the industry wishes to mitigate and eliminate LMA.

In the absence of any data establishing a detrimental effect of LMA on quality, there are now strong incentives to develop alternative simple, robust and high throughput tests that can discriminate between LMA and PHS. Such a test would need to be quick, inexpensive and appropriate for use at grain receival. One consequence would be to allow the resources of breeders to be used more efficiently in delivering enhanced varieties for growers. Given the importance that LMA has for the global wheat industry and the economic activities and livelihoods that stem from it, a more thorough understanding of the effect of LMA on wheat quality is needed. The findings of this study, together with previous studies, demonstrates that the detrimental impacts of LMA on flour and product quality are difficult to discern and points to the need for further evaluations of this contention and other assumptions surrounding LMA.

DATA AVAILABILITY

Complete dataset is available in a data access portal (Ral et al., 2018a).

AUTHOR CONTRIBUTIONS

MN and J-PR were involved in the design and coordination of the study, conceived and performed the experiments, analyzed the data, and wrote the manuscript. AZ and AW analyzed the

data and wrote the manuscript. JM, JP, and SD-C performed the experiments and analyzed the data related to the LMA assessment. MS, EL, and KI performed the experiments and analyzed the data related to the baking quality assessment. DD generated biological material. All authors read and approved the manuscript.

FUNDING

This work was supported by CSIRO Agriculture and Food and Grain Research and Development Corporation (GRDC).

ACKNOWLEDGMENTS

We would like to acknowledge Dr. Phil Larkin for his helpful discussions. We would like to thank to the Grain Research and Development Corporation (GRDC) of Australia for their financial support, through CSP00144, that allowed the baking quality assessments of the MAGIC wheat samples. We would also like to thank Australian Export Grains Innovation Centre (AEGIC) and George Weston Milling for their technical assistance.

SUPPLEMENTARY MATERIAL

The Supplementary Material for this article can be found online at: https://www.frontiersin.org/articles/10.3389/fpls.2018.01356/full#supplementary-material

FIGURE S1 | Boxplots of raw values for bread quality traits from commercial varieties, as well as tall and semi-dwarf MAGIC RILs grown at Yanco, Narrabri, and Wongan Hills. Horizontal lines indicate the median and interquartile ranges of the observed values.

REFERENCES

AACC International Approved Methods 10-05.01 (2000). *AACC International Approved Methods of Analysis, Method. Measurement of Volume by Rapeseed Displacement*. Washington, DC: AACC.

AACC International Approved Methods 10-09.01 (2008). *AACC International Approved of Analysis, Method Basic Straight-Dough Bread-Baking Method–Long Fermentation*. Washington, DC: AACC.

AACC International Approved Methods 10-10.03 (2009). *AACC International Approved of Analysis, Method. Optimized Straight-Dough Bread-Making Method*. Washington, DC: AACC.

AACC International Approved Methods 22-08.01 (1995). *AACC International Approved of Analysis Method Measurement of alpha-Amylase Activity with Rapid Visco Analyser*. Washington, DC: AACC.

Ainsworth, C. C., Doherty, P., Edwards, K. G. K., Martienssen, R. A., and Gale, M. D. (1985). Allelic variation at alpha-amylase loci in hexaploid wheat. *Theor. Appl. Genet.* 70, 400–406. doi: 10.1007/BF00273745

Barnard, A., and Smith, M. F. (2012). Determination of the influence of climate on falling number of winter wheat in the dryland production areas of the Free State Province of South Africa. *Euphytica* 188, 15–24. doi: 10.1007/s10681-012-0673-5

Barnard, A., van Deventer, C. S., and Maartens, H. (2005). Comparison between methods for estimating sprout damage in wheat. *South Afr. J. Plant Soil* 22, 44–48. doi: 10.1080/02571862.2005.10634679

Barrera, G. N., Tadini, C. C., Leon, A. E., and Ribotta, P. D. (2016). Use of alpha-amylase and amyloglucosidase combinations to minimize the bread quality problems caused by high levels of damaged starch. *J. Food Sci. Technol.* 53, 3675–3684. doi: 10.1007/s13197-016-2337-2

Barrero, J. M., Mrva, K., Talbot, M. J., White, R. G., Taylor, J., Gubler, F., et al. (2013). Genetic, hormonal, and physiological analysis of Late Maturity alpha-Amylase in wheat. *Plant Physiol.* 161, 1265–1277. doi: 10.1104/pp.112.209502

Best, S., and Muller, R. (1991). Use of Hagberg Falling Number apparatus to determine malt and barley quality. *J. Inst. Brew.* 97, 273–278. doi: 10.1002/j.2050-0416.1991.tb01068.x

Bettge, A. (2018). Low falling Numbers in the Pacific Northwest wheat growing region: preharvest Sprouting, late maturity amylase, falling number instrument, or low protein? *Cereal Foods World* 63, 12–16. doi: 10.1094/CFW-63-1-0012

Borner, A., Nagel, M., Agacka-Moldoch, M., Gierke, P. U., Oberforster, M., Albrecht, T., et al. (2018). QTL analysis of falling number and seed longevity in wheat (*Triticum aestivum* L.). *J. Appl. Genet.* 59, 35–42. doi: 10.1007/s13353-017-0422-5

Brandolini, A., Hidalgo, A., and Plizzari, L. (2010). Storage-induced changes in einkorn (*Triticum monococcum* L.) and breadwheat *(Triticum aestivum* L. ssp *aestivum*) flours. *J. Cereal Sci.* 51, 205–212. doi: 10.1016/j.jcs.2009.11.013

Buchanan, A. M., and Nicholas, E. M. (1980). Sprouting, alpha-amylase, and breadmaking quality. *Cereal Res. Commun.* 8, 23–28. doi: 10.1007/BF00293343

Butler, D., Cullis, B., Gilmour, A., and Gogel, B. (2009). *ASReml-R Reference Manual, version 3*. Brisbane, QLD: The Department of Primary Industries and Fisheries.

Cavanagh, C. R., Taylor, J., Larroque, O., Coombes, N., Verbyla, A. P., Nath, Z., et al. (2010). Sponge and dough bread making: genetic and phenotypic relationships with wheat quality traits. *Theor. Appl. Genet.* 121, 815–828. doi: 10.1007/s00122-010-1352-3

Chakraborty, M., Hareland, G. A., Manthey, F. A., and Berglund, L. R. (2003). Evaluating quality of yellow alkaline noodles made from mechanically abraded sprouted wheat. *J. Sci. Food Agric.* 83, 487–495. doi: 10.1002/jsfa.1403

Cheng, C. R., Oldach, K., Mrva, K., and Mares, D. (2014). Analysis of high pI *α-Amy*-1 gene family members expressed in late maturity α-amylase in wheat (*Triticum aestivum* L.). *Mol. Breed.* 33, 519–529. doi: 10.1007/s11032-013-9968-z

Cockburn, D., Nielsen, M. M., Christiansen, C., Andersen, J. M., Rannes, J. B., Blennow, A., et al. (2015). Surface binding sites in amylase have distinct roles in recognition of starch structure motifs and degradation. *Int. J. Biol. Macromol.* 75, 338–345. doi: 10.1016/j.ijbiomac.2015.01.054

Edwards, R. A., Ross, A. S., Mares, D. J., Ellison, F. W., and Tomlinson, J. D. (1989). Enzymes from rain-damaged and laboratory-germinated wheat.1. Effects on product quality. *J. Cereal Sci.* 10, 157–167. doi: 10.1016/s0733-5210(89)80044-x

Farrell, A. D., and Kettlewell, P. S. (2008). The effect of temperature shock and grain morphology on alpha-amylase in developing wheat grain. *Ann. Bot.* 102, 287–293. doi: 10.1093/aob/mcn091

Gooding, M. J., Uppal, R. K., Addisu, M., Harris, K. D., Uauy, C., Simmonds, J. R., et al. (2012). Reduced height alleles (Rht) and Hagberg falling number of wheat. *J. Cereal Sci.* 55, 305–311. doi: 10.1016/j.jcs.2012.01.003

Gubler, F., Millar, A. A., and Jacobsen, J. V. (2005). Dormancy release, ABA and pre-harvest sprouting. *Curr. Opin. Plant Biol.* 8, 183–187. doi: 10.1016/j.pbi.2005.01.011

Hagberg, S. (1960). A rapid method for determining alpha-amylase activity. *Cereal Chem.* 37, 218–222.

He, H., and Hoseney, R. C. (1991). Gas retention in bread dough during baking. *Cereal Chem.* 68, 521–525.

Huang, B. E., George, A. W., Forrest, K. L., Kilian, A., Hayden, M. J., Morell, M. K., et al. (2012). A multiparent advanced generation inter-cross population for genetic analysis in wheat. *Plant Biotechnol. J.* 10, 826–839. doi: 10.1111/j.1467-7652.2012.00702.x

Janecek, S., Svensson, B., and MacGregor, E. A. (2014). alpha-Amylase: an enzyme specificity found in various families of glycoside hydrolases. *Cell. Mol. Life Sci.* 71, 1149–1170. doi: 10.1007/s00018-013-1388-z

Kingwell, R., and Carter, C. (2017). Economic issues surrounding wheat quality assurance: the case of late maturing alpha-amylase policy in Australia. *Australas. Agribus. Rev.* 2:14.

Kiszonas, A. M., Engle, D. A., Pierantoni, L. A., and Morris, C. F. (2018). Relationships between Falling Number, alpha-amylase activity, milling, cookie, and sponge cake quality of soft white wheat. *Cereal Chem.* 95, 373–385. doi: 10.1002/cche.10041

Kweon, M., Slade, L., Levine, H., and Souza, E. (2010). Application of RVA and time-lapse photography to explore effects of extent of chlorination, milling extraction rate, and particle-size reduction of flour on cake-baking functionality. *Cereal Chem.* 87, 409–414. doi: 10.1094/cchem-03-10-0046

Lindahl, L., and Eliasson, A. C. (1992). Influence of added enzymes on the rheological properties of a wheat-flour dough. *Cereal Chem.* 69, 542–546.

Lunn, G. D., Kettlewell, P. S., Major, B. J., and Scott, R. K. (2001). Effects of pericarp alpha-amylase activity on wheat (*Triticum aestivum*) Hagberg falling number. *Ann. Appl. Biol.* 138, 207–214. doi: 10.1111/j.1744-7348.2001.tb00104.x

Luo, J. X., Ahmed, R., Kosar-Hashemi, B., Larroque, O., Butardo, V. M., Tanner, G. J., et al. (2015). The different effects of starch synthase IIa mutations or variation on endosperm amylose content of barley, wheat and rice are determined by the distribution of starch synthase I and starch branching enzyme IIb between the starch granule and amyloplast stroma. *Theor. Appl. Genet.* 128, 1407–1419. doi: 10.1007/s00122-015-2515-z

Mares, D., and Mrva, K. (2008). Late-maturity alpha-amylase: low falling number in wheat in the absence of preharvest sprouting. *J. Cereal Sci.* 47, 6–17. doi: 10.1016/j.jcs.2007.01.005

Mares, D. J., and Mrva, K. (2014). Wheat grain preharvest sprouting and late maturity alpha-amylase. *Planta* 240, 1167–1178. doi: 10.1007/s00425-014-2172-5

Marti, A., Cardone, G., Nicolodi, A., Quaglia, L., and Pagani, M. A. (2017). Sprouted wheat as an alternative to conventional flour improvers in bread-making. *LWT Food Sci. Technol.* 80, 230–236. doi: 10.1016/j.lwt.2017.02.028

Martinez, S. A., Godoy, J., Huang, M., Zhang, Z. W., Carter, A. H., Campbell, K. A. G., et al. (2018). Genome-Wide association mapping for tolerance to Preharvest Sprouting and low Falling Numbers in wheat. *Front. Plant Sci.* 9:141. doi: 10.3389/fpls.2018.00141

Mieog, J., Janeček, Š., and Ral, J. P. (2017). New insight in cereal starch degradation: identification and structural characterization of four α-amylases in bread wheat. *Amylase* 1, 35–49. doi: 10.1515/amylase-2017-0004

Mieog, J. C., Howitt, C. A., and Ral, J. P. (2013). Fast-tracking development of homozygous transgenic cereal lines using a simple and highly flexible real-time PCR assay. *BMC Plant Biol.* 13:71. doi: 10.1186/1471-2229-13-71

Milczarski, P., Masojc, P., Krajewski, P., Stochmal, A., Kowalczyk, M., Angelov, M., et al. (2017). QTL mapping for benzoxazinoid content, preharvest sprouting, alpha-amylase activity, and leaf rust resistance in rye (*Secale cereale* L.). *PLoS One* 12:e0189912. doi: 10.1371/journal.pone.0189912

Mohler, V., Albrecht, T., Mrva, K., Schweizer, G., and Hartl, L. (2014). Genetic analysis of falling number in three bi-parental common winter wheat populations. *Plant Breed.* 133, 448–453. doi: 10.1111/pbr.12177

Mrva, K., and Mares, D. J. (1999). Regulation of high pI alpha-amylase synthesis in wheat aleurone by a gene(s) located on chromosome 6B. *Euphytica* 109, 17–23. doi: 10.1023/a:1003696026410

Mrva, K., and Mares, D. J. (2001). Quantitative trait locus analysis of late maturity alpha-amylase in wheat using the doubled haploid population Cranbrook x Halberd. *Aust. J. Agric. Res.* 52, 1267–1273. doi: 10.1071/ar01047

Patel, M. J., Ng, J. H. Y., Hawkins, W. E., Pitts, K. F., and Chakrabarti-Bell, S. (2012). Effects of fungal alpha-amylase on chemically leavened wheat flour doughs. *J. Cereal Sci.* 56, 644–651. doi: 10.1016/j.jcs.2012.08.002

Posner, E. S., and Hibbs, A. N. (eds). (2011). "Wheat: the raw material," in *Wheat Flour Milling*, 2nd Edn. Eagan, MN: AACCI, 1–46.

Ral, J. P., Whan, A., Larroque, O., Leyne, E., Pritchard, J., Dielen, A. S., et al. (2016). Engineering high alpha-amylase levels in wheat grain lowers Falling Number but improves baking properties. *Plant Biotechnol. J.* 14, 364–376. doi: 10.1111/pbi.12390

Ral, J. P., Whan, A., Zwart, A. B., and Newberry, M. (2018a). Viscosity and related traits from wholemeal and white flour. *CSIRO.* doi: 10.25919/5b751069334e9

Ral, J. P. F., Sun, M., Mathy, A., Pritchard, J. R., Konik-Rose, C., Larroque, O., et al. (2018b). A biotechnological approach to directly assess the impact of elevated endogenous alpha-amylase on Asian white-salted noodle quality. *Starch Starke* 70:1700089. doi: 10.1002/star.201700089

Sanz-Penella, J. M., Laparra, J. M., and Haros, M. (2014). Impact of alpha-amylase during breadmaking on in vitro kinetics of starch hydrolysis and glycaemic index of enriched bread with bran. *Plant Foods Hum. Nutr.* 69, 216–221. doi: 10.1007/s11130-014-0436-7

Simsek, S., Ohm, J. B., Lu, H. Y., Rugg, M., Berzonsky, W., Alamri, M. S., et al. (2014). Effect of pre-harvest sprouting on physicochemical changes of proteins in wheat. *J. Sci. Food Agric.* 94, 205–212. doi: 10.1002/jsfa.6229

Verity, J. C. K., Hac, L., and Skerritt, J. H. (1999). Development of a field enzyme-linked immunosorbent assay (ELISA) for detection of alpha-amylase in preharvest-sprouted wheat. *Cereal Chem.* 76, 673–681. doi: 10.1094/cchem.1999.76.5.673

Viksø-Nielsen, A., Blennow, A., Jorgensen, K., Kristensen, K. H., Jensen, A., and Moller, B. L. (2001). Structural, physicochemical, and pasting properties of starches from potato plants with repressed r1-gene. *Biomacromolecules* 2, 836–843. doi: 10.1021/bm0155165

Whan, A., Dielen, A. S., Mieog, J., Bowerman, A. F., Robinson, H. M., Byrne, K., et al. (2014). Engineering alpha-amylase levels in wheat grain suggests a highly sophisticated level of carbohydrate regulation during development. *J. Exp. Bot.* 65, 5443–5457. doi: 10.1093/jxb/eru299

Conflict of Interest Statement: The authors declare that the research was conducted in the absence of any commercial or financial relationships that could be construed as a potential conflict of interest.

VII. ABSTRACTS OF THE 13TH INTERNATIONAL SYMPOSIUM ON PRE-HARVEST SPROUTING IN CEREALS

13TH INTERNATIONAL SYMPOSIUM ON PRE-HARVEST SPROUTING IN CEREALS

PERTH, WESTERN AUSTRALIA, 16-18 SEPTEMBER 2016

INTERNATIONAL COMMITTEE:

CHENGDAO LI (CHAIR, MURDOCH UNIVERSITY, AUSTRALIA)
HIRO NONOGAKI (OREGON STATE UNIVERSITY, USA)
JEAN-PHILIPPE RAL (CSIRO, AUSTRALIA)
JIRUI WANG (SICHUAN AGRICULTURAL UNIVERSITY, CHINA)
JOSE BARRERO (CSIRO, AUSTRALIA)
LEE HICKEY (UNIVERSITY OF QUEENSLAND, AUSTRALIA)
OLUWASEYISHORINOLA (JOHN INNES CENTRE, UK)
ROBERT BENECH-ARNOLD (UNIVERSITY OF BUENOS AIRES, ARGENTINA)
SHINGO NAKAMURA (INSTITUTE OF CROP SCIENCE, JAPAN)

LOCAL ORGANIZING COMMITTEE:

PROFESSOR CHENGDAO LI (MURDOCH UNIVERSITY, INTERNATIONAL CHAIR)
DR DEAN DIEPEVEEN (DEPARTMENT OF AGRICULTURE AND FOOD, LOCAL CHAIR)
MS DEBORAH BOXALL (AUSTRALIAN EXPORT GRAIN INNOVATION CENTRE)
MR STEPHAN HARASYMOW (AUSTRALIAN EXPORT GRAIN INNOVATION CENTRE)
MR TROY ADRIANSZ (AUSTRALIAN EXPORT GRAIN INNOVATION CENTRE)
DR LARISA CATO (AUSTRALIAN EXPORT GRAIN INNOVATION CENTRE)
DR BEN BIDDULPH (DEPARTMENT OF AGRICULTURE AND FOOD)
DR DARSHAN SHARMA (DEPARTMENT OF AGRICULTURE AND FOOD)
MS SUE BRUGHTON (DEPARTMENT OF AGRICULTURE AND FOOD)
DR FRANK GUBLER (CSIRO)
DR JOSE BARRERO (CSIRO)
DR DION BENNETT (AUSTRALIAN GRAIN TECHNOLOGY)
DR DAN MULLAN (INTERGRAINS)
DR GLEN FOX (UNIVERSITY OF QUEENSLAND)
DR LEE HICKEY (UNIVERSITY OF QUEENSLAND)
DR ANYOU LIU (CBH GROUP)
PROFESSOR YONGLIN REN (MURDOCH UNIVERSITY)
MS RUTH ABBOTT (MURDOCH UNIVERSITY)

Dormancy in Cereals: About The Mechanisms Behind This Trait

Roberto L. Benech-Arnold

IFEVA/Cátedra de Cultivos Industriales, Universidad de Buenos Aires/CONICET, Argentina

Email: benech@agro.uba.ar

To adjust the dynamics of dormancy release in cereal grains in order to adequate it to the necessities of the industry and farmers, is an aim of crop breeding. This adjustment is particularly difficult in grains whose industrialization requires a high germination capacity immediately after harvest (i.e. malting barley) since a release from dormancy taking place too early exposes the grain to suffer pre-harvest sprouting damage. For this reason, identifying and evidencing regulatory mechanisms for this trait is always an opportunity for their manipulation and consequent adjustment to our necessities. Because the ancestors of cereal species evolved under very diverse environments worldwide, different mechanisms have arisen as a way of sensing an appropriate germination environment (a crucial factor for winter or summer annuals such as cereals). In addition, different species (and even different varieties within the same species) display diverse grain morphology, allowing some structures to impose dormancy in some cereals but not in others. As in seeds from many other species, the antagonism between the plant hormones abscisic acid and gibberellins is instrumental in cereal grains for the inception, expression, release and re-induction of dormancy. However, the way in which this antagonism operates is different for the various species and involves different molecular steps as regulatory sites.

In this presentation I will show how we have elucidated different mechanisms in our model system grain sorghum, using different approaches (i.e. physiological, molecular, genetics). In particular, I will be referring to the crosstalk between abscisic acid signaling and gibberellins metabolism and its role in the determination of dormancy in this cereal. In addition, I will discuss which is the probability of finding these mechanisms operating in other species (cereals or else) and which are the methodological ways we are exploring to continue evidencing new dormancy mechanisms.

Grain in the Rain: East Asia as a Nursery for PHS Tolerance Genes in Wheat and Barley

Shingo Nakamura

Institute of Crop Science, NARO / Kannondai 2-1-2, Tsukuba, 305-8518, Japan

Email: shingo@affrc.go.jp

The rainy season in East Asia, including Japan, happens around the harvest season for wheat and barley, potentially causing pre-harvest sprouting (PHS) and thus substantial economic damages. Therefore, improving PHS tolerance is one of the most important tasks for wheat and barley breeding programs. To study the mechanism of PHS tolerance, The TRS (1001) project was launched as part of 'Genomics-based Technology for Agricultural Improvement" sponsored by the Ministry of Agriculture, Forestry, and Fisheries of Japan. The TRS(1001) project aims to identify the genes responsible for natural variation in seed dormancy in wheat and barley. Recently, three independent research groups that participate in TRS(1001) identified the causal genes for three major seed dormancy quantitative trait loci (QTL), *SD1* and *SD2* on chromosome 5H in barley, and *Phs1* on chromosome 4A in wheat (Sato et al. 2016; Nakamura et al. 2016; Torada et al. 2016). The studies revealed that an alanine aminotransferase gene (*ALT*) is the causal gene for *SD1* (*Qsd1*), and a *Mitogen-activated Kinase Kinase 3* gene (*MKK3*) is the causal gene for *SD2* (*Qsd2-AK*) and *Phs1*. In addition, we previously identified *Mother of FT and TFL1* (*MFT*) as the causal gene for the wheat major seed dormancy QTL *QPhs.ocs-3A.1* on chromosome 3A (Nakamura et al. 2011). These studies identified single-nucleotide polymorphisms (SNPs) as the causes of these QTL; genotyping these SNPs gives us information about their dormant or non-dormant genotypes, thus enabling marker-assisted selection to improve PHS tolerance using these genes. Moreover, the results for the barley QTL *Qsd1* and *Qsd2-AK* give us a clue for the improvement of PHS tolerance in wheat because their dormant alleles are recessive. The allohexaploid nature of wheat can mask the phenotype of recessive alleles because the other two homeologs can compensate for any recessive mutation. Therefore, introducing the recessive mutations into all the wheat homeologs may provide a novel method to increase seed dormancy in wheat cultivars. We analysed the distribution of the SNPs in *MFT* and *MKK3* in cultivars worldwide (Nakamura et al. 2015; Nakamura et al. 2016). The results suggest that the natural mutations for the dormant alleles occurred after domesticated wheat and barley reached East Asia from the Fertile Crescent, where their early domestication occurred. Cultivars with alleles giving stronger seed dormancy may be more adapted to the environment of East Asia, particularly the coincidence of the harvest and rainy seasons, which might lead to the prevalence of these alleles in East Asia.

Prevention of Preharvest Sprouting Through Hormone Engineering

Mariko Nonogaki and Hiro Nonogaki
Department of Horticulture, Oregon State University, Corvallis, OR 97331, USA

While vivipary, germination of seeds on the maternal plant, is observed in nature and provides ecological advantages in certain wild species, precocious seed germination in agricultural crops, such as preharvest sprouting (PHS) in cereals, is a serious issue. PHS reduces grain quality and causes economical losses to farmers. PHS can be prevented by translating the basic knowledge of hormone biology in seeds into technologies. Biosynthesis of abscisic acid (ABA), which is an essential hormone for seed dormancy, can be engineered to enhance dormancy and prevent PHS. Enhancing nine-*cis*-epoxycarotenoid dioxygenase (*NCED*), a rate-limiting enzyme of ABA biosynthesis gene, through a chemically induced gene expression system, has successfully been used to suppress germination of Arabidopsis seeds. The more advanced system *NCED* positive-feedback system, which amplifies ABA biosynthesis in a seed-specific manner without chemical induction, has also been developed. The proofs of concept established in the model species are now ready to be tested in crops. A potential problem is recovery of germination from hyperdormant crop grains. Hyperdormancy induced by these systems can be reversed by inducing counteracting genes, such as *NCED* RNA interference or gibberellin (GA) biosynthesis genes. Alternatively, seed sensitivity to ABA can be modified to rescue germination using the knowledge of chemical biology. ABA antagonists, which were developed recently, have great potential to recover germination from the hyperdormant seeds. Combination of the dormancy-imposing and -alleviating approaches will establish a comprehensive technology for PHS prevention and germination recovery.

Engineering High Alpha-Amylase Levels in Wheat Grain Lowers Falling Number but Improves Baking Properties

Jean-Philippe Ral[1], Alex Whan[1], Oscar Larroque[1], Emmett Leyne[1], Jeni Pritchard[1], Anne-Sophie Dielen[2], Crispin A Howitt[1], Matthew K Morell[3] and Marcus Newberry[1]

[1]CSIRO Agriculture Flagship, GPO Box 1600, Canberra ACT 2601, Australia

[2]Research School of Biology, The Australian National University, Canberra, ACT 0200, Australia

[3]Current Address: International Rice Research Institute, Manilla, The Philippines

Some wheat genotypes are prone to Late Maturity alpha-Amylase (LMA) and Pre Harvest Sprouting (PHS). When finishing environments have triggered these conditions, the grain is characterized by elevated levels of alpha-amylase isoforms. The enhanced expression of alpha-amylases results in a reduction in Falling Number, a test of gel viscosity, and a reduction in price for growers. The Falling Number test is unable to distinguish between LMA and PHS, thus both defects are treated similarly when grain is traded. Consequently any grain sample that has a low Falling Number is automatically considered poor for baking quality. While there is clear evidence linking PHS with poor baking quality, no such relationship has been demonstrated with LMA. Our work has demonstrated that wheat in which one isoform of alpha-amylase (TaAmy3), was overexpressed in the endosperm of developing grain to levels of up to 100 fold higher than the wild-type, resulted in low Falling Number similar to those seen in LMA or PHS affected grains. This increase had no detrimental effect on starch structure, flour composition and enhanced baking quality, in small scale 10g baking tests. In these tests loaf volume was increased and Maillard related browning was enhanced even without added baking improver, to levels higher than those seen in control flours when baking improver was added. These findings highlight the need for a better understanding of the impact of alpha-amylase expression alone on end product quality.

Changes in Some Physiological Parameters of Wheat (Triticum Aestivum L.) Genotypes Under Pre-harvest Sprouting Conditions

Ahmadpour Malakshaha and H. Pirdashtib

Department of Environmental Science University of Pune, India

Department of Agronomy, Genetics and Agricultural Biotechnology Institute of Tabarestan, Sari Agricultural Sciences and Natural Resources University, Sari, Iran

The evaluation of pre-harvest sprouting (PHS) is one of the most important breeding program for yield and grain quality of spring wheat in northern part of Iran (Mazandaran Province) . The PHS tolerance is determined by environmental, physiological, biochemical and enzymological factors and interaction between the genotypes and environment. Therefore, to screening and understand the role(s) of different physiological factors in PHS, an experiment was conducted using five spring wheat genotypes under three of mist irrigation conditions (MI, 7, 14 and 21 days after physiological maturity) at Agriculture Research Station of Baye Kola. The experimental design was a randomized complete block design with three replications. Changes physiological attributes in wheat grains such as carbohydrates, sugars, starch and phenols and proline under MI may serve as the reliable physiological markers to identify the PHS tolerant or sensitive genotypes. It is seems that MI is highly suitable and most practicable method for screening the different wheat genotypes. The PHS tolerance in selected wheat genotypes may be probably due to more carbohydrates and starch as well as less sugars, coupled with very high accumulation of phenols and proline. Consequently, these traits playing key role in PHS tolerance, which may assist the breeders to identify PHS tolerance in spring wheat genotypes.

Factors Affecting Pre-Harvest Sprouting Tolerance (PHST) in Spring Wheat (Triticume aestivume L.)

Ahmad Ahmadpour Malakshah and Hemmatollah Pirdashti

Department of Environmental Science, SPPU Pune, India & Agriculture research center of Mazandaran Agricultural Sciences and Natural Resources University, Sari, Iran

Pre-harvest sprouting (PHS) is one of the most important abiotic factors affecting the yield and grain quality of spring wheat in northern part of Iran (Mazandaran Province) due to rainfall and humidity at the harvesting time.

To investigate the effect of mist irrigation (MI) at the harvesting time of wheat, on yield, physiological, biochemical and enzymological attributes of spring wheat during PHS, field experiment was conducted in Northern Iran using forty wheat genotypes. Results of multivariate analysis indicated that there was a highly significant interaction between mist irrigation (MI) period (AB) and genotypes toward PHS tolerance/sensitiveness in all the varieties. The similarity level and mean comparison analysis indicated that about 17 genotypes showed more tolerance to PHS after 21 days of MI. The regression analysis indicated that, sugars and total amylase were increased but yield and starch were decreased after 21 days MI. The traits like, damage percentage, harvest index, biological yield, kernel density per spike and spike number per plot had high negative direct effects on grain yield. While, duration of MI, damage severity, kernel weight, number of kernels per spike, sugars and total amylase had shown indirect effect on grain yield.While, the grain yield and starch decreased after MI.

Phenotypic Stability of Barley Seed Germination

Tefera Tolera Angessa[*], Lee-Anne McFawn[**] and Chengdao Li[*, **]

[*]Western Barley Genetics Alliance, School of Veterinary and Life Sciences (VLS), Murdoch University, 90 South Street, Murdoch, WA6150, Australia

[**]Grains Industry, Department of Agriculture and Food, 3 Baron-Hay Court, WA, Australia

Four hundred and sixty eight barley genotypes of diverse origin were studied for germination percentage in nine different environments. The environments included Esperance 2014, Geraldton 2013 and 2014, Katanning 2013 and 2014. One hundred seeds per genotype were spread on a layer of two filter papers in a 90mm petri dish. Four ml deionized water was added to each petri dish, covered with its lid and placed in an incubator with no light at 20º C temperature. Seeds with any sign of germination were counted after 72 hours of incubation. Further germination environments were created with seeds harvested from Geraldton 2013 and Katanning 2013. One hundred seeds per genotype were incubated in 4 ml and 8 ml deionized water, and germinated seed counted after 48 hours. Germinated seeds from all environments were expressed in percentage and phenotypic stability of barley genotypes assessed using PLABSTAT. The analysis of variance revealed very highly significant differences between barley genotypes and also between environments. Environmental effect was observed to be very strong. Mean germination percentage across genotypes was as low as below 60% in Geraldton 2013 4 ml water 48 hours incubation, Geraldton 2013 4 ml water 72 hours incubation, 2013 and 2014 Katanning 4 ml water 72 hours incubation. The highest germination percentage was recorded in Geraldton 2013 4 ml water 48 hours incubation (91.4%), and Katanning 2013 4 ml water 48 hours incubation (95.5%). This was in contrary to low germination percentage in 8 ml in both Geraldton 2013 and Katanning 2013 environments. Germination percentage variation between genotypes was also substantial. It was observed to be as low as below 40% in VB0330, Beecher, Molloy, and Tilga, in contrary to higher than 95% germination percentage in WI4705, CDC Kendall, and Granifen. When phenotypic stability of barley genotypes was considered, genotypes exhibited high degree of variability in response to environmental change. Some genotypes such as Doolup, WI4892, and CDC Sisler were the most unstable ones. On the other extreme, Commander with an across environment germination percentage of 74% was the most stable genotype with the lowest MS of interaction. Genotypes with high germination percentage across environments showed very low degree of interaction. Spearmen's rank correlation coefficient analysis of germination percentage with days to awn appearance appeared to show no correlation between these two important traits. Overall, barley genotypes included in this study did not show specific adaptability to specific environments as revealed by AMMI analysis. Germination is one of the most important traits of barley. This trait is important agronmically for plant population establishment in the field, for plants to stay dormant after maturity and before harvest, and also in the malt house. About 40.5% of 468 genotypes included in this study showed pre-harvest sprouting in 2015 Esperance Environment of WA. Association mapping of sets of barley genotypes from this study revealed that germination is a trait under genetic control (Gaofeng et al., a paper in this conference). Genotypes with very stable high germination percentage across environments would play substantial roles in advancing our genetic understanding of barley pre-harvest sprouting and in future barley improvements.

A Modelling Framework for Predicting the Risk for Late Maturity Alpha-Amylase (LMA) Across the Main Wheat Producing Shires of Australia

Robert Armstrong[1], Andries Potgieter[1], Graeme Hammer[2],Daryl Mares[3] and Jason Brider[4]
[1]Queensland Alliance for Agriculture and Food Innovation, University of Queensland, 203 Tor Street, Wilsonton Heights, Toowoomba, QLD, Australia, 4350, r.armstrong1@uq.edu.au
[2]Queensland Alliance for Agriculture and Food Innovation, University of Queensland, Room 3.300, Level 3, Qld Bioscience Precinct [#80], Brisbane, QLD, Australia, 4350, g.hammer@uq.edu.au
[3]School of Agriculture Food & Wine, University of Adelaide, Waite Campus, Urrbrae, SA, 5064, daryl.mares@adelaide.edu.au
[4]Department of Agriculture and Fisheries, 203 Tor Street, Wilsonton Heights, Toowoomba, QLD, Australia, 4350, jason.brider@gmail.com

Late maturity alpha-amylase (LMA) is a genetic defect that can result in high levels of alpha-amylase in ripe wheat grain in the absence of weather damage and pre-harvest sprouting. In cultivars susceptible to LMA a low temperature shock can trigger enzyme production during a critical period of grain filling about 25-35 days after flowering. The accumulation of alpha-amylase may result in a low Falling Number that does not meet the specifications for grain receival and export. Varieties with this trait may be unsuitable for classification and represent a significant cost to wheat breeders and the wheat industry. To help industry better understand the incidence risk of LMA, existing associations of certain genotypes to identified triggers (including temperature) obtained from experimental glasshouse studies will aid in the development of an LMA predictive modelling framework. The main goal of this project is to determine the likely frequency of LMA expression for different environments at regional scale across the main wheat growing regions of Australia. This will be achieved through the incorporation of causative LMA triggers, derived from the glasshouse studies, into a biophysical wheat crop model, followed by simulation analysis with historical weather records. The incidence of simulated LMA outputs will be compared with measured data obtained from experimental trial sites across Australia and the triggering criteria adapted to give the best fit. Future outcomes of the project will also be discussed, including the development of risk 'footprint' maps, which will inform industry regarding the degree of LMA risk for specific regions due to the prevailing environmental conditions. This research project is funded by the Grains Research and Development Corporation (GRDC; Project ID: UQ00077).

High and Low Temperature Effects on Grain Dormancy in Wheat

Jose Barrero and Frank Gubler
CSIRO Agriculture and Food / GPO Box 1600, Canberra ACT 2601, Australia

jose.barrero@csiro.au

Environmental cues have a deep influence on grain development and germination with temperature being a major cue affecting both grain dormancy onset and release. We have observed that high temperatures during mid-grain maturation were able to supress the development of grain dormancy making the crop more susceptible to pre-harvest sprouting. We have analysed the responses to high temperature in sets of near-isogenic wheat lines segregating for a major dormancy QTL located on chromosome 4AL, concluding that this QTL is suppressed by heat. Also, following recent discoveries in the model plant Arabidopsis, we have analysed the role of flowering and of grain pigmentation in relation with the effects of temperature on dormancy. By generating a wheat population segregating for a mutation in the flowering gene FT, grain colour and the 4AL QTL we will examine GxE interactions in a major cereal crop species.

Development of a Rapid Sprout Test on a New Falling Number Instrument

Mark L. Bason
Perten Instruments Australia, PO Box 70, North Ryde BC, NSW 1670, Australia

mbason@perten.com

Sprout testing to classify and segregate wheat and other cereals at harvest is a key requirement for grading and trading. For over half a century the Perten Falling Number (FN) instrument has provided this function following standardisation approvals by the ISO, AACCI, ICC and many country-specific regulators. While the standard Hagberg-Perten FN test will continue to be used into the foreseeable future, time pressures at the elevator during harvest make faster testing desirable. To meet these needs, Perten has developed a new model of the Falling Number that is capable of running both the standard FN test and a rapid version through the addition of novel force sensing technology. Analysis of 80 Australian grain and flour samples indicated equivalency to prior models using the standard test. The instrument was also able to detect sound samples in one minute by assessing the force characteristics of the gelling starch during the mixing phase, when the key processes of starch gelatinisation, pasting, thixotropic shearing, enzymatic hydrolysis and thermal denaturation occur. The new method offers significant advantages for time-constrained grain elevators. Other improvements include automatic elevation correction and bath level control, pre-set test time limitation, improved insulation, LIMS handling and touch interface for better accuracy, safety and ease of use.

Using Rainfall Simulators, Germination Index (Gi) and Field Results for the Development of Robust PHS Susceptibility Classifications For New-Release Wheat Varieties in Western Australia

Jeremy Curry[1], Kevin Young[2], Ben Biddulph[1], Dion Nicol[1] and Mario D'Antuono[1]
[1]Department of Agriculture and Food, Western Australia, Australia
[2]GxE Crop Research, Australia

Jeremy.curry@agric.wa.gov.au

Testing varieties for PHS tolerance in field is complicated due to unreliability of rainfall at harvest/maturity and the differences in the maturity of varieties. While GI gives an indication of PHS susceptibility, it doesn't correlate well with observed PHS susceptibility in the field. This is likely due to the low levels of dormancy commonly observed in commercial varieties (GI>0.4). So how can PHS susceptibility be ranked reliably in the seasons prior to the release of a new variety?

Five times of sowing were used to coincide dates of grain filling and maturity for the different varieties. At maturity, samples of 50 heads from 3 replicates of each variety were subjected to a range of artificial rainfall treatments. Linear mixed model was used to incorporate the variability from the field and the rainfall simulator to produce the variety mean dose response (spline) curves (for FN against increasing intensity of rainfall treatments). These fitted curves, produced for each variety at each harvest time, as well as GI and natural field weathering data, were used to rank new or untested varieties against varieties with known variation (Eagle Rock, Mace, Yitpi, Calingiri, Magenta and Westonia, from less to more susceptible).

From the 2015 dataset, DS Newton (tested as ADV08.0065) appears to have the lowest PHS susceptibility of the tested varieties. Scepter (tested as RAC2182) had similar performance to the widely grown and generally low risk variety Mace. Spatial variability in the field and laboratory (rainfall simulator) has been identified and will be the focus of ongoing work.

A combination of artificial weathering, GI and natural field assessments in comparison to well-known varieties suggests the relative PHS risk of new varieties can be developed within 2 seasons. The preliminary 2015 results will be presented to illustrate the responses of the various varieties tested.

Scoring LMA Using SNP Analysis From Elite Australian Breeding Lines

Rudi Appels, Dean Diepeveen, Kerry Forrest and Matthew Hayden

Rudiappels5@gmail.com Australia
Dean.diepeveen@agric.wa.gov.au Australia
Kerry.forrest@ecodev.vic.gov.au Australia
Mathew.hayden@ecodev.vic.gov.au Australia

LMA classification is a major impact on the release of new varieties in Australia due to technology required to assess plant response. Recent research has been focused on a genetic solution to variety classification requirements in Australia. In view of the developmental nature of the LMA phenotype, the pathways associated with LMA are expected to be complex and subject to environmental conditions that are required to trigger LMA response. Australian growing conditions for crops vary and often an LMA responsive variety does not express LMA under comparable conditions. This elevates the need for a more detailed genetic description of factors associated with expression of LMA in order to manage the LMA risk factor in the field.

Our research (McNeil et al, 2009) examined the use of a genetic score based on the presence of a series of genetic markers in order to define the parentage associated with LMA expression. The research uses several sets of discriminating LMA breeding and commercial cultivars from all Australian breeding companies that have been sequenced using the latest high resolution SNP-based wheat maps. Based on phenology results from breeding programs, predicted breeding values (ie LMA scores) are associated with chromosome regions for LMA expressive cultivars. Using cross-validation methods that iterate to develop better associations with the phenotype LMA scores, a clearer association between smaller chromosome regions and LMA scores was determined. The results from these analyses indicated an extremely complex suite of markers are likely to associate with a high risk factor for LMA expression. The study confirmed the significance of the 7BL locus previously identified but this was against a background of many marginal associations. In particular the study supported the conclusions by McNeil et al (2009) that "it is feasible to develop a risk factor for a variety to express LMA using molecular marker data from the 7BL ... LMA regions identified". Overall it was much more reliable to identify non-LMA breeding lines.

Development of Australia's First High-Protein Milling Wheat With Tolerance to Pre-Harvest Sprouting for the Northern Region

Mark Dieters[1,2], Lee Hickey[2] and Nick Willey[3]
[1] *The University of Queensland, School of Agriculture and Food Sciences, Australia*
[2] *Queensland Alliance for Agriculture and Food Innovation, Brisbane, Qld. 4072, Australia*
[3] *Dow AgroSciences Australia Ltd, Unit 12A, 84 Barnes Street Tamworth NSW 2340, Australia*

m.dieters@uq.edu.au

The University of Queensland (UQ) in collaboration with Dow AgroSciences (DAS) expects to release Australia's first wheat variety with increased tolerance to pre-harvest sprouting (PHS) for the northern region during 2016. This variety combines excellent yield potential and rust resistance, with high levels of grain dormancy in a high protein milling wheat (Australian Prime Hard, APH classification), providing for the first time, excellent protection against PHS in a premium milling wheat adapted to the northern wheat growing regions of Australia.

Adverse wet weather at harvest can result in losses in productivity and profitability of wheat producers. After the most recent widespread wet harvest during 2010, GRDC estimated losses of approximately AUD$100 million due to PHS (GRDC, Ground Cover, Feb. 2016). Grain dormancy provides the best option for protection of wheat from pre-harvest sprouting, and is routinely used as a selection criterion in wheat breeding programs. The variety Yitpi (adapted to the southern zone, released in 1999 and classified as Australian Hard, AH) has long been the only Australian wheat variety demonstrating improved levels of grain dormancy with moderate tolerance to PHS. More recently, two APW (Australian Premium White) varieties have been released in Australia: AGT Estoc (2010 release) with high levels of grain dormancy, and DS Pascal (2015 release) with market-leading levels of grain dormancy. Nevertheless, difficulty in the development of cultivars combining high levels of grain dormancy (e.g. equivalent to or better than AGT Estoc) in high protein, hard white cultivars (e.g. APH) has resulted in limited options for northern wheat producers looking for tolerance to PHS.

A proof-of-concept project was initiated at UQ in 2009 using rapid generation advance and high throughput glasshouse screening. We aimed to backcross grain dormancy into an elite Australian APH cultivar (EGA Gregory), using continuous light and controlled temperature conditions, combined with phenotypic screening for grain dormancy in large segregating generations. All crossing and selection was conducted exclusively in the greenhouse, with 10 plant generations completed in the 4 years between 2009 and 2012, with selection for grain dormancy in 4 of the generations. Selected BC3F3:5 rows were grown in the field for the first time in 2012. Lines have been evaluated by DAS in multi-environment yield trials since 2013, with the most promising lines entered into the National Variety Testing scheme in 2015, less than six years after making the F1 crosses. Pending the outcome of variety classification, it is anticipated that one or more high protein milling varieties will be released before the end of 2016, with the first commercial production in 2017. This represents a significant milestone for the northern cropping region of Australia.

The success of this project clearly demonstrates the ability of the rapid generation advance methodology (i.e. 'speed breeding') to quickly and efficiently transfer grain dormancy into an elite spring wheat variety and deliver value to grain producers.

Relationship Between Head Characteristics, Grain Dormancy and Pre-Harvest Sprouting in an Elite Bread Wheat Breeding Population

Karen Graham and Mark Dieters
The University of Queensland St Lucia Campus Hartley Teakle Building St Lucia, Brisbane, Queensland 4072, Australia

karen.graham@uq.edu.au

Grain dormancy and pre-harvest sprouting (PHS) were assessed on 35 lines from a wheat (*T. aestivum* L.) breeding population that had been grown in both field and controlled glasshouse conditions during 2015 in the University of Queensland facilities. The objectives of the study were to ascertain if any correlations exist between head characteristics, sprouting tolerance, and grain dormancy, and identify if there are likely to be any correlated responses in head traits from selection of grain dormancy and sprouting tolerance. Three heads from each genotype were harvested at maturity upon collapse of the first node in a stratified format from the glasshouse and during a single event from the field. Grain dormancy was assessed on threshed grain using the Germination Index (GI7; Walker-Simmons 1987) over a period of seven days. Intact heads were screened for PHS in a misting chamber over multiple days and then dried overnight at 60^0C. In-ear sprouting was calculated from each head by counting the number of individual grain that had sprouted and was scored as a proportion. A series of head and glume characteristics that are frequently used in variety classification were also assessed on heads grown in the field during 2015.

Weak to moderate correlations were observed between some head characteristics, PHS, and GI7. Moderately negative correlations occurred between head density and PHS (-0.30 to -0.33) and GI7 (-0.25), and head length and PHS (-0.25 to -0.33), and GI7 (-0.24). Weak correlations were observed between awn length, PHS (-0.20 to -0.27), and GI7 (-0.11), between glume beak length, PHS (0.14 to 0.21), and GI7 (0.22), and between proportion of glumes open and PHS (0.18 to 0.24). As expected, the strongest correlation occurred between GI7 and PHS (0.65 to 0.81). Heads harvested from the glasshouse showed a stronger correlation with GI7 than those harvested from the field, presumably due to the stratified harvest regime in the glasshouse.

The measure of grain dormancy (GI7) was the only trait that influenced the prediction of PHS. A regression model accounted for 62.1% of variability of the data when GI7 was regressed against the mean estimate of PHS from heads grown in glasshouse conditions.

Based on this study, phenotypes of heads demonstrating superior seed dormancy and reduced in-ear sprouting tended to be long and lax with shorter beaks, longer awns and closed glumes. However, these traits did not influence PHS. Grain dormancy made a significant contribution to expression of PHS but did not account for all of the variation, suggesting a strong contribution of environmental conditions either in conjunction with, or independent of other unmeasured head characteristics. The GI7 method for selection for grain dormancy continues to be a reliable method for improving tolerance to PHS and has the benefit of being a highly heritable trait (0.83).

Speeding Up Development of Adapted Wheat Germplasm Incorporating Sprouting Tolerance and Disease Resistance

Lee Hickey[1] and Mark Dieters[1,2]
[1]The University of Queensland, Queensland Alliance for Agriculture and Food Innovation, Brisbane, QLD 4072, Australia
[2]The University of Queensland, School of Agriculture and Food Sciences, Brisbane, QLD 4072, Australia

l.hickey@uq.edu.au

Pre-harvest sprouting (PHS) is a major problem for the Australian wheat industry because the majority of cultivars lack adequate tolerance. Introduction of grain dormancy into elite cultivars could minimise the impact of PHS by preventing germination in response to rainfall or high humidity at crop maturity. However, this is a challenging task because sources of grain dormancy are relatively unadapted, high levels of dormancy are conferred by multiple genes, and expression is influenced by environmental factors. Further, traditional screening techniques are laborious and selection is typically performed late in the breeding cycle, when variation is limited.

Here, we report a recurrent selection pre-breeding program that sought to develop adapted germplasm incorporating tolerance to pre-harvest sprouting and multiple disease resistance.

A panel of elite donor lines for grain dormancy developed at The University of Queensland were crossed to generate donor F1s, which were then crossed to three Australian adapted wheat cultivars; Suntop, Mace and Lang. This resulted in a series of 3-way crosses (i.e. DxD x A). Populations were developed using the rapid generation advance technology 'speed breeding', where plants were grown in a temperature controlled glasshouse using continuous light to accelerate plant development.

Two cycles of recurrent selection were performed. Each cycle involved: 1) selection for agronomic traits such as plant height and maturity performed in the field at Gatton, Queensland, 2) phenotyping for grain dormancy, and 3) screening for tan spot and leaf rust diseases under controlled conditions. Between and within family selection was performed for agronomic traits and grain dormancy. Intercrossing was carried out under speed breeding conditions, where selected plants within each of the three genetic backgrounds were inter-mated (Suntop, Mace and Lang). Yield testing of selected lines from this program will begin in 2017.

We anticipate this strategy will accelerate the development of adapted wheat germplasm incorporating grain dormancy for tolerance to pre-harvest sprouting and multiple disease resistance.

Highly Sprouting Tolerant Wheat Grain Exhibits Extreme Dormancy and Cold Imbibition Resistant Accumulation of Abscisic Acid

Naoto Kawakami, Yu-ichi Kashiwakura and Daisuke Kobayashi

Department of Life Sciences, School of Agriculture, Meiji University, 1-1-1 Higashimita, Tama-ku, Kawasaki 214-8571, Japan

kawakami@meiji.ac.jp

Pre-harvest sprouting (PHS) of wheat (*Triticum aestivum* L.) grains induces hydrolyzing enzymes such as α-amylase, which considerably decreases wheat product quality. The largest wheat-producing region in Japan is Hokkaido, which is a northern island that often experiences cool and wet weather conditions during the wheat harvest season (i.e., August). The wheat-growing areas are often affected by severe PHS. Seed dormancy has been regarded as a major factor affecting resistance to PHS. It is well known that wheat grains do not show dormancy when imbibed at low temperature, so that the unseasonable weather may brake dormancy and induce germination of the grains in the ear. In this study, we used Japanese PHS tolerant varieties, Gifu-komugi (Gifu) and OS38, to characterize the mechanisms of both dormancy breakage and dormancy maintenance at low temperatures. Physiologically mature Gifu grains exhibited dormancy after imbibition at 20°C, but germinated at 15°C. In contrast, OS38 grains remained dormant even at temperatures as low as 5°C. Embryo half-grains cut out from the dormant Gifu grains germinated by imbibition at 20°C, similar to conventional varieties worldwide. However, OS38 embryo half-grains were still dormant. Hormonome and pharmacological analyses suggested that abscisic acid (ABA) and gibberellin (GA) metabolism are important for temperature dependent dormancy maintenance and breakage. Imbibition at 15°C decreased ABA levels but increased GA levels in embryos of freshly harvested Gifu grains. Additionally, low temperatures induced expression of the ABA catabolism genes, *TaABA8'OH1* and *TaABA8'OH2*, and the GA biosynthesis gene, *TaGA3ox2*, in the embryos. However, in embryos of freshly harvested OS38 grains, ABA levels were increased while GA levels were suppressed at 15°C. In these dormant embryos low temperatures induced the *TaNCED* ABA biosynthesis genes, but suppressed *TaABA8'OH2* and *TaGA3ox2*. These results show that the regulatory mechanism influencing the expression of ABA and GA metabolism genes may be critical for dormancy maintenance and breakage at low temperatures. Our findings should help improve PHS resistant wheat breeding programs.

Relationship Between the Denso Gene and Seed Dormancy

Xiaoxue Liu[1], Xue Gong[2], Yanhao Xu[1], Qiaojun Jia[3] and Chengdao Li[4]
[1]Yangtze University, Jingzhou, Hubei, China 434025
[2]University of Adelaide, Adelaide, South Australia, Australia 5005
[3]Zhejiang Sci &Tech University, Hangzhou, Zhejiang, China 310018
[4]Murdoch University, Murdoch, Western Australia, Australia 6150

Email: x.liu@murdoch.edu.au

The denso gene has been used around the world to develop malting barley varieties and it exists in more than 40% of modern European barley varieties. We have identified that the denso gene encodes a GA-20-oxidase. As the GA is important for seed germination, we investigated if the denso gene affects seed dormancy. A DH population with 178 lines was developed from a cross of Baudin (denso) x Ac Metcalfe. The population was phenotyped for seed germination under 43 different growing and germination conditions. In 24 tests, the denso gene has increased seed dormancy. This is especially true when the germination was conducted under dark condition. Thus, the denso gene may have negative impact on barley germination in the malting plants.

Strategies to Recover Germination From PHS-Resistant Hyperdormant Seeds

Mariko Nonogaki and Hiro Nonogaki
Department of Horticulture, Oregon State University, Corvallis, OR 97331, USA

mariko.nonogaki@oregonstate.edu

Enhanced expression of the ABA biosynthesis gene *NCED* (*nine-cis-epoxycarotenoid dioxygenase*), through inducible expression or a positive feedback mechanism, has been demonstrated to be successful for imposing hyperdormancy in Arabidopsis seeds and offers potential for PHS prevention in cereals. However, the hyperdormancy approach cannot be introduced to cereals without developing strategies for germination recovery. Therefore, strategies for germination recovery were also investigated. Chemical induction of anti-*NCED* or an ABA deactivation gene can reduce ABA levels in seeds, which is expected to break dormancy. However, dormant seeds do not exhibit testa (seed coat) rupture, which might hinder the entry of chemical ligands to seeds. A different system of inducible gene expression using nitrate, a testa-permeable ligand, was examined in Arabidopsis seeds. Results indicated that the nitrate-inducible system was capable of causing expression of a test gene in seeds even before testa rupture. A separate chemical biology approach was also tested for germination recovery. Application of an ABA antagonist, which blocks ABA perception and the signal transduction downstream, recovered germination from the *NCED*-induced hyperdormant seeds in a dose-dependent manner, suggesting that induction of temporal ABA insensitivity could be an alternative to inducible expression of counteracting genes. Combination of the hyperdormancy approach through the enhanced ABA pathways and the germination recovery strategy through counteracting gene induction or chemical biology could provide a comprehensive technology for PHS prevention.

Exploring Protein Expression in Dormant and Germinating Barley

Sarah Osama[1], Ben Schultz[1], Alison Kelly[1,2] and Glen Fox[1]
[1]QAAFI, The University of Queensland, St Lucia, Queensland, Australia
[2]Department of Agriculture and Fisheries, Toowoomba, Queensland, Australia

Barley germination is required for producing malt for brewing. Maltsters require a minimum of 98% germination over the whole processing season which can be more than one year. When germination efficiency drops off unexpectedly there is a major cost to the malting industry and potential for subsequent problems in brewing. To study this loss of viability in barley, germination of the variety Sterling was assessed over a period of three days. Seeds were sampled before germination, 24 h after germination, and 72 h after germination. For comparison purposes, three groups were sampled at 72 h: seeds which had failed to germinate; seeds that had just germinated; and seeds which germinated after 24 h and had been growing for 72 h. Using mass spectrometry, 128 unique proteins were identified. Comparison with SWATH–MS revealed protein abundance differences within the groups sampled. Many large differences were identified along the time course of germination. The samples which failed to germinate were similar for a large number of proteins to the samples which had been growing for 72 h. However, there were some proteins which were very different in abundance between these samples. These differences may contribute to failure of the onset of germination in these seeds. The identification of these essential proteins supporting germination which are absent in the dormant seeds could help tackle the gap of knowledge in dormancy.

Genetic Gain in Pre-Harvest Sprouting Tolerance Amongst Commercial, White Grained Wheat

A. Rattey[1*], N. Willey[2], A. Mitchell[2], R. Chambers[3], S. Shorter[4] and R. Richards[5]
[1]*Dow Seeds, Canberra, Australia*
[2]*Dow Seeds, Canberra, Australia*
[3]*Dow Seeds, Sydney, Australia*
[4]*New Zealand Plant and Food Research, Australia*
[5]*CSIRO, Canberra, Australia*

[*]*Corresponding author: arattey@dow.com*

Rain at harvest causes industry losses through harvest delays, reduced test weight and can cause pre-harvest sprouting (PHS). 2010 was the most recent widespread 'wet harvest', with GRDC estimating losses of approximately $100 million due to PHS. Currently, limited genetic tolerance to PHS exists amongst Australian wheat lines; for years, Yitpi and a related line (Estoc) have been considered the benchmark for PHS tolerance amongst commercial white grained wheat varieties grown in Australia. High levels of grain dormancy, or reduced PHS effects, should be seen as an 'insurance' to limit the impact of PHS. Dow Seeds has been targeting genetic improvements in grain dormancy, estimated using germination index (GI) as a surrogate attribute. This has been achieved via targeted introgression of novel germplasm, where crosses between elite germplasm and the donor have been coupled with intensive phenotyping for the low GI amongst large populations. These populations have then enabled identification of sufficient numbers of individuals with acceptable commercial ideotype to be tested for their adaptation to the growing regions of Australia. As a consequence of these efforts, Dow Seeds have launched a variety called DS Pascal that has GI similar to SUN325B and drastically lower than Estoc and Yitpi (Fig. 1). DS Pascal is highly adapted to earlier sowing opportunities across much of Southern Australia. Dow Seeds will also be launching a line in Northern Australia (DS Faraday) with very low GI from a different donor line in the near future. These drastic reductions for GI amongst DS Pascal and DS Faraday, and their subsequent use in recurrent breeding for all attributes important to Australian wheat, should help reduce the effects of PHS on industry profitability.

High-Resolution Mapping and Haplotype Analysis of Diverse Germplasm Highlights a Causal Role of *Tamkk3* as the Major 4Al Pre-Harvest Sprouting Resistance Locus *Phs-A1*

Oluwaseyi Shorinola[1], Nicholas Bird[1,5], James Simmonds[1], Simon Berry[2], Tina Henriksson[3], Peter Jack[4], Peter Werner[5], Tanja Gergets[6], Duncan Scholefield[6], Barbara Balcárková[7], Miroslav Valárik[7], Michael Holdsworth[6], John Flintham[1] and Cristobal Uauy[1*]

[1]*John Innes Centre, Norwich Research Park, NR4 7UH, UK*
[2]*Limagrain UK Ltd, Woolpit Business Park, IP30 9UP, UK*
[3]*Lantmannen, SE-268 81, Svalov, Sweden*
[4]*RAGT Seeds, Essex, CB10 1TA, UK*
[5]*KWS UK Ltd, Hertfordshire, SG8 7RE, UK*
[6]*Division of Plant and Crop Sciences, School of Biosciences, University of Nottingham, LE12 5RD, UK*
[7]*Centre of Plant Structural and Functional Genomics, Olomouc, 783 71, Czechia*

Pre-harvest Sprouting (PHS) is a grain defect that is characterised by premature seed germination before harvest which is detrimental to global wheat production. While PHS is a complex multi-genic trait, a significant proportion of the natural variation for sprouting is controlled by a few major QTL, including *Phs-A1* on chromosome arm 4AL. Two candidate genes including the tandem *PM19* genes and *TaMKK3* have recently been proposed to underlie this major QTL. However, it is presently unclear whether independent natural variations at these two loci individually or together account for this QTL effect. To characterise the *Phs-A1* locus and to examine the causal effects of these candidate genes, we constructed an extended physical map of the *Phs-A1* locus. This physical map information along with high-resolution fine-mapping in two independent UK populations supports a causal role of *TaMKK3*, and not the *PM19* genes, in *Phs-A1* effect. Using diverse progenitor, historic and modern germplasm, we show that the susceptible *TaMKK3* mutation originates from the diploid A-genome progenitor - *Triticum urartu*, and that this allele has increased in frequency through domestication and breeding. Finally, analysis of exome capture data of diverse hexaploid wheat populations highlights a finite number of distinct haplotypes at the *TaMKK3* locus. The molecular marker as well as haplotype information reported in this study will advance more precise deployment of this major PHS resistance locus into elite germplasm.

Amylab FN, a New Alternative to Measure Hagberg Falling Number

Gregory VERICEL, Product Manager, CHOPIN Technologies
20 avenue Marcellin Berthelot, 92390 Villeneuve-la-Garenne, France

Contact email : gvericel@chopin.fr

The Amylab FN measures the activity of starch degrading enzymes (alpha-amylases) to detect sprout damage in wheat or rye. It uses the standard Hagberg Falling Number method or the new, unique and faster Testogram method.

Reminder: The Falling number method is based on the ability of α-amylase to liquefy a starch gel. The activity of the enzyme is measured by falling number (FN), defined as time in seconds required to stir and allow stirrer to fall a measured distance through a hot aqueous flour or meal gel undergoing liquefaction. α-amylase activity is associated with kernel sprouting, and both of these are inversely correlated with FN. The method is applicable to both meal and flour of small grains and to malted cereals.

The Amylab FN features several key innovations. Instead of a standard boiling water bath, the Amylab FN uses an induction heating system, that is safer (no boiling water) and less sensitive to environment variations such as altitude or water level. Consequently, results are more accurate. Also, instead of a standard glass tube (breakable, difficult to clean), the Amylab FN uses a test tube made of aluminum, with a removable bottom, which makes it very quick and easy to clean.

Finally, the Amylab FN features a new testing method called Testogram. Instead of measuring the time required for the plunger to fall down the tube and go through the starch gel sample (which takes between 60 and 500 seconds depending on the sample, average 325 seconds), it records the consistency during 90 seconds of constant shaking and determines if there is sprout damage in the sample.

The Testogram method provides results that are on average 66% faster compared to the standard Falling Number Method.

Sprouting Tolerance in Barley in Victorian Mallee

Linda Walters
Birchip Cropping Group, 73 Cumming Avenue Birchip VIC 3483, Australia

linda@bcg.org.au

Specific varieties can differ in their susceptibility to the effects of a delayed and wet harvest. The amount, timing and duration of rainfall events, related humidity and temperatures can influence sprouting. When this occurs in the grain, it results in an increase in alpha-amylase, causing the breakdown of starch content. Grain that has sprouted is not suitable for malting or sowing because of potential loss of seed viability, reduced capacity for long storage time and a decline in feed value. With the risk of unknown weather patterns at harvest, sprouting is not common but can pose significant losses in susceptible varieties when it does occur.

The trials were conducted to determine the sprouting tolerance of new and existing barley varieties in field based trials, in 2014 and 2015 in the northern Victorian Mallee. It was sown under overhead irrigation sprinklers, including three different water treatments (total of irrigation and rainfall). In 2014 this included a control (0mm), 20mm and 48mm treatments. In 2015 the treatments were control (0mm), 50mm and 76mm. These treatments were applied in split irrigation applications and actual rainfall. Harvest was delayed with each of these treatments.

The irrigation was targeted when actual rainfall was forecast and conditions were humid with lower temperatures and low wind speed (to maintain consistency in irrigation) to better simulate a 'rainfall' event.

In 2014 the trial consisted of six barley varieties, Compass, La Trobe, Fathom, Scope CL, Schooner and Skipper. In 2015, Spartacus CL, Hindmarsh, Commander, La Trobe, Scope CL and Compass were trialled. Grain quality, yield and falling numbers was carried out on the varieties.

In 2015, conditions at harvest were more conducive to sprouting. Falling numbers in Commander, Spartacus CL, La Trobe and Hindmarsh, declined significantly in the presence of rainfall. Scope CL was the most tolerant variety in both years.

Consequently, as harvest was delayed and grain became favourable to sprouting, test weight decreased, however wasn't significant between varieties. In 2015 field fungi and dark tipping were also present in the grain, which consequently leads to further downgrades at grain receival sites.

By determining which varieties pose a greater susceptibility, growers can manage their variety selections and timeliness in their harvesting program.

Characterization of Two Stable Qtls *qphs.sicau-1B* and *qphs.sicau-3D* From Synthetic Wheat, and Their Application for Wheat Breeding

Jian Yang[1,†], Chao Tan[1,†], Zaoxia Wang[1], Lianquan Zhang[1], Dengcai Liu[1] and Jirui Wang[1*]
[1]Triticeae Research Institute, Sichuan Agricultural University, Chengdu-Wenjiang, Sichuan 611130, China

Email: wangjirui@gmail.com

Pre-harvest sprouting was a seriously problem leading to quality deterioration, as well as yield decreasing. Similarly, accumulation of amylase in the later stage of grain development also cause many losses as pre-harvest sprouting. In order to characterize the genes associated with pre-harvest sprouting in synthetic wheat Axiom™ wheat 660k Arrays was applied for QTL mapping, and nine QTLs were detected at more than one environments. Two of the 8 QTLs *qPHS.sicau-3D* and *qPHS.sicau-1B* on chromosome on 3DL and 1BS were stable at 15 and 8 environments, which were form *Aegilops tauschii* and *Triticum turgidum* respectively. Physical mapping of *qPHS.sicau-3D* revealed that it was co-located with *TaMyb10-D* gene. The expression of *TaMyb10-D* was significant different between two parents at the beginning of grain development. While the *qPHS.sicau-1B* may harbor novel gene(s) for pre-harvest sprouting. In additional, transcripts variation of *TaAmy1* was also measured, and one eQTLs for *TaAmy1* was detected at both DPA25 and DPA30 that was overlapped with QTL *qPHS.sicau-1B*. It demonstrated that this QTL/eQTL could confer PHS resistance of wheat according to decrease *TaAmy1* transcripts quantity. Furthermore, a new registered wheat (in 2016) cultivar "Shumai 580" showed high pre-harvest sprouting resistance as its synthetic wheat parent, which carried regions containing *qPHS.sicau-3D* and partial *qPHS.sicau-1B*. It was indicated that these QTLs derived from synthetic wheat would improve PHS resistant breeding for wheat.

Conferring Resistance to Pre-Harvest Sprouting in Durum Wheat by a QTL Identified in Triticum Spelta

Yujiao Liu[1,2,†], Yaxi Liu[1,†], Yong Zhou[1], Charlene Wight[2], Zhien Pu[1], Pengfei Qi[1], Qiantao Jiang[1], Mei Deng[1], Zaoxia Wang[1], Yuming Wei[1], Wenguang Cao[2], Dengcai Liu[1], Youliang Zheng[1], Chunji Liu[3], Judith Frégeau-Reid[2] and Jirui Wang[1*]

[1]Triticeae Research Institute, Sichuan Agricultural University, Chengdu-Wenjiang, Sichuan 611130, China
[2]Agriculture & Agri-Food Canada, Eastern Cereal and Oilseed Research Centre, Ottawa, Ontario, K1A 0C6, Canada
[3]CSIRO Agriculture Flagship, 306 Carmody Road, St Lucia 4067, QLD, Australia

Email: wangjirui@gmail.com

Pre-harvest sprouting (PHS) causes significant yield loss and degrade the end-use quality of wheat, especially in regions with prolonged wet weather during the harvesting season. Unfortunately, there is inadequate genetic resource in *Triticum durum* (tetraploid durum wheat) for PHS resistance. Therefore finding out new genetic resources from other wheat species to develop PHS resistance in durum wheat is of importance. A major PHS resistance QTL, *Qphs.sicau-3B.1*, was mapped on chromosome 3BL in a recombinant inbred line population derived from 'CSCR6' (*Triticum spelta*), a PHS resistant hexaploid wheat and 'Lang', a PHS susceptible Australian hexaploid wheat cultivar. This QTL, *Qphs.sicau-3B.1*, is positioned between DArT marker *wPt-3107* and *wPt-6785*. Two SCAR markers (Ph3B.1 and Ph3B.2) were developed to track this major QTL and were used to assay a BC2F8 tetraploid population derived from a cross between the durum wheat 'Bellaroi' (PHS susceptible) and 'CSCR6' (PHS resistant). Phenotypic assay and marker-assisted selection revealed five tetraploid lines which were highly stable PHS resistant. This study has successfully established that PHS-resistance QTL from hexaploid wheat could be efficiently introgressed into tetraploid durum wheat. This tetraploid wheat germplasm could be useful in developing PHS resistant durum cultivars with high yield and good end-use quality.

Genome-Wide Association Analysis for Pre-Harvest Sprouting Resistance in a Large Germplasm Collection of Chinese Wheat Landrace

Yong Zhou[1], Mengping Cheng[1], Zhongxu Chen[1], Zhanyi Li[1], Shang Gao[1], Yaxi Liu[1], Yuming Wei[1], Youliang Zheng[1,2] and Jirui Wang[1*]

[1]Triticeae Research Institute, Sichuan Agricultural University, Chengdu 611130, China
[2]Ministry of Education Key Laboratory for Crop Genetic Resources and Improvement in Southwest China, Sichuan Agricultural University, Yaan, Sichuan 625014, China

Email: wangjirui@gmail.com

Pre-harvest sprouting (PHS) is considered a worldwide disaster that reduces the production and damages quality of wheat. In China, the wheat in Huai River Valleys and Southwestern China are usually suffered by PHS. The germination levels of 717 Chinese wheat landraces from all 10 wheat growing zones were extensively examined in 2011-2015. Genetic architecture of PHS tolerance in a genome-wide association study using DArT-seq and Wheat660 SNP assay was also conducted. After four years' trait evaluation, 194 varieties had stable PHS tolerance (mean GR < 0.200), including 9 white kernel-grain varieties. Landraces from 3 south China wheat growing zones showed the highest PHS tolerance (mean GR < 0.300). While landraces from Xingjinag in northwest China showed the lowest tolerance to PHS with an average germination rate of 0.678. About 9,740 high-quality polymorphisms DArT-seq markers and 178,803 Wheat660 SNP markers of the whole genome with minor allele frequency (MAF) > 0.05 were selected for genome-wide association analysis (GWAS). Eight DArT-seq markers and 89Wheat660 SNP markers were significantly associated with PHS resistance, among which 3 DArT-seq markers and 24 SNP markers were newly identified. Strong signals were observed on chromosomes 3A, 3B, 3D, 5D and 7D from at least two environments. In total, four favor/elite types and nine favor/elite alleles for PHS tolerance were identified by DArT-seq and SNP markers respectively. The favor types and alleles appeared at one environment could be utilized for PHS breeding at other environments.

A Pyramiding Effect of Major Pre-Harvest Sprouting Resistance Qtls in Wheat and Development of Near-Isogenic Lines for Genetic Characterisation of the Trait

Xingyi Wang, Hui Liu, Kadambot H. M. Siddique and Guijun Yan
Company/address: School of Plant Biology and The UWA Institute of Agriculture, Faculty of Science, The University of Western Australia, 35 Stirling Hwy, Crawley, WA 6009, Australia

Contact email: guijun.yan@uwa.edu.au

Marker-assisted selection (MAS) is an important means of improving the selection efficiency in plant breeding. In this study, four large effect alleles responsible for PHS resistance were investigated for their separate or joint effects in 42 Australian wheat cultivars to validate their potential for MAS. Four PCR markers *Xgwm155*, *Vp1B3*, *Xzxq118* and *Xgwm495* associated with alleles located on 3AL, 3BL, 4AL and 4BL, respectively, were used for the investigation. The results confirmed that each resistant allele contributed positively to pre-harvest sprouting (PHS) resistance. The PHS scores for the genotypes with PHS resistant alleles from the four markers were 3.14, 2.47, 3.13 and 2.78, respectively, which were significantly higher than those with susceptible alleles that were 2.17, 1.50, 2.15 and 2.00, respectively ($p<0.05$) among the scale of 1 (susceptible) to 4 (resistant). Of the PHS resistance alleles, a pyramiding effect - the more resistance alleles, the higher the PHS resistance-were observed indicating the positive interactions among the resistance alleles. Near-isogenic lines for three QTLs located on 3AL, 4AL and 4BL have been developed using a fast generation cycling system and MAS. The isolines are being characterised phenotypically and by transcriptomic, proteomic and metabolomic approaches.

Analysis of Chromosome 5HL Genes for Seed Dormancy and Malting Quality

Xiao-Qi Zhang[1], Sue Broughton[2], Penghao Wang[1], Gaofeng Zhou[1], Qisen Zhang[3], Lee-Anne McFawn[2], Roberto Barrero[1] and Chengdao Li[1,2]

[1]WA State Agricultural Biotechnology Centre, School of Veterinary and Life Sciences, Murdoch University, South Street, Murdoch, WA 6150, Australia

[2]Department of Agriculture and Food Western Australia, [3]Baron-Hay Court, South Perth, WA 6151, Australia

[3]Australian Export Grains Innovation Centre, [3]Baron-Hay Court, South Perth, WA 6151, Australia

The telomere region of chromosome 5HL has been identified as a hot spot for multiple QTLs controlling seed dormancy and malting quality. We sequenced 25 BAC clones and assembled a scaffold with 1.68 million base pairs covering the QTL region. There are 44 genes annotated including three copies of AWPM-19-like family protein and two copies of protein kinase superfamily protein. These two gene families have been indicated as important members controlling seed dormancy. We further conducted whole genome transcriptomic analysis of 24 and 48 hr germinating barley (green malt) from Australian and Canadian barleys with different seed dormancy and malting quality. There were seven genes with differential expression, including three members of the AWPM-19-like family gene. Over 100 INDEL and SNP molecular markers were developed and tested in two doubled haploid populations and over 600 barley varieties. The protein kinase gene appears to be more important in controlling seed dormancy while the AWPM-19-like genes play only minor roles in certain environments. Six haplotypes of the gene combinations were identified and allele-specific molecular markers were developed for molecular marker-assisted selection.

Genetic Analysis of Seed Dormancy in Barley

Gaofeng Zhou, Xiao-Qi Zhang, Lee-Anne Mcfawn, Sue Broughton and Chengdao Li

[1] WA State Agricultural Biotechnology Centre, School of Veterinary and Life Sciences, Murdoch University, South Street, Murdoch, WA 6150, Australia

[2]Department of Agriculture and Food Western Australia, [3]Baron-Hay Court, South Perth, WA 6151, Australia

[3]Australian Export Grains Innovation Centre, [3]Baron-Hay Court, South Perth, WA 6151, Australia

Seed dormancy plays a pivotal role in pre-harvest sprouting in barley. A total of 830 barley accessions were collected from all over the world and used in the present study. The lines were sown in Esperance, Geraldton, and Katanning in 2013 and 2014. Around 17,000 DArT markers were applied to genotype this population. By filtering the data with callrate and PIC value, 4071 molecular markers were used for association mapping analysis. The locus on chromosome 5HL was identified as a major QTL for seed dormancy in three locations. Novel loci were detected on chromosome 2HL, 3HL and 6HL in Geraldton (2014) and Esperance (2014) environments. Furthermore, we also detected the QTL for loss of germination on chromosome 2HS, 3HS, 5HL, 6H and 7HL.

Abscisic Acid-Catalase2-Reactive Oxygen Species Cycle is Involved in Dormancy and Germination of Barley Seeds

Gaku Watabe[1], Nozomi Aoki[1], Kyohei Kai[1], Reisa Tomokiyo[2], Norimitsu Hamaoka[1,2], Mari Iwaya-Inoue[1,2] and Yushi Ishibashi[1,2*]

[1]*Graduate Sch. Biores. Bioenviron. Sci.,Kyushu University, Japan*
[2]*Faculty of Agriculture, Kyushu University, Japan*

Contact email: yushi@agr.kyushu-u.ac.jp

Reactive oxygen species (ROS) release seed dormancy and promote seed germination in several cereal crops. ROS produced in barley (*Hordeum vulgare* L.) seed after imbibition regulate germination by enhancing gibberellin (GA) biosynthesis and abscisic acid (ABA) metabolism in non- dormant seeds. However, the mechanism of ROS regulation in dormant seeds is not yet well-known. In nine barley cultivars that have different dormancy levels, germination index (GI) and ROS contents in embryo showed positive correlation. Therefore, we focused on the expression of ROS production and catabolism related-genes in dormant seeds. The expression of *catalase2* (*HvCAT2*) gene, one of the antioxidant enzymes, was up-regulated in dormant seeds during imbibition. Furthermore, GI and *HvCAT2* expression in the nine cultivars demonstrated negative correlation. To clarify the role of *HvCAT2* in seed dormancy, we examined the transient assay in isolated mature embryo and found that led to decrease in germination rate. These results indicated that *HvCAT2* was involved in regulation of barley seed germination.

It has been reported that ABA insensitive5 (ABI5), ABA responsive transcription factor, is bound to ABA-responsive transcriptional factor (ABRE) (Casaretto et al. 2003) which domain was found at 500bp up-stream of *HvCAT2* promoter region. *HvCAT2* and *HvABI5* expressions were induced by exogenous ABA. In addition, high ABA contents and *HvABI5* expression levels were confirmed in dormant seeds during imbibition. Using electrophoresis mobility shift assay, it was confirmed that ABI5 was able to bind to ABRE at *HvCAT2* promoter region. In this study, it was suggested that dormant seeds maintained high ABA contents promoting *HvCAT2* expression through ABI5 for ROS catabolism. In addition, ABA catabolism gene, ABA 8'-hydroxylases1 (*HvABA8'OH1*), was induced by exogenous ROS.

Therefore, dormant seeds showed low ROS contents with decreased *HvABA8'OH1* expression to maintain high ABA contents. Thus, the ABA-*HvCAT2*-ROS cycle might play an important role in dormancy mechanism.

Rapid Prediction of Wheat Falling Number by Multivariate Analysis of Rva Data

Jennifer M.C. Dang and Mark L. Bason
Perten Instruments Australia, PO Box 70, North Ryde BC, NSW 1670, Australia

jdang@perten.com

Preharvest sprouting in wheat results in increased amylase activity, which leads to many problems in processing and final product quality. The Falling Number (FN) test is widely used to measure sprout damage, however a simpler and faster method would benefit time-constrained grain receival sites. Although the three-minute Stirring Number (SN) test, using the Rapid Visco Analyser (RVA), shows good correlation to FN results, the test time is still considered too long and it has had limited success in replacing the FN. This study investigates the feasibility of using multivariate analysis on the RVA viscosity curve to more rapidly predict FN. SN and FN tests were performed on 211 Australian wheat samples with a wide range in α-amylase content. For the critical grading range of FN $\leq$ 350 s (n = 119), univariate correlation of FN and SN (viscosity at 180 s) gave a root mean square (RMS) of residuals of the fit of 19.1 s (R2 = 0.95). For the same data set, the univariate correlation of FN versus the single RVA viscosity point at 60 s gave an RMS of 27.7 s (R2 = 0.90). Partial least squares (PLS) regression of raw data points from 20 to 60 s of the RVA profile was able to predict FN with an error of 25.1 s (R2 = 0.93) for samples with FN $\leq$ 350 s. The results indicate that a one-minute RVA method, in combination with multivariate analysis of the raw data points, can be used to estimate the FN of wheat, with minimal loss of prediction accuracy. The shorter test will benefit time-constrained grain receival sites.

Starch pasting properties by Mixo Lab of wheat samples differing in Falling Numbers

L. Cato and J. Ng
Australian Export Grains innovation Centre (AEGIC), South Perth, WA, Australia

larisa.cato@aegic.org.au

Pre-harvest sprouting or weather damage in wheat can cause processing problems for the affected grain due to actions of various enzymes such as amylases, proteases and lipases in the grain endosperm. These enzymes accelerate the breakdown of starch granules and protein in the endosperm. Wheat that is weather damaged has a significantly lower market value as it can impact the quality of end-products for example loaf structure and volume, or noodle colour and cooking quality. Eight wheat varieties were collected from each of the three locations from the Esperance region in Western Australia from 2015-16 growing season. One of the three locations (Neridup) has received unwanted harvest rain and thus resulted in samples with very low Falling Numbers (ranging from 62 to 283 seconds). Falling numbers at the second site (Salmon Gums) ranged from 452 to 502 and from 298 to 449 seconds at the third site (Cascade). The MixoLab is a device developed for the quality control of cereals. It measures dough and flour quality by exposing a sample to predetermined heating and cooling cycles while placing the sample under a strain field (Chopin Technologies, France). The MixoLab was used in this study to evaluate mixing properties (protein) and pasting properties (starch) of wheat flour samples milled on a Buhler mill at 60% flour extraction for noodle making. Wheat protein content at Salmon Gums, Neridup and Cascade ranged from 9.4 to 11.5, 10.1 to 11.7 and 8.4 to 9.5 respectively. Noodle brightness was lowest at Neridup as expected due to low Falling Numbers. Starch pasting properties as measured by MixoLab will be discussed as related to noodle cooking and eating properties.

Advantages of publishing in Frontiers

OPEN ACCESS
Articles are free to read for greatest visibility and readership

FAST PUBLICATION
Around 90 days from submission to decision

HIGH QUALITY PEER-REVIEW
Rigorous, collaborative, and constructive peer-review

TRANSPARENT PEER-REVIEW
Editors and reviewers acknowledged by name on published articles

Frontiers
Avenue du Tribunal-Fédéral 34
1005 Lausanne | Switzerland

Visit us: www.frontiersin.org
Contact us: info@frontiersin.org | +41 21 510 17 00

REPRODUCIBILITY OF RESEARCH
Support open data and methods to enhance research reproducibility

DIGITAL PUBLISHING
Articles designed for optimal readership across devices

FOLLOW US
@frontiersin

IMPACT METRICS
Advanced article metrics track visibility across digital media

EXTENSIVE PROMOTION
Marketing and promotion of impactful research

LOOP RESEARCH NETWORK
Our network increases your article's readership